

**A LITERATURE SURVEY**  
**ON**  
**Study the Effects of ESIPT and TICT Mechanism on the**  
**Fluorescence Behavior of Organic Luminogen**



**Submitted by**

**Abhisek Saikia**

**Exam Roll No.: PS-191-808-0047**

**Registration number: 283922 of 2016-17**

**M.Sc. 4th semester**  
**Gauhati University**

**Supervisor**

**Dr. Rupam Jyoti Sarma**

**Associate professor**

**Department of Chemistry, Gauhati University**

## **Certificate**

This is to certify that the literature survey report, entitled “**Study the Effects of ESIPT and TICT Mechanism on the Fluorescence Behavior of Organic Luminogen**” is submitted by **ABHISEK SAIKIA**, M. Sc 4th semester, Gauhati University in partial fulfillment of the requirement for the degree of Master in Science in Chemistry. The literature survey is a bonafide work carried out by her under my supervision and guidance.

**Dr. Rupam Jyoti Sarma**

**Associate professor**

**Department of Chemistry**

**Gauhati University**

## **ACKNOWLEDGEMENT**

I would like to express my special appreciation to my project supervisor **Dr. Rupam Jyoti Sarma**, Associate professor, Department of Chemistry, Gauhati University, for his constant guidance, congenial help and unfailing support throughout my literature survey work.

I would like to take the opportunity to thank **Dr. Chitrani Medhi**, Head of the Department, Chemistry, for giving me the opportunity to do the literature survey work and providing timely support.

I am pleased to convey my hearty thanks to Krishnamoni Deka and Garima Saikia for their help and encouragements during various stages of completion of the literature survey.

**Date: 08/09/2021**

**Abhisek Saikia**

**Roll no.: PS-191-808-0047**

**Registration number: 283922 of 2016-17**

**M. Sc. 4<sup>th</sup> Semester**

**Department of Chemistry**

**Gauhati University**

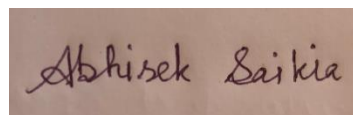
## **DECLARATION**

I, **Abhisek Saikia** student of M.Sc. 4<sup>th</sup> semester, studying at Gauhati University, Guwahati, hereby declared that the M.Sc. project report on “**Study the Effects of ESIPT and TICT Mechanism on the Fluorescence Behavior of Organic Luminogen**” submitted to Gauhati University is the work conducted by me.

This report is not being submitted to any other University for award of any other Degree, Diploma and Fellowship.

**Date:** 08/09/2021

**Place:** Guwahati

A rectangular box containing a handwritten signature in dark ink. The signature is written in a cursive style and reads "Abhisek Saikia".

(Abhisek Saikia)



## **CONTENTS**

## **Page No.**

<b>1. Introduction</b>	<b>1</b>
<b>2. Examine how ESIPT and TICT works</b>	<b>2</b>
<b>3. Detailed mechanical explanation of     ESIPT and TICT</b>	<b>5</b>
<b>4. Conditions which favor</b>	
<b>4.1</b> ESIPT process	11
<b>4.2</b> TICT process	12
<b>5. Examine the role of</b>	
<b>5.1</b> Molecular structure & Geometry (Conformation)	13
<b>5.2</b> Solvent effect	23
<b>5.3</b> Intra/intermolecular interaction	30
In the process of ESIPT and TICT	
<b>6. Conclusion</b>	<b>34</b>
<b>7. References</b>	<b>35</b>

# Study the Effects of ESIPT and TICT Mechanism on the Fluorescence Behavior of Organic Luminogenes.

**Abstract:** Charge transfer and separation are foremost processes governing numerous chemical reactions. Basic understanding of those processes and therefore the underlying mechanism is essential for chemical science and photochemistry. Excited-state intramolecular proton transfer (ESIPT) and twist intramolecular charge transfer (TICT) are the two most fundamental dynamic processes, associated with biological and chemical reactions. ESIPT and TICT are an electron transfer process that occurs upon photoexcitation in molecules that usually contain both donor and acceptor part linked by a single bond. Here, I have discussed the mechanisms of Excited State Intramolecular Proton Transfer (ESIPT) and Twisted Intramolecular Charge Transfer (TICT) and their effects on the Fluorescence behaviour of Organic Luminogenes. Apart from these, I have added little information regarding the favorable conditions for occurrence of ESIPT and TICT and role of structure, geometry, solvent and intra/inter molecular interaction.

## 1. Introduction

Luminescence-based applications become one amongst the foremost and promising topics in materials science, have led to great development of fluorescent and phosphorescent molecules. Since the light properties of molecules are key factors governing application options, understanding and management of radiative and nonradiative decay processes aren't solely demanded to optimize the present performance, however conjointly expected to encourage novel and innovative application ideas.

The intra- and inter- molecular chemical bond (H-Bond), a noncovalent weak fundamental interaction, widely exists in numerous branches owing to its elementary importance in chemical science (photophysics & photochemistry) and photobiology, a lot of attention has been dedicated to the investigation of H-Bonding interaction [1]. H-Bond intensity is closely associated with proton donor acidity and proton acceptor basicity. Upon the photoexcitation, each the acidity and also basicity of the donor and acceptor become stronger, respectively [2]. Thus the H-Bond is enhanced within the excited state, that can promote excited state

intramolecular and intermolecular proton transfer, that is, the enhancing HB provides driving force for the ESIPT reaction process [3].

The dynamic processes of ESIPT are an enormous challenge in theoretical and experimental investigations. Since the first appearance of the ESIPT reaction in the late 1940s [40], the correlation mechanisms and potential applications have become more and more attractive. Photoinduced proton transfer in proteins and enzymes of photosynthesis and respiration has attracted much attention, which is also an important task in bioengineering [4]. ESIPT systems widely used in sensors for humidity, mostly luminescent solar collectors [5], they are also used for proton transfer lasers [6] as well as photo stabilizers and devices based on thermally activated delayed fluorescence [7], moreover they used as white light generation [8], organic lightemitting diodes (WOLED) [9] as well as suitability in sensing of anion and cations, photochromic switching [10] and even understanding of fading of colorants in art. [11]

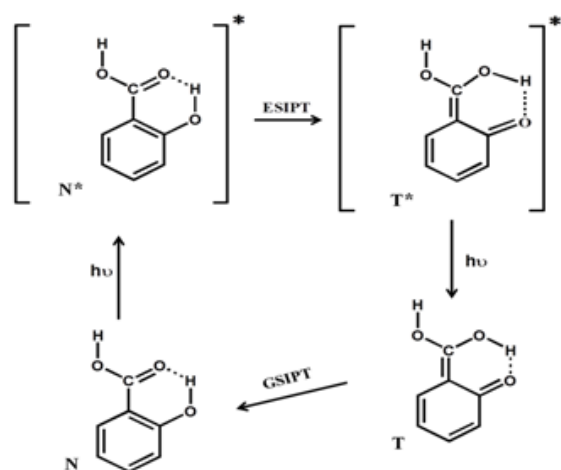
Numerous donor–acceptor substituted aromatic compounds show dual fluorescence and is explained by the twisting of the donor relative to the acceptor group [12]. The decoupling of the two groups that results from the twisting process, i.e. separation of donor and acceptor, that usually results in the considerable charge transfer and results in a highly polar, charge separated state commonly known as the twisted intramolecular charge transfer (TICT) state [13]. Besides being an elementary photophysical phenomenon, TICT has found applications that embody pH and ion indicators, highly sensitive for specific ions, fluorescent probes, liquid crystals, fluorescent solar collectors, and volume sensing in polymers. Recently, it was found that there is a stabilization of the charge separation process by the TICT state in case of the dye-sensitized solar cells (DSSCs) usually via a little charge recombination rate [31].

## **2. Examine how ESIPT and TICT works**

As a general definition, molecules, that contain each proton donating or accepting groups, can undergo excited-state intramolecular proton transfer (ESIPT) due to magnified acidity/basicity. In SA (salicylic acid), as an example, the hydrogen of the hydroxyl group becomes more electropositive but the oxygen of the carboxylic group attains more

electronegative character within the excited-state. That leads to the proton translocation from the hydroxyl group to the carboxylic group. The schematic illustration of ESIPT in salicylic acid is given in Scheme 1, where N and T denoted the ground state normal and tautomer (obtained as a result of the ESIPT) forms, respectively. Their analogous excited state forms are denoted as N\* and T\*. The zwitter ion that results from this translocation involving electron transfer and in some cases, it leads to the partial or complete hydrogen transfer (ESIHT) state, when it is displaced.[ 11]

Traditionally, ESIPT is taken into account as a method where the proton is exchanged through intramolecular H-bonding between the proton donating and accepting groups within the molecule. There are also systems, where the proton donating and accepting sites aren't adjacent and hence the proton is transferred over a significantly long distance. For this specific case, the PT can be a result either from solvent or concentration assisted and ultimately a proton is transferred within the same molecule, termed as pseudo-intramolecular [29].



**Scheme1.** Representative photocycle of excited-state intramolecular proton transfer (ESIPT) in Salicylic acid (SA).

Some chemical groups of family such as carboxylic acids which can be used as proton transfer systems are hydroxybenzoic acids & esters [14], hydroxynaphthoic acids & anthranilic acid and its esters [15]. Besides carboxylic acids, alternative compounds closely related to the family of hydroxyflavones, quinoline and anthraquinones, 7-azaindole and derivatives, hydroxyl

phenylbenzoxazole (HBO) derivatives. One of the mostly studied compounds is the Azo dyes and also Schiff bases and are well documented in the literature [11].

TICT might be a comparatively common process for molecules that contain a D–A (such that D and A within the context of charge transfer refers to electron donating or accepting groups rather than donors or acceptors of the excitation energy) connected by a single bond (Fig. 1). In polar solvents, fast intramolecular electron transfer can results from the donor to the acceptor part of the molecule from such fluorophores. This electron transfer is associated with an intramolecular D–A twisting around the single bond (Fig. 1) and results in a relaxed perpendicular structure. There is a process known as dual fluorescence that usually results from the equilibration between a relaxed perpendicular conformer and a coplanar conformer, i.e., a relaxation from a high energy band to the locally excited (LE) state and from a lower energy band because of the emission from the TICT state [16]

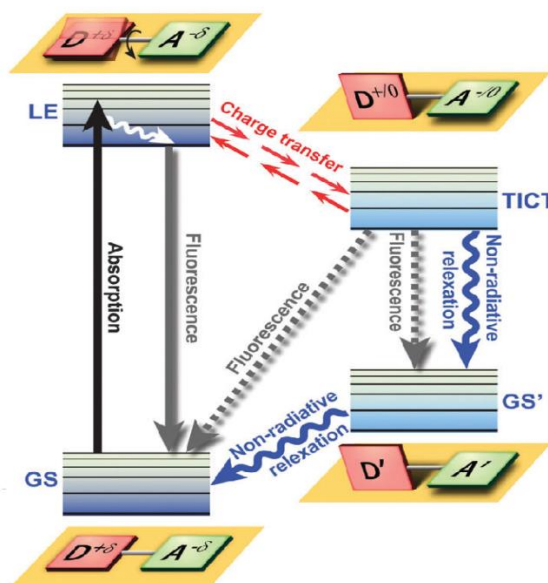


**Fig 1:** Twisted Intramolecular Charge Transfer (TICT) dynamics.<sup>11</sup> Upon excitation from the GS, the LE state equilibrates rapidly with the TICT state after fast charge transfer. GS ground state; GSD = ground state donor; GSA = ground state acceptor;

### 3. Detailed mechanical explanation of ESIPT and TICT

The hydrogen bond, one of the important weak interactions, has been indicated to play an important role in excited-state intramolecular proton transfer and thus has attracted more attention because its excited-state reinforcement can promote intramolecular proton transfer. [17]

A large Stokes shift is the most important photophysical property of the ESIPT chromophores. The large Stokes shift is a desired feature for fluorophores because the self-absorption, or the inner filter effect, can be avoided and the fluorescence analysis can be improved with this kind of fluorophores. The transient ground state character of the emissive species of the ESIPT chromophores, i.e. the keto tautomer is also a unique feature of the ESIPT chromophores. The schematic representation of the basic photophysical process of the ESIPT chromophores is illustrated in Fig. 2, by 2-(2-hydroxyphenyl)-benzothiazole (HBT). The ESIPT chromophores that exist in the cis-enol form at the ground state, that can lead to the formation of intramolecular H-bond. Upon photoexcitation, mostly the excited singlet state of the enol form is populated. Then an important ultrafast ESIPT process occurs and results in the formation of cis-keto at the singlet excited state that is stabilized by the intramolecular hydrogen bond. Since the ESIPT is much faster than the radiative fluorescence process the fluorescence observed for the ESIPT chromophores is very often due to the keto tautomer, although exceptions do exist. [17]

Besides the radiative decay, the deactivation channel for the cis-keto form is intersystem crossing (ISC), which leads to the triplet excited state of the keto tautomer (Fig. 2). Another important deactivation route is the isomerization of the trans-keto form (Fig. 1, KZ). Transformation of the trans-keto form into the cis-keto form will have to cross an energy barrier, thus the trans-keto to cis-keto is a slow process. The relatively slow decay of the triplet excited state and the trans-keto to cis-keto processes are at a similar time-scale (up to ms scale) [37].

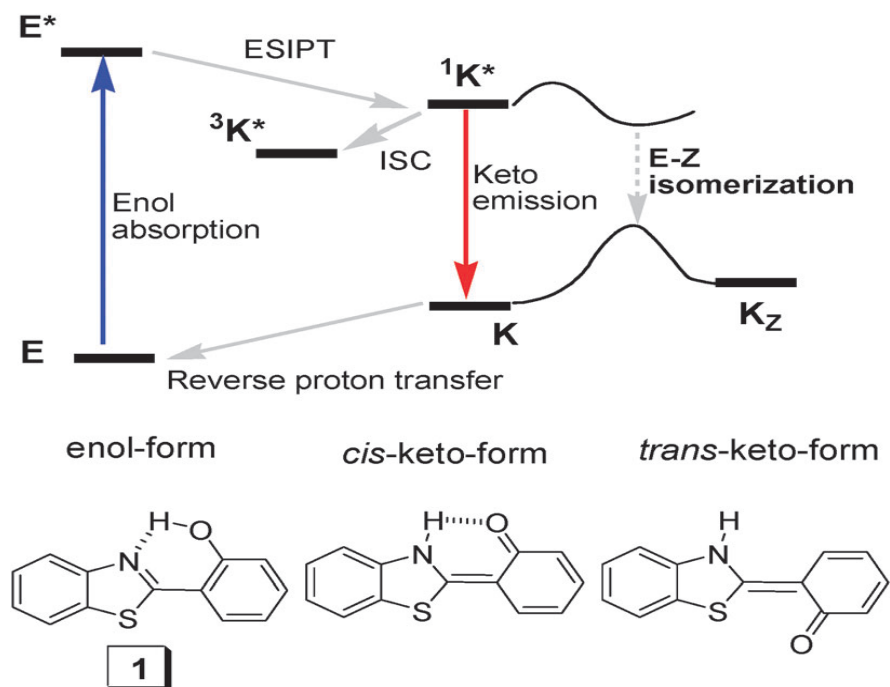


**Fig.2:** Principal Photophysics of ESIPT. Illustrated by 2-(2-hydroxyphenyl)- benzothiazole 1 (HBT).

Weller found that there is an asymmetric double-well potential curve (Figure 3) for the ESIPT in SA and for its derivative methyl salicylate (MS) to clarify the observed normal (with small Stokes shift) from  $P^*$  and enormous Stokes shifted emission ensuing from the tautomer  $T^*$  after ESIPT. [11]

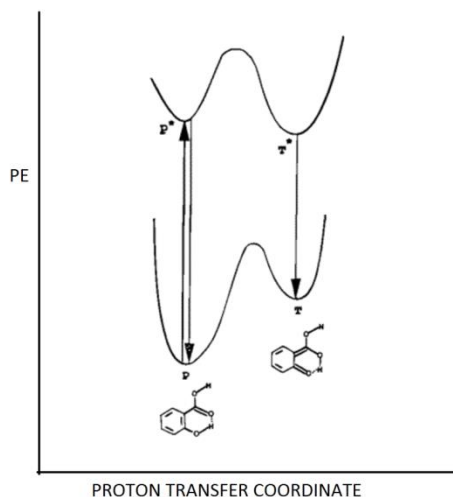


**Figure 3:** Asymmetric double-well potential for ESIPT in SA and methyl salicylate (MS) proposed by Weller

However, later, excitation spectra and also the time-resolved studies showed that the double-well potential wasn't correct in these cases, but actually the normal and tautomer emissions result from two totally different conformers in which one with a proper intramolecular H-bond (IHB) to undergo ESIPT (P form) leading to T form and the other lacking this sturdy IHB and giving rise to normal emission (R form) [30] as shown in Figure 4 [11].

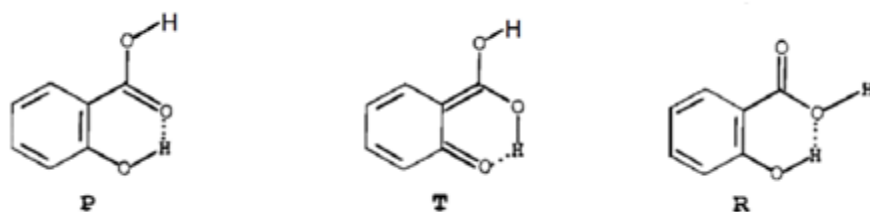


**Figure 4:** P R and T form of SA

The proton transfer is relatively tough for 1,2-Dihydroxyanthraquinone (ALR-E) in S<sub>0</sub> state to convert to ALR-K because of the relatively high barrier of 5.85 kcal/mol and the endothermal process. However, the ground-state reverse proton transfer (RPT), that's the transition of ALR-K to the ALR-E, is an almost barrierless process. So due to its high energy or instability, the ALR-K exists less in the ground state. Therefore, the enol-keto isomerization of



ALR should be attributed to the excited-state proton transfer and ground-state reverse proton transfer.[ 17]

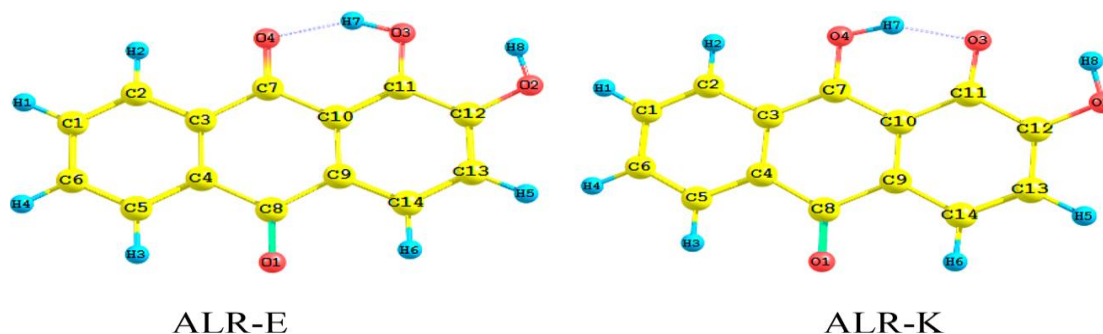


**Fig5:** Optimized Molecular Structures of ALR-E and Its Corresponding Keto-Isomer ALR-K

Franck–Condon (FC) state, wherever the 1,2-Dihydroxyanthraquinone (Alizarin-ALR) is unstable, then relaxes to the minimum  $S_1$  state (ALR-E ( $S_1$ )). After that, a section of ALR-E ( $S_1$ ) transitions back to ground state with a  $\sim 574$  nm fluorescence emission, and another part of ALR-E ( $S_1$ ) increases the ESIPT due to the reinforcement of intramolecular hydrogen bond to form the ALR-K ( $S_1$ ). Then, the first excited-state ALR-K jumps to the ground state via  $\sim 673$  nm radiative transition. Finally, the ground-state ALR-K quickly returns to the enol form through the ground-state reverse proton transfer with very little barrier FIG 6 [17].

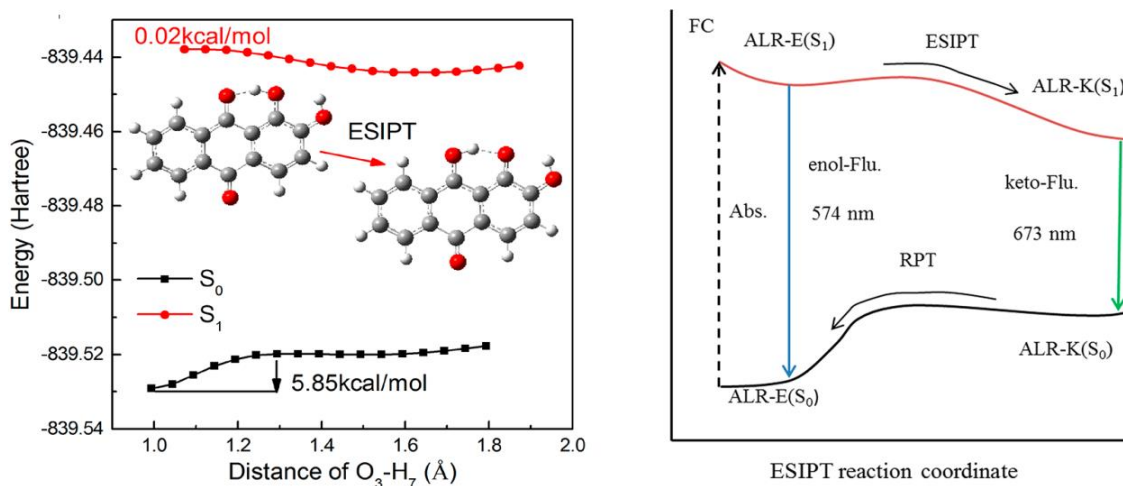


**Figure 6:** Enol-keto tautomerism mechanisms for ALR.

If linked by a single bond, the D<sup>+</sup> and A<sup>-</sup> subsystems have a very limited degree of freedom. Internal rotation around the central bond, as in large amplitude torsional motion or twist, seems to be the first choice of the vibrational mode for a relaxation that involves in a change in the excited state electronic structure. Along with the twist angle, the distance changes between D<sup>+</sup> and A<sup>-</sup>, i.e., the central bond length. [12]

In case of an adiabatic energy surface of the charge transfer (CT) state of an excited D–A system, two distinct excited states exert opposite forces; between them the force that twisted the D–A junction has an electron transfer (ET) character, whereas the force that favours a coplanar conformation is the results of mixing with a locally excited (<sup>1</sup>LE) state (Fig. 7). The <sup>1</sup>ET state is accompanying the pair of HOMO and LUMO frontier orbitals, where a single electron is transferred from the HOMO to LUMO. As for that D–A systems, an electron is promoted from the HOMO to the LUMO upon photoexcitation, resulting in the formation of a biradicaloid pair (Fig. 7a). As the interaction of Frontier orbitals increases, there is an increase the excitation energy required for the <sup>1</sup>ET state and consequently a perpendicular conformation minimises the excitation energy. In case of a perpendicular conformation, the relative energy level of the <sup>1</sup>ET state can also be approximated by subtracting the electron affinity of LUMO from the ionisation potential of the HOMO and thus strong donors and acceptors stabilize the <sup>1</sup>ET state. The <sup>1</sup>ET state is found in D–A systems as well as in those that contain isomerisable double bonds. In contrast, mesomeric interaction between p-subsystems ( $\Psi_1$  and  $\Psi_2$ ) stabilizes the <sup>1</sup>LE state in a coplanar conformation (Fig. 7a).

Resonance stabilization and accompanying planarization between p-subsystems is particularly enhanced in the excited state; multiple interactions between whole occupied and unoccupied p-orbitals of  $\Psi_1$  and  $\Psi_2$  enhance the HOMO level and reduce the LUMO level that results in a lower <sup>1</sup>LE level. These competing two forces enhance the division of the <sup>1</sup>CT surface to generate either single or multiple minima (Fig. 7b). When the ET character of <sup>1</sup>CT outweighs the LE character of S<sub>1</sub>, the <sup>1</sup>CT minimum distinctly becomes a TICT state. [16]

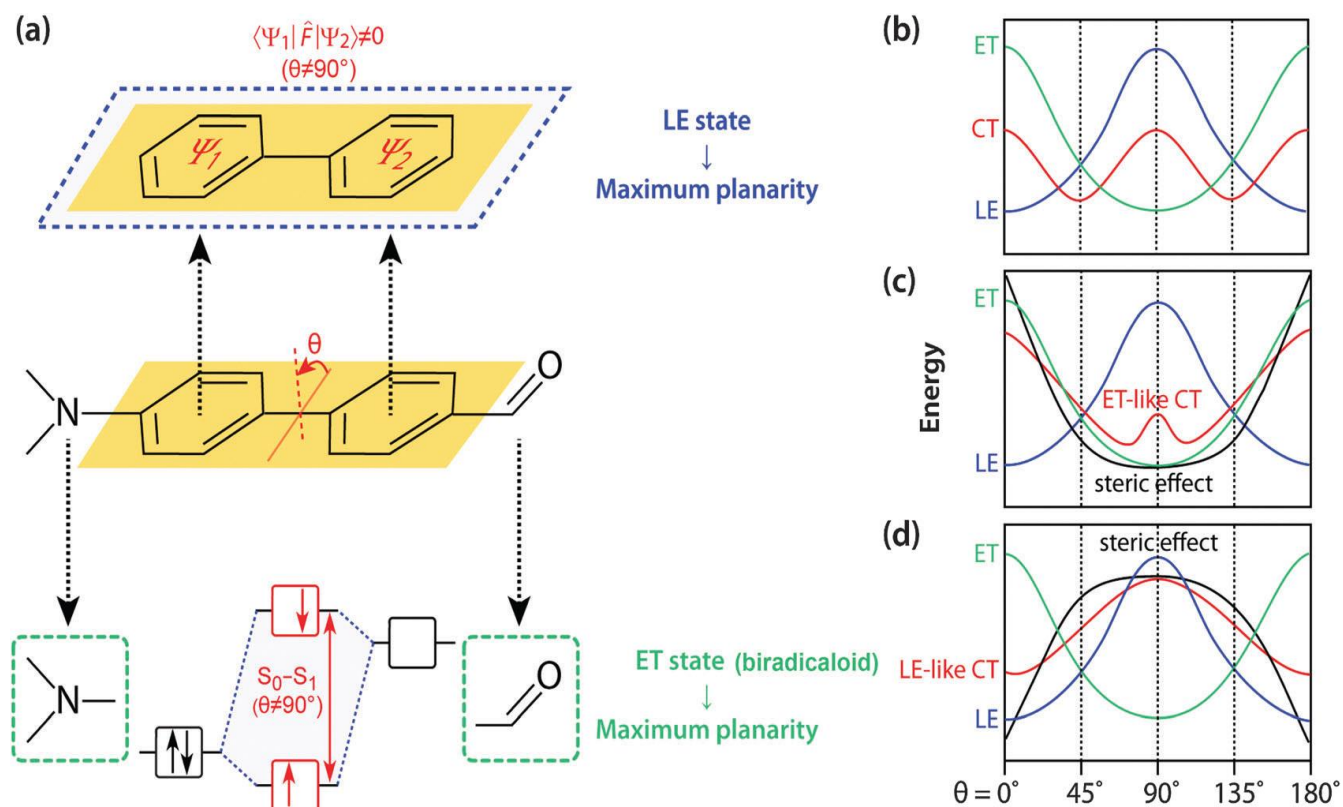


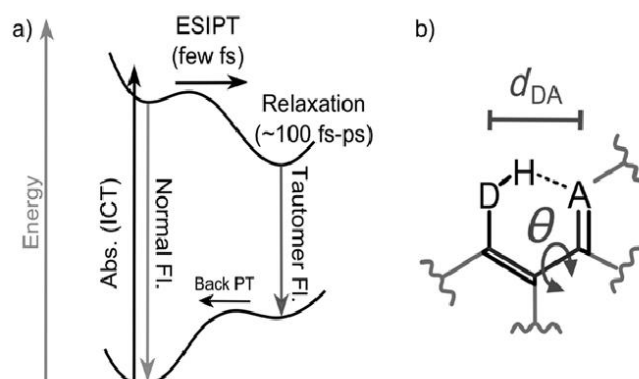
**Fig.7** (a) Preferred geometries of  $^1\text{LE}$  and  $^1\text{ET}$  states. Schematic energy diagrams of the  $^1\text{LE}$  (blue),  $^1\text{ET}$  (green) and  $^1\text{CT}$  (red) states when: (b)  $^1\text{LE}$  and  $^1\text{ET}$  character are comparable to each other, (c) when the steric restriction (black) is introduced to twist the D–A junction (e.g. an alkyl group at ortho position) and (d) when the D–A junction is made coplanar (e.g. a carbon bridge).

The introduction of steric hindrances like that associated with an alkyl group at the ortho position of the D–A junction deforms the  $^1\text{CT}$  surface to find its minima at a severely twisted conformation (Fig. 7c). During this conformational change, there is a total destabilization within the  $^1\text{LE}$  state because of the mixing efficiently with the  $^1\text{ET}$  state that leads to a highly twisted and polarised state (i.e. TICT state) because of the  $^1\text{CT}$  minimum. On the opposite hand, if there's a steric hindrance like the carbon bridge between a donor and an acceptor the D–A junction tends to be coplanar, the  $^1\text{LE}$  state is sufficiently stabilized in order that the  $^1\text{CT}$  minimum is governed by  $^1\text{LE}$  character (i.e. coplanar ICT state, Fig. 7d) [16]

## 4. Conditions which favor such processes

Excited state proton transfer (ESPT) is one of the important processes in biology and also in commercial technologies. A special case of ESPT that occurs when the proton is transferred intramolecularly (ESIPT), which is the key process in the function of white OLEDs and optoelectronic technologies. The process of ESIPT takes place in case of H-bonded conjugated ring system is typically accompanied by photoinduced tautomerization. Formation of the photoinduced tautomer requires the molecule to undergo the following processes (Scheme 2a).

- The presence of intra-molecular H-bonds, the rate of ESIPT increases with the strength of the H-bond. [18]
- Light absorption to form an intramolecular charge-transfer state (ICT), leading to an electron density redistribution that provides the driving force for ESIPT.
- Adiabatic proton transfer on the excited state surface, on a time scale as fast as tens of femtoseconds. [19]
- Relaxation of the newly formed strained molecule by intramolecular vibrational redistribution (IVR) within hundreds of femtoseconds and subsequent excess energy dissipation to the solvent environment (vibrational cooling) within a few and up to tens of picoseconds. Relaxation of the resulting strained molecule causes rearrangement of the atomic positions and concomitant electronic redistribution, typically involving bond-order alternation. [19]



**Scheme2.** a) General energy diagram of photoinduced tautomerization (Fl.= fluorescence). b) Intramolecular H-bond in a conjugated ring, where  $d_{DA}$  is the proton donor–acceptor distance and  $\theta$  is the dihedral angle.

The driving forces behind the twisted intramolecular charge transfer (TICT) are

- i. Polar solvents, it stabilizes TICT states with large dipole moments.
- ii. The most decisive factor is the energy gap difference between the planar and twisted conformations. For all of the considered molecules, TICT only occurred if the twisted structure had a smaller energy gap than the planar structure. (Figure8)

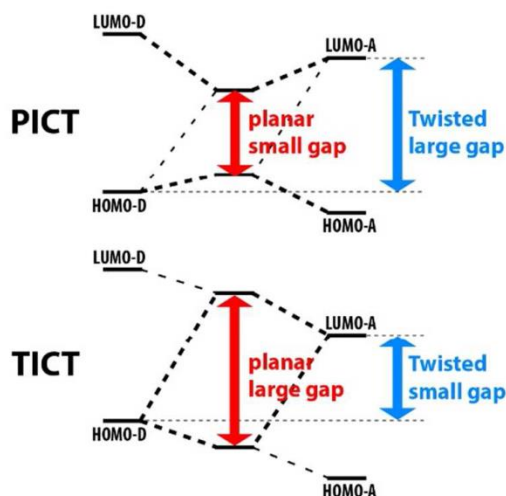


**Fig.8:** The energy gap of twisted or planar state.

- iii. Going from planar to twisted conformation, the separation of hole and electron decrease both Coulombic attraction (contributes to PICT) and exchange – correlation repulsion (contributes to TICT). Under most circumstances, the separation distance in twisted state is insufficiently large and there is considerable HOMO-LUMO overlap in planar state, so the exchange – correlation term exceeds the Coulomb term and contributes to TICT. This term contributes less with larger hole-electron distances in the twisted conformation or a smaller HOMO-LUMO overlap in the planar conformation. (Fig.9)

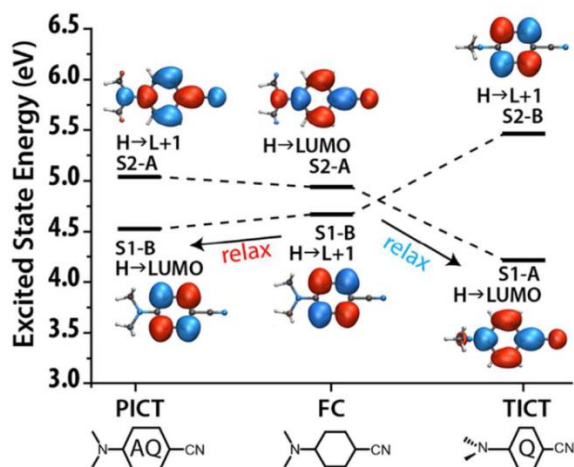


**Figure9.** Excited state and corresponding orbitals for **DMABN** in its FC, PICT, and TICT states. S1 and S2 refer to the first and second singlet excited states, respectively.

Going from planar to twisted conformation, the separation of hole and electron decrease both Coulombic attraction (contributes to PICT) and exchange – correlation repulsion (contributes to TICT). Under most circumstances, the separation distance in twisted state is insufficiently large and there is considerable HOMO-LUMO overlap in planar state, so the exchange – correlation term exceeds the Coulomb term and contributes to TICT. This term contributes less with larger hole-electron distances in the twisted conformation or a smaller HOMO-LUMO overlap in the planar conformation. (Fig.9)

## 5. Examine the role of molecular structure, geometry (conformation), solvent effect and intra/intermolecular interaction

### 5.1 Molecular structure and Geometry

The pre-requisite for ESIPT is the formation of intramolecular H-bonding between proton donor and acceptor within the molecule. The drastic electronic and structural changes through ESIPT often produced strong fluorescence in the solid state with a large Stokes shifts without self-absorption. The majority of the p-conjugated organic molecules that showed strong fluorescence in solution become weak or non-fluorescence in the solid state due to aggregation caused quenching.

Absorption spectra of 1 (Fig.10) in DMF showed  $\lambda_{\text{max}}$  at 406 nm that could be assigned for n-p\* transition. Introducing electron donor methoxy group at ortho position (2) slightly red shift the absorption to 418 nm [21] whereas hydroxyl attached 3 exhibited further red shift of absorption ( $\lambda_{\text{max}} = 425$  nm). In contrast, phenyl hydrazine based 4 showed blue shifted absorption ( $\lambda_{\text{max}} = 380$  nm) [42]. Interestingly, 1 and 2 showed very weak fluorescence in DMF whereas 3 exhibited highly enhanced emission. The strong fluorescence of compound 3 in comparison to the compound 1 and 2 is expected to be due to the ESIPT as the structure of 3 can form an intramolecular H-bonding between phenyl hydroxyl donor and imine acceptor whereas in case of 1 and 2, they could not form such intramolecular H-bonding because of the non-availability of hydroxyl functional group.[ 43]

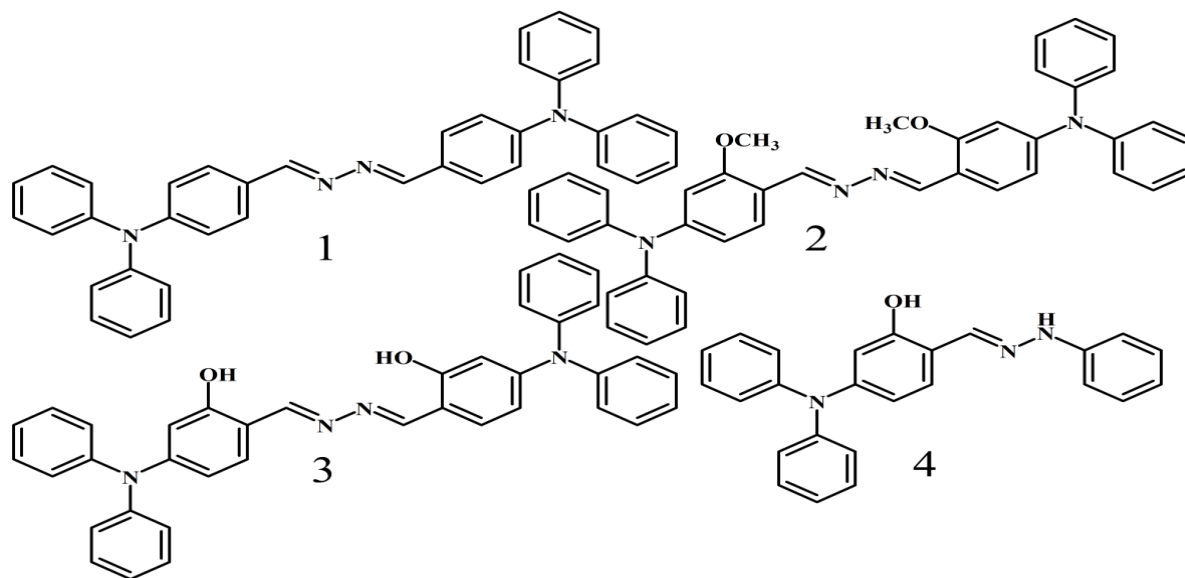


**Fig.10:** Compounds 1-4

Intramolecular hydrogen bonds of Salicylic Acid (SA) can be formed between  $C_7=O_1$  and  $O_2-H_{pt}$  in the ground state, whereas they can be formed between  $C_3=O_2$  and  $O_1-H_{pt}$  in the excited state. In addition, the key geometric parameters of different electronic states and their numerical values can be found in Table 2. Particularly, upon exciting to  $S_1$  excited state the distance between  $O_1$  and  $H_{pt}$  decreases from 1.76 Å to 1.03 Å, while that between bond length  $O_2$

and  $H_{pt}$  increases from 0.99 Å to 1.56 Å, respectively (Table1). The excited state bond angles  $C_3C_2C_7$  and  $C_2C_3O_2$  are both smaller than the corresponding ground state bond angles. The excited state distance between  $O_1$  and  $O_2$  becomes shorter than the corresponding ground state distance. The changes of bond length and bond angles of the SA indicate that from the ground state to the singlet excited state, the intramolecular  $C_7=O_1$  -  $H_{pt}-O_2$  breaks, concomitantly accompanying with the formation of an intramolecular  $C_3-O_2---H_{pt}-O_1$ . The most reasonable explanation is that after the exciting the H-bonded quasi-aromatic chelating ring system becomes smaller. As the distance between the two atom decreases, the interactions increased. Therefore, the intramolecular hydrogen bond in the SA molecule facilitates the ESIPT process. [22]

<b>Table1</b>	$C_2-C_7$	$C_7-O_1$	$O_1-H_{pt}$	$O_2-H_{pt}$	$O_1-O_2$	$C_3-O_2$	$\angle C_3C_2C_7$	$\angle C_2C_3O_2$
S0	1.45	1.23	1.76	0.99	2.64	1.34	120.32	121.88
S1	1.44	1.32	1.03	1.56	2.51	1.28	118.26	120.10

The geometric structures of methyl salicylate in the ground state  $S_0$  and the first singlet excited state  $S_1$  have been optimized using DFT and TD-DFT method, respectively. Intramolecular hydrogen bonds  $C_1=O_2---H_3-O_4$  and  $O_2-H_3---O_4=C_5$  can be formed in normal methyl salicylate (MSn) and its proton-transferred tautomer (MSt), respectively. From the listed dihedral angles table1, it is inferred that ester group of MSn is almost on the plane of the aromatic ring in the both states  $S_0$  and  $S_1$ , while in the  $S_1$  state of MSt, the dramatical torsion occurs between the ester group and aromatic ring. (Fig.11)



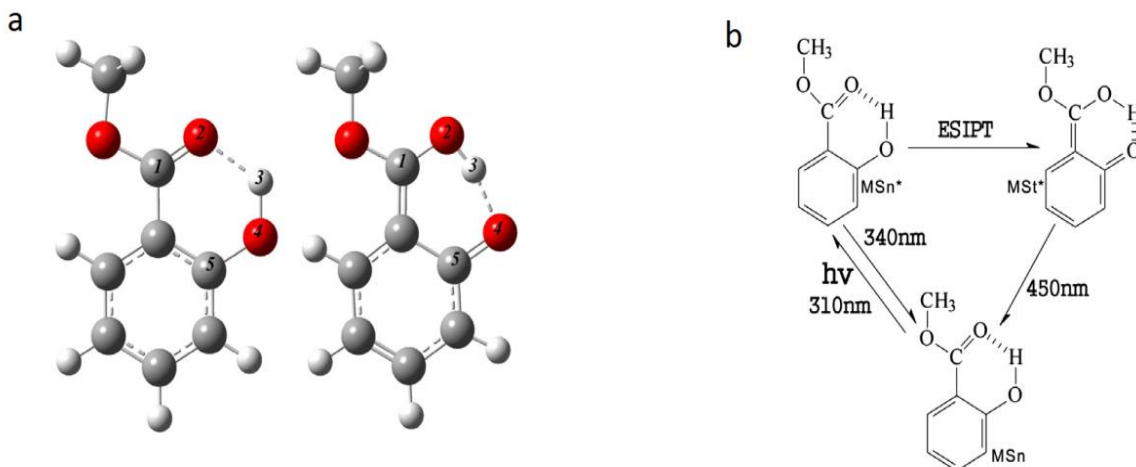


**Fig.11:** **a.** geometric structures of normal methyl salicylate (MSn<sub>g</sub>) and its tautomer (MSt<sub>g</sub>) in the excited state **b.** Photophysical scheme proposed by Weller to explain the dual-fluorescence behavior of methyl salicylate (MS).

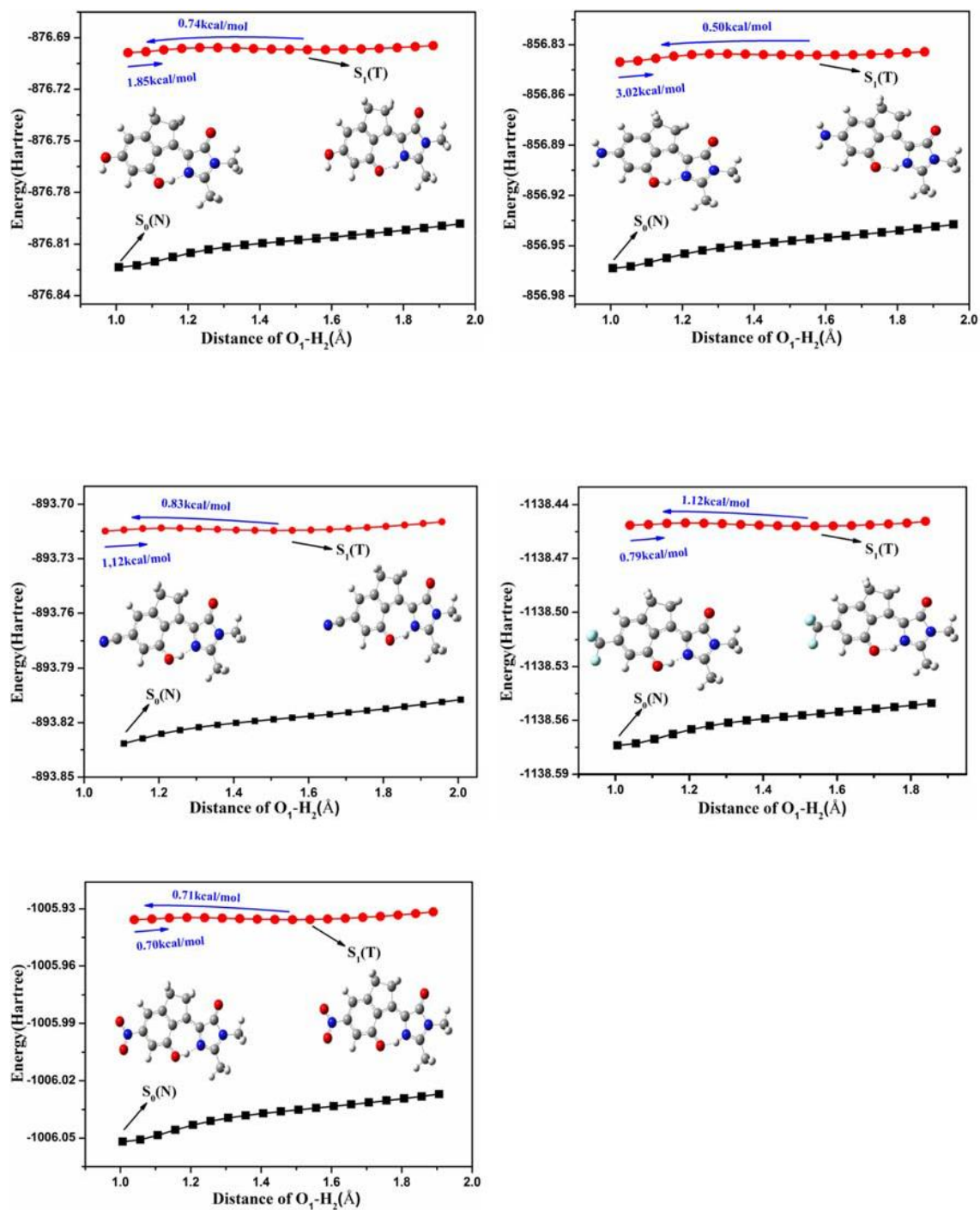
The listed bond lengths indicated that the distance between O<sub>2</sub> and H<sub>3</sub> in IMHB C<sub>1</sub>=O<sub>2</sub>---H<sub>3</sub>-O<sub>4</sub> is significantly shortened upon excitation from 1.738 Å in the ground state to 1.468 Å in the excited state. Meanwhile, the bond lengths of both groups C<sub>1</sub>=O<sub>2</sub> and H<sub>3</sub>-O<sub>4</sub> in the excited state are slightly increased in comparison to those in the ground state. The result testifies that the intramolecular hydrogen bond C<sub>1</sub>=O<sub>2</sub>---H<sub>3</sub>-O<sub>4</sub> is significantly strengthened upon excitation to the S<sub>1</sub> state. The experimental results have indicated that the proton transfer process occurs in the S<sub>1</sub> state. Besides, the excited state proton transfer of MS that takes place through the intramolecular H-bond C<sub>1</sub>=O<sub>2</sub>---H<sub>3</sub>-O<sub>4</sub>. Hence, the reaction of proton transfer can be speed up by the excited-state hydrogen bond strengthening in the S<sub>1</sub> state. As for the proton-transferred tautomer MSt, one new intramolecular hydrogen bond C<sub>5</sub>=O<sub>4</sub>---H<sub>3</sub>-O<sub>2</sub> is formed between new enol group and carbonyl group. Moreover, it is noted that in the S<sub>1</sub> state the hydrogen bond length of C<sub>5</sub>=O<sub>4</sub>---H<sub>3</sub>-O<sub>2</sub> is longer than that of C<sub>1</sub>=O<sub>2</sub>---H<sub>3</sub>-O<sub>4</sub>. This indicates that the hydrogen bond in the S<sub>1</sub> state of MSn is more significantly strengthened than in MSt (Table 2). The weak hydrogen bond results in the difficulty of reversion. [23]

Table2	S <sub>0</sub>	S <sub>1</sub>	
		MSn	MSt
L <sub>C1=O2</sub>	1.233	1.278	–
L <sub>H3-O4</sub>	0.989	1.064	–
L <sub>C5=O4</sub>	–	–	1.295
L <sub>O2---H3</sub>	1.738	1.468	–
L <sub>O4---H3</sub>	–	–	1.495
L <sub>O2-H3</sub>	–	–	1.061
<O2=C1-C-C5	-0.058	0.003	–
<O2-C1=C-C5	–	–	6.132

Ni et al. [24] by DFT and TD-DFT method modelled the effect of substitution on the behaviour of ESIPT in the derivatives 4- (2-hydroxybenzylidene)-1,2-dimethyl-1H-imidazol-5(4H)-one (o-LHBDI). Proton transfer process in the substituted o-LHBDI derivatives cannot occur in the S<sub>0</sub> state since the potential barrier of the S<sub>0</sub> state increases with the elongating of the O1–H2 bond distance without any local maxima. However, with the increasing the bond length of O1–H2 in S<sub>1</sub> state, the potential energy curve of 4R-o-LHBDI (R: OH, NH<sub>2</sub>, CN, CF<sub>3</sub>, NO<sub>2</sub>) can exist in a relatively stable structure (Fig.12).

The calculated potential barriers of the S<sub>1</sub> state for 4(OH)- o-LHBDI, 4(NH<sub>2</sub>)- o-LHBDI, 4(CN)-o-LHBDI, 4(CF<sub>3</sub>)-o- LHBDI, and 4(NO<sub>2</sub>)-o-LHBDI are 1.85, 3.02, 1.12, 0.79, and 0.70 kcal/mol, respectively. No matter which substituent is used in o-LHBDI, the ESIPT potential barrier of 4R o- LHBDI (R: OH, NH<sub>2</sub>, CN, CF<sub>3</sub>, NO<sub>2</sub>) is 0.34~2.32 kcal/mol bigger than that value of o-LHBDI. These results indicate that ESIPT in the 4R-o-LHBDI (R: OH, NH<sub>2</sub>, CN, CF<sub>3</sub>, NO<sub>2</sub>) is a slightly difficult to proceed than that in the case of o-LHBDI. It also can be seen that the potential barrier of 4R-o-LHBDI (R: CN, CF<sub>3</sub>, NO<sub>2</sub>) and 4R-o-LHBDI (R: OH, NH<sub>2</sub>) is average 0.51 and 2.08 kcal/mol larger than the barrier of o-LHBDI, respectively.[ 24]

Thus it was concluded that the ESIPT barrier decreases with the stronger electron withdrawing ability or weaker electron-donating ability of the substituent.



**Fig.12:** Potential energy curves of 4R-o-LHBDI (R: OH, NH<sub>2</sub>, CN, CF<sub>3</sub>, NO<sub>2</sub>) in the S<sub>0</sub> and S<sub>1</sub> states

Compounds from 1–5 and 8 also have only one stable structure. Compounds 1, 4, and 8 prefer ESIPT while the others prefer TICT, in line with the experiments. Both ESIPT and TICT equilibrium geometries were obtained for compounds 6 and 7, which have two channels (Fig.13).

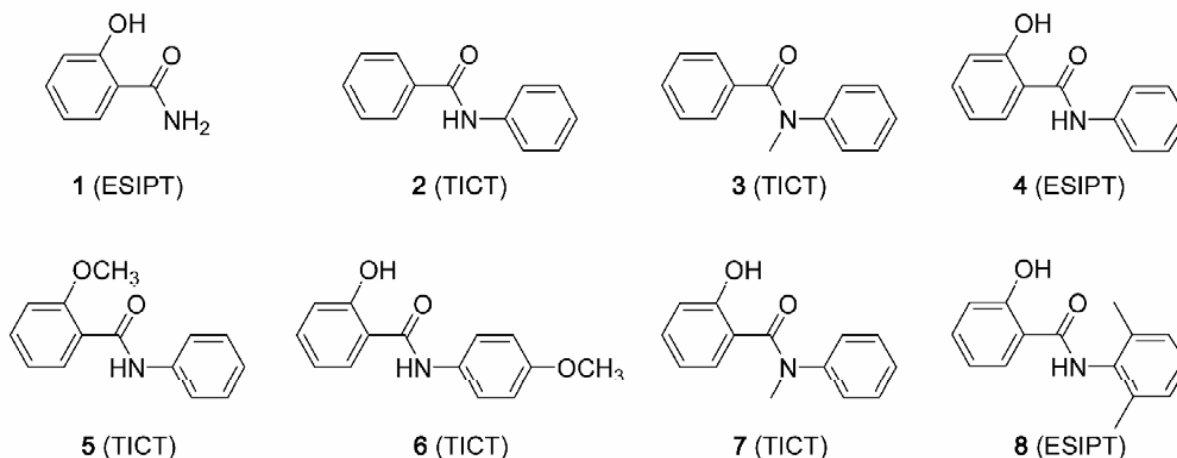


**Fig.13:** Structural formulas of salicylanilide analogues (1–3) and derivatives(4–8). For compounds 2, 3, and 5–7, twisted intramolecular charge transfer (TICT) occurs when the molecules are excited in non-polar solvents, whereas, for the other compounds, excited-state intramolecular proton transfer (ESIPT) occur.

The remarkable difference between the ESIPT and TICT structures of the S1 states is that anilino moiety twists from benzoyl moiety by a large angle in the latter structure. Compounds 6 and 7 in Fig.14 were taken as examples. Dihedral angle  $\theta_{O1C1N1H2}$  in compound 6 and  $\theta_{O1C1N1C2}$  in compound 7 are  $72^\circ$  and  $77^\circ$  in TICT structures, respectively. In ESIPT structures, anilino moiety twists from benzoyl moiety slightly. Dihedral angle  $\theta_{O1C1N1H2}$  in compound 6 and  $\theta_{O1C1N1C2}$  in compound 7 are  $168^\circ$  and  $13^\circ$ , respectively. In the former it is the trans form and the latter it is the cis form. In the ESIPT reaction, H1 atom transfers from O2 to O1 (Fig.14).

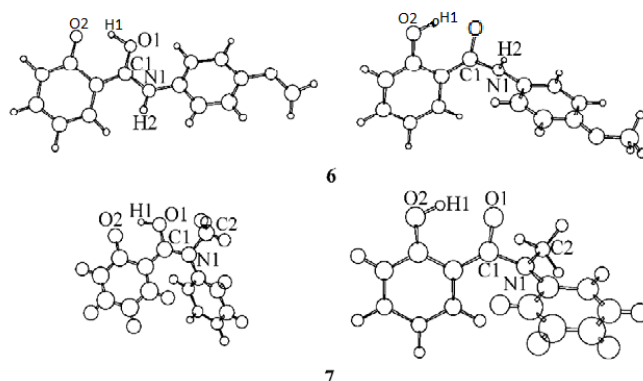


**Fig.14:** Compounds 6 and 7

In S1 geometries of compounds 1, 4, and 8, the bond lengths of H1–O2 are 0.1580–0.1606 nm, about one and a half of the normal single-bond length. The bond lengths of H1–O1 are 0.1003–0.1007 nm, which is comparable with the bond length of normal single-bond. After PT, the breaking of the H1–O2 bond and there is a formation of H1–O1 bond. Thus, the intramolecular proton bond transforms from O2–H1···O1 to O2···H1–O1. The bond length that links anilino and benzoyl moieties of N1–C1 is 0.1351–0.1342 nm. Although in the case of compounds 6 and 7, they have CT and PT channels, but PT does not concomitantly occur in TICT structures as shown in Fig.2. It can be shown from the shorter equilibrium bond lengths of H1–O2 in TICT structures than that of H1–O1 in ESIPT that the former is a little stronger. In the TICT structures the bond strengths of N1–C1 are considerably weaker than in the case of ESIPT that can be found on an inspection of the bond lengths. Vibrational frequency analysis for S1 geometries of these eight compounds confirmed that they are all minima on potential energy surfaces. The frequencies of H1–O1 stretch in ESIPT structures are considerably smaller than those of H1–O2 ones in TICT structures, coincident with the differences of H–O bond lengths and strengths between ESIPT and TICT structures.[ 25]

The geometric configurations of coumarin E-8-((4 (dimethylamino) phenylimino) methyl)-7-hydroxy-4-methyl-2H-chromen-2-one (CDPA) in the S0, S1-TICT and S1-ESIPT states are shown in Fig. 5. For comparison, the intramolecular hydrogen bond (IMHB) of O18-

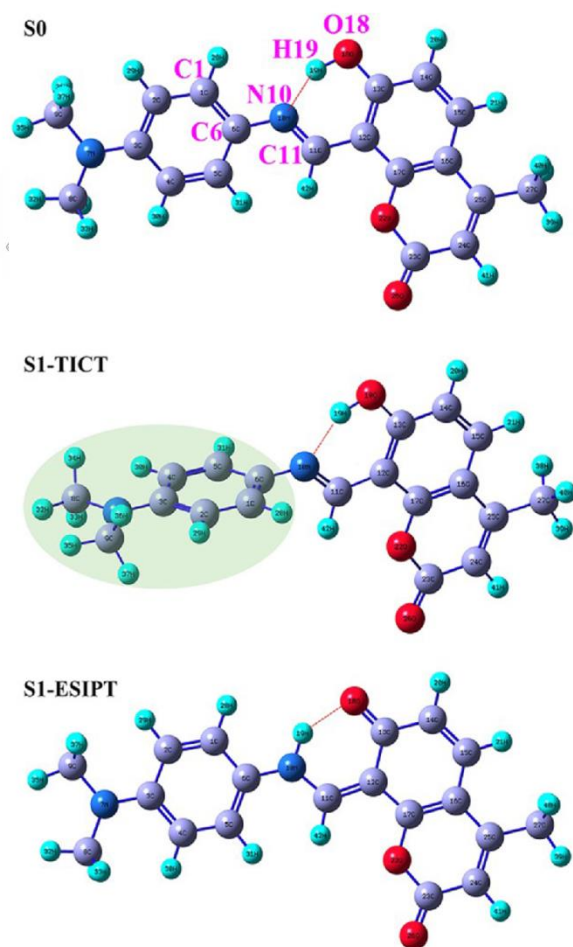
H19...N10 and also the dihedral angle (C1-C6-N10-C11) parameters of CDPA in n-Hexane, THF and ACN solvents are also summarized in Table 3.

**Table 3:** Calculated intramolecular hydrogen-bond lengths (Å) and dihedral angles (°) of CDPA in n-Hexane, THF and ACN solvents

CDPA	O18-H19...N11		C1-C6-N10-H11		
	S0	S1-TICT	S0	S1-TICT	
n-Hexane	1.622	1.761	160.20	92.04	68.16
THF	1.614	1.668	162.04	119.00	44.04
THF	1.610	1.640	162.44	153.80	8.64

With the increase of solvents polarity from n-Hexane, THF, and to ACN, the hydrogen bond (H19...N10) length was increased from 1.622 Å, 1.614 Å and 1.610 Å in the S0 state to 1.761 Å, 1.668 Å and 1.640 Å in case of the S1-TICT state, respectively. The lengthening of the bond length indicated that the excited-state intramolecular H-bonds of CDPA were weakened in these solvents. Furthermore, it was found that the bond length of intramolecular H-bonds in n-Hexane is slightly longer than that in ACN solvent both in the case of S0 and S1-TICT states, which indicated that the strength of intramolecular H-bonds in ACN is stronger than that in the case of n-Hexane solvent. Meanwhile, after the photoexcitation, there is a dramatic torsion shown by dihedral angle C1-C6-N10-C11 of CDPA in n-Hexane which is from 160.20° in the S0 state to 92.04° in the S1-TICT state. Similarly, in THF solvent, the dihedral angle C1-C6-N10-C11 changes from 162.04° to 119° when there is a translation of the molecular structure of CDPA from the S0 state to S1-TICT state. It is worth noting that the optimized geometric

configuration only presents an 8.64° twist from S0 to S1-TICT state indicates the CDPA in ACN is closer to the plane.



**Scheme3.** Optimized geometric configurations of CDPA in different electronic states.

It can be seen that the highest occupied molecular orbital (HOMO) has the  $\pi$  character and the lowest unoccupied molecular orbital (LUMO) has the  $\pi^*$  character, which indicates S0  $\rightarrow$  S1 transition is predominantly  $\pi\pi^*$  type transition. As we saw, the noticeable ICT character in these solvents was observed when there is a transition of CDPA from HOMO to LUMO. In ACN the charge of the CDPA is mainly distributed over the HOMO of the donor group i.e. dimethylaniline moiety, which in the LUMO is transferred to the coumarin fragment (acceptor



group) (Fig.15). Similar is the case in ACN, the same trend of charge transfer is also seen in THF solvent. However, there is huge difference in the charge distribution of the CDPA in n-Hexane than that in ACN. The orbital interaction between fragment molecular orbital of electron-donating and accepting moieties is prevented by the twisted structure of the CDPA in n-Hexane. Obviously, the phenyl group torsion along the C-N bond has a greater influence on the electric charge distribution.[26]

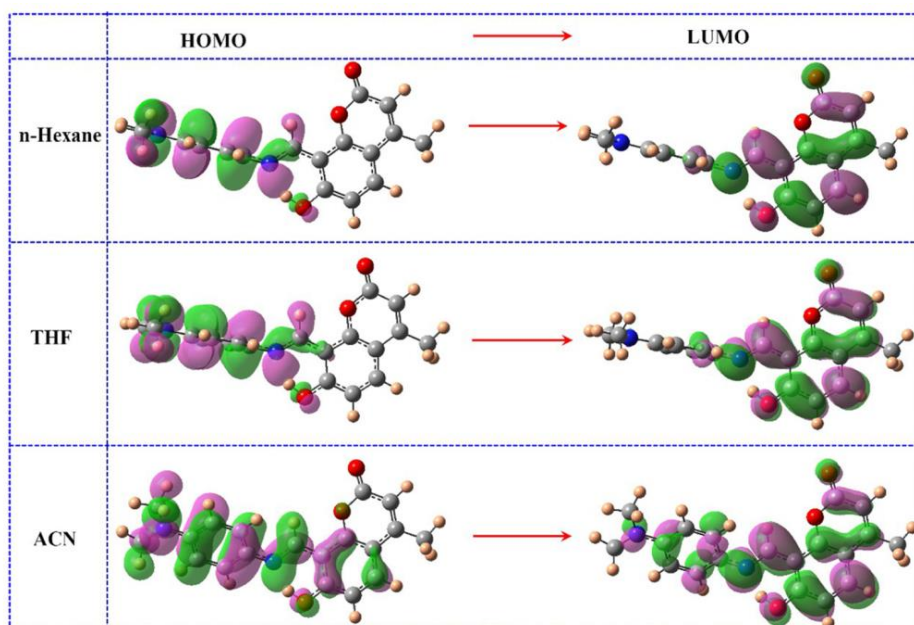


**Fig.15:** The frontier molecular orbital of CDPA in n-Hexane, THF and ACN solvents.

## 5.2 Solvent Effect

Solvent polarity reinforces charge relocation, which provides the driving force of ESIPT [41]. The fluorescence spectra of CDPA in different polar solvents are depicted in Fig. 16. Obviously, the fluorescence intensity decreases as the solvent polarity increases from n-Hexane, THF to ACN. The measured fluorescence quantum yield of CDPA in n-Hexane, THF to ACN solvents is 6.47%, 0.86% and 0.35%. Moreover, from these three solvents two fluorescence peaks were observed. Specifically, the short-wavelength fluorescence peak is found at 535 nm,



549 nm and 570 nm but there is also the long-wavelength fluorescence peak that is located at 567 nm, 588 nm and 600 nm when there is a change in the solvent from n-Hexane, THF and to ACN. The short-wavelength fluorescence herein was assigned into the TICT state and the long-wavelength fluorescence into ESIPT state. Furthermore, the fluorescence intensity from the TICT state was higher than that from the ESIPT state in n-hexane and THF solvents. However, in ACN, the fluorescence intensity from the TICT state was less than that from ESIPT state. These findings demonstrated that the TICT process was dominating over ESIPT process in n-Hexane and THF solvents, which in contrast thereto in ACN solvent. Therefore, the solvent polarity has different effects on ESIPT and TICT processes for the CDPA system.[26]

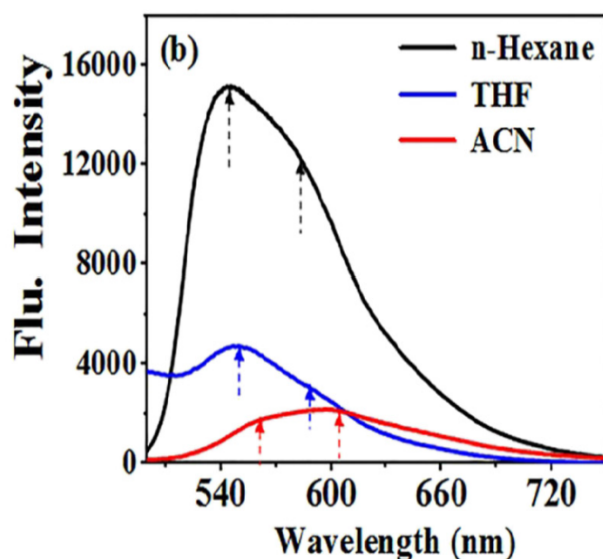


**Fig 16:** fluorescence (b) spectra of CDPA in n-Hexane, THF and ACN solvents.  $\lambda_{ex}$  = 405 nm.

In the study of effects of water on the ESIPT mechanism of 1,2-Dihydroxyanthraquinone (Alizarin-ALR) shows that the formation of a hydrated hydrogen bond between the carbonyl oxygen and a water molecule weakens the intramolecular hydrogen bond associated with proton transfer, increases the barrier height of ESIPT Fig.17, and thus hinders the transition of ALR-E to ALR-K in the excited state the intramolecular hydrogen bond attenuates with the increase in water molecules which results in the reduction of emission intensity as the water proportion in binary solvent increases. [17]

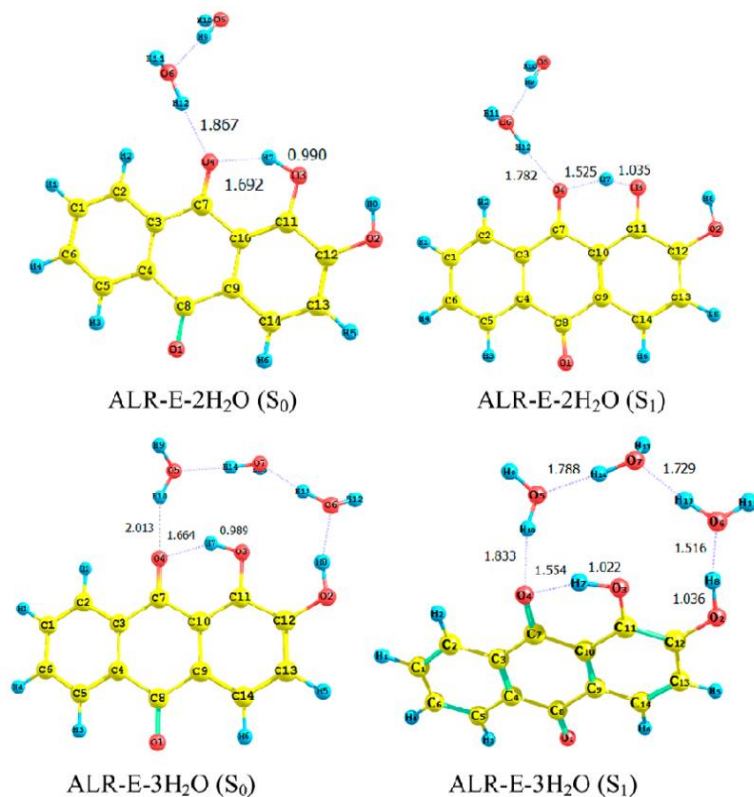


**Fig.17** Optimized Structures of ALR-E-2H<sub>2</sub>O and ALR-E- 3H<sub>2</sub>O in the S<sub>0</sub> and S<sub>1</sub> States

The scanned potential energy curves are shown in Figures 18a and 18b for ALR-E-2H<sub>2</sub>O and ALR-E-3H<sub>2</sub>O, respectively. In a water environment, the ground- and excited-state barrier heights of intramolecular proton transfer are all increased compared with that of ALR-E [39]. This conformably shows that the intermolecular hydrogen bond formed by carbonyl oxygen with water molecules impedes the ESIPT [38]. In addition, interestingly, we found that the ESIPT barrier height increases with the increase in number of water molecules. That means the transition from ALR-E to ALR-K will become difficult with increase in water. [17]

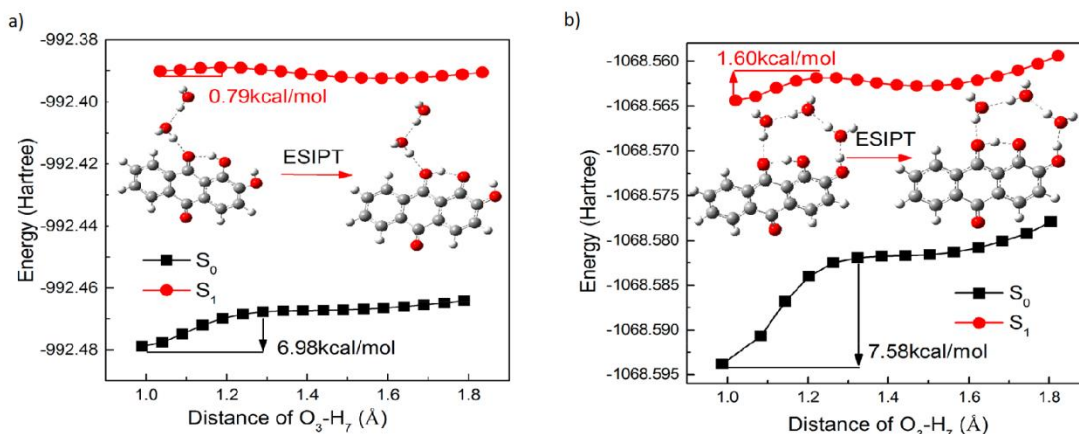


**Figure 18:** Ground- and excited-state potential energy curves of proton transfer a) for the ALR-E linked with two  $H_2O$  molecules and b) for the ALR-E linked with three  $H_2O$  molecules

The relative quantum yield of the “nonpolar” and the TICT emission of dimethylaminobenzonitrile (DMABN) relative to those in pure propionitrile as a function of solvent composition is given in figs. 19a and 19b respectively. It is readily seen that with increase in relative proportion of propionitrile (and hence polarity) there is a gradual decrease in the yield of “nonpolar” emission. This can be easily explained in terms of the polarity dependent energy barrier between the “nonpolar” and therefore the TICT states. According to Eisenthal and coworkers the energy barrier for the TICT process decreases with increase in the solvent polarity, presumably because of the increased solvation of the TICT state and of the transition state leading to it [44]. Thus the rate of TICT state formation increases with polarity and since TICT is the main nonradiative pathway in the “nonpolar” excited state of DMABN acceleration of TICT process automatically implies a decrease within the yield of emission from the “nonpolar” state.

In pure n-octane DMABN doesn’t exhibit any TICT emission, obviously because at such low polarity the barrier for TICT is just too high to be surmounted. As the polarity of the medium increases the yield of the TICT emission increases up to a  $ET(30)$  value of 40.5 (10% propionitrile, v/v) and the yield gradually decreases with further increase in the polarity. To explain this, it’s necessary to think about two competing processes – formation of the TICT state

from the “nonpolar” one and therefore the subsequent nonradiative decay of the TICT state. According to the energy gap law of non radiative transitions a decrease in the energy gap results in an increase in the nonradiative rates. Thus, with increase in solvent polarity the rate of nonradiative transitions from the TICT state to the low lying triplets and/or ground state increases. [27]

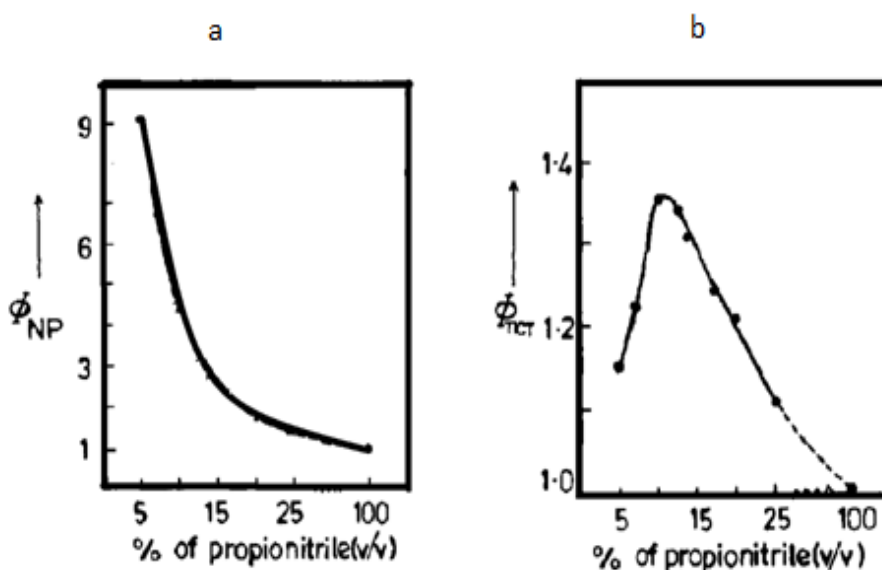


**Fig.19** Yield of “nonpolar” emission of DMABN as a function of solvent composition. Ordinate gives ratio of yield of “nonpolar” emission to that in pure propionitrile. Relative yield of TICT emission of DMABN as a function of solvent composition

The influence of specific solvent fluorophore interactions on emission of 1–5 in methanol–water mixtures of different compositions has been monitored and the spectra are illustrated in Fig. 20. The addition of water to the methanol–water mixture remarkably enhances the emission with a red shift and this may be due to a combined effect of hydrogen bonding and polarity of the medium. Mixing of the lowest closely lying 2twosinglet states ( $n, p^*$  and  $p, p^*$ ) favours the IST(the intersystem crossing) of phenanthrimidazole derivatives.

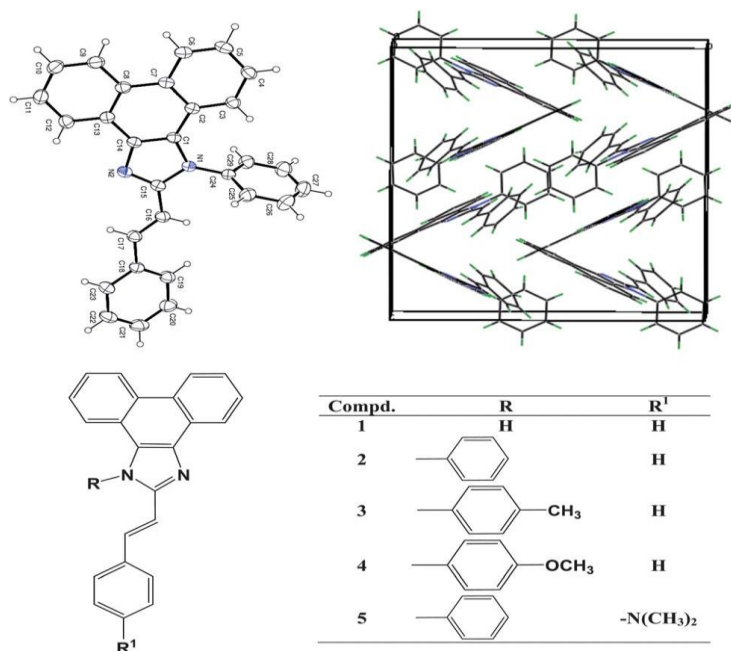
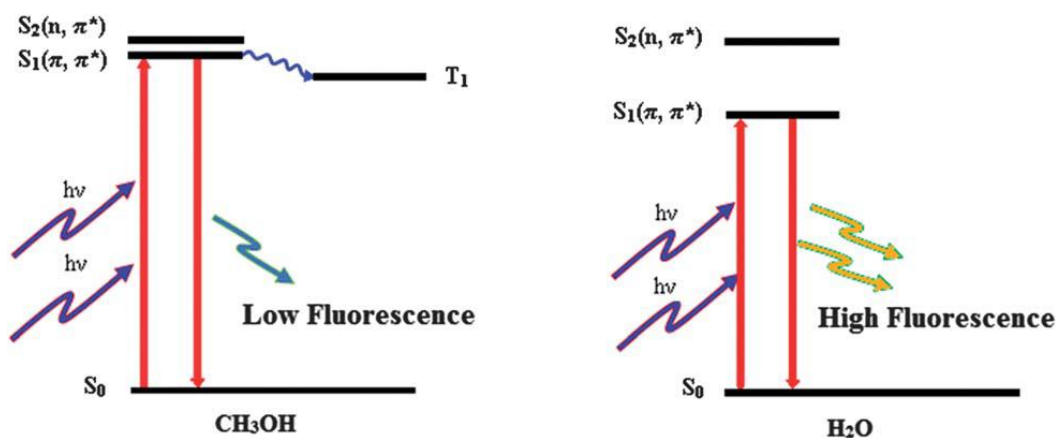


**Fig.20:** 1-phenyl-2-styryl-1H-phenanthro[9,10-d]-imidazole.

As the polarity of the medium is increased, the intermolecular hydrogen bonding interaction within the excited state stabilized the  $p, p^*$  state and enhanced the energy between the two states, which diminishes the blending between the 2 states (Scheme 4). As a result intersystem crossing from  $S_1$  to  $T_1$  decreases and an enhancement of fluorescence is observed. [28]



**Scheme4.** Schematic demonstration of modulation of the close-lying lowest singlet  $n, p^*$  and  $p, p^*$  states with solvent polarity in the excited state.

The TICT state can be well examined through energy evolutions of several excited singlet states as a function of the twist angle between the donor and the acceptor parts of the molecule 9 (Fig.21).

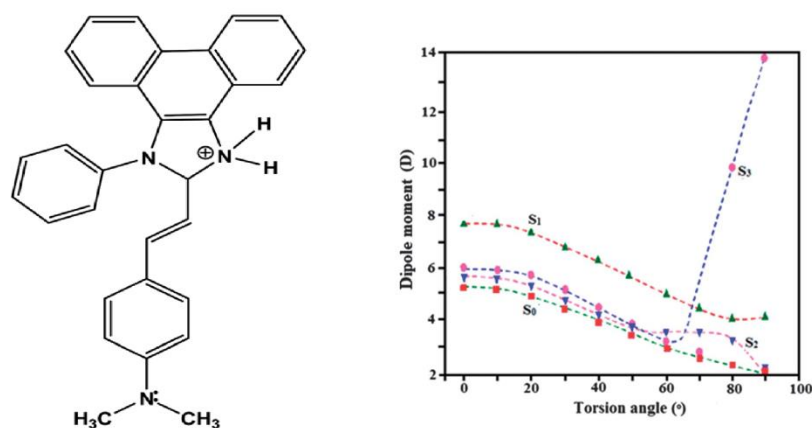


**Fig. 21:** Compound 9 and Change in the dipole moments of the different singlet states with the variation of the torsion angle

DFT calculations have been used to find out the excited singlet state that is responsible for the increasing TICT emission. Rotation of the  $N(CH_3)_2$  moiety in the molecule, keeping the rest of the molecule in the trans planar form, it can be observed that at an angle of  $90^\circ$ , a very high dipole moment (14.23 D) is acquired by the S3 state of the molecule. The change in the dipole moments of the different singlet states with the variation of the torsion angle is illustrated by Fig.21.

The remarkable lowering of energy of the S3 state has been observed at a twist angle,  $\theta=90^\circ$ , which is consistent with the increase in dipole moment of the S3 state at the same twist angle. The effect of solvation by each polar solvent results in the lowering of energy of the S3 TICT state, even lower than S1 LE as well as S1 TICT states, at a critical polarity that makes S3 TICT state responsible for anomalous fluorescence. These calculations suggest the presence of TICT state and highly Stokes shifted fluorescence in polar solvents and also support the experimental observations. [28]

### 5.3 Intra/Intermolecular Interaction

The dependence of the ESIPT reaction has been found on external hydrogen bonding. For SA it can be seen that the existing dimers broken when there is an external hydrogen bonding with diethyl ether ( $\text{Et}_2\text{O}$ ) and only the enhanced intensity monomeric emission from tautomer has been observed. In the study of the influence of chemical bond (H-bond) geometry on the dynamics of ESIPT in phenol-quinoline compounds it was found that with the increased in the donor-acceptor distance there is increased in PT barrier whereas a large dihedral angle (angle between the planes having proton donor-acceptor subunits) leads to a deactivation channel after ESIPT. In the case of quinolone derivatives hydrogen bonding wires/bridge formation, because of the non-adjacent of the proton donor and acceptor groups, has been reported to be a prerequisite for ESIPT. It has been found that 6-hydroxyquinoline (6-HQ) and 7-hydroxyquinoline (7-HQ) undergo ESIPT in water, methanol: water and acetic acid through the formation hydrogen bridge [32].

It was also found that in case of the 4'-N,N-dimethylamino-3-hydroxyflavone (DMHF) the effect of intermolecular interactions on ESIPT is doped in acetonitrile crystals [33]. It was found that the modulation of the potential energy surface can explain the prominent differences in two different crystalline phases (Figure 22).

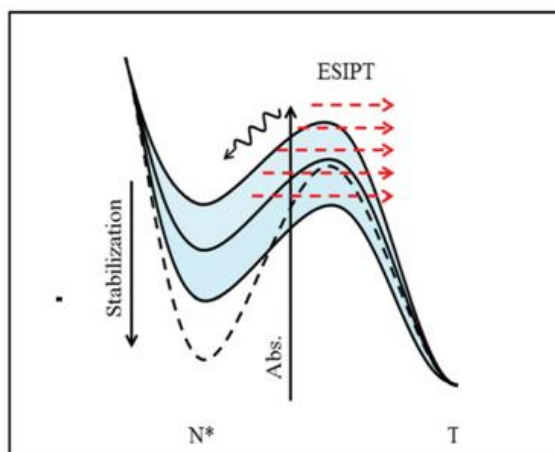
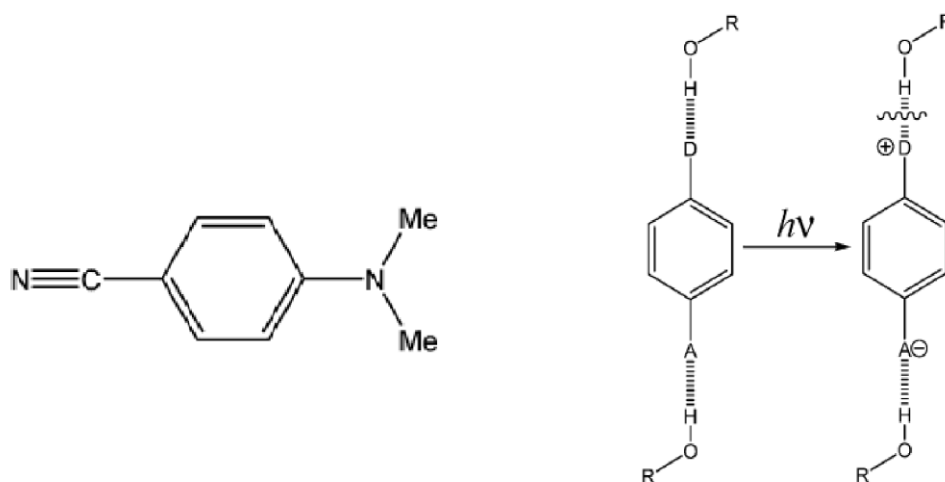


**Figure22:** Modification of potential energy surface (PES) by crystalline phases of acetonitrile from reference [85]. Solid and dotted lines show potential energy curves for low and high-temperature crystalline phases respectively.

Because of the complicated interactions, the hydrogen bonding significantly affects the ICT state in protic solvents of 10 (Scheme 4). It is commonly accepted that the charge donor makes hydrogen bonding with protic solvents within the ground state (GS). The donor acquires a positive charge in the excited ICT state and the hydrogen bond between the protic solvent and the positively charged donor is expected to break (Scheme 5). On the opposite hand the solvent molecules strengthen the prevailing H-bonds and/or form a completely new H-bond with the electron acceptor within the ICT state. The bond breaking and bond forming processes results in the slower rate of formation of the ICT state from the LE state for 10 in alcohols [34].



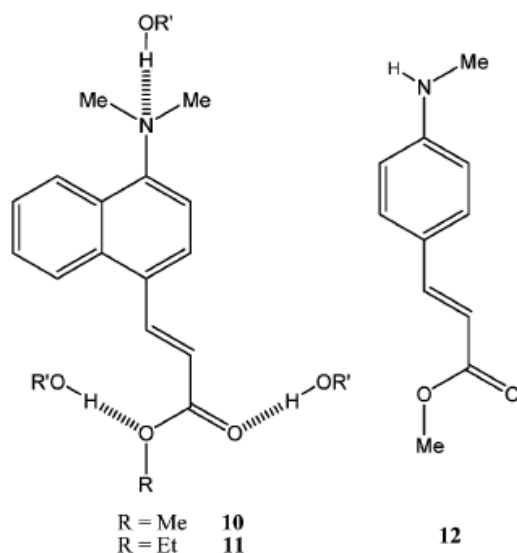
**Scheme5.** Compound 10

The results of the hydrogen bonding of the solvent with a charge donor moiety is the twisted conformers in the ground state, that twisted conformers can emit ICT fluorescence upon excitation. The hydrogen bonding that enhanced the formation of the twisted conformer within the ground state with the donor is the essential condition to obtain ICT emission in the excited state.



It was suggested that 10 form two kinds of hydrogen bonded complexes with water or  $\text{CF}_3\text{H}$ . The hydrogen bonded cyano site of the complex absorbs light but doesn't form the ICT state and therefore the hydrogen bonded complex from the amino site hardly absorbs light, but interestingly favors the ICT state formation.

It was showed that ICT emission in ethyl and methyl esters of N,N-dimethylaminonaphthyl-(acrylic)-acid (10 and 11) linearly depends on hydrogen bond donating capacity of the solvent. The absorption spectra of 10 and 11 were blue shifted in aqueous medium compared to that in polar aprotic solvents reported red shift in the absorption spectrum.

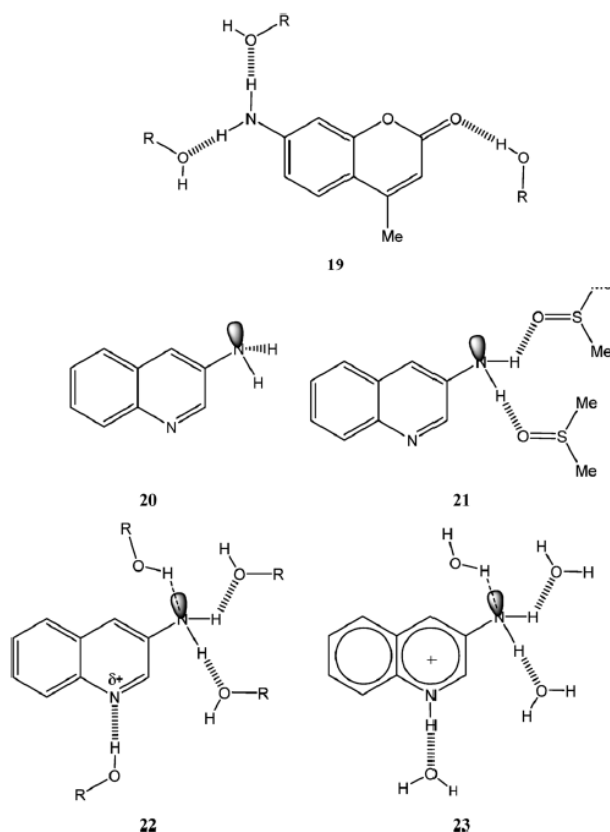


Further it was shown that there are linear dependence on hydrogen bond donating capacity of the solvents by the band maxima of the ICT fluorescence as in the case of compound 12 [35].

Interestingly different types of hydrogen bonding in some of the aminocoumarins between the ground state amino group and the solvents are proposed, in which the electron donating amino group behaves like a donor of hydrogen bond (19).[36] However, such hydrogen

bonds thus favoring the formation of the ICT state by increasing the electron donating capacity of the amino group,.

The protic solvents favours the ICT emission process of 3-aminoquinoline (20) as in the case of dimethyl sulfoxide by a identical sort of hydrogen bonding (21). On the opposite hand, there is an inhibition to the ICT emission because of the hydrogen bonding of 20 in protic solvents, where the charge donor behaves like a hydrogen bond acceptor 22, but the ICT process is enhances the protonation of the acceptor (23).



In the case of ICT state, Hydrogen bonding plays an important role in the formation and stabilization. In the ICT state the hydrogen bonding of the solvent with the donor breaks but with the acceptor is strengthens. A dynamic equilibrium is expected to establish between the free ICT state and the hydrogen bonded ICT state which is very similar to the equilibrium between the LE state and the. The promotion for the formation of the ICT state doesn't come from the hydrogen bonding in the condensed phase; rather inhibits its formation. However the crucial role of the hydrogen bonding promotion in the gaseous phase between the donor with the solvent in

the formation of ICT may not be ruled out, as it may necessarily provide a path for the dissipation of the energy. Hydrogen bonding between the solvent molecules and the electron acceptors lead to the stabilization of the ICT state; thereby it also enhances the internal conversion that ultimately leads to the quenching of the ICT state in many molecules. Though in several molecules the formation of the TICT state may results from the solvent polarity alone such as aminophenylpyridoimidazoles, the hydrogen bonding with the protic solvents is a prerequisite to obtain dual emission. In aminophenylpyridoimidazoles hydrogen bonding of electron acceptors with the protic solvents increases the electron withdrawing capacity of the acceptor, thus leading to the formation of the TICT state. The ICT processes significantly influenced by the proton transfer occurring via hydrogen bonding. In some cases the formation of the TICT state of the phototautomer lead to the opening of nonradiative decay channels for some of the ESIPT molecules. [34]

## Conclusion

In summary I theoretically explore and elaborate the process of Excited state Intramolecular Proton Transfer (ESIPT) and Twisted Intramolecular Charge Transfer (TICT). I have also investigated the effect of different kinds of solvents on ESIPT and TICT processes and their bond lengths and bond angles in various type of compounds. It is found that the ICT can promote the occurrence of ESIPT and the larger electronic energies can cause blue shift in absorption and emission. From the study of various factors that govern such process I found that ground state H-bond is prerequisite for them and also solvent polarity enhances their occurring possibility. Structures that favor the formation of H-bonding and excited state structural relaxation can also promote the ESIPT and TICT processes. The excited state flattening of the molecules along with more or less twisted in their ground states (the steric nonbonding interactions between D and A usually leads to the deviation from planarity) clearly occurs in numerous cases of large aromatic donors or/and acceptors. Above all, with the decreasing in the dielectric constant, more favorable for the ESIPT reaction to occur and the TICT is important for dual fluorescence.

## References:

1. Yu Zhao, Yong Ding, Yunfan Yang, Wei Shi, Yongqing Li, Fluorescence deactivation mechanism for a new probe detecting phosgene based on ESIPT and TICT; Journal Name, 2012, 00, 1-3.
2. Guang-Jiu Zhao, Ke-Li Han, Hydrogen Bonding in the Electronic Excited State, Acc. Chem. Res. 2011, 45, 404-413.
3. G. J. Zhao, K. L. Han, Competitive excited-state single or double proton transfer mechanisms for bis-2,5-(2-benzoxazolyl)-hydroquinone and its derivatives, J. Chem. Phys. 2007, 127, 024306.
4. Hao Dong, Jinfeng Zhao, Huan Yang, Yujun Zheng, Fluorescence deactivation mechanism for a new probe detecting phosgene based ESIPT and TICT, ACS Applied Bio Materials, 2019, 2, 8, 3622–3629
5. Jinfeng Zhao, Hao Dong, Huan Yang, Yujun Zheng, Determinant of ESIPT mechanism by the structure designed for symmetric and unsymmetric molecules, ACS Applied Bio Materials, 2019, 2, 2060-2068
6. Yan, C.-C., Wang, X.-D., Liao, L.-S., Organic Lasers Harnessing Excited State Intramolecular Proton Transfer Process, ACS Photonics, 2020, 7, 1355–1366
7. Long, Y., Mamada, M., Li, C., dos Santos, P.L., Colella, M., Danos, A., Adachi, C., Monkman, A. Excited State Dynamics of Thermally Activated Delayed Fluorescence from an Excited State Intramolecular Proton Transfer System, J. Phys. Chem. Lett, 2020, 11, 3305–3312.
8. Moraes, E.S., Teixeira Alves Duarte, L.G., Germino, J.C., Atvars, T.D.Z. Near Attack Conformation as Strategy for ESIPT Modulation for White-Light Generation, J. Phys. Chem. C, 2020, 124, 22406–22415.
9. Zhang, Z., Chen, Y.-A., Hung, W.-Y., Tang, W.-F., Hsu, Y.-H., Chen, C.-L., Meng, F.-Y., Chou, P.-T., Control of the Reversibility of Excited-State Intramolecular Proton Transfer (ESIPT) Reaction: Host-Polarity Tuning White Organic Light Emitting Diode on a New Thiazolo[5,4- d ]Thiazole ESIPT System, Chem. Mater, 2016, 28, 8815–8824.
10. Sobolewski, A.L., Reversible Molecular Switch Driven by Excited-State Hydrogen Transfer, Phys. Chem. Chem. Phys. 2008, 10, 1243

11. Hem C. Joshi <sup>1</sup>, Liudmil Antonov <sup>2</sup>, Excited-State Intramolecular Proton Transfer: A Short Introductory Review *Molecules*, 2021, 26, 1475.
12. Zbigniew R. Grabowski, Krystyna Rotkiewicz, Structural Changes Accompanying Intramolecular Electron Transfer: Focus on Twisted Intramolecular Charge-Transfer States and Structures, *Chem. Rev.* 2003, 103, 3899-4031.
13. Ahmed M. El-Zohry, Esam A. Orabi, Martin Karlsson, Burkhard Zietz; Twisted Intramolecular Charge Transfer (TICT) Controlled by Dimerization: An Overlooked Piece of the TICT Puzzle, *The Journal of Physical Chemistry A*, 2021, 125, 2885–2894.
14. Tiwari, A.K.; Sathyamurthy, N., Structure and Stability of Salicylic Acid-Water Complexes and the Effect of Molecular Hydration on the Spectral Properties of Salicylic Acid, *J. Phys. Chem. A* 2006, 110, 5960–5964.
15. Blodgett, K.N., Fischer, J.L., Zwier, T.S., Sibert, E.L., The Missing NH Stretch Fundamental in S 1 Methyl Anthranilate: IR-UV Double Resonance Experiments and Local Mode Theory, *Phys. Chem. Chem. Phys.* 2020, 22, 14077-14087.
16. Shunsuke Sasaki, a Gregor P. C. Drummen, Gen-ichi Konishi, Recent advances in twisted intramolecular charge transfer (TICT) fluorescence and related phenomena in materials chemistry *Journal of Materials Chemistry C*, 2016, 4, 2731—274 .
17. Yajing Peng, Yuqing Ye, Xianming Xiu, Shuang Sun, Mechanism of Excited-State Intramolecular Proton Transfer for 1,2-Dihydroxyanthraquinone: Effect of Water on the ESIPT, *J. Phys. Chem. A* 2017, 121, 5625–5634.
18. Xin Lan, Dapeng Yang , Xiao Sui, Dandan Wang, Time-dependent density functional theory (TD-DFT) study on the excited-state intramolecular proton transfer (ESIPT) in 2-hydroxybenzoyl compounds: Significance of the intramolecular hydrogen bonding, *Spectrochimica Acta Part A: Molecular and Biomolecular Spectroscopy* 102 (2013) 281–285
19. Giovanni A. Parada,[a] Todd F. Markle,[b] Starla D. Glover,[a] Leif Hammarström,[a] Sascha Ott and Burkhard Zietz, Control over Excited State Intramolecular Proton Transfer and Photoinduced Tautomerization: Influence of the Hydrogen Bond Geometry, *Chem. Eur. J.* 2015, 21, 6362 – 6366.
20. Cheng Zhong; The driving forces for twisted or planar intramolecular charge transfer; *Physical Chemistry Chemical Physics*, 2012, 10.1039.

21. Riju Davis, N. S. Saleesh Kumar, Shibu Abraham, C. H. Suresh, Nigam P. Rath, Nobuyuki Tamaoki, Suresh Das, Molecular Packing and Solid-State Fluorescence of Alkoxy-Cyano Substituted Diphenylbutadienes: Structure of the Luminescent Aggregates, *J. Phys. Chem. C* 2008, 112, 2137-2146.
22. Hang Yin, Ying Shi, Ye Wang; Time-dependent density functional theory study on the excited-state intramolecular proton transfer in salicylaldehyde, *Spectrochimica Acta Part A: Molecular and Biomolecular Spectroscopy*, 2014, 129, 280–284.
23. Xin Lan, Dapeng Yang, Xiao Sui, Dandan Wang, Time-dependent density functional theory (TD-DFT) study on the excited-state intramolecular proton transfer (ESIPT) in 2-hydroxybenzoyl compounds: Significance of the intramolecular hydrogen bonding, *Spectrochimica Acta Part A: Molecular and Biomolecular Spectroscopy* 102 (2013) 281–285.
24. Ni, M., Su, S., Fang, H., Substituent Control of Photophysical Properties for Excited-State Intramolecular Proton Transfer (ESIPT) of o-LHBDI Derivatives: A TD-DFT Investigation, *J. Mol. Model*, 2020, 26, 108.
25. Yilei Wang, Guoshi Wu, Electronic Structure Characteristics of ESIPT and TICT Fluorescence Emissions and Calculations of Emitting Energies, *Acta Phys. -Chim. Sin*, 2008, 24(4): 552–560.
26. Jianhui Han, Bifa Cao, You Li, Qiao Zhou, Chaofan Sun, Bo Li, Hang Yin, Ying Shi, *Spectrochimica Acta Part A: Molecular and Biomolecular Spectroscopy*, 2020, 231, 1386-1425.
27. Ashis NAG, Tapanendu Kundu, Kankan Bhattacharyya, Effect of Solvent Polarity on The Yield of Twisted Intramolecular Charge Transfer (TICT) Emission. Competition between Formation and Nonradiative Decay of the TICT State, *Chemical Physics Letters*, 1989, 160, 3.
28. V. Thanikachalam, A. Arunpandiyan, J. Jayabharathi, P. Ramanathan, Photophysical properties of the intramolecular excited charge-transfer states of p-expanded styryl phenanthrimidazoles – effect of solvent polarity, *RSC Adv.*, 2014, 4, 6790.
29. Konijnenberg, J., Ekelmans, G.B., Huizer, A.H., Varma, C.A.G.O. Mechanism and Solvent Dependence of the Solvent-Catalysed Pseudo-Intramolecular Proton Transfer of

- 7-Hydroxyquinoline in the First Electronically Excited Singlet State and in the Ground State of Its Tautomer, *J. Chem. Soc. Faraday Trans.2*, 1989, 85, 39–51.
30. Maheshwari, S., Chowdhury, A., Sathyamurthy, N., Mishra, H., Tripathi, H.B, Panda, M, Chandrasekhar, J. Ground and Excited State Intramolecular Proton Transfer in Salicylic Acid: An Ab Initio Electronic Structure Investigation, *J. Phys. Chem. A* 1999, 103, 6257–6262.
31. El-Zohry, A. M., Alturki, A., Yin, J.; Mallick, A., Shekhah, O., Eddaoudi, M., Ooi, B. S., Mohammed, O. F., Tunable Twisting Motion of Organic Linkers Via Concentration and Hydrogen-Bond Formation, *J. Phys. Chem. C* 2019, 123, 5900–5906.
32. Mehata, M.S., Joshi, H.C., Tripathi, H.B., Excited-State Intermolecular Proton Transfer Reaction of 6 Hydroxyquinoline in Protic Polar Medium.,*Chem. Phys. Lett.*, 2002, 359, 314–320
33. K. Furukawa, N. Yamamoto, K. Hino, H. Sekiya, Excited-state intramolecular proton transfer and conformational relaxation in 4'-N,N-dimethylamino-3-hydroxyflavone doped in acetonitrile crystals, *Phys. Chem. Chem. Phys.*, 2016,18, 28564-28575
34. Francis A. S. Chipem, Anasuya Mishra, G. Krishnamoorthy, The role of hydrogen bonding in excited state intramolecular charge transfer, *Phys. Chem. Chem. Phys.* 2012,14, 8775-8790.
35. A. Chakraborty, S. Kar, D. N. Nath, N. Guchhait; Photoinduced Intramolecular Charge Transfer Reaction in (E)-3-(4-Methylamino-phenyl)-acrylic Acid Methyl Ester: A Fluorescence Study in Combination with TDDFT Calculation; *J. Phys. Chem. A*, 2006, 110, 12089–12095.
36. M. J. Kamlet, C. Dickinson, R. W. Taft; Linear Solvation Energy ~La~Ions~~S. Solvent Effects on Some Fluorescence Probes, *Chem. Phys. Lett.*1981, 77, 69–72.
37. Jianzhang Zhao, Shaomin Ji, Yinghui Chen, Huimin Guo, Pei Yang; Excited state intramolecular proton transfer (ESIPT): from principal photophysics to the development of new chromophores and applications in fluorescent molecular probes and luminescent materials, *Phys. Chem. Chem. Phys.*, 2012, 14, 8803–8817.
38. Zhao, G. J.; Han, K. L. Hydrogen Bonding in the Electronic Excited State. *Acc. Chem. Res.* 2012, 45, 404–413.

39. Zhao, G. J., Han, K. L., Excited State Electronic Structures and Photochemistry of Heterocyclic Annulated Perylene (HAP) Materials Tuned by Heteroatoms: S, Se, N, O, C, Si, and B. *J. Phys. Chem. A* 2009, 113, 4788–4794.
40. Hao Dong, Jinfeng Zhao, Huan Yang, and Yujun Zheng, Determinant of ESIPT Mechanism by the Structure Designed for Symmetrical and Unsymmetrical Molecule *ACS Applied Bio Materials*, 2019, 2, 8, 3622–3629.
41. Hao Dong, Huan Yang, Jinfeng Zhao, Xiaoyan Liu, Yujun Zheng; Modulation of excited state proton transfer *Journal of Luminescence*, 2021, 231, 117840.
42. Doose S, Neuweiler H, Sauer M, Fluorescence Quenching by Photoinduced Electron Transfer: A Reporter for Conformational Dynamics of Macromolecules, *ChemPhysChem*, 2009, 10, 1389-1398.
43. Anu Kundu, Subraminain Karthikeyan, Dohyun Moon, Savarimuthu Philip Anthony; *Journal of Molecular Structure*, 2018, 05, 042.



**A LITERATURE SURVEY**  
**ON**  
**DESIGN AND DEVELOPMENT OF CARBON DOTS FOR**  
**LUMINESCENT APPLICATIONS**



Submitted by

**Anima Deori**

Exam roll no: PS-191-808-0049

Registration no: 19000056

Supervisor

**Dr. Rupam jyoti Sharma**

Associate professor

Department of chemistry, Guahati University

## **DECLARATION**

I hereby declare that the matter embodied in this literature survey entitled, ***“Design and development of carbon dots for luminescent applications”*** is the result of survey of scientific literature carried out by me at the Department of Chemistry, Gauhati University, Guwahati, Assam under the supervision of **Dr. Rupam jyoti sharma** and that it has not been submitted elsewhere for the award of any degree or diploma.

As a general practice of writing scientific reports, due acknowledgement has been made to all the authors whose works have been discussed in this survey and unintentional omission, if any, is highly regretted.

Date:6/09/21

Place: Gauhati University

**Anima Deori**

M.Sc. 4<sup>th</sup> Semester

## **CERTIFICATE**

This is to certify that **Anima Deori**, Examination Roll No. PS-191-808-0049, M.Sc. 4<sup>th</sup> semester, student of Department of Chemistry, Gauhati University has successfully carried out literature survey on the topic “***Design and development of carbon dots for luminescent applications***” under my supervision. This literature survey is a partial fulfillment of requirement for obtaining M.Sc. Degree from the Department of Chemistry, Gauhati University.

I would like to certify that the literature survey submitted has been carried out independently by her under my guidance.

Date:

Dr. Rupam jyoti Sharma

Department of Chemistry  
Gauhati University,

# CONTENTS

<b>1. Introduction</b>	<b>3</b>
1.1 Discovery of Carbon dots	4
1.2 Structure of Carbon dots	4
<b>2. Methods of synthesis of Carbon dots</b>	<b>5</b>
2.1 Top down approaches	5
2.1.1 Arc discharge	6
2.1.2 Electrochemical/chemical oxidation	7
2.2.2 Laser ablation	8
2.2.3 Ultrasonic treatment	10
2.2 Bottom up approaches	11
2.2.4 Hydrothermal treatment	12
2.2.5 Microwave synthesis	13
2.2.6 Thermal decomposition	13
2.2.7 Carbonization	14
<b>3. Purification and size control of Carbon Dots</b>	<b>14</b>
3.1 Column chromatography	15
3.2 Anion exchange high performance liquid chromatography	16
3.3 Reversed phase high performance liquid chromatography technique	18
3.4 Gel electrophoresis	19
3.5 Density gradient centrifugation	20
3.6 Size control confined pyrolysis	21
<b>4. Characterization of Carbon Dots</b>	<b>21</b>
4.1 Scanning probe microscope	22
4.2 Scanning and transmission electron microscopy	23
4.3 Fourier transform infrared spectroscopy(FTIR)	24
4.4 Nuclear magnetic resonance (NMR)	25

4.5	Photoluminescence	26
4.6	UV spectroscopy	26
5.	Application of luminescent Carbon dots	27
5.1	Photocatalysis	28
5.2	Light emitting diodes(LEDs)	29
5.3	Metal ion probe	30
5.4	Carbon dots in photovoltaics	31
5.4.1	Light harvesting	32
5.4.2	Electron collector	33
5.4.3	Solar cells	34
6.	Conclusion	
7.	Future perspective	35
8.	Acknowledgment	36
9.	References	36

# DESIGN AND DEVELOPMENT OF CARBON DOTS FOR LUMINESCENT APPLICATION

**ABSTRACT:** Luminescent carbon dots are highly on demand due to their non toxic, environmentally friendly compounds for variety of applications in photonics, optoelectronics, bio imaging, photo voltaic applications and drug delivery etc. Carbon dots (CDs) are recently developed kind of luminescent nanomaterial which is emerged as potential competitors for inorganic quantum dot and other toxic, heavy metal based materials due to their remarkable characteristics like eco friendly, low toxicity, biocompatible, easy to obtain, and inexpensive, with a stable and widely tunable emission. In this review we have summarized the synthesis of Carbon dots with various synthetic methods, and also discussed about various separation techniques to separate the unwanted species and get the desired carbon dots and later we have discussed about some characterization techniques and lastly discussed about the various applications of luminescent carbon dots and their future perspective.

## INTRODUCTION

Carbon dots (CDs) have emerged useful and high promising class of materials in the field of nanotechnology because of outstanding properties and applications. By observing the current situation it is very important to obtain such materials which have low toxicity, low preparing cost and conduct good performance, CDs is such an example.

The carbon based materials which have 0 dimensions and size having less than 10 nm commonly known as carbon nano dots, C- dots or Carbon quantum dots [1].

These materials are obtained from organic compounds and are stable in aqueous solution which is extremely significant in terms of biological point of view [2]. Because of the good photostability, high quantum yield, biocompatibility low toxicity, water solubility, good conductivity, and environmental friendliness of CDs gains outstanding advantages over other materials [3]. They exhibit different size reliant optical properties such as photoluminescence, chemiluminescence, electrochemical luminescence and photo induced electron transfer due to the electron donor and electron acceptor behavior [4]. Besides, it have various applications such as explosive detection, chemical sensing food safety ,bioimaging, drug delivery energy conversion, and photocatalysis, metal detection and many others [5].these properties of CDs are being employed for wastewater treatment and hydrogen generation .

### **1.1 Discovery of Carbon dots:**

In 2004, during electrophoretic purification of single walled carbon nano tubes (SWCNTs) carbon nano particles were accidentally discovered by Xu et al. [6]. Sun et al. synthesized first stable photoluminescent carbon nano particle, and in the same year they prepared water soluble CDs passivated with poly-propionylethylenimine -co-ethylenimine (PPEI-EI). And these prepared CDs are utilized to detect human breast cancer MCF-7 cells [7].

### **1.2 Structure of Carbon Dots:**

Among the different nanomaterials that have been reported till now CDs is the smallest category, and mostly having spherical shape and diameter less than 10 nm. CDs consist of both  $sp^2$  and  $sp^3$  carbon hybridization and quantum confinement effect. they can easily combined with hydroxyl group, carbonyl, amino, and epoxy groups on the surface of CDs which is binds via either

hydrophilic or hydrophobic character which helps to provide a thermodynamic stabilities in different solvents especially in water. Beside of this, pure CDs cannot exhibit any kind of photoluminescent activities but with the surface modification of CDs lead to exhibit strong photoluminescence activity. The modification of surface CDs by different functionalities, Passivating agent, and solvents lead them to a smart material with variation properties [8]. In the fig 1 shows the generalized structure of CDs on the surface of which various functional groups were attached.

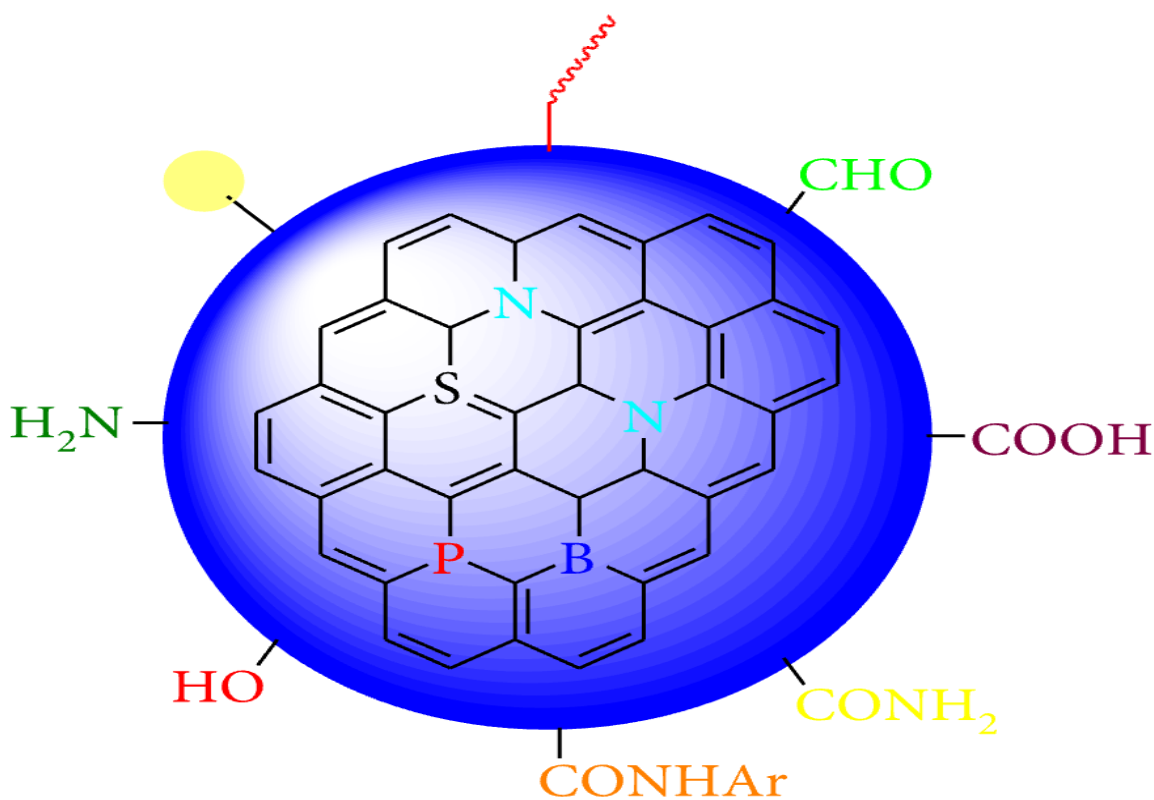


Fig 1: generalized structure of CDs

There are mainly two types of methods are available for synthesis of CDs; i.e top-down approach and bottom up approach. Top down approach refers to breaking down larger carbon structures, such as carbon nano tubes and graphite into smaller carbon structure having dimensions less than 10 nm using arc discharge, laser ablation and electrochemical methods [9]. Wang et al synthesized CDs via



electrochemical method from MWCNTs [10]. Bottom-up approach refers to the synthesis of CDs from smaller carbon units (small organic molecules) by electrochemical/chemical oxidation, laser ablation, hydrothermal/ solvothermal treatment, microwave irradiation, ultrasonic treatment, and thermal decomposition techniques. For example, Zhu et al. synthesized CDs via by heating a solution of poly (ethylene glycol) and saccharide in 500W microwave oven for 2 to 10 min [12]. Various chemical precursors have been identified as the source of CDs, such as citric acid [13], glycerol [14], L-ascorbic acid [15], glucose [16], citric acid urea [17]. To convert these precursors into luminescent CDs various synthetic processes are used, such as ultrasonication [34,35], arc discharge [6], solvothermal [20], hydrothermal [21], chemical oxidation [22], and laser ablation [23]. A lot of efforts have been made to expand the usability of CDs to fulfill the growing demand for high-performance techniques, such as in electronics hole collection, drug-gene delivery, chemical sensing, as well as photocatalysis. However, it is also necessary to regulate the dimensions of CDs during its synthesis to attain uniform properties for a particular application. A large number of reports established the methods of purifying the as-prepared CDs via post-treatment, for example, centrifugation, filtration, gel-electrophoresis and column chromatography [24]. Besides, monitoring the dimensions of CDs during its formation is also preferred. In the past few years, many review articles have been published on the synthesis, properties and applications of CDs which are derived from either small organic molecules (chemical) or green sources [25]. There are various method also present for the characterization of CDs namely scanning probe microscopy, transmission electron microscopy, scanning electron microscopy, NMR, FTIR, Raman spectroscopy etc. from which we can determine the functional group present in them, their optical properties, morphology and size of the CDs can be determined, elemental composition can also be characterized, fluorescence lifetime and decay status can be detected.

In this current review, we have described mainly about the possible synthesis of CDs using top down and bottom up approaches, separation techniques to remove the unwanted species and get the desired CDs and discussed about the characterization of CDs using various technique to know about their shape size, structure and chemical composition and the designing of carbon dots for various luminescent applications molecule and their future perspective.

## **2. Methods of synthesis of carbon dots**

There are various methods for preparing CDs. It can be synthesized mainly through two approaches (1) top-down approach and (2) bottom up approach (fig :2) top down approaches refers to the breaking down larger carbon structure via chemical oxidation, discharge, electrochemical oxidation, and ultra sonic methods. Bottom up approaches refers to the conversion of smaller carbon structure into CDs to desired size. This bottom up approaches consists of hydrothermal treatment, carbonization, Microwave synthesis and solvothermal method [26]. Here we will discuss both the top-down approach and bottom up approach for synthesis of CDs

### **2.1 Top down approach:**

The methods which come under top down approach are viz; arc discharge, laser ablation, electrochemical oxidation, ultrasonic treatment.

#### **2.1.1 Arc discharge method:**

This method was originated in 2004 by xu et.al obtained three kind of carbon nano particles with different relative molecular mass and fluorescence properties accidentally when preparing single walled nano carbon tubes by arc discharge method[6]. The as prepared CQDs can emit blue green yellow and orange fluorescence at 365 nm. Later on the experiment demonstrated that the surface of CQDs obtained by this method have good water solubility, however in general

they possess a large particle size distribution in view of different sizes of carbon particles are formed during the discharge process. The large particle size would extensively decrease the specific surface area of CQDs, which may limit the active reaction sites during the electro catalytic process.

### **2.1.2 Electrochemical oxidation**

Electrochemical oxidation is the most used top down synthesis of CDs due to several remarkable advantages such as high yield, high purity, low cost and easy control over size. Zhou et al. demonstrated the first synthesis of CDs from carbon nano tube via electrochemical oxidation method[12] later Ray et al. used carbon soot as the carbon source for synthesis of CDs, and this approach can be used for the mg scale synthesis of CDs[27].

Peng et al. fabricated TTDDA passivated CDs with an average size of 5 nm from carbohydrates by dehydrating with conc.  $\text{H}_2\text{SO}_4$  [37]. Fabricated CDs from low molecular weight alcohols was reported by Deng et al.[28] they observed that the diameter of CDs was highly dependent upon applied potentials. Hou et al. synthesized CDs from sodium citrate, and urea and the observed diameter of CDs were in the range of 1.0 to 3.5 nm with 11.4% quantum yield [29]. Liu et al. used graphite electrode as the carbon source of synthesized CDs with an average diameter of  $4 \pm 0.2$  nm [30]

**2.1.3 Laser ablation:** This is a standard method for preparing CDs used by the researchers Yu et al. prepared CDs from toluene through the laser irradiation technique [31]. By using femtosecond laser ablation method Nguyen et al. prepared CDs where graphite power is used as carbon source and they observed that size of CDs and photoluminescence properties could easily be controlled by changing the parameters including spot size, irradiation time and laser fluence. Smaller size CDs can be synthesized by increasing the irradiation time [32].

the laser ablation method (kuzmin et al. 2010, Liu et al. 2015, Xiao et al, 2017; donate Buendia et al, 2018) uses a high energy laser pulse to irradiate the surface of the target to a thermodynamic state in which high temperature and high pressure are generated, rapidly heats up and evaporates into a plasma state, and then the vapor crystallizes to form nano particles it is an effective method to prepare CQDs with narrow size distribution, good water solubility, and fluorescence characteristics. However its complicated operation and cost limit its application [33].

#### **2.1.4 Ultrasonic treatment:**

Ultrasonic treatment is a very convenient method as the larger carbon materials can be broken down by action of very high energy of ultrasonic sound wave. Wang et al. synthesized N-doped CDs from ascorbic acid and ammonia via ultra sonic treatment [34]. Dang et al. fabricated CDs using oligomer- polyamide resin as the carbon source by ultrasonic treatment. The as- prepared CDs were well dispersed, has low crystallinity, and functional groups at the surface [35]. In table 1 summarized the various top down methods from which CDs can be synthesized and their sources the color they exhibit and the size.

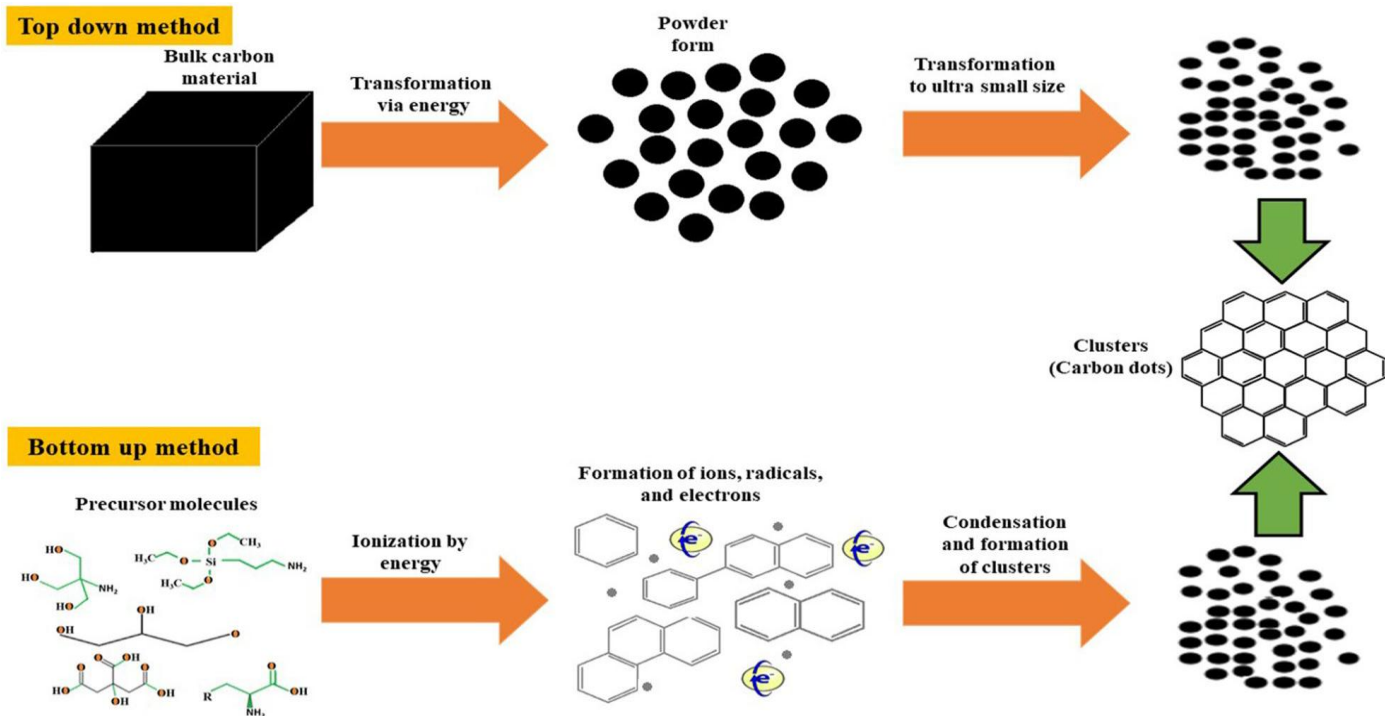


Fig 2: General synthesis methods of CDs, bottom up approach; CDs are synthesized from smaller carbon units. Top down approach; CDs are synthesized by transforming of larger carbon structure into small fragments

Table 1: synthesis of CDs from small organic molecules via top-down approach

Sl no	Source	Method of preparation	Doping(d)/surface Passivating	Color	Size	Refs no.
1	Carbon nanotube	Electrochemical synthesis		Blue	2.8	[27]
2	Carbon soot	Chemical oxidation		green	2-6	[28]
3	carbohydrates	Chemical oxidation	(TTDDA) 4,7,10-tridecanediamine	Red, blue, green and yellow	5	[37]
4	Low molecular	Electrochemical		Red and	2.1,2.9,3.5,and	[29]

	weight alcohol	synthesis		blue	4.3	
5	Sodium citrate and urea	Electrochemical synthesis		Blue	1.0-3.5	[30]
6	Graphite electrode	Electrochemical synthesis		Bright yellow	4+-0.2	[31]
7	Toluene	Laser ablation		Red, black, blue	2-3.9,3-10.0,10-17.21	[32]
8	graphite powders	Laser ablation		Red black blue	1.5,1.6,and 1.8	[33]
9	Oligomer polyamide resin	Ultrasonic treatment	Silane coupling agent	Bright yellow	2-4	[36]
10	Ascorbic acid and ammonia	Ultrasonic treatment	N(d)	Blue green	3.36	[35]

## 2.2 Bottom up approaches

### 2.2.1 Hydrothermal treatment:

Hydrothermal treatment is commonly used because it is cheap, eco friendly and low cost route to synthesize CDs. It can be synthesize from various sources such as Saccharides, amines, organic acids and their derivatives. In a typical approach, small organic molecules or polymers are dissolved in water or organic solvent to form the reaction precursor, which was then transferred to a Teflon-lined stainless steel autoclave. The organic molecules or polymers merged together at high temperature to form carbon seeding core and then grow into CQDs with particle of size less 10nm. Different researchers have used different types of precursors for the preparation of CDs. Zhang et al. synthesized fluorescent CDs for the first time from small organic molecule, L-ascorbic acid via hydro thermal method. They heated the aqueous solution ascorbic acid at constant 180 °C temperature for 4 hrs in an autoclave and purified the water phase solution viz

dialysis using 8000-1400 MWCO membrane. The diameter of prepared CDs is 2 nm [36]. Qu et al. synthesized CDs from dopamine at 180 °C for 6 hrs in an autoclave and purified via centrifugation. The synthesized CDs were mostly spherical with an average diameter of about 3.8 nm [37]. Li et al. fabricated water soluble Nitrogen-doped CDs using ammonium citrate and ethylenediamine. They heated the aqueous solution of ammonium citrate and ethylenediamine at a constant 200°C for 5 hrs. The average diameter found to be 4.8 nm with quantum yield of 66.8% [38]. Many researchers have used this method for the synthesis of CDs ref (39-41)

### **2.2.2 Microwave synthesis:**

Microwave synthesis method is a low cost method for the synthesis of CDs via the irradiation of electromagnetic radiations having a wavelength ranging from 1 mm to 1m which can provide intensive energy to break the chemical bonds of a substrate. This process can reduce the reaction time and provide homogeneous heating which leads to uniform size of the prepared CDs. Zhu et al. [42] synthesized CDs for the first time by using this method. They heated the aqueous solution of saccharides and polyethylene glycol in a domestic microwave (500W) for nearly 3 min. with increasing time the solution changes from colorless to yellow, and final color is dark brown. The size of the synthesized CDs is ~ 3.7 nm. Liu et al. [44] synthesized multi color photoluminescence CDs with an average size ~ 5nm using glycerol as the carbon source and 4, 7, 10- trioxa-1, 13-tridecanediamine (TTDDA) as the passivating agent. Cao et al. (2018) synthesized CDs from the aqueous solution of glucose and arginine using microwave oven (700W) for nearly 10 min. The average diameter of the obtained CDs was between 1 and 7 nm [43].

### **2.2.3 Thermal decomposition:**

It is another standard bottom up method for the synthesized of CDs. Here substance decomposes chemically by the action of heating. This method is easy to operate, less time consuming, low cost and large scale production. Thermal decomposition is generally endothermic. Wang et al. synthesized highly luminescent CDs by the thermal decomposition of citric acid as the carbon source and organosilane, N ( $\beta$ -aminoethyl)- $\gamma$ -amino propyl methyl dimethoxy silane (AEAPMS) as the passivation agent. They heated the reaction mixture for only 1 min, and the observed diameter of CDs was  $\sim 0.9$  nm. Later, Wang et al. synthesized CDs by this method from citric acid. They heated citric acid on a hot plate at 200°C for 30 min; neutralized with sodium hydroxide solution, and finally dialyzed for purification. The size of CDs was range from 0.7 to 1 nm [45]. These CDs showed both excitation-dependent as well as independent photoluminescence properties and different QY depending on synthesis conditions.

#### **2.2.4 Carbonization synthesis:**

carbonization method is also used for the synthesis of CDs. Carbonization is a chemical process in which solid residues with higher content of carbon are formed from organic materials by prolonged pyrolysis in an inert atmosphere. Carbonization of the precursor molecule is one of the best method because it is very simple inexpensive and ultra fast one step method to synthesized CDs. Wei et al. synthesized N-doped CDs using this ultrafast method within 2 min from glucose as a carbon source, and ethylenediamine as the nitrogen source. The observed size of the CDs was 1 to 7 nm with 48% of QY [46]. In table 2 summarized the various bottom up techniques and their sources the color they exhibit and their size.

Table 2: synthesis of CDs from small organic molecule from various bottom up approaches



S.no	Source	Method of preparation	Doping (d) Surface	Color	Size (nm)	Refs. No
1	Saccharides and Polyethylene glycol	Microwave synthesis		Blue	3.7	[42]
2	Glycerol	Microwave synthesis	TTDDA(p)	Blue,turquoise, Green,and red	5	[43]
3	Glucose and argnine	Microwave synthesis		Blue green yellow,red	1-7	[44]
4	Citric acid	Thermal decomposition	organosilane	Blue	0.9	[45]
5	Citric acid	Thermal decomposition	NaOH	Blue, yellow,red, Green	1.0-3.5	[45]
6	Glucose	Carbonization	Ethylene diamine Phosphoric acid	Green	1-7	[46]
7	L-Ascorbic	Hydrothermal treatment		Violet	2	[36]
8	Dopamine	Hydrothermal treatment		Blue, yellow, Green	3.8	[37]
9	Ammonium citrate	Hydrothermal treatment	Ethylene Diamine	Blue	1.59	[38]
10	L-serine ,L-cysteine	Hydrothermal treatment	N,S (d)	Orange	2.6	[40]
11	Citric acid, NH <sub>3</sub> -H <sub>2</sub> O	Hydrothermal treatment	N(d)	Blue	2	[39]
12	Folic acid Phosphoric acid	Hydrothermal treatment	Folic acid, Phosphoric acid	Indigo	13.2	[41]

### 3. Purification and size control of carbon dots:

Purification is done to separate various unwanted species such as amorphous carbon, residual catalyst and chemicals. It can be done filtration, dialysis, centrifugation, gel electrophoresis and chromatography methods.

#### 3.1 Column chromatography Technique:

In this technique there is a stationary phase and mobile phase in column chromatography. Silica gel will be the stationary phase and water will be the

mobile phase. In the fig 1 it is shown that how silica column gel is prepared first of a glass wool is placed in the base of the column. Then we put silica gel as stationary phase. When a sample to be purified is dissolved in small amount of mobile phase and introduced in the column, the various components separate as they move down the column as additional mobile phase is added. The larger particles (i.e the carbon dot) which cannot enter the pores in silica gel, move more quickly and elute earlier while the smaller particles (i.e) the starting material) which do enter the pores, move much more slowly, thus separating the materials. A chromatographic separation based on size, like this, is referred as the size exclusion chromatography [47].

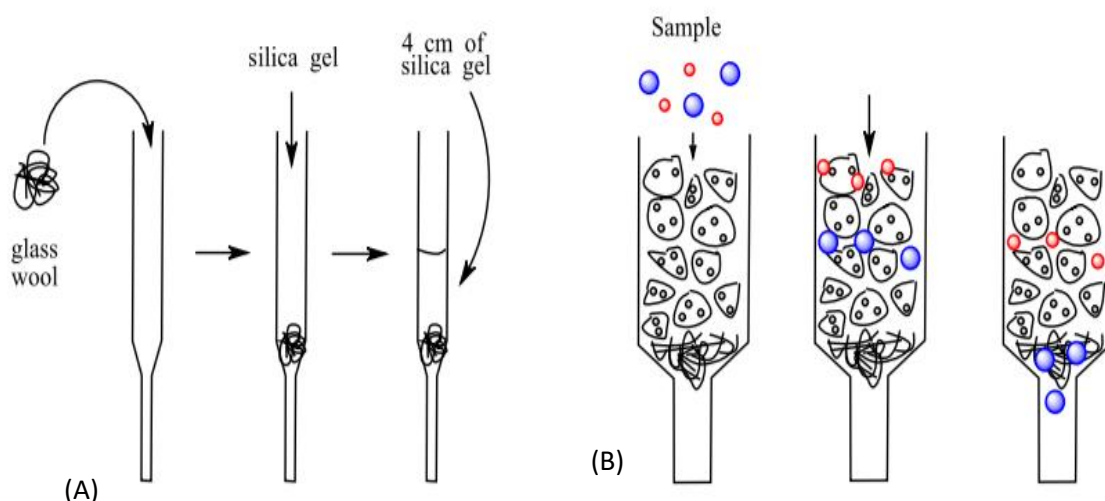


*Fig 3: (A) Building a silica gel column (B) the size exclusion separation process*

### **3.2 Anion exchange High performance liquid chromatography ( AE-HPLC):**

This technique is mainly useful for the separation of negative ions. This allows the separation of negatively charged ions or molecules according to their affinity to the ion exchange resin containing positively charged groups. The first AE-HPLC

was used by Vinci and colon in combination with the UV detection at 250 nm and laser induced photoluminescence detection (LIP) at  $\lambda_{ex}/\lambda_{em}$  of 325/350 nm to separate C-dot products obtained starting with generated during combustion of paraffin oil in a flame. The fractionated CDs mixture strong anion – exchange column and ammonium acetate is used eluent. The fractions of CDs were collected for further characterization by PL spectroscopy and TEM [48] (fig C)

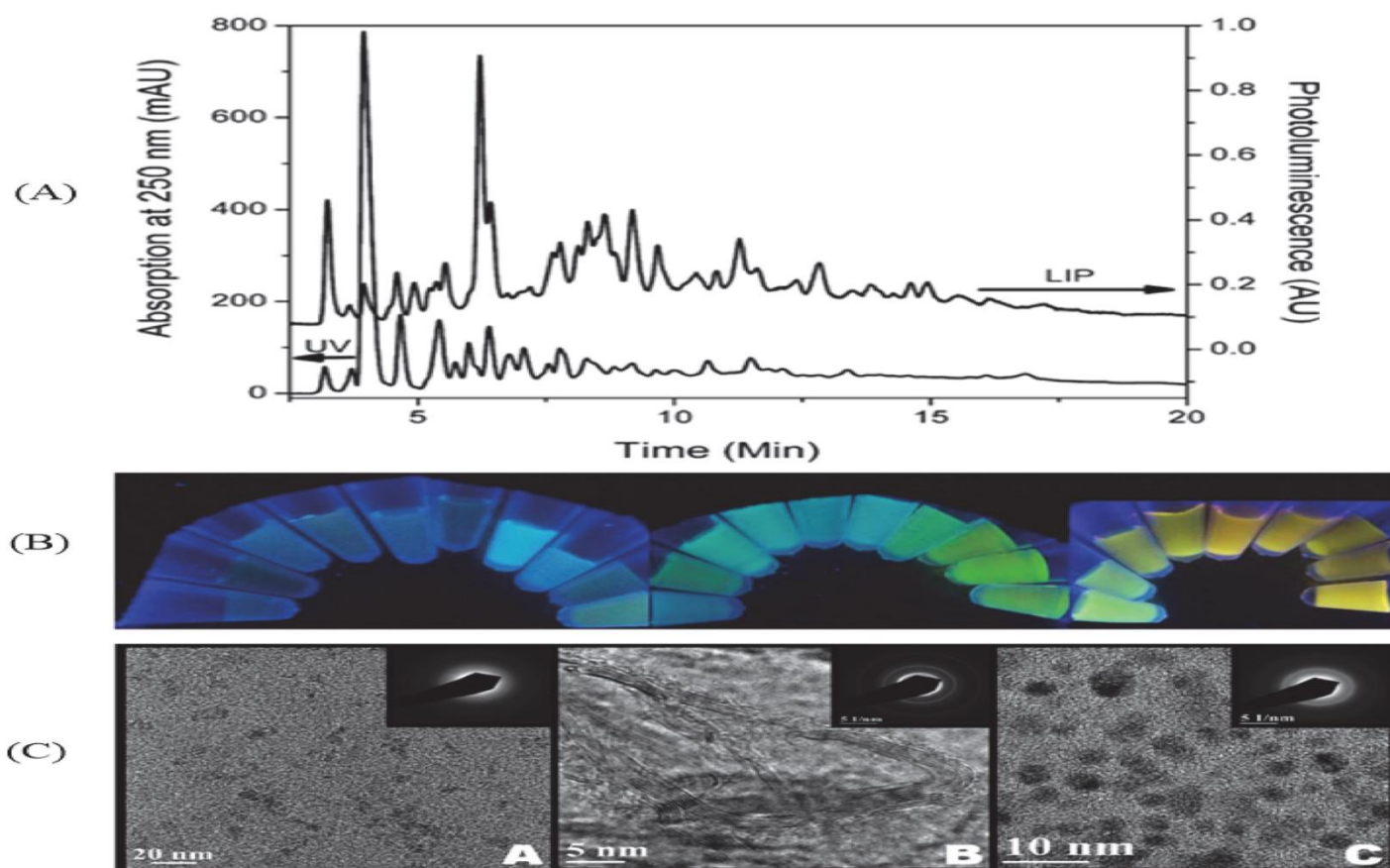


Fig 4 : (A) AE-HPLC chromatograms of the soot derived CDS sample monitored by UV detection at 250 nm and LIP detection at  $\lambda_{ex}/\lambda_{em}$  of 325/350 nm. (B) photographic images of 29 separated CDs fractions under a hand held UV lamp.(C) TEM images and electron diffraction pattern of selective CDs fraction.

### 3.3 Reversed phase high performance liquid chromatography technique:

RP-HPCL is a separation technique where polarity of the mobile phase is higher than the stationary phase. X gong et al. reported the RP-HPLC technique where

CDs is prepared by hydrothermal carbonization of chitosan with UV detection at 300 nm and fluorescence detection at  $\lambda_{ex}/\lambda_{em}$  of 300/405 nm. In this method C18 column is used with methanol and Milli-Q water as the mobile phase (fig A).

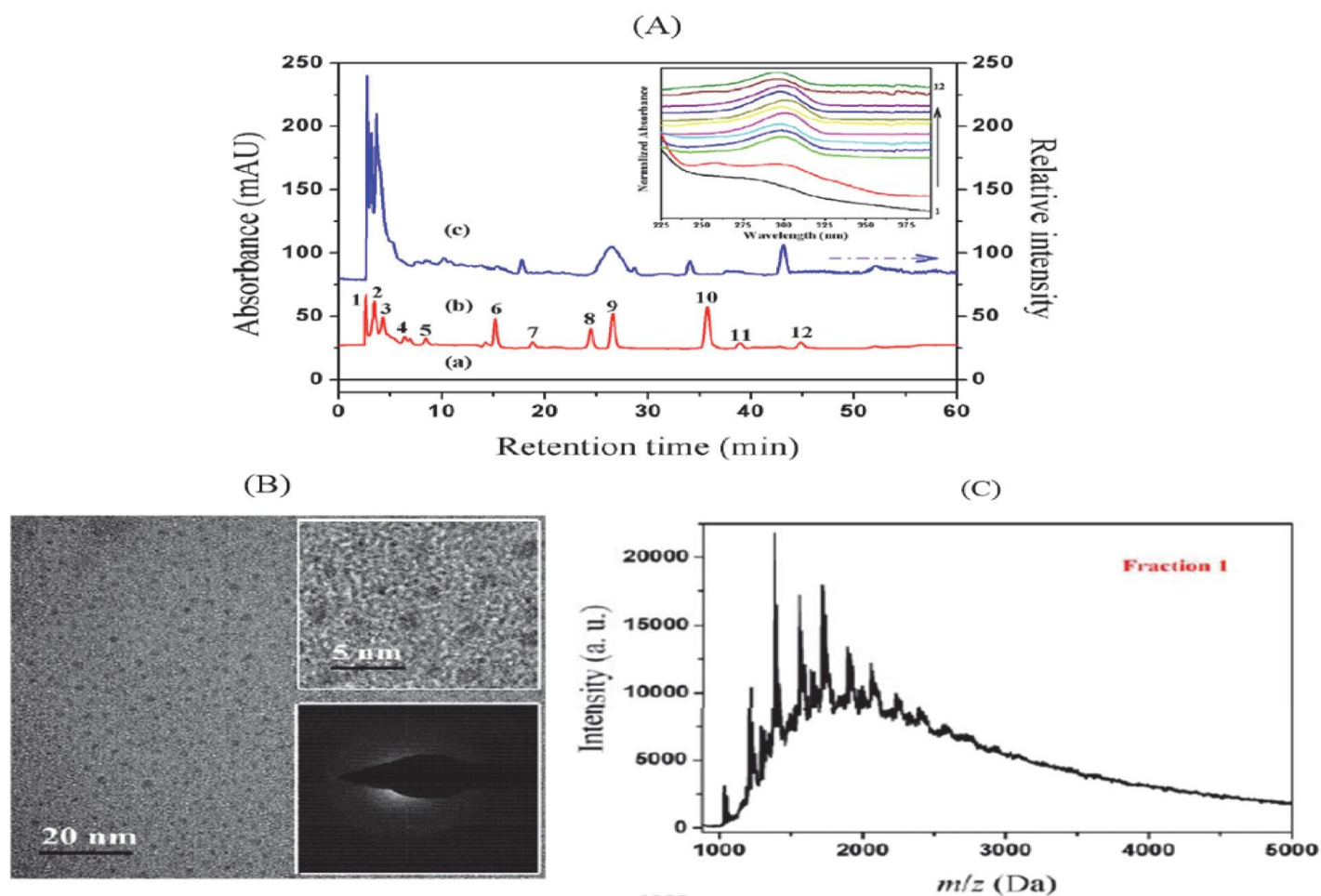


Fig 5: (A) Absorption chromatograms of (a) chitosan and acetic acid in MeOH/water (1 : 19 v/v) and (b) C-dots solution monitored at 300 nm. (c) Fluorescence chromatogram of C-dots solution monitored at  $\lambda_{ex}/\lambda_{em}$  of 300/405 nm. The inset displays the absorption spectra of the 12 separated C-dots fractions. (B) and (C) are the TEM image and MALDI-TOF MS spectrum of fraction 1

In both cases, the electronic and optical properties of CDs were measured by UV visible and PL spectroscopy Fig (A) and TEM (fig (b)). MALDI –TOF-MS was applied to elucidate the surface attached functionalities of CDs fractions by examining their fragmentation pattern in fig (c). later they adopted RP-HPLC method coupled with fluorescence detection for the fractionation of CDs prepared from citric acid and 1, 2-ethylenediamine using 10mM NH<sub>4</sub>Ac buffer and MeOH as the mobile phase .their group further reported the separation of hollow CDs by using RP-HPLC method using UV detection 300 nm with a binary solvent mixture of MeOH and 10 Mm NH<sub>4</sub>Ac buffer as the mobile phase. And it is found that multi color emissive, displaying red, green and blue fluorescence under UV radiation (365nm). The characterization of chemical structure and the elucidation of the molecular formulas of CDs simultaneously ESI-Q-TQF-MS/MS is used [48].

### **3.4 Gel electrophoresis:**

Gel electrophoresis is a fractionation technique which separated the analytes according to the different migration behavior of analytes by sieve effects under the influence of an electric field. The rate of migration is proportional to size, smaller fragments move more quickly, and wind up at the bottom of the gel. Xu et al. used first this method to purify SWCNT which are prepared by arc discharge method [6]. They separated by using 20% denaturing gel that is prepared by using 8 M urea and 1x TBE running buffer and by applying 600 V at 55°C in electrophoresis unit. As

shown in the fig 6 (A) observed under the UV light that the candle soot

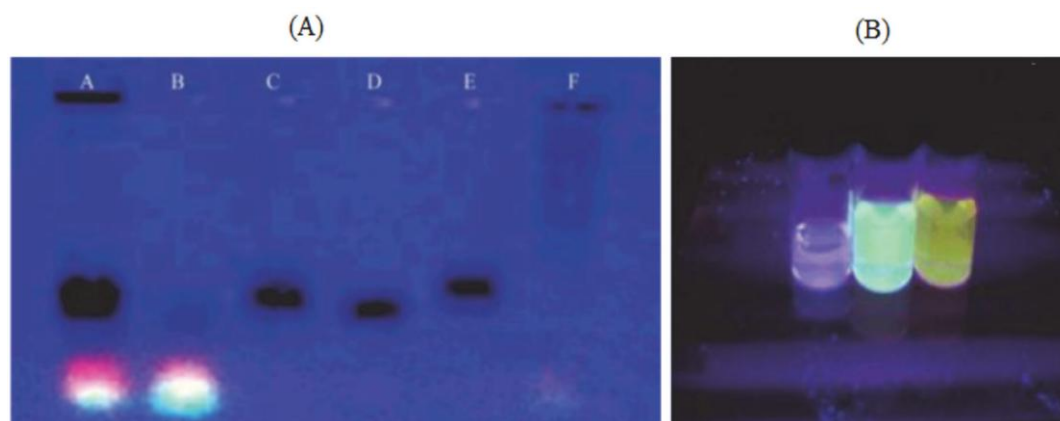


*Fig 6: (A) electrophoretic profile of C dots in 1% agarose gel under 365 nm UV light. (B) photographic images of 3 fractions of fluorescent C- dots species under 365nm*

dispersion was separated into 3 class of nanomaterial, that is agglomerates which did not penetrate the gel, slow moving dark bands of short tubular carbons and fast moving multicolor bands of fluorescent nanomaterials. The multicolor fluorescent bands were further divided into 3 discrete bands which is displaying different colors in order of their elution and increasing size. Shown in the fig6 (B), after separation the separated CDs fractions were passed through a  $0.45\ \mu\text{m}$  PVDF filter and extensively dialyzed against distilled water for purification and subjected to further characterization by elemental analysis, FTIR, PL spectroscopy, and AFM. Liu et al. reported for the separation of CDs used sodium dodecyl sulphate (SDS) polyacrylamide gel electrophoresis (PAGE) method. The observation were found similar to Xu et al. it is found that the electrophoretic mobilities of CDs fractions were highly related to their fluorescence color, with the faster migration CDs species emitted at shorter wavelength. Many researcher were used this method for further exploration of the CDs and other component.

### **3.5 Density gradient centrifugation:**

Density gradient centrifugation method is a routine technique used to separate bio macromolecules. Density gradient is made up of sucrose, glycerol, cesium

chloride, and other aqueous solutions. When sample is put on the top of the density gradient the solutions are sequentially form layered with different densities. When the samples were centrifuged the particles were deposit in the density gradient according to their sizes, shapes or densities. Pandey et al. [49] used sucrose density gradient centrifugation (SDGC) to isolate CDs from other carbonaceous materials. Pure sucrose is taken in a test tube and the sample mixture was fractionated in a density gradient shown in fig7 (a) particulate CDs were found on the basis of the size of the CDs. Under the observation of UV light the obtained fragments exhibited blue and green fluorescence.

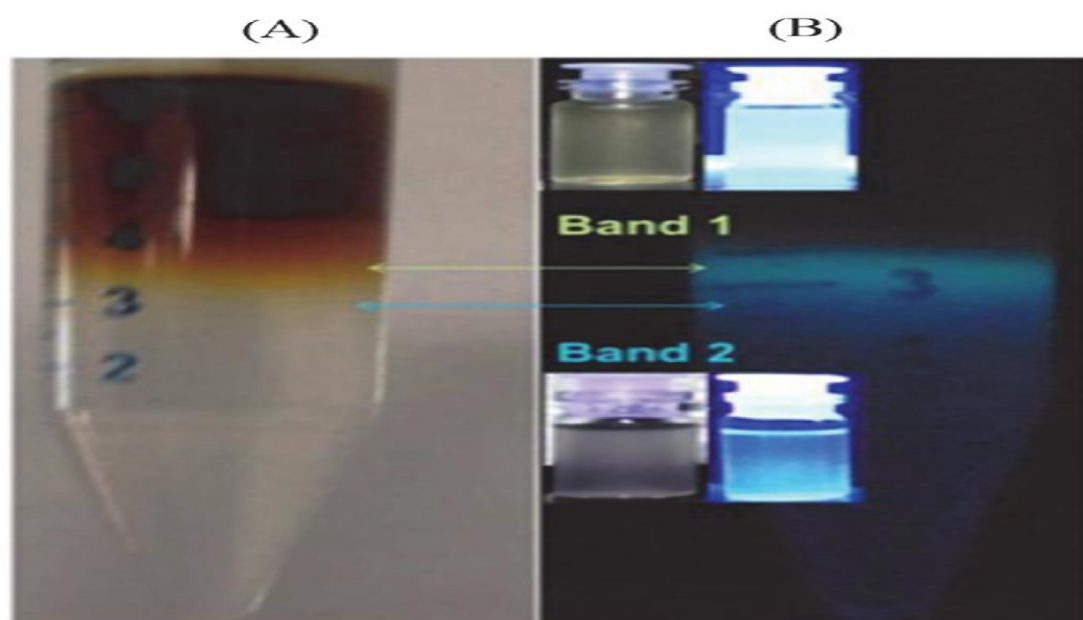


*Fig 7 : (A) SDGC separation of CDs from sonication of cane juice (B) the image of separated CDs bands under ambient and UV light.*

**3.6 Size control-confined pyrolysis:** It is very important to control the size of the carbon dot to get uniform properties. Size control processes are done in three steps as follow:



- i. Here organic precursor is absorbed into porous nano - reactor via capillary force.
- ii. Organic precursors confined are pyrolysis in the nano reactor into carbonaceous matter.
- iii. Release of the synthesized CQDs by removing the nano reactor. The size produced and size distribution from this method is detected by texture parameter of the nano reactor.

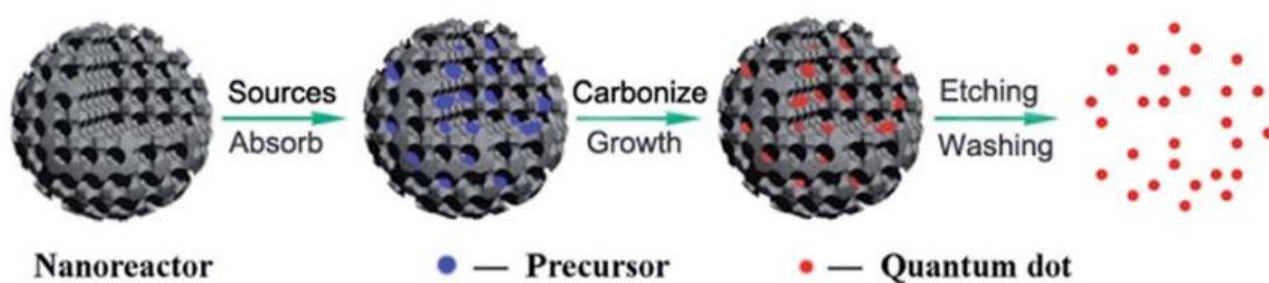


*Fig 8: schematic illustration of the preparation of CQDs via confined pyrolysis of an organic precursor in nano reactors.*

Porous silicas are the most widely used nano reactors for their various, tunable and easily obtained textures fig (8) [50]. Zhu et al. synthesized hydrophilic CDs with mesoporous silica nanospheres as nano reactors by using citric acid as precursor [51]. When it is pyrolysis for 2 hrs at 300 °C in air, after that silica gel is removed and dialysis and obtained CDs with uniform size of 1.5-2.5 nm. And the prepared CDs showed good photostability, low toxicity, excellent luminescent and up conversion properties.

#### **4. Characterization of carbon dots:**

It is very important know the chemical composition, shape and size of carbon dot to find out its properties. There are various routes to characterize CDs some of them are mention below:



#### 4.1 Scanning probe microscope:

AFM is a high resolution scanning probe microscopy that gives surface dimensional images of CDs at lower resolution around 1 nm. AFM produces both 2D and 3D images of CDs. From the 2D image of CDs dimensions can be determined by counting the height of the particles on the image and from the 3D image we get information about the surface morphology of the CDs, in the fig9 (A) and fig9 (B) under the investigation of CDs both the 2D and 3D topographic AFM images of CDs were achieved by the interaction between the AFM cantilever tip and CDs. Fig9 (C) depicts the height profile along lines I, II, III in the 2D image of CDs.

It is important to note that although microscopy based technique are highly accurate and have good performance, the electron microscopy requires intricate preparation and to acquire excellent images is really difficult. This is due to the fact that this microscopy based technique has large potential due to which imaging artifacts were formed [52] .

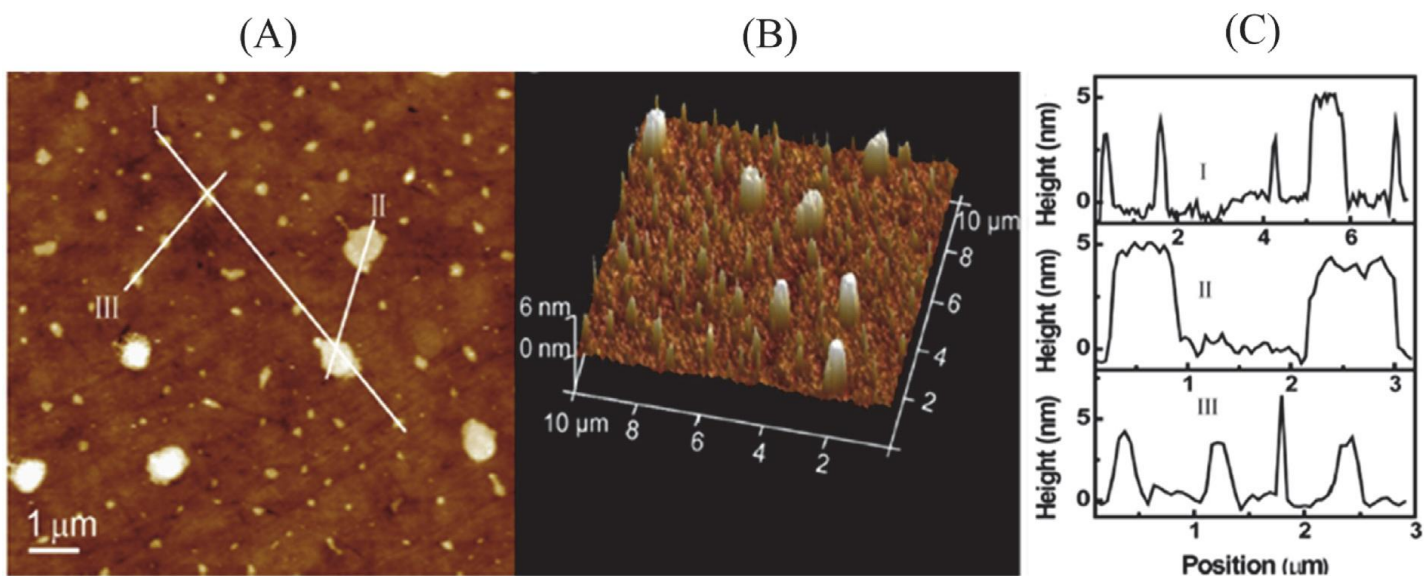


*Fig 9 : (A)AFM topography image of a bulk sample of CDs on quartz substrate (B) AFM 3D image of (A) fig (C) height profile along I, II, and III in (A)*

## 4.2 Scanning and transmission electron microscopy.

To determine the information about the particle size, size distribution and morphology of CDs SEM and TEM is very useful technique, and also to inquiry whether the agglomeration of particles is present or the good dispersion of the particle is achieved with both TEM and SEM image is used. SEM image is produced by scanning the surface of CDs sample with a focused electron beam which interacts with the atom of CDs during which the charges are gather to form an image. Fig10 (A) is an example of SEM image of CDs [52]. And in TEM the image is produced when a beam of high energy electrons is applied to the attained images of sample based on electron transmission of CDs shown on fig10 (B). To analyzed CDs structures and lattice imperfection high resolution transmission electron microscopy (HRTM) fig10(C) is used which used both transmitted and scattered beam to create an interface image, and the analyzing of the image has been extensive and successful

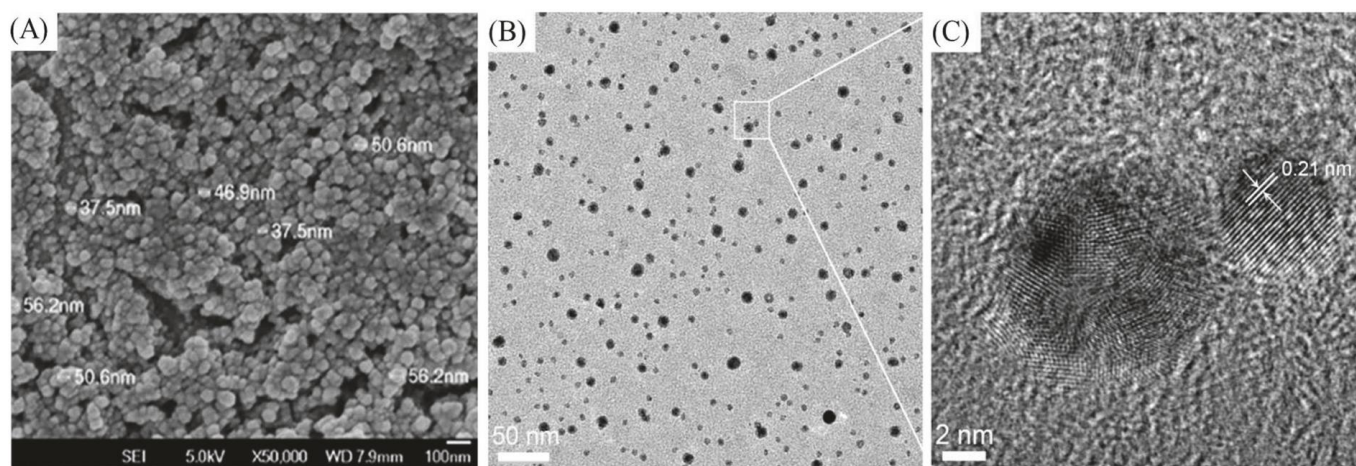


*Fig 10: (A) image formed by SEM. Fig (B) image formed by TEM fig (C) image formed by HRTEM*

## 4.3 Fourier Transform infrared spectroscopy (FTIR):

FTIR is used to for the determination of functional group present on the surface of the CDs. Due to the development of CDs by the partial oxidation of a carbon

precursor there are abundant of carboxyl or carboxylic acid groups, hydroxyl groups and ether/epoxy are present on the surface of the CDs and for the investigation of oxygen group FTIR is very useful device. Before applying, changes were required to be made with CDs for balancing out potentials wells on the energy surface, lesser cytotoxicity, and higher fluorescence QY. Peng et al. developed CDs of size 1-4 nm through the compound oxidation of the carbon strands of one micron, 1-4nm CDs, the particles that formed are broke up in a polar solvent and they were soluble in water, dimethyl sulfoxide and dimethyl formamide are examples. And IR recorded was found that peaks of characteristics absorption at  $1724\text{ cm}^{-1}$  and  $3307\text{ cm}^{-1}$  proposed carboxyl groups, appearance on their surface, the present double bond was shown by the peak of absorption at  $1579\text{ cm}^{-1}$  and the presence of ether linkage was implied by an absorption peak at  $1097\text{ cm}^{-1}$ [52]

#### **4.4 Nuclear magnetic resonance:**

NMR method is usually used to determine the structural information of CDs, hybrid type of C- atoms in the crystalline network and binding mode between the C- atoms. Tian et al. prepared CDs from the natural gas burning sediment which is used as a carbon source and conducted the refluxing with nitric acid and it is found that the aromatic ( $\text{sp}^2$ ) carbon shows resonance in the region expanded from 90-180 ppm, whereas the aliphatic carbon indicated the resonance expanded the region from 8-80 ppm. By distinguishing the  $\text{sp}^3$  carbon from those of  $\text{sp}^2$  the structural insight of CDs is determine with the help of NMR measurement.  $^{13}\text{C}$  NMR range was indicated the absence of aliphatic carbon, which depicted the absence of the single peak below ppm. In the region expanded from 120-150 ppm, order of peaks were appeared and it is found that most of the peaks were seems to come from aromatic carbon. From the  $^{13}\text{C}$  NMR spectroscopic analysis it is conclude that the CDs had developed from  $\text{sp}^2$  carbons [52].

## 4.5 Photoluminescence

Photoluminescence (PL) character is one of the best characters of CDs which occurs from the quantum confinement effect. The quantum yield of bare CDs declined (>10%) which is due to the emissive trap on surface. And it has been observed that the quantum yield can be increase by surface passivation or modification. Many researchers were tried to synthesis various CDs with different method and PL color, in the range between UV visible light or near the infrared area but it is challenging to determine the optical and luminescence mechanism of CDs.

The emission peak could change with regard to the excitation wave length and leads to an interesting while confused excitation behavior and arises debate about luminescence feature. A typical characteristic of photoluminescence in the CDs has been considered to be the obvious  $\lambda_{ex}$  dependence of the emission wave length and also its intensity. Therefore, via applying the surfactant modified silica sphere as the carrier and resols as the carbon precursors, the CDs with a size range of 1.5 to 2.5 nm have been synthesized and later the surface passivation has been performed with PEG1500N. Therefore, QY of the passivated CDs has been indicated as equal to 14.7%. In addition, suspending the passivated CDs exhibited robust blue luminescence with excitement at 365 nm. Moreover, the CDs had wide emission spectra, in a range between 430 and 580 nm so that exhibited  $\lambda_{ex}$  dependent photoluminescence emission. Consequently, the vibrant and brilliant photoluminescence of the CDs could be explained due to the presence of the surface energy trap established via the surface passivation [53].

## 4.6 UV Spectroscopy:

CDs shows strong absorption peak on UV region due to present of  $\pi$ - $\pi^*$  transition of the C=C bonds. And these bonds shows strong absorption peak in

the region (260 to 320 nm). Li et al. prepared active carbon (4.0 g) into 70 mL of  $H_2O_2$  to make a suspension and sonicated it for 2 hrs at room temperature. And after the filtration a diameter range of 5-10 nm fluorescent water soluble CDs were obtained, and a typical absorption of an aromatic Pi framework was represented by common UV visible absorption peak at 250-300 nm. Tang et al. prepared CDs by conducted pyrolysis of glucose solution by assisted microwave techniques, obtained CDs diameter was 1.65 nm with fluorescence QY of 7-10%. The aqueous solutions of CDs were indicated two evident UV absorption peak at 228 and 282 nm. The intensity of both UV absorption peaks was increased by extending the microwave heating time, whereas the peak positions remained unaltered and showed no connection with NPs size [52].

## **5. Application of luminescent carbon dots:**

Luminescent carbon dots have been rises as versatile carbon nanostructures with wide range of potential applications. They are utilized as favorable materials in different field due to their intriguing and fascinating properties such as biocompatibility, water solubility, and high stability. CDs are promising materials and find various applications such as bio imaging, photocatalysis, sensors (biosensor, chemical sensor), drug delivery, energy conversion supercapacitors, LEDs, and many others, and it is also found that CDs have shown great achievements in the field of food science in terms of food safety, nutrient management and food toxicity [53]. The surface functionalizations with suitable reactive made them productive materials. CDs are efficient in several biomedical applications such as in vivo and in vitro fluorescent probes and bio makers. The applicability of CDs in biological and chemical sensing shows excellent results with respect to sensitivity, selectivity, stability, reproducibility, and response time[45].

### **5.1 Photocatalysis:**

CDs efficiently used as photocatalysts for harnessing solar energy in organic pollutant degradation due to their efficient redox properties. CDs upon irradiation generate electron hole pairs, which can be later on utilized for multiple applications in pollutant degradation, reduction of CO<sub>2</sub>, and photocatalytic water splitting[54]. CDs have been as excellent photocatalyst with strong absorption in the wide range of electromagnetic spectrum. However the application is hindered because of the poor electron transfer inside the CDs. In order to increase the efficiency of the CDs and to make them better photocatalyst, their electronic structure is modified by adopting several strategies, such as heterostructure formation, metal ion doping, composite formation and many others. When CDs is doped, shows efficient electronic properties with a strong visible light absorption and show low recombination of charge carriers. Nitrogen-doped CDs in comparison with pure CDs show efficient light photo catalytic degradation of methyl orange. It has also reported that CDs in the size of 1-4 nm showed good photocatalytic oxidation of benzyl alcohol to benzaldehyde in the presence of hydrogen peroxide [55]. The conversion efficiency under NIR light was observed to be 92-100%, confirming better redox properties of CDs. The proposed mechanism of the conversion has been demonstrated in fig 11

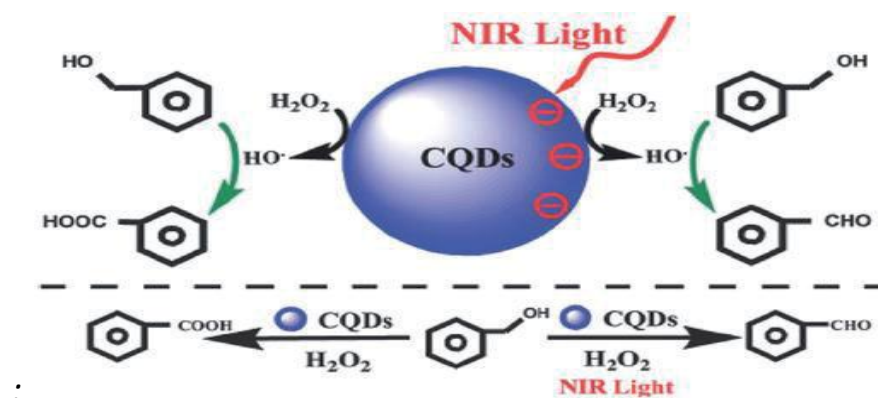


*Fig11: CDs supported oxidation of benzyl alcohol to benzaldehyde in the presence of NIR light*

## 5.2 LED Devices:

Guo et al. by the thermolysis of epoxy group conducting polystyrene microspheres synthesized a series of multicolor CDs. Under the temperature of 200, 300, and 400°C the prepared CDs could emit blue, orange, and white fluorescence with the excitation of single wavelength ultraviolet respectively. And the fluorescent quantum yield is 47%. Those mentioned above CDs could be used as three color LED devices with excellent properties.

Wang et al. also prepared CDs from citric acid which is used as carbon source in octadecene coupled with 1-cetylamine as surface passivator. The maximum quantum yield of these CDs made white light emitting devices reach 0.083% under the irradiation of 5 Ma/cm<sup>2</sup> ampere density [56].

## 5.3 Metal ion probe: CDs can be used as metal ion probe, in the solution easily

quenched efficiently by electron acceptor and thus it can successfully detect metal ions which is present in the solution and it can also determine the concentration of metal ions in a certain concentration range.

Hg<sup>2+</sup> is one of the most toxic heavy metal ion in our environment. Therefore to detect Hg<sup>2+</sup> varieties CDs based sensor is developed by the scientists. Lu et al. [57] prepared new type of CDs from grapefruit peel through hydrothermal method. As the Hg<sup>2+</sup> can effectively quench the fluorescence of CDs, new method of Hg<sup>2+</sup> was developed, the detection limit of 0.23 nm, and this method has been successfully applied to the detection to the detection of Hg<sub>2</sub><sup>+</sup> in the river. Liu et al. prepared CDs with excellent fluorescent stability by the polyethylene glycol(PEG) refluxed with NaOH, and these prepared CDs used as sensor can specifically detect Hg<sub>2</sub><sup>+</sup> in solution and the detection limit reaches 1



fM shown in fig12. this method can was successfully detected  $\text{Hg}^{2+}$  in the rivers, lakes, and tap water samples and the sensitivity is very high.

Zhang and Chen prepared CDs where vitamin B is used as carbon and nitrogen source and prepared a high fluorescence yield and nitrogen rich fluorescence CDs by hydrothermal method [36]. And it is found that  $\text{Hg}^{2+}$  can be able to bind specially with these CDs, the use of this fluorescent probe to established a new method for label free detection of  $\text{Hg}^{2+}$ .scientists have also developed variety of methods to detect  $\text{Cu}^{2+}$ ,  $\text{Fe}^{3+}$ ,  $\text{Pb}$  and  $\text{Ag}^{+}$

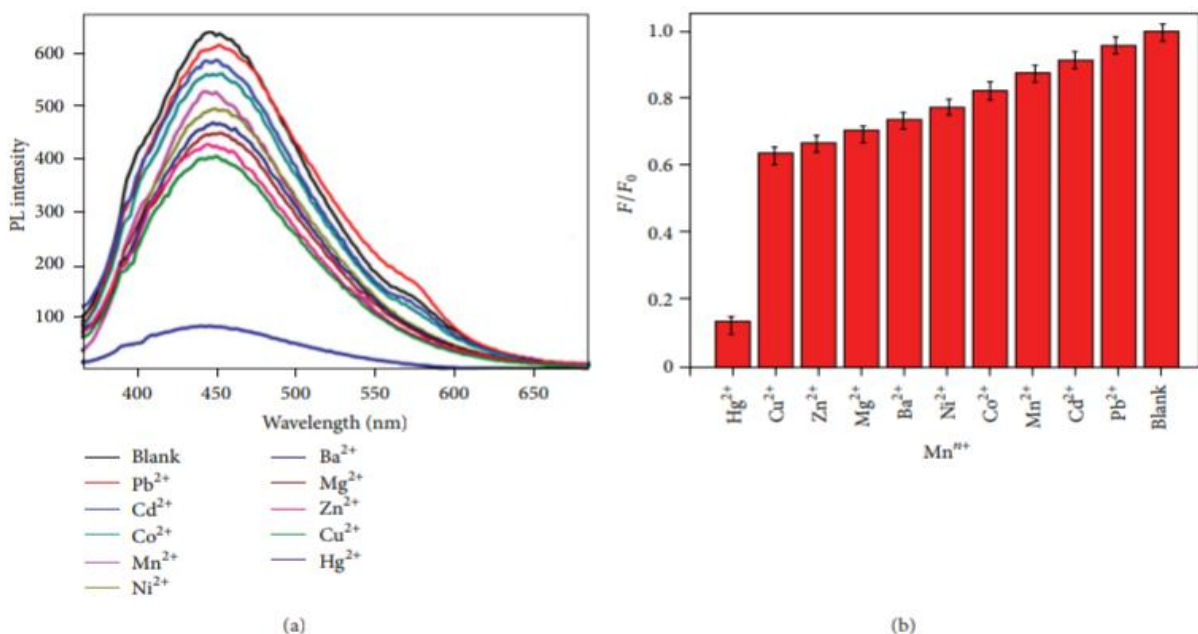
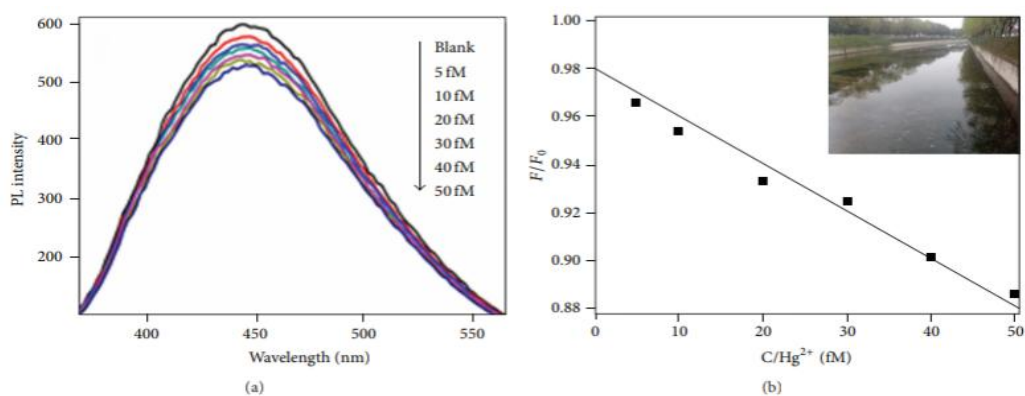


Fig 12: PL spectra and the different PL intensity ratio ( $F/F_0$ ) of FCDs with various metal ions.





*Fig 13: (a b) PL spectra and the different PL intensity ratio ( $F/F_0$ ) of the FCDs with various  $Hg^{2+}$  ions concentration in the range of 0-50 fM in river water.*

## **5.4 Carbon dots in photovoltaics:**

The light harvesting abilities and conducting properties of CDs have prompted researchers to use them in variety of roles in solar cell.

### **5.4.1 Light harvesting:**

The spectral absorption features of the CDs in the UV region have led their application as single absorber in several photovoltaics cells. Briscoe and co-workers studied the construction of low cost sustainable structured cells making use of CDs obtained from biomass. They prepared CDs by hydrothermal carbonization of chitin, chitosan or glucose which led to samples with features that reflected the parent reactant. Thus chitin and chitosan led to N-doped CDs (10% and 8% respectively). The surface was functionalized by amides if chitin was used, amines if chitosan was used and hydroxyl if glucose was used. There will be difference during deposition onto ZnO nanorods because the best coverage was obtained with chitosan and glucose. Finally CuSCN was added as HTL giving rise to cell configuration FTO/ZnO nanorod/CDs/CuSCN/Au. When chitosan derived is used the efficiencies is best. It was observed that the nature of the precursors and surface functionalizations heavily influences the performance of the diodes. For further optimization, the researchers combined two types of CDs to integrate their best properties and increase optical absorption. It is very important to note that the combination needed to be done with great care to prevent the series resistance from increasing and the short circuit density ( $J_{sc}$ ) from decreasing. Therefore results were best with a

combination of chitosan and chitin-derived CDs, for which efficiency was 0.077[58].

CDs have been also applied in nanostructured silicon solar cells. Xie et al. intended to broaden the absorption range of the silicon wire by creating core/shell heterojunctions with CDs. The nano particle were synthesized by electrochemical etching methods and added to 5 layers of CDs. The overall structure of the device was In-Ga/Si/CD/Au and reached an efficiency of 9.1% which is much higher than the references prepared with planar silicon and 5 layers of CDs or silicon nanowires without CDs. The reason for the enhanced performance of the device were the increase in optical absorption in the UV region and the fact that the recombination was lower because of blocking layer action of CDs shown in figure: 14

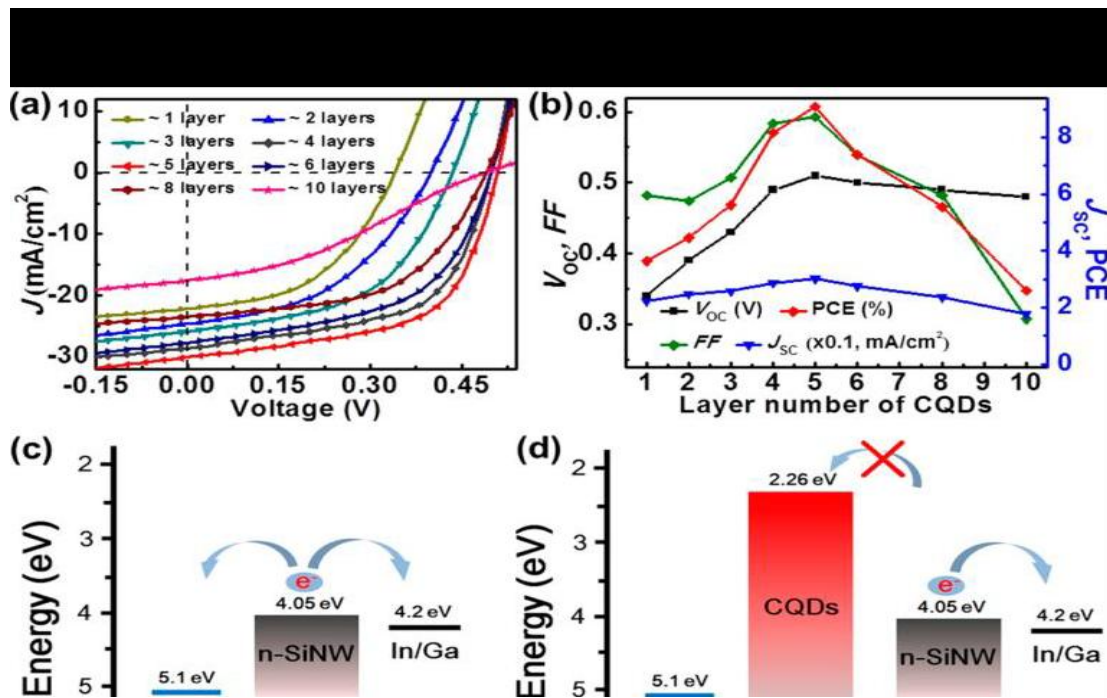


Fig 14: (a) variation of the JV curve (b) variation of cell parameters(c) with increasing layers of CDs; energy level alignments of the cells without CDs (d) energy level alignment of the cells with CDs

### 5.4.2 Electron collector:

In the solar cell the potential contribution of CDs to the charge transport which led to the nanocrystals used as electron acceptor. Kwon and coworkers examine oleylamine-capped CDs in combination with the electron donor P3HT to form the structure ITO/PEDOT:PSS/P3HT:CDs/Al. Compared to 1.99% efficiency of the P3HT/PCBM references, the 0.23% obtained points to the insulating character of the oleylamine as the origin of the lower  $J_{sc}$  values.

To enhance the charge transport of CDs Narayanan prepared a device which is made up of quantum dots ZnS/CdS/ZnS which act as an exciton generator, and the small molecule CuPc as electron acceptor. The quantum dots absorb light in the blue green region of the spectrum and transferred the energy via Förster resonance to the red absorber phthalocyanine. The addition of the CDs to the heterojunction accelerated the charge transfer towards the electrode and decreased the electron recombination rate, which was reflected in the increase in IPCE. Thus, the resulting  $J_{sc}$  was 5.76 times higher than the reference prepared without CDs. open circuit voltage ( $V_{oc}$ ) was also enhanced, and the efficiency increased to 0.35%. The carbon nanocrystals measured 16 nm and were closely connected to CDs and CuPc, as observed by HRTEM [58].

### 5.4.3 Solar cells:

The composite with CDs luminescence and exhibits a luminescent down shifting (LDS) property. The P3HT: PCBM based solar cell harvests sunlight from 480 to 650 nm, only covering a part of visible light (380-780) that contains the peak of the sun's irradiance output. The remaining portions (380-480 nm and 650-780 nm) are not effectively utilized. The CDs filled polysiloxane composite is able to emit light from 400 to 650 nm under the excitation from 320 to 450 nm, because of the emission wavelength range of the composite coincidence with

the response curve of the P3HT: PCBM- based BHJ solar cell, the power conservation efficiency is raised by 12% and the absorption is enhance near ultra violet and blue-violet portions of sunlight [59] shown in fig 15

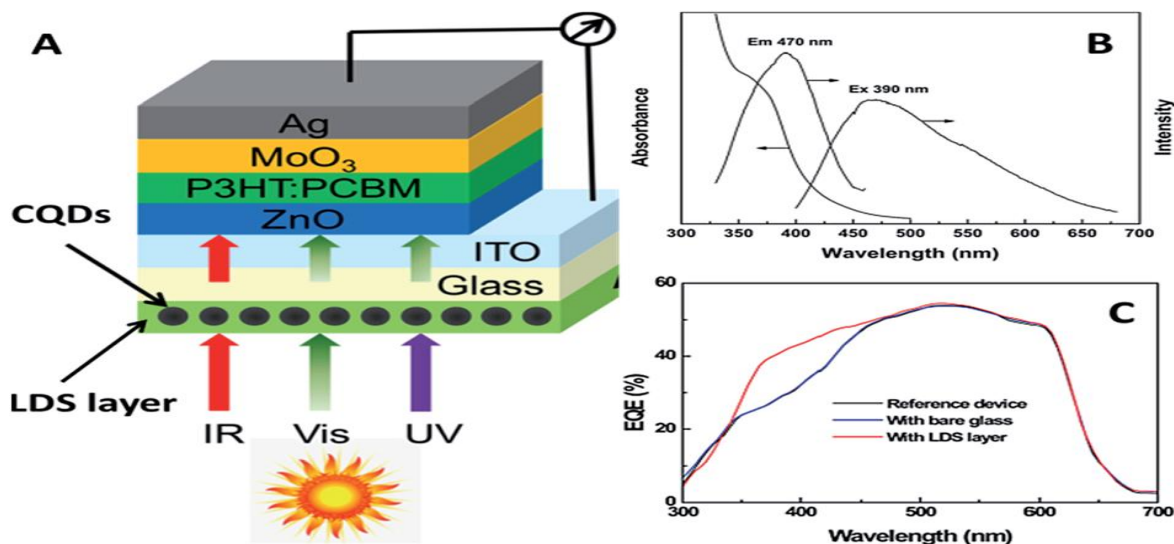


Fig 15: (A) Schematic architecture of the BHJ solar cell with LDS layer.(B) UV-visible absorption and PL spectra of the CQDs filled polysiloxane composite 20  $\mu\text{m}$  thick) coated on glass. (C) Wavelength dependences of external quantum efficiency of the P3HT: PCBM-based solar cell with and without the LDS layer.

## 6. CONCLUSION :

This review is aim to give a general information about CDs. Here I have putted the information of the synthesis of CDs using various synthetic techniques used by the researchers namely top down and bottom up approaches, and discussed about various separation techniques such as column chromatography, gel electrophoresis, centrifugation. and further also mentioned about the different characterization techniques of CDs it is shown that synthesized of different CDs shows different characteristics such as composition structure luminescent character which can be applied in different applications such as in optoelectronics, LED device, metal ion detection, in photovoltaics applications also such as light harvesting, electron collector, solar cells and many others.

At the last by analyzing the various applications and properties of the CDs we have concluded that luminescent CDs will give a remarkable application in future by further investigating the properties

## **7. FUTURE PERSPECTIVE:**

Luminescent carbon dots fascinating applications in the field of chemical sensor, bioimaging, optoelectronics, drug delivery electro catalysis and many others. However significant development has been done over the past, at present their applications as well as their synthesis are limited due to numerous physical and chemical phenomena are still unexplored.

The synthetic variability hinders reproducibility and affects the efficiency so the size and surface molecules need to be fine tuned if efficient device are to prepared, these material are expected to play a important role in energy harvesting device help to decrease CO<sub>2</sub> emissions and lower the cost of renewable energy.

It is important to understand the real mechanism of CDs formation which is not understood fully till date. Therefore simple and controllable surface modifications are still crucial problems, which may help for designing CDs with excellent photoluminescence property and other application with high efficiency. Another one, it is important to study the lifetime and decay profiles of the CDs and identify system with desirable fluorescence emissions which is very useful for the study of photovoltaic applications. Finally, the use of CDs in the area of energy storage is needed to explored, so that CDs will gain significant interest in future.

## ACKNOWLEDGEMENT

I would like to thank **prof Dr. Rupam jyoti Sharma** for guiding me through the course of this project as my supervisor; for giving me the opportunity to work on this topic and for helping me out with my queries. I would like to pay my heartfelt gratitude to **Miss Pirbika engtipi** and **Mr. Abhisekh saikia**, for supporting me from all aspects and giving me suggestions for making this report better. Finally, I would like to thank all the supporting hands and **Dr. Chitrani medhi**, Head of the Department of Chemistry, Gauhati University, for providing me this opportunity of working on this project as a part of my program curriculum.

## References

- [1] Anish khan, Mohamod Jawaidd, Inamuddin, Abdullah Mohammad Asiri, Carbon dots: preparation ,properties and application ,*appl.surf.sci*, **2** , 2019 , 651-676
- [2 ] S. Y. Lim, W. Shen, and Z. Gao, “Carbon quantum dots and their applications,” *Chem.soc.rev*,44, 1,362–381, **2015**
- [3] J. Geys, A. Nemmar, E. Verbeken et al., “Acute toxicity and prothrombotic effects of quantum dots: impact of surface charge,” *Environmental Health Perspectives*, 116, **12**. 1607–1613, **2008**.
- [4] anirudh, joydeep das ,Small molecules derived carbon dots: synthesis and applications in sensing, catalysis, imaging, and biomedicine , **2,2019**
- [5] Peng H, Zhang L, Kjällman THM, Soeller C. DNA hybridization detection with blue luminescent quantum dots and dye-labeled single-stranded DNA. *Communication*. **2007**;129,11,3048–9.
- [6] X. Xu, R. Ray, Y. Gu et al., “Electrophoretic analysis and purification of fluorescent single-walled carbon nanotube fragments,” *J Am Chem Soc.*, 126, 40, 12736-12737, **2004**.

- [7] L. Cao, X. Wang, M. J. Meziani et al., "Carbon dots for multiphoton bioimaging," *J Am. Chem. Soc.*, 129, 37, 11318-11319, **2007**
- [8] F. Yuan, S. Li, Z. Fan, X. Meng, L. Fan, and S. Yang, "Shining carbon dots: synthesis and biomedical and optoelectronic applications," *Nano Today*, 11, 5, 565–586, **2016**
- [9] Lim SY, Shen W, Gao Z. Carbon quantum dots and their applications. *Chem Soc Rev.* **2015**;1:362–81.
- [10] Wang CI, Wu WC, Periasamy AP, Chang HT. "Electrochemical synthesis of photoluminescent carbon nanodots from glycine for highly sensitive detection of hemoglobin". *Green Chem.* **2014**;5,:2509–14.
- [12] Zhou J, Booker C, Li R, Zhou X, Sun X, Ding Z," An electrochemical avenue to blue luminescent nanocrystals from multiwalled carbon nanotubes (MWCNTs)". *J Am Chem Soc.* **2007**;4:744–5.
- [13] Zeng Q, Shao D, He X, Ren Z, Ji W, Shan C, Qu S, Li J, Chen L, Li Q. Carbon dots as a trackable drug delivery carrier for localized cancer therapy in vivo. *J Mater Chem B.* **2016**;30,5119–26.
- [14] Rai S, Singh BK, Bhartiya P, Singh A, Kumar H, Dutta PK, Mehrotra GK."Lignin derived reduced fluorescence carbon dots with theranostic approaches: nano-drug-carrier and bioimaging". *J Luminescence.* **2017**;190:492–503.
- [15] Qian Z, Shan X, Chai L, Ma J, Chen J, Feng H." Si-doped carbon quantum dots: a facile and general preparation strategy, bioimaging application, and multifunctional sensor" *ACS Appl Mater Interfaces*, 2014;6,:6797–805
- [16] Li H, He X, Liu Y, Huang H, Lian S, Lee S, Kang Z. "One-step ultrasonic synthesis of water-soluble carbon nanoparticles with excellent photoluminescent properties". *Carbon.* **2011**;2,:605–9
- [17]. Bourlinos AB, Trivizas G, Karakassides MA, Baikousi M, Kouloumpis A, Gournis D, Bakandritsos A, Hola K, Kozak O, Zboril R, Papagiannouli I, Aloukos P, Couris S. Green and simple route toward boron doped carbon dots with significantly enhanced non-linear optical properties. *Carbon.* **2015**;83:173–9.
- [18] Dang H, Huang LK, Zhang Y, Wang CF, Chen S. Large-scale ultrasonic fabrication of white fluorescent carbon dots, *Ind Eng Chem Res.* **2016**;18:5335–41.

- [21] Wang S, Chen ZG, Cole I, Li Q. Structural evolution of grapheme quantum dots during thermal decomposition of citric acid and the corresponding photoluminescence. *Carbon*. 2015;82:304–13.
- [22] Zhang Y, Ma D, Zhuang Y, Zhang X, Chen W, Hong L, Yan Q, Yu Huang S. One-pot synthesis of N-doped carbon dots with tunable luminescence properties. *J Mater Chem*. 2012;22(33):16714–8.
- [23] Qu K, Wang J, Ren J, Qu X. Carbon dots prepared by hydrothermal treatment of dopamine as an effective fluorescent sensing platform for the label-free detection of iron (III) ions and dopamine. *Chem A Eur J*. 2013;19(22):7243–9
- [24] Wang X, Shen X, Li B, Jiang G, Zhou X, Jiang H. One-step facile synthesis of novel beta amino alcohol functionalized carbon dots for the fabrication of selective. *RSC Adv*. 2016;6(22):18326–32.
- [25] Molinero, A. A., Enright, M., & Cossairt, B. Preparation and Characterization of Carbon Quantum Dots And Their Application to Fingerprint Imaging.
- [26] Shafi, A., Bano, S., Sabir, S., Khan, M. Z., & Rahman, M. M. Eco-Friendly Fluorescent Carbon Nanodots: Characteristics and Potential Applications. In *Carbon-Based Material for Environmental Protection and Remediation*. IntechOpen, 2020
- [27] Ray S, Saha A, Jana NR, Sarkar R. Fluorescent carbon nanoparticles: synthesis, characterization, and bioimaging application. *J Phys Chem C*. **2009**;113(43):18546–51
- [28] Deng J, Lu Q, Mi N, Li H, Liu M, Xu M, Tan L, Xie Q, Zhang Y, Yao S. Electrochemical synthesis of carbon nanodots directly from alcohols. *Chem A Eur J*. 2014;17:4993–9.
- [29] Hou Y, Lu Q, Deng J, Li H, Zhang Y, One-pot electrochemical synthesis of functionalized fluorescent carbon dots and their selective sensing for mercury ion, *Anal Chim Acta*. **2015**;866:69–74
- [30] Liu M, Xu Y, Niu F, Gooding JJ, Liu J. Carbon quantum dots directly generated from electrochemical oxidation of graphite electrodes in alkaline alcohols and the applications for specific ferric ion detection and cell imaging. *Analyst*. **2016**;9:2657–64
- [31] Yu H, Li X, Zeng X, Lu Y., Preparation of carbon dots by non-focusing pulsed laser irradiation in toluene. *Chem Commun*, **2015**;4:819–22.



- [32] Nguyen V, Yan L, Si J, Hou X. Femtosecond laser-induced size reduction of carbon nanodots in solution: effect of laser fluence, spot size, and irradiation time. *J Appl Phys.* 2015;117(8):084304.
- [33] Wang X, Feng Y, Dong P and Huang J, A Mini Review on Carbon Quantum Dots Preparation, Properties, and Electrocatalytic Application, *Front. Chem*, 5, **2019**:671.
- [34] Wang F, Wang S, Sun Z, Zhu H. Study on the ultrasonic single-step synthesis and optical properties of nitrogen-doped carbon fluorescent quantum dots. *Fullerenes Nanotubes Carbon Nanostruct.* 2015;23(9):769–76.
- [35] Dang, H., Huang, L. K., Zhang, Y., Wang, C. F., & Chen, S. Large-scale ultrasonic fabrication of white fluorescent carbon dots. *Ind. Eng. Chem. Res.* 55(18), 5335-53 ;41. **2016**
- [36] Zhang B, Liu C, Liu Y, A novel one-step approach to synthesize fluorescent carbon nanoparticles. *Eur J Inorg Chem*; **2010**,28,:4411–4.
- [37] Qu K, Wang J, Ren J, Qu X. Carbon dots prepared by hydrothermal treatment of dopamine as an effective fluorescent sensing platform for the label-free detection of iron (III) ions and dopamine, *Chem A Eur J.* **2013**;19(22):7243–9.
- [38] Li Z, Yu H, Bian T, Zhao Y, Zhou C, Shang L, Liu Y, Wu L, Tung C, Zhang T. Highly luminescent nitrogen-doped carbon quantum dots as effective fluorescent probes for mercuric and iodide ions. *J Mater Chem C.* **2015**;9,1922–8.
- [39] Zhang Y, Cui P, Zhang F, Feng X, Wang Y, Yang Y, Liu X. Fluorescent probes for “off-on” highly sensitive detection of Hg<sup>2+</sup> and l-cysteine based on nitrogen-doped carbon dots. *Talanta*;2,288–300, **2016**
- [40] Zeng Y, Ma D, Wang W, Chen J, Zhou L, Zheng Y, Yu K, Huang S. N, S co-doped carbon dots with orange luminescence synthesized through polymerization and carbonization reaction of amino acids. *Appl Surf Sci.* **2015**;342:136–43
- [41] Campos BB, Oliva MM, Cáceres RC, Castellón ER, Jiménez JJ, da Silva JCGE, Algarra M. Carbon dots on based folic acid coated with PAMAM dendrimer as platform for Pt(IV) detection. *J Colloid Interface Sci.* 7, **2016**;465,165–73.
- [42] Zhu H, Wang X, Li Y, Wang Z, Yang F, Yang X. Microwave synthesis of fluorescent carbon nanoparticles with electrochemiluminescence properties. *Chem Commun*,10, **2009**

- [43] Cao X, Wang J, Deng W, Chen J, Wang Y, Zhou J, Du P, Xu W, Wang Q, Wang Q, Yu Q, Spector M, Yu J, Xu X. Photoluminescent cationic carbon dots as efficient non-viral delivery of plasmid SOX9 and chondrogenesis of fibroblasts. *Scientific Rep.* **2018**;8,7057.
- [44] Liu C, Zhang P, Zhai X, Tian F, Li W, Yang J, Liu Y, Wang H, Wang W, Liu W. Nanocarrier for gene delivery and bioimaging based on carbon dots with PEI passivation enhanced fluorescence. *Biomaterials*,**2012**;13,3604–13.
- [45] Wang F, Xie Z, Zhang H, Liu CY, Zhang YG. Highly luminescent organosilane-functionalized carbon dots. *Adv Funct Mater*, **2011**;21,1027–31
- [46] Wei X, Xu Y, Li Y, Yin X, He X. Ultrafast synthesis of nitrogen-doped carbon dots via neutralization heat for bioimaging and sensing. *RSC Adv.* 2014;**84**,44504–8.
- [47] Anthony A. Molinero‡, Michael Enright§, and Brandi Cossairt, Preparation and Characterization of Carbon Quantum Dots And Their Application to Fingerprint Imaging,4,
- [48] Qin Hu,1 Xiaojuan Gong,2 Lizhen Liu,3 and Martin M. F. Choi1, Characterization and Analytical Separation of Fluorescent Carbon Nanodots, Miguel A. Garcia,2-16,**2017**,
- [49] S. Pandey, A. Mewada, G. Oza et al., “Synthesis and centrifugal separation of fluorescent carbon dots at room temperature,” *Nanoscience and Nanotechnology Letters*, 5, 7, 775–779, **2013**
- [50] Ramalingam Senthil, Mukund Gupta, Shahab Makda, The Synthesis and Production Challenges of Quantum Dot Based Solar Cells, *Int. J.Mech Eng.*,240, **2018**, 236–244
- [51]Ortega liebana, M C, Chung, NX,Lipens,R,Gomez L, Hueso,JL ,Santamaria, “uniform luminescent carbon nano dotes prepared by rapid pyrolysis of organic precursors confined with nanoporous templating structure,117,**2017**,437-446
- [52] J. J. Huang, Z. F. Zhong, M. Z. Rong, X. Zhou, X. D. Chen, and M. Q. Zhang, “An easy approach of preparing strongly luminescent carbon dots and their polymer based composites for enhancing solar cell efficiency,” *Carbon*,70,190–198,**2014**.
- [53] Somayeh Tajik,a Zahra Dourandish,b Kaiqiang Zhang,cd Hadi Beitollahi,Quyet Van Le,Ho Won Jang, and Mohammadreza Shokouhimehr, Carbon and graphene quantum dots: a review on syntheses, characterization, biological and sensing applications for neurotransmitter determination, *RSC Adv.*, **2020**, 10, 15406

- [54] Adil Shafi, Sayfa Bano, Suhail Sabir, Mohammad Zain Khan and Mohammed Muzibur Rahman, Eco-Friendly Fluorescent Carbon Nanodots: Characteristics and Potential Applications, *IntechOpen*, 16, 89474
- [55] Li H, Liu R, Lian S, Liu Y, Huang H, Kang Z. Near-infrared light controlled photocatalytic activity of carbon quantum dots for highly selective oxidation reaction. *Nanoscale*. **2013**;8,3289-3297
- [56] X. Guo, C.-F. Wang, Z.-Y. Yu, L. Chen, and S. Chen, "Facile access to versatile fluorescent carbon dots toward light-emitting diodes," *Chemical Communications*, 48, 21 2692– 2694, **2012**
- [57] Jun Zuo, Tao Jiang, Xiaojing Zhao, Xiaohong Xiong, Saijin Xiao, and Zhiqiang Zhu, Preparation and Application of Fluorescent Carbon Dots, Hindawi Publishing Corporation, 6-7, **2015**, 787862
- [58] Paulo, S., Palomares, E., & Martinez-Ferrero, E, Graphene and carbon quantum dot-based materials in photovoltaic devices: From synthesis to applications. *Nanomaterials*, 7-8, 157, **2016**
- [59] ] Li, W., Hendriks, K. H., Furlan, A., Wienk, M. M., & Janssen, R. A,. High quantum efficiencies in polymer solar cells at energy losses below 0.6 eV. *J Am Chem.Soc*, 137(6), 2231-2234. **2015**





# **Polymorphic Pharmaceutical Cocrystals and Its Limitations in Pharmaceutical Industry**



**A literature review submitted to the Department of Chemistry, Gauhati University in partial fulfillment of the requirements for the award of degree of Master of Science in chemistry with specialization in organic chemistry.**

**Submitted by**

**DEBASHISH DAS**

Roll number: PS-191-808-0058

Registration number: 288205 of 2016-17

M.Sc 4<sup>th</sup> Semester, Gauhati University

**Under the Supervision of**

**DR. RANJIT THAKURIA**

**Assistant Professor**

**Department of Chemistry, Gauhati University**

## **DECLARATION**

I, Debashish Das, do hereby declare that the subject matter in this literature review entitled, **“Polymorphic Pharmaceutical Cocrystals and Its Limitation in Pharmaceutical Industry”** is the result of survey of scientific literature carried out by me with full integrity, honesty and concentration under the supervision of Dr. Ranjit Thakuria, Assistant professor, Department of Chemistry, Gauhati University, in the fulfillment of project dissertation.

As a general practice of writing scientific reports, due acknowledgement has been made to all the authors whose works have been discussed in this survey and unintentional omission, if any, is highly regretted.

Date: 08/09/2021

Place: Guwahati

**Debashish Das**

M.Sc 4<sup>th</sup> semester

## **Certificate**

This is to certify that the literature survey report, entitled “**Polymorphic Pharmaceutical Cocrystals and Its Limitations in Pharmaceutical Industry**” is submitted by Debashish Das, M.sc 4<sup>th</sup> semester, Organic chemistry specialization, in partial fulfillment for the requirement of degree of Masters in Science in Chemistry. The literature survey is a bonafied work by him under my supervision and guidance.

**I wish him success in life.**

Date:

Place:

**Dr. Ranjit Thakuria**

Assistant Professor

Department of Chemistry

Gauhati University



## **Acknowledgement**

I would like to express my special appreciation to my project supervisor **Dr. Ranjit Thakuria**, Assistant Professor, Gauhati University, for his constant guidance, congenial help and unfailing support throughout my literature survey work.

My sincere thanks goes to **Dr. Chitrani Medhi**, Prof. and Head of the department, Chemistry for giving us the opportunity to do the literature survey work staying in home in this difficulty time of **COVID19 pandemic**.

I would like extend my thanks to my friends who always put their hands to help me whenever it is needed and my sincere gratitude goes to **Poonam Deka**, a research scholar as she put a lot of energy and time on completion my work.

Last, but not the least, I would like to thank my **parents, brother and sister** who have been very cooperative and supportive in my study time.

Date: 08/09/2019

Place: Guwahati

**Debashish Das**

M.Sc 4<sup>th</sup> semester

## **Contents**

	PAGE NO.
<b>1. Introduction</b>	1
1.1. What is cocrystal?	1-2
1.2. What is pharmaceutical cocrystal?	2
 <b>2. Design of Cocrystals</b>	 2-4
 <b>3. Different strategies of cocrystal formation</b>	 5
3.1. Solid-state methods	5-6
3.1.1. Contact crystallization	6
3.1.2. Solid-state grinding	6
3.1.2.1. Neat grinding	6-7
3.1.2.2. Liquid-assisted grinding	7-8
3.1.3. Hot Melt Extrusion Technique	8
3.2. Solvent-based methods	8-9
3.2.1. Solvent Evaporative crystallization	9-10
3.2.2. Slurry Crystallization	10
3.2.3. Anti-Solvent Method	10
3.2.4. Ultrasound Aided Cocrystallization	10-11
3.2.5. Cooling Crystallization	11
3.2.6. Reaction Crystallization	11
 <b>4. Physicochemical properties and application of cocrystals</b>	 11
4.1. Physical stability	11

4.1.1. Melting points	11
4.1.2. Hygroscopicity	12
4.2. Chemical stability	12
4.3. Mechanical properties	12
<b>5. Polymorphs of cocrystal showing distinct physicochemical properties</b>	12-13
<b>6. Structural studies</b>	13
6.1. Single crystal X-ray diffraction (SCXRD)	13
6.2. Powder X-ray diffraction (PXRD)	13
6.3. Fourier-Transform Infrared Spectroscopy (FTIR)	13
6.4. Thermal Gravimetry Method	13
<b>7. Conclusion and Future Outlook</b>	14-15
<b>8. References</b>	15-19

## 1. Introduction

Why only less than 1% active pharmaceutical compounds come out in the marketplace? It is not due to the toxicity but it is because of the poor biopharmaceutical properties.<sup>1</sup> Poor water solubility and low oral bioavailability of an active pharmaceutical ingredient (API) are the major restrictions during the development of new drugs.<sup>2</sup> The Supramolecular chemistry is the entities of organization that results from the association of two or more chemical species held together by non-covalent interactions.<sup>3</sup> The idea of cocrystal engineering is the knowledge of intermolecular interactions in crystal packing and in the implementation of such process to design the new solids with enhanced physical and chemical properties. The most important issue from the pharmaceutical point of view is to improve the properties such as solubility, stability, dissolution rates, hygroscopicity, mechanical properties, bioavailability etc. of a drug.<sup>4</sup> Among these, solubility and dissolution rate plays an important rule to determine the activity and efficacy of a drug.<sup>5</sup> Physical modification often aims to increase the particle surface area, improve solubility or wetting of powder and improving the stability of an API. To overcome the conventional drug discovery which were only based on the traditional remedies or coincidental discoveries, there has been a growing interest in pharmaceutical cocrystals.<sup>6</sup> The main aim of discovery of pharmaceutical cocrystals is to obtain a drug with optimal physicochemical, pharmaceutical and biological properties.

### 1.1 What is co-crystal?

There is currently some debate to the definition of a cocrystal. Most literature agrees that a cocrystal is a crystalline structure, composed of at least two components.<sup>7</sup> According to the definition of US Food and Drug Administration (FDA), crystalline materials composed of at least two different neutral components that are solid under ambient conditions present in definite stoichiometric amounts.<sup>8, 9, 10</sup> FDA's definition of cocrystal would be much more restrictive than any other definitions currently used by scientific community. Further this definition could be hazy since every molecular crystal must be defined as having two or more molecules in the crystal lattice in order to exhibit repeating rearrangement of molecules that define crystal. There were a lot of arguments pointed by a number of publications on this definition. A recent perspective authored by a group of scientists aimed to come to consensus on the exact definition of a cocrystal. According to their viewpoint, the solids that are in crystalline form having single phase comprised of two or more different molecular or ionic compounds in a definite stoichiometric ratio which are either solvates or a simple salt are defined as cocrystal. As per literature, quinhydrone was the first cocrystal synthesized, which is mixture of benzoquinone and hydroquinone in 1:1 ratio.<sup>11, 12</sup>

Polymorph refers to the different crystalline forms of a same chemical compound.<sup>13</sup> Polymorphism provides an opportunity to study about the structure-properties relationship of the same compound in different supramolecular environment. It is important to investigate the polymorphic behavior of an active pharmaceutical ingredient in the process of drug

development.<sup>13</sup> There are more than 50% drugs available in market exist as polymorphic. Therefore, study about polymorphic cocrystal attains a lot of interest in recent time. It is important to mention that a cocrystal is different in definition from a pharmaceutical cocrystal.

## **1.2 Pharmaceutical cocrystals**

Pharmaceutical co-crystal is simply a cocrystal in which at least one of the cocrystal components acts as an active pharmaceutical ingredient (API) in conjunction with another component which is called a coformer. It is useful to mention that the non-API part should be a non-toxic compound which has no adverse side effects.<sup>14</sup> The API and the coformer interact via non-covalent bonding such as ionic interactions, hydrogen bonding, and Vander Waals interactions. In the cocrystal synthesis, the selection of coformer which is compatible with particular active pharmaceutical ingredients is one of the main challenges to be handling with care.

## **2. Design of cocrystals**

The design and prediction of new crystals are typically performed using the concept of supramolecular synthons and crystal engineering principles.<sup>15</sup> The principle is generally applied to select an appropriate coformer to form a cocrystal with the active compound in order to enhance the physical and chemical properties.<sup>16</sup> A common strategy is to investigate the crystal structure of the target compound and to evaluate which non-covalent interactions could aid in the formation of new supramolecular synthons between the APIs and coformers.<sup>17</sup> Besides this, the ability of an API to cocrystallize in the presence of a coformer depends on some controlling parameters such as the stoichiometry ratio (API/coformer) i.e. the composition of the cocrystal components, the solvent employed for cocrystallization, temperature, the crystallization techniques and the solubility of the components. Usually, an API is more prone to cocrystallize when possessing donor and acceptor sites able to form reliable hydrogen bonding (supramolecular synthons) with the coformer. The selection of an appropriate coformer is done mainly on the basis of hydrogen bond propensities, molecular recognition, etc. Identification of complementary sites of an API and coformer that can form hydrogen bonds is the approach one should follow for the design and synthesis of pharmaceutical cocrystal.<sup>18</sup>

During the experimental process, one cannot ensure that the formation of desired polymorphs will take place. Different possible outcomes are there in a cocrystal experiment. The formation of a single crystal component is the undesirable outcome if cocrystal formation is the desired target. In the cocrystallization process, sometimes serendipitous discovery includes the formation of new polymorphs provides an advantage in expanding the diversity of solid forms and providing patent life protection. For example, the result of a serendipitous discovery of novel polymorphs of a single crystal during the crystallization of aspirin, curcumin, and nicotinamide (NCT).<sup>19</sup> In addition to this, in an attempted cocrystallization process the formation of hydrates and solvates of a cocrystal is not uncommon. Recently, a lot of such alternative solids have been reported. Solid solutions and eutectics are the two other outcomes in the process of cocrystallization. Solid

solutions are formed between the materials that are isomorphous or isostructural; eutectics are formed between the non-isomorphous materials.

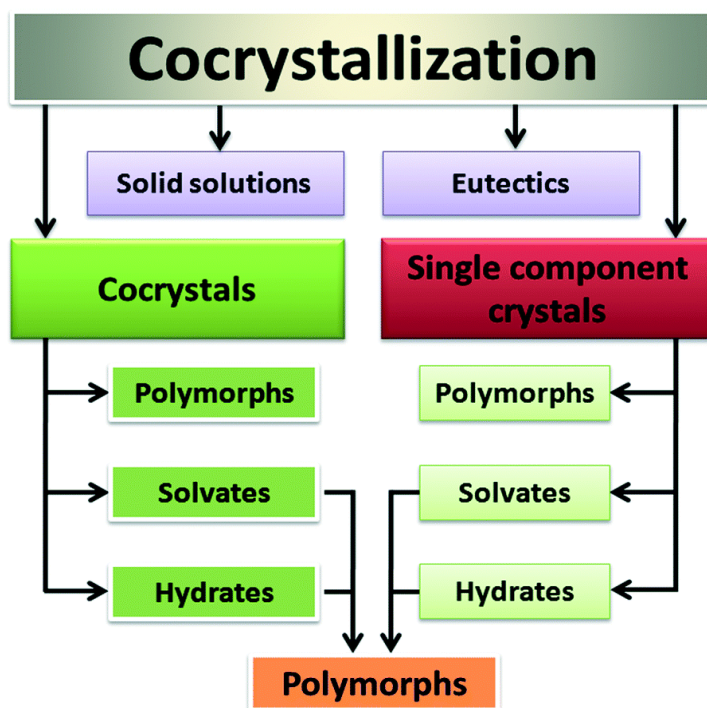


**Figure 1.** Various possible outcomes of an attempted cocrystallization experiment<sup>19</sup>

Different theoretical approaches have been employed such as hydrogen bonding propensity, Cambridge Structure Database (CSD), supramolecular synthons, pKa values and Hansen solubility parameters to know the exact mechanism of cocrystal formation. Cocrystals design is based on the principle of the supramolecular synthesis which provides a strong approach for the discovery of novel pharmaceutical solid forms. For the rapid success of cocrystallization, it is important to highlight the two most significant reasons as a method of constructing advanced materials are (i) the supramolecular synthons that form cocrystals following a simple design (ii) the management and improvement of the design can exchange of cocrystal components with the intention of improving a particular solid-state property.<sup>20</sup>

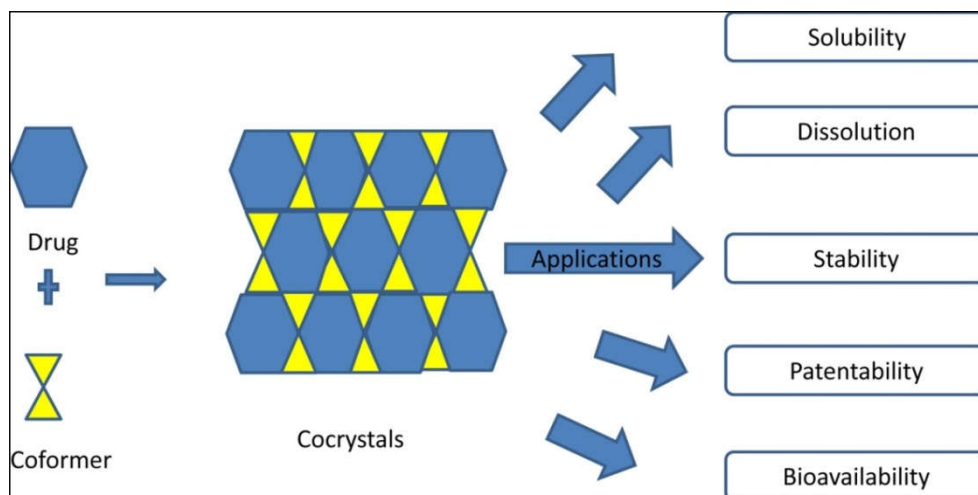


**Figure 2.** Cocystal formation and its application.<sup>20</sup>

In cocrystals, drug and coformers interact with each other by non-covalent interactions such as vander waals forces, hydrogen bonding, or  $\Pi$ - $\Pi$  stacking interactions.<sup>20</sup> Hydrogen bonding is the main interaction and is responsible for the cocrystals formation. The interaction is in between the functional groups present on an API and the functional groups present on the coformers and finally they will lead to the formation of cocrystal. The common functional groups of API and coformers are carboxylic acids, amides and alcohols. The most common supramolecular synthons in the Crystal Engineering are Homosynthons,<sup>21</sup> formed between two same functional group, e.g. carboxylic acid dimers, amide dimers, and hydroxyl dimers, whereas heterosynthon are formed between two different functional groups, e.g. carboxylic acid and amide group,<sup>22</sup> carboxylic acid and aromatic nitrogen (pyridine), hydroxyl and cyano group, alcohol and ether group, carboxylic acid and hydroxyl group, hydroxyl and aromatic nitrogen (pyridine) in hydrogen bond formation. Hydrogen bonding is involved in which the functional groups having all good proton donors and acceptor.<sup>23</sup>

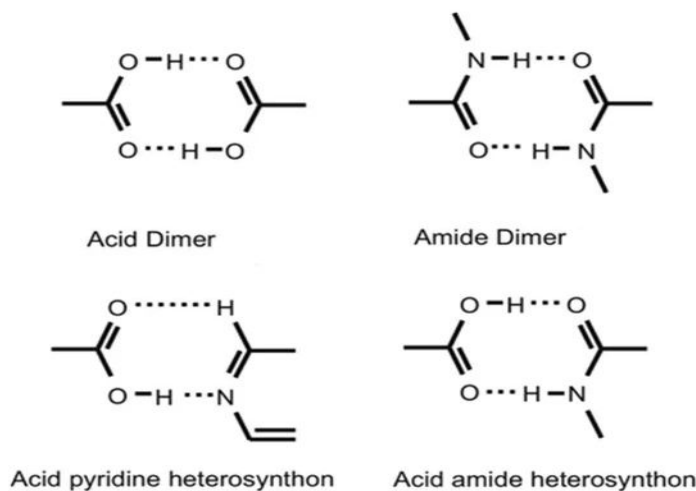


**Figure 3.** Homosynthon dimers and heterosynthesis dimers.<sup>24, 25</sup>

### 3. Different strategies of cocrystal formation

To date, a large number of methods have been recognized for the preparation of cocrystal. Solid-based methods and solution-based methods are the most widely used methods for the cocrystallization process. Different kinds of strategies such as solid-state grinding, slurry conversion, crystallization technique, anti-solvent addition, solvent evaporation, reaction crystallization methodology have been employed for the cocrystal formation. Recently, some new strategies are being used for the formation of cocrystals, such as area unit ultrasound aided methodology, the critical fluid atomization technique, spray-drying technique and the hot soften extrusion technique have begun to appear. However, the selection of an appropriate cocrystallization method is a challenging work.

In solution-based methods, for dissolving the cocrystal components high solvent consumption is required. The choice of solvents can affect the results of cocrystallization, because solvent can change the intermolecular interactions between API and coformer. Conversely, solid-state methods offer the potential to eliminate the requirement of using solvent in cocrystal formation whether no or less solvent may require.

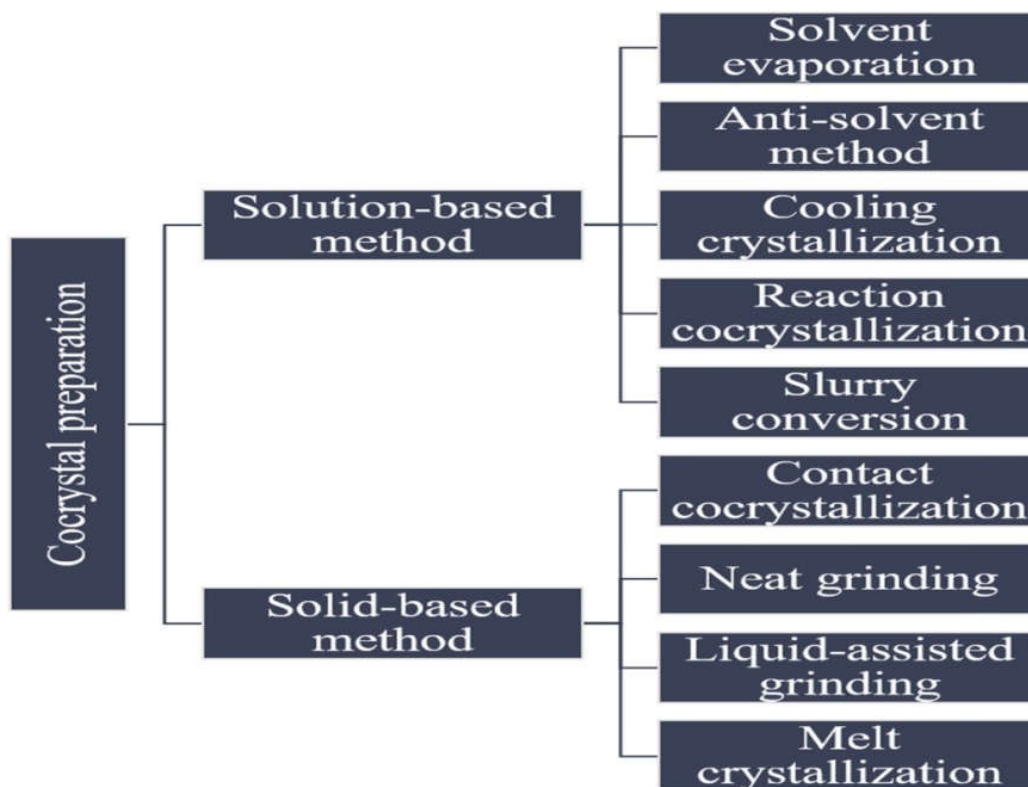


**Figure 4.** Common methods of cocrystal preparation.<sup>26</sup>



### 3.1. Solid-state methods

The solid-state formation of pharmaceutical cocrystals has gained significant interest over the last few years due to the advantages associated with these processes. Solid state crystallization methods are very effective and environmentally friendly in cocrystal formation as they need no solvent or very little solvent. The cocrystal forms through direct contact or grinding with higher energy inputs. It generally includes solid phase grinding, melt extrusion, and sonication from 80 to 85°C. In this method, the cocrystal components are melted and mixed in a fixed stoichiometric ratio, resulting in the formation of the cocrystal. The mechanism of cocrystallization in the presence of moisture at deliquescent conditions usually consists of three stages: (a) moisture uptake, (b) dissolution of reactants, and (c) cocrystal nucleation and growth.<sup>28</sup>

#### 3.1.1. Contact cocrystallization

The interactions between API and coformer could occur after soft mixing of the starting materials.<sup>29</sup> The possible mechanisms explaining spontaneous crystallization by contact are vapor diffusion of two solids, eutectic phase formation, moisture sorption, long-range anisotropic molecular migration.<sup>30</sup> Higher temperature, higher humidity and smaller particle sizes of raw materials could enhance the cocrystal formation. MacFhionnghaile et al. reported that caffeine-urea cocrystals were formed within three days by mixing separately premilling raw materials at 30% relative humidity and at room temperature.<sup>31</sup> It was explained that the key factor for the formation of caffeine-urea cocrystals was the interparticle surface contact between the solids. The phase transformation of theophylline-nicotinamide mixture to cocrystal formation was conducted without the assistance of any mechanical grinding was demonstrated by Ervasti et al.<sup>32</sup>

#### 3.1.2. Solid State Grinding

The solid-state grinding methods are widely used to generate cocrystal powder samples. In this method, the constituents of a cocrystal are ground together resulting in the generation of fine powder having higher surface area which increases the diffusion rate of the cocrystals. Two formats are accomplished in this method: neat or dry grinding and liquid-assisted grinding. Neat grinding is a cocrystallization method that is performed without a solvent. The method need some energy put in to form the cocrystal by manual grinding or by mechanical milling. The solid materials that will result in the cocrystal are mixed in appropriate stoichiometric amounts, pressed and crushed together with a mortar, and pestle, or a ball mill or a vibrator mill.<sup>32</sup>

With this method, numerous cocrystals can be prepared, and any failure of cocrystal formation is commonly due to the use of improper settings or non-stoichiometric ratio of constituents used. Reducing the particle size increases the specific surface area of interaction between the materials for the formation of intermolecular bonds.

### 3.1.2.1. Neat grinding

It is already demonstrated that the active potential mechanisms of cocrystal formation by neat grinding method include molecular diffusion and the formation of a eutectic and the transient amorphous intermediate. A mobile solid surface is created by grinding which causes the energy transfer or vaporization. So, high vapor pressure ( $10^{-1}$  to  $10^{-4}$  mm Hg) of the solid components is necessary in the neat grinding process. Hence, cocrystals can be formed on the crystal surface due to gas phase diffusion. Further, grinding can offer energy for surface diffusion and migration to remove the generated cocrystal from the reactant surface to create a fresh surface for more cocrystallization. Rastogi et al.<sup>33</sup> were able to found the cocrystal forming from the mixture picric acid and aromatic hydrocarbons by molecular diffusion with the help grinding.

### 3.1.2.2. Liquid-assisted grinding (LAG)

LAG method is a useful method for generating the cocrystal products with high yields and high crystallinity as compared to neat grinding. This technique is a modification of neat grinding method. The method is good for rapid cocrystal screening, which is independent of the solubility of the raw materials. In this method a small amount of liquid is being added to increase the molecular diffusion, for accelerating the cocrystal formation.<sup>34</sup> The effect of the solvent can be described as catalytic, because very small amount of liquid is needed and is not a part of the final product. The formation of solid products and the quality of crystals depends on the amount of liquid taken and the selection of liquid.

Its advantages lie in its increased performance, in the ability to control the production of polymorphs, and in the improved crystallinity of the product, while a large number of coformers are suitable for this cocrystallization. This method enhances the cocrystallization rate, as some cocrystals showed poor performance in cocrystal formation following neat grinding for a considerable amount of time. This method can be used to prepare high-purity cocrystals with a significant reduction in the preparation time.<sup>35</sup> It also allows the synthesis of selective polymorphic forms of cocrystals. This allows interconversion between crystalline forms of polymorphic organic components, according to polarity of the solvent. Limitations of liquid-assisting grinding include the fact that it is a small-scale technique, requires high energy consumption, and has a low performance in terms of product purity. Fischer et al.<sup>36</sup> Investigated the effect of solvent properties on 1:1 caffeine-anthranilic acid cocrystal polymorphs and observe that the formation of form I appeared in the most of solvents and form II was found only in solvents with high polarity such as of carbonyl or nitrile groups. The coordination of solvent molecules with the amino group of anthranilic acid led to the torsion of the caffeine at the amino-carbonyl hydrogen bond, thus form II with zigzag structure was formed rather than form I with a planar structure. It was explained that the solvent molecules occupied many sites so that the interaction between caffeine molecules and the amino group of anthranilic acid could not take place in the same planar layer, causing caffeine twisting at around  $30^\circ$ .

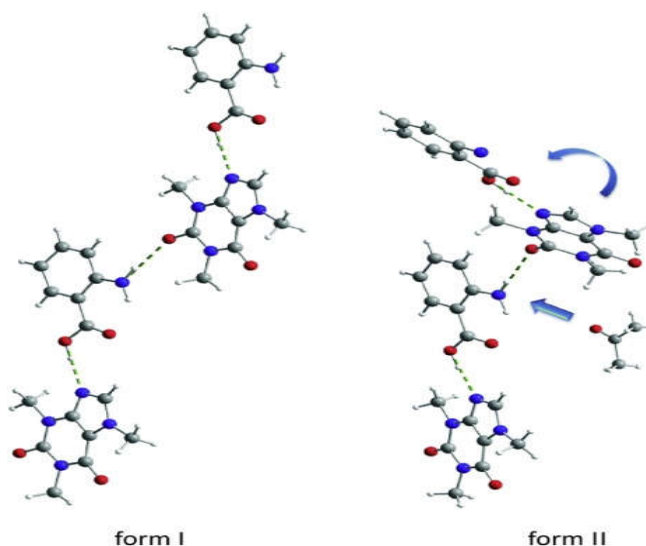


**Figure 5.** Crystal structure of caffeine-anthranilic acid.<sup>36</sup>

### 3.1.3. Hot Melt Extrusion Technique

Hot-Melt Extrusion (HME) is a simpler method that combines cocrystal formation and drug formulation process, provide a simpler way to manufacture a drug product. It can be consider as green approach for the synthesis of pharmaceutical cocrystal. In the Hot Melt Extrusion (HME) technique, the unit area of cocrystal is prepared by heating the constituents with intense energy which improved the surface interactions without using any solvent. Specific temperature is used for heating in the method so that only the desired matrix is softened and melted. Cocrystal formation using HME method requires a catalyzing agent to improve the product formation played by softened or melted matrix. Suitable matrices for HME method must have some common qualities; (a) have low glass transition (T<sub>g</sub>) temperature, lower than melting point of cocrystal to ensure a lower processing temperature, (b) have limited non-covalent interaction with drug or conformer, (c) exhibit a rapid solidification step. The disadvantage of this methodology is that each coformer and API is not compatible with the liquefied kind and cannot be used for unstable medicine. Melatonin-pimelic acid cocrystals were synthesized in this process by Yan et al.<sup>37</sup> When molten mixture of melatonin and pimelic acid were put in the temperature range of 50-70°C, the melatonin-pimelic acid cocrystals were formed. The carbamazepine-nicotinamide cocrystal was synthesized by melting the mixture of drug and coformer at 160°C and then cooling the mixture to the ambient temperature for crystal growth.<sup>38</sup>

### 3.2. Solvent-based methods

There are a large number of methods working with solvent for cocrystallization. In these methods the major driving force for cocrystallization is the supersaturation of the mixture. There are ternary phases in the solution (API, coformer and solvent) and the perfect state is that the cocrystals are supersaturated while the reactants (API and coformer) are saturated or undersaturated under the experimental conditions. The degree of supersaturation with respect to

solution is the key parameter for cocrystallization and can be adjusted by the concentration of API and coformer.<sup>39</sup> The thermodynamic stability of the ternary phase must be established by a phase diagram which gives a proper guide for the cocrystal formation.

The figure shows the ternary phase diagram, which describes how to find the supersaturation of cocrystals, when the reactants are in a saturated or unsaturated state. In figure (a) similar solubilities between reactant A and B and saturated in the solvent, thus cocrystal can be formed in an equivalent reactant concentration. In figure (b) reactants have different solubilities saturated with solvents, in which cocrystal can be formed by nonequivalent reactant concentrations to reach the cocrystal stable region.<sup>40</sup>

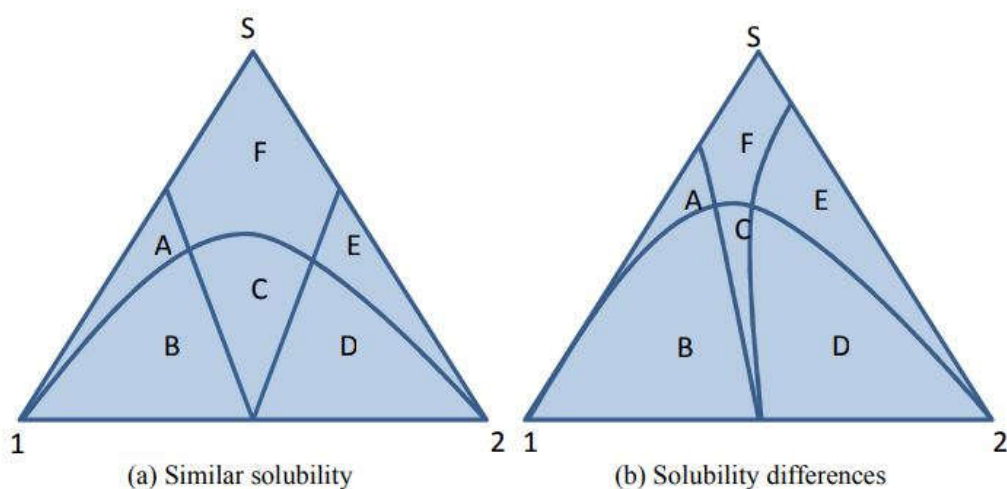


**Figure 6.** Schematic representation of isothermal ternary phase diagram: (a) similar solubilities of reactant 1 and 2 in solvent; (b) different solubilities of reactant 1 and 2 in solvent. In region 1) component A and solvent; in region 2) 1 and cocrystal: In region 3) Cocrystal: In region 4) mixture of 2 and cocrystal: In region 5) 2 and solvent and in region 6) solution.<sup>40</sup>

### 3.2.1. Solvent Evaporative Cocrystallization

Solvent evaporative cocrystallization is the most frequently used method of generating cocrystals, particularly used for single cocrystal formation which can be easily analyzed by single crystal X-ray diffraction. It is the most commonly used technique in the field of cocrystallization typically applied for high quality single crystal synthesis. In this technique, stoichiometric amounts of the cocrystal components are dissolved in a suitable solvent of appropriate ratio and then evaporate the solvent to obtain the cocrystal.<sup>41</sup> In this process, cocrystallization depends on the selection of solvents, which impacts the solubility of the reactants. The cocrystal components should be soluble in the solvent used. If two incongruently soluble components are involved in the cocrystallization process, then the less soluble component precipitates preferentially, resulting in the formation of a solid mixture of cocrystal or a failure of forming cocrystals. The principle is based on when different molecules having

complementary functional groups can form hydrogen bonds with each other that are more favorable than each of the individual molecular components; the product formed is thermodynamically more favored. A lot of cocrystals have already been synthesized by solvent evaporation methods.<sup>42</sup> For example, a block-shaped single crystal of a 1:1 febuxostat-piroxicam cocrystal, which interacted through carboxylic acid-azole synthons, was prepared by slow evaporation of acetonitrile at room temperature for 3-5 days. The cocrystal formed having higher solubility and better tableability than the parent components.<sup>43</sup>

### **3.2.2. Slurry Crystallization**

The solution-mediated phase transformation process known as the slurry conversion method involves the addition of excess components of cocrystal to the solvent in order to form the suspension of raw materials. During the formation of suspension, the components dissolve gradually and start forming complex. The reactant concentrations are decreased during the formation of cocrystal and lead to undersaturation. The ternary phase diagram controls the operational range of components concentration and temperature, which guides for attaining the supersaturation phase of cocrystal. The solvent is pouring out and then the solid material is dried under a flow of nitrogen for 5 min and can be characterized by using powder X-ray diffraction. This methodology is used for the preparation of cocrystals once the drug and coformer are stable within the solvent.

### **3.2.3. Anti-Solvent Method**

The method has been considered an effective approach to control the particle sizes, quality and properties of cocrystals. The Anti-solvent method also known as vapor diffusion is the method in which antisolvent is used for the synthesis of high quality cocrystals. In this method, a solvent in which the compound is less soluble is often added to another solution, favoring the precipitation of the solids. During this process, supersaturation is generated by adding a second liquid to a solution of the drug-coformer to be crystallized, which is miscible with the solvent and in which the cocrystals are insoluble or sparingly soluble. The resulting suspension is filtered, and the collected solid can be characterized by PXRD. Disadvantages of this method are its lower performance as compared to grinding as well as the large volume of solvent required. By this method, cocrystals of iodomethacin-saccharin were synthesized by Chun et al.<sup>44</sup>

### **3.2.4. Ultrasound Aided Cocrystallization**

Ultrasound aided cocrystallization or sonocrystallisation is another liquid assisted technology that has been employed for the synthesis of nano cocrystals. In this technique drug and coformers are dissolved in an appropriate solvent. Cold water is passing throughout the sonication process to take care of the constant temperature of the sonicator and forestall fragmentation. The energy that is imparted to the sample during irradiation causes a rapid rise in temperature in a short period of time, which leads to melting of crystalline material, followed by material mixing and then rapid recrystallization upon cooling. One proposed condition for the coformer material

which can be used for this method is that the coformer must be in sublimable condition in order to support a nucleation process through the vapor phase. Pure cocrystals were obtained by using this methodology.

### **3.2.5. Cooling crystallization**

Cooling crystallization involves varying the temperature of the crystallization system which has recently attracted much more attention for potential of a large scale of cocrystal production. First a large amount of reactants and solvents are mixed in a reactor typically a jacketed vessel and then the system is heated to higher temperature to make sure all solutes dissolved in the solvent and is followed by a cooling down step. Cocrystal will precipitate when solution become supersaturated with respect to cocrystal as the temperature drops down.

### **3.2.6. Reaction Crystallization**

Reaction crystallization is suitable for cocrystal formation when the cocrystal components possess different solubilities; the reactants with nonstoichiometric concentrations are mixed to generate supersaturated solutions of cocrystal, leading to cocrystal precipitation. In this method, the nucleation and growth of cocrystals are controlled by the ability of reactants to decrease the solubility of cocrystals.

## **4. Physicochemical properties and application of cocrystals**

### **4.1. Physical stability**

Physical change is the change in the state of the substance without any change in the chemical composition of the substance. Physical properties of the solid state materials include melting point, hygroscopicity, solubility, hardness, plasticity, elasticity etc.<sup>45</sup> Cocrystallization is a powerful approach for improving the physical properties and maintaining the physical stability of drug substance.

#### **4.1.1. Melting Points**

Solid forms of drugs provide a convenient way to purify, identify, transport and store. Solid forms of drugs are more convenient to administration than liquid drugs. However some drugs exist as liquid at room temperature due to their low melting points. Cocrystallization has the potential to alter the melting points of liquid drugs by incorporating a suitable coformer into the crystalline lattices.

#### **4.1.2. Hygroscopicity**

The hygroscopicity of a drug must be thoroughly investigated because it could impact the physicochemical properties, e.g. solubility, dissolution rate, stability, bioavailability and mechanical properties. Maintaining the hygroscopic stability of the anhydrous form is one of the

major challenges during drug development. Several strategies have been applied to tackle this challenge, including applying proper packing for reducing moisture uptake or coating the drug product by enteric polymers. Some studies have demonstrated that cocrystal formation could improve the hygroscopic stability of the drugs.

#### **4.2. Chemical stability**

Chemical degradation of drug substances tends to occur during the manufacturing and storage stages, which challenges the development of a stable pharmaceutical formation. It is critical to develop an effective strategy to eliminate or minimize drug degradants. Recently, pharmaceutical cocrystals have emerged as a prospective approach to overcome the chemical instability of APIs in the solid state. Chemical stability involves the mechanisms by which cocrystallization solves the problem of chemical degradation through changing the crystal packing of APIs.

#### **4.3. Mechanical properties**

The mechanical properties of crystalline materials are critical attributes to various manufacturing processes of solid dosage forms, such as blending, milling, granulation, tableting and coating. For solid materials, the mechanism of mechanical deformation consist of elastic, plastic, viscoelastic and fragmentation. Generally, materials with better plasticity properties could exhibit superior compressibility.

### **5. Polymorphs of cocrystal showing distinct physicochemical properties**

As it has been already documented that polymorphism can change the properties of materials. It is well known to impact the properties such as stability, solubility, dissolution rates, bioavailability, mechanical properties, etc. It is always expected that the change in the crystal structure of a cocrystal may lead to specific changes in the performances of the cocrystals. Recently, polymorphs of sulphonamide antibiotic, SACT and ACT have been reported by Goud and Nangia. Crystal structure analysis has confirmed that the two polymorphs have the hydrogen bonding,  $\text{N-H} \cdots \text{O}_{\text{sulfonamide}}$   $\text{N-H} \cdots \text{O}_{\text{carbonyl}}$ <sup>46</sup> The dissolution studies confirmed that the dissolution rate of form **I** and form **II** of SACT-ACT are 1.6 times and 1.3 times faster than the dissolution SACT in aqueous buffer solution at P<sup>H</sup> 7.

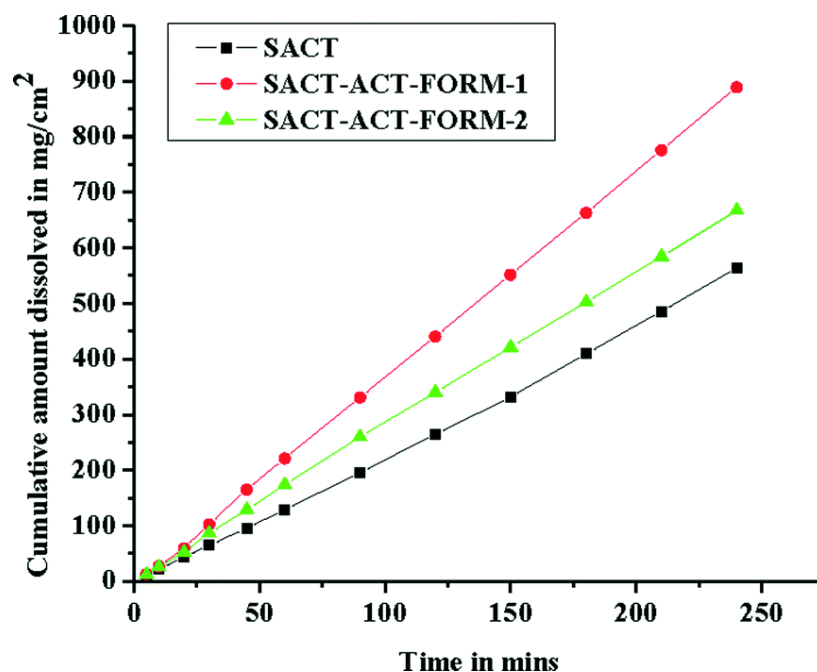


**Figure 7.** Comparison of dissolution rates of SACT and SACT-ACT polymorphs at P<sup>H</sup> 7 buffer medium.<sup>46</sup>

Polymorphism brings stability to caffeine with respect to humidity. Generally caffeine is unstable with respect to humidity, which forms crystalline hydrate. Trask et al. have reported the two polymorphs of cocrystal of caffeine with glutaric acid show different physical stability at elevated humidity conditions. Form II shows higher resistance to hydration under high RH conditions, whereas form II converts to form I at low RH and completely to caffeine hydrate at high RH conditions.<sup>47, 48</sup>

## 6. Structural studies

The physicochemical properties of cocrystal can generally be characterized by crystallographic studies.

### 6.1. Single crystal X-ray diffraction (SCXRD)

Single crystal X-ray diffraction is the most preferable technique to obtain information about molecular recognitions, hydrogen bonding patterns, assembly and packing of pharmaceutical cocrystals. It is known as gold standard technique in terms of cocrystal characterization. SCXRD is an excellent technique to make distinction between formation of cocrystal, multi component salts and salt-cocrystal continuum forms. It not only gives information about the crystal structure but also it gives the 3D representation of the crystal with the elucidation of supramolecular synthons. Single crystal X-ray diffraction is based on the diffraction of X-ray from the electron density of the cocrystal and hence it is relatively insensitive to the cocrystal forming from less electron density atom. In most of the cases obtaining suitable single crystals for X-ray diffraction



is not easy, so other analytical techniques must be used to gain information about the formation of cocrystals. Among these other techniques for characterization of cocrystal, Powder X-ray diffraction (PXRD) is extensively used for characterization of different multi component solid forms: cocrystal or salts, eutectic or solid mixtures, coamorphous, allowing understanding the structural properties of this materials.<sup>49</sup>

## **6.2. Powder X-ray diffraction**

As single crystal X-ray diffraction gives information only for the single crystal component, and so it is good to practice to elucidate the solid that are formed from the bulk materials by using PXRD. For drug design and structure based functional studies to aid the development of therapeutic agents and medicines, the knowledge of exact molecular structure is the pre-requisite demand. To characterize an active pharmaceutical ingredient (API), it is important to establish the crystal structures of the API; SCXRD is a traditionally used technique for this purpose. But because of simplicity in the performance of PXRD, it is the predominant tool for study and characterization of polycrystalline API forms. Distinct PXRD pattern correspond to different crystal structures so it is considered as fingerprints of specific crystal phases.<sup>50</sup>

It follows that the PXRD analysis can detect phase transitions between polymorphs of same APIs or distinguishes between cocrystal and corresponding salt phases, which differ due to proton transfers in intermolecular hydrogen bonding.

## **6.3. Fourier-Transform Infrared Spectroscopy (FTIR)**

In addition to crystallographic methods, the spectroscopic data can also provide the characteristic fingerprint of a particular group present in the cocrystal. As cocrystals, salts, solvates and polymorphs are solid chemical substances, so they can be studied by solid-state spectroscopic methods. Vibrational spectroscopy is one of the methods primarily used for this purpose as it depends on the vibrational modes of the bonds present in the solid state environment. It can be used for the prediction and determination of chemical conformation, intermolecular interactions between API and coformers. FTIR works in the microwave ranges of wavelength  $400\text{--}4000\text{cm}^{-1}$ . Analysis of the API, coformers, and cocrystals has been performed in this range. It is always a powerful tool to distinguish cocrystal from salts, as a functional group gives a different stretching frequency than its salt form. For example, a neutral carboxylic group has a strong carbonyl( $\text{C}=\text{O}$ ) stretching peak at around  $1700\text{cm}^{-1}$  and a weak C-O stretching peak at around  $1200\text{cm}^{-1}$ . If deprotonation occurs then carboxyl group will convert to carboxylate anion which has only a single C-O stretch in the fingerprint region.

## **6.4 Differential Scanning Calorimetry (DSC) and Thermal Gravimetry Analysis (TGA)**

DSC technique compares the power needed to maintain the sample and reference at a temperature. The technique is used in detecting the phase changes that do not involve in the mass change. DSC gives an accurate value for melting point temperature and thermal data such as

enthalpy of melting; glass temperature. DSC data is useful in constructing energy-temperature relationship. The technique TGA records mass loss of sample during heating. TGA method is used for determining the decomposition temperature of cocrystals. Stoichiometry can be confirmed by measuring the loss of volatile components in this method. Prediction of crystal purity, solvates/hydrates forms of cocrystals, thermal stability and compatibility can be possible with thermal gravimetry method.

## 7. Conclusion and Future Outlook

Pharmaceutical cocrystals have become an important solid form in pharmaceuticals industry. It is evident from a number of research papers, review articles published in various journals that a cocrystal enhances the stability of parent drugs. From the industrial point of view the number of patent file throughout the world by various research group and pharmaceutical industries are increasing at a faster rate. Cocrystals are an excellent alternative for drug development in order to enhance stability, solubility, bioavailability and, processability. However, several challenges are still being faced by the researchers, including coformer selection, physicochemical characterization and formulation. Careful drug conformer screening and formulation design can lead to a successful cocrystal development. A wide range of technologies applied for the experimental screening, synthesis and manufacture of pharmaceutical cocrystals in order to overcome poor physical properties of APIs is already mentioned in this review.

During early development, cocrystallization processes mainly were focused on traditional methods, such as solvent evaporation, grinding and slurry method. However, as time has gone and the field has progressed, scientist in this field have developed newer methods which are increasingly simple to enable the cocrystallization processes to overcome their previous limitations. Novel methods that can be used for cocrystallization are hot melt extrusion, spray drying, supercritical fluid technology, laser irradiation, etc.

## 8. References

- [1] Qiao, N.; Li, M.; Malek, N.; Davies, A.; Pharmaceutical cocrystals: An Overview. *Int. J. Pharm.***2011**, *419*, 1-11.
- [2] Nanda, A.; Kumar, S.; Pharmaceutical Cocrystals: An Overview. *Ind J. Pharm. Sci.***2017**, *79*, 858-871.
- [3] Gadade, D. D.; Pekamwar, S. S.; Pharmaceutical Cocrystals: Regulatory and Strategic Aspects, Design and Development. *Adv. Pharm. Bull.***2016**, *6*, 479-494.
- [4] Aitipamula, S.; Chow, P. S.; Tan, R. B. H. Polymorphism in cocrystals: a review and assesment of its significance. *CrystEngComm.***2014**, *16*, 3451-3465.
- [5] Vioglio, P. C.; Chierotti, M.R.; Gobetto, R.; Pharmaceutical aspects of salt and cocrystal forms of APIs and characterization challenges. *Adv. Drug Deliv. Rev.***2017**, *117*, 86-110.

- [6] Schultheiss, N.; Newman, A.; Pharmaceutical cocrystals and their physicochemical properties. *Cryst. Growth. Des.***2009**, *9*, 2950-2967.
- [7] Aakeröy, C. B.; Salmon, D. J.; Building co-crystals with molecular sense and supramolecular sensibility. *CrystEngComm***2005**, *7*, 439-448.
- [8] Lindeman, J. A.; Patents and the US FDA's definition of 'cocrystal': an ordinary and customary meaning?. *Pharm. Pat. Analyst***2012**, *1*, 513-515.
- [9] Bond, A. D.; What is a co-crystal? *CrystEngComm***2007**, *9*, 833-834.
- [10] Bhogala, B. R.; Nangia, A.; Ternary and quaternary co-crystals of 1,3-cis,5-cis-cyclohexanetricarboxylic acid and 4,4'-bipyridines. *New J. Chem.***2008**, *32*, 800-807.
- [11] Brittain, H.G. Cocrystal systems of pharmaceutical interest. *Cryst. Growth Des.***2011**, *12*, 1046-1054.
- [12] Jones, W.; Motherwell, W.S.; Trask, A.V. Pharmaceutical cocrystals: An emerging approach to physical property enhancement. *MRS Bull.***2006**, *31*, 875-879.
- [13] Bernstein, J.; Polymorphism in Molecular Crystals, Clarendon. *Oxford***2002**.
- [14] Shaikh, R.; Singh, R.; Walker, G. M.; Croker, D. M.; Pharmaceutical Cocrystal Drug Products: An Outlook on Product Development. *Trends in Pharm. Sci.***2018**, *39*, 1033-1048.
- [15] Desiraju, G. R.; Crystal and co-crystal. *CrystEngComm***2003**, *5*, 466-467.
- [16] Zhang, S.; Rasmuson, A. C.; Thermodynamics and Crystallization of the Theophylline-Glutaric Acid Cocrystal. *Cryst. Growth. Des.***2013**, *13*, 3, 1153-1161.
- [17] Kavanagh, O. N.; Croker, D. M.; Walker, G. M.; Zaworotko, M. J.; Pharmaceutical cocrystals: from serendipity to design to application. *Drug Discov. Today***2019**, *24*, 796-804.
- [18] Perlovich, G. L.; Manin, A.; Design of pharmaceutical cocrystals for drug solubility improvement. *Russ. J. Gen. Chem.***2014**, *2*, 84, 407-414.
- [19] Aitipamula, S.; Chow, P.S.; Tan, R. B. H.; Pharmaceutical cocrystals of ethebamide: structural, solubility and dissolution studies. *CrystEngComm***2012**, *14*, 8515-8524.
- [20] Anand, R.; Kumar, A.; Nanda, A.; Pharmaceutical Co-Crystals - Design, Development and Applications. *Drug Deliv. Lett.***2020**, *10*, 169-184.
- [21] Shattock, T. R.; Arora, K. K.; Vishweshwar, P.; Zaworotko, M. J.; Hierarchy of supramolecular synthons: persistent carboxylic acid...pyridine hydrogen bonds in cocrystals that also contain a hydroxyl moiety. *Cryst. Growth. Des.***2008**, *8*, 4533-4545.

- [22] Walsh, R.D.B.; Bradner, M. W.; Fleischman, A. S.; Morales, L. A.; Zaworotko, M. J.; Crystal engineering of the composition of pharmaceutical phases. *Chem. Comm.***2003**, 9, 186-187.
- [23] Goud, N. R.; Nangia, A.; Synthon polymorphs of sulfacetamide–acetamide cocrystal based on N–H $\cdots$ O=S and N–H $\cdots$ O=C hydrogen bonding. *CrystEngComm*.**2013**, 15, 7456-7461.
- [24] Karagianni, A.; Malamataris, M.; Kachrimanis, K.; Pharmaceutical Cocrystals: New Solid Phase Modification Approaches for the Formulation of APIs. *Pharmaceutics*.**2018**, 10, 18, 133-146.
- [25] Reddy, L. S.; Nangia, A.; Lynch, V. M.; Phenylperfluorophenyl synthon mediated cocrystallization of carboxylic acids and amides. *Cryst. Growth. Des.***2004**, 4, 89-94.
- [26] Blagden, N.; Berry, D.J.; Parkin, A.; Javed, H.; Ibrahim, A.; Gavan, P.T.; De Matos, L. L.; Seaton, C. C.; Current directions in co-crystal growth. *New J. Chem.***2008**, 32, 1659-1672.
- [27] Guo, M.; Sun, X.; Chen, J.; Cai, T.; Pharmaceutical cocrystals: A review of preparations, physicochemical properties and applications. *Acta Pharm. Sin. B*.**2021**, 11, 2537-2564.
- [28] Garala, C.K.; Buddhadev, S. S.; Pharmaceutical Cocrystals—A Review. *Proceedings*.**2021**, 62.
- [29] Nagapudi, K.; Umanzor, E.Y.; Masui, C.; High-throughput screening and scale-up of cocrystals using resonant acoustic mixing. *Int. J. Pharm.***2017**, 521, 337-345.
- [30] Kaupp, G.; Solid-state molecular syntheses: complete reactions without auxiliaries based on the new solid-state mechanism. *CrystEngComm*.**2003**, 5, 117-133.
- [31] Maheshwari, C.; Jayasankar, A.; Khan, N.A.; Amidon, G.E.; Rodríguez-Hornedo, N.; Factors that influence the spontaneous formation of pharmaceutical cocrystals by simply mixing solid reactants. *CrystEngComm*.**2009**, 11, 493-500.
- [32] Macfheonnghaile, P.; Crowley, C.M.; Mcardle, P.; Erxleben, A.; Spontaneous solid-state cocrystallization of caffeine and urea. *Cryst. Growth. Des.***2020**, 20, 736-745.
- [33] Aitipamula, S.; Chow, P. S.; Tan, R. B. H.; Co-crystals of caffeine and piracetam with 4-hydroxybenzoic acid: Unravelling the hidden hydrates of 1 : 1 co-crystals. *CrystEngComm*.**2012**, 14, 2381-2385.
- [34] Leiserowitz, L.; Nader, F.; The molecule packing modes and the hydrogen-bonding properties of amide-dicarboxylic acid complexes. *Acta Crystallogr.***1977**, B33, 2719–2733.
- [35] Reddy, L. S.; Nangia, A.; Lynch, V. M.; Phenylperfluorophenyl synthon mediated cocrystallization of carboxylic acids and amides. *Cryst. Growth. Des.***2004**, 4, 1, 89-94.

- [36] Fischer, F.; Scholz, G.; Benemann, S.; Klaus Rademann, K.; Emmerling, F.; Evaluation of the formation pathways of cocrystal polymorphs in liquid-assisted syntheses. *CrystEngComm*.**2014**, *16*, 8272-8278.
- [37] Fischer, F.; Scholz, G.; Benemann, S.; Rademann, K.; Emmerling, F.; Evaluation of the formation pathways of cocrystal polymorphs in liquid-assisted syntheses. *Cryst. Eng. Comm.***2014**, *16*, 8272-8278.
- [38] Y, Yan.; Chen, J.M.; Lu, T.B.; Thermodynamics and preliminary pharmaceutical characterization of a melatonin–pimelic acid cocrystal prepared by a melt crystallization method. *Cryst. Eng. Comm.***2015**, *17*, 612-620.
- [39] Liu, X.; Lu, M.; Guo, Z.; Huang, L.; Feng, X.; Wu, C.; Improving the chemical stability of amorphous solid dispersion with cocrystal technique by hot melt extrusion. *Pharm. Res (N Y)*.**2012**, *29*, 806-817.
- [40] Jafari, K. M.; Padrela, L.; Walker, M. G.; Croker, M. D.; Creating Cocrystals: A review of Pharmaceutical Cocrystal Preparation Routes and Applications. *Cryst. Growth. Des.***2018**, *18*, 10, 6370-6387.
- [41] Blagden, N.; Berry, D.J.; Parkin, A.; Javed, H.; Ibrahim, A.; Gavan, P.T.; De Matos, L. L.; Seaton, C. C.; Current directions in co-crystal growth. *New J. Chem.***2008**, *32*, 1659-1672.
- [41] Chiarella, R.A.; Davey, R.J.; Peterson, M.L.; Making co-crystals the utility of ternary phase diagrams. *Cryst. Growth. Des.***2007**, *7*, 1223-1226.
- [42] Weyna, D.R.; Shattock, T.; Vishweshwar, P.; Zaworotko, M.J.; Synthesis and structural characterization of cocrystals and pharmaceutical cocrystals: mechanochemistry vs slow evaporation from solution. *Cryst. Growth. Des.***2009**, *9*, 2, 1106-1123.
- [43] Basavoju, S.; Boström, D.; Velaga, S.P.; Pharmaceutical cocrystal and salts of norfloxacin. *Cryst. Growth. Des.***2006**, *6*, 2699-2708.
- [44] Modani, S.; Gunnam, A.; Yadav, B.; Nangia, A.K.; Shastri, N.R.; Generation and evaluation of pharmacologically relevant drug–drug cocrystal for gout therapy. *Cryst. Growth. Des.***2020**, *20*, 3577-3583.
- [45] Roy, S.; Bhatt, M. P.; Nangia, A.; Kruger, G. J.; Stable Polymorph of Venlafaxine Hydrochloride by Solid-to-Solid Phase Transition at High Temperature. *Cryst. Growth. Des.***2007**, *7*, 476–480
- [46] Goud, N. R.; Khan, A. R.; Nangia, A.; Modulating the solubility of sulfacetamide by means of cocrystals. *CrystEngComm*.**2014**, *16*, 5859–5869.

- [47] Desiraju, G. R.; Supramolecular synthons in crystal engineering-a new organic-synthesis. *Angew. Chem. Int. Ed. Engl.***1995**, *34*, 2311-2327
- [48] Blagden, N.; Berry, D. J.; Parkin, A.; Javed, H.; Current directions in co-crystal growth. *New J. Chem.***2008**, *32*, 1659-1672.
- [49] Childs, S. L.; Stahly, G. P.; Park, A.; The Salt–Cocrystal Continuum: The Influence of Crystal Structure on Ionization State. *Mol. Pharm.***2007**, *4*, 323–338.
- [50] Steed, W. J.; The role of co-crystals in pharmaceutical design. *Trends in Pharm. Sci.***2013**, *34*, 185-193.

**MECHANOSYNTHESIS OF AGRO-BASED COCRYSTAL  
FOR  
IMPROVED NITROGEN MANAGEMENT**



A literature review submitted to the Department of Chemistry, Gauhati University in partial fulfilment of the requirements for the award of degree of Master of Science in Chemistry

Submitted by

**Minakshi Gohain**

**Roll number:PS-191-808-0072**

**Registration number: 19000063**

**MSc.4<sup>th</sup> semester**

**Gauhati university, Assam**

**UNDER THE SUPERVISION OF**

**Dr. RANJIT THAKURIA**

**ASSISTANT PROFESSOR**

**DEPARTMENT OF CHEMISTRY**

**GAUHATI UNIVERSITY**

**GUWAHATI, ASSAM 781014, INDIA**

## **CERTIFICATE**

This is to certify that the literature survey report, entitled “**Mechanosynthesis of Agro-based Cocrystal for Improved Nitrogen Management**” is submitted by **Minakshi Gohain**, M. Sc 4th semester, organic chemistry specialization in partial fulfilment of the requirement for the degree of Master in Science in Chemistry. The literature survey is a bonafide work carried out by her under my supervision and guidance. I wish her success in life.

**Dr. RANJIT THAKURIA**  
**ASSISTANT PROFESSOR**  
**DEPARTMENT OF CHEMISTRY**  
**GAUHATI UNIVERSITY**



## DECLARATION

I, Minakshi Gohain, student of MSc.4th semester, Gauhati University, Guwahati, hereby declare that the MSc. project report on “**Mechanosynthesis of Agro-based Cocrystal for Improved Nitrogen Management**” is a record of work done by me under the guidance of Dr. Ranjit Thakuria, Assistant Professor, Department of Chemistry, Gauhati University. The information and data given in the report is authentic to the best of my knowledge. The report is not being submitted to any other university for award of any other Degree, Diploma and Fellowship.

Date:08/09/2021

Place: Guwahati

*Minakshi Gohain*

Minakshi Gohain

## ACKNOWLEDGEMENT

I would like to express my sincere gratitude to my project supervisor **Dr. Ranjit Thakuria**, Assistant Professor, Gauhati University, for his constant guidance, congenial help and unfailing support throughout my literature survey work.

I would like to take the opportunity to thank **Prof. Chitrani Medhi**, Head of the Department, Chemistry, for giving me the opportunity to do the literature survey work and providing timely support and I would also like to thank all the teachers of Chemistry department for their support.

Finally, I am pleased to convey my hearty thanks to research scholar **Diptajyoti Gogoi** and friends for their helps and encouragements during various stages of completion of the literature survey.

**Minakshi Gohain**

**MSc.4<sup>th</sup> semester**

**Department of Chemistry**

**Gauhati University**

## ABSTRACT

Urea is the most common and widely used nitrogen fertilizer in various agricultural practices. The solubility of urea is very high and it is swiftly hydrolyzed to ammonium ( $\text{NH}_4^+$ ) and bicarbonate ( $\text{HCO}_3^-$ ) in presence of catalyst like the nickel-dependent enzyme urease after decomposition in the soil. The hydrolysis causes a rapid pH increase in the medium that leads to the formation of gaseous ammonia ( $\text{NH}_3$ ) and consequent N loss from soil. It has been suggested that only 47% of the applied fertilizer nitrogen is taken up by the plants whereas nearly 50% of fertilizer nitrogen lost to the environment which causes heavy disturbance in the biodiversity as well as brings negative impact to the economy. Therefore, use of agro based cocrystals as a fertilizer is very important to improve the management of nitrogen and mechanochemical synthesis of these cocrystals is an effective approach as it involves green synthesis process. This review deals with the mechanochemical synthesis of various calcium and magnesium containing urea cocrystals and zinc-urea-thiourea cocrystal. It is suggested that these cocrystals have the capability to improve nitrogen fertilization efficiency providing global solution to upgrade the management of nitrogen.

# CONTENTS

Table of contents	Page number
1. Introduction.....	1-2
2. Synthesis	
2.1 Importance of cocrystal .....	3-4
2.2 Mechanochemical synthesis .....	4-5
2.2.1Mechanosynthesis of agro- based cocrystal .....	5-8
3. Characterization .....	9-14
4. Conclusion .....	15
5. Reference .....	16-19

## 1. INTRODUCTION

Nitrogen (N) is one of the essential nutrients in the field of agriculture and food production. The proper growth and productivity of a plant depends on the requisite supply of nitrogen. The human activities have a significant impact on the global nitrogen cycle.<sup>1</sup>Burning fossil fuels, application of nitrogen-based fertilizer and other activities dramatically increase the amount of biologically available nitrogen in the ecosystem. In agricultural systems, fertilizers are used extensively to increase plant production, but unused nitrogen generally in the form of nitrate can leach out of the soil, enter streams and rivers and eventually make its way into our drinking water.<sup>2</sup>The process of making synthetic fertilizers for use in agriculture by the reaction between  $N_2$  and  $H_2$ , known as the Haber-Bosch process has increased significantly over the past several decades. In fact, today, nearly 80% of the nitrogen found in human tissues originated from the Haber- Bosch process.<sup>3,4</sup> Much of the nitrogen applied to agricultural and urban areas finally enters rivers and nearshore coastal systems. In nearshore marine systems, increases in nitrogen can often lead to anoxia (no oxygen) or hypoxia (low oxygen), changes in food-web structure, general habitat degradation which leads to biodiversity alteration.<sup>4</sup>

[CO (NH<sub>2</sub>)<sub>2</sub>] (Urea) is a well-known N fertilizer and has the highest nitrogen content of all solid nitrogenous fertilizers in familiar use. Urea accounts for more than 60% of the global nitrogen fertilizer use.<sup>5</sup> It is produced via ammonia (NH<sub>3</sub>) as an intermediate formed using the Haber process. In this process hydrogen reacts with  $N_2$  in presence of a catalyst under high temperature and pressure.<sup>6</sup> Fertilizer nitrogen may be lost from the soil in several different ways, including ammonia volatilization, nitrate leaching and nitrate denitrification. Factors affecting these losses include fertilizer compound, fertilizer form, type of application, timing of application, soil properties, rainfall amount and intensity, temperature and wind after application.<sup>7</sup>The high solubility of urea in water (110–170 g/100 ml, in the 20–40 °C range) and rapid moisture uptake after application make it particularly susceptible to mobility and runoff. As a result, excessive amounts of urea are frequently used to ensure that sufficient quantities are available to plants and crops. <sup>8</sup> Urea is swiftly hydrolyzed to ammonium (NH<sub>4</sub><sup>+</sup>) and bicarbonate (HCO<sub>3</sub><sup>-</sup>) in presence of catalyst like the nickel-dependent enzyme urease after decomposition in the soil.<sup>9,10</sup> The hydrolysis causes a rapid pH increase in the medium that leads to

the formation of gaseous ammonia ( $\text{NH}_3$ ) and consequent N loss from soil. These losses can be greater if the soil has a high pH or if the soil is wet when the urea is applied. The reason -wet soil makes the losses worse is twofold-one is that applying urea to wet soil insures the pellet dissolves almost instantly and makes the urea subject to attack by urease enzyme that causes loss and another is that the urease enzyme that is responsible for the loss is more prevalent in wet soil than in dry soil.<sup>11,12</sup> The ammonium ion is a major inorganic nitrogen source for plants and it promotes plant growth, but high amount of this ion can Cause toxicity.  $\text{NH}_4^+$  undergoes an aerobic nitrification process carried out either by a mutualistic symbiosis involving ammonia oxidizing bacteria (AOB) and Archaea (AOA) with nitrite-oxidizing bacteria (NOB)<sup>11</sup> or directly by complete ammonia-oxidizing (Comammox) bacteria which results in the formation of nitrate ( $\text{NO}_3^-$ ) via nitrite ( $\text{NO}_2^-$ ).<sup>12,13</sup> In all these cases, the copper-dependent ammonia monooxygenase (AMO) catalyze the initial oxidation of  $\text{NH}_4^+$  to hydroxyl amine ( $\text{NH}_2\text{OH}$ ) which leads to the formation of nitrite ( $\text{NO}_2^-$ ), and finally nitrate ( $\text{NO}_3^-$ ) is formed via nitrite, catalyzed by the molybdenum-dependent nitrite oxidoreductase (NIX).<sup>14</sup> Nitrate thus formed in these processes is taken up by plant roots or enters an anaerobic denitrification route and converts back to nitrite by the Mo-dependent nitrate reductase (NAR); nitrite is then transformed to gaseous forms of N such as nitric oxide (NO), ammonia ( $\text{NH}_3$ ), nitrous oxide ( $\text{N}_2\text{O}$ ), dinitrogen ( $\text{N}_2$ ), while an enormous portion of nitrate is also eventually leached into groundwater.<sup>15,16</sup> As a consequence of these, nearly 50% of nitrogen fertilizer applied to the soil is not used by plants and is lost to the environment, some of the released species are the cause of greenhouse effect<sup>17</sup>, eutrophication is also seen due to leached nitrate.<sup>18</sup> Along with the environmental degradation, the farmers suffer significant economic loss due to these issues.<sup>19</sup> To reduce the problems mechanochemical synthesis of agro- based cocrystal is done which is one of the effective way to improve nitrogen management.<sup>20</sup>

## 2.SYNTHESIS

### 2.1 Importance of cocrystal:

In the cocrystal technology, the crystalline environment of a compound is altered without changing its molecular structure which in principle makes it possible to access desirable physical properties. Co-crystals have been used to develop new anticancer, antiviral, antidepressant and anticonvulsant drugs with enhanced aqueous solubility.<sup>21</sup> Cocrystallisation is also applicable to non-ionizable molecules where salt formation is not possible. Compared to amorphous solid forms, cocrystals tend to be more stable and have a predictable behavior.<sup>22</sup> These are also less prone to polymorphic transformations due to the higher complexity of their crystal structure when compared to single component system.<sup>23</sup> Liquids, pastes and oily products can turn into solid form as a result of cocrystallisation leading to more robust and efficient manufacturing process. Cocrystals do not involve structural modification of the parent molecules, for that reason, in case of designing cocrystals their development programs will be significantly shorter and less risky than those of new chemical entities.<sup>24</sup> Cocrystal technologies can also be used to prevail over solubility problems associated with agrochemicals such as herbicides, pesticides and insecticides which in turn cap their negative impacts.<sup>25</sup>

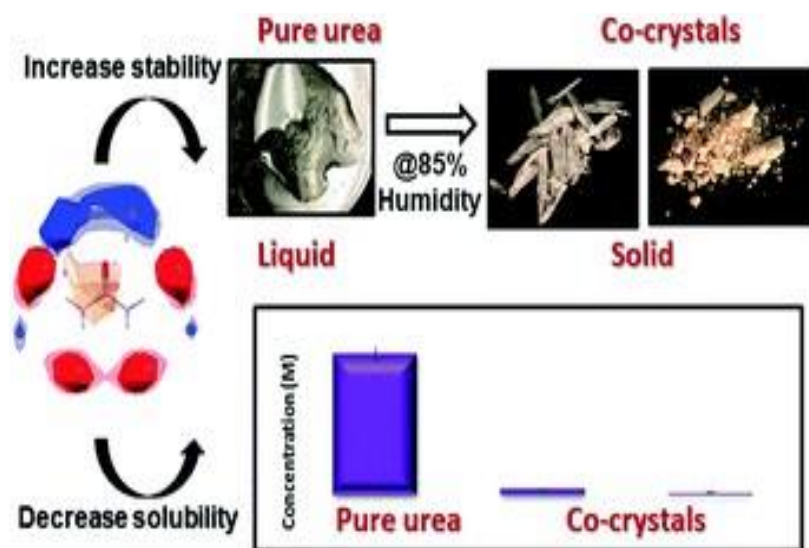


**Figure1:** formation of solid urea cocrystal having low solubility in water.<sup>26</sup>

Co-crystals can provide new solid forms of urea with substantially reduced aqueous solubility and lowered hygroscopicity, which may limit environmental degradation and come up with ease storage and handling of a chemical that is used globally on a multi-ton scale each year.<sup>27</sup>

## 2.2 Mechanochemical synthesis:

Mechanochemical synthesis is a processing technique of solids in which mechanical and chemical phenomena are coupled on a molecular scale. A formal definition by IUPAC states “*a mechanochemical reaction is a chemical reaction that is induced by mechanical energy*”.<sup>28</sup> This process enables to produce a desired product using only a mechanical action like high pressure and mechanical stress between reactants and balls at room temperature or at temperatures lower than traditional solid-state synthesis.<sup>29</sup> Mechanochemical synthesis can be performed under different conditions which includes use of reactive atmosphere such as reactive ball milling, under cryogenic conditions (cryomilling) or in a solvent. Moreover, other experimental parameters can be controlled that influence the characteristics of the final material which are milling time, powder to ball weight ratio, milling temperature, milling frequency, milling atmosphere and pressure of the selected gas, etc.<sup>30</sup> Depending on the synthesis parameters, different products can be obtained, such as metastable phases, high-pressure phases, and amorphous and disordered phases, leading to the development of different compounds.<sup>30,31</sup> Mechanochemical synthesis does not make use of heat to cause chemical reactions, starting reagents are placed in a high-energy mill where mechanically induced chemical changes take place under the high load and strain rate conditions found at the contact points between the milling media.<sup>32</sup>

The amount of energy which can be imparted to a system under mechanical activation can be significant i.e. certainly sufficient to break chemical bonds but can also be reduced when working with systems such as soft molecular crystals in order to minimize chemical activation while still enabling processes such as the conversion of a crystalline solid to an amorphous product or the readjustment of molecules within a lattice. Such readjustments may lead to the introduction of lattice imperfections, to polymorphic transformations or to the intimate mixing of two separate crystalline molecular solids to create a crystalline multicomponent product indistinct from that which would be obtained by conventional solution crystallization.<sup>32,33</sup>



Mechanochemistry is considered as an alternative attractive greener approach to prepare diverse molecular compounds and has become an important synthetic tool in different fields like physics, chemistry, and material science since is considered an ecofriendly procedure that can be carried out under solvent free conditions or in the presence of minimal quantities of solvent which means in catalytic amounts.<sup>33</sup> Furthermore, the products are of high purity and the reactions periods are typically completed within minutes. Mechanochemistry has gained increasing importance for the synthesis of novel compounds in recent years. These sustainable methods have an enormous impact on a great variety of chemistry fields, including catalysis, organic synthesis, metal complexes formation, preparation of multicomponent pharmaceutical solid forms etc.<sup>34</sup>

### **2.2.1 Mechanosynthesis of agro-based cocrystal:**

Applying the mechanochemical process agrochemical cocrystals can be synthesized that are typically based on inexpensive but poorly soluble ionic starting materials. To improve nitrogen management, synthesis of urea cocrystal is very necessary as it is the widely used fertilizer in agriculture field.<sup>35</sup>

Typically, the inorganic acids or their metal salts, such as Calcium or magnesium phosphates, sulfates and nitrates are used for the preparation of urea molecular ionic cocrystal. The general procedure includes mixing of Ca or Mg salt and urea with the corresponding molar ratios and loaded into a stainless-steel jar together with stainless steel balls and ground for few minutes in mixer mill.<sup>36</sup>

These urea ionic cocrystals are capable of decreasing  $\text{NH}_3$  emissions to the environment in comparison to pure urea. Moreover, urea molecular ionic cocrystals with inorganic Ca and Mg salts also contain other primary and secondary nutrients, such as calcium, phosphorus, magnesium and Sulphur which are important for a balanced nitrogen uptake. Mainly these urea ionic cocrystals have been synthesized from saturated aqueous solution.<sup>36,37</sup> Some examples of calcium and magnesium salt containing agro based urea ionic cocrystals fertilizers are  $\text{Ca}(\text{H}_2\text{PO}_4)_2 \cdot 4\text{CO}(\text{NH}_2)_2$ ,

$\text{CaSO}_4 \cdot 4\text{CO}(\text{NH}_2)_2$ ,  $\text{Ca}(\text{NO}_3)_2 \cdot 4\text{CO}(\text{NH}_2)_2$ ,  $\text{MgSO}_4 \cdot 6\text{CO}(\text{NH}_2)_2 \cdot 0.5\text{H}_2\text{O}$ ,  $\text{Mg}(\text{H}_2\text{PO}_4)_2 \cdot 4\text{CO}(\text{NH}_2)_2$ ,  $\text{Mg}(\text{NO}_3)_2 \cdot 4\text{CO}(\text{NH}_2)_2 \cdot x\text{H}_2\text{O}$  etc. The crystalline water in the reactant has a major role in the final product structure and the alternative polymorphs can be generated by selecting different precursors.<sup>37</sup>

Particularly, importance is given to the Co-crystallization of neutral organic molecules and inorganic salts such as alkali and alkaline earth halides, sulfates, phosphates etc. .The ionic cocrystal thus formed are similar to the classical coordination compounds (complexes) in terms of structure and intermolecular bonding features and effectiveness of the organic–inorganic assembly to enhance thermal stability, improve particle size and morphology , significant change in solubility and dissolution rate with respect to those of the pure active ingredients brings more interest to synthesize this type of cocrystal. Figure 2 shows organic-inorganic assembly of ionic cocrystal.<sup>38</sup>

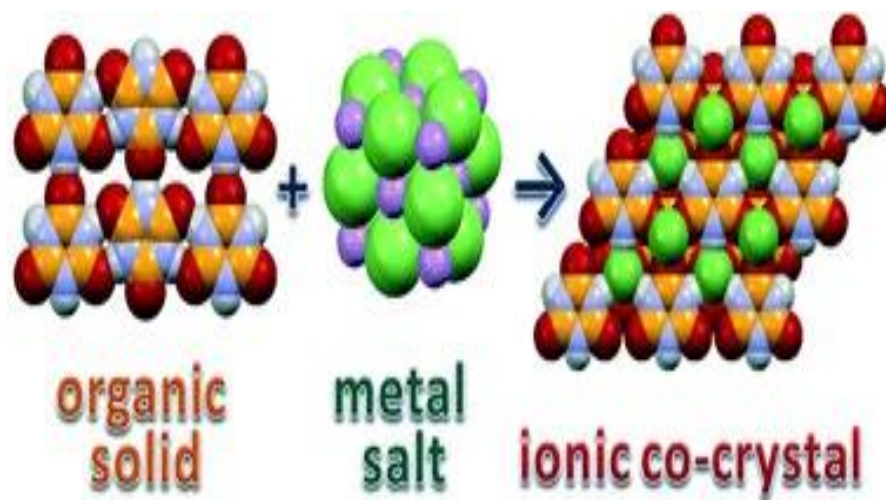


**Figure2:** Formation of ionic cocrystal from organic solid and metal salt.

### Ca (H<sub>2</sub>PO<sub>4</sub>)<sub>2</sub>·4CO (NH<sub>2</sub>)<sub>2</sub> synthesis:

The green synthesis of Ca [CO (NH<sub>2</sub>)<sub>2</sub>]<sub>4</sub>(H<sub>2</sub>PO<sub>4</sub>)<sub>2</sub> (calcium urea phosphate) can be done using mechanochemical process which is an excellent example of agrochemical ionic cocrystal. This cocrystal is highly advantageous as a fertilizer because of its stability, reduction in ammonia loss, while providing three critical nutrients and good moisture stability from very poorly soluble inorganic precursors.<sup>38,39</sup> The calcium urea phosphate cocrystal is formed by the reaction of Co(NH<sub>2</sub>)<sub>2</sub>[urea], Co(NH<sub>2</sub>)<sub>2</sub>H<sub>3</sub>PO<sub>4</sub> [urea phosphate] and either calcium hydroxide or calcium oxide as shown in fig.3. CaCO<sub>3</sub> or Ca(OH)<sub>2</sub>, urea and urea phosphate are taken in 1: 2: 2 respective stoichiometric ratio for this cocrystal synthesis. The neutralization reaction leads to the formation of calcium urea phosphate along with water and carbon dioxide as byproducts.<sup>39</sup>

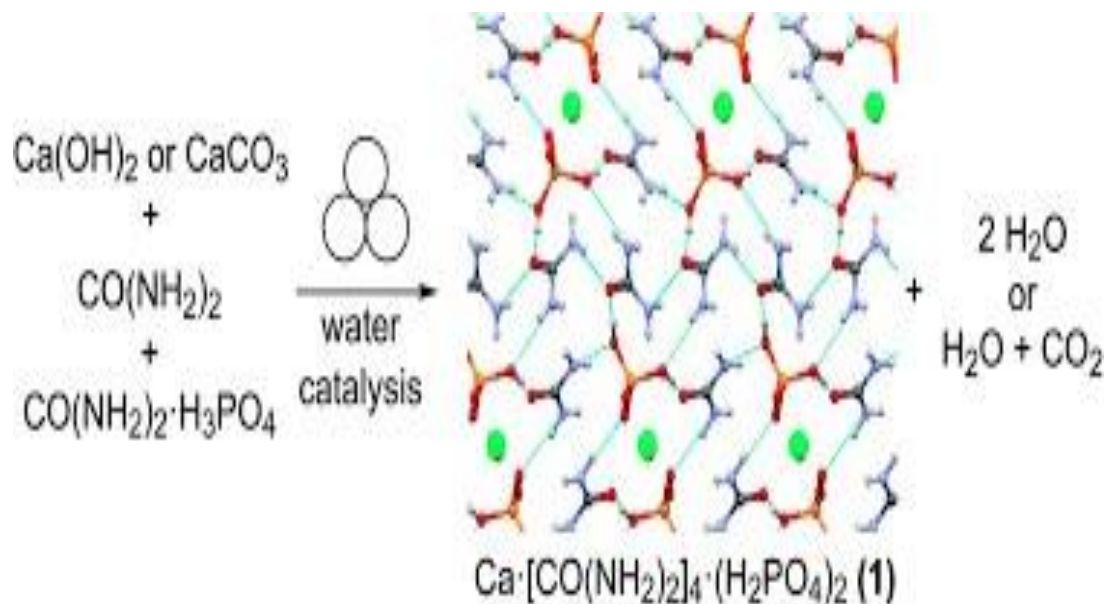


**Figure3:** Mechanochemical synthesis of the agrochemical cocrystal 1 from urea, urea phosphate and either calcium hydroxide or carbonate. Calcium ions are shown in green and hydrogen bonding interactions are displayed in light blue.<sup>39</sup>

### Synthesis of [Zn (thiourea)(urea)Cl<sub>2</sub>], (ZnTU) by using mechanochemistry:

The procedure for Small Scale Synthesis of ionic cocrystal ZnTU via Mechanochemistry involves ball milling of Urea (16.54 mg, 0.28 mmol) with thiourea (20.96 mg, 0.28 mmol) and ZnCl<sub>2</sub> (42.49 mg, 0.28 mmol), in a 1:1:1 stoichiometry ratio with the addition of 50  $\mu$ L of water, in an agate jar for 60 min at 20 Hz. [Zn (thiourea)(urea)Cl<sub>2</sub>] is considered as a novel material for improving N fertilization efficiency which provides agricultural practice in an ecofriendly way. The molecular structure of ZnTU in the solid state is shown in Figure 4 and hydrogen bonding motifs in this cocrystal is shown in figure5.<sup>40</sup>

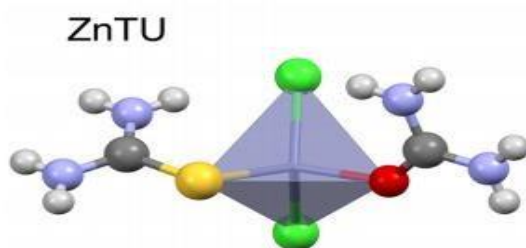


**Figure 4:** Molecular structure of ZnTU. Color code: Zn- black; O- red; S- yellow; C- dark gray; N-blue; H- light gray; Cl- green.

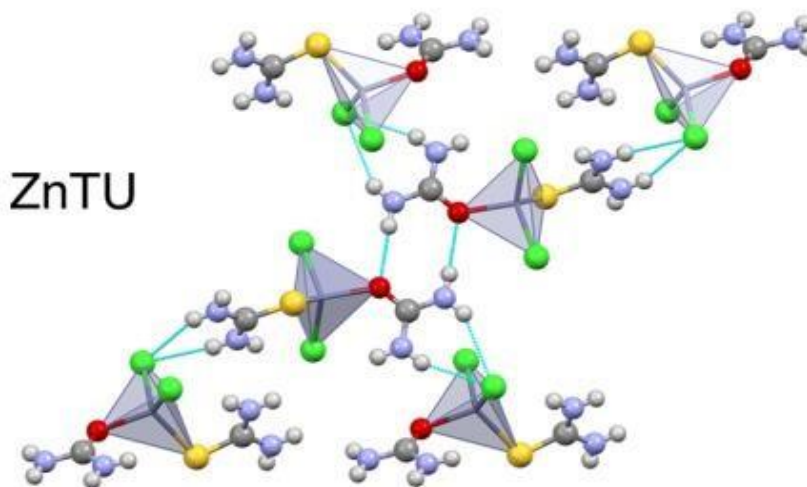


**Figure 5:** Hydrogen bonding motifs in ZnTU. Color code: Zn- black; O- red; S- yellow; C- dark gray; N- blue; H- light gray; Cl- green.

### 3.CHARACTERIZATION:

The techniques such as powder X-ray diffraction, Differential Scanning Calorimetry, Thermogravimetric analysis, Raman spectroscopic technique etc. are used for the characterization of agro based ionic cocrystals.<sup>41</sup>

#### 3.1 Powder X-ray diffraction technique (XRPD):

The crystalline nature of the reactant and the ionic cocrystal formed are confirmed by powder X-ray diffraction. The ZnTU phase identification can be done with the help of XRPD patterns.<sup>40</sup>

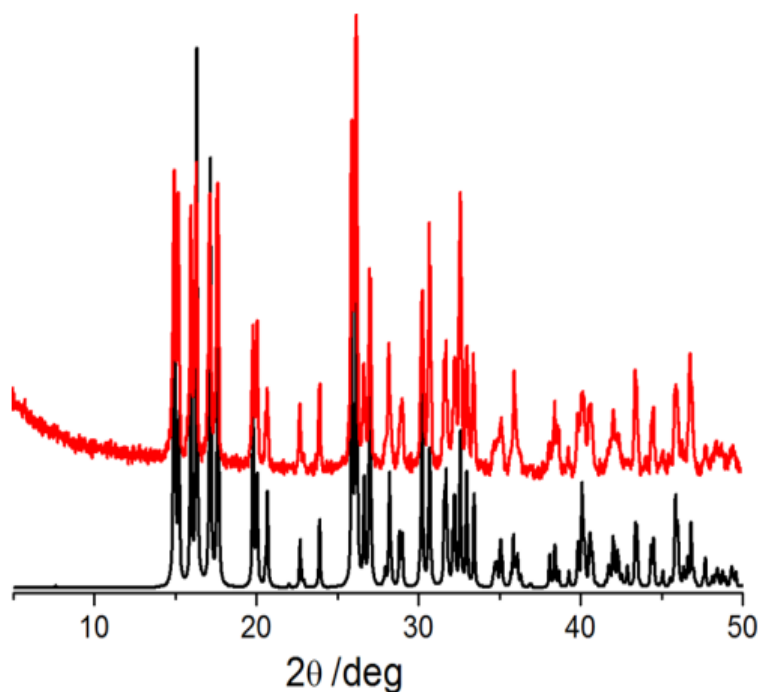


**Figure6:** Comparison between the experimental pattern measured for ZnTU as obtained by solid-state synthesis (red line) and the pattern calculated on the basis of the single crystal structure (black line).<sup>40</sup>

The XRPD shows crystalline nature of various Ca and Mg salt–urea ionic cocrystal materials and this unique single crystalline structure fertilizer material contains N–Ca–S, N–P–Ca, N– Ca, N–Mg–S, N–P–Mg, N–Mg macronutrients etc. It is seen that the XRPD patterns obtained match those simulated of the crystals obtained using conventional solution-based routes.<sup>41</sup>

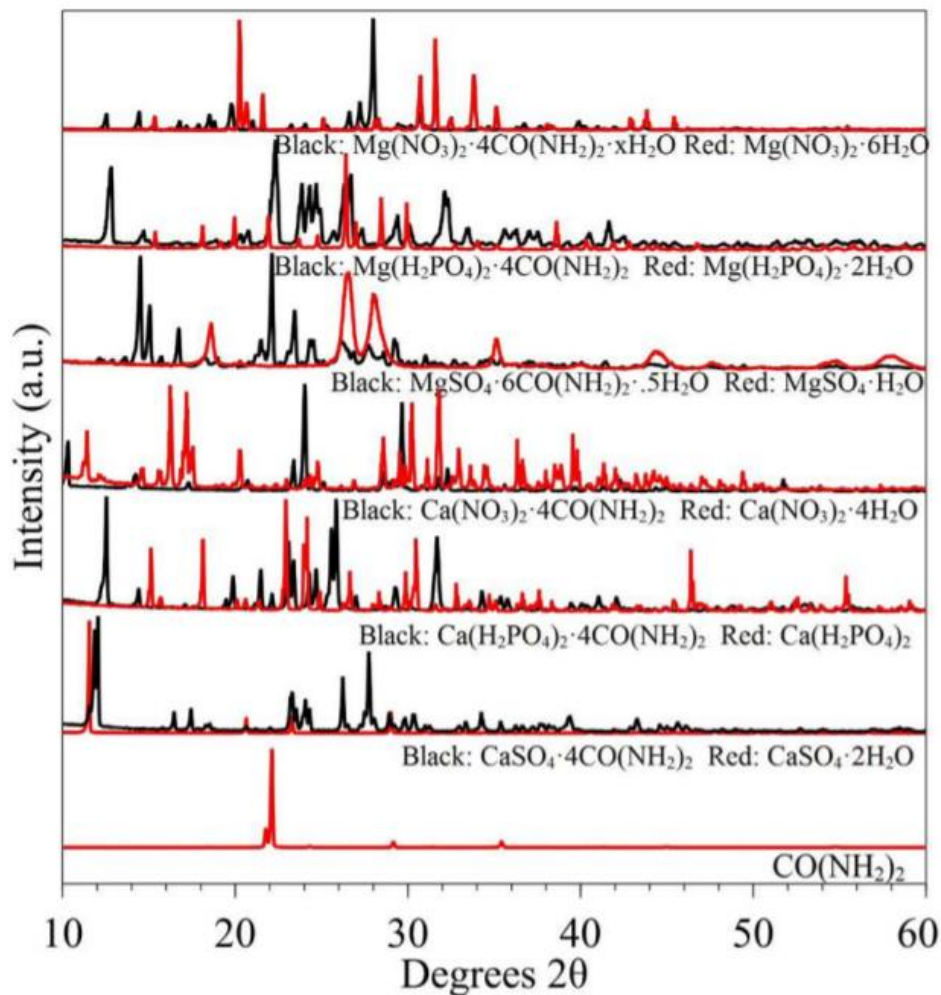


**Figure7:** Powder XRD patterns of urea, magnesium or calcium salt reactants and the corresponding Mg or Ca-urea ionic cocrystal products.<sup>41</sup>

### 3.1 Differential scanning Calorimetry (DSC):

Differential scanning calorimetry analysis is done to characterize the thermal stability of an ionic cocrystal. With the help of DSC, heat associated with melting of the cocrystal formed can be quantified. DSC analysis shows that cocrystallisation of the organic molecules with  $\text{ZnCl}_2$  significantly reduces the melting point (peak temperatures) particularly in the three-components cocrystal ZnTU ( $\sim 100^\circ\text{C}$ ) as compared to the melting point of urea ( $137^\circ\text{C}$ ) and thiourea ( $179^\circ\text{C}$ ). No thermal event is observed in the DSC trace of ZnTU before melting.<sup>40</sup>

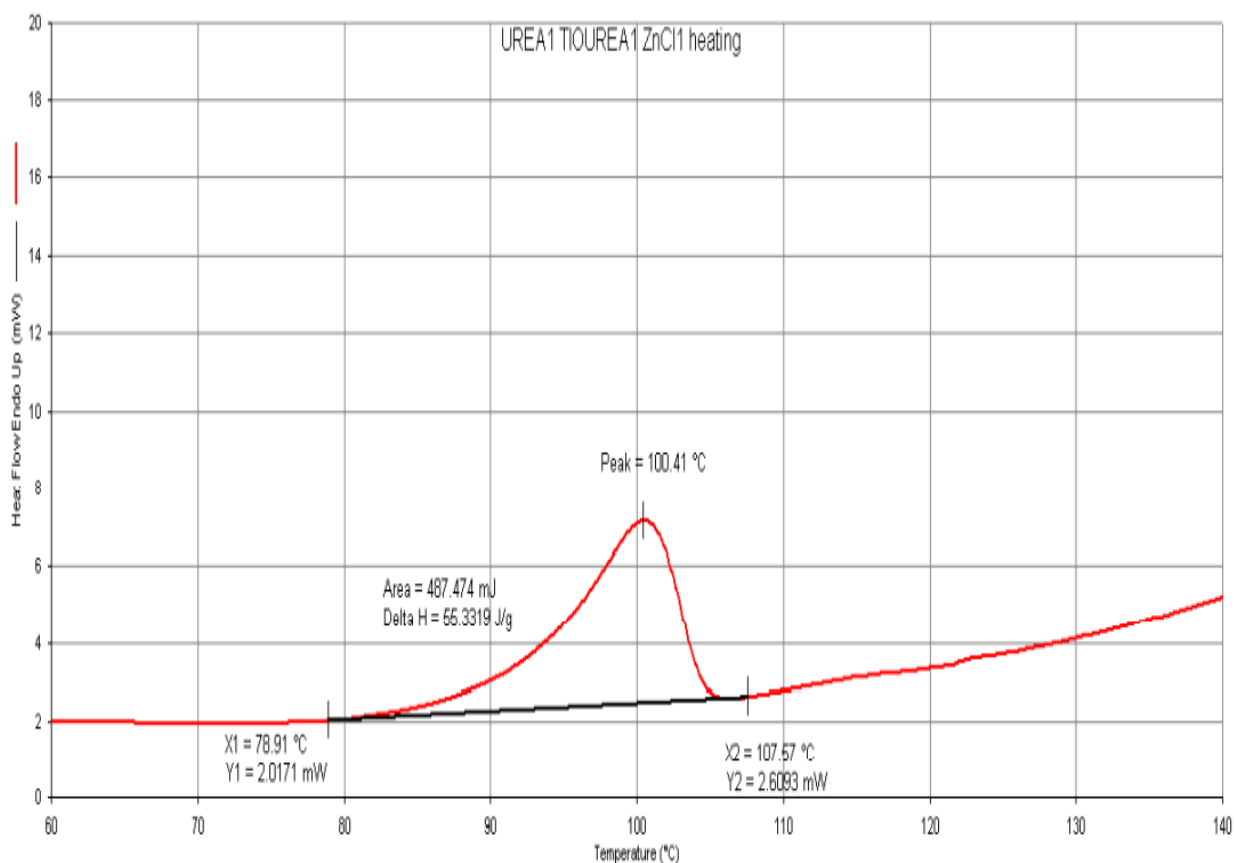


**Figure8:** DSC trace for [Zinc(thiourea)(urea) $\text{Cl}_2$ ] (ZnTU).<sup>40</sup>



An understanding of how urea is stabilized within this hybrid organic-inorganic crystal is provided by Differential scanning calorimetry (DSC) curves of the ionic cocrystals.<sup>37</sup>

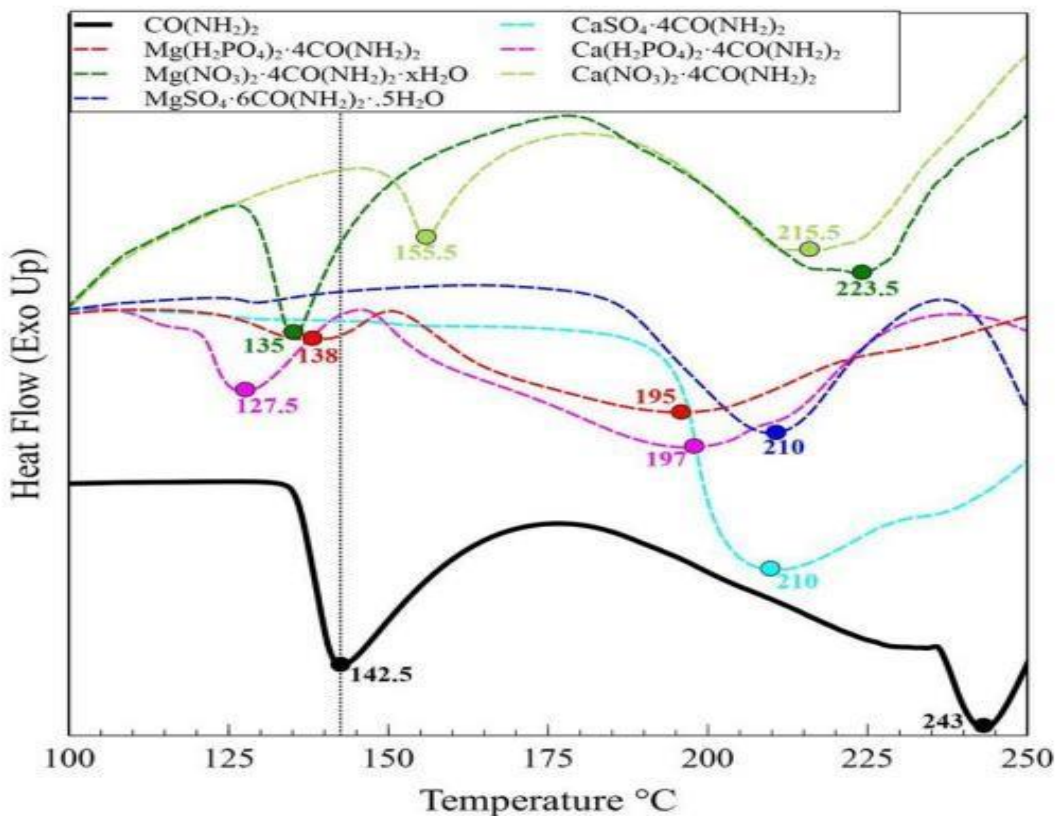


**Figure9:** DSC curve of urea and magnesium or calcium salt-urea ionic cocrystal products.<sup>37</sup>

Urea starts melting 132 °C and peak value in DSC curve of 142.5 °C, as shown in Figure 9. It is generally accepted that urea thermal decomposition also begins at the same temperature although melting is commonly reported to occur first.<sup>42</sup> The changes in this melting temperature can be associated with the stabilization of urea within the new crystal structure due to the formation of different types of bonds and from the curves obtained (in figure.9), a series of interesting observations can be collected. Both metal sulfate ionic cocrystals,  $\text{MgSO}_4 \cdot 6 \text{CO (NH}_2)_2 \cdot 0.5\text{H}_2\text{O}$  and  $\text{CaSO}_4 \cdot 4\text{CO(NH}_2)_2$ , exhibit absence of the typical 132°C peak and new melting peaks towards higher temperatures with the endothermal transition peaks at 210°C. Metal phosphate ionic cocrystals also lack well-defined pure urea melting peaks at 132 °C with apparent new peaks at



195°C –197 °C although smaller peaks at 127.5°C and 138°C are apparent. These are expected to result from the melting of the corresponding urea phosphate fragments.<sup>42,43</sup> Distinct endothermal peaks are apparent at 135°C and 155 °C for  $\text{Mg}(\text{NO}_3)_2 \cdot 4\text{CO}(\text{NH}_2)_2 \cdot x\text{H}_2\text{O}$  and  $\text{Ca}(\text{NO}_3)_2 \cdot 4\text{CO}(\text{NH}_2)_2$  respectively. The former is because of the crystalline water melting and the latter is due to the boiling of the resulting liquid calcium nitrate. In all the cases, nevertheless the absence of a strong endothermal transition with the onset at 132°C can be observed suggesting that urea is incorporated into the new crystal structure trigger to the stronger bonding.<sup>44</sup>

### 3.2 Thermogravimetric analysis (TGA):

Thermogravimetric analysis is done to determine the thermal stability of the ionic cocrystal formed. In TGA weight change of the product can also be monitored. Thermogravimetric measurement for ZnTU is performed using a PerkinElmer TGA7 thermogravimetric analyzer, in the 30–300 °C temperature range, under a  $\text{N}_2$  gas flow at a heating rate of  $5.00^\circ\text{C min}^{-1}$ . TGA trace for ZnTU shows that the compound is stable up to 100 °C.<sup>40</sup>

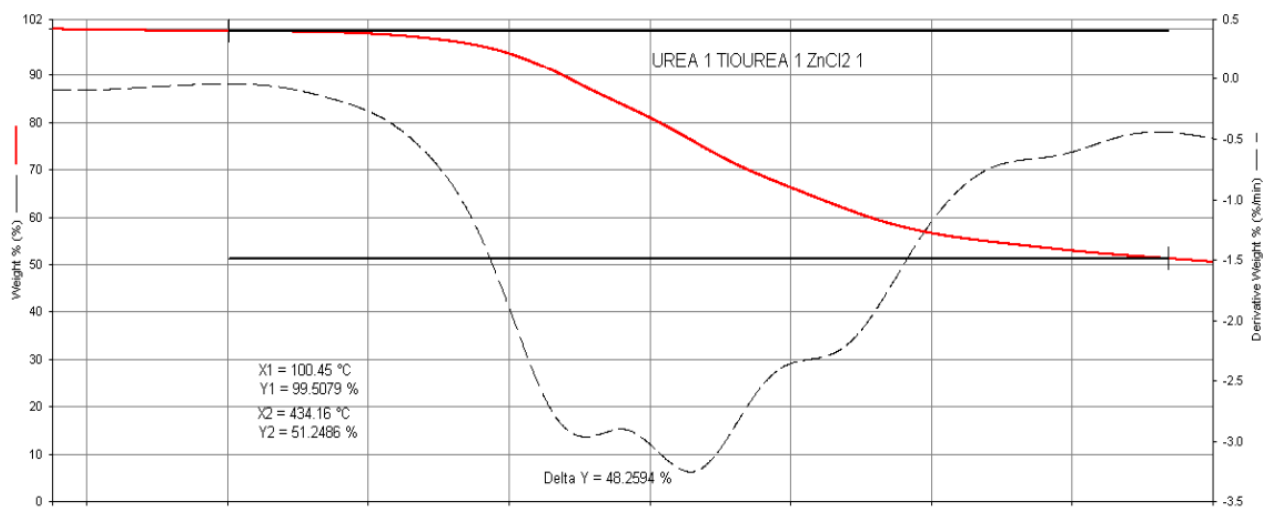


**Figure10:** TGA trace for ZnTU.<sup>40</sup>

### 3.3 Raman spectroscopic technique:

Raman spectroscopy is a useful vibrational technique for characterization of cocrystals. The measurement obtained by this technique is noninvasive, nondestructive and rapid.<sup>45</sup> Real-time Raman spectroscopy monitoring of the reaction involving  $\text{CaCO}_3$ , urea, and urea phosphate in 1: 2: 2 respective stoichiometric ratios revealed the appearance of calcium urea phosphate after 5 minutes milling. In spite of the considerable overlap of Raman bands for reactants and product, formation of this cocrystal is clearly observable by the appearance of the characteristic band at  $1083\text{cm}^{-1}$ .<sup>39,40</sup>

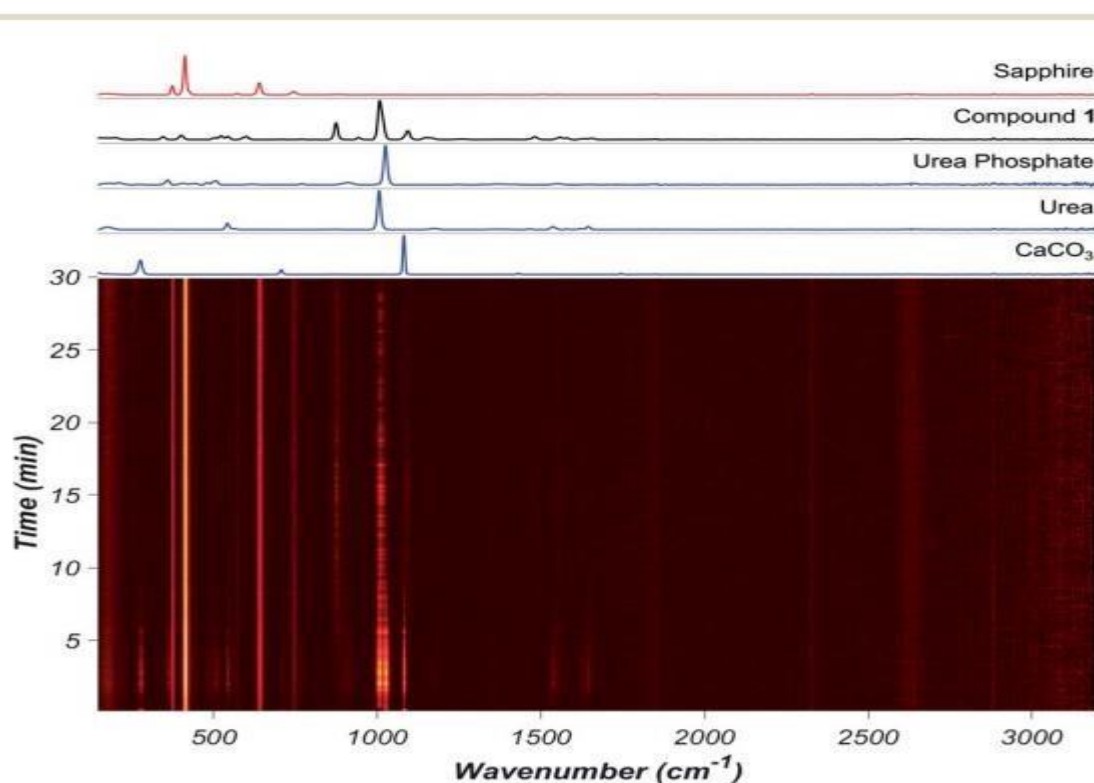


**Figure11:** (Bottom) In situ Raman spectra of the neat milling reaction between  $\text{CaCO}_3$ , urea, and urea phosphate. Brighter color denotes higher intensity. (Top) Raman spectra of reactants (blue), the product (black), and background from the sapphire milling jar (red) with individual spectra of reactants and product above the 2D.<sup>40</sup>

#### 4. CONCLUSION:

Urea is the most commonly used fertilizer in the agriculture field and it has the highest nitrogen content of all solid fertilizer. However, it has been put forwarded that only 47% of the applied fertilizer nitrogen is taken up by the crops whereas nearly 50% of fertilizer nitrogen lost to the environment yields underactive atmospheric  $N_2$ . This is because of the inherent mismatch between the nutrient supply and plant demand which results in nutrient loss through leaching or volatilization and poor plant growth.<sup>18</sup> To improve the management of nitrogen, synthesis of agro based cocrystal is very much necessary and mechanosynthesis is an effective way for it as this involves a greener approach.<sup>37</sup> Generally, the agro based urea cocrystal includes Calcium or Magnesium-urea ionic cocrystals. These cocrystals have the capability to decrease  $NH_3$  emissions than that of pure urea.<sup>41</sup>  $[Zn(thiourea)(urea)Cl_2]$  cocrystal is also regarded as a novel material for improving nitrogen fertilization efficiency which provides ecofriendly agricultural practice.<sup>40</sup> Therefore, it can be said that the mechanosynthesis of different agro based cocrystals will provide global solution to upgrade nitrogen management.<sup>41</sup>

## 5. REFERENCES

1. Roy, R.N.; Finck, A.; Blair, G. J.; Tandon, H. L. S. *Plant Nutrition for Food Security*; Food and Agriculture Organization of the United Nations: Rome, **2006**; p 348
2. Beeckman, F.; Motte, H.; Beeckman, T. Nitrification in agricultural soils: impact, actors and mitigation *Curr. Opin. Biotechnol.* **2018**, 50, 166–173
3. Biyun, F.; Fangming, L.; Chuanfeng, Z.; Chunyan, L.; Jun, N.; Wang, X.; Jianxin, L.; Bingyu, L.; Lilong, J. Sacrificial Sucrose Strategy Achieved Enhancement of Ammonia Synthesis Activity over a Ceria-Supported Ru Catalyst. *ACS Sustainable Chemistry & Engineering* **2021**, 9 (27), 8962–8969.
4. Johnson, P. T. J. *et al.* Linking environmental nutrient enrichment and disease emergence in humans and wildlife. *Ecological Applications* **20**, 16–29 (2010) .
5. Stein, L. Y.; Klotz, M. G. The nitrogen cycle. *Curr. Biol.* **2016**, 26 (3), R94–8.
6. Patil, B. S.; Wang, Q.; Hessel, V.; Lang, J. Plasma N<sub>2</sub>-fixation: 1900–2014. *Catal. Today* **2015**, 256, 49–66.
7. Bacon, P.E.; Freney, J.R. (1989) Nitrogen loss from different tillage systems and the effect on cereal grain-yield *Fertilizer Research* **20**(2), 59–66.
8. Ruark, M.; *Advantages and disadvantages of controlled release fertilizers*, Department of Soil Science, University of Wisconsin-Madison, WI FFVC, **2012**, pp. 1–33
9. Maroney, M. J.; Ciurli, S. Nonredox nickel enzymes: Chem. Rev. 2014, 114 (8), 4206–28.
10. Mazzei, L.; Musiani, F.; Ciurli, S. Urease In The Biological Chemistry of Nickel; Zamble, D.; Yrek, Ž.; Kozłowski, M. *Royal Society of Chemistry: London*, **2017**; pp 60–97
11. Paulot, F.; Jacob, D. J. Hidden cost of U.S. agricultural exports: particulate matter from ammonia emissions. *Environ. Sci. Technol.* **2014**, 48 (2), 903–908
12. Daims, H.; Lebedeva, E. V.; Pjevac, P.; Han, P.; Herbold, C.; Albertsen, M.; Jehmlich, N.; Palatinszky, M.; Vierheilig, J.; Bulaev, A.; Kirkegaard, R. H.; von Bergen, M.; Rattei, T.; Bendinger, B.; Nielsen, P. H.; Wagner, M. Complete nitrification by Nitrospira bacteria. *Nature* **2015**, 528, 504.
13. van Kessel, M. A. H. J.; Speth, D. R.; Albertsen, M.; Nielsen, P. H.; Op den Camp, H. J. M.; Kartal, B.; Jetten, M. S. M.; Lü cker, S. Complete nitrification by a single microorganism. *Nature* **2015**, 528, 555.
14. Bremner, J. M.; Douglas, L. A. Decomposition of Urea Phosphate in Soils1. *Soil Sci, Soc, Am, J.* **1971**, 35 (4), 575–578.

15. Maia, L. B.; Moura, J. J. How biology handles nitrite. *Chem. Rev.* **2014**, 114 (10), 5273–357.
16. Tilman, D.; Fargione, J.; Wolff, B.; Antonio, C.; Dobson, A.; Howarth, R.; Schindler, D.; Schlesinger, W. H.; Simberloff, D.; Swackhamer, D. Forecasting Agriculturally Driven Global Environmental Change. *Science* **2001**, 292 (5515), 281.
17. Galloway, J. N.; Cowling, E. B. Reactive Nitrogen and The World: 200 Years of Change. *Ambio* **2002**, 31 (2), 64–71.
18. Maia, L. B.; Moura, J. J. How biology handles nitrite. *Chem. Rev.* **2014**, 114 (10), 5273–357.
19. Duce, R. A.; LaRoche, J.; Altieri, K.; Arrigo, K. R.; Baker, A. R.; Capone, D. G.; Cornell, S.; Dentener, F.; Galloway, J.; Ganeshram, R. S.; Geider, R. J.; Jickells, T.; Kuypers, M. M.; Langlois, R.; Liss, P. S.; Liu, S. M.; Middelburg, J. J.; Moore, C. M.; Nickovic, S.; Oeschies, A.; Pedersen, T.; Prospero, J.; Schlitzer, R.; Seitzinger, S.; Sorensen, L. L.; Uematsu, M.; Ulloa, O.; Voss, M.; Ward, B.; Zamora, L. Impacts of Atmospheric Anthropogenic Nitrogen on the Open Ocean. *Science* **2008**, 320 (5878), 893
20. Fenn, L. B.; Richards, J. Ammonia loss from surface applied urea-acid products. *Fert. Res.* **1986**, 9 (3), 265–275
21. Karimi-Jafari, M.; Padrela, L.; Walker, G.M.; Croker, D.M. Creating Cocrystals: A Review of Pharmaceutical Cocrystal Preparation Routes and Applications. *Cryst. Growth Des.* **2018**, 18, 6370–6387.
22. Aitipamula, S.; Banerjee, R.; Bansal, A.K.; Biradha, K.; Cheney, M.L.; Choudhury, A.R. Polymorphs, Salts, and Cocrystals: What's in a Name? *Cryst. Growth Des.* **2012**, 12, 2147–2152.
23. Grant, D.J.W. Theory and origin of polymorphism. In *Polymorphism in Pharmaceutical Solids*, 2nd ed.; Brittain, H.G., Ed.; Marcel Dekker Inc.: New York, NY, USA, **1999**; Volume 95, pp. 1–33.
24. Stanton, M.K.; Bak, A. Physicochemical Properties of Pharmaceutical Co-Crystals: A Case Study of Ten AMG 517 Co-Crystals. *Cryst. Growth Des.* **2008**, 8, 3856–3862.
25. Mazzeo, P.P.; Carraro, C.; Monica, A.; Capucci, D.; Pelagatti, P.; Bianchi, F.; Agazzi, S.; Careri, M.; Raio, A.; Carta, M.; et al. Designing a Palette of Cocrystals Based on Essential Oil Constituents for Agricultural Applications. *ACS Sustain. Chem. Eng.* **2019**, 7, 17929–17940.

26. Plasson, R.; Brandenburg, A.; Jullien, L.; Bersini, H. *J. Phys. Chem. A*, **2011**, 115, 8073–8085
27. Honer, K.; Kalfaoglu, E.; Pico, C.; McCann, J.; Baltrusaitis, J. Sustainable ammonia production *ACS Sustainable Chem. Eng.*, **2017**, 5, 8546–8550
28. James, S. L.; Adams, C. J.; Bolm, C.; Braga, D.; Collier, P.; Friščić, T.; Grepioni, F.; Harris, K. D. M.; Hyett, G.; Jones, W.; Krebs, A.; Mack, J.; Maini, L.; Orpen, A. G.; Parkin, I. P.; Shearouse, W. C.; Steed, J. W.; Waddell, D. C. Mechanochemistry: opportunities for new and cleaner synthesis. *Chem. Soc. Rev.* **2012**, 41, 413–447
29. Takacs, L. The historical development of mechanochemistry. *Chem. Soc. Rev.* **2013**, 42, 7649–7659
30. Friščić, T.; Jones, W. Recent advances in understanding the mechanism of cocrystal formation via grinding *Cryst. Growth Des.* **2009**, 9, 1621–1637
31. Baig, R. B. N.; Varma, R. S. Microwave-Assisted Chemistry: synthetic applications for assembly of nanomaterials and organics. *Chem. Soc. Rev.* **2012**, 41, 1559–1584
32. Jörres, M.; Mersmann, S.; Raabe, G.; Bolm, C. Organocatalytic solvent-free hydrogen bonding-mediated asymmetric Michael additions under ball milling conditions. *Green Chem.* **2013**, 15, 612–616
33. Hasa, D.; Miniussi, E.; Jones, W. Mechanochemical Synthesis of Multicomponent Crystals: One Liquid for One Polymorph? A Myth to Dispel *Cryst. Growth Des.* **2016**, 16, 4582–4588
34. Sharma, L.; Kiani, D.; Honer, K.; Baltrusaitis, J. Mechanochemical synthesis of magnesium and calcium salt-urea ionic cocrystal fertilizer materials for improved nitrogen management. *ACS Sustainable Chem. Eng.* **2019**, 7, 6802–6812
35. James, S. L.; Adams, C. J.; Bolm, C.; Braga, D.; Maini, L.; Steed, J. W.; Collier, P.; Orpen, A. G.; Hyett, J.; Waddell, D. C. Mechanochemistry: opportunities for newer and cleaner synthesis. *Chem. Soc. Rev.*, **2012**, 41, 413–447
36. Braga, D.; Maini, L.; Grepioni, F. Mechanochemical preparation of co-crystals. *Chem. Soc. Rev.*, **2013**, 42, 7638–7648.
37. Gracin, D.; Strukil, V.; Friščić, T.; Halasz, I.; Zarević, K. Laboratory real time in situ monitoring of mechanochemical milling reaction by Raman spectroscopy. *Angew. Chem., Int. Ed.*, **2014**, 53, 6193–6197.
38. Braga, D.; Grepioni, F.; Shemchuk, O. Organic-inorganic ionic co-crystals: a class of multipurpose compounds. *CrystEngComm*, **2018**, 32, 7418–7598

39. Honer, K.; Pico, C.; Baltrusaitis, J. Reactive mechanosynthesis of urea ionic cocrystal fertilizer materials from abundant low solubility magnesium and calcium containing materials. *ACS Sustainable Chem. Eng.*, **2018**, 6, 4680–4687
40. Karki, S.; Frišcić, T.; Jones, W.; Motherwell, W. D. S. Characterization and quality control of pharmaceutical cocrystals. *Mol. Pharm.*, **2007**, 4, 347–354
41. Kulla, H.; Greiser, S.; Benemann, S.; Rademann, K.; Emmerling, F. Mechanochemistry: A green approach in the preparation of pharmaceutical cocrystal. *Molecules*, **2016**, 21, 917.
42. Jones, J. M.; Rollinson, A. N. Thermogravimetric evolved gas analysis of urea and urea solutions with nickel alumina catalyst. *Thermochimica Acta* **2013**, 565, 39–45.
43. McCullough, J. F.; Sheridan, R. C.; Frederick, L. L. Pyrolysis of urea phosphate. *J. Agric. Food Chem.* **2013**, 426, 41–58
44. Navizaga, C.; Boecker, J.; Sviklas, A. M.; Galeckiene, J.; Baltrusaitis, J. Adjustable N:P<sub>2</sub>O<sub>5</sub> Ratio Urea Phosphate Fertilizers for Sustainable Phosphorus and Nitrogen Use: Liquid Phase Equilibria via Solubility Measurements and Raman Spectroscopy. *ACS Sustainable Chem. Eng.* **2017**, 5 (2), 1747–1754. 1978, 26 (3), 670–675
45. Bolton, B. A.; Prasad, P. Characterization of new cocrystal by Raman Spectroscopy, powder X-ray Diffraction, Diffraction Scanning Calorimetry and Transmission Raman Spectroscopy *Pharm. Sci.* **1984**, 73, 1849–1851

# **A STUDY ON IONIC LIQUID BASED HYDROGELS**



*A project report submitted by the Department of Chemistry, Gauhati University in partial fulfillment of the requirements for the award of degree of Master of Science in Chemistry*

## **SUBMITTED BY**

**MITALI DEKA**

**ROLL NO: PS-191-808-0073**

**REGISTRATION NO: 270338**

**M.Sc 4<sup>th</sup> SEMESTER**

**DEPARTMENT OF CHEMISTRY**

**GAUHATI UNIVERSITY**

## **UNDER SUPERVISION OF**

**Dr. DILIP KUMAR KAKATI**

**PROFESSOR**

**DEPARTMENT OF CHEMISTRY**

**GAUHATI UNIVERSITY**

**GUWAHATI**

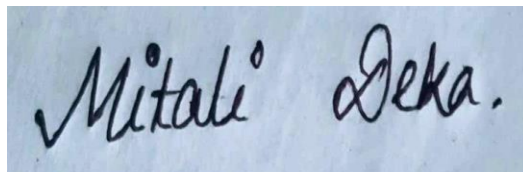


## DECLARATION

I, Mitali Deka student of M. Sc 4<sup>th</sup> semester, studying at Gauhati University, Guwahati, hereby declare that the M.Sc project report (Literature Review) on “**Ionic Liquid Based Hydrogels**” submitted to Gauhati University is the work conducted by me.

The information and the data given in the report are authentic to the best of my knowledge.

This report is not being submitted to any other university for award of any other Degree, Diploma and Fellowship.

A photograph of a handwritten signature in black ink on a light blue background. The signature reads "Mitali Deka." with a period at the end.

**Date** – 08-09-2021

(Mitali Deka)

**Place-** Guwahati



## GAUHATI UNIVERSITY

Department of Chemistry  
Gauhati University  
Guwahati – 781 014  
Assam: India

Email: dkk.chem@gauhati.ac.in  
Mobile: (0) 98643-28857  
Email: dilip\_kakati2003@yahoo.co.in

---

D. K. Kakati, Ph.D. (LONDON) DIC  
Professor

### CERTIFICATE

This is to certify that the review work on “Ionic liquid based hydrogels” compiled by Mitali Deka, in partial fulfillment of the requirement for the degree of Master of Science was done under my supervision. I would also like to certify that the survey work submitted herein is the result of extensive literature survey carried out independently by her.

I wish her success in life.

(Dilip Kumar Kakati)

Date: 08-09-2021

## ACKNOWLEDGEMENT

*I feel immensely privileged to take this opportunity to acknowledge my profound sense of gratitude and regards to my esteemed guide, **Dr. Dilip Kumar Kakati**, Professor, Gauhati University, for his valuable guidance and supervision throughout the project work. He has been a constant source of inspiration, guidance and supervision without which my task of preparing the project report would not have been possible. I am extremely grateful to him for his constant encouragement and relentless support at each and every step of my project work. I want to express my deep sense of gratitude and heartfelt thanks to him.*

*I feel indebted to Dr. Citrani Medhi, Head of the Department of Chemistry, for providing the necessary facilities required for preparing this project report.*

*Finally, I wish to express my special thanks to my friends who always encourage me in any situation whenever needed to prepare this report.*

Date: 08/09/2021

**Mitali Deka**

Roll no: PS-191-808-0073

M. Sc. 4<sup>th</sup> Semester

Department of Chemistry

Gauhati University

# CONTENTS

## 1. Introduction

1.1 Hydrogel.....	1
1.2 Classification of Hydrogels.....	1-2
1.3 Characteristic features of Hydrogels.....	2
1.4 Ionic liquids.....	2-3
1.5 Ionic liquid based .....	4
1.6 Importance of Ionic liquid based Hydrogel.....	4-5
1.7 Applications of Ionic liquid based Hydrogels.....	5

## 2. Literature Review

2.1 Introduction.....	6
2.2 ILs Hydrogels as Adsorbent and Catalyst.....	7-11
2.3 Polymerized Ionic liquid Hydrogels in Medical fields.....	11-14
2.4 Thermoresponsive Poly(ionic liquid) Hydrogels.....	14-16
2.5 Rheological properties of IL Hydrogels.....	16-17
2.6 IL/PILs based Hydrogels as flexible electrolytes and devices.....	17-19

## 3. Conclusion.....20-21

## 4. References.....21-24

# **CHAPTER 1**

## **INTRODUCTION:**

### **1.1 Hydrogels-**

Hydrogels have received considerable attention in the last few years, both from academia and industries, because of their potential applications in several areas. These polymers swell in water and have partially cross linked polymeric structure where the fluid or dispersion medium is water. In 1960, hydrogel was first reported by Wichterle and Lim <sup>[1]</sup> fundamentally hydrogel is a three dimensional network of hydrophilic polymers that can swell in water and grasp a large quantity of water while maintaining the structure due to chemical or physical cross linking of individual polymer chains. These are prepared by simple reaction of one or more monomers through association bonds like hydrogen bonds and strong van der Waals interactions between polymeric chains. The water content in hydrogels by definition must be at least 10% of the total weight or volume of the material. Due to their significant water content the hydrogels also have a comparable degree of flexibility as natural tissue. The hydrogels possess hydrophilic nature due to the presence of hydrophilic groups such as  $-\text{CONH}$ ,  $-\text{NH}_2$ ,  $-\text{COOH}$ ,  $-\text{SO}_3\text{H}$ , and  $-\text{OH}$ , <sup>[1]</sup>.

Exploiting the chemical and/or physical cross linking it is possible to modulate the properties like surface morphology, hardness, resilience to temperature, stiffness, biocompatibility, biodegradability, self healing behavior which makes them attractive materials for medical applications<sup>[2]</sup>.

Hydrogels can undergo significant volume phase transition or gel- sol phase transition in response to physical stimuli like temperature, electric and magnetic fields, solvent composition, light intensity, pressure and chemical stimuli like pH etc. In most cases the conformational transitions are reversible and therefore the hydrogels are capable of returning to their initial state after a reaction as soon as the trigger is removed. The response of hydrogels to external stimuli is mainly determined by the nature of the monomer, charge density, the degree of cross linking. The magnitude of response is also directly proportional to the applied external stimulus.

### **1.2. Classification of Hydrogels-**

Hydrogels can be divided into different classes on the basis of different parameters.

1. Hydrogels could be particle, powder, membrane, crystalline, semi crystalline and emulsions in nature on the basis of configurations.

2. Hydrogels can be divided into two categories, on the basis of physical or chemical nature of the crosslinks.
3. The hydrogel can be divided into natural, semi synthetic polymer or synthetic in accordance with the nature of chemical used for its synthesis.
4. The hydrogels can be divided on the basis of type of polymerization methods used such as graft polymerizations, cross-linking polymerization and radiation polymerization.
5. Hydrogels can also be classified according to electrical charge located on the cross-linked chains such as (a) nonionic, (b) ionic, (c) amphoteric and (d) zwitterionic.
6. On the basis of polymeric compositions hydrogels can be classified as (a) homopolymeric hydrogels (b) copolymer hydrogels, (c) multipolymer interpenetrating polymeric hydrogels.
7. Hydrogels are called “smart materials” if they are responsive to the change in the environment. Smart hydrogels are classified according to their sensitivity to temperature, electric current, light, sound, magnetic field, and pH.

### **1.3. Characteristic features of hydrogels:**

- They have quite good absorption capacity
- They show highest absorbency under load.
- Low soluble content and residual monomer.
- They show pH neutrality after swelling in water.
- They have durability and stability in the swelling environment and during the storage.
- They are biodegradable without formation of toxic species following the degradation.
- They possess rewetting capability.
- They are colorless, odorless, non-toxic in nature and possess photo stability.<sup>[3]</sup>

### **1.4. Ionic liquids:**

In 1994, the first ionic liquid ethyl ammonium nitrate was developed by Paul Walden. Ionic liquids are non-molecular compounds solely composed of ions, in which the ions are poorly coordinated, which results in these solvents being liquid below 100° C or even at room temperature ( room temperature ionic liquids, RTIL's ).<sup>[5]</sup> At least one ion should have delocalized charge and another part is organic, which helps in preventing the formation of a stable crystal lattice. These substances are also termed as ionic fluids, liquid electrolytes, ionic melts, fused salts, ionic glasses, or liquid salts. Ionic liquids are organic salts that contain organic cations such as pyridinium, imidazolium, pyrrolidinium or ammonium derivatives.<sup>[6]</sup> These can be associated with

organic anions such as  $\text{CH}_3\text{COO}^-$  or inorganic anions such as  $\text{Cl}^-$ ,  $\text{Br}^-$ ,  $\text{I}^-$  or  $\text{BF}_4^-$  to prepare a particular IL.

They are typically moderate to poor conductors of electricity, non ionizing, highly viscous and frequently exhibit low pressure. Their other properties are low combustibility, excellent thermal stability, wide liquid regions, and favourable solvating properties for a wide range of polar and non polar compounds.

These are extensively used in organic chemistry, electrochemistry, catalysis <sup>[4]</sup>, physical chemistry, and life science and material science. They are outstanding green solvents and electrically conducting fluid. Salts that are liquid at near ambient temperature are important for electric battery applications, and have been considered as sealants due to their very low vapour pressure. Approximately 50% of commercial pharmaceuticals are organic salts; ionic liquid forms of number of pharmaceuticals have been investigated. Combining a pharmaceutically active anion leads to a Dual Active ionic liquid in which the actions of two drugs are combined.

Ionic liquids have earned a great deal of interest in academic research field as they possess unique physiochemical properties such as high ionic conductivity, non-flammability and thermal, electrochemical and chemical stability. Moreover, their freezing points can be tuned by adjusting the respective structures of the paired organic cation and inorganic or organic anion. All the properties of ionic liquids make the scientist to study the synthesis and utilisation of ionic liquids for the development of the diverse fields from academic research to industrial research. The ionic liquids being electrochemically stable over a great potential range are good candidates to be studied for application in supercapacitors, electrochemical and biosensor, batteries.

Ionic liquid also possess biocompatible behaviour as they can form hydrogen and electrostatic interactions with biomolecules and can be used in immobilisation and stabilization of enzymes, proteins and living cells thus retaining the activities the of the biomolecules for a longer period of time. Researchers of various fields of chemistry are interested in ILs as it can be used as a “green solvent” minimising the hazardous effect of the conventional solvents that are being used in many industries.

Though ILs contains so many attractive properties yet it has some disadvantages too. These are relatively expensive, have low recovery from the reaction mixture and are not reusable. Thus development of less costly ionic liquids has a great importance for the large scale application of ionic liquids in catalysis and electrochemistry. In recent year poly (ionic liquid) is getting more importance in the fields of catalysis, energy and environmental applications, analytical chemistry, material science etc. These poly (ionic liquid) are basically formed by the polymerization of IL monomeric repeating units linked to polymeric backbone. The research on PILs discloses many novel properties and applications, such as:

- Engineering-coatings, lubricants, dispersing agent, compatibilities, plasticizer.
- Biological- drug delivery, biocides, biomass processing, embalming.
- Electrochemistry- batteries, metal plating, solar panels, fuel cells.
- Solvent and catalysis, nanochemistry, microwave chemistry.

### **1.5. Ionic liquid based Hydrogels:**

Ionic liquid hydrogel is a composite material consisting of an ionic liquid immobilized by a hydrogel. The composite material shows quality of maintaining high ionic conductivity in the solid form. After polymerization with ILs due to ionic interactions inside the ionic liquids, these hydrogels combine strong and weak crosslinks. The hybrid hydrogels formed are tough, stretchable, flexible and self recoverable in nature. Many mechanical tests done on different ILs hydrogels has certified the superior mechanical properties.

The basis of cross linking of ionic liquids is that reactive functional groups in it contain cations and anions. Due to these ionic crosslinking agents ionic liquids gets the advantageous properties such as conductivity, thermal stability, low volatility in the crosslinked polymer. In addition this will increase the hydrogen bond sites in the polymeric matrices. This is helpful to improve the swelling rate and mechanical properties of the hydrogels. The extra level of design provided by the ionic liquid enhances the tunability and the strength of the gel. The high cost of ionic liquid cross linking agent and not so easy degradability in normal environment which can bring environmental protection issues could be the major disadvantages of this hydrogels.

However , the nature and properties of this ILs hydrogels yet to be fully explored and further studies should be carried out on the role ionic liquid plays in the structural properties of the gel-based materials as it is poorly understood . The topic is still in its early stage so further studies are expected to be done on the various properties and applicability of the ILs hydrogels.

### **1.6. Importance of Ionic Liquid based Hydrogel:**

The hydrogels that are based on ionic liquids show some excellent electrochemical properties which remain stable under different phenomena like bending, folding, compressing or twisting. The combination of properties of hydrogel ( such as biocompatibility, great mechanical strength ,flexibility, good swelling properties) and ionic liquid ( ionic conductivity, great chemical and thermal stability, negligible volatility, non-toxicity, biodegradability) gives ionic liquid hydrogels huge applicability in a diverse field of science which could be academic to industrial, medical to commercial applications.



These polymeric gels are of great importance in the field of medical or pharmaceutical industries as drug delivery systems, as antibacterial material, bone substitutes, coatings, contact lens and implants. They are also industrially important materials as they can be used in manufacturing smart electronic devices such as actuator and sensors. Also PIL hydrogels have been used in immobilization of enzymes and organocatalysts. Also these materials have importance as chemical absorbent. The removal of toxic heavy metal found in aqueous media which are produced from different industrial processes can be done by this hydrogels more easily. The reduction of heavy metal pollution from water sources have great scientific and practical significance and thus important for good ecological and environmental as well as public health. So many ILs/PILs hydrogels are being studied to know more about the structural properties of these gels and enhance the use of these polymeric gels in various fields.

### **1.7. Applications of Ionic Liquid based Hydrogels**

The properties like freeze- resistance, heat resistance, high tensile strength, biocompatibility, flexibility makes the ionic liquid based hydrogels applicable on many fields from industrial to biological field. Such applications of this hydrogel are listed below:

- Poly ionic liquid based hydrogel coatings support the formation of a full covering cell layer and may therefore have a mitigating influence on the foreign body reaction to implants. In combination with mechanical properties and the ability to swell in water contact, hydrogel coatings are of special interest for implant applications such as stent or pacemaker coatings.
- Hydrogels based on ionic liquids can be applied as conductor material. (ionic liquids have excellent ionic conductivity up to their decomposition temperature.)
- Poly (ethylene glycol) dimethacrylate based hydrogels are used as potential bone regeneration material.
- Antibacterial wound dressings play an important role in wound healing and infection treatment. The poly (ionic liquid) hydrogel dressing does not release antibacterial agents. Since this hydrogel dressing exhibits effective antibacterial ability and good mechanical property, thus these can be used as antibacterial wound dressing.
- Vinylimidazonium based poly (ionic liquid) hydrogel in comparison to natural polymer hydrogels are better for catalyst immobilisation.
- This IL hydrogels are proven to be good dye adsorbent, thus can be used in heavy metal removals, toxic components removals from various effluents, recovery of dyes.
- These materials can be used in production of actuators and sensors.

## **CHAPTER 2**

Presented below a literature review on several aspects of ionic liquid based hydrogels.

**2.1. INTRODUCTION:** A hydrogel is a three-dimensional (3D) network of hydrophilic polymers that can swell and store a considerable amount of water while preserving structure due to chemical or physical cross-linking of individual polymer chains. Because of their tunable mechanical properties, excellent electrical conductivity, and low interfacial resistance, hydrogels have such a lot of potential.

For practical applications, hydrogels with exceptional strength and broad thermal compatibility are desired, and in the last decade, significant progress has been made in preparing tough hydrogels utilising a number of methodologies.<sup>[7-9]</sup> Double-network (DN) hydrogels, which have a brittle initial sacrificial network and a tough, covalently cross-linked second network, have the highest elasticity and toughness of all of them.<sup>[10-11]</sup> Li et al. developed alginate-polyacrylamide-based DN hydrogels with ionic and covalently cross-linked polymeric networks. The elastic modulus and fracture energy of the DN gel were both high. Most DN gels are prepared using a two-step procedure, according to Kamio et al., which results in inhomogeneous spatial network clusters within their respective parent-gels, restricting the improvement of mechanical qualities.<sup>[12]</sup> Li et al. further mentioned that controllable gelation allows for the formation of a more homogenous sacrificial network in a single stage, which increases the resilience and fracture energy of DN gels.<sup>[13]</sup> As a result, developing a one-step, controlled polymerization process for preparing DN gels under ambient circumstances is desirable.

Hydrogels had previously been observed to freeze at sub zero temperatures and dehydrate at high temperatures, both of which significantly limit their practical applicability. Anti-freezing and non-drying hydrogels for long-term applications have been found to be due to the utilisation of an organic solvent system.<sup>[14]</sup> For practical applications, freeze- and heat-resistant gels are preferred.

Ionic liquids (ILs) are composed of cation-anion pairings of an organic ion and inorganic counter ion.<sup>[15]</sup> Because of their extraordinary physicochemical features, such as strong ionic conductivity, non-flammability and thermal, electrochemical and chemical stabilities, they have attracted a lot of interest in academic research. Furthermore, by modifying the structures of these paired cations and anions, their freezing points can be adjusted. Poly (ionic liquid)s (PILs) are polymers with IL monomers as their backbones. PILs have received a lot of attention in the polymer and materials sciences because they combine polymer chain durability with small-molecule IL functionality.

## 2.2. ILs hydrogels as adsorbent and catalyst

Hydrogels are recognized as efficient adsorbent materials for the removal of heavy metal ions from the polluted water due to their available design at a molecular level, swelling network for guest molecule diffusion and convenient operation. Traditional hydrogels produced by traditional polymerization methods (i.e. free radical copolymerization of vinyl monomers and cross-linking monomers) typically have such a random cross-linked network structure, which leads to entanglements of their molecular chains and trying to bury the adsorption sites in the interior of the network, limiting the hydrogel's adsorption performance. Recent research on hydrogel adsorbents has concentrated on the design and fabrication of innovative network architectures that favour the exposure of internal adsorption sites in order to improve adsorption capacity. Hyperbranched topology is a promising option for enabling the exposure of internal functional groups and increasing the use of internal functional groups on guest molecules due to their three-dimensional highly branched structure and numerous intramolecular cavities.

Another major strategy for improving the adsorption capabilities of hydrogels is to increase the interaction between functional groups and adsorbates. A large number of studies have demonstrated that using ILs-based functional groups as adsorption sites in adsorbents can greatly improve their adsorption performance due to their superior structural tunability and strong interaction with pollutants.<sup>[16,17]</sup> By using  $\gamma$ -radiation-induced polymerization, a new polymeric ionic liquid gel (PIL gel) for the removal of hazardous pollutants has been developed. Through anion exchange, the resulting PIL gels demonstrated enhanced Cr (VI) adsorption capacity. Similarly, Khiratkar et al. developed and synthesised a benzimidazolium-based PIL for the removal of Cr (VI) from wastewater using a copolymerization and alkylation procedure. With a maximum adsorption capacity of 40 mg g<sup>-1</sup>, the developed PIL demonstrated good adsorption ability.

In 2018, Miao et al. developed a novel imidazolium-based ionic liquid hydrogel containing hyperbranched topology for the first time via a one pot A<sub>3</sub>+B<sub>3</sub> method.<sup>[18]</sup> The resulted hbGel-PEG-TTIm<sup>+</sup>Br<sup>-</sup> showed advantages of facilitating the exposure of internal IL functional groups and increasing the utilization of internal functional groups on guest molecules. Compared with other adsorbents, hbGel-PEG-TTIm<sup>+</sup>Br<sup>-</sup> possessed fast and efficient adsorption properties with the maximum adsorption capacity of appx. 238 mg g<sup>-1</sup>. Adsorption kinetics and isotherm results indicated that the adsorption process of Cr (VI) by hydrogels was chemical adsorption and monolayer adsorption. In addition, the recycling experiment proved that the hydrogels had good reusability. Yildiz et al. done a research on IL hydrogels for in situ metal nanoparticle preparation of Co and Cu and then used as catalyst for the reduction reactions of 4-nitrophenol, 4-nitroaniline,

and 4-nitrobenzaldehyde to their corresponding amines.<sup>[19]</sup> The ILs hydrogel templates were based on inherently cationic p (APTMAcI) matrices with different size and morphologies, such as microgel, bulk gel, and cryogel. They prepared matrices of different dimensions and porosities with same monomer and crosslinker but employing different polymerization techniques and catalytic performance of their metal nanoparticle-containing forms for nitro compounds were determined. The rate for the reduction of nitro compound found to be depending on the hydrogel dimension and morphology, as well as the metal nanoparticles. In this investigation it was found that the activation energy for the reduction of 4-NP was 44.74, 34.02, and 40.7 kJ mol<sup>-1</sup> catalyzed by p(APTMAcI)-Cu IL composite bulk gel, cryogel, and microgel, respectively, signifying the role of porosity due to the lower activation energy obtained for cryogel composite systems. In addition, the TOF values for 4-NP reduction catalyzed by p(APTMAcI)-Cu IL composite at various reaction temperatures (30–70 °C) varied between  $0.59 \pm 0.01$  and  $6.71 \pm 0.51$  mol 4-NP (mol catalyst min)<sup>-1</sup>, and found to increased with the increase in reaction temperature. The p(APTMAcI)-Cu IL composite cryogel and microgel catalyst systems gave the highest TOF values. The p (APTMAcI) IL composites were also very effective in the reduction of other nitro compounds containing different functional groups. In a nut shell, This study demonstrated that the p(APTMAcI)-M (M: Co and Cu) IL composite hydrogels with variable sizes and morphologies offer great potential for diverse metal nanoparticles in addition to Cu and Co and can be used for a variety of catalytic reactions in the synthesis of organic compounds or for environmentally toxic species.

Some of the best characteristics of the ionic liquid hydrogel as an appropriate candidate for absorption of nanoparticles is that they are environmental friendly and insensitive to toxic particles as well as they are low in cost and have high efficiency ; which helps them gaining huge interest. As conventional ILs hydrogels show some drawbacks like brittleness and mechanical defects, Lv et.al prepared novel entrapped pattern and structural transformation of ILs within a copolymer of acrylamide/*N,N*-dimethylaminoethyl methacrylate bromododecan hydrophobic monomers p(AM/DMLB)- based hydrogels through changing the filling pattern of ILs to form hydrophobic association of hydrogels.<sup>[46]</sup> The resulted hydrogels possessed high mechanical properties, tensile strength, elongation and toughness reached 0.49MPa, 23005, and 4.9MJ/m<sup>3</sup>, respectively. The properties such as biocompatibility, remoldability and fatigue resistance give the p(AM/DMLB)ILs-LPs hydrogels/Pd with recycled and reused performances, enabling sample with any desired shape and ability to act as catalysts for promising convenient applications. Thus, the pioneering design tactic for ionic liquids' latex sphere particles as the only joint center of a dual physically cross-linked network could be used to build up tough and stretchable hydrogel materials for catalytic use in manure disposal industry. Li and coworkers prepared cellulose/chitosan

hydrogel bead by extruding and regenerating the blends from IL 1-ethyl-3-methylimidazolium acetate ([Emim]Ac) in ethanol.<sup>[20]</sup> The analysis found that the beads were nonporous with diameter from 10 to 20 nm with maximum adsorption capacity of 40 mg/g for congo red (CR) dye removal from aqueous solutions, which was more proficient than most of the natural biosorbents that has been reported. This efficient adsorption property of the cellulose/chitosan hydrogel beads can be used in removal of dye contaminant from wastewater. Hydrogels due to their assortment of highly fascinating properties like tautness, surface hardness, pliability to temperature and solvent attacks as well as the swelling behavior and biocompatibility, they are of great interest in the medical and pharmaceutical industry as well as in the other engineering aspects.

Since hydrogels exhibits properties like biocompatibility, non-toxicity, biodegradability and potential self healing nature the hydrogel based materials are attractive for medical purposes. By controlling the mechanical properties and swelling behavior we can use hydrogels in a variety of aspects. It is important to study the swelling properties and diffusion mechanism happening in this material for the optimal applications. Ann Jastram and coworkers studied the swelling and diffusion behavior of the hydrogel synthesized by radical polymerization of imidazolium-based ionic liquids via gravimetric swelling as well as sorption experiments implanted in water, ethanol, n-heptanes and THF. <sup>[21]</sup> They found strong swelling in water and ethanol, and also found that the varying counter ion and chain length of the cation influences the process. It was observed the diffusion coefficient delivered values in the range of  $10^{-10}$  to  $10^{-12} \text{ m}^2 \text{ s}^{-1}$ . A visualization of the water diffusion front within the hydrogel should help to further illumination the diffusion acquire in the imidazolium – based hydrogel.

A current approach for more durable and stable hydrogel synthesis is the use of monomers derived from ionic liquids which are polymerized to yield polyelectrolyte. These compounds are of huge interest as the innate properties can be easily fine tuned by carefully selecting and combining different ionic functionalization to specifically exploit the advantages of both ionic and solid polymer structure, enhancing mechanical stability, improved processibility and durability. Moreover ionic liquids carry excellent ionic conductivity up to their decomposition temperature. Therefore ionic liquid based hydrogels can be applicable as conductor material. In addition polyionic liquid based hydrogel coatings support the formation of full covering cell layer, and may therefore have extenuating influence on foreign body reaction to implants. Thus the hydrogel materials are suitable matrix for cell growth due to their excellent biocompatibility and outstanding mechanical strength.

The recent advancement in the use of ILs in synthesizing polymeric gels (ionogels) and smart hydrogels mainly involve ILs and PILs that are stimuli responsive such as magnetic field, critical solution temperature, pH, and thermo reversibility. The tunability and flexibility of ILs associated

with the features of natural polymer such as chitin or cellulose and/or synthetic polymers have attracted scientist to study them and disclose new paths to process them not only as hydrogels, but also as matrices with different shapes and sizes.<sup>[22]</sup> Polymeric hydrogels processed in ILs can be useful for a wide range of applications from the elimination of anionic dyes to biomaterials. However, with reference to biomedical applications, despite showing potential result, little has been reported concerning the in vitro and in vivo biocompatibility of the developed matrices, which could limit their possible use as biomaterials.

A good number of the study that has been reported suggests the use of ILs as a tool not only in the dissolution or processing of polymers in large amount of matrices but also to pull out biopolymers directly from biomass promoting the economic reduction of the process as well as the increase in the quality of the obtained biopolymer. The PILs synthesis has also making ways to certain developments in the creation of responsive hydrogels though the developments are in their early stage. Still more developments are being expected in near future.

Polymer composed with ILs often shows responsive phenomena. Thus, SR hydrogels have also been developed by assimilation of thermo sensitive polymers like PNIPAAm and PBzMA into PILs. PNIPAAm is the extensively studied thermo sensitive polymer in temperature responsive hydrogels and shows a lower critical solution temperature (LCST)-type phase separation in aqueous solutions at almost same with the body temperature. These kinds of materials have potential use in highly diverse areas ranging from controlled drug release to chemo-mechanical actuators or sensors, catalysis, and other applications.<sup>[23]</sup>

The fusion of ILs with polymers allows the creation of smart soft materials. T. Ueki has reviewed the thermodynamic aspects and recent developments in stimuli-responsive polymers in ILs, as a new class of smart soft materials.<sup>[24]</sup> It is suggested that polymers in ILs need extended periods to get thermodynamic equilibrium as a result of the high viscosity of ILs. Thus, the viscosity of polymer/IL composites must be concealed to achieve a fast response time for the ensuing soft materials.

PILs have also been used as a way of finding dual-responsive hydrogels. These systems are produced by incorporating two functional monomers that respond to different stimuli, offering additional functional control. Gallagher and coworker described the sIPN hydrogels prepared by using different concentrations of linear pNIPAAm incorporated into a thermally responsive PIL hydrogel tributyl-hexyl phosphonium 3-sulfopropylacrylate (P-SPA).<sup>[25]</sup> The swelling and shrinking responses of the hydrogels prepared were modulated by the presence of linear pNIPAAm in the polymer matrix.

Feng and co-workers prepared dual-responsive highly swellable hydrogels, that were consisted of thermo-responsive PNIPAM and redox-responsive poly (ferrocenylsilane) (PFS)-

based PILs, which were produced by photo-polymerization.<sup>[26]</sup> By changing the counter ion type the swelling ability and thermo-responsivity of the hydrogels could be tuned. It is due to the presence of the poly (ionic liquid) part. This hydrogel has been in use as a reducing environment for the in situ fabrication of gold nanoparticles (AuNPs), forming AuNP–hydrogel composites. Another report of preparation of responsive PILs based hydrogel has been described by Tudor et al, where semi-interpenetrating (sIPN) hydrogels were synthesized by adding escalating amounts of poly(N-isopropylacrylamide-co-spiropyran-co-acrylic acid) to a cross-linked PIL template. All of the hydrogels, polymerized for approximately 120s, have different mechanical properties which can be modulated through the content of the copolymer.

According to other authors PNIPAAm-based ionic hydrogels could be synthesized by free-radical polymerization with N-isopropylacrylamide (as a monomer) and imidazolium-based dicationic IL (as a cross-linker).<sup>[27]</sup> The hydrogels obtained from the synthesis had good swelling properties and exhibited strongly interfacial interaction with anionic dyes such as thymol blue, methyl blue, methyl orange, orange G, Congo red and bromothymol blue in aqueous solution. This performance was dependent on the chemical structure of the anionic dyes in solution.

### **2.3. Polymerized Ionic Liquid based Hydrogels in Medical fields:**

Smart hydrogels which undergo structural changes in response to pH, temperature or light have promising biomedical applications as delivery systems, particularly for the locally controlled discharge of drugs. To omit the cytotoxicity, poor solubility, and biodegradability of components of the conventional electroconductive hydrogels, engineering of new kind of hydrogels are must needed. Noshadi et al. reported a Bio-IL conjugated hydrogel with high tunability, high electrical conductivity and biocompatibility, which can be implemented in different tissue engineering as well as biomedical applications.<sup>[28]</sup> Fang et al reports an easy approach to synthesis a antimicrobial PIL/PVA hydrogel wound healing dressing with high strength of chemical polymerization and physical crosslinking.<sup>[29]</sup> Yu et al. designed multifunctional antibacterial hydrogel where pyrrolidinium IL was used as antibacterial drug, where they found that hydrogels that contains ILs with longer alkyl chain shows great antibacterial properties.<sup>[30]</sup>

Mounting demand in controlled release of drugs in pharmaceutical industry requires growth of new and consistent drug delivery system. Embedding of drugs in hydrogels can be the cleverest way of drug delivery. Such ground-breaking systems allow the smart delivery of bioactive molecules from drugs for an oral route of administration. Synthesis of stable poly (ionic liquid) based hydrogel as drug carrier by radical polymerization according to Mildner et al. showed reversible compression up to 90% without crack formation. Initial findings also show little to no toxicity subsequent to polymerization.<sup>[31]</sup> A elevated mechanical strength and with a favorable pH

dependent swelling behavior is also required. There could be more than a few variation potential during the synthesis causing crucial effect on the synthesis of the hydrogel like content and type of cross-linker, water content and the ionic liquid. Researchers has developed a hydrogel which was imidazolium- based ionic liquid bearing a vinyl group is polymerized with cross linker *N,N'*-methylenebisacrylamide. <sup>[32]</sup> The embedding of a drug can be achieved by adding a dynamic pharmaceutical element. The properties of the yielded hydrogels depend on several factors such as preparation methods, volume fraction of polymers, degree of cross linking, length of cross-linker chain and swelling agent. The mechanical properties of the hydrogels are chiefly controlled by the type of monomer and are only somewhat dependent on the type of cross-linker. By adjusting the concentration of monomer and cross-linker; desired mechanical properties can be achieved. Moreover the drug release can be controlled pH- dependent swelling behavior. A noteworthy lower swelling can be achieved by decreasing the pH-value of the solution. By functionalizing the PIL's- based hydrogels an increased pH responsive drug release can be obtain. Recently Kuddushi and co-workers have developed a pH and temperature dual – responsive smart polymeric hydrogel with an ester – functionalized ionic liquid (C<sub>16</sub> EMorphBr) as one of the additives to advance the efficiency of anticancer drug doxorubicin encapsulation and localized delivery. <sup>[33]</sup> The in vitro cytotoxicity and drug release study was depicted by measuring the swelling and phase transition performance of the hydrogel under temperature 37° C and pH 5.0. The final results showed that the hybrid hydrogel based on ionic liquid is more effectively killed cancerous cells, and the targeted release of doxorubicin occurred at intercellular acidic pH. DOX- infused polymeric hydrogels give respond to intracellular biological stimuli, showed higher encapsulation, cytotoxicity and drug uptake towards the MCF-7& HeLa cell lines. A selective drug release from hydrogels at particular location in a specific time duration in order to control period of action while derogating unwanted effects outside the site of action; is the basic concept behind the development of the ILs or PILs - based hydrogel which are able to omit the disadvantages of the existing intelligent hydrogels.

Till now researchers have been synthesised quite a good amount of PILs-based hydrogels that have medical importance as a drug releaser. It has been showed that mechanical properties hydrogel are affected by IL monomer, composition, cross-linking density degree of drying or swelling. Simultaneous absorption of water and desorption of a drug via swelling controlled diffusion mechanism is the one of the key factor of drug release. Batra and co-worker described preparation and polymerization of IL based on methylimidazolium which was incorporated in the terminus C<sub>8</sub> alkyl chain of an acryloyl moiety. <sup>[34]</sup> The hydrogel prepared by self assembly and polymerization of IL, was demonstrated to adopt ordinary lamellar structure when studied under SAXS. Studies showed that this polymer can show good swelling property with large amount of



water absorption also swelling studies showed that this polymer can be swollen by a range of organic solvents. PILs based hydrogels have also been reported as anti-bacterial agent. PILs based on imidazolium, quaternary ammonium, and pyridinium and have special effects against a wide range of bacteria as well as fungi and algae. Combining the designable properties of both PILs and hydrogels; hydrogels based on poly(ionic liquids) they have been showing mechanical properties as well as good biocompatibility and been used for the immobilization of enzymes as well as other medical applications like drug delivery systems, materials for contact lenses and tissue engineering. Claus et al has described the inherent antibacterial activity of 11 different polymerized ionic liquid based hydrogels as well as their corresponding monomers in a broad screening.<sup>[35]</sup> In that study two distinct representative of gram-positive and gram-negative bacteria respectively (methicillin- resistant) MRSA Xen 30 and *P. aeruginosa* Xen 5 were chosen as test microorganisms. Out of the 11 monomers six were able to wipe out more than 80% of *P. aeruginosa* Xen 5 cells in suspension. The antibacterial property of the cationic gels retained with just about 100% eradication of chosen microorganisms even at least amount tested, but after polymerization the anionic, neutral and zwitterionic representatives lost their functionality. By cross linking them to three dimensional networks can be possible way to improve the weak antibacterial activities. The result that the researchers had found clearly incited that the hydrogels possessed strong killing efficiencies of at least 68% and even at low hydrogel volume fractions, the PILs hydrogels were able to maintain activity

The killing efficiency of the PILs based hydrogels can be found in their mechanism of action. There is a possibility that the studied monomers probably interact with certain components of the cell membrane unlike the conventional antibiotics that exerts their antibacterial activities by inhibiting DNA replication and RNA synthesis of essential metabolites or blocking bacterial protein synthesis. The scientist have assumed that the cationic substances come into contact with the negatively charged phosphate and carboxylate groups of the cell wall by means of electrostatic interactions and ultimately the storage of the hydrophobic parts of the compounds resulting in the cell death. So the cationic species increased with the intensity of the interactions. Evidently cationic monomers such as poly (TMA-VB) and Imidazolium based hydrogels have terrific killing efficiencies of at least 97.7%. Poly (AE-TMA) and poly (MAE-TMA) also had a fine effect, killing approximately 72% of bacteria. Among all the monomers used in the experiment Poly (VEImBr) showed best performance with cell viability ~98%.

For an adequate application it is crucial to know the length of time of action. It was found that Imidazolium – based hydrogels as well as poly (TMA-VB) retained their killing efficiencies of 100 % for at least one week. Furthermore, it could be shown that storing the hydrogels in an airtight container for 14 days does not have a major effect on the antibacterial effect. Incubation

tests proved that the inherent antibacterial activity of monomers and hydrogels lasts for several days. That means freshly prepared or stored hydrogels both are equally useful. Studies have showed that all hydrogels with a cationic framework have a very good intrinsic antibacterial activities against both gram negative and gram positive bacteria. Imidazolium based hydrogels have outstanding antibacterial properties with killing efficiency 95%. Poly (VBI<sub>m</sub>Cl) and poly (VBI<sub>m</sub>Br) have high killing effects even at the lowest hydrogel content.

Poor mechanical properties of self-healing hydrogels limited their biomedical and industrial applications. He et al. has prepared and studied a series of self-healing polymeric ionic liquid (PIL) hydrogels. These PILs based hydrogels with high mechanical strength and electrical conductivity were produced through hydrophobic association. In the production of these hydrogels hydrophilic monomer vinyl ionic liquids (VILs) based on choline and amino acids, acrylamide (AAM) and hydrophobic monomers stearyl methacrylate (C18) were copolymerized in a micellar solution of sodium dodecyl sulphate (SDS).<sup>[36]</sup> The bacterial cellulose was introduced to improve the mechanical strength of hydrogels. The prepared hydrogels, without any external interference showed outstanding mechanical strength of 5.8 MPa, extensive elongation property and excellent self-healing efficiency which is up to 85%. They found that tensile strength of most hydrogels could reach 2.5–3.9 MPa after healaton and because of the incorporation of ILs in hydrogels, resultant hydrogels possessed good electrical conductivity (a maximum of 1.258 S/m). Nunes et al. used [Hmim][HSO<sub>4</sub>] ionic liquid (IL) and bio-renewable sources as chitosan (CHT) and chondroitin sulfate (CS) to yield hydrogel-based materials (CHT/CS).<sup>[37]</sup> CHT/CS blended hydrogels characterized and achieved with excellent stabilities (in the 1.2–10 pH range), well-built swelling capacities, as well as devoid of cytotoxicity towards the normal VERO and diseased HT29 cells indicating various applications in many technological purposes, like medical, pharmaceutical, and environmental fields.

#### **2.4. Thermoresponsive Poly (ionic liquid) Hydrogels**

Gel materials where the polymeric network is filled with ionic liquid phase may attain some remarkable properties due to the combination of characteristics of polymer and with those of IL. Researchers demonstrated that the thermo-responsive PIL hydrogels can be used as smart draw agent for forward osmosis desalination.<sup>[38,39]</sup> These include appearance of Lower Critical Solution Temperature (LCST) of the gel network that allows the shrinkage of the gel when temperature is raised higher than the LCST. LCST behavior arises mainly due to the changes in the hydration forces between the polymer chain and aqueous medium, and the attractive forces between the polymers chain themselves.<sup>[40]</sup> Recently LCST behavior has been reported PILs and due to such temperature sensitive behavior new potential for using these PILs as well-designed fluids has been

opened up. Amusingly out of many different cation–anion combinations, the majority of the thermoresponsive ILs reported are based on variation of phosphonium cations, such as tetrabutyl or tributyl-hexyl phosphonium. The most frequent anions used to make LCST ILs are mainly the derivatives of benzenesulphonic acid.

A new and captivating family of thermoresponsive monomeric ILs have been used to synthesize first ever thermo responsive poly IL hydrogel. This hydrogel display surprisingly broad LCST and volume transition manners compared to standard thermoresponsive gels and linear ILs. With increasing gel cross linker concentration showed some decreasing LCST property.<sup>[22]</sup> It has been anticipated that these thermoresponsive monomeric ILs can be polymerized into hydrogel to form thermoresponsive poly IL hydrogels and these materials should act similarly to the well known thermoresponsive poly (*N*-isopropylacrylamide) (NIPAAm) hydrogels, but modifications in properties due to the presence of IL component. These materials with the temperature sensitive behavior disclosed new possibilities for using them as functional fluids, microfluid flow controller and actuators, controlled absorber, release and delivery materials etc.

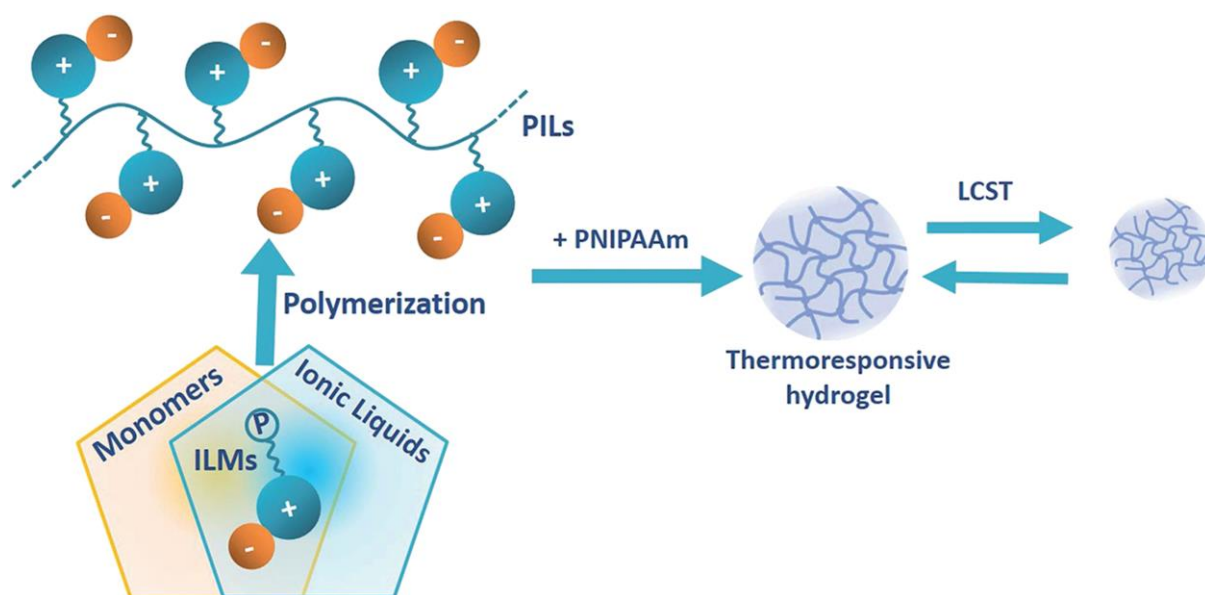


Figure: Schematic illustration of the relationship between ionic liquids and Poly (ionic liquid)s, and the formation of a thermoresponsive hydrogel. Adapted from *Progress in Polymer Science*, J. Yuan, D. Mecerreyes, M. Antonietti, Poly (ionic liquid)s: An update, 1009–1036

In recent years, several groups have demonstrated the microfluidic integration of a variety of stimuli – responsive materials that respond to changes in their external environment, such as temperature, light, pH, or variation in electrical potential and pressure. Tudor et.al for the first time, of the phosphonium based crosslinked PIL tributylphosphonium sulfpopropylacrylate (PSPA) to produce a poly (ionic liquid) hydrogel that features a lower critical solution temperature.<sup>[41]</sup> The depiction of the hydrogel indicates that the hydrogel shrinks by up to 58% of

its swollen area when temperature is raised from 20 to 70° C and when the temperature is raised from 20 to 50° C it shrinks up to 39% . The shrinkage over this broad range of temperature attributed to the lack of freedom that the bulky and highly charged polymer backbone experiences in the cross linked hydrogel state. In addition it is necessary to determine the burst pressure of hydrogel too. The cross linked polyILs show a considerable broadening of the temperature range over which the LCST behavior occurred. This extensive LCST interval of the PIL hydrogels could create a new tool box for the development of simple and low- cost temperature responsive microfluidic actuators or as temperature modulated flow regulators.

Liu et al designed anti freezing hydrogel based on a zwitterionic poly (ionic liquid) was fabricated artificial skin for the application of soft robots.<sup>[42]</sup> Both positively charged and negatively charged groups in one unit that is in the zwitterionic PIL, is the key for the preparation of this hydrogel. With the super stretchability of about 900%, ability of self healing, and a high conductivity at low temperature such as -20°C and workability at ultimate tensions, these non-releasing zwitterionic PIL hydrogels are expected to be used in more sophisticated stimuli responsive skin design and development with multifunctionality and adaptability to different environmental conditions. This PIL hydrogel based artificial ionic skin includes capacitive mode, resistive mode as well as triboelectric sensing mode in it (which is stable under wide range of temperature) and are easily switched in a single device simultaneously.

### **2.5. Rheological properties of IL based Hydrogel:**

Over the past years studies of hydrogel based on polymerized ionic liquids have increased as they are increasingly used in medical and pharmaceutical industry as implants, drug delivery systems, contact lens materials and coatings. That is why they require being biocompatible, flexible as well as resistant to external stress. So there is a huge interest in designing, synthesizing and characterizing of such kind of polymers with good mechanical performance. The significance of the rheological analysis is that (a) rheological study can supply a relative analysis of similar material but does not say anything about whether investigated material is good or bad, (b) rheological study can provide some parameters which can be helpful to recognize the physical or chemical structure of the material, (c) modeling the vibrant behavior and flow of the materials using obtained rheological properties.

Currently there is a rising demand for ILs in polymeric gels due to the retainment of useful properties of ILs within polymeric matrix. Jastram and coworkers in their analysis on rheological behavior of chemically cross-linked hydrogels based on PILs investigated mechanical properties such as gelation kinetics, shear strain resistance, and response to compression and stretching of the ten different PILs based hydrogels.<sup>[43]</sup> The results showed a broad range of critical strains in

stretching measurement leading to  $4.8 \pm 1.1$  to  $47.9 \pm 15.1\%$  and in compression measurement critical strain from  $7.8 \pm 3.6$  to higher than  $59.8 \pm 17.3\%$ , as well as linear viscoelastic range in shear from  $14 \pm 8$  to  $267 \pm 26\%$ . The mechanical properties can be improved by changing concentration of the cross linker. Interestingly the gelation rate depends on the stability of the monomer; the more labile monomer radicals improved the polymerization. On the other hand more stable radical showed inhibiting effect. Poly (VB-TMA) due to high compressibility to be compresses and non-invasively introduced into the human bodies could be an attractive material. Due to their fast shape recovery and additional swelling behavior, this hydrogel can expand inside human body beyond its initial extend. In a nutshell these properties provide a good groundwork for research of these hydrogels for medical applications. Ziółkowski et.al reported an interesting strategy to prepare ionogels by polymerizing *N*- isopropylacrilamide monomer in five different ILs with or without adding cross-linker. <sup>[44]</sup> The results showed that the nature of the IL had a strong effect on the viscosity of the polymerization medium and the polymerization speed. Rheological analysis of the prepared ionogels showed reversible increase in modulus as a function of temperature above its lower critical solution temperature (LCST). As far as structural changes are concerned, rheology enables the study of the thermodynamics and dynamics of polymer chains in ILs. Hydrogels are also useful as rust removal agent for cleaning of cultural remainder. Many cross linking agents were used as monomers to synthesize hydrogel which showed good liquid absorption properties, resistant to rust . But adsorption performance was very poor shown by these hydrogels. An ionic liquid dimethylaminoethyl methacrylate maleate (DMAEMA-MA) was used as the cross linking agent in IC-P hydrogel , the increase in amount of (DMAEMA-MA) from 0 to 1.%, the swelling rate of the IC-P hydrogel was also increased from 115.78 to 235.97%, and had certain pH and temperature responsiveness. Moreover the conductivity hydrogel also increased with increase the amount of the (DMAEMA-MA) which reached  $\sim 58.8 \mu\text{S cm}^{-1}$ . Also the rust removal effect which was the main focus was shown to have gradually increased with increase dose of (DMAEMA-DM)( Sun et. al)<sup>[45]</sup>

## 2.6. As flexible electrolytes and devices:

The growing demand and popularity of flexible devices, such as wearable electronic devices, smart mobile devices, roll-up displays and implantable biosensors due to their better characteristics like being portable, lightweight, bending ability has inspired the progress in the corresponding flexible energy storage and conversion devices with elevated performance. Each component of this flexible energy storage and conversion devices must contain mechanical stability, flexibility and some superior electrochemical properties like high conductivities and electrochemical stabilities. Manufacturing idyllic flexible electronic devices are still in their early stage of development. Gao

et al. designed and developed a self healing hydrogel with conductive, adhesive and mechanical properties by introducing polydopamine nanoparticles and ionic liquids in the hydrophobic association polyacrylamide. The resultant hydrogels seems to show excellent capacitance after self healing indicating that it could be a great flexible material which can be used in flexible sensors and super capacitors.<sup>[46]</sup>

Ionic liquids are getting more popularity over the past years in many fields due to their interesting physicochemical properties like high ionic conductivity, negligible vapor pressure high chemical and thermal stability, non-inflammability, non toxicity, non volatility, wide electrical windows, environmental friendly property. There has been research going on making polymer electrolytes based on ionic liquids. Though ionic liquids can be good option for being used as an electrolyte, but researchers are more interested in making portable electrolytes without any leakage problem. For this electrolyte should be in solid form with desirable shape and sizes. This problem can only be solved by combining two the properties high conductivity, high electrochemical and thermal stability of ionic liquids and good mechanical stability of polymers such as hydrogels maintaining the individual properties of the materials. In this polymeric matrix significant amount of liquid electrolytes can be entrapped in the polymeric network which improves the safety performance reducing the risk of ignition of solution by chemical reaction. As ionic liquids contain ions for conduction and can also improve segmental motion of polymer, the combination of ionic liquid and hydrogel can be used in making polymer electrolytes. The preparation can be done by incorporating the ionic liquid in hydrogel matrix or by hydrogel or polymer containing ionic liquid. The new polymeric matrix carries both cohesive property of the solid electrolyte and diffusive properties of the liquid electrolyte.

. Though ionic liquid based super capacitors shows very high specific capacitance of  $244 \text{ F g}^{-1}$  at room temperature, the leakage problems caused by ionic liquids limits their application in practical use. As a sub- discipline of ionic liquids, poly (ionic liquid)s have attractive mechanical characteristics of polymers while retaining the superior physicochemical properties of ionic liquids. This special feature can help to overcome the leakage problem and poor mechanical limitations of ionic liquid. However incorporation of poly (ionic liquid)s into functional devices commonly requires their shaping into processable materials, such as thin films and gels. Studies on incubation of PILs on gel polymers such as hydrogels are going on to make portable electronic devices with great ionic conductivity. This category of materials in future is going to opened up the possibilities of developing electronic devices, because of their high ionic conductivities and great mechanical strength in comparison to liquid electrolytes.

Gels that are freeze-resistant and heat-resistant and have ultimate tensile strength are desirable in practical applications due to their potential in designing flexible energy storage

devices, actuators, and sensors. Ren et al reported simple method for fabricating ionic liquid (IL)–based on click-ionogels using thiol-ene click chemistry under ambient condition which was based on the concept of DN.<sup>[47]</sup> They selected ionic interaction interactions between poly (1-butyl-3-vinyl imidazolium fluoborate) (PIL-BF<sub>4</sub>) and benzene tetracarboxylic acid (BTCA) to form a sacrificial network. The click-ionogels prepared persist excellent mechanical properties and resilience after 10,000 fatigue cycles. Furthermore, due to numerous exceptional properties of ILs and the formation of a hydrogen bond between IL-BF<sub>4</sub> and polymer network, these click-ionogels display high ionic conductivity, good optical transparency, and non-flammability performance over a wide range of temperature (from –75° to 340°C). Click-ionogel–based triboelectric nanogenerators exhibit outstanding mechanical, freeze-thaw, and heat stability. For the potential features of click-ionogels, they are going to be good candidate to promote new applications in designing of flexible and safe device.

It is found that strong and weak cross–link (ionic bonds) can promote gels’ mechanical properties. Zhou et.al managed to prepare flexible poly (ionic liquid) hydrogel electrolytes with a noble ionic liquid, 3-(1-vinyl-3-imidazolio) propanesulphonate/2-acrylamido-2-methylpropane sulphonic acid (ZIW/AMPS).<sup>[48]</sup> As both the cations and anions of the novel ionic liquid have carbon- carbon double bonds, these poly (ionic liquid) hydrogels merge both strong and weak cross-links after polymerization. The amalgamation makes these hydrogel electrolytes tough, flexible and self recoverable tested by mechanical measurements. Due to the functional mechanism, these poly (ionic liquid) hydrogels exhibit high mechanical strength, excellent elongation and flexibility and good self recoverable property after successive and large compressive strain and thus they hold good electrical stability. Apart from the mechanical properties, the hydrogel based on poly (ZIW/AMPS) exhibit excellent electrical properties too. Remarkably these hydrogels exhibit superior electrochemical properties, which can remain stable under different bending angles and successive bending, folding, compressing and twisting and under mechanical strain. Feng, Yi, Zhang, Niu, and Xu by using chitosan crosslinkinking with redox-PIL Poly(1-vinyl-3-propionate imidazole phenothiazine sulfonic acid [Poly(VPI+PTZ-(CH<sub>2</sub>)<sub>3</sub>SO<sup>3-</sup>)], produce a redox-responsive poly(ionic liquid) (redox-PIL) hydrogel Poly(1-vinyl-3-propionate imidazole phenothiazine sulfonic acid)- chitosan Poly[(VPI+PTZ-(CH<sub>2</sub>)<sub>3</sub>SO<sup>3-</sup>)-CS] with good electron catalytic ability, ionic conductivity, and electron conductivity.<sup>[49]</sup> Fusion of properties of hydrogel with redox–PIL, Poly(VPI+PTZ-(CH<sub>2</sub>)<sub>3</sub>SO<sup>3-</sup>)-CS seems to offer intrinsic porous conducting frameworks and promoting the transport of molecules, charge and ions; showing good electrochemical properties.

## CHAPTER 3

### CONCLUSIONS

In this literature review work a brief review on some of the recent advances in the use of ILs in the process of synthesizing hydrogels has been given. The tunability and adaptability of ILs associated with the features of natural (such as chitin or cellulose) and/or synthetic polymers have given new directions to process them as hydrogels as well as matrices with different sizes and shapes. These hydrogels are being used as efficient adsorbent in water bodies to remove toxic metals, and dyes, as well as they are of interesting subject in medicinal ,pharmaceuticals and industrial sectors.

Majority of the studies and research reports suggest the use of ILs in hydrogels increase in the quality of the obtained polymer. Studies have shown that polymeric hydrogels processed in ILs can be helpful for a wide range of applications from the removal of anionic dyes to biomaterials. Despite of the promising results shown by the materials, it is a bit early for wider use in the concerned biomedical applications as little has been reported about the in vitro and in vivo biocompatibility of the so far developed matrices. This could limit the potential use of these materials as biomaterials. The nontoxicity and effect of the surface morphology on the cell growth and viability should be taken into account while considering the use in the field of medical applications.

By controlling the monomer or crosslinker concentration, desired mechanical properties of the hydrogels can be achieved though it is practically limited by the solubility of the monomer and crosslinker. The hybrid ILs hydrogels imparts the diffusive properties of the liquids and the cohesive properties of the solids in the formation of the polymer gel electrolyte. The polymer gel electrolytes overcome the low ionic conductivity of polymeric gels or hydrogels in solid electrolytes and the leakage and evaporation problems of ionic liquid in liquid electrolytes. Which is a useful criteria in the making of electronic devices and research has been carried out in development of this field.

To make hydrogels more practical in special fields, researchers are still focusing on adjusting durability, degradability as well as mechanical properties and swelling behavior. Therefore new approaches for hydrogel synthesis are of utmost importance. In many technological applications ionic liquid gel are utilized as these materials are a combination of controlled assembly of gels with the vast application of ionic liquids. This enables the designing of a heady combination of functional tailored materials, which will lead to the development of more task



specific ionic liquid gels. This material has the potential to develop functional materials for green and sustainable chemistry, medicine, energy, catalysis, electronics and many more.

PILs synthesis has also contributed to firm developments in the manufacture of responsive hydrogels. Although very few reports can be found in the literature suggesting that it is at an early stage; due to its potential and many extraordinary properties of ILs/PILs hydrogel more developments are expected in the upcoming years.

## References –

1. M Bahram , N Mohseni and M Moghtader . “An introduction to hydrogels and some recent applications.” *Emerging Concepts in Analysis and Applications of Hydrogels*, edited by Sutapa Biswas Majee, 2016, pp 10-13 DOI: 10.5772/61692
2. Q Chai , Y Jiao and X Yu “ *Hydrogels for biomedical applications: Their characteristics and mechanisms behind them.*”. *Gels* 2017,3,6
3. E M. Ahmed . A review on Hydrogels: Preparation, Characterization, and applications. *Journal of Advanced Research* (2015)**6**, 105-121
4. Z Lei, B Chen, Y M Koo, D R. MacFarlane(2017) Introduction: Ionic Liquids *Chem. Rev.*2017, 117,10,6633-6635
5. P. Wasserscheid, W. Keim *Ionic Liquids- New Solutions for Transision Metal catalysis. Angew. Chem.. Int. Ed. Engl.* 2000, 39, 3772.
6. Freemantle, Michael An Introduction to Ionic liquid. *Royal Society of Chemistry* ISBN 978-1-184755-161-0 (2009)
7. W. Kong, C. Wang, C. Jia, Y. Kuang, G. Pastel, C. Chen, G. Chen, S. He, H. Huang, J. Zhang, S. Wang, L. Hu, Muscle-inspired highly anisotropic, strong, ion-conductive hydrogels. *Adv. Mater.* **30**, e1801934 (2018).
8. Y. Wu, D. Wang, I. Willner, Y. Tian, L. Jiang, Smart DNA hydrogel integrated nano channels with high ion flux and adjustable selective ionic transport. *Angew. Chem.* **130**, 7916–7920 (2018).
9. Y. Zhang, H. Gao, H. Wang, Z. Xu, X. Chen, B. Liu, Y. Shi, Y. Lu, L. Wen, Y. Li, Z. Li, Y. Men, X. Feng, W. Liu, Radiopaque highly stiff and tough shape memory hydrogel microcoils for permanent embolization of arteries. *Adv. Funct. Mater.* **28**, 1705962 (2018).

10. H. Wu, Y. Cao, H. Su, C. Wang, Tough gel electrolyte using double polymer network design for the safe, stable cycling of lithium metal anode. *Angew. Chem. Int. Ed. Engl.* **57**, 1361–1365 (2018).
11. L. Chu, C. Liu, G. Zhou, R. Xu, Y. Tang, Z. Zeng, S. Luo, A double network gel as low cost and easy recycle adsorbent: Highly efficient removal of Cd(II) and Pb(II) pollutants from wastewater. *J. Hazard. Mater.* **300**, 153–160 (2015).
12. E. Kamio, T. Yasui, Y. Iida, J. P. Gong, H. Matsuyama, Inorganic/organic double-network gels containing ionic liquids. *Adv. Mater.* **29**, 1704118 (2017).
13. H. Li, D. Hao, J. Fan, S. Song, X. Guo, W. Song, M. Liu, L. Jiang, A robust double-network hydrogel with under sea water super oleophobicity fabricated *via* one-pot, one-step reaction. *J. Mater. Chem. B* **4**, 4662–4666 (2016).
14. Q. Rong, W. Lei, J. Huang, M. Liu, Low temperature tolerant organohydrogel electrolytes for flexible solid-state super capacitors. *Adv. Energy Mater.* **8**, 1801967 (2018).
15. J. Yuan, D. Mecerreyes, M. Antonietti, Poly(ionic liquid)s: An update. *Prog. Polym. Sci.* **38**, 1009–1036 (2013).
16. Khiratkar AG, Senthil Kumar S, Bhagat PR Designing a sulphonic acid functionalized benzimidazolium based poly(ionic liquid) for efficient adsorption of hexavalent chromium. *RSC Adv* 6(44):37757–37764(2016)
17. Mi H, Jiang Z, Kong JHydrophobic poly(ionic liquid)for highly effective separation of methyl blue andchromium ions from water. *Polymers* 5(4):1203–1214 (2013)
18. K Li , L Qian, W Song , M Zhu , Y Zhao , & Z Miao . Preparation of an ionic liquid-based hydrogel with hyperbranched topology for efficient removal of Cr (VI). *Journal of Materials Science*, 53(20), 14821-14833. (2018).
19. S Yildiz , M Sahiner , N Sahiner. Macromolecular Nanotechnology Ionic liquid hydrogel templates: Bulkgel, cryogel, and microgel to be used for metal nanoparticle preparation and catalysis. *European Polymer Journal* 70,66,-78. (2015)
20. M Li, Z Wang, B Li . Adsorption behaviour of congo red by cellulose/chitosan hydrogel beads regenerated from ionic liquid *Desalination and Water Treatment* 57 (36), 16970-16980( 2016)
21. A Jastram , T Lindner , C Luebbert , G Sadowski and U Kragl Swelling and Diffusion in Polymerized Ionic Liquids-Based Hydrogels *Polymers*2021, 13, 1834. (2021)
22. S S Silva, R L Reis Ionic Liquids as Tools in the Production of Smart Polymeric Hydrogels . *Polymerised Ionic Liquids* (pp 304-318), Published by The Royal Society of Chemistry(2018)

23. M A Haq, Y Su, D Wang. A review on mechanical properties of PNIPAM based hydrogel *Metarial science and engineering volume 70, part 1, 2017, pages 842-855* (2016)
24. T Ueki (2014) Stimuli Responsive polymers in ionic liquids *Polymer Journal* 46, 64-655
25. A Tudor, L Florea, S Gallagner, J Burn. Poly(ionic Liquid) Semi-interpenetrating network multi-responsive hydrogels *Sensors* 16(2):219 (2016)
26. X Feng, K Zhang, P Chen, X Sui, M A Hempenius, B Liedberg, G Julius Vancso Highly Swellable, Dual-Responsive Hydrogels Based on PNIPAM and Redox Active Poly (ferrocenylsilane) Poly (ionic liquid) s: Synthesis, Structure, and Properties *Macromolecular rapid communications* 37 (23), 1939-1944, 2016
27. X Zhou, J Wang, J Nie, B Du. Poly( N-isopropylamide)- based ionic hydrogels: Synthesis, Swelling properties, Interfacial adsorption and release of dyes. *Polymer Journal* 48, 431-438 (2016)
28. I Noshadi, B W. Walker, R Portillo-Lara, E S Sani, N Gomes, M R Aziziyan & N Annabi Engineering Biodegradable and Biocompatible Bio-ionic Liquid Conjugated Hydrogels with Tunable Conductivity and Mechanical Properties *Scientific Reports* 7, article number : 4345 (2017)
29. H Fang, J Wang, L Li, L Xu, Y Wu, Y Wang, X Fei, J Tian, Y Li. A novel high-strength poly(ionic liquid)/PVA hydrogel dressing for antibacterial applications *Chemical Engineering Journal Volume 365, , Pages 153-164* (1 June 2019)
30. Y Yu, Z Yang, S Ren, Y Gao, L Zheng. Multifunctional hydrogel based on ionic liquid with antibacterial performance *Journal of Molecular Liquids* 299, 112185 (2020)
31. A. Mildner, L. Henke, T. Gerdes, J. Großeheilmann Hydrogels based on polymerized ionic liquids as innovative drug carriers in controllable and individualized dosage forms <https://doi.org/10.24355/dbbs.084-202001221322-09> (2019)
32. J Claus, A Brietzke, C Lehnert, S Oschatz, N Grabow, U Kragl. Swelling characteristics and biocompatibility of ionic liquid based hydrogels for biomedical applications. *PLoS ONE* 15(4): e0231421 (2020)
33. M Kuddushi, D Ray, V Aswal, C Hoskins, N Maleka Poly(vinyl alcohol) and Functionalized Ionic liquid Based Smart Hydrogel for Doxorubicin Release *ACS Applied Bio Materials* 3 (8), 4883-4894, 2020
34. D Batra, Hay, and M A. Firestone, Formation of a Biomimetic, Liquid-Crystalline Hydrogel by Self-Assembly and Polymerization of an Ionic Liquid *Chem. Mater.* 2007, 19, 18, 4423-4431

35. J Claus, A Jastram, Ewelina Piktel, Robert Bucki, Paul A. Janmey, Udo Kragl Polymerized ionic liquids-based hydrogels with intrinsic antibacterial activity: Modern weapons against antibiotic-resistant infections. *J Appl Polym Sci.* 2021;138:e50222(2020)
36. X He, X Sun, H Meng, S Deng. Self healing polymeric ionic liquid hydrogels with high mechanical strength and ionic conductivity *Journal of Material Science* 59(17); 1-18 ,(2021)
37. C S Nunes, K B Rufato, P R Souza, E A.M.S. de Almeida, M. J.V da Silva, D B Scariot, C V Nakamura, F A Rosa, A F Martins, E C. Muniz. *Carbohydrate Polymer volume 170, pages 99-106*(2017)
38. X Fan, H Liu, Y Gao, Z Zou, V SJ Craig, G Zhang, G Liu. Forward-Osmosis Desalination with Poly (Ionic Liquid) hydrogels as smart draw agents *Advanced Materials* 28 (21), 4156-4161. (2016)
39. C H Hsu, C Ma, N Bui, Z Song, A D Wilson, R Kostecki, K M Diederichsen, B D McCloskey, J J Urban. Enhanced forward osmosis desalination with a hybrid ionic liquid/hydrogel thermoresponsive draw agent system *ACS omega* 4 (2), 4296-4303(2019)
40. A Tudor, L Florea, S Gallagner, J Burn. Poly(ionic Liquid) Semi-interpenetrating network multi-responsive hydrogels *Sensors* 16(2):219(2016)
41. A Tudor, J Saez, L Florea, F Benito-Lopez, D Diamond. Poly(ionic liquid) thermo-responsive hydrogel microfluidic actuators, *Sensors and Actuators B: Chemical* <http://dx.doi.org/10.1016/j.snb.2017.03.045> (2017)
42. Z Liu, Y Wang, Y Ren, G Jin, C Zhang, W Chend and F Yan Poly(ionic liquid) hydrogel-based anti-freezing ionic skin for a soft robotic gripper *Material Horizons* 7(3), 919-927, 2020
43. A. Jastram a, J. Claus , P.A. Janmey , U.Kragl Rheological properties of hydrogels based on ionic liquids. *Polymer Testing*, <https://doi.org/10.1016/j.polymertesting>. 2020.106943
44. B Ziolkowski and D Diamond (2013) Thermoresponsive poly(ionic liquid) hydrogels *Chem. Commun.*, 49, 10308, DOI : 10.1039/c3cc45862h
45. J Sun, J Wang, H Wang, D Li, H Gao and Z Jin (2021) Properties of ionic liquid cross-linked hydrogels and their application of derusting. *Bull. Matter. Sci.* (2021) 44:183 <https://doi.org/10.1007/s12034-021-02471-w>
46. Z Gao, L Kong, R Jin, X Liu, W Hu, G Gao Mechanical, adhesive and self-healing ionic liquid hydrogels for electrolytes and flexible strain sensors *Journal of Materials Chemistry C* 8 (32), 11119-11127, 2020
47. Y Ren, J Guo, Z Liu, Z Sun, Y Wu, L Liu, F Yan. Ionic liquid-based click-ionogels *Sci. Adv.* 5, eaax048 (2019)

48. T Zhou,<sup>a</sup> X Gao,<sup>a</sup> B Dong,<sup>b</sup> N Suna and L Zheng (2015) Poly(ionic liquid) hydrogels exhibiting superior mechanical and electrochemical properties as flexible electrolytes *J. Mater. Chem. A*, 2016,**4**, 1112
49. X Feng, J Yi, W Zhang, Y Niu, L Xu. A redox poly (ionic liquid) hydrogel: Facile method of synthesis and electrochemical sensing *Journal of Applied Polymer Science* 136 (42), 48051. (2019)

# USE OF NITRILES FOR THE SYNTHESIS OF HETEROCYCLIC COMPOUNDS



A dissertation submitted to the Department of Chemistry, Gauhati  
University for the partial fulfilment of the degree of Masters of Science  
(M.Sc.) in Chemistry, 2021

## **SUPERVISOR**

**PROF. PRODEEP PHUKAN**

**Department of Chemistry**

**Gauhati University,**

**Guwahati-781014**

## **SUBMITTED BY**

**MOITREYEE BHATTACHARJEE**

**M.Sc. 4<sup>th</sup> SEMESTER**

**Exam Roll No: PS-191-808-0075**

**Registration No. 217057**

**Department of Chemistry**

**Gauhati University,**

**Guwahati – 781014**



# DEPARTMENT OF CHEMISTRY

**Gauhati University,**

**Guwahati-781014, Assam, India**

**Dr. Prodeep Phukan**

**E-mail: pphukan@gauhati.ac.in**

**Professor (Chemistry)**

---

## **CERTIFICATE**

This is to certify that the work described in the project entitled, **“USE OF NITRILES FOR THE SYNTHESIS OF HETEROCYCLIC COMPOUNDS”** was carried out in the **Department of Chemistry, Gauhati University**, by **Moitreyee Bhattacharjee** under my supervision and guidance. This project was carried out for partial fulfilment of requirements for obtaining the **Masters of Science (M.Sc.) Degree** from the **Department of Chemistry, Gauhati University**.

I would like to certify that the work submitted here is the outcome of the literature survey carried out by her.

**Date:**

**Dr. PRODEEP PHUKAN**

**Supervisor**

## **DECLARATION**

The project entitled “**USE OF NITRILES FOR THE SYNTHESIS OF HETEROCYCLIC COMPOUNDS**” submitted for the award of the **Masters Degree in Chemistry** is a presentation of my work which has been carried out under the guidance of Dr. Prodeep Phukan, Professor, Department of Chemistry, Gauhati University. Wherever contributions of others’ work are involved, every effort is made to indicate this clearly, with due reference to the literature, and acknowledgement of collaborative research and discussions. I would like to declare that this project work has not been submitted to any other University or Institution for the award of any degree.

*Moitreyee Bhattacharjee*

**Date:**

**MOITREYEE BHATTACHARJEE**

**M.Sc. 4<sup>th</sup> Semester**

**PS-191-808-0075**

In my capacity as supervisor of the candidate’s work, I certify that the above statements are true to the best of my knowledge.

**Dr. PRODEEP PHUKAN**



## **ACKNOWLEDGEMENT**

It has been quite a learning experience for me to carry out the project work in the Department of Chemistry, Gauhati University. In the successful completion of this project work there are the contributions of various persons to be acknowledged, without whose help, I would have never been able to complete my project work.

I feel immense pleasure in expressing my sincere gratitude to my supervisor Dr. Prodeep Phukan, Professor, Department of Chemistry, Gauhati University for his valuable guidance, constant support and patience which enabled me to complete this study. He encouraged me through my project work. He made every possible effort to bring the best out of me and gave me full freedom in my work and also provided me with necessary materials.

I deeply admire all the faculty members and staff of this department for their helping attitude and acknowledge their efforts in building up an active research environment in the department with their encouragement, insightful comments and suggestions for my overall improvement. I would also like to thank the Head of the Department of Chemistry, Gauhati University for allowing me to carry out my literature survey. I am also thankful to Gauhati University for implementing this project work in our M.Sc. curriculum which has helped us to learn a lot.

Last but not the least, I am thankful to all my batchmates who extended their encouraging support and helped me in building a symbiotic environment.

*Moitreyee Bhattacharjee*

**MOITREYEE BHATTACHARJEE**

**Department of Chemistry (M.Sc. 4<sup>th</sup> SEM)**

**Gauhati University**

**Date:**

**Place: Guwahati**

## Contents

<b>Topics</b>	<b>Page No.</b>
<b>1. Introduction</b>	<b>1-4</b>
<b>2. Synthesis of three-membered heterocyclic compounds</b>	<b>5-7</b>
2.1. Azirine Derivatives	5-6
2.2. Epoxide Derivatives	6-7
<b>3. Synthesis of four-membered heterocyclic compounds</b>	<b>8-9</b>
3.1. Thietane Derivatives	8
3.2. Azetidine Derivatives	9
<b>4. Synthesis of five-membered heterocyclic compounds</b>	<b>9-53</b>
4.1. Pyrrole and its derivatives	9-19
4.2. Thiophene and its derivatives	20-25
4.3. Furan and its derivatives	25-29
4.4. Imidazole and its derivatives	29-35
4.5. Pyrazole and its derivatives	36-39
4.6. Thiazole and its derivatives	39-41
4.7. Oxazole and its derivatives	41-46
4.8. Triazole and its derivatives	46-48
4.9. Tetrazole and its derivatives	49-50
4.10. Thiadiazole and its derivatives	50-53

<b>5. Synthesis of six-membered heterocyclic compounds</b>	<b>54-74</b>
5.1. Pyran and its derivatives	54-60
5.2. Pyridine and its derivatives	60-65
5.3. Pyrimidine and its derivatives	66-71
5.4. Pyrazine and its derivatives	71-72
5.5. Triazine and its derivatives	73-74
<b>6. Synthesis of fused heterocyclic compounds</b>	<b>74-86</b>
6.1. Indole and its derivatives	74-77
6.2. Quinoline and its derivatives	78-83
6.3. Quinazoline and its derivatives	84-86
<b>7. Conclusion</b>	<b>87</b>
<b>8. Reference</b>	<b>88-96</b>

# USE OF NITRILES FOR THE SYNTHESIS OF HETEROCYCLIC COMPOUNDS

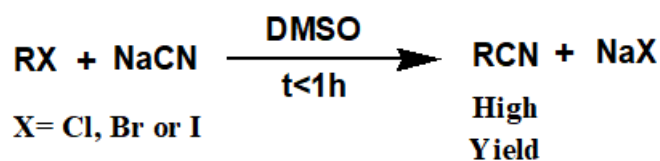
## 1. Introduction

Heterocycles form the foremost division of organic chemistry. They are omnipresent in all kinds of compounds of interest and there are several synthetic methods of introducing them into a structure. The field of heterocyclic chemistry has no distinct demarcations and are an inextricable part of life processes. Their extensive importance in biological, medicinal and industrial processes are attributed to their structural uniqueness and abundance in our surroundings. Moreover, they also owe their importance in the understanding of life processes and thus improving the quality of life. Some of the most common synthetic pathways for heterocyclic compounds involve cyclization, cycloaddition and photochemical reactions. Their synthesis involves starting materials such as organometallic compounds, nitrogen, sulphur, oxygen and phosphorous containing compounds and ylides. But, a large number of these synthetic pathways include the use of nitriles for the synthesis of various classes of heterocyclic compounds among which many of them are environmentally benign procedures [1].

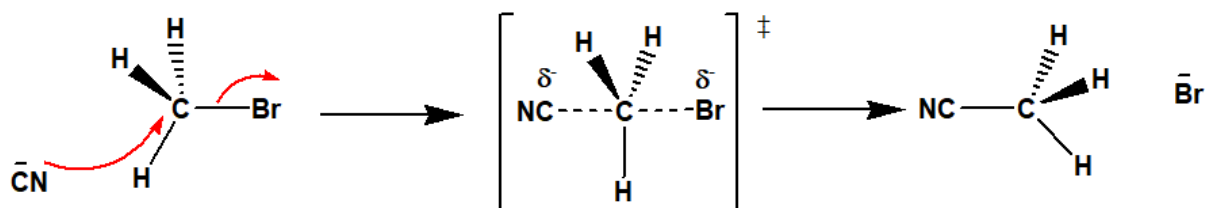
Nitriles are the organic compounds, bearing the functional group  $\text{--C}\equiv\text{N}$  and are thus referred to as the derivatives of hydrocyanic acid. The prefix “Cyano” is often used to denote this functional group. Both the carbon and the nitrogen atom in nitriles exhibit  $\text{sp}$  hybridization thereby forming a triple bond (one  $\sigma_{\text{sp-sp}}$  and 2  $\pi$  bonds). The first syntheses of nitriles were reported in 1832 by Wöhler and Liebig, who successfully prepared benzoyl cyanide and benzonitrile, and by Pelouze in 1834, who synthesized propionitrile. It took nearly another century for the research in the field of nitrile chemistry to reach considerable proportions. A significant factor for such slow progress was the low availability and high price of the inorganic cyanide raw materials. But, later on, during the period from 1920 to 1935 the average number of work on nitrile chemistry increased four times and this has continued at an ever-increasing trend over years [2].

Presently, there are numerous synthetic pathways for production of nitriles, some of which includes treatment of alkyl halides with sodium cyanide (Kolbe nitrile synthesis) via a  $\text{S}_{\text{N}}2$

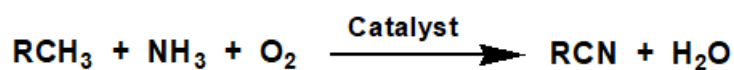
mechanism [3], dehydration of amides, ammoxidation of hydrocarbons [4] and addition of hydrogen cyanide to unsaturated organic compounds.



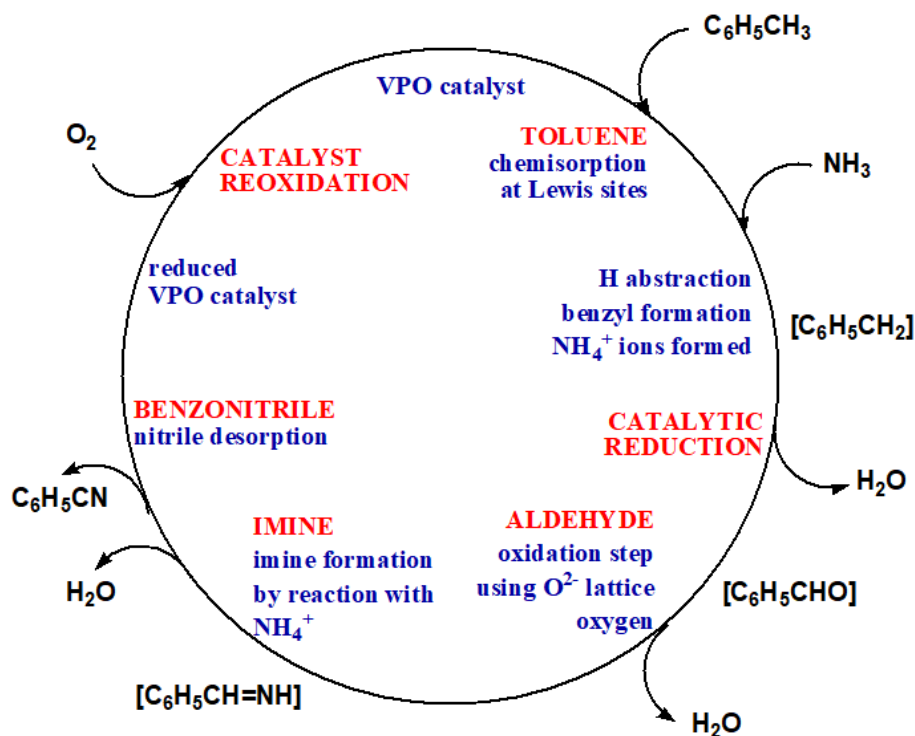
Scheme 1



Possible Reaction Pathway for Scheme 1



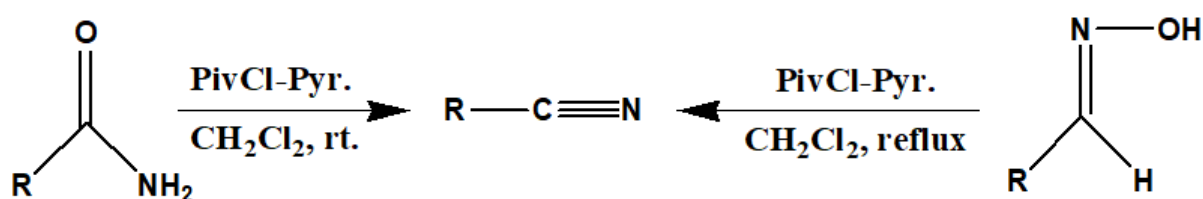
Scheme 2



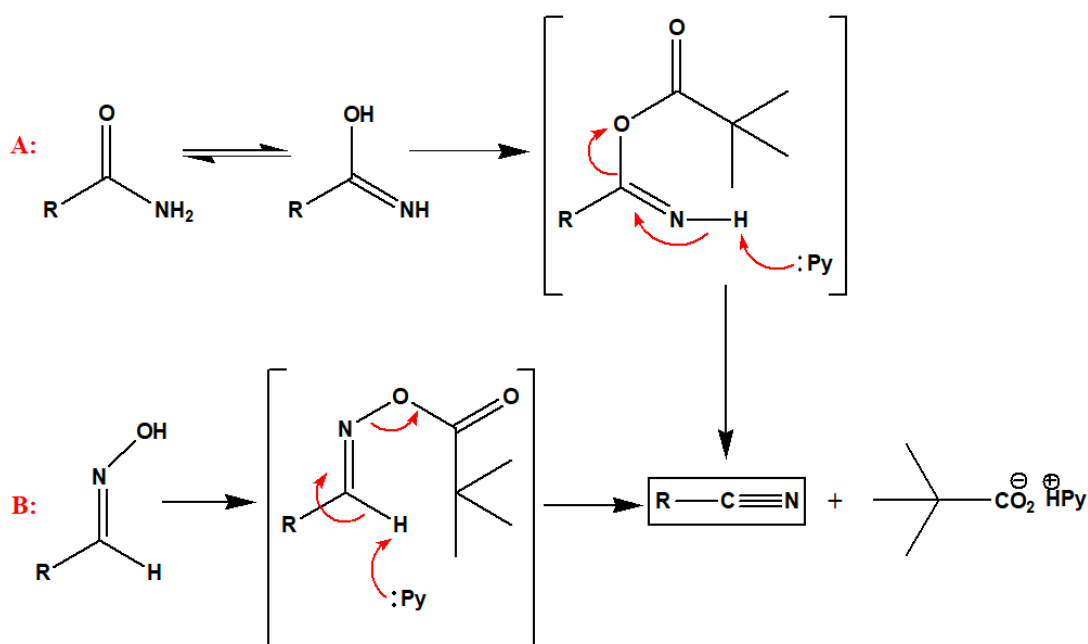
Possible Reaction Pathway for Scheme 2

They have numerous applications in the fields of synthetic resin, pharmaceuticals, dyes, plastics, vitamins, special solvents, other chemical compounds, war gases, and insecticides. Such widespread applications are attributed to the fact that most of the nitriles are relatively stable and inexpensive and are supports a variety of substituents and thus can be transformed into different functional groups and heterocycles by various pathways. But on the contrary nitriles show toxicity to the extent that on the entering our body may be metabolized to liberate cyanide and thus care must be taken in order to avoid inhalation, ingestion or direct skin contact [2].

Some other recent and more efficient methods of nitrile synthesis include the one reported by Narsaiah and Nagaiah, that involves the preparation of nitriles with excellent yields from primary amides and aldoximes using pivaloyl chloride-pyridine system as an efficient reagent to carry out the synthesis under mild reaction conditions (Scheme 3) [5].

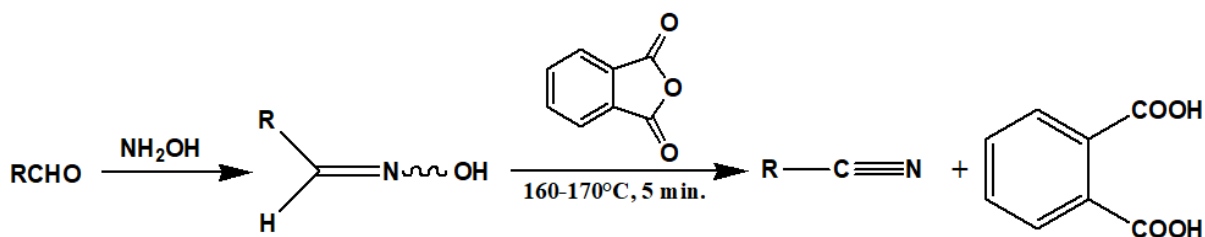


Scheme 3

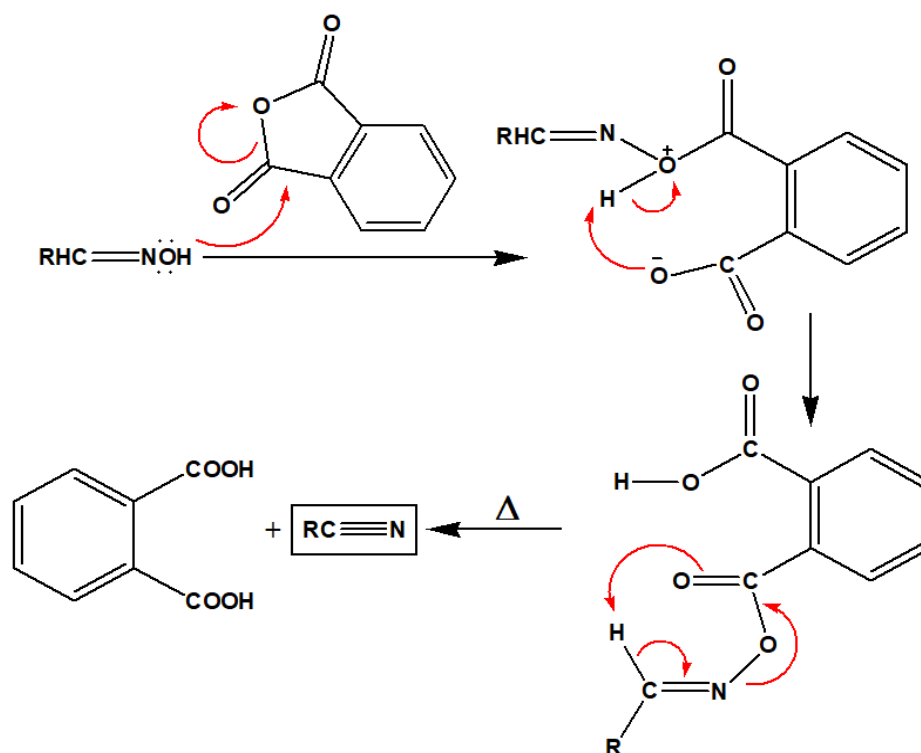


Possible Reaction Pathway for Scheme 3

Another efficient synthetic method for generating nitriles was reported by Wang et al. The synthesis proceeds with the fusion of phthalic anhydride with aldoximes resulting in a fast and efficient conversion into nitriles with excellent yields (over 85%) within a time period of 5 minutes (Scheme 4) [6].



**Scheme 4**



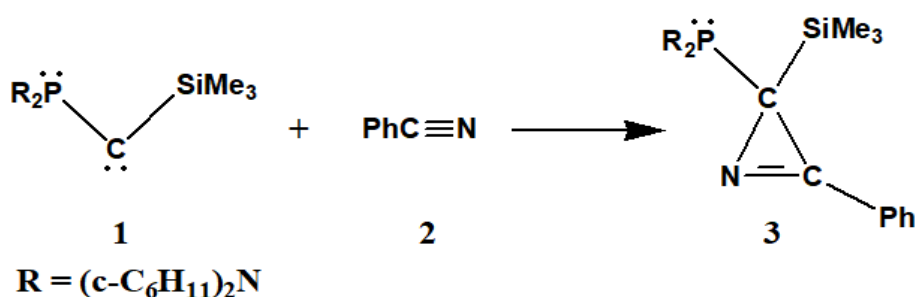
**Possible Reaction Pathway for Scheme 4**

Nitriles are an important and versatile building block in organic synthesis. This particular synthon finds its application in the synthesis of a variety of heterocyclic compounds. The use of nitrile bearing building blocks for the synthesis of various classes of heterocycles are briefly described below.

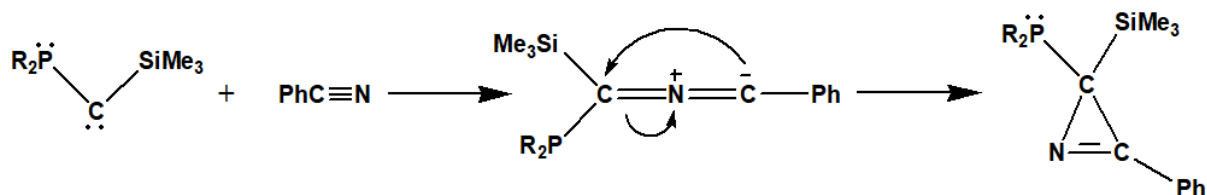
## 2. Synthesis of three-membered heterocyclic compounds

### 2.1 Azirine Derivatives

Alcaraz et al. reported an efficient carbene-type reaction pathway using transient carbenes for the synthesis of 2H-azirine through a [2+1] cycloaddition reaction. In this method the phosphinocarbene **1** is allowed to react at room temperature with an excess of benzonitrile **2** in toluene to obtain the desired compound **3** with a yield of 85% (Scheme 1). A  $^{31}\text{P}$  NMR spectrum implied that the reaction attained completion after 18 hours without the formation of any intermediate. The product obtained **3** was confirmed to be 2H-azirine with the help of X-ray diffraction study. An elemental analysis and a mass Spectrum showed that compound **3** was a 1,1-adduct of the carbene **1** along with benzonitrile **2** (Scheme 5) [7].



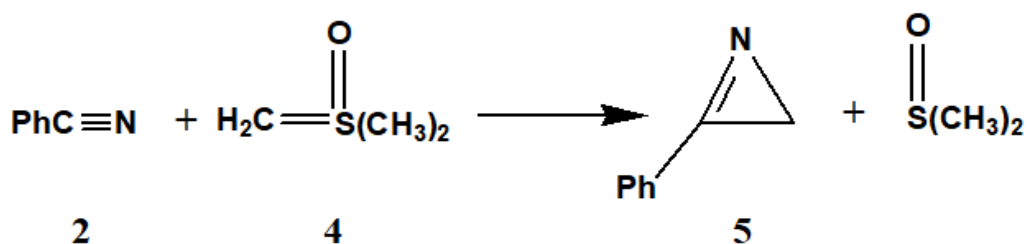
Scheme 5



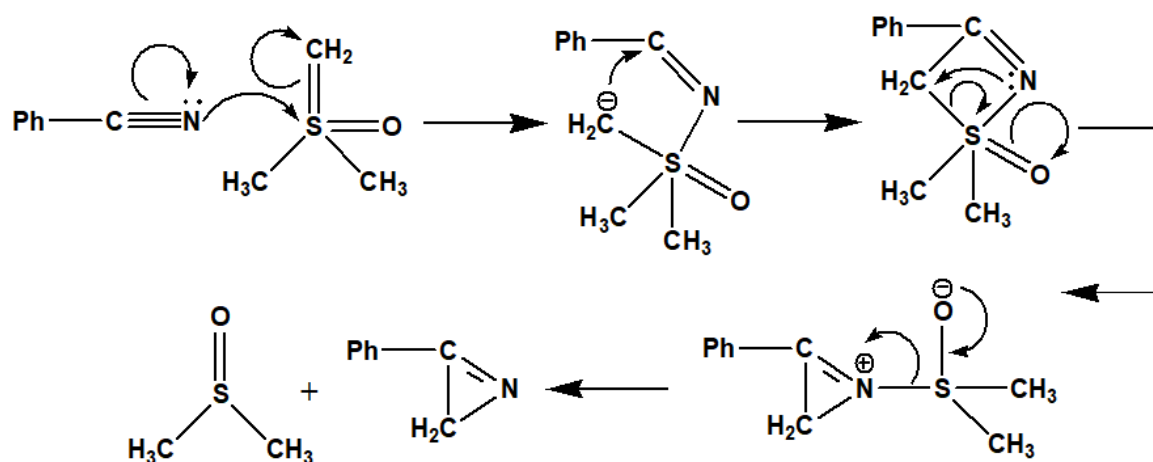
Possible Reaction Pathway for Scheme 5

Koenig et al. illustrated a simplified approach for synthesizing 2-phenylazirine **5** due to the reaction of benzonitrile **2** with dimethyl oxo sulfonium methylide **4** (Scheme 6) [8].





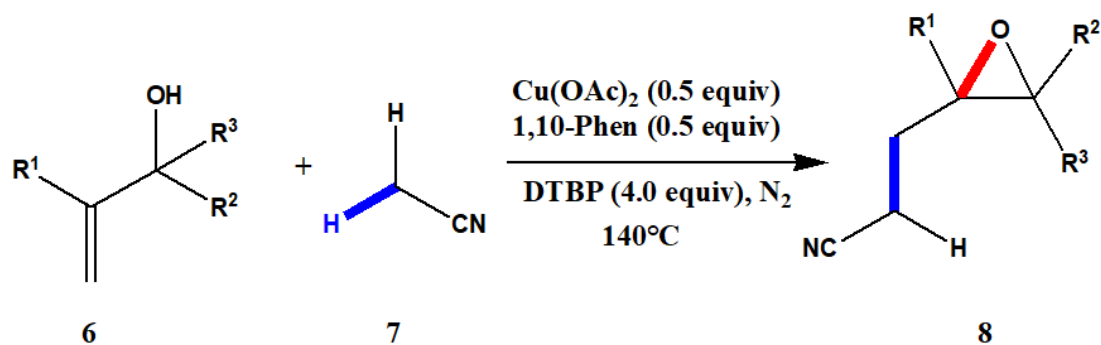
Scheme 6



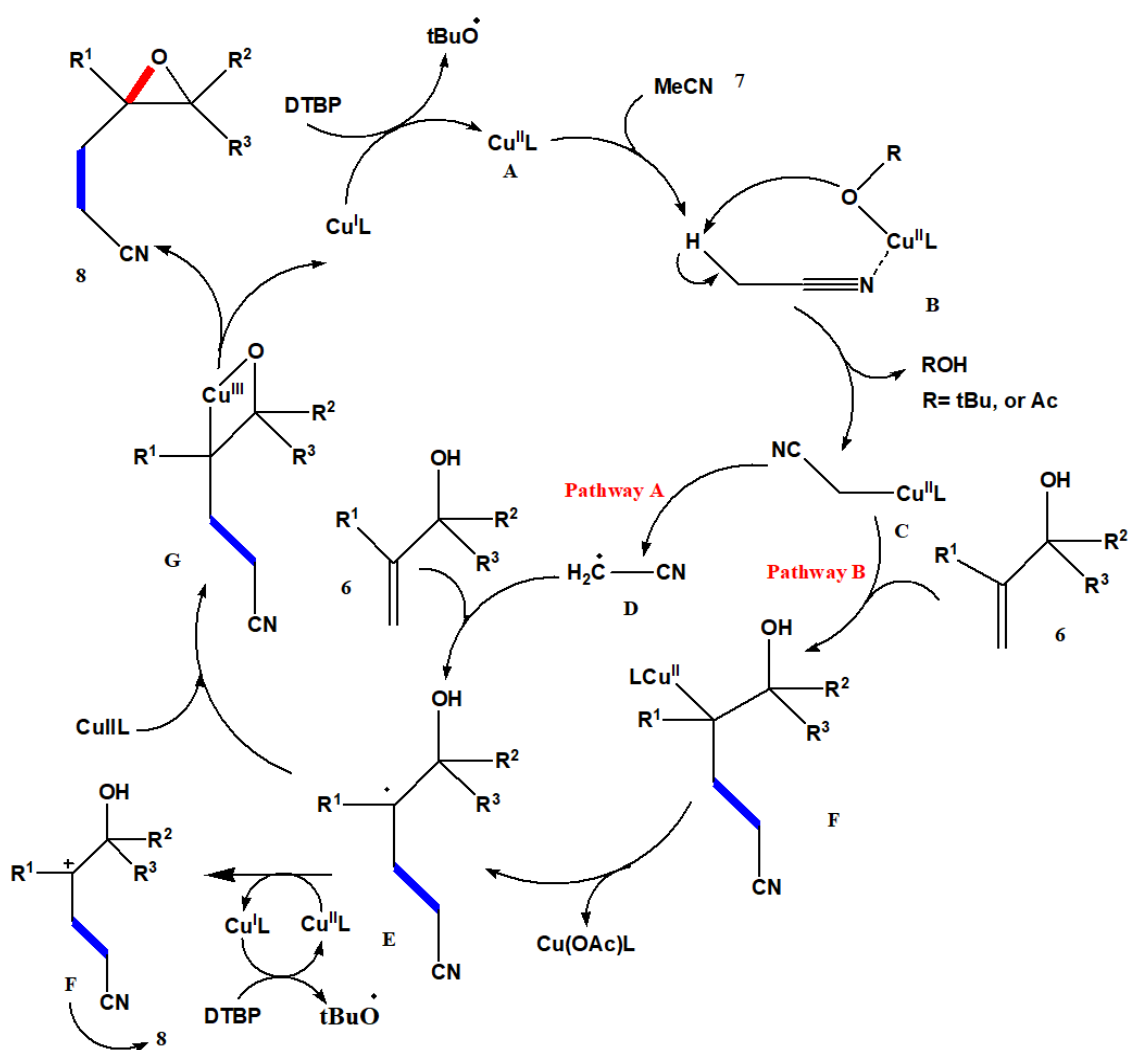
Possible Reaction Pathway for Scheme 6

## 2.2 Epoxide Derivatives

Bunescu et al. reported an efficient synthetic route for the generation of tri- and tetra-substituted epoxides **8** with moderate to excellent diastereoselectivity. The synthesis involves oxyalkylation of allylic alcohols **6** using nonactivated alkyl nitriles **7** using copper as a catalyst. The reaction sequence involves the generation of an alkyl nitrile radical which then adds to a double bond resulting in a copper-mediated formation of C(sp<sup>3</sup>) – O bond (Scheme 7) [**9**].



Scheme 7

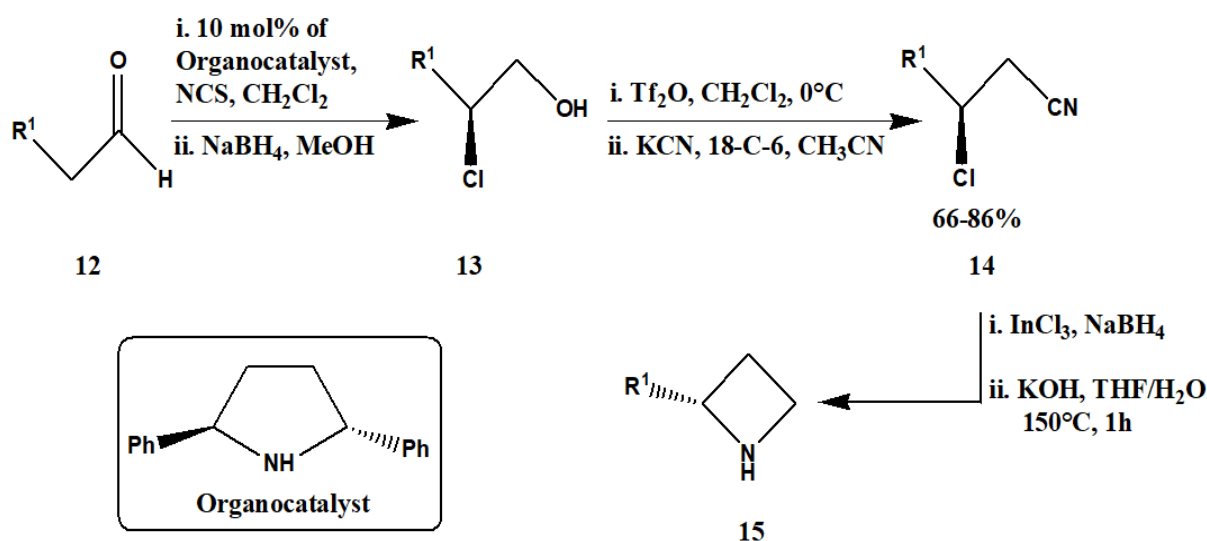


Possible Reaction Pathway for Scheme 7

### Possible Reaction Pathway for Scheme 8

### 3.2 Azetidine Derivatives

Senter et al. reported a short and high yielding methodology for an enantioselective  $\alpha$ -Chlorination of aldehydes **12** using an organocatalyst, prepared using a cost-efficient route. It is then subjected to  $\text{NaBH}_4$  reduction to form 2-chloro alcohol intermediate **13** and is then transformed into  $\beta$ -chloro nitrile intermediates **14** with about 66-86% yield, using 18-crown-6 additives. These nitrile intermediates are then used for the preparation of functionalized azetidines **15** in 22-32% overall yield and with 84-92% ee (Scheme 9) [11].

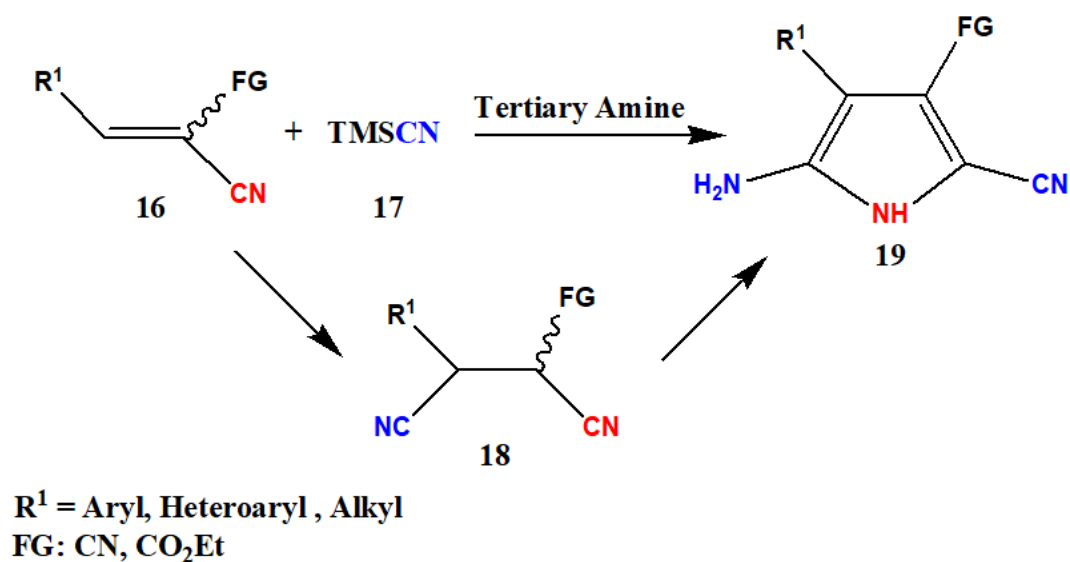


Scheme 9

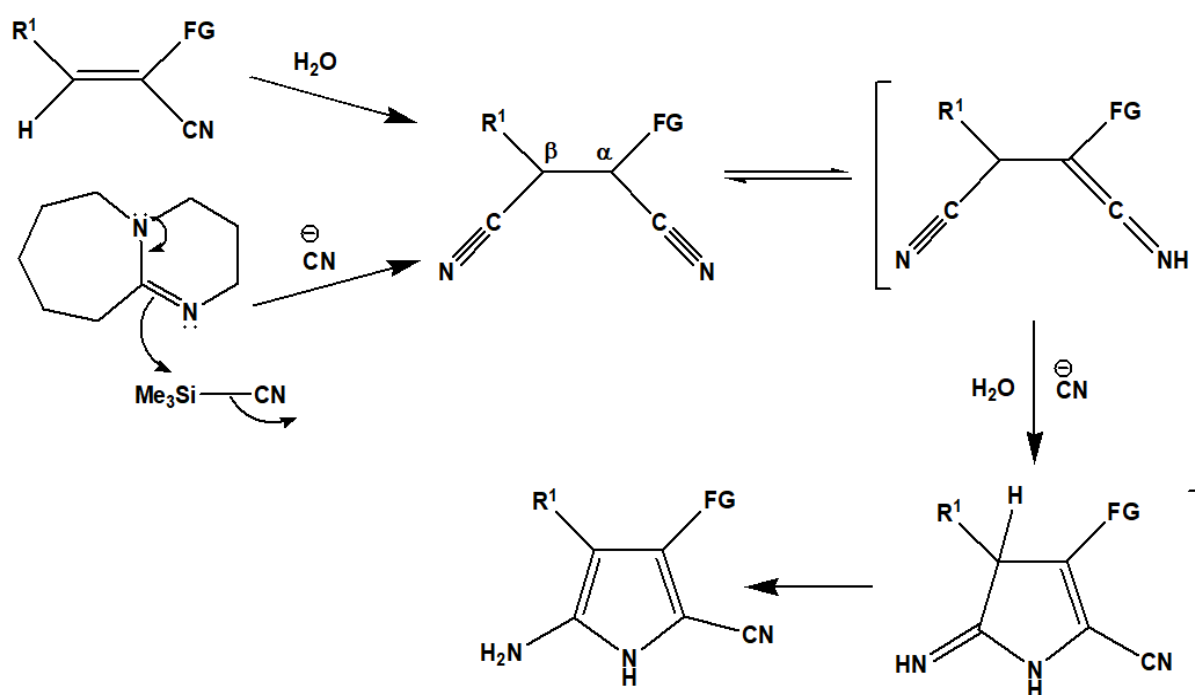
## 4. Synthesis of five-membered heterocyclic compounds

### 4.1 Pyrrole and its derivatives

Guchhait et al. developed a new approach for the synthesis of polyfunctionalized NH-pyrroles **19** via a Tandem reaction to generate vic-dinitrile **18** using Michael addition and intramolecular cyanide-mediated nitrile to nitrile cyclocondensation reaction using gem-diacetylated acrylonitrile **16** and TMS-CN **17**. The synthesis is carried out under aqueous conditions and generates a yield of 90% with appreciable chemoselectivity (Scheme 10) [12].



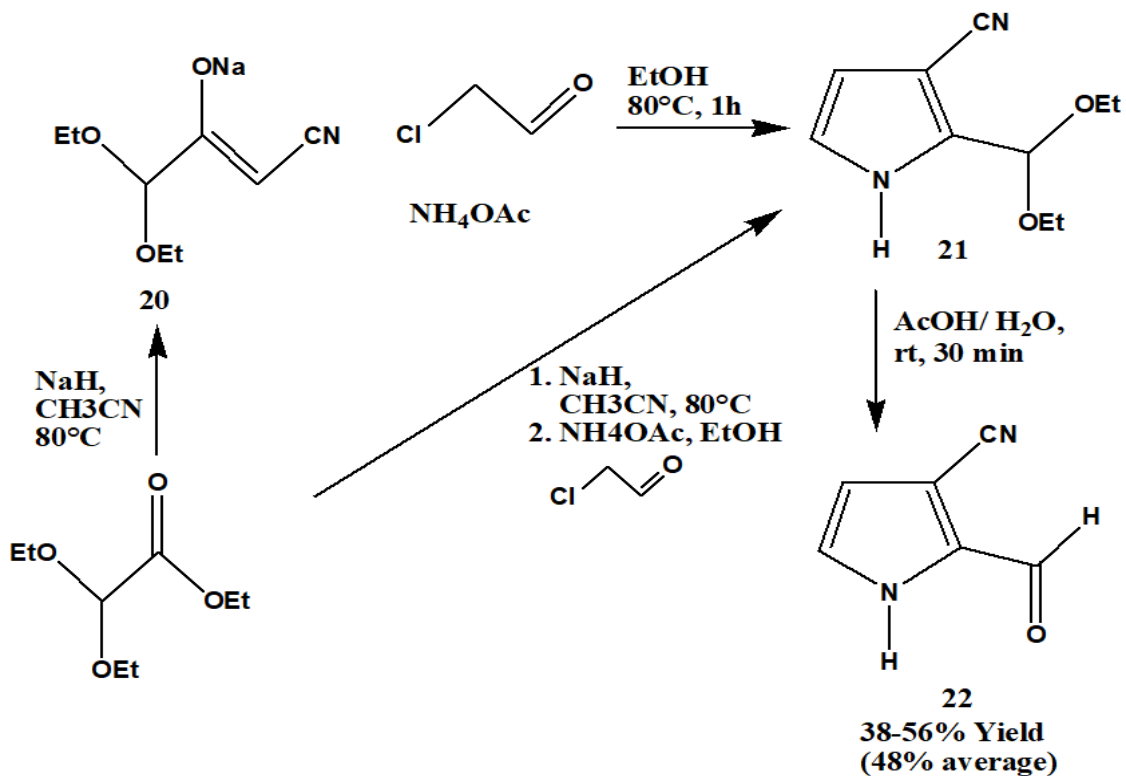
Scheme 10



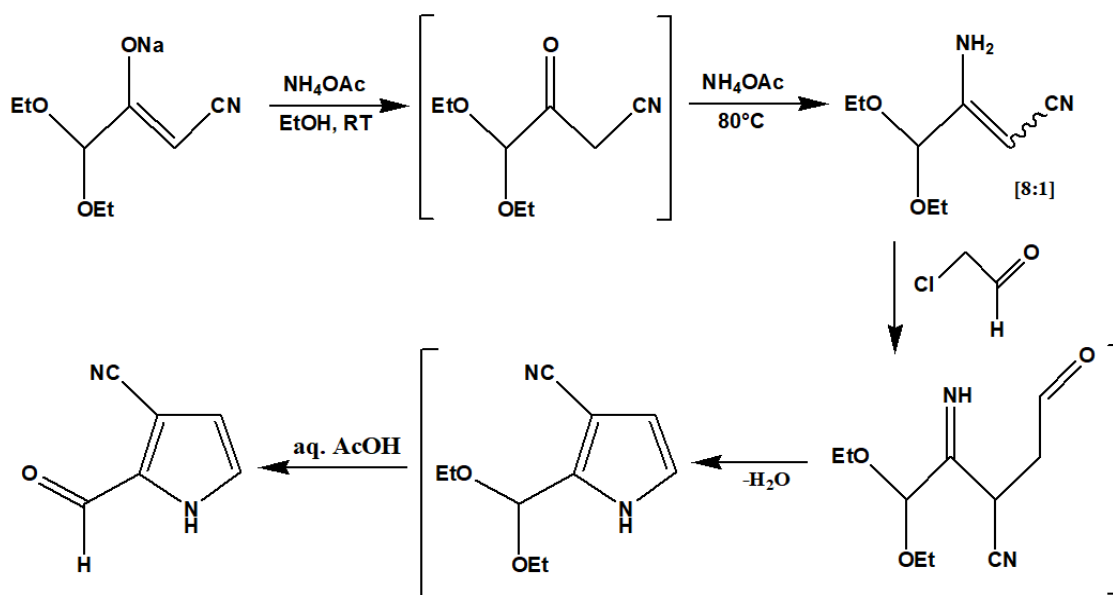
Possible Reaction Pathway of Scheme 10

The Hantzsch synthesis has been modified for the preparation of specific classes of pyrroles which are otherwise not easily obtained. Thus, Moss and Nowak reported the synthesis of pyrroles bearing carbonyl substituents **22** at C-2 and C-3 positions by reacting sodium enolate of 4,4-diethoxy-3-oxobutanenitrile **20**, ammonium acetate and chloroacetaldehyde. The

reaction can also be carried out using a four-component protocol in which acetonitrile and ethyl-2,2-diethoxyacetate are used as the precursor for 4,4-diethoxy-3-oxobutanenitrile **20** thereby facilitating a one-pot process (Scheme 11) [13].

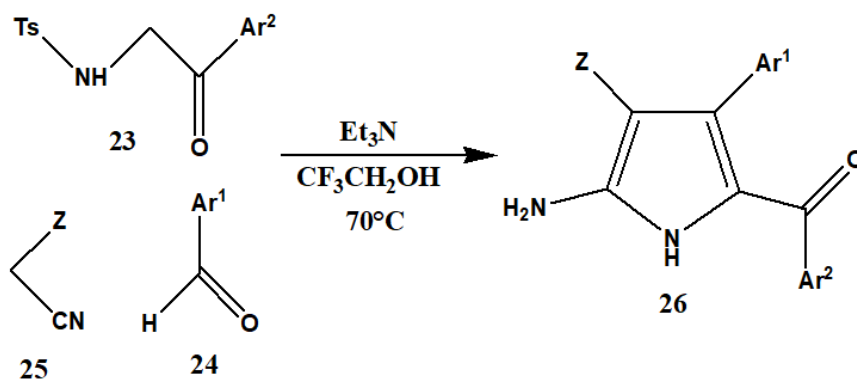


Scheme 11

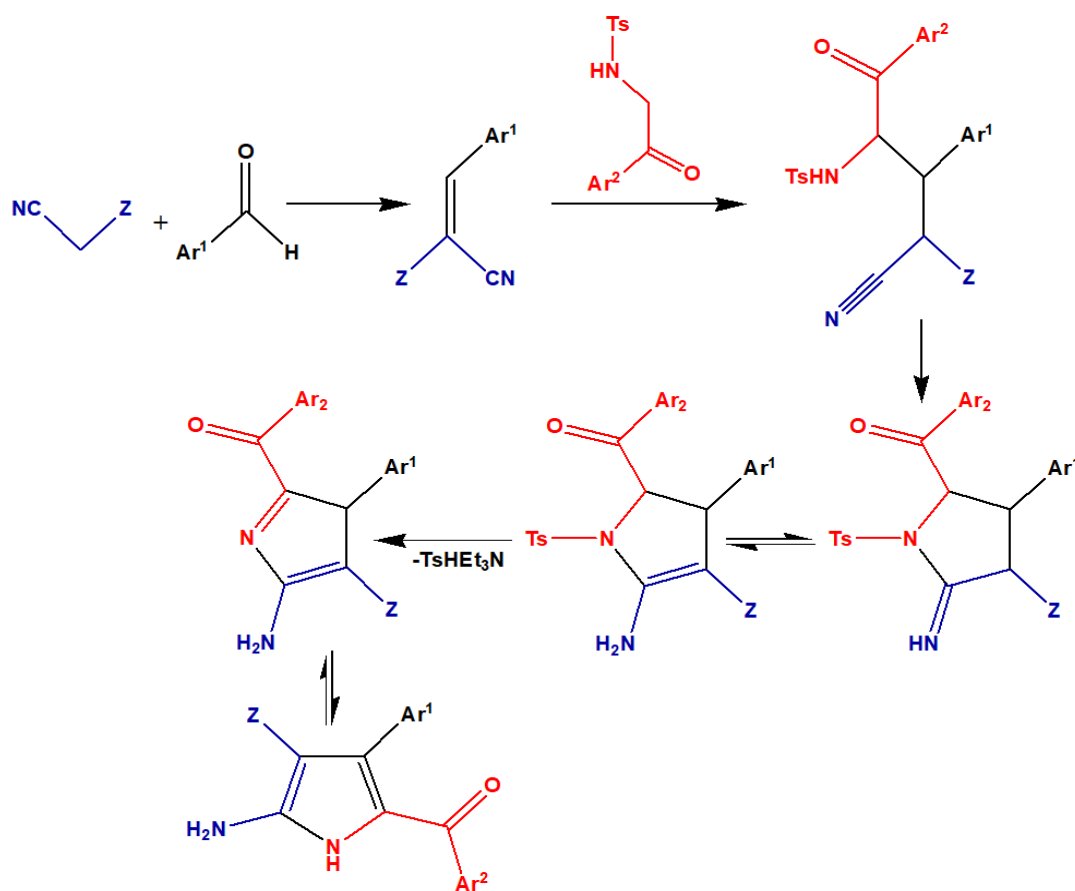


Possible Reaction Pathway for Scheme 11

Wang and Dömling reported a very efficient synthetic pathway for the preparation of the derivatives of 2-amino-5-ketoarylpyrrole **26** scaffold because of their high pharmaceutical potential. In this method, a mixture of N-protected  $\alpha$ -amino acetophenones **23**, aromatic aldehydes **24** and malonodinitrile **25** or cyanoacetic acid derivatives are refluxed in trifluoroethanol for about 12 hours and the product pyrroles precipitated out of the reaction mixture, thereby eliminating the need for chromatographic separation (Scheme 12) [14].

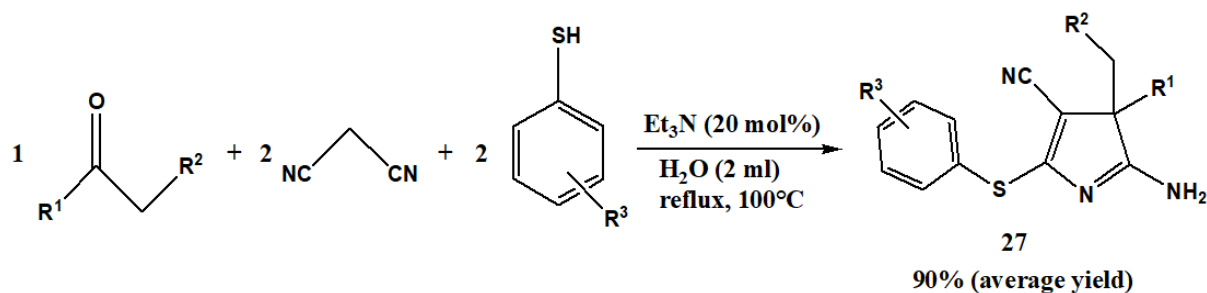


Scheme 12

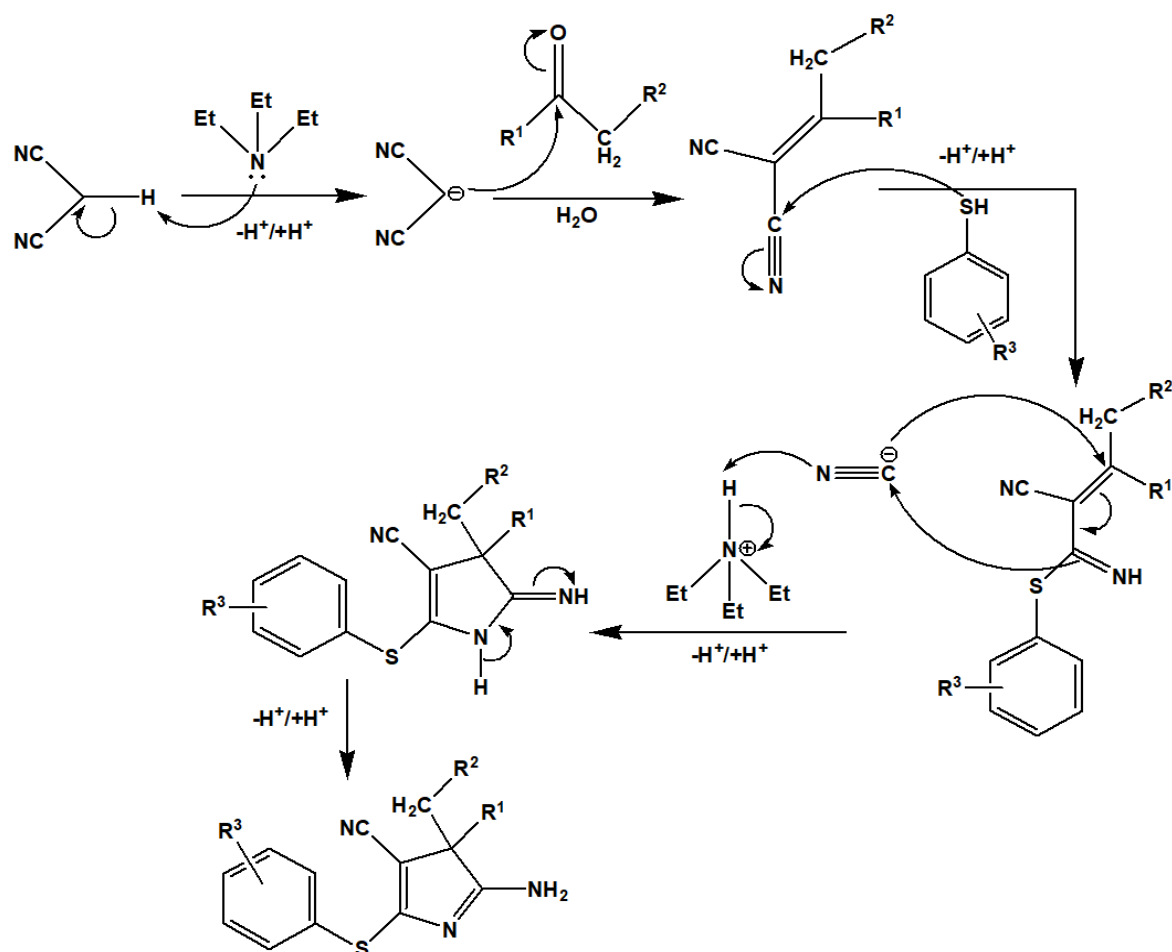


Possible Reaction Pathway for Scheme 12

Recently, Mukhopadhyay and his co-workers reported an innovative one-pot multicomponent synthesis with the aid of an organocatalyst (triethylamine) for the generation of 3H-pyrroles **27** with an average yield of 90%. This method uses ketones, thiols and malononitrile in water as a solvent which leads to an unprecedented coupling that results in the formation of nitrogen containing ring with initiating from any amine moiety. This method exploits the ability to act both as an electrophile and a nucleophile (Scheme 13) [15].



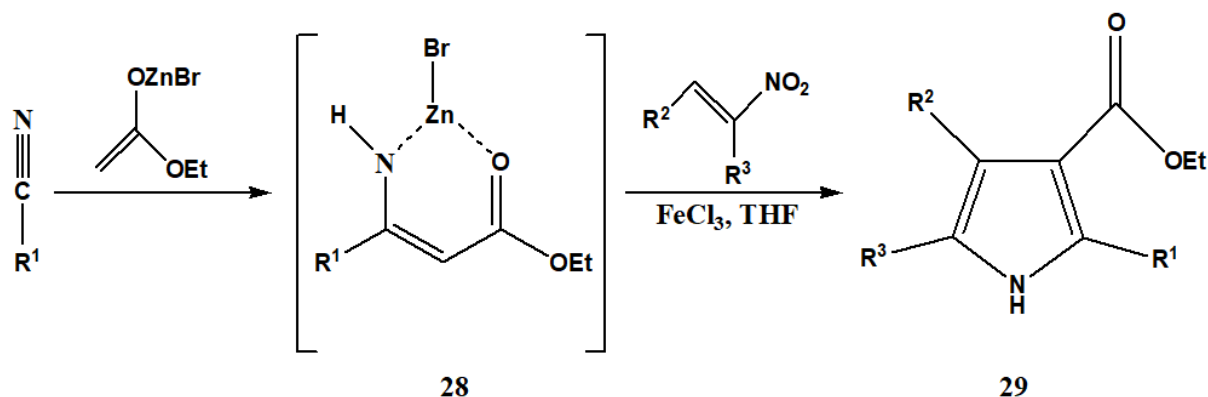
Scheme 13



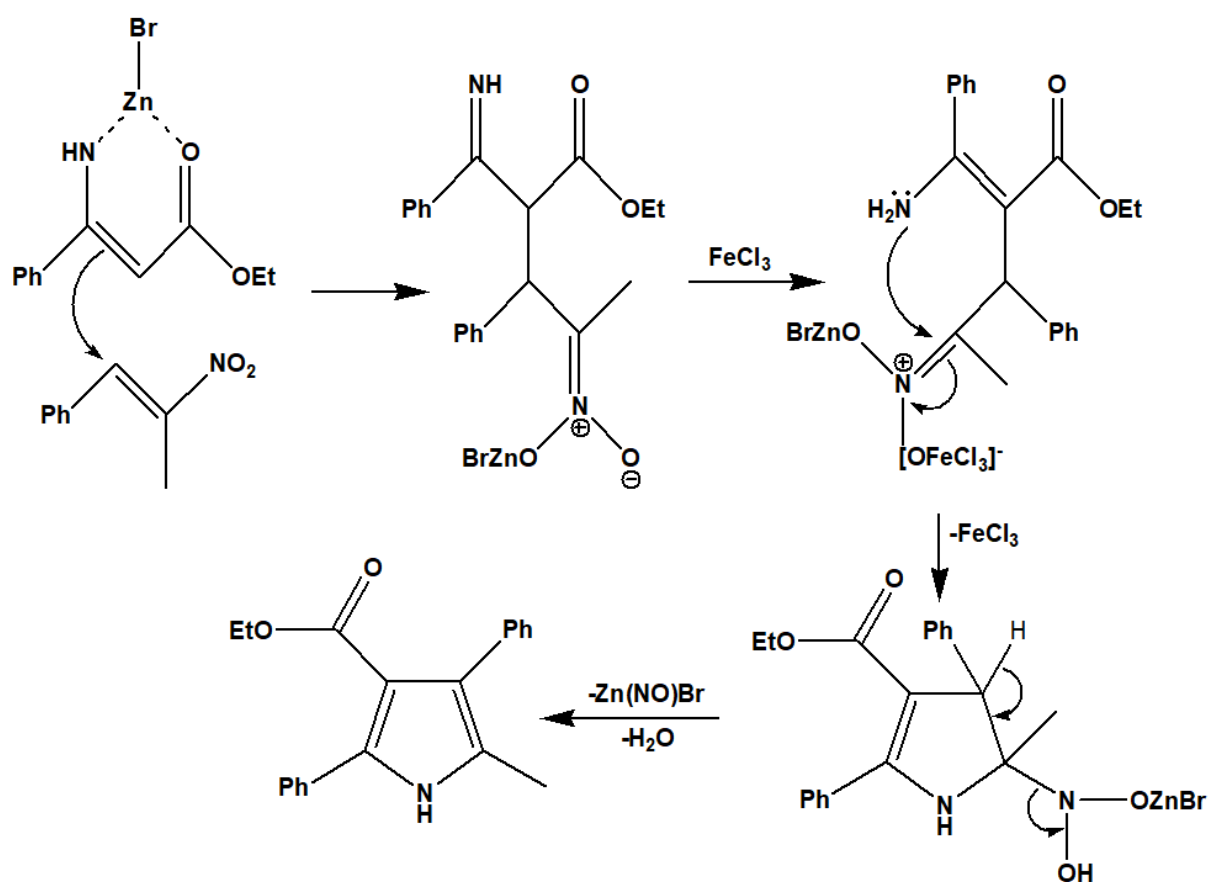
Possible Reaction Pathway for Scheme 13



Zhao et al. recently reported the synthesis of highly functionalized NH-pyrroles **29** from nitriles in a tandem one-pot reaction protocol. The process involves an iron catalyzed addition and cyclization of the Blaise reaction intermediate **28** and nitro olefins. This reaction produces a broad spectrum of substituted pyrroles in good yields. Thus, in order to obtain the Blaise intermediate, a mixture of nitriles and ethyl 2-bromoacetate is refluxed in the presence of zinc. Moreover, this reaction exhibits good functional group tolerance (Scheme 14) [16].

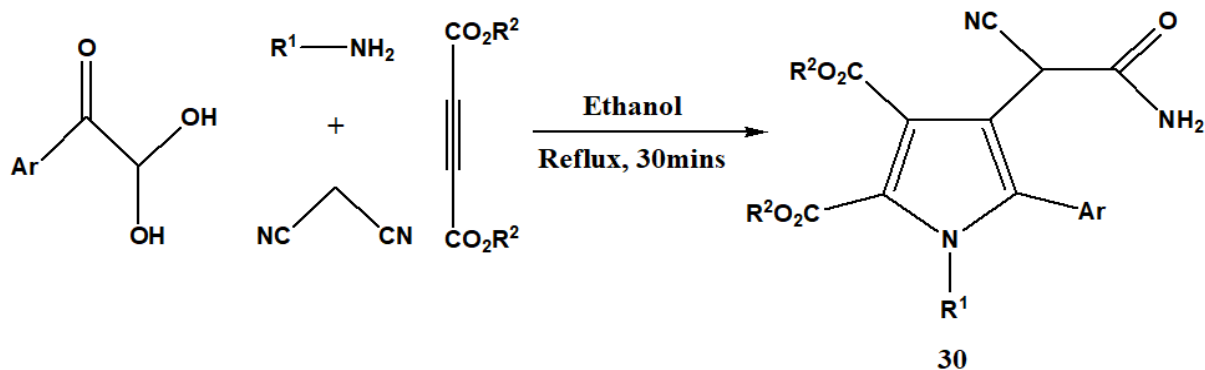


Scheme 14

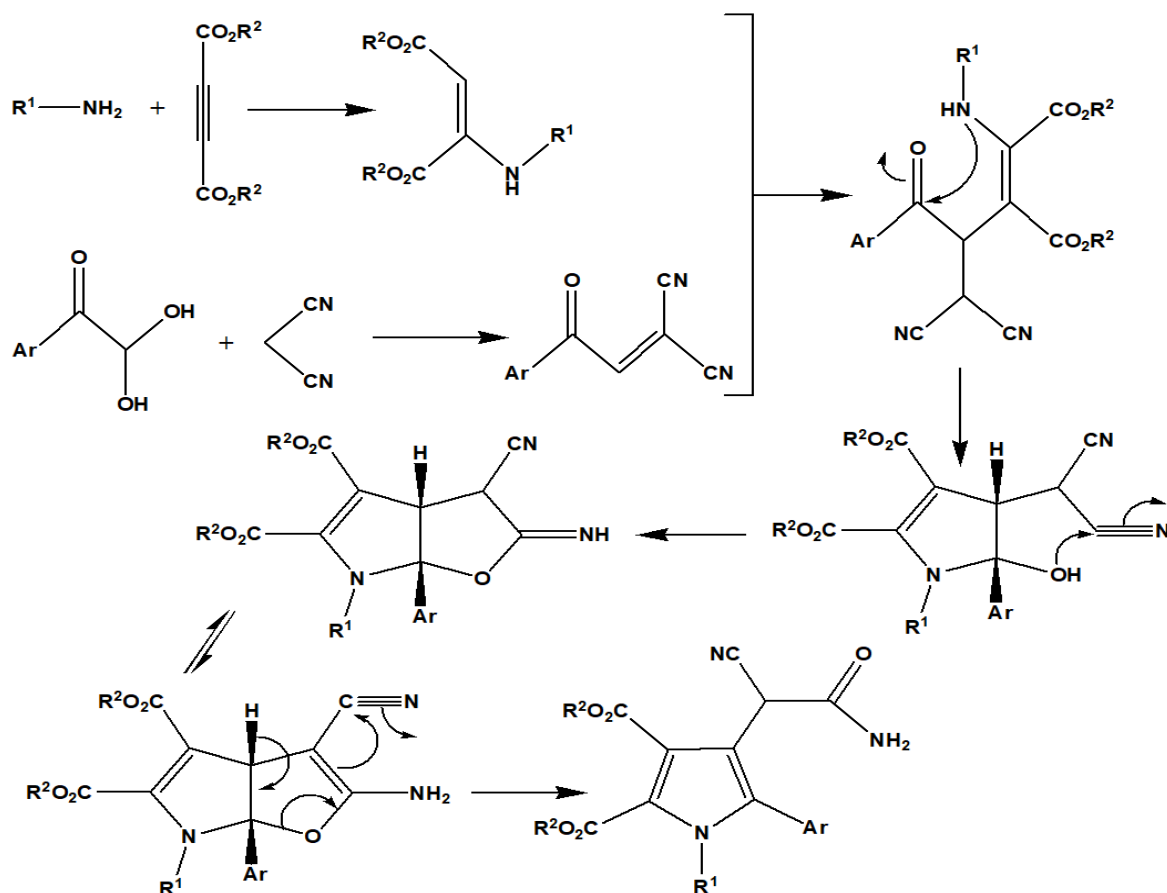


Possible Reaction Pathway for Scheme 14

Recently, Feng et al. reported a highly efficient catalyst-free synthetic pathway for the generation of polysubstituted pyrroles **30** through a novel four-component domino reaction using arylglyoxal monohydrate, an aniline, a dialkyl but-2-ynedioate and malononitrile. The reaction is carried out by refluxing in ethanol for 30 mins and thereby generating an average yield of about 77%. Thus, this method is used to rapidly produce a diverse collection of polysubstituted pyrroles with excellent yields (Scheme 15) [17].

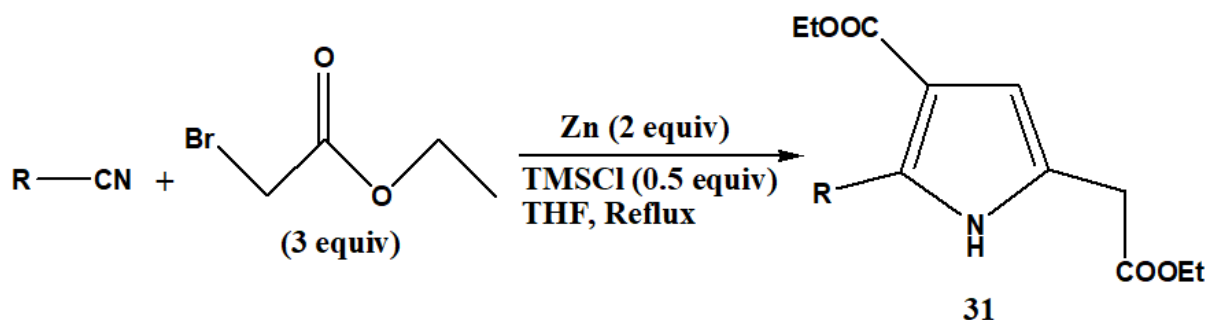


Scheme 15

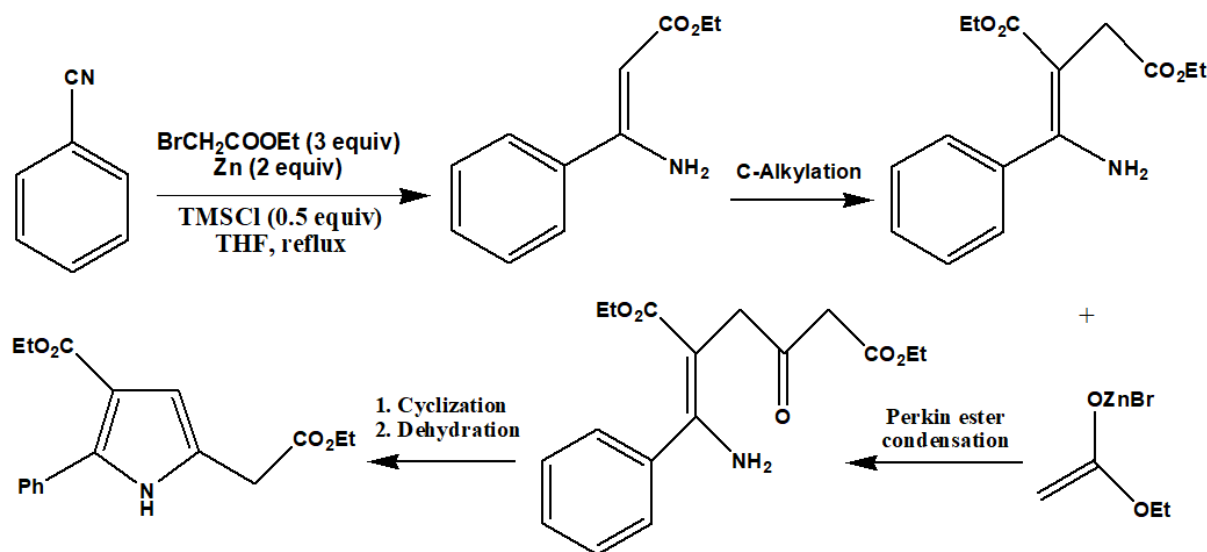


Possible Reaction Pathway for Scheme 15

Rao and Desai reported an efficient one-pot synthesis of 2,3,5-trisubstituted pyrrole diesters **31** through a zinc mediated pseudo four-component reaction using readily available aromatic/ benzylic/ aliphatic nitriles and ethyl bromoacetate and trimethylsilyl chloride as the catalyst. It is a straightforward CN+3C procedure and consist of modifying the classic Blaise reaction thereby furnishing pyrroles with yields up to 90% (Scheme 16) [18].



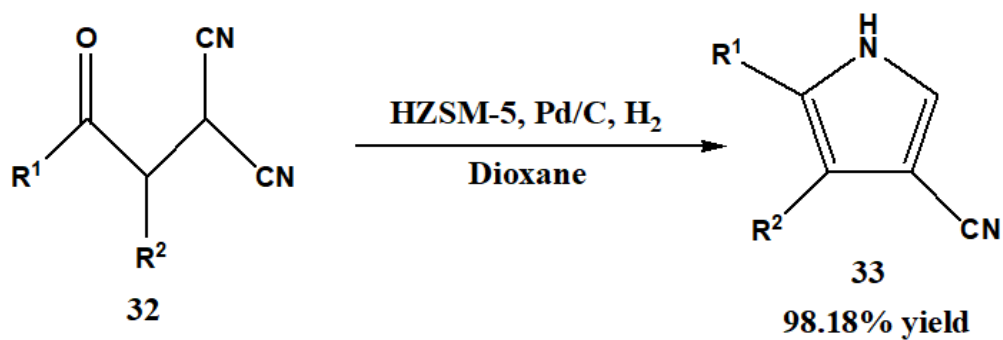
Scheme 16



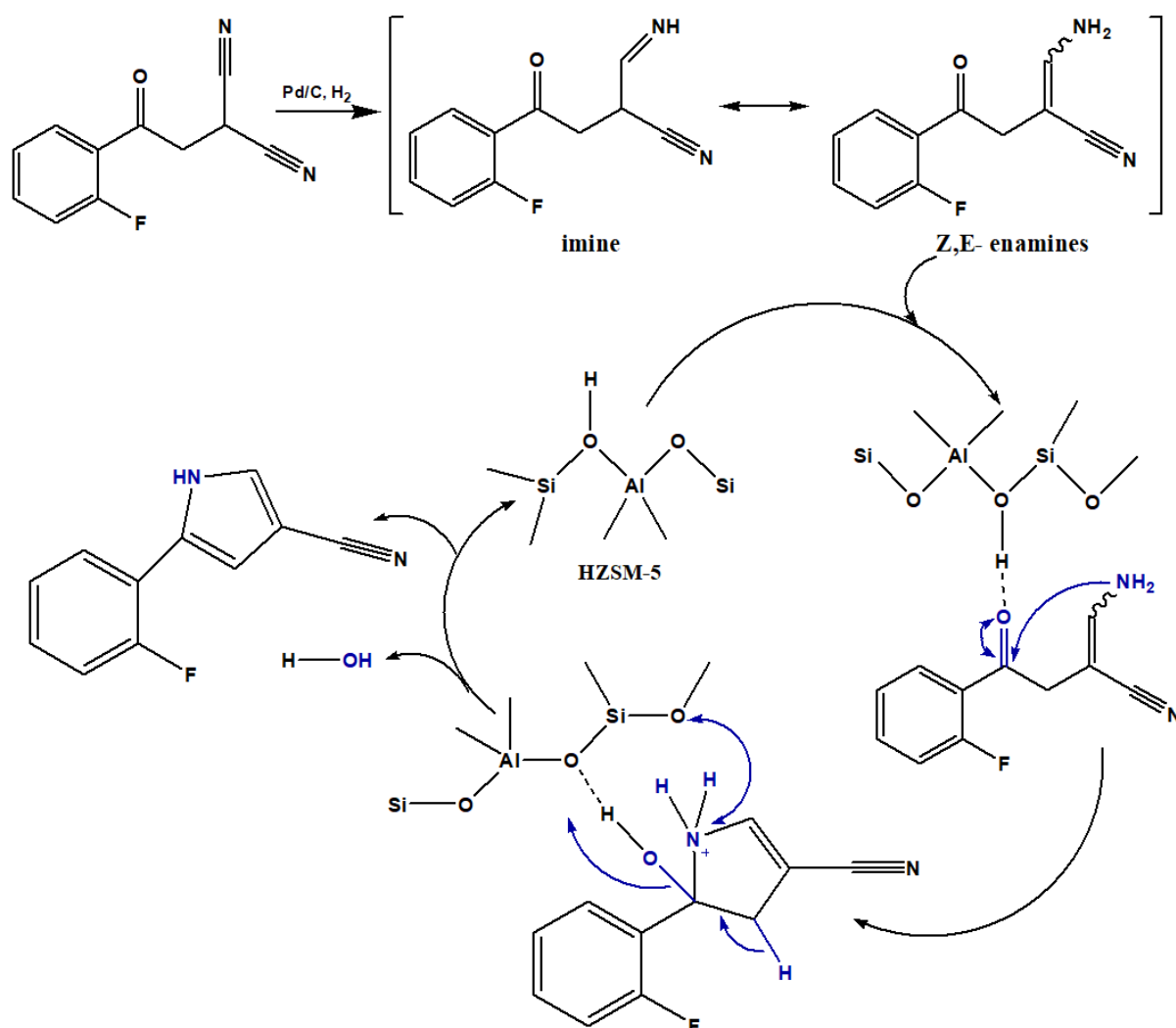
Possible Reaction Pathway for Scheme 16

Chen and his co-workers reported an efficient and eco-friendly approach for the synthesis of 4,5-substituted 1H-pyrrole-3-carbonitriles **33** with excellent yields (up to 98%) by using 2-(2-oxo-2-ethyl)malononitriles **32** and commercially available HZSM-5 and Pd/C as the recyclable heterogeneous catalyst instead of traditional liquid acids. The product obtained is a key

intermediate in the synthesis of vonoprazan which adds to the practical utility of this synthetic pathway (Scheme 17) [19].

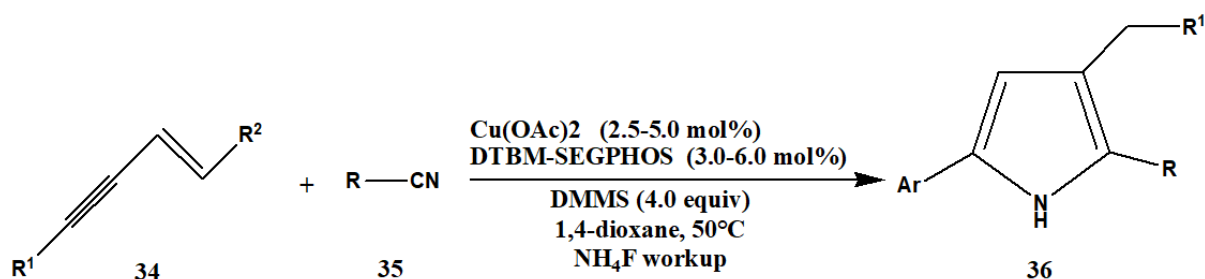


Scheme 17

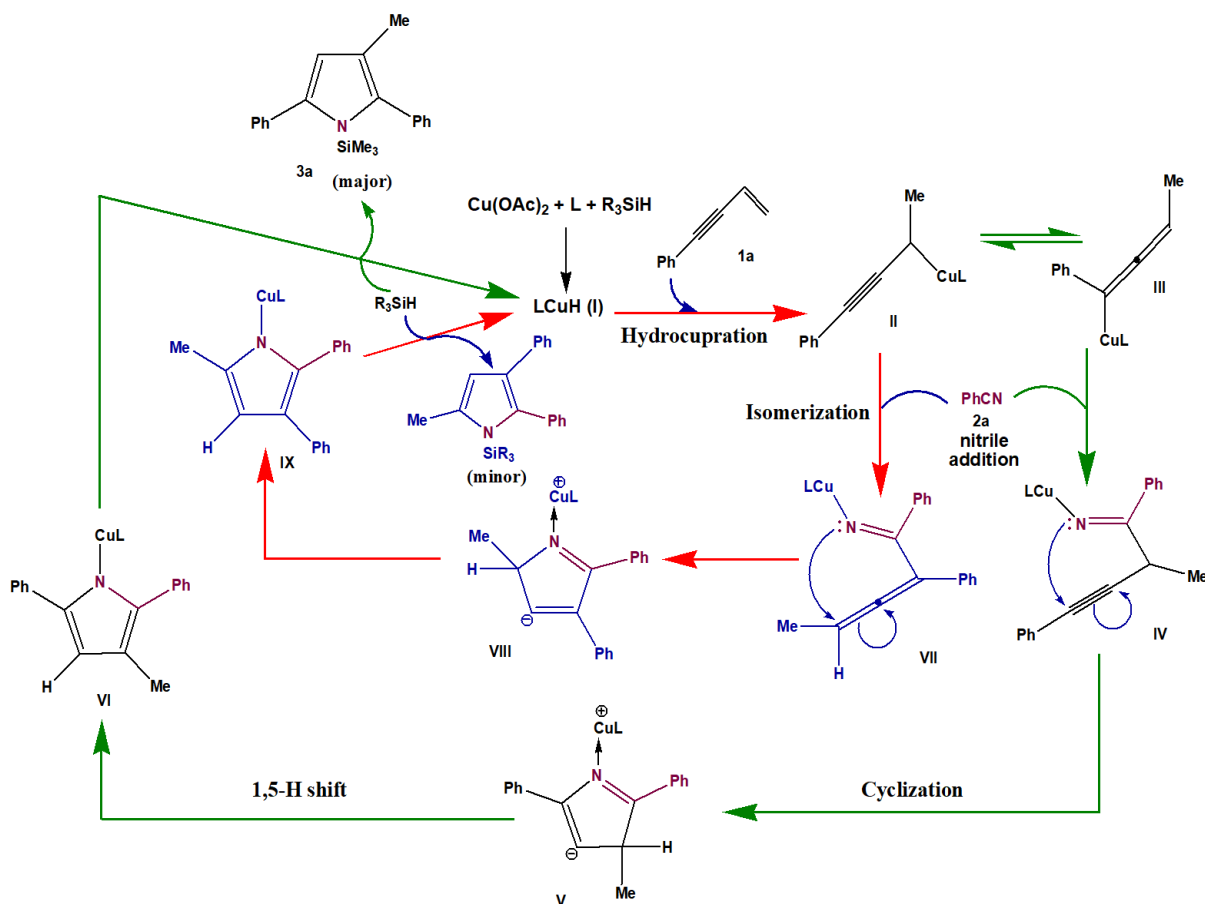


Possible Reaction Pathway for Scheme 17

Zhou et al. reported the synthesis of polysubstituted pyrroles **36** via an efficient copper-hydride (CuH)-catalyzed coupling reaction between enynes **34** and nitriles **35**. The protocol involves both aromatic and aliphatic substrates along with a broad range of functional groups. The product pyrrole is obtained in good yield and high regioselectivity. The proposed mechanism ascertains that the Cu-based catalyst enhances both the initial reductive elimination and the cyclization steps. The reaction mechanism was elucidated using DFT calculations (Scheme 18) [20].

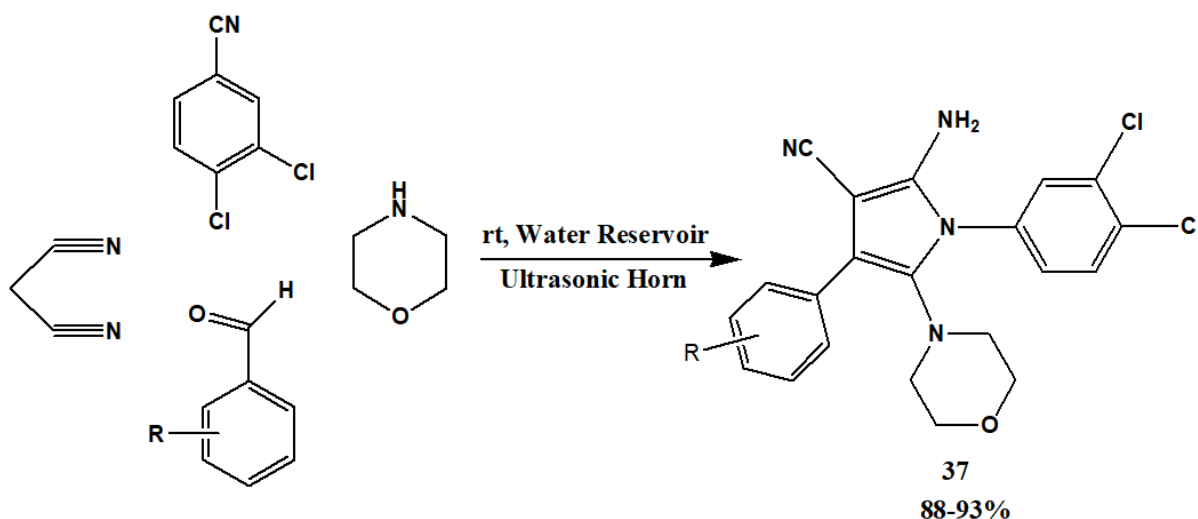


Scheme 18

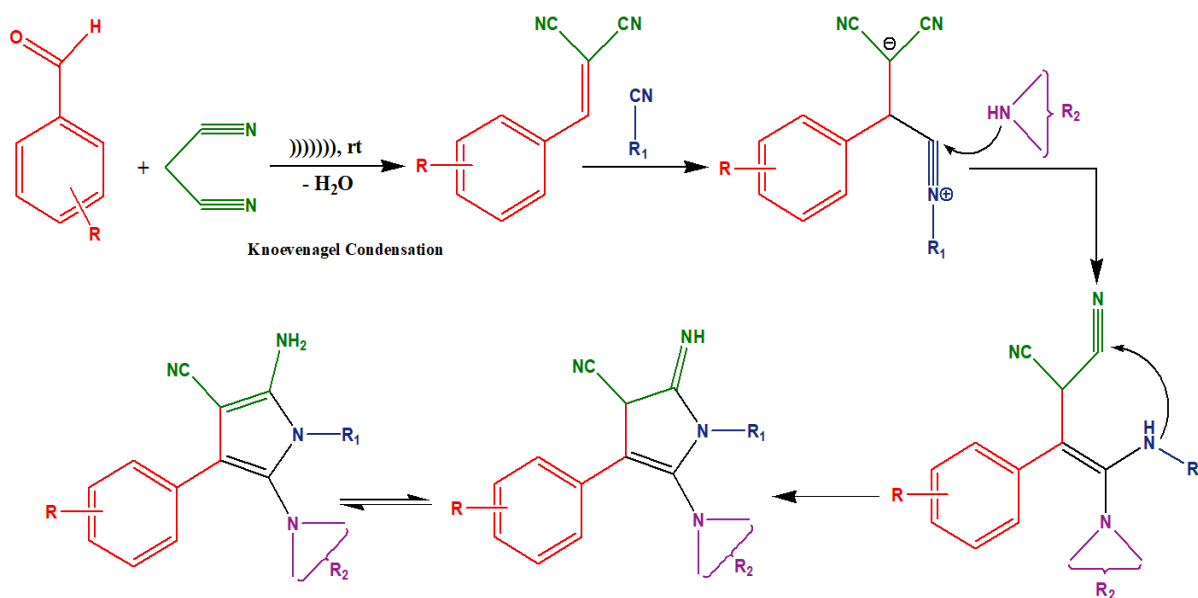


Possible Reaction Pathway for Scheme 18

Pagadala and Anugu reported a one-pot synthesis of polyfunctional pyrroles using green chemical methods. The reaction sequence involves the standard Knoevenagel condensation which is followed by Michael type reaction under ultrasonic energy and with water as an excellent solvent. It has been termed as a green method because of its catalyst free reaction system, short reaction time, excellent yields (88-93%), use of ultrasound in water medium, easy workup, high atom economy and economically efficient (Scheme 19) [21].



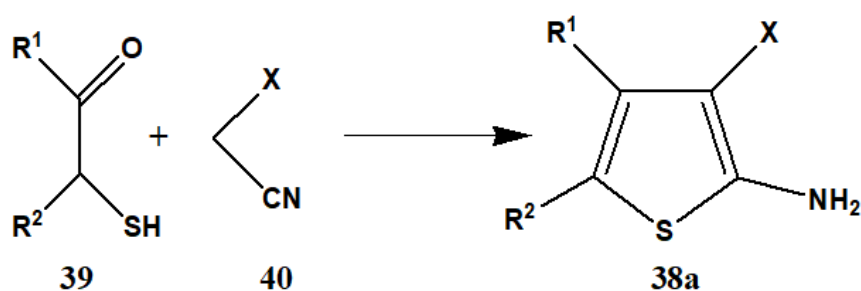
**Scheme 19**



**Possible Reaction Pathway for Scheme 19**

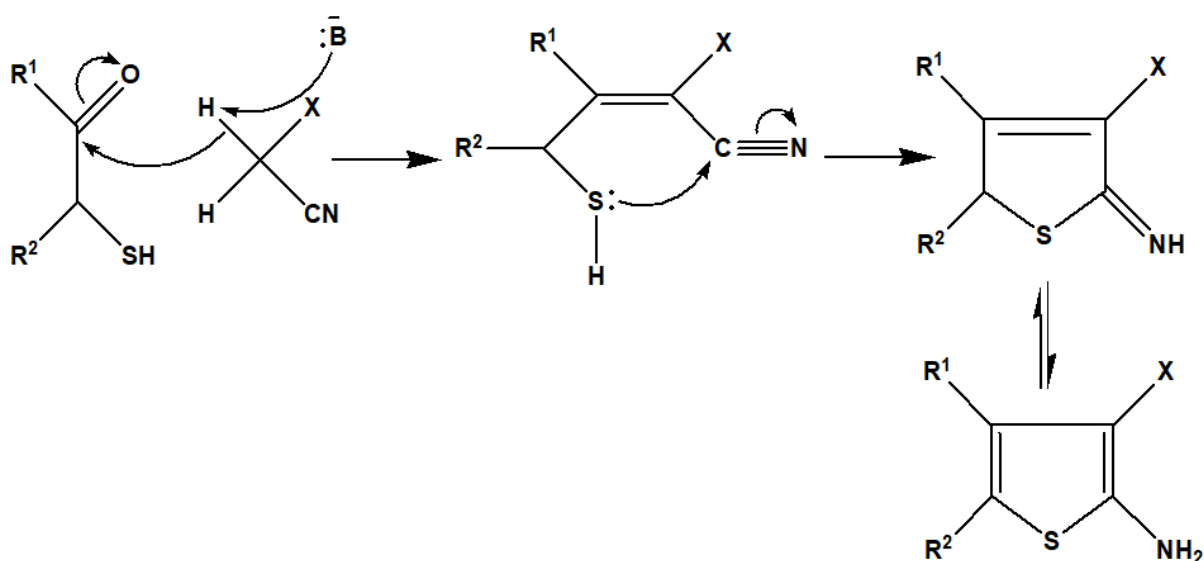
## 4.2 Thiophene and its derivatives

Gewald developed the most promising and facile set of synthetic pathways to form 2-aminothiophenes **38a,b,c** with electron withdrawing groups viz. cyano, carboethoxy, carboxamido etc. in position 3 and alkyl, aryl and hetaryl groups in the 4<sup>th</sup> position. In one such synthetic route,  $\alpha$ -mercaptoaldehyde or  $\alpha$ -mercaptoketone **39** are allowed to react with an activated nitrile **40** bearing an electron withdrawing group in the presence of basic catalyst viz. triethylamine, piperidine at 50°C in solvents such as water, ethanol, DMF, dioxane etc. The major disadvantage of this route is that the starting material used are unstable and are difficult to be prepared. Additionally, it was found that non-activated nitriles fail to undergo this reaction (Scheme 20a) [22].



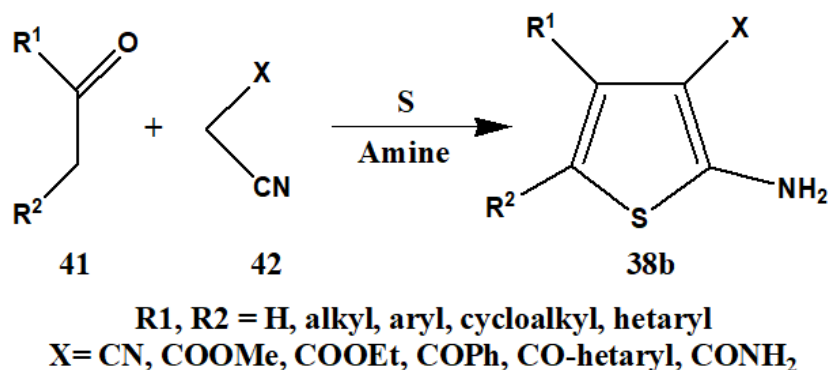
$R^1, R^2 = H, \text{ alkyl, aryl, cycloalkyl, hetaryl}$   
 $X = CN, COOMe, COOEt, CPh, CO\text{-hetaryl}$

Scheme 20a



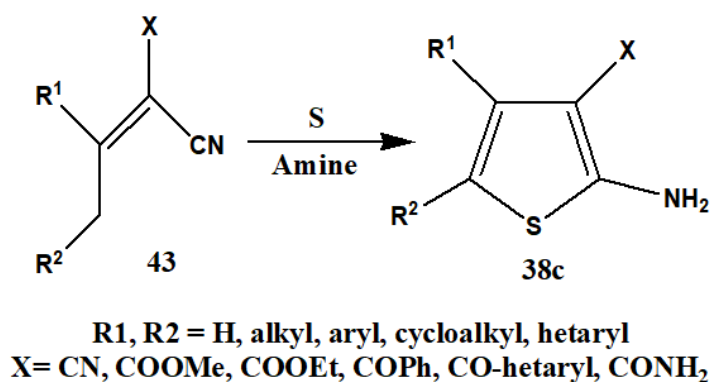
Possible Reaction Pathway for Scheme 20a

The second route is a convenient technique and is thus extensively used for the synthesis of 2-aminothiophenes **38b**. It is a one-pot reaction pathway which includes the condensation of aldehydes, ketones or 1,3-dicarbonyl **41** with activated nitriles **42** in the presence of sulfur and amine at room temperature. The commonly used solvents are ethanol, DMF, dioxane etc. This route generates a higher yield and also overcomes the drawbacks of the previous version as it uses starting materials that are commercially available (Scheme 20b) [22].



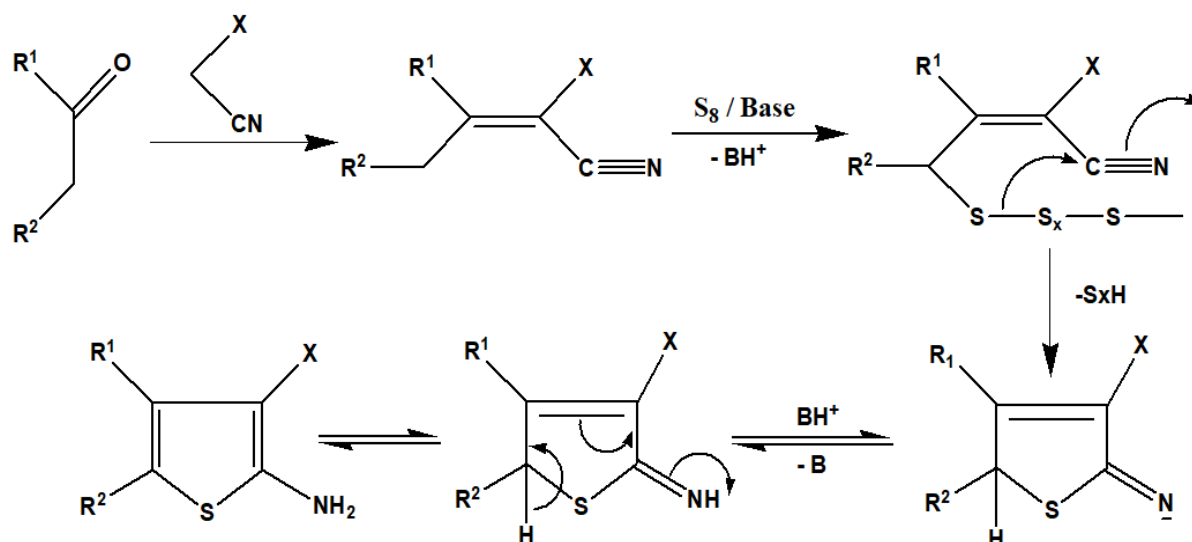
Scheme 20b

The third synthetic route is a two-step procedure which involves the initial synthesis of an  $\alpha,\beta$ -unsaturated nitrile **43** through a Knoevenagel-Cope condensation which is then treated with sulfur and amine. This route produces even higher yields (Scheme 20c) [22].



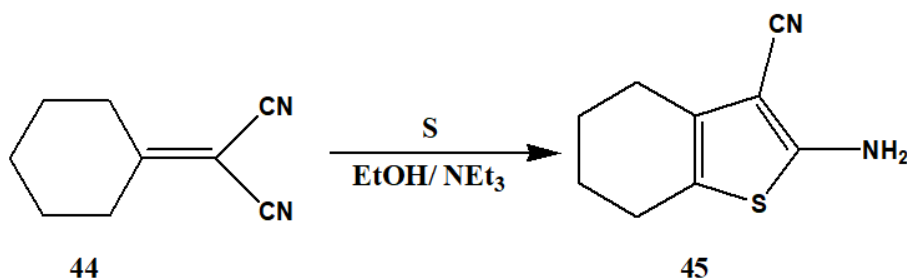
Scheme 20c





### Possible Reaction Pathway for Scheme 20b & 20c

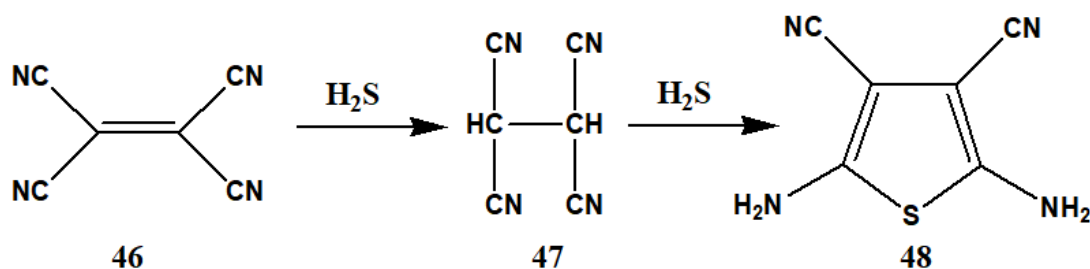
Goudic reported the synthesis of thiophene derivatives obtained by thiolation of α,β-unsaturated nitriles. One such example is the treatment of the arylidene derivative of cyclohexanone **44** with elemental sulfur thereby yielding the enaminothiophene derivative **45**. It is carried out in the presence of a base viz. triethylamine and ethanol as the solvent (Scheme 21) [23].



Scheme 21

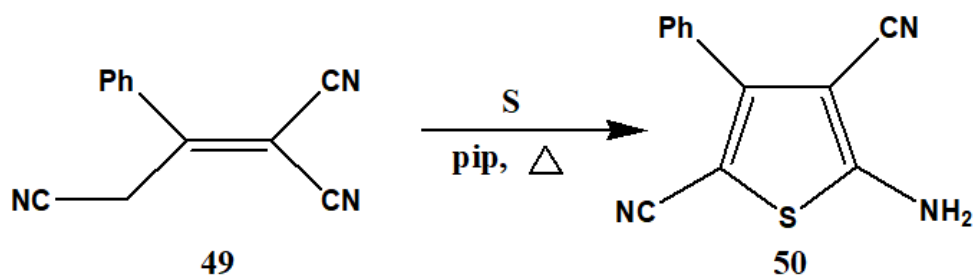
Middleton et al. designed a synthesis for the preparation of 2,5-Diamino-3,4-dicyanothiophene by reacting tetracyanoethylene **46** with hydrogen sulphide in the presence of a basic catalyst. It is a two-step synthesis which involves the initial formation and isolation of tetracyanoethane **47** which is then followed by the conversion into of 2,5-Diamino-3,4-dicyanothiophene **48**. It was found that the use of sodium sulfide eliminated the need an added catalyst in the second step, whereas the use of hydrogen sulfide demands the use of catalyst to

carry it to completion. The commonly encountered catalyst are viz. triethylamine, pyridine and sodium hydroxide (Scheme 22) [24].



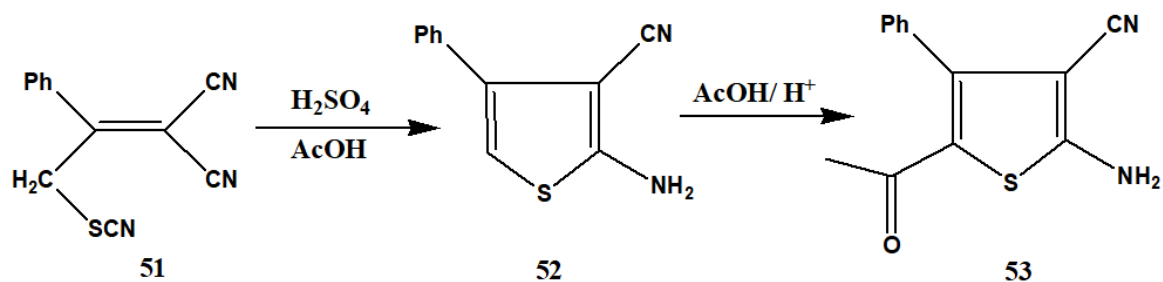
Scheme 22

Reux and Pochat reported a simple route for the synthesis of 5-amino-3-phenylthiophene-2,4-dicarbonitrile **50** from 3-dicyanomethylene-3-phenylpropionitrile **49**. In this route, compound **49** was allowed to react with elemental sulfur and refluxed in ethanol with a catalytic amount of piperidine (Scheme 23) [25].

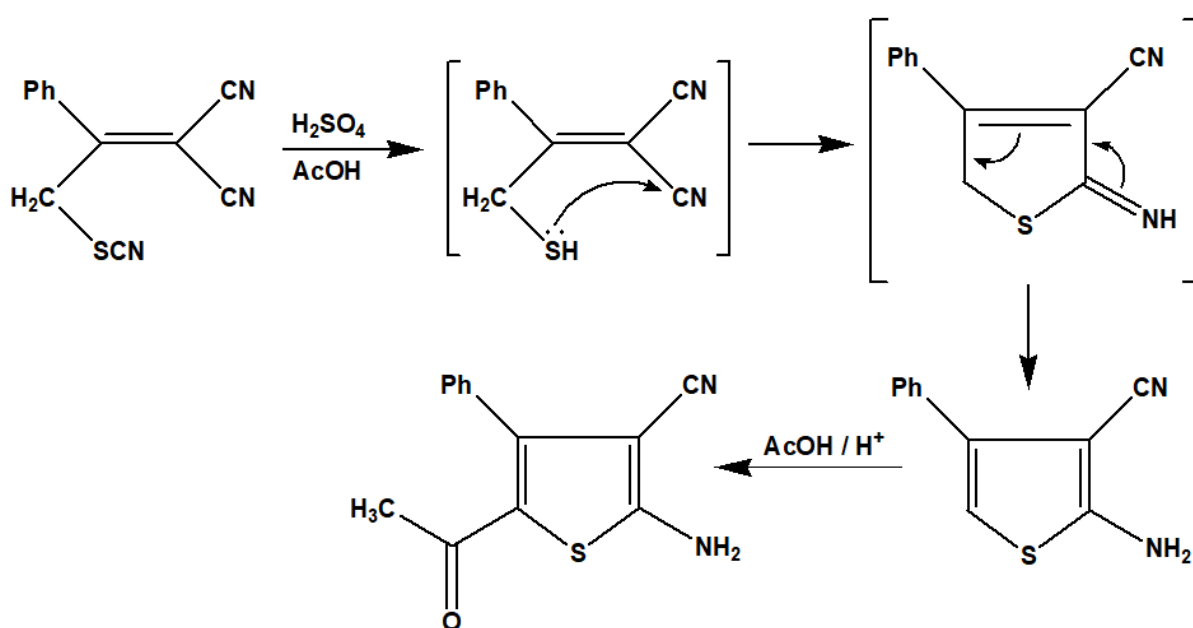


Scheme 23

Abdelrazek and Ead developed a reaction pathway for the transformation of  $\alpha$ -Cyano- $\beta$ -thiocyanatomethyl cinnamionitrile **51** into 5-acetyl-2-amino-4-phenylthiophen-3-carbonitrile **53**. This is carried out by refluxing compound **51** in a mixture of acetic acid and sulfuric acid thereby yielding a greenish product. The product was confirmed through elemental analysis and spectral data. It was assumed that the reaction proceeds with an initial hydrolysis of the thiocyanate group into  $-\text{SH}$  group which is then accompanied by intramolecular addition to the neighbouring CN to yield compound **52**. This resultant compound **52** is not separated and therefore undergoes acylation in the same reaction vessel thereby producing compound **53** (Scheme 24) [26].

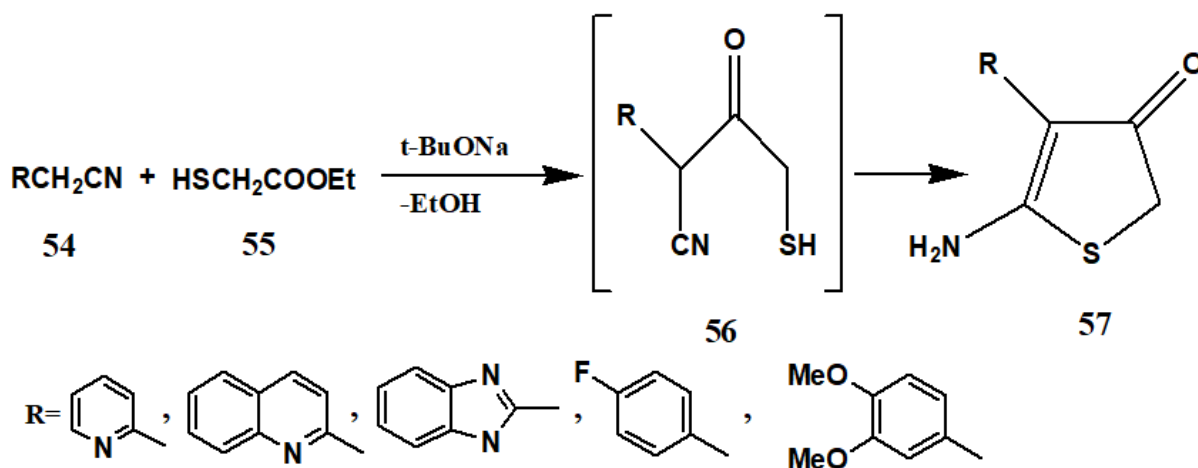


Scheme 24



Possible Reaction Pathway for Scheme 24

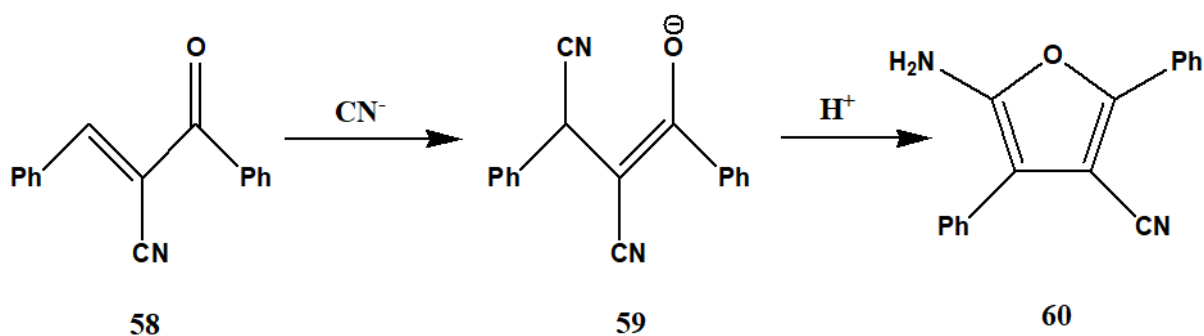
Volovenko et al. devised a new method for the synthesis of 2-amino-4(5H)-oxothiophenes **57** that contains aryl and hetaryl substituents in the 3<sup>rd</sup> position. This method is based on the acylation of aryl- and azahetarylacetonitriles **54** using mercaptoacetic ester **55** and is carried out in tert-butyl alcohol in the presence of sodium tert-butyrate. Spectral data suggested that compound **57** existed in the keto form instead of the tautomeric enol form (Scheme 25) [27].



Scheme 25

### 4.3 Furan and its derivatives

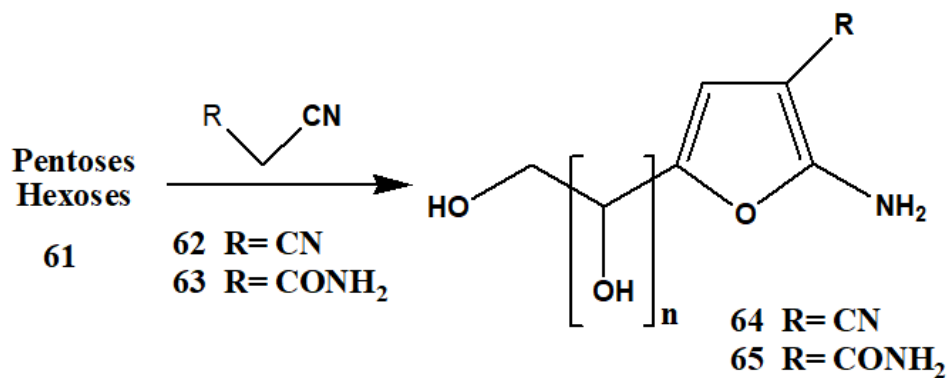
Recently, Aran and Soto reported the formation of furan derivatives **60**. They carried out the same by heating 2-benzoyl-3-phenyl-acrylonitrile **58** with cyanide ion (Scheme 26) [28].



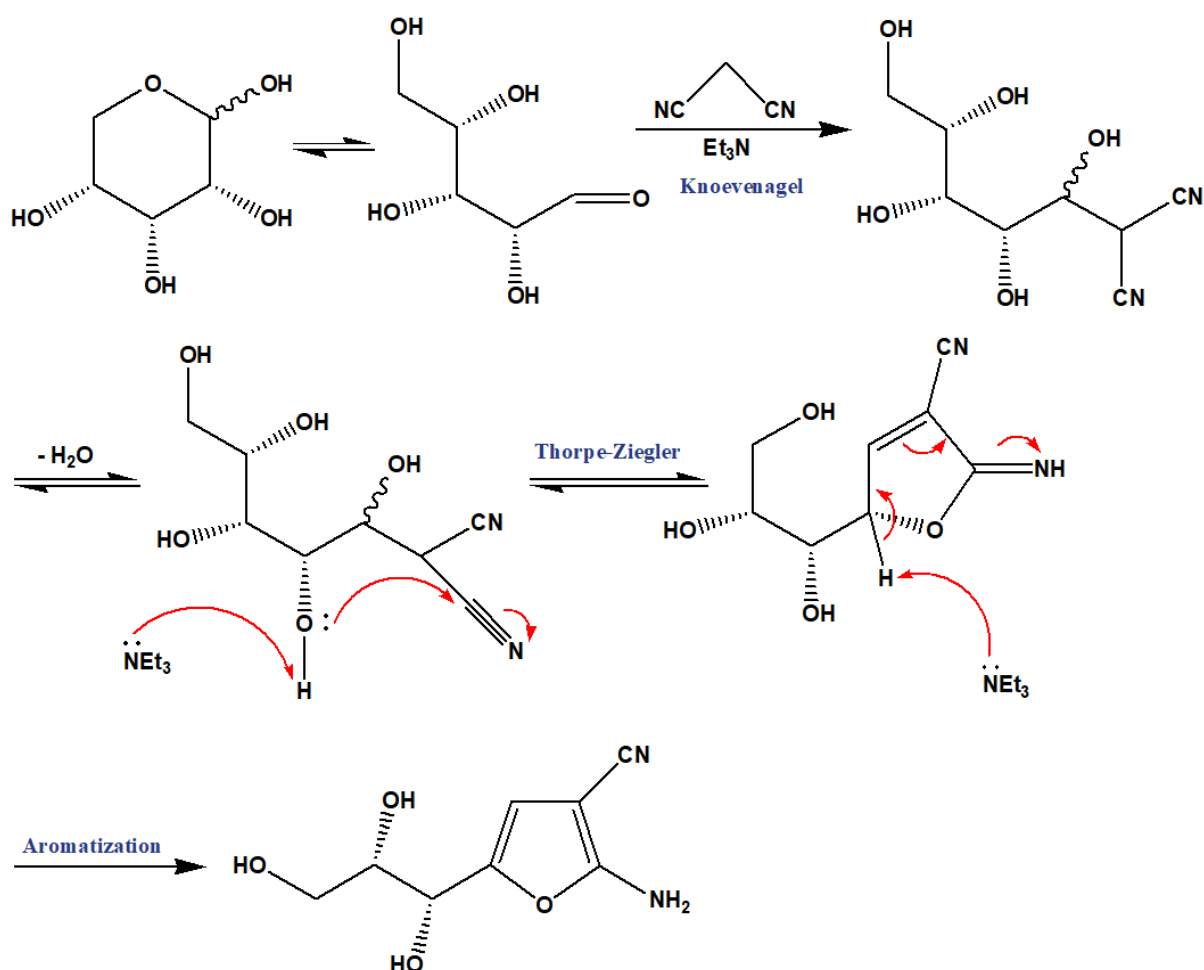
Scheme 26

Lambu and Judeh devised a one-pot condensation reaction of unprotected carbohydrates **61** with malononitrile **62** or malonamide nitrile **63** in basic medium to generate densely functionalized, polyhydroxyalkyl 2-amino-3-furanonitriles **64** and polyhydroxyalkyl 2-amino-3-furanocarboxamides **65** with 84-98% yields. On the basis of the rate of formation of the furans, the ability of the bases to catalyze the reaction was estimated and was found to have the

following order -  $\text{Et}_3\text{N} > \text{DBU} > \text{K}_2\text{CO}_3 > \text{NaOMe}$ . The synthesis is simple, metal-free and proceeds with exclusive chemo-, regio-, and stereo- selectivity. It is carried out under environmentally benign conditions and holds large-scale applications (Scheme 27) [29].

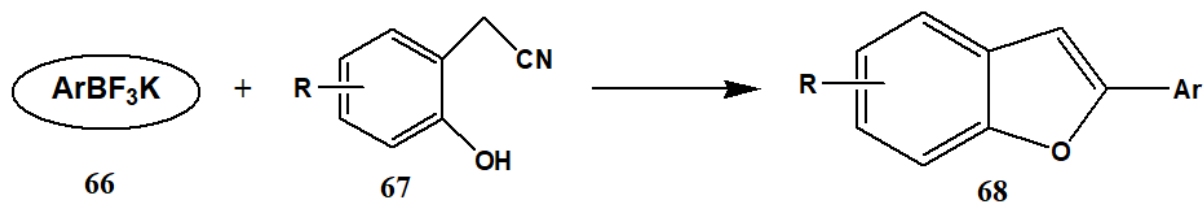


Scheme 27



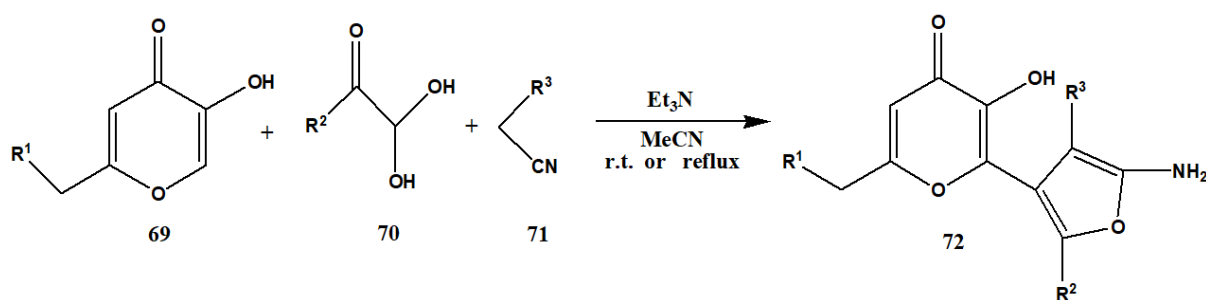
Possible Reaction Pathway for Scheme 27

Wang et al. reported a synthetic pathway for the preparation of 2-Arylbenzo[b]furans **68** which involves a palladium-catalyzed addition of potassium aryltrifluoroborates **66** to nitriles **67** and resulted in formation of moderate to excellent yields of the product. This is a one-step synthesis that proceeds through a sequential addition and intramolecular annulation reaction. The methodology is widely accepted and is a much-developed approach for the synthesis of furans (Scheme 28) [30].

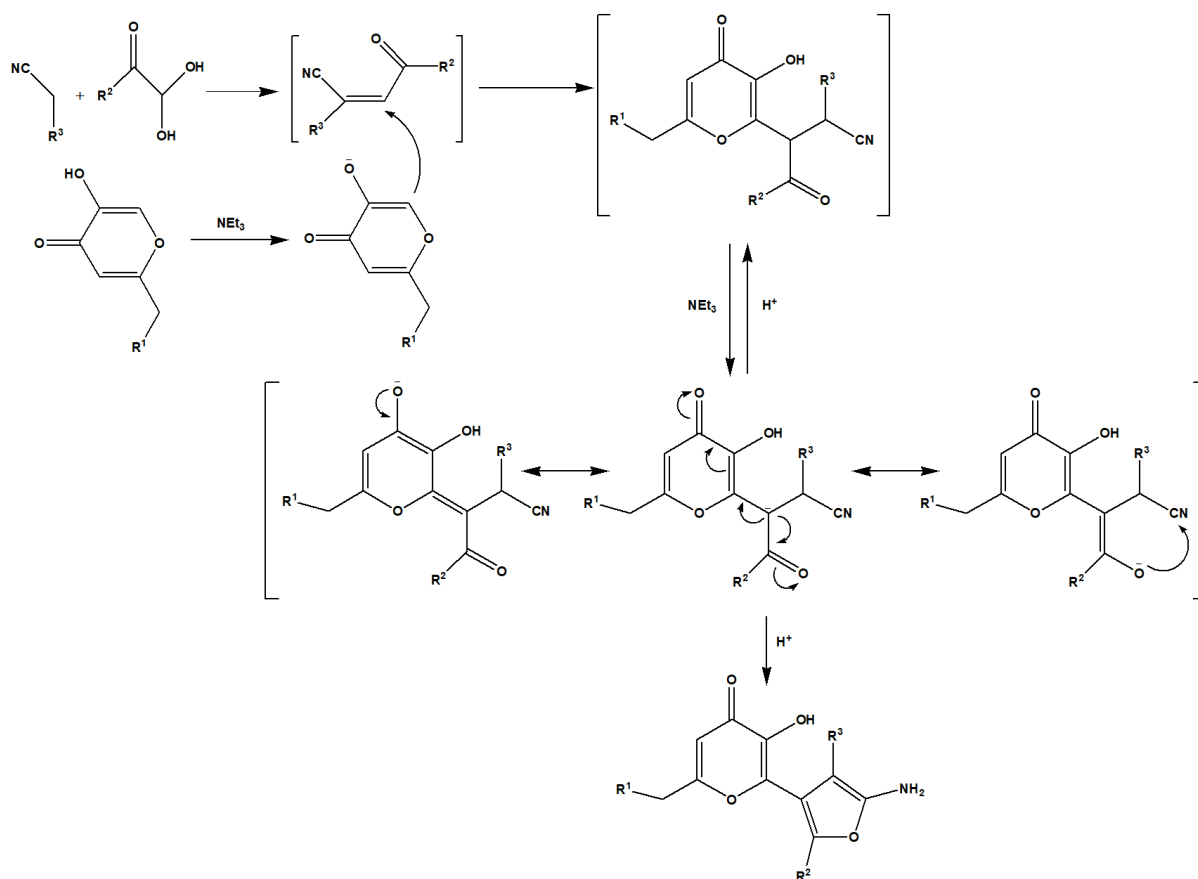


Scheme 28

Komogortsev et al. developed an efficient one-pot synthetic route for the preparation of 2-aminofurans **72**. It is a multicomponent reaction that includes 3-hydroxy-4H-pyran-4-ones **69**,  $\alpha$ -ketoaldehydes **70** and methylene active nitriles **71**. The major advantages of this synthesis are that it produces high yields and can be carried out under mild reaction conditions with high atom economy. Moreover, the product does not demand any chromatographic purification (Scheme 29) [31].

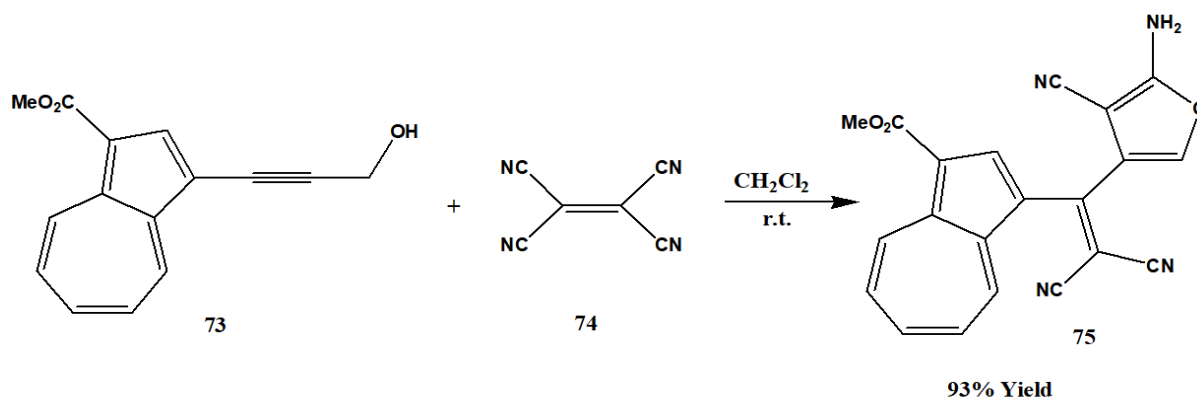


Scheme 29

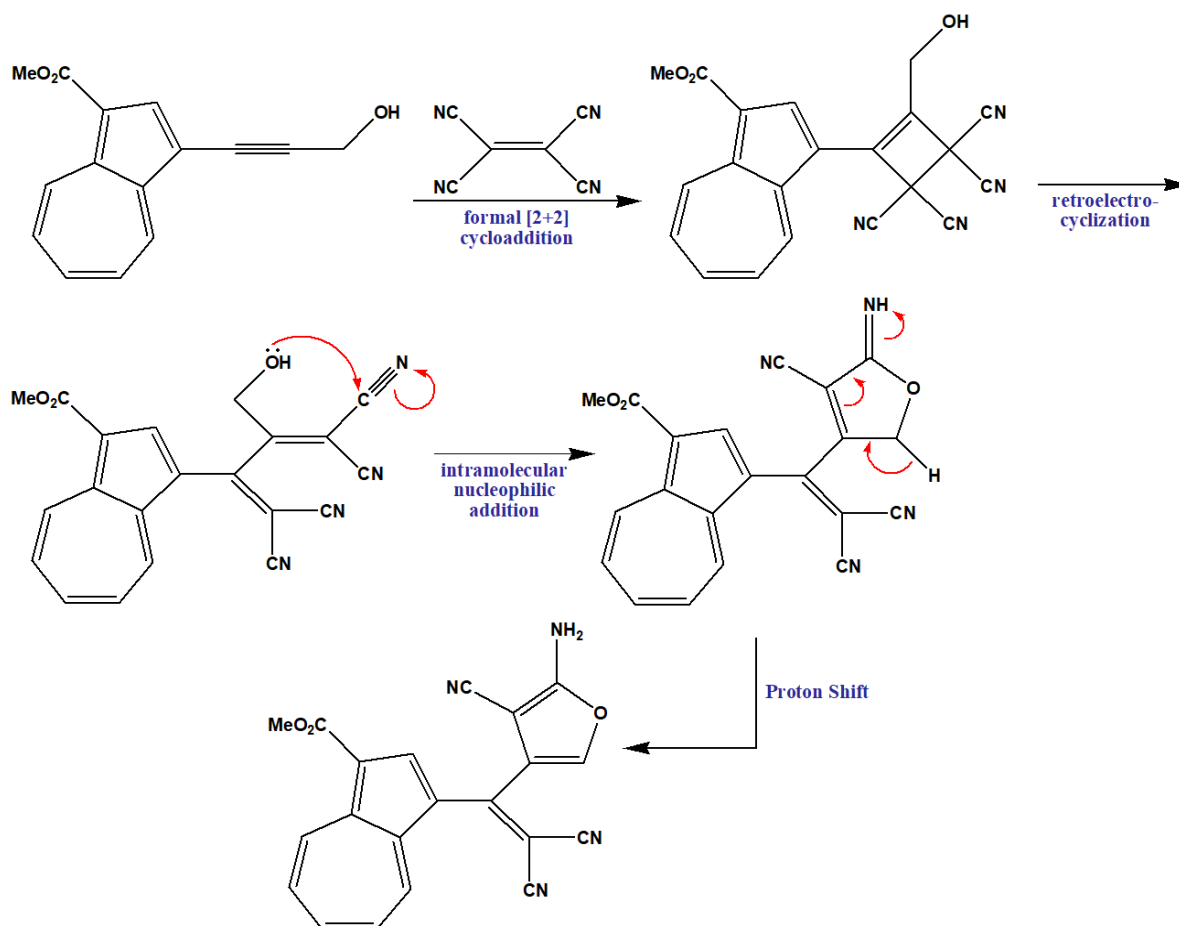


### Possible Reaction Pathway for Scheme 29

Shoji and his co-workers put forward sequential [2+2] cycloaddition-based synthesis of 2-aminofurans **75** in excellent yields (93%). It proceeds with a formal cycloaddition-retroelectrocyclization of 3-(1-azulenyl or N,N-dimethylanilino)-2-propyn-1-ols **73** and tetracyanoethylene **74**. It is a highly efficient procedure as it proceeds under mild conditions with short reaction period and yields products that become readily available with simple purification (Scheme 30) [32].



Scheme 30

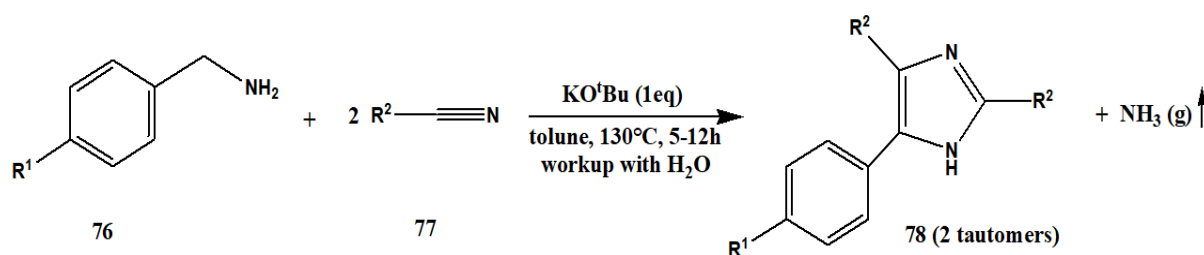


**Possible Reaction Pathway for Scheme 30**

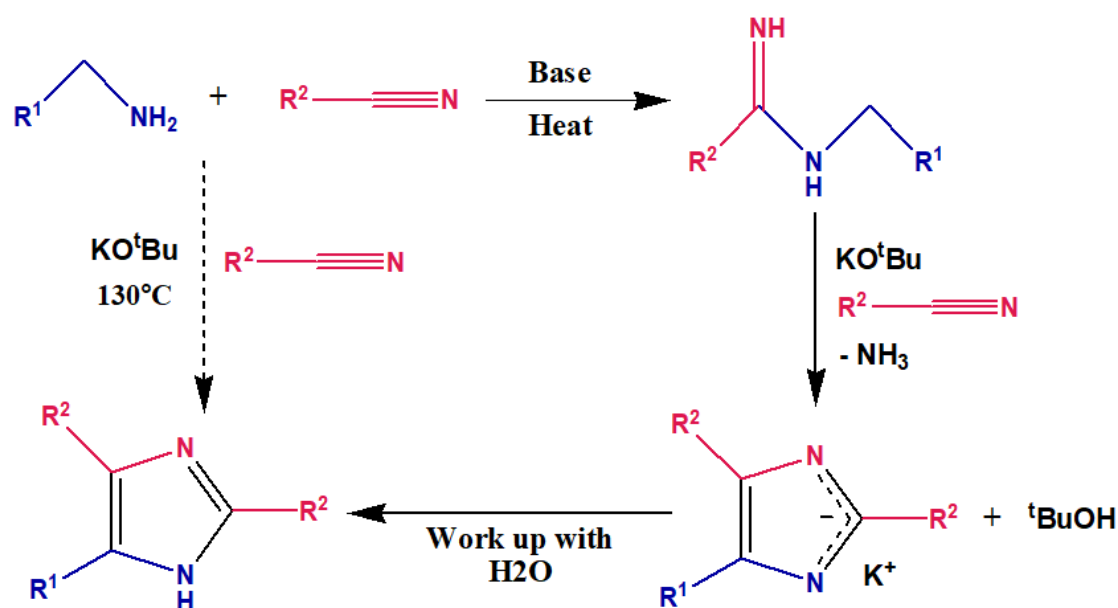
#### 4.4 Imidazole and its derivatives

Das and his co-workers designed a straightforward transition metal free synthetic pathway for the generation of substituted imidazoles. It is a one-step synthesis of 2,4,5-trisubstituted imidazoles **78** which involves a base promoted deaminative coupling of benzylamines **76** with nitriles **77** with the liberation of ammonia. The major advantage of this method was the ability to synthesize valuable imidazole derivatives from readily available starting materials (Scheme 31) [33].



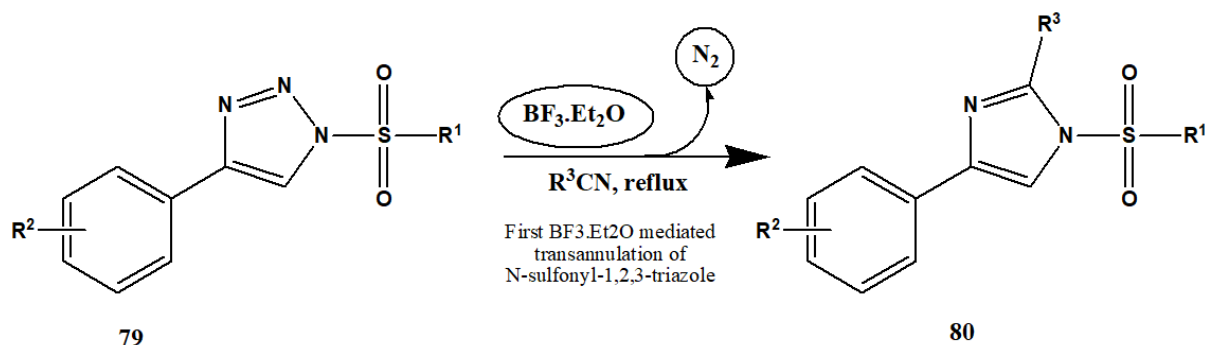


Scheme 31

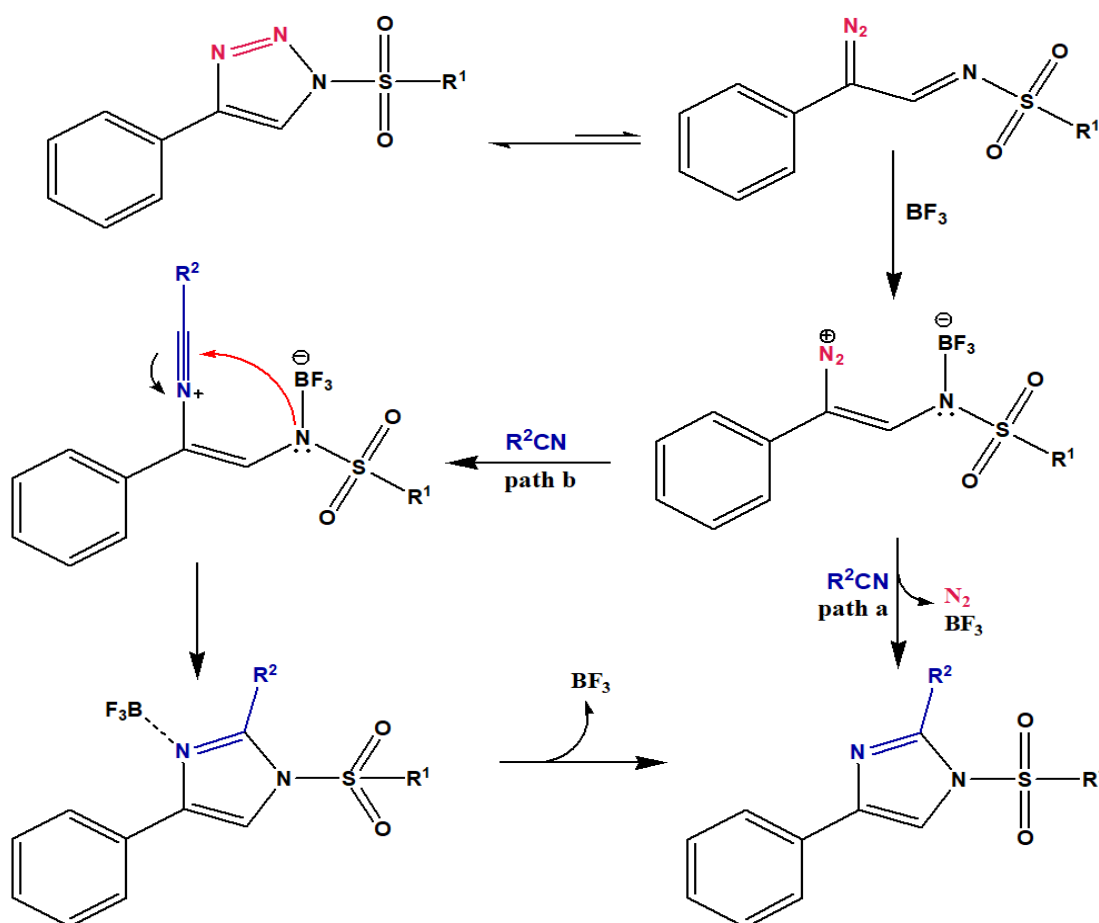


Possible Reaction Pathway for Scheme 31

Yang et al. devised the first BF<sub>3</sub>.Et<sub>2</sub>O mediated, metal-free synthesis of substituted imidazoles **80** by transannulation of N-sulfonyl-1,2,3-triazole **79**. In this method, instead of using transition metals, BF<sub>3</sub>.Et<sub>2</sub>O was used to facilitate the formation of α-diazoimines from N-sulfonyl-1,2,3-triazole in nitriles, ultimately leading to the formation of various imidazoles. This reaction protocol favours a broad range of functional groups and can also be applied for late-stage modification of bioactive molecules, thereby proving its significance in organic synthesis (Scheme 32) [34].

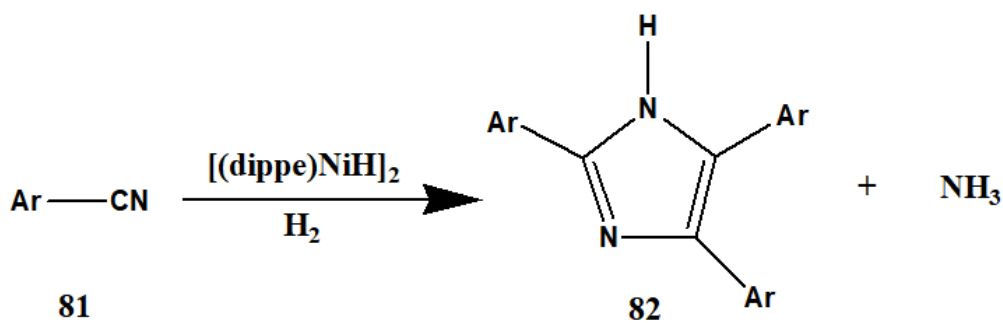


Scheme 32

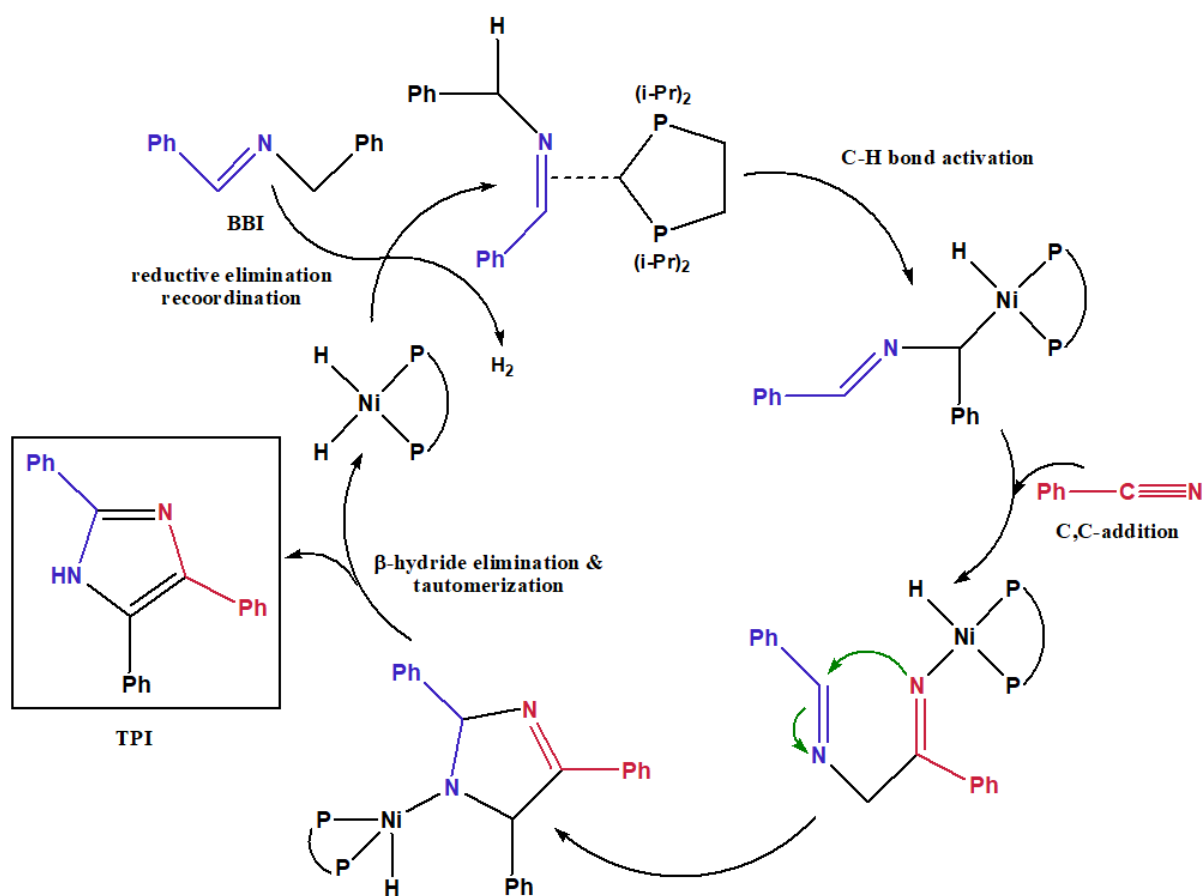


Possible Reaction Pathway for Scheme 32

Garcia et al. reported a one pot, nickel(0) catalyzed, synthesis to produce substituted imidazoles **82** in good to high yields. The reaction uses benzonitrile, p-substituted benzonitriles and 4-cyanopyridines as the starting materials **81**. The reaction is generally carried in a stainless-steel autoclave, pressurized at an indicated pressure (psi) of  $\text{H}_2$ . The obtained yield depends on the substrate used, the reaction time, temperature and pressure of  $\text{H}_2$  (Scheme 33) [35].



Scheme 33



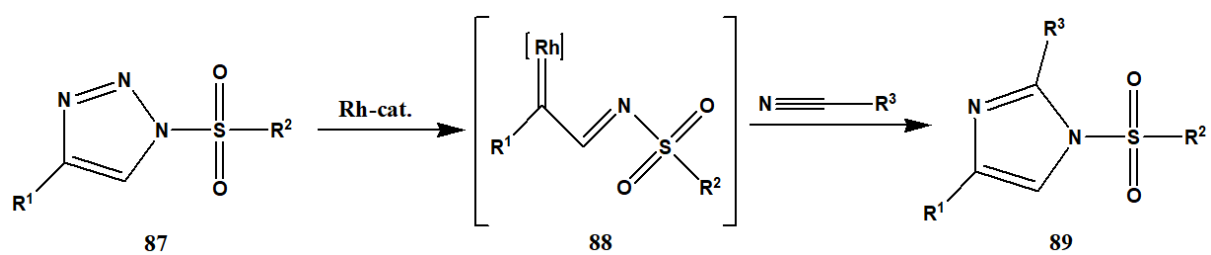
Possible Reaction Pathway for Scheme 33

Wang et al. devised an efficient base promoted nitrile-alkyne domino-type reaction. It involves a multicomponent cyclization assembly of alkynes **83**, nitriles **84** and  $\text{tBuOK}$  **85** resulting in the formation of imidazoles **86**. The reaction can be carried out even in the absence of a solvent, on a gram scale with 100% atom economy from readily available starting materials (Scheme 34) [36].

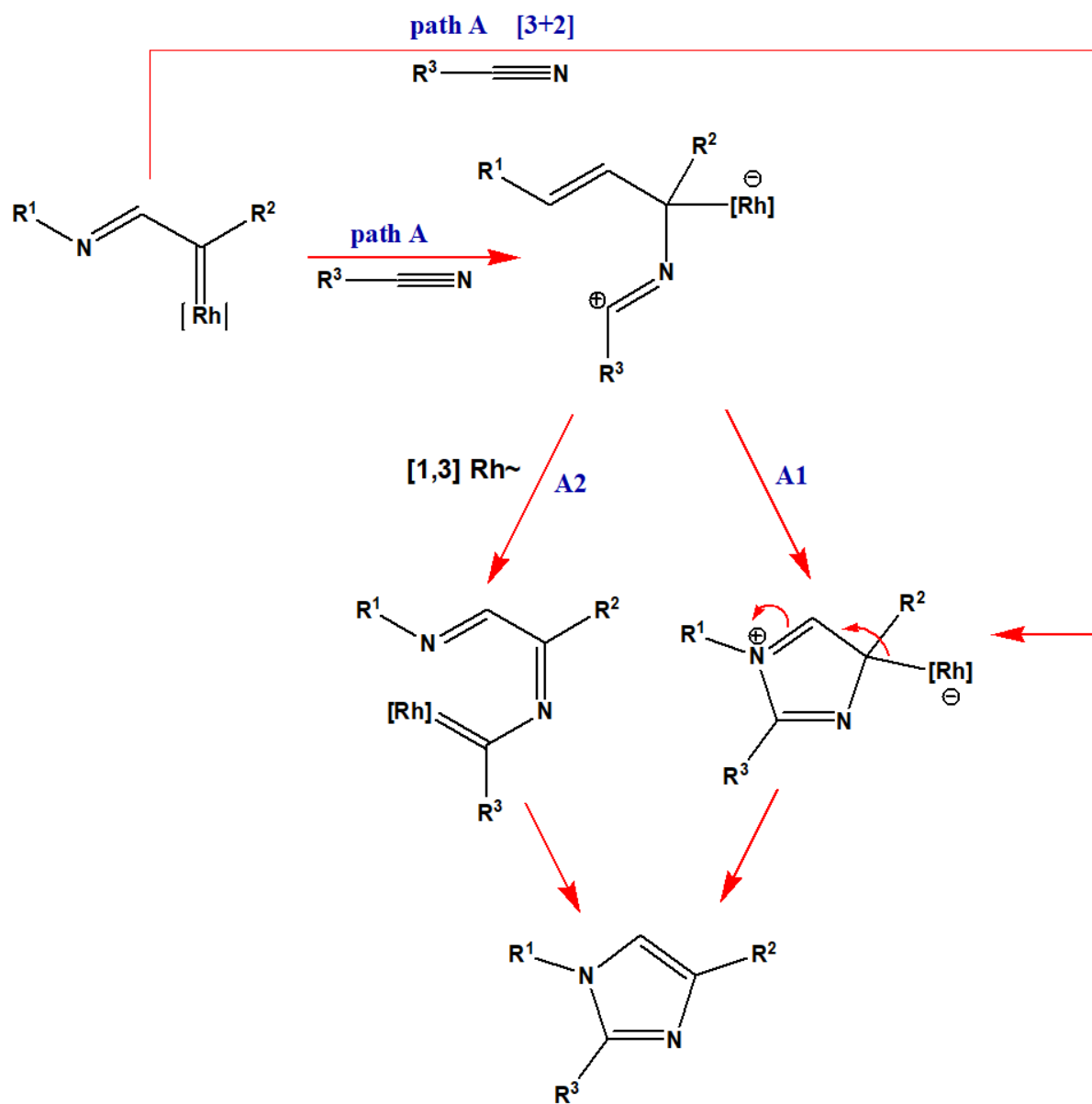
The proposed mechanism for the synthesis of 1,2,4,5-tetraphenyl-1H-imidazole involves the following steps:

- Deprotonation:** 1-phenyl-2-(tert-butoxy)-1-propyne reacts with  $t\text{-BuOK}$  to form a propargyl anion intermediate.
- Alkylation:** The propargyl anion reacts with two equivalents of 2,5-diphenyl-1H-imidazole-3-yl potassium salt to form a bis-alkylated intermediate.
- Deprotection:** The bis-alkylated intermediate is treated with  $t\text{-BuOH}$  and  $\text{H}^+$  to remove the tert-butoxy groups, yielding a bis-alkyne intermediate.
- Cyclization:** The bis-alkyne intermediate undergoes cyclization to form the final product, 1,2,4,5-tetraphenyl-1H-imidazole.

Horneff et al. devised a synthesis using Rh(II) complexes as a catalyst for ring opening of N-sulfonyl 1,2,3-triazoles **87** to form the Rh-iminocarbenoids **88**. These iminocarbenoids then react with nitriles to produce imidazoles **89** in good to excellent yields (Scheme 35) [37].

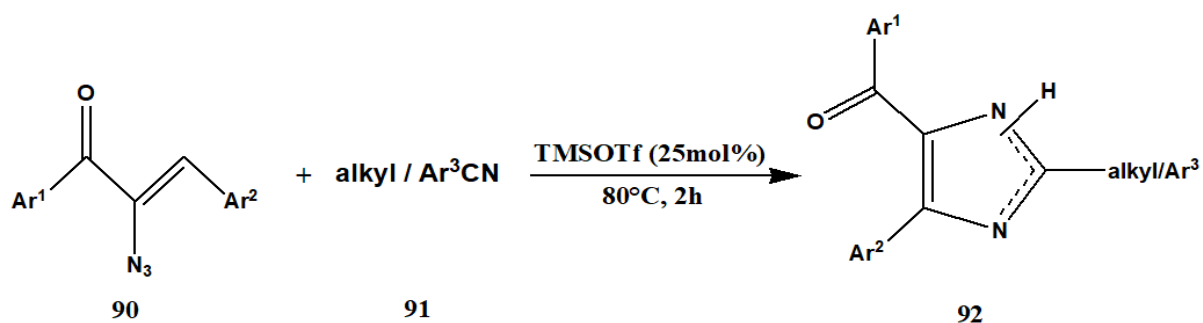


### Scheme 35

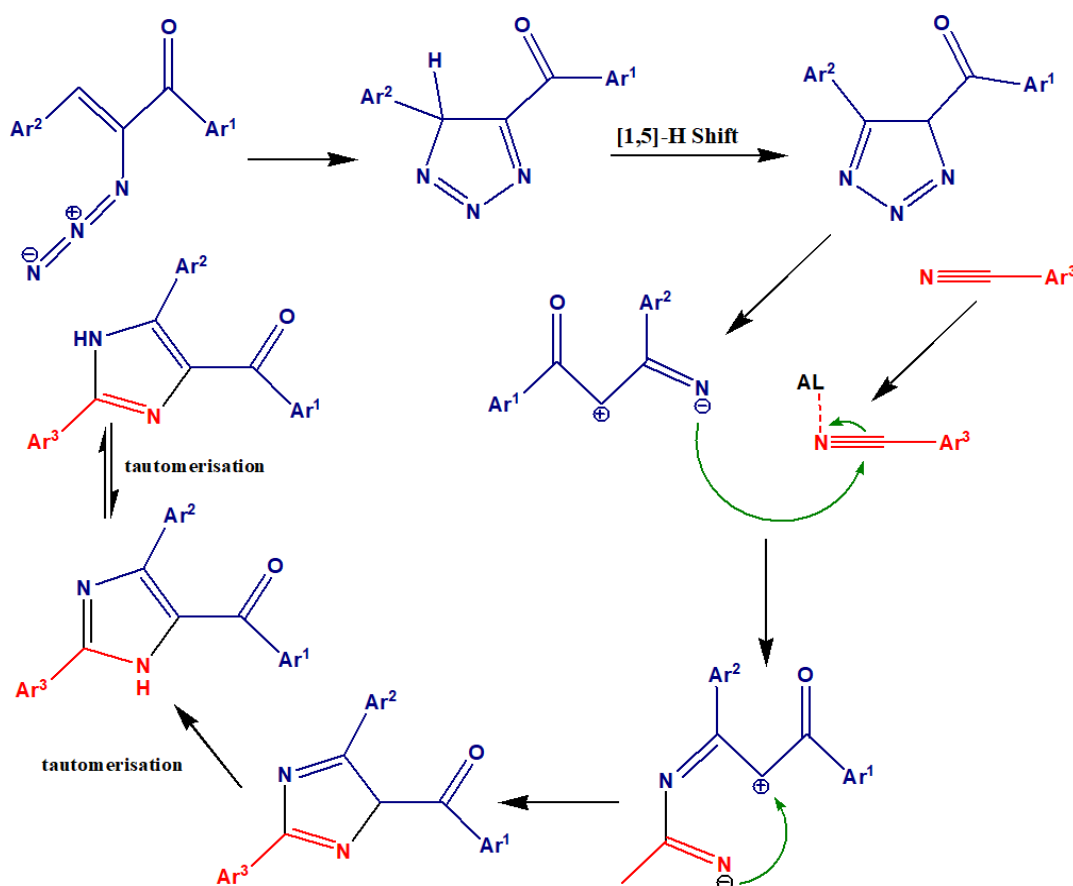


### Possible Reaction Pathway for Scheme 35

Harisha et al. devised a TMSOTf-catalysed synthetic pathway for the generation of 2,4,5-trisubstituted imidazoles **92**. It proceeds via a [3+2] addition reaction between azido chalcones **90** and organic nitriles **91** under mild reaction conditions resulting in the generation of two new C-N bonds. It can also be carried out under microwave conditions. Additionally, it also presents an excellent scope of substrate as a great number of vinyl azides and aromatic and aliphatic nitriles take part in this reaction. (Scheme 36) [38].



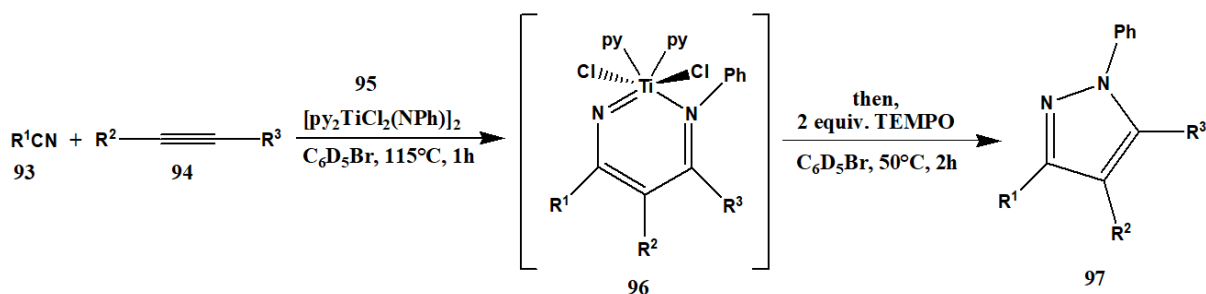
Scheme 36



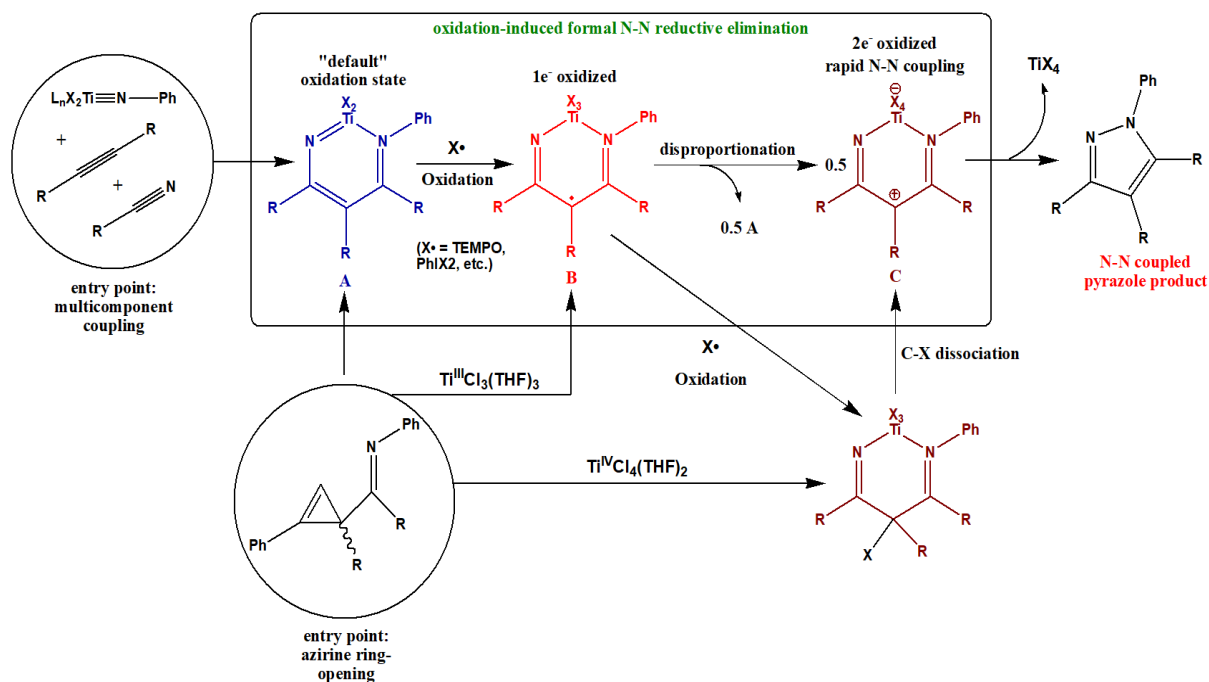
Possible Reaction Pathway for Scheme 36

## 4.5 Pyrazole and its derivatives

Pearce et al. successfully reported a multicomponent synthesis for the generation of polysubstituted pyrazoles **97** using nitriles **93**, alkynes **94** and Titanium imido complexes **95**. The major advantage of this pathway is that it avoids the use of potent hazardous reagents like hydrazine, which is conventionally used for the insertion of an intact N–N bond into pyrazole. In this method, the N–N bond fragment is introduced in the last step as a critical transformation via 2-electron oxidative coupling on Titanium and is thus a rare example of formal N–N coupling on metal center that proceeds through an electrocyclic mechanism. The reaction mechanism has been studied in details through stoichiometric reactions (Scheme 37) [39].

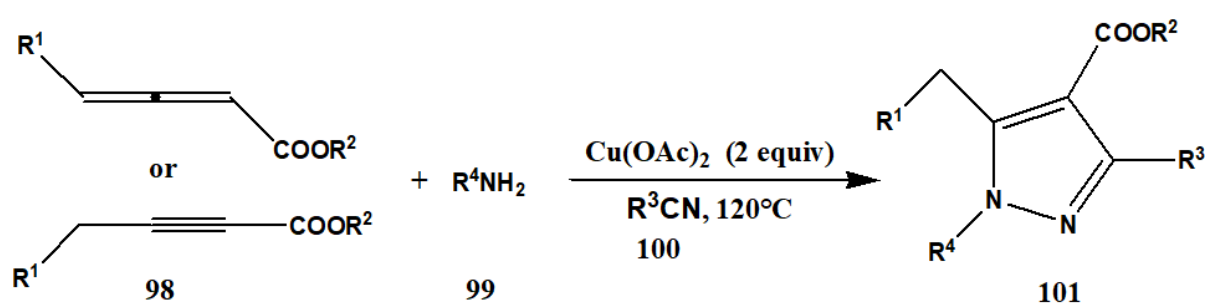


Scheme 37

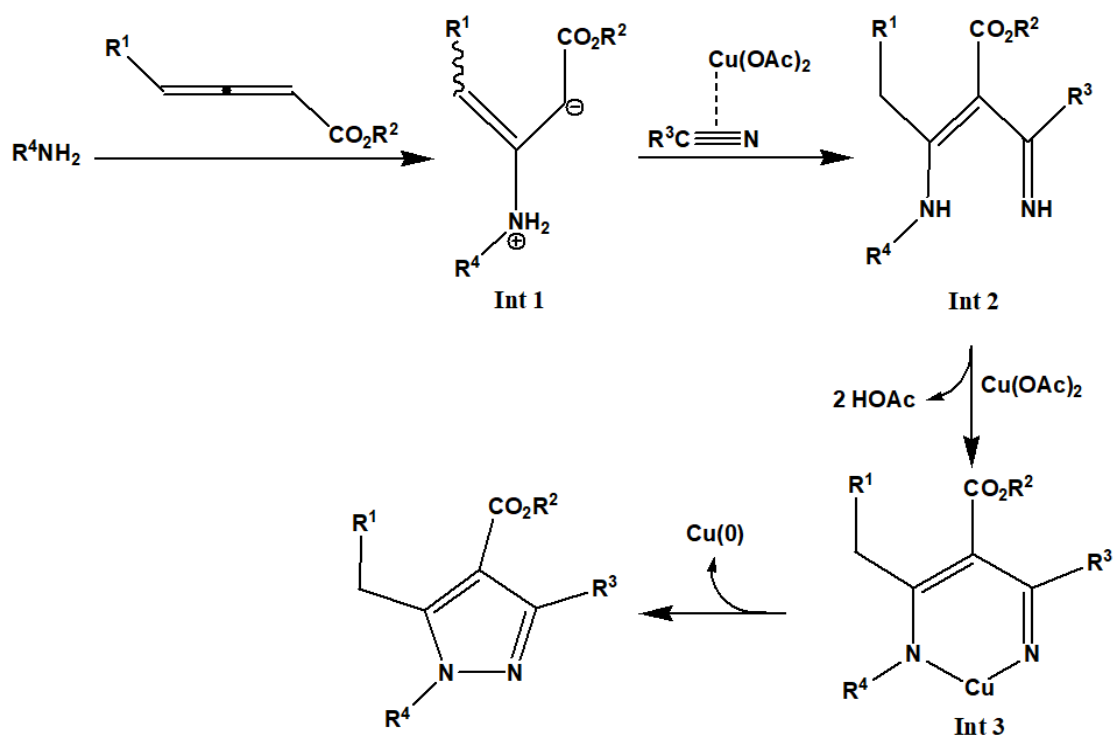


Possible Reaction Pathway for Scheme 37

Chen et al. devised an efficient pathway of the generation of fully substituted pyrazoles **101** with excellent diversity. It is a three-component copper-mediated reaction of 2,3-allenoates or 2-alkynoates **98**, amines **99** and nitriles **100**. Details mechanistic studies have suggested that the reaction proceeds with a tandem conjugate addition, 1,2-addition and a N–N bond formation. This reaction is of great interest for the organic and medicinal chemists because of the easy availability of the starting material and easy transformation of the carboxylic ester functionality and high potential of the products (Scheme 38) [40].



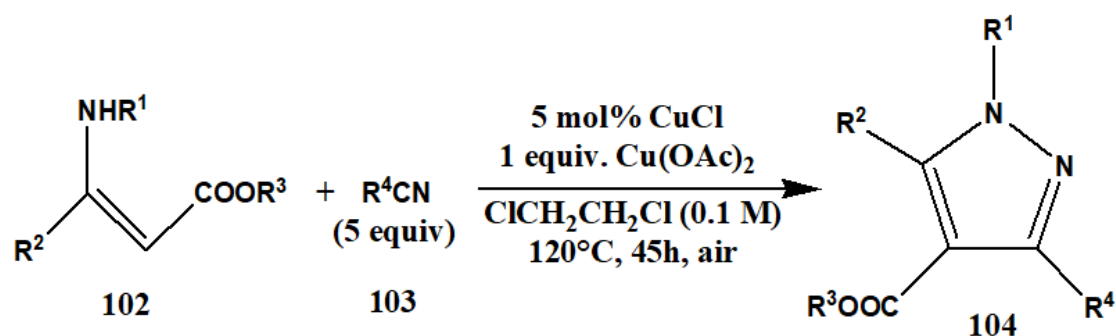
Scheme 38



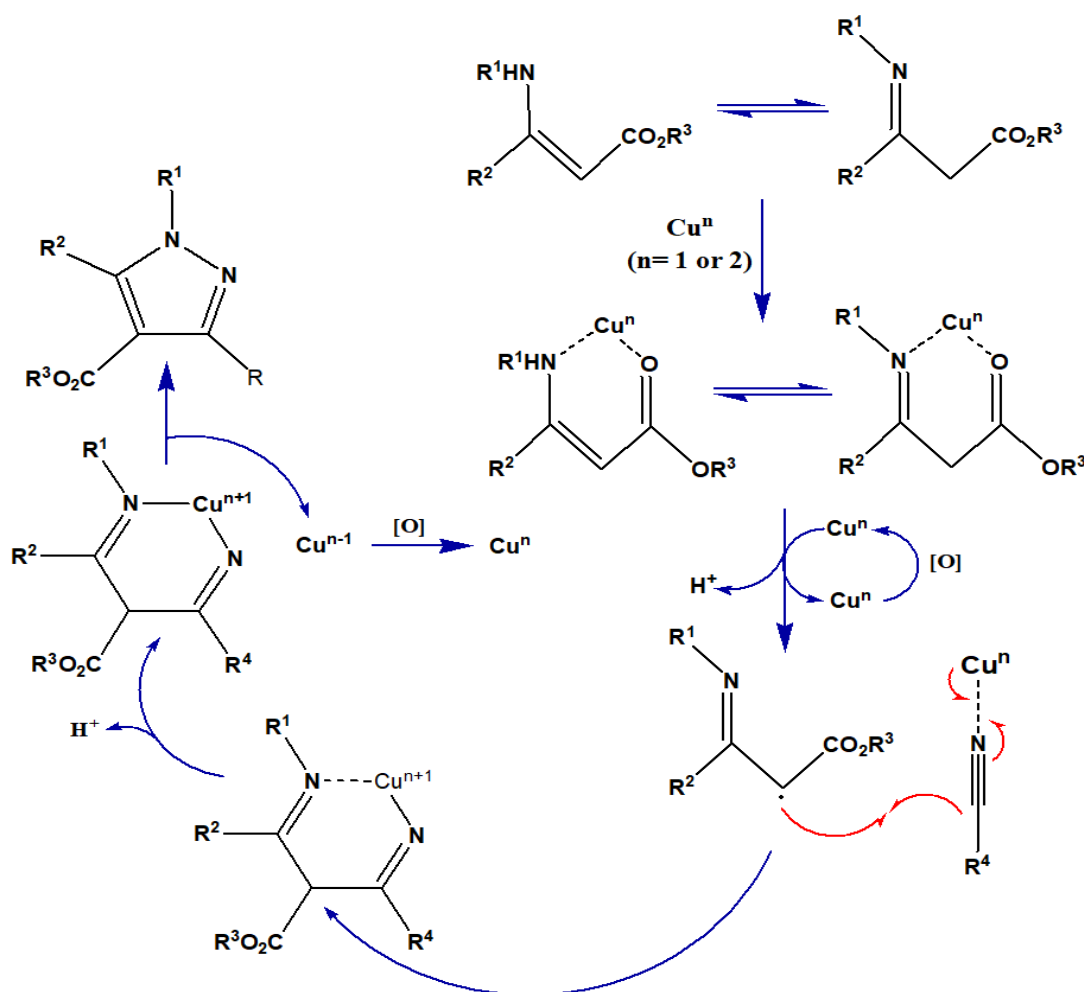
Possible Reaction Pathway for Scheme 38



Jang et al. reported an oxidant-controlled divergent synthetic pathway for generating pyrazoles **104**. The reaction involves a copper(I)-catalyzed oxidative annulation of  $\beta$ -enamino esters **102** to form fully substituted pyrazoles, by sequential formation of C–C and N–N or C–N bonds in the presence of nitriles **103** as reagent and cosolvent. The mechanism involves the formation of radical intermediates due to single-electron transfers (SET) (Scheme 39) [41].

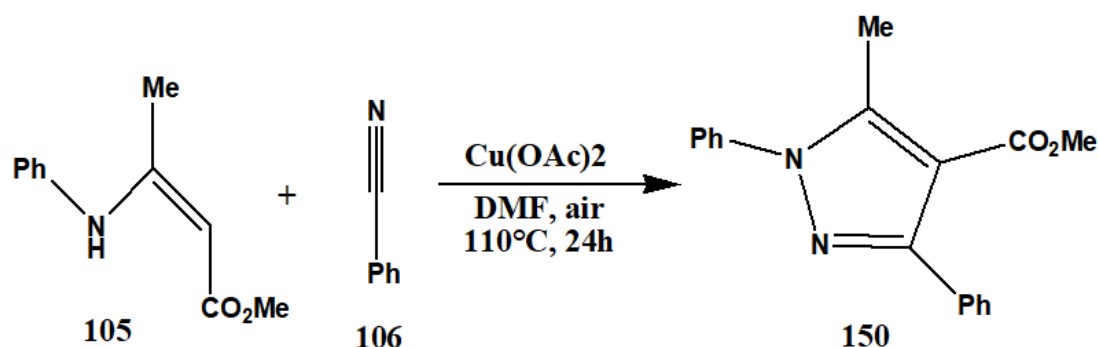


Scheme 39

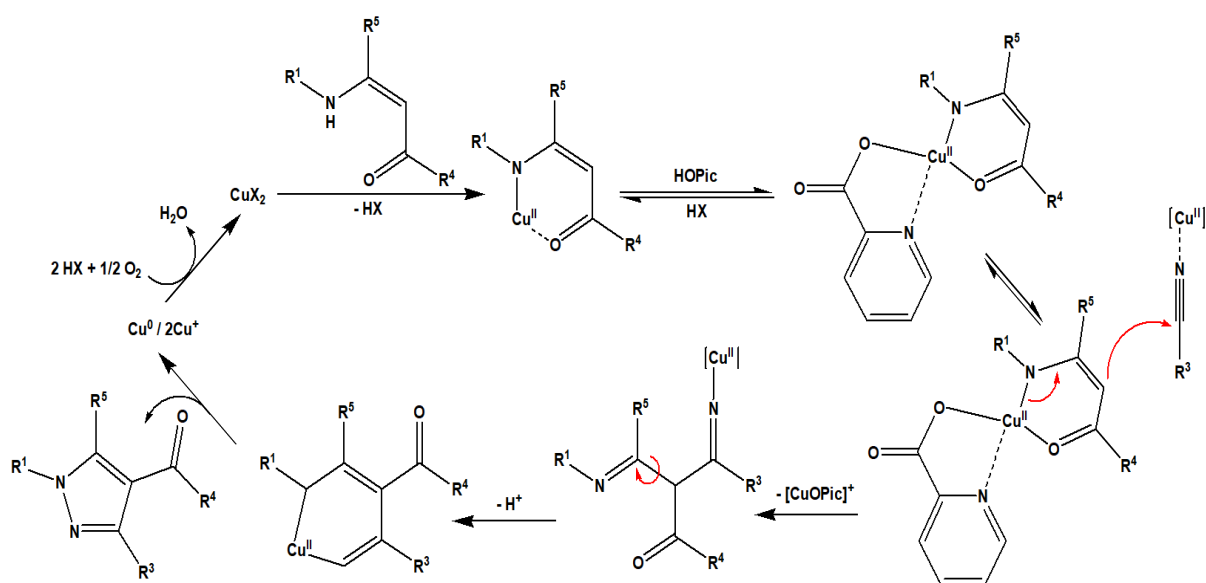


Possible Reaction Pathway for Scheme 39

Suri et al. has developed an efficient copper-catalyzed pathway for the synthesis of tetra-substituted pyrazoles **107**, using readily available enamines **105** and nitriles **106** as the substrates and oxygen as the oxidant. The reaction proceeds with the formation of C–C and N–N bonds and is highly atom economic. Additionally, the use of oxygen as the oxidant adds to the economic and environmental advantage of this process (Scheme 40) [42].



Scheme 40

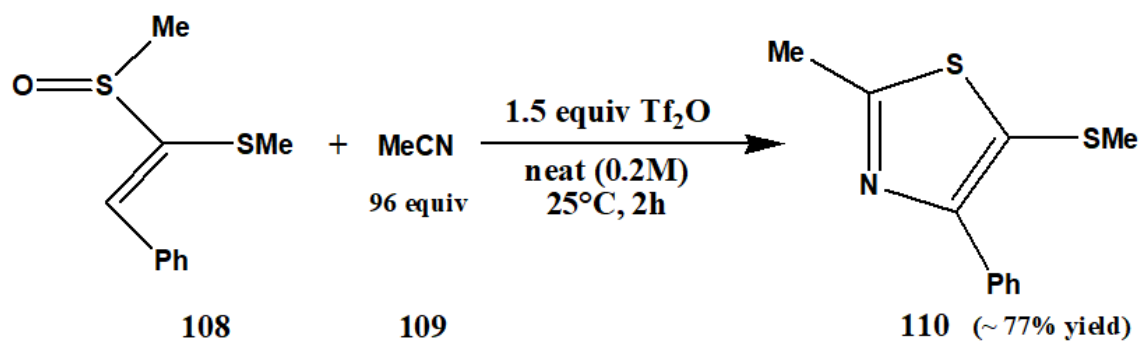


Possible Reaction Pathway for Scheme 40

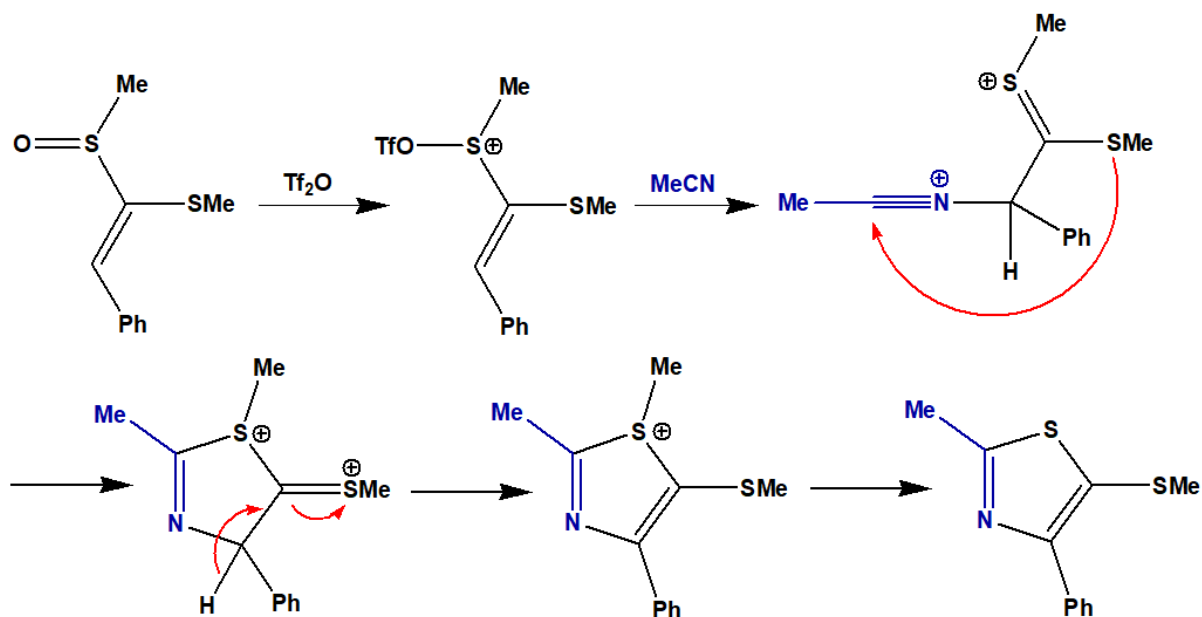
#### 4.6 Thiazole and its derivatives

Hori et al. reported a Pummerer-based annulative synthesis of thiazoles using alkenyl sulfoxides **108**, mainly KDMs, and nitriles **109**. The use of trifluoromethanesulfonic anhydride

( $\text{Tf}_2\text{O}$ ) as an activator and the additive Pummerer reaction followed by a C–S bond forming cyclization from the nitrilium intermediates leads to formation of the corresponding thiazoles **110** (Scheme 41) [43].

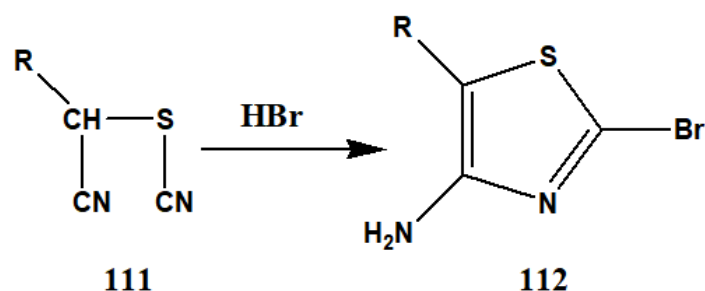


Scheme 41



Possible Reaction Pathway for Scheme 41

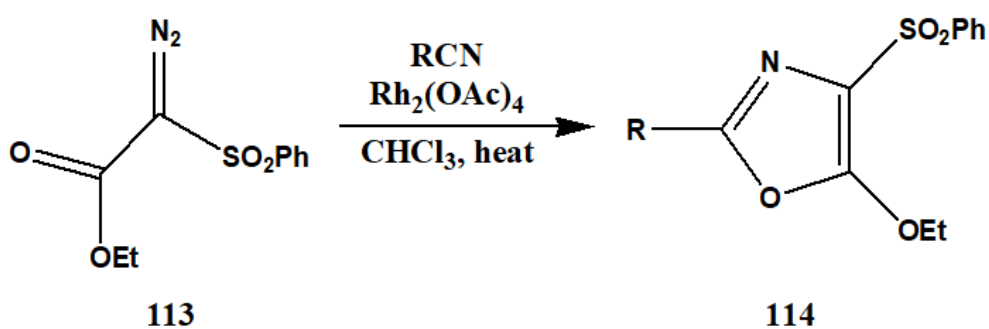
Johnson and Nasutavicus reported a new synthetic pathway for generating thiazoles by cyclization of nitriles using halogen acids.  $\alpha$ -Cyanoalkyl thiocyanates **111** undergo cyclization to produce 2-bromo-4-aminothiazole **112** derivatives by means of hydrogen bromide, whereas hydrogen chloride proved to be an unsatisfactory cyclizing agent (Scheme 42) [44].



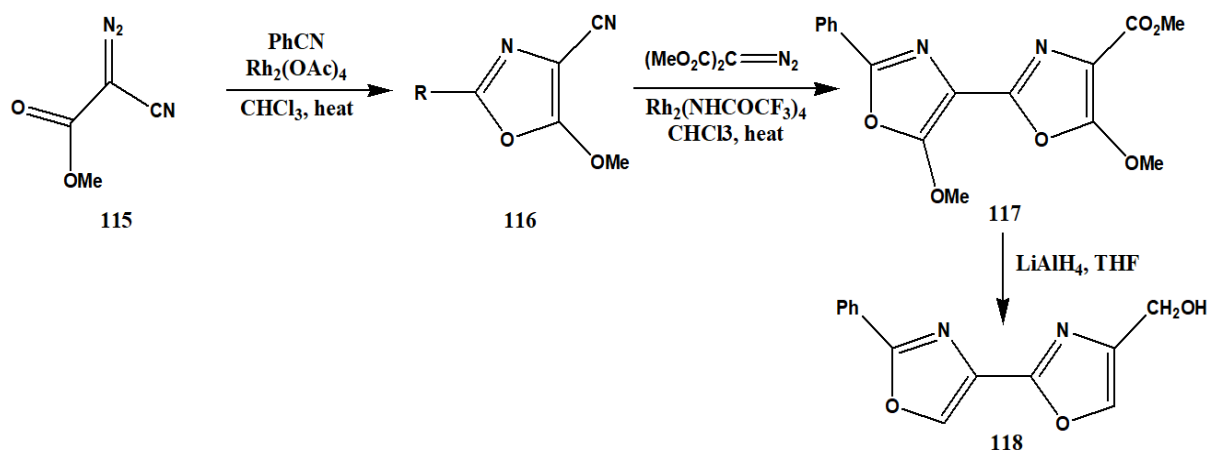
Scheme 42

#### 4.7 Oxazole and its derivatives

Doyle and Moody reported the synthesis of substituted oxazoles, particularly oxazole-4-sulfones and -nitriles by rhodium(II) catalyzed addition of nitriles with the corresponding diazo compounds. Diazosulfone **113** reacts with a wide range of nitriles to produce 4-benzenesulfonyloxazoles **114** in varying yields. On the other hand, methyl diazocynoacetate **115** reacts with benzonitrile in the presence of rhodium(II) acetate and refluxing chloroform to produce 4-cyanooxazole **116** with 35% yield. Additionally, reaction of 4-cyanooxazole **116** with dimethyl diazomalonate using rhodium(II) trifluoroacetamide, yields bis-oxazole **117** with 53% yield. Finally, the concomitant reduction of the ester using lithium aluminium hydride yields bis-oxazole **118** (Scheme 43a, 43b) [45].

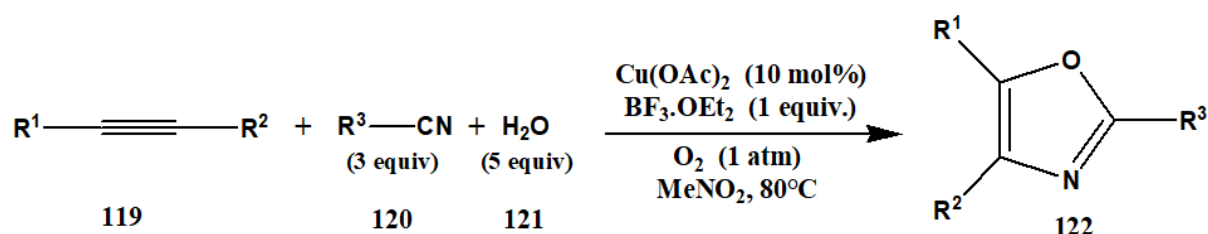


Scheme 43a

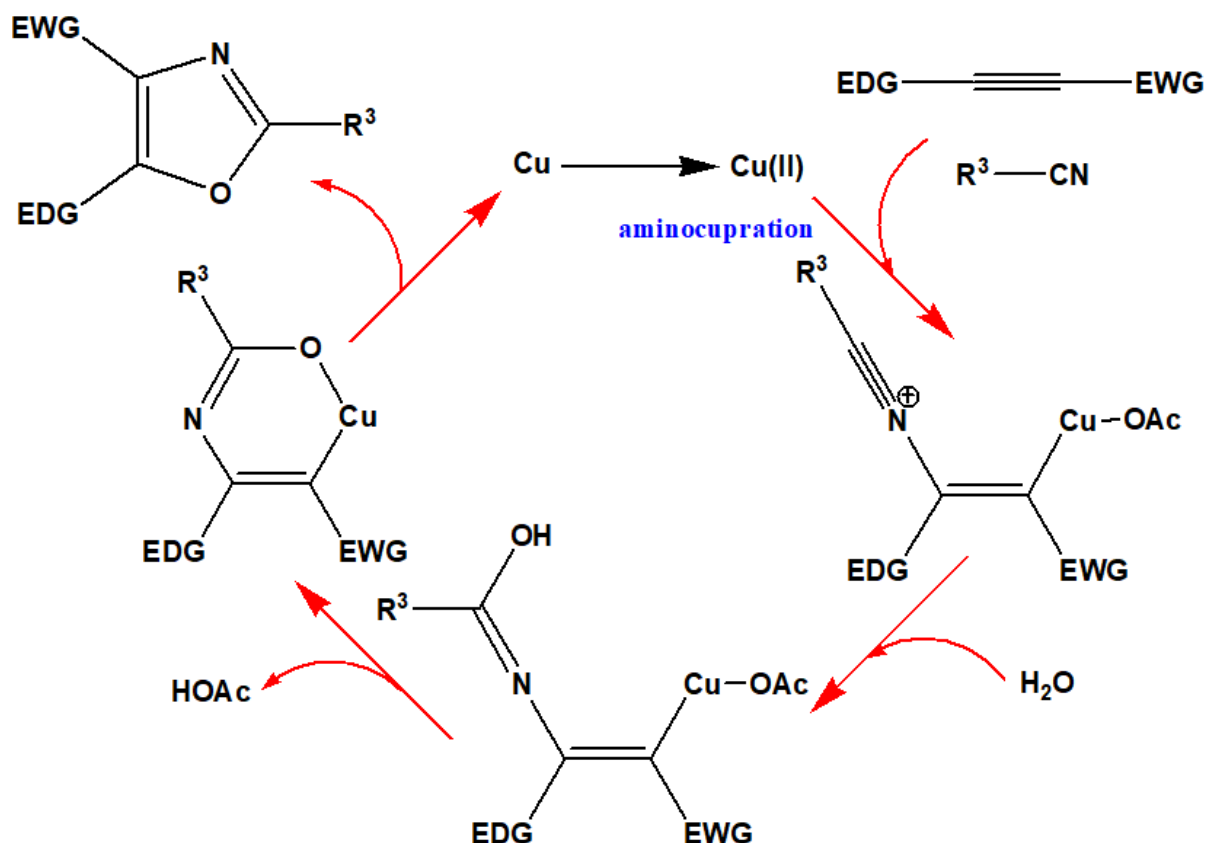


Scheme 43b

Li et al. reported a highly efficient oxidative copper(II)-catalyzed [2+2+1] cycloaddition reaction for the synthesis of 1,3-oxazoles **122** using internal alkynes **119** and nitriles **120**. The reaction is highly robust and regioselective and is thought to proceed via the formation of an enamide intermediate. Water **121** substantially takes part in this reaction. Additionally, the reaction exhibits high functional group tolerance under mild reaction conditions (Scheme 44) [46].

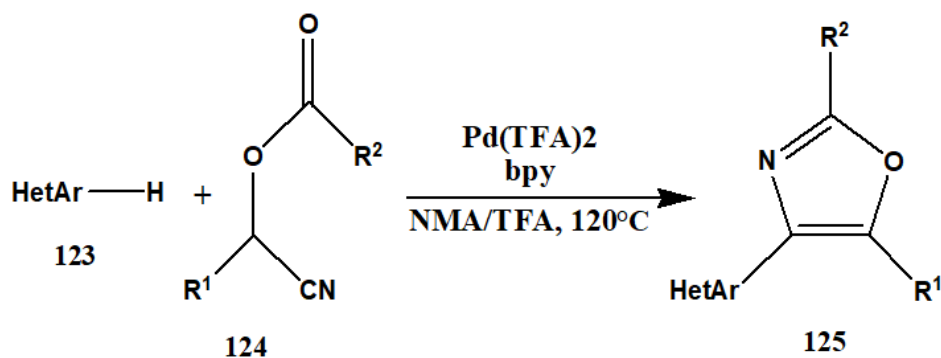


Scheme 44

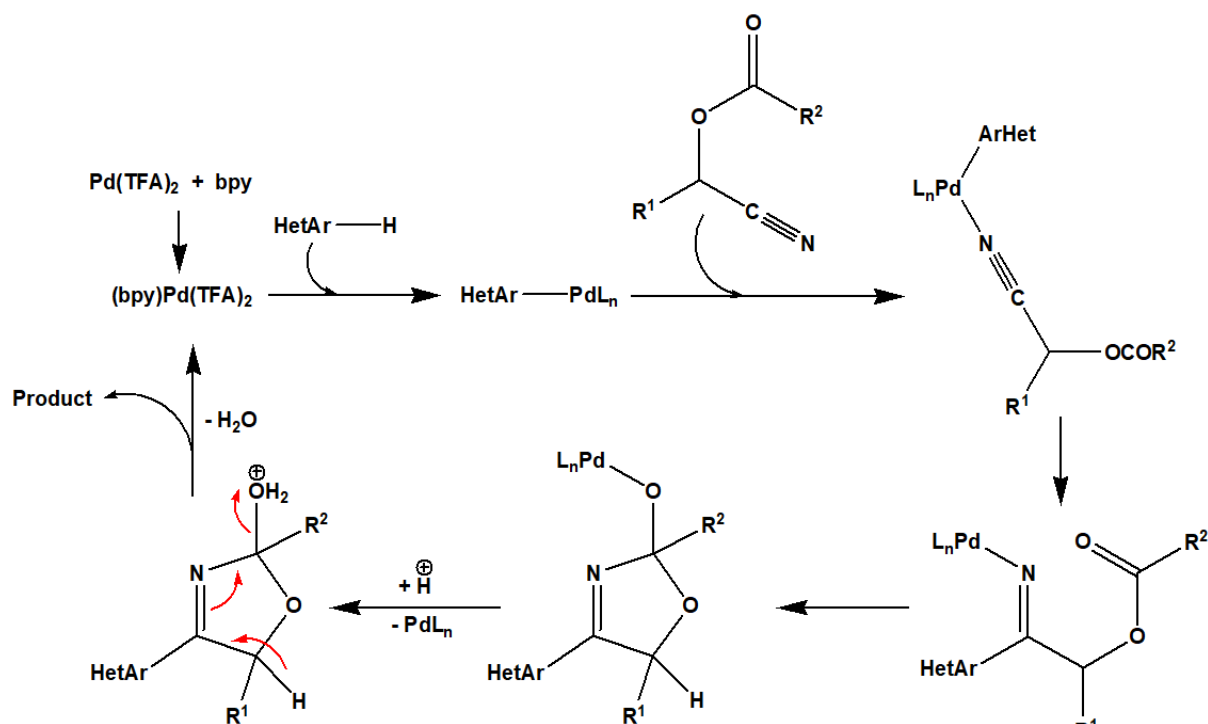


Possible Reaction Pathway for Scheme 44

Zhang et al. devised a synthetic pathway for the diverse Pd-catalyzed synthesis of 2,4,5-trisubstituted oxazoles **125** via a flexible and practical intermolecular protocol from readily available starting materials. The synthesis involves a direct C–H addition of electron-rich heteroarenes **123** to O-acyl cyanohydrins **124** bearing an  $\alpha$ -hydrogen. It was found that under redox neutral conditions, a wide range of trisubstituted oxazoles were obtained in good to high yields with high efficiency and great tunability (Scheme 45). [47]

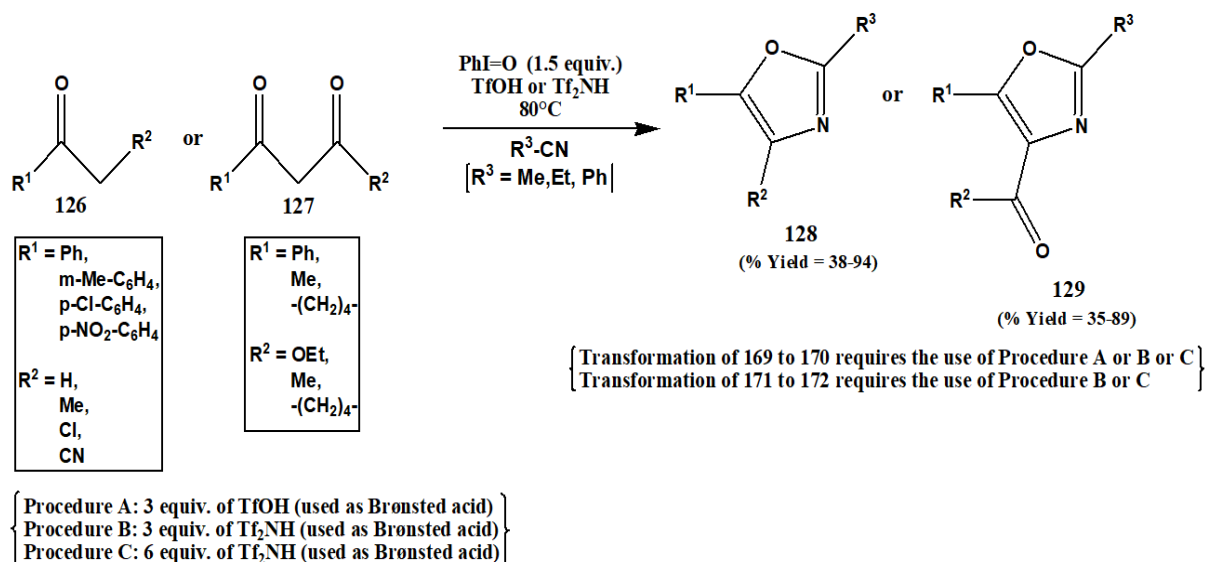


Scheme 45

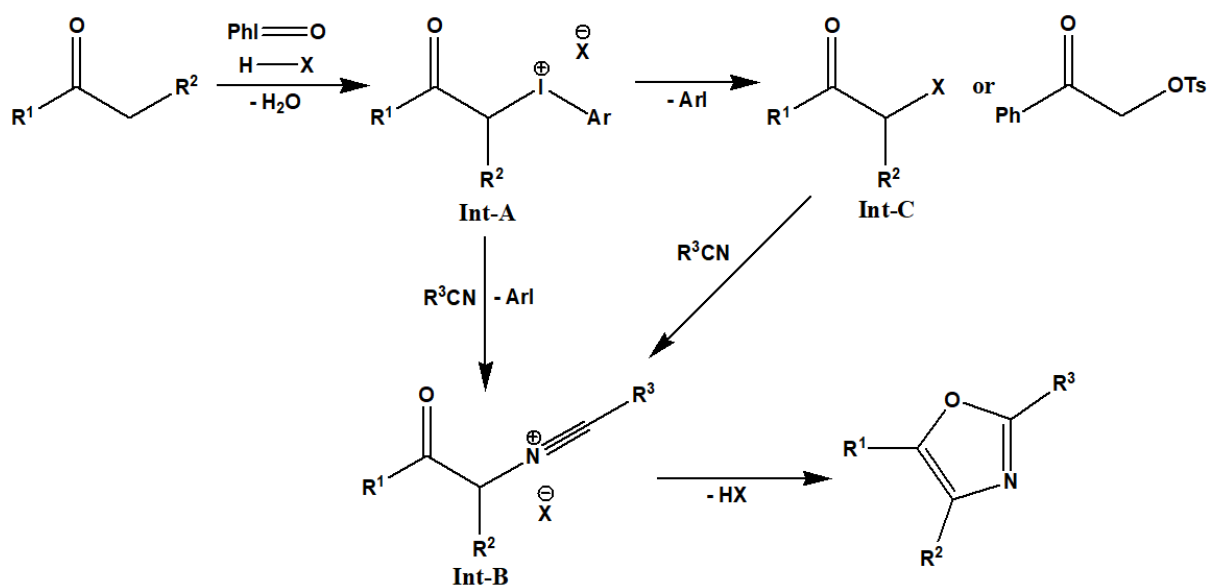


#### Possible Reaction Pathway for Scheme 45

Saito et al. reported the synthesis of highly substituted oxazoles by reaction of ketones and nitriles using iodine(III) as a catalyst. In this process, iodosobenzene ( $\text{PhI=O}$ ), in the presence of trifluoromethanesulfonic acid ( $\text{TfOH}$ ) or bis(trifluoromethanesulfonyl)imide ( $\text{Tf}_2\text{NH}$ ), promotes the reaction of both mono **126** and dicarbonyl compounds **128** with nitriles to yield 2,4-disubstituted and 2,4,5-trisubstituted oxazoles **127** & **129** in a single step under mild reaction conditions (Scheme 46) [48].



Scheme 46

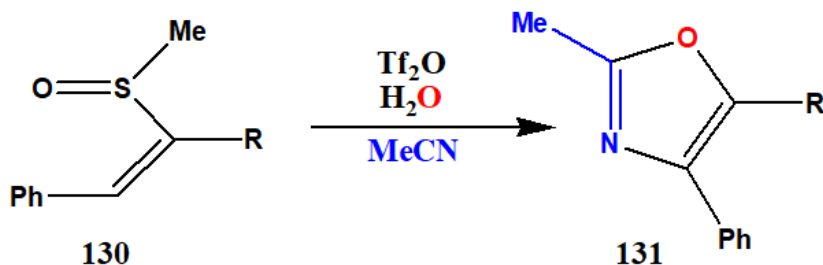


Possible Reaction Pathway for Scheme 46

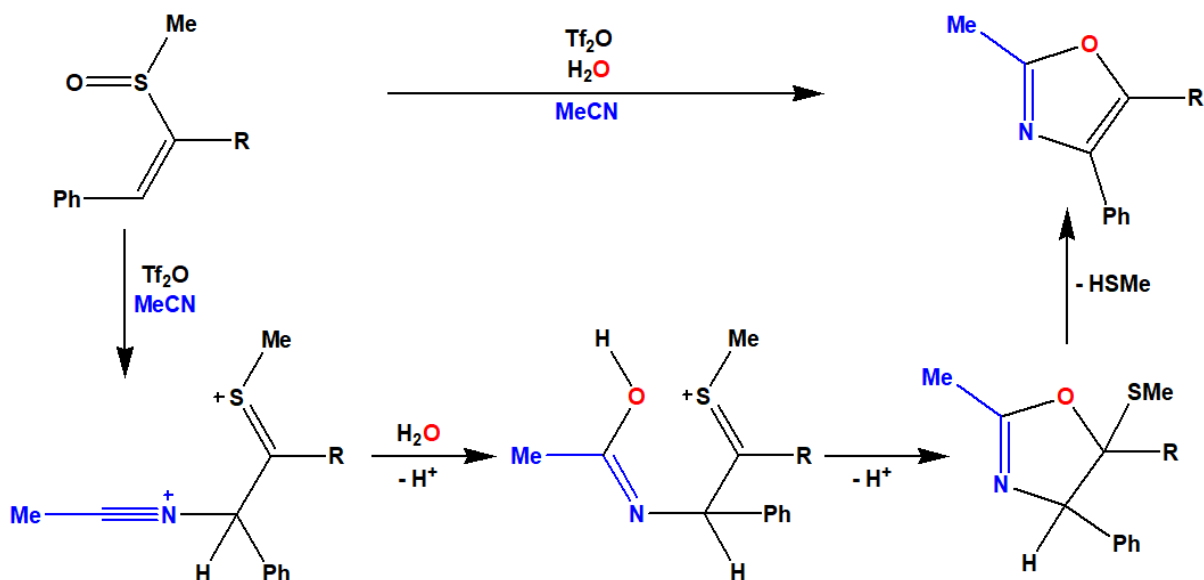
Hori et al. reported a Pummerer-based annulative synthesis of oxazoles using alkenyl sulfoxides **130** and nitriles. The use of trifluoromethanesulfonic anhydride (Tf<sub>2</sub>O) as an activator and the additive Pummerer reaction resulted in the formation of the nitrilium intermediates which ultimately lead to formation of the corresponding oxazoles **131** on addition of water as an oxygen source. It was predicted that the reaction proceeds with the nucleophilic attack of H<sub>2</sub>O on the nitrilium intermediate to yield a thionium intermediate,



which then undergoes subsequent C–O– bond forming cyclization and a removal of methanethiol, ultimately resulting in the formation of oxazole (Scheme 47) [49].



Scheme 47

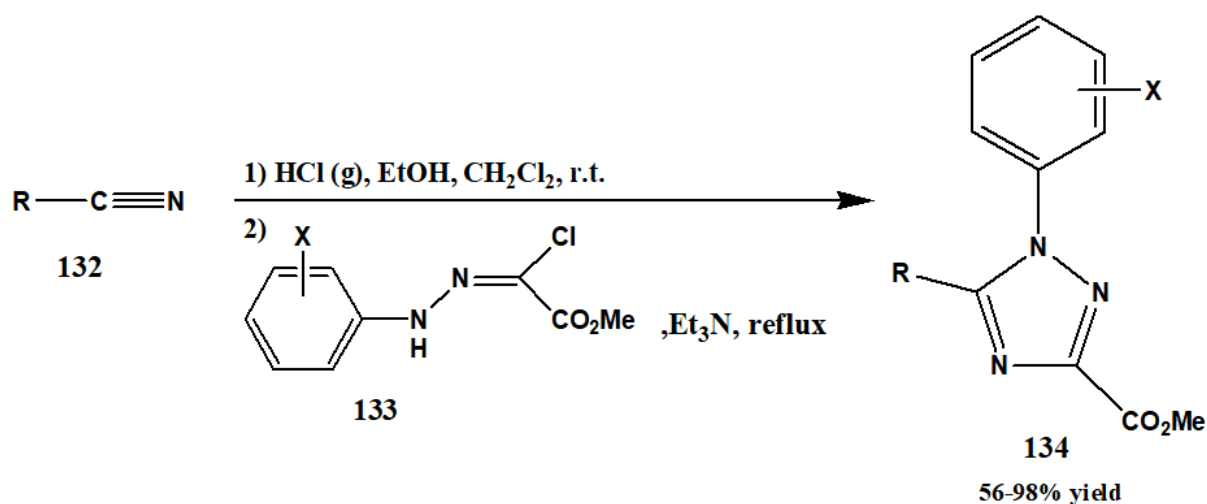


Possible Reaction Mechanism for Scheme 47

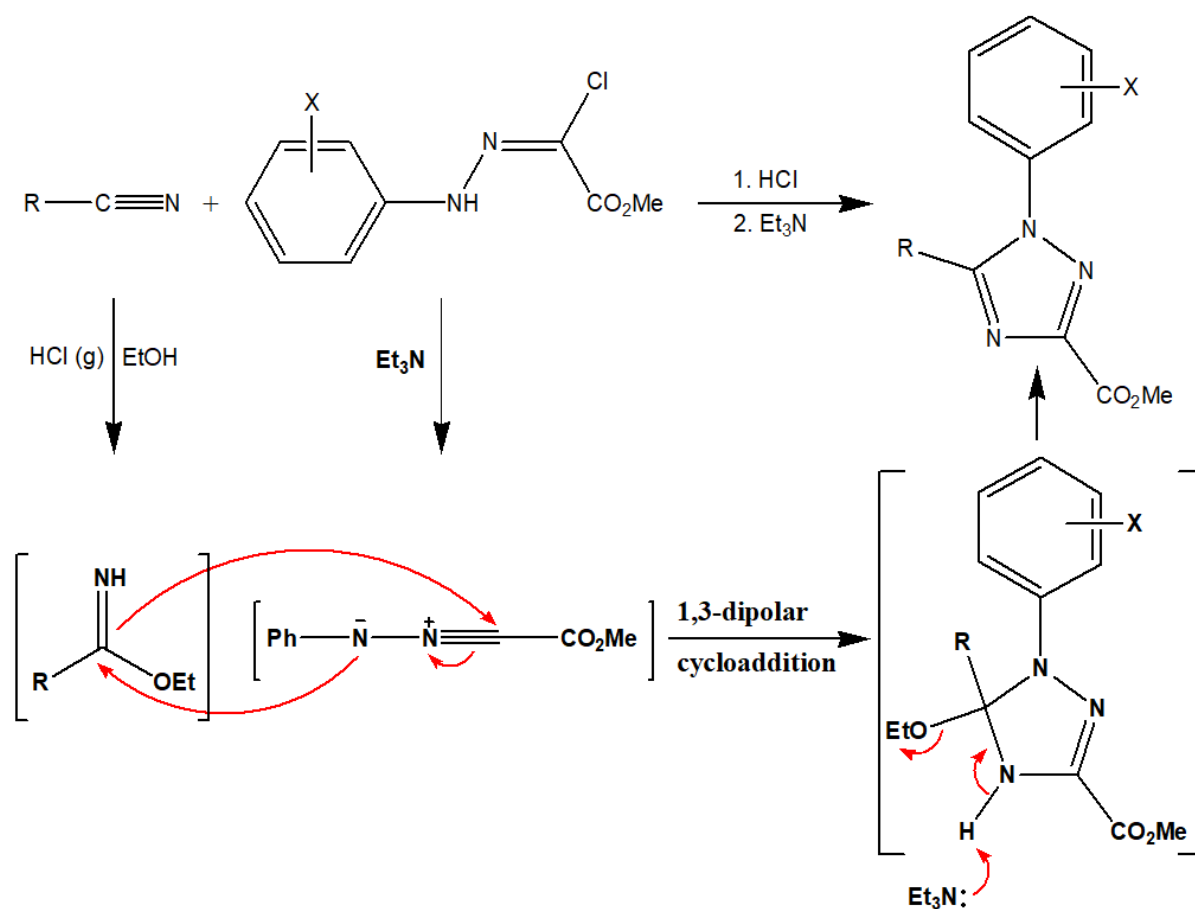
#### 4.8 Triazole and its derivatives

Wang et al. reported a one-flask 1,3-dipolar cycloaddition reaction involving nitriles **132** and hydrazonoyl chlorides **133** for the generation of 1,3,5-trisubstituted 1,2,4-triazoles **134**. The synthesis is carried out under basic conditions and exhibits excellent product yields (56-98%). The imidate and nitrilimine produced from its corresponding nitriles and N-arylhydrazonoyl chloride respectively undergoes the actual 1,3-dipolar cycloaddition to yield the final product.

The synthesis can be carried out for both aromatic and aliphatic nitriles as well as for N-phenylhydrazonoyl chlorides having ester or acetyl groups (Scheme 48) [50].

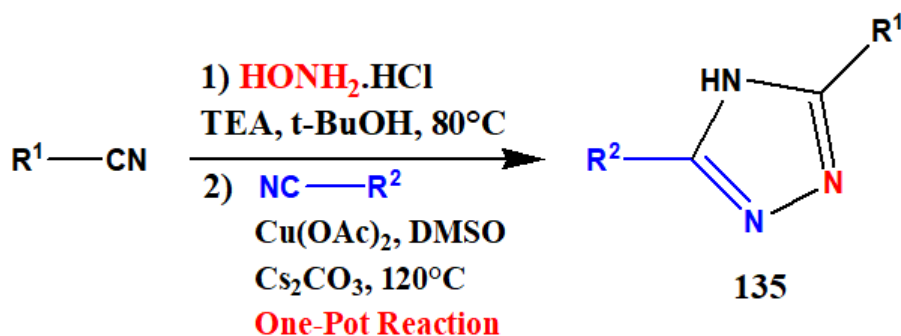


Scheme 48

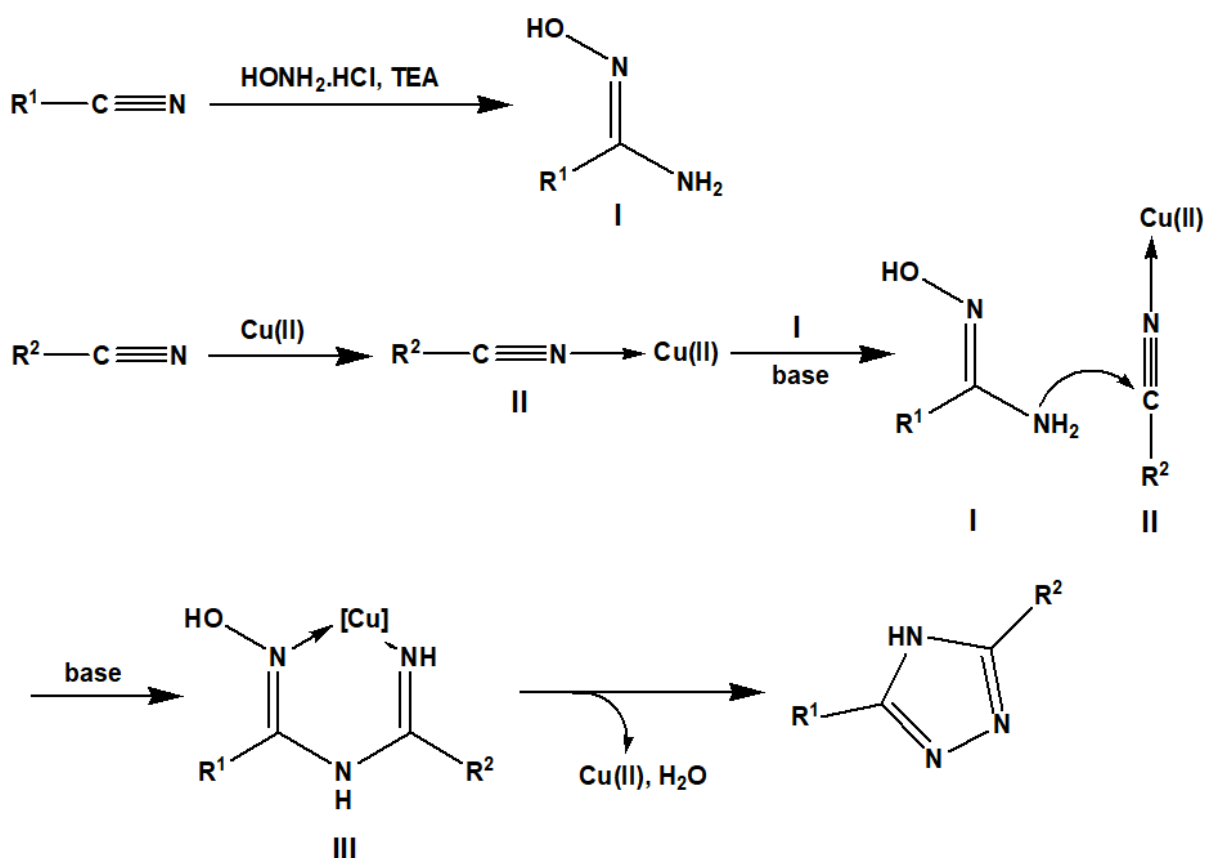


Possible Reaction Pathway for Scheme 48

Xu et al. reported a copper-catalyzed simple and efficient one-pot synthesis using two nitriles and hydroxylamine to produce 1,2,4-Triazoles **135**. The synthesis uses readily available nitriles and relatively inexpensive catalyst  $\text{Cu}(\text{OAc})_2$  to generate triazoles with moderate to good yields. The reaction protocol proceeds with the intermolecular addition of hydroxylamine to one nitrile to produce amidoxime which then further reacts with another nitrile via an intramolecular dehydration cyclization to yield the final product (Scheme 49) [51].



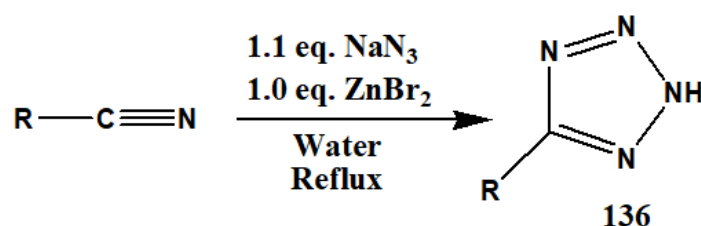
Scheme 49



Possible Reaction Pathway for Scheme 49

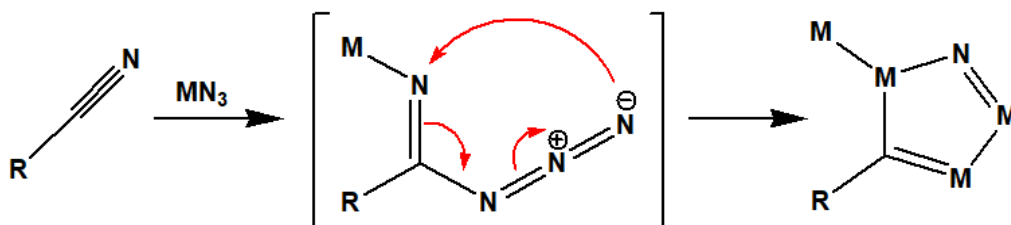
## 4.9 Tetrazole and its derivatives

Demko and Sharpless reported an efficient and simple synthesis of 1H-Tetrazoles **136** by the addition of sodium azides into nitriles using zinc salts as catalyst in water. The substrate scope of the reaction is very broad as it includes the use of a number of aromatic nitriles, activated and unactivated aliphatic nitriles, thiocyanates, cyanamides and various substituted vinyl nitriles. Although the starting materials are relatively insoluble in water, yet it is used as a solvent in this process (Scheme 50) [52].

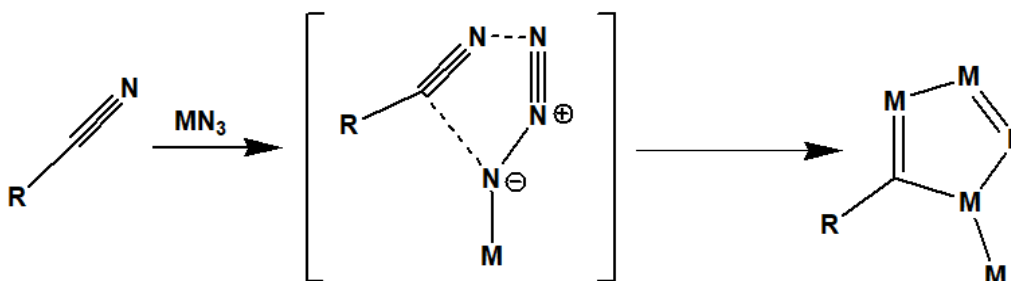


Scheme 50

### Two-Step Mechanism



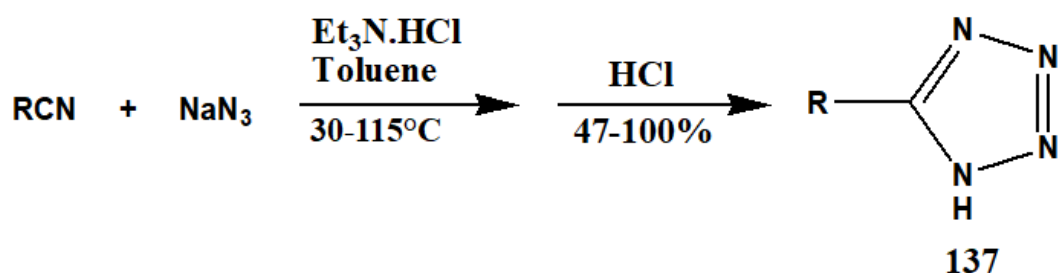
### Concerted Mechanism



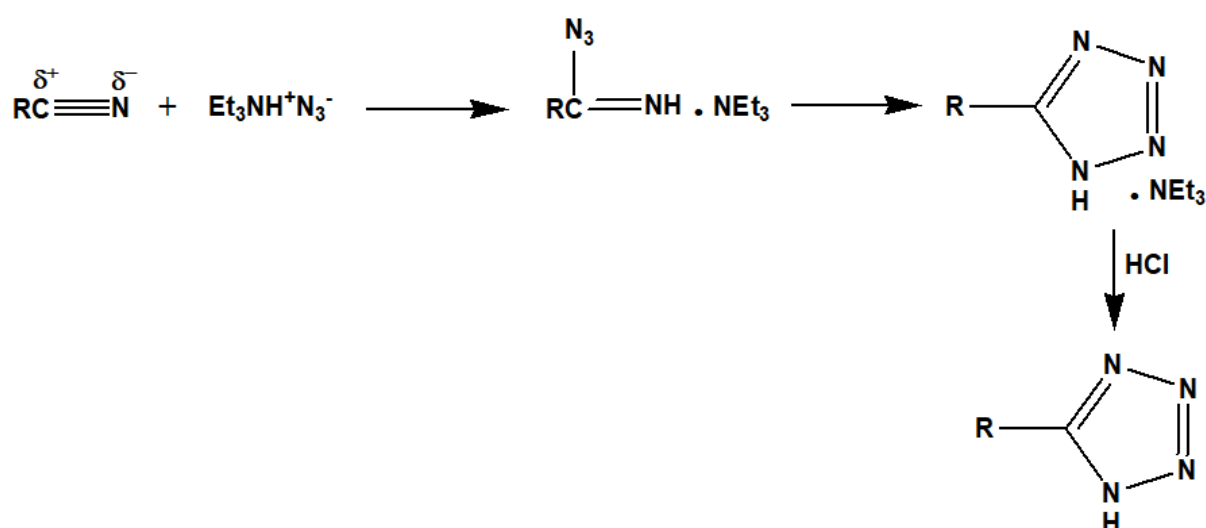
$\text{M} = \text{H}, \text{L}_n\text{Zn}, \text{Other metals}$

Possible Reaction Pathway for Scheme 50

Koguro et al. reported the efficient novel synthesis of 5-substituted tetrazoles by reacting sodium azides with nitriles in the presence of an amine salt in an aromatic solvent. The synthesis uses commercially available reagents and is a safe, cost-efficient and facile synthetic pathway. This method can be used for generating a variety of 5-substituted tetrazoles (Scheme 51) [53].



Scheme 51

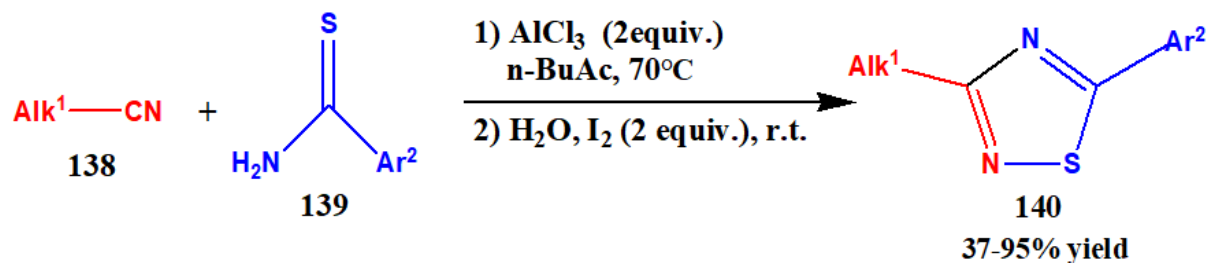


Possible Reaction Pathway for Scheme 51

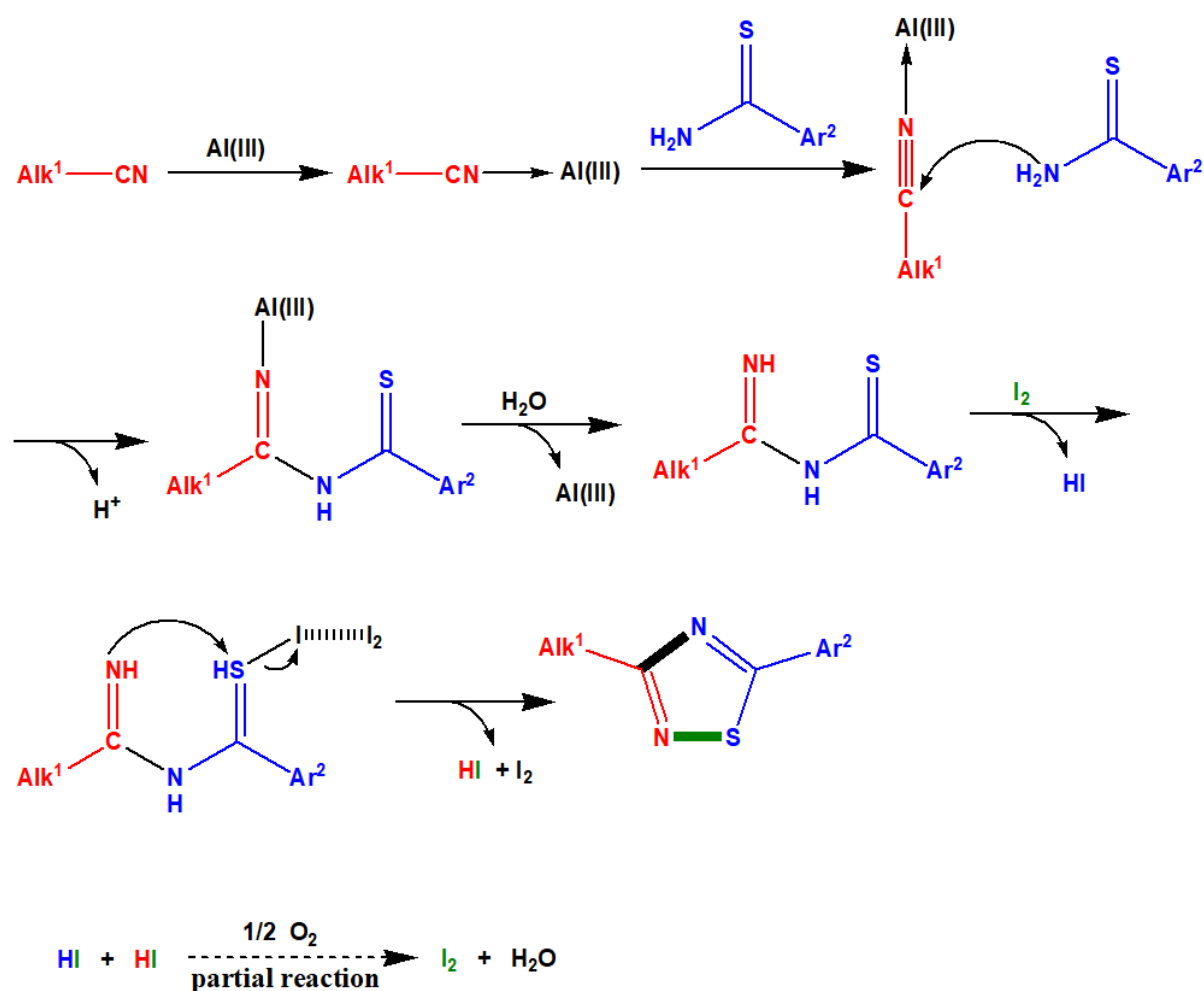
#### 4.10 Thiadiazole and its derivatives

Chai et al. reported an efficient one-pot synthesis using nitriles **138** and thioamides **139** to produce 3,5-disubstituted 1,2,4-thiadiazoles **140** in good yields (37-94%) with a variety of functional groups. The reaction protocol involves the oxidative formation of an N–S bond mediated by  $\text{I}_2$  i.e., it involves the intermolecular addition of thioamide to nitriles followed by

molecular iodine mediated intramolecular oxidative coupling of N–H and N–S bonds. The synthesis uses readily available substrates and uses I<sub>2</sub> as the oxidant which is eco-friendly and readily available (Scheme 52) [54].

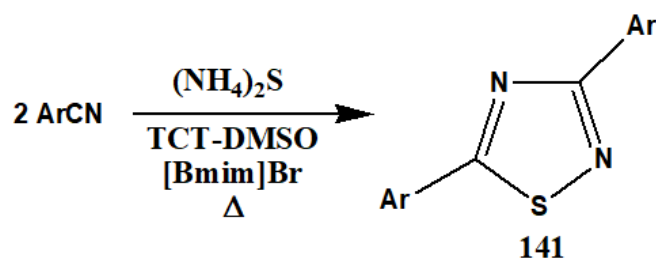


Scheme 52



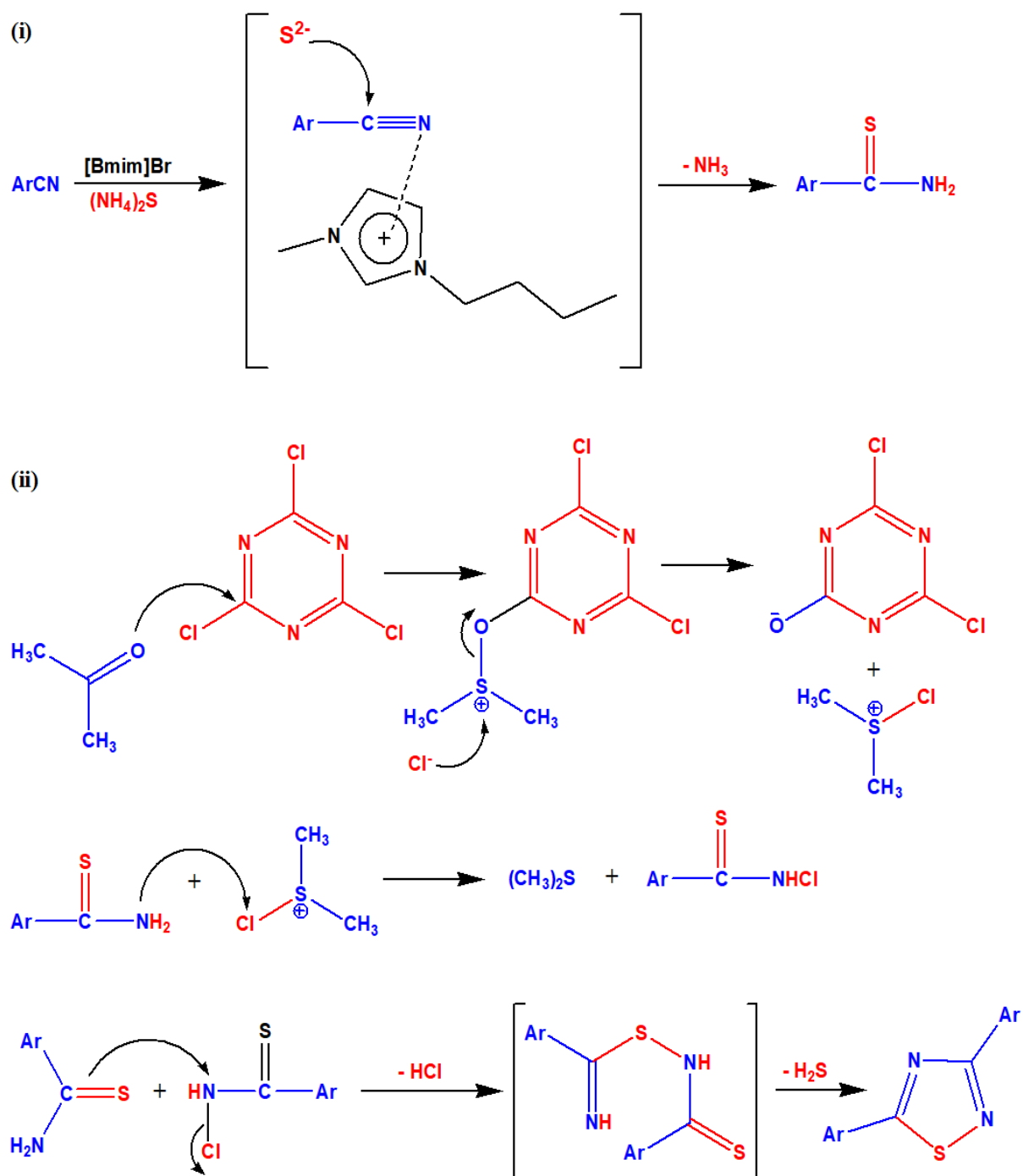
Possible Reaction Pathway for Scheme 52

Noei and Khosropour reported a simple, novel and efficient telescoped method for the generation of 3,5-diaryl-1,2,4-thiadiazoles **141** in high yields under mild reaction conditions by the reaction of aryl nitriles in a  $(\text{NH}_4)_2\text{S}$  and TCT-DMSO promoted ionic liquid i.e., 1-butyl-3-methylimidazolium bromide. Although this reaction happens very slowly in organic solvents, it proceeds rapidly in ionic solvents (Scheme 53) [55].



Scheme 53

Contd.



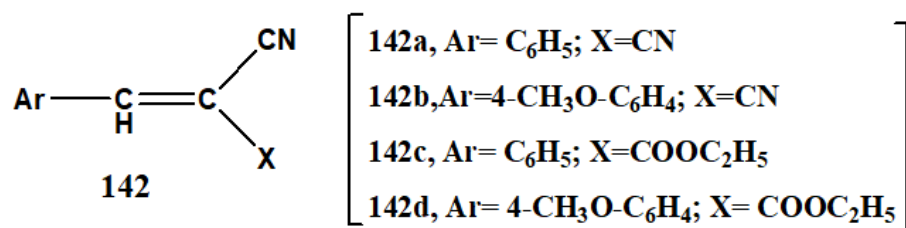
Possible Reaction Pathway for Scheme 53



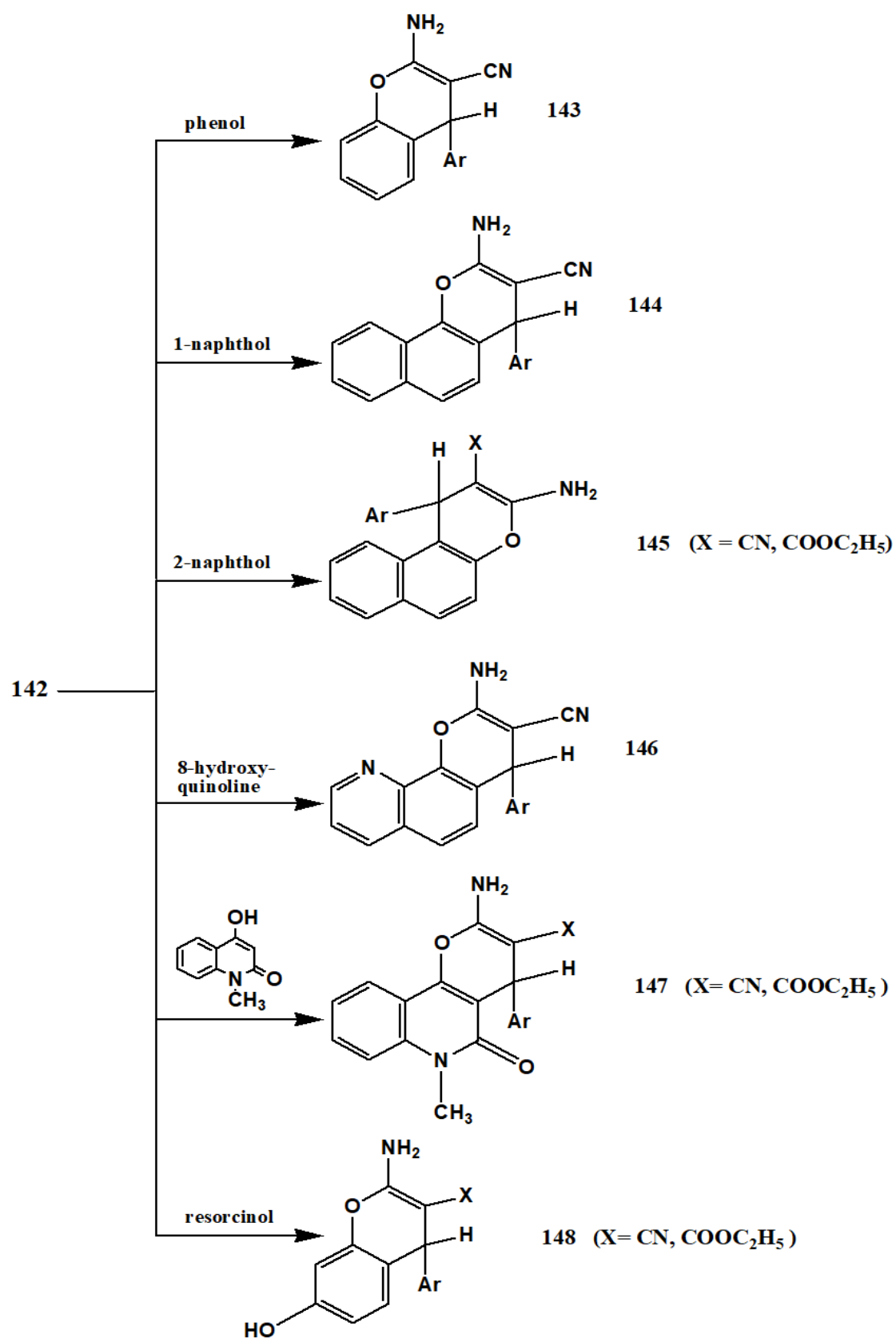
## 5. Synthesis of six-membered heterocyclic compounds

### 5.1 Pyran and its derivatives

Elagamey et al. reported the synthetic potential of  $\alpha,\beta$ -unsaturated nitriles **142** in the novel synthesis of Benzo[b]pyrans **143**, Naphtho[1,2-b]pyrans **144**, Naphtho[2,1-b]pyrans **145**, Pyrano[3,2-h]quinolines **146** and Pyrano[3,2-c]quinolines **147**. It was found that on reacting cinnamonnitriles with anions of phenols, naphthols and other hydroxy  $\pi$ -deficient heterocycles, 4H-pyrans were produced in high yields. Mechanistic studies suggested that the  $\alpha,\beta$ -unsaturated moiety of the nitrile reacts with phenol C-2 to generate acyclic Michael adduct which subsequently cyclizes via the addition of the hydroxy function to the cyano group, finally yielding 4H-benzopyran derivatives. In the similar manner, the  $\alpha,\beta$ -unsaturated nitriles reacts with 1-, 2-naphthols, 8-hydroxyquinoline and 1-methyl-4-hydroxy-2-quinoline to generate the rest of the pyrano derivatives (Scheme 54) [56].

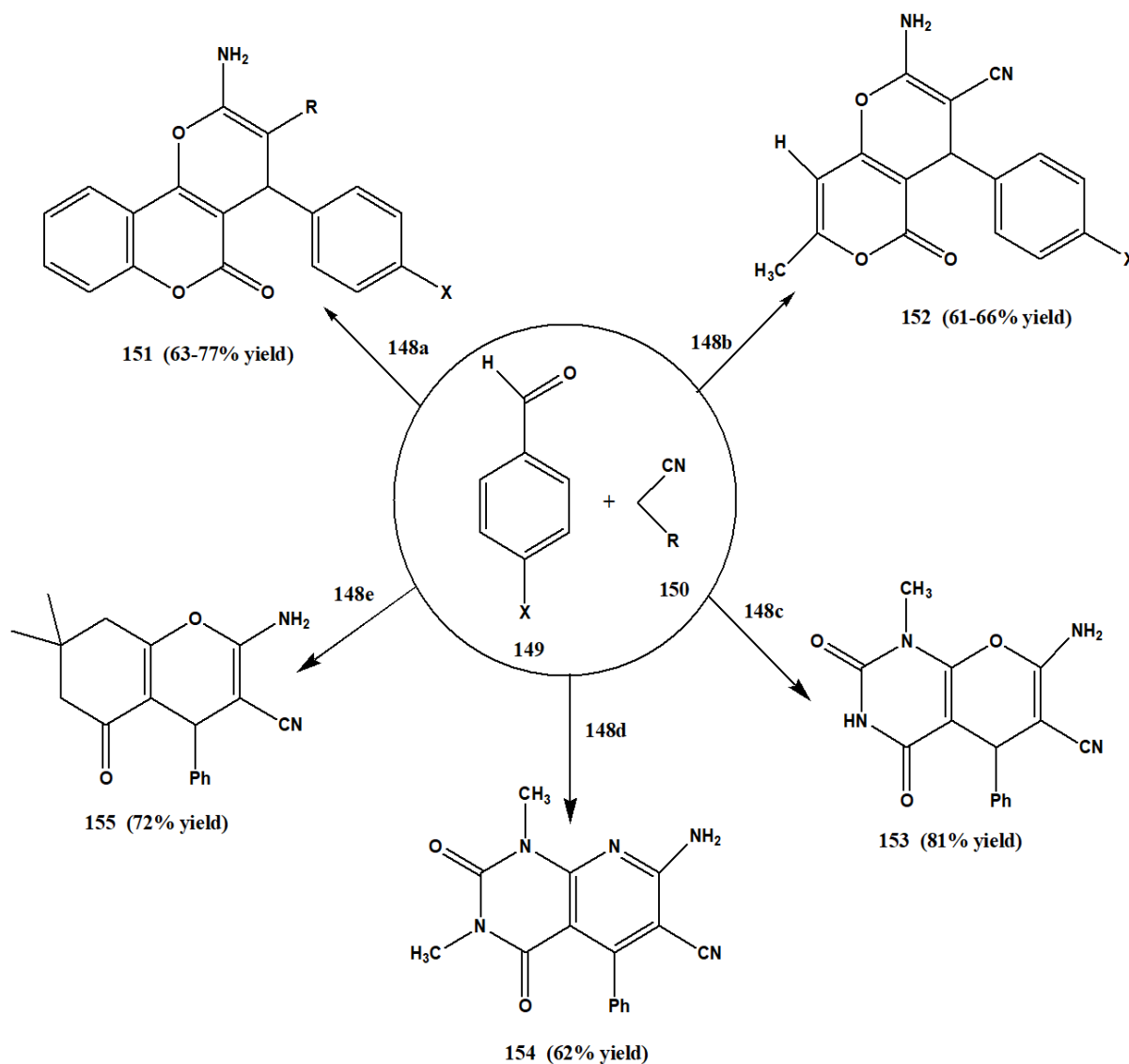


Contd.



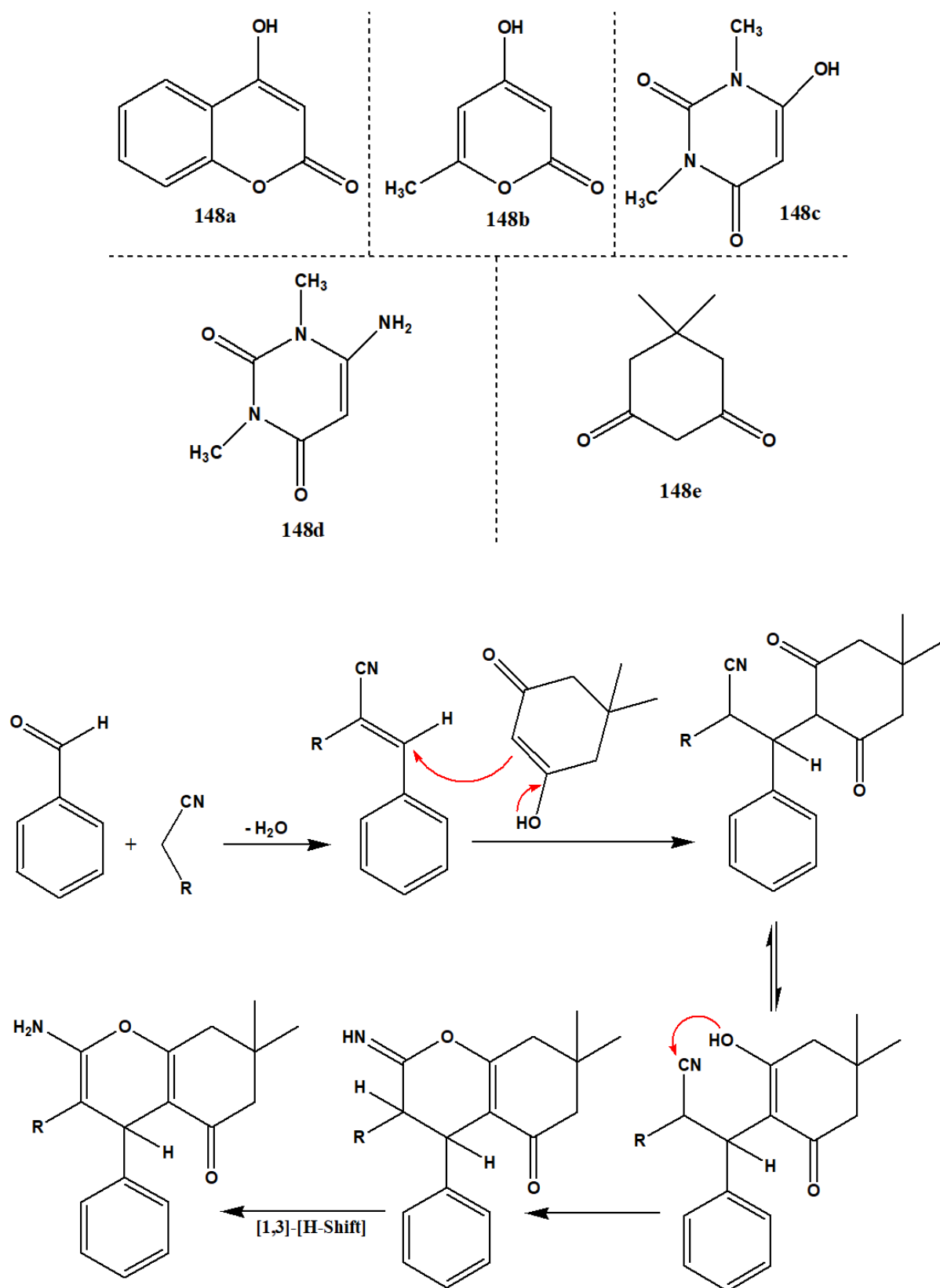
Scheme 54

Shaabani et al. devised a one-pot condensation reaction pathway using an activated C–H acid **148a,b,c,d,e**, an aldehyde **149**, and alkyl nitriles **150** in water as a green solvent to generate the corresponding pyran annulated heterocycles in good yields. The reaction is environmentally friendly, eco-compatible, avoids the use of any additional catalyst and results in easy separation of the products obtained (Scheme 55) [57].



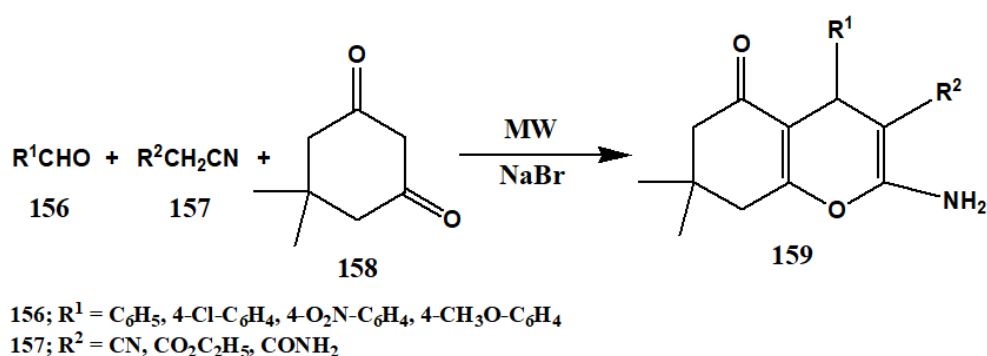
**Scheme 55**

The activated C–H acids are as follows-

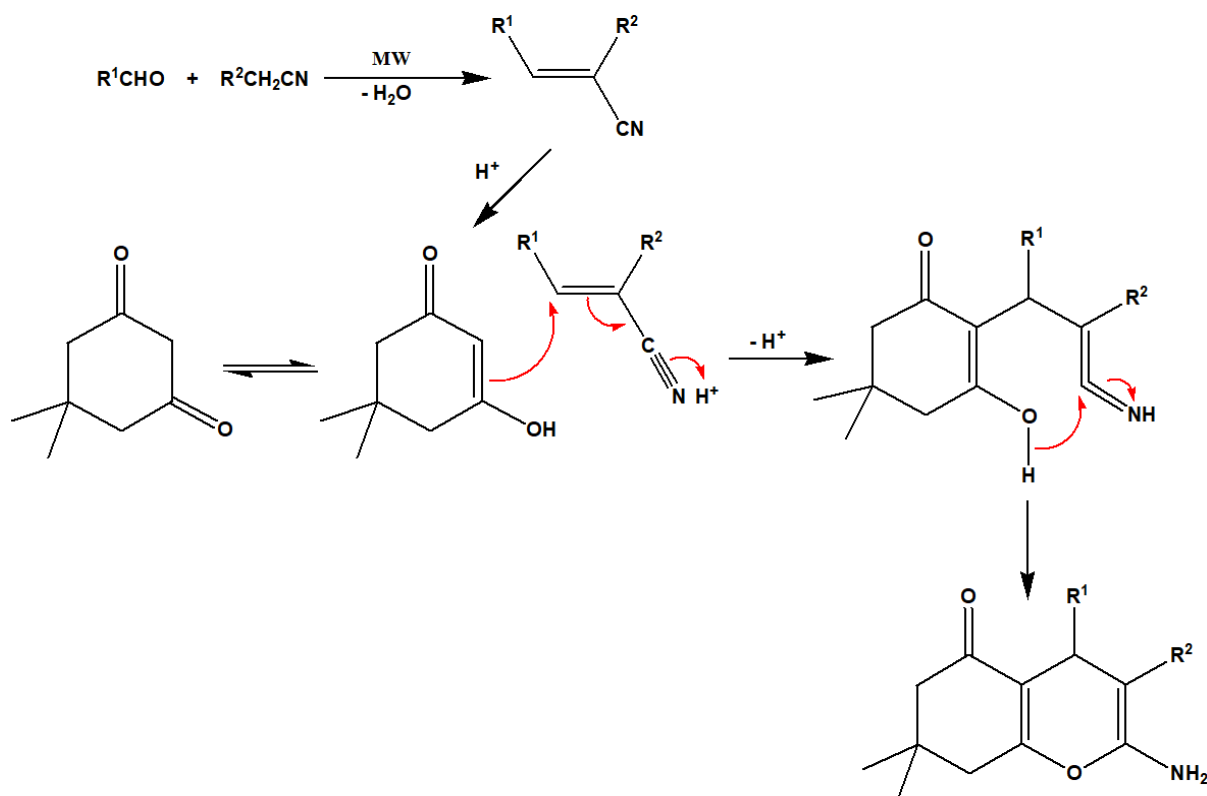


Possible Reaction Pathway for Scheme 55

Devi and Bhuyan reported a one-pot synthesis of highly functionalised tetrahydrobenzo[b]pyrans **159** in high yields via a NaBr catalyzed cyclocondensation reaction of three components, viz. aryl aldehydes **156**, alkyl nitriles **157** and dimedone **158** under microwave irradiation at 70-90°C in the absence of a solvent. Mechanistic studies suggests that the reaction proceeds with the formation of the cyano olefin, the condensation product of aryl halide **156** and alkyl nitrile **157**. The cyano olefin then reacts with **158** to generate an intermediate which undergoes cyclization to yield the final product (Scheme 56) [58].

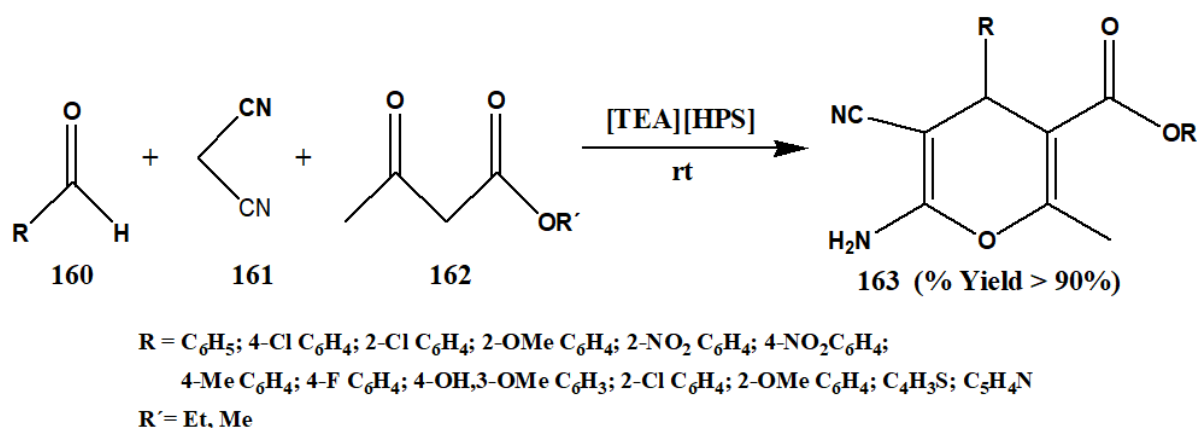


Scheme 56



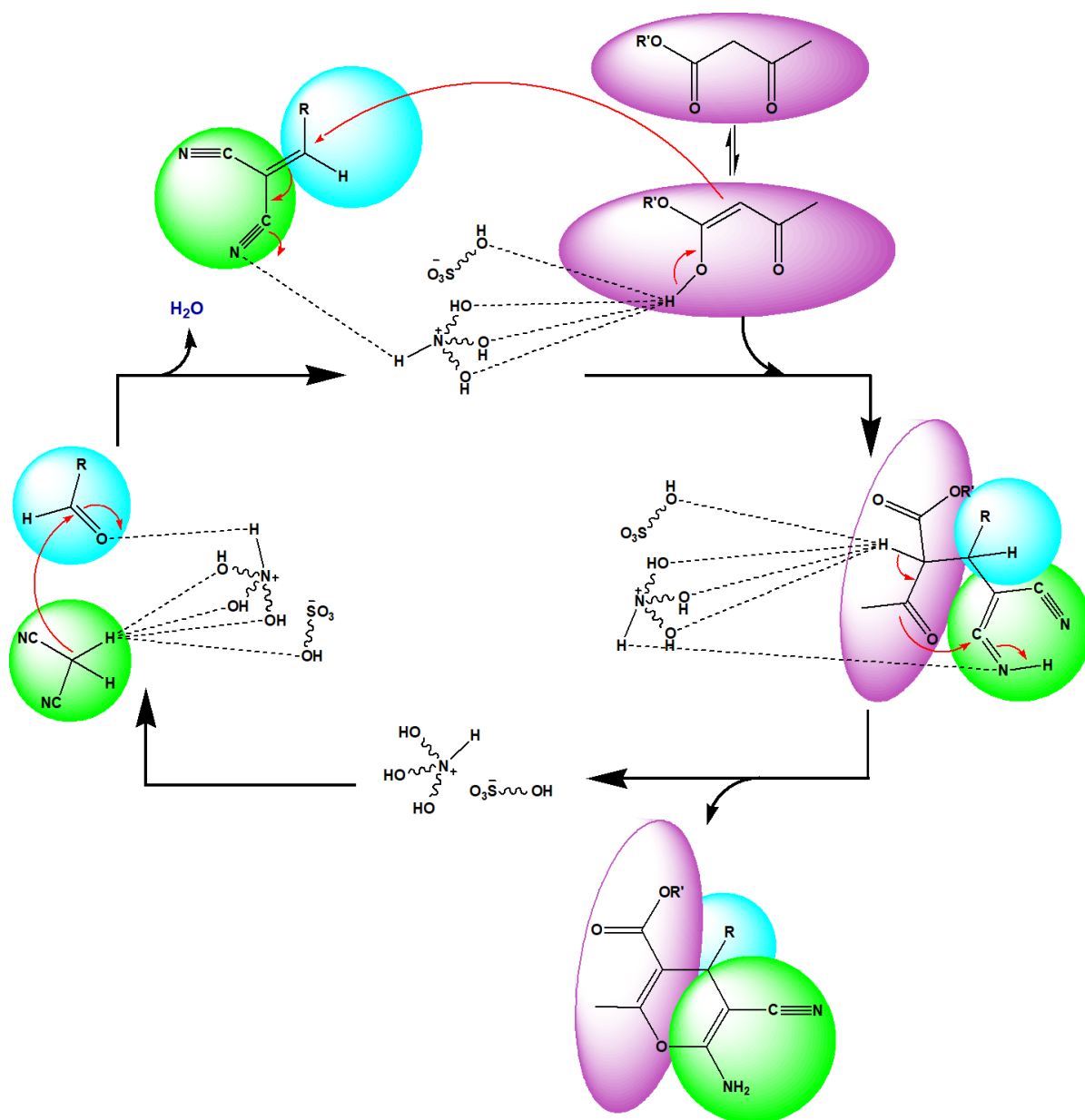
Possible Reaction Pathway for Scheme 56

Honarmand et al. in their recent work on the synthesis of novel multi-OH functionalized ionic liquid, triethanolammonium 3-hydroxypropane-1-sulfonate [TEA][HPS], also demonstrated the use of the ionic liquid as a catalyst and solvent in the one-pot synthesis of 4H-pyran **163** using a three-component reaction between aldehydes **160**, malononitrile **161** and alkyl acetoacetate **162** at room temperature. Experimental observations suggested that [TEA][HPS] could be easily recycled and reused without any appreciable loss of activity for about six times and has an acceptable biodegradability. Additionally, it was found to be successful in synthesizing six new 4H-pyran derivatives (Scheme 57) [59].



Scheme 57

Contd.

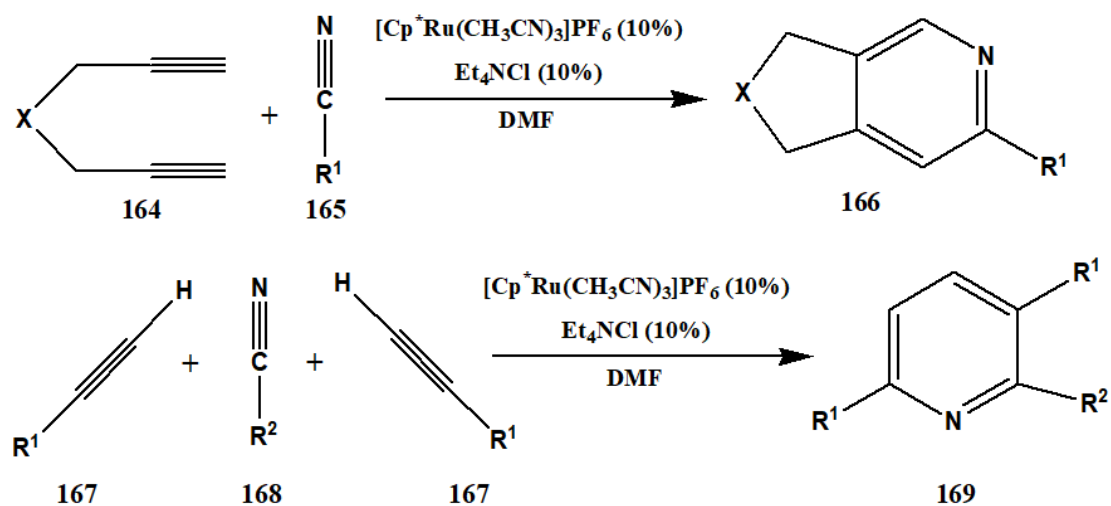


Possible Reaction Pathway for Scheme 57

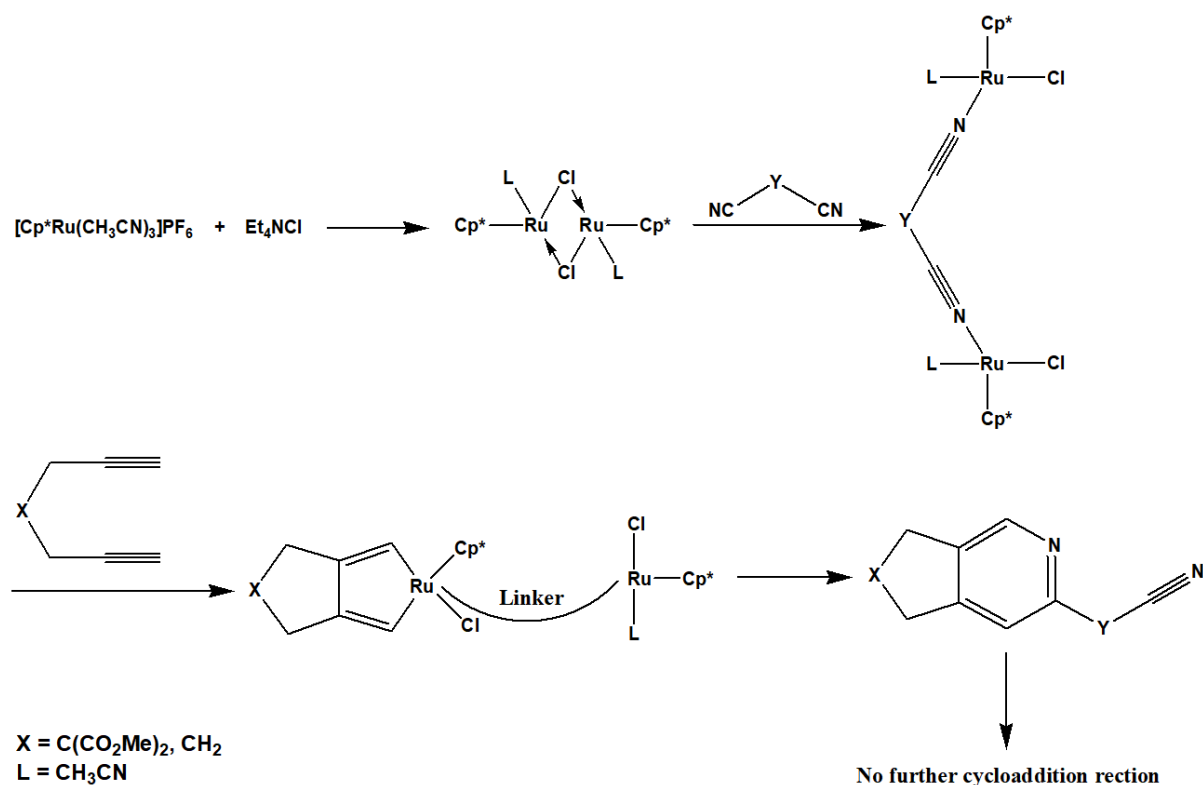
## 5.2 Pyridine and its derivatives

Varela et al. reported the ruthenium(II)-catalyzed synthetic pathway for generation polysubstituted pyridines **166** & **169** in good yields. It was found that that pyridines can be efficiently synthesized by two different reaction pathways both of which are catalyzed by Ru(II) compounds, viz. the [2+2+2] cycloaddition between 1,6-diynes **164** and  $\alpha,\omega$ -dinitriles **165** and the [2+2+2] cocyclization of electron-deficient alkynes

**167** and nitriles **168**. Detailed mechanistic studies implied that the reaction of dinitriles proceeds with the formation of a ruthenacyclopentadiene intermediate whereas, the one involving electron-deficient nitriles proceed via the formation of azaruthenacyclopentadienes (Scheme 58) [60].



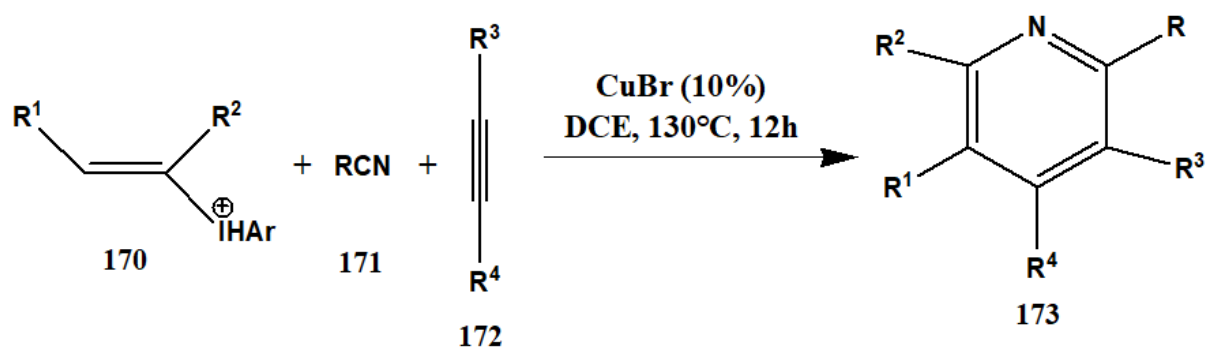
Scheme 58



Possible Reaction Pathway for Scheme 58

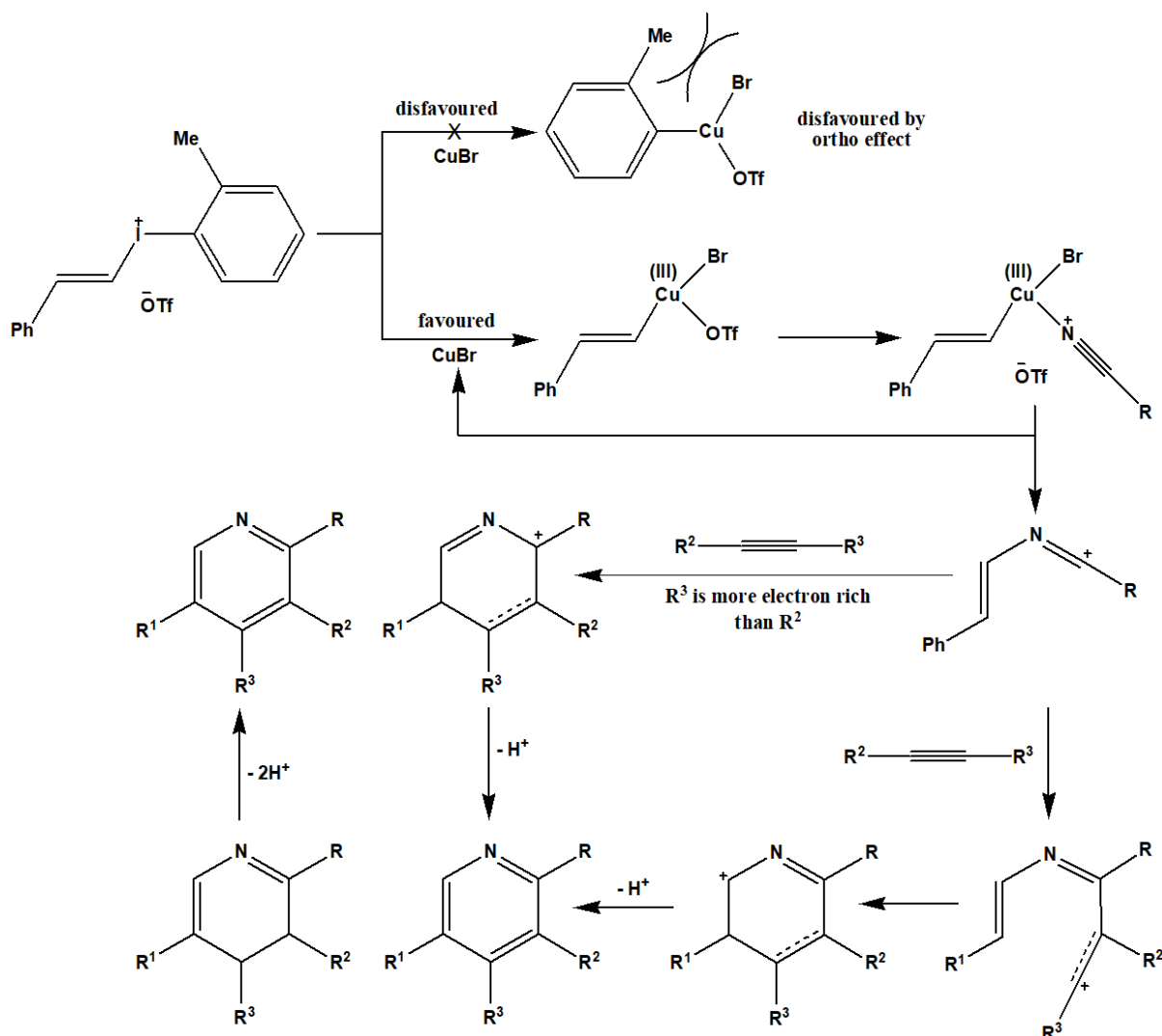


Sheng et al. reported an efficient copper-catalyzed [2+2+2] modular synthetic pathway for the generation of highly regioselective polysubstituted pyridines **173** using three components viz. vinyl iodonium salts **170**, nitriles **171**, and alkynes **172**. The synthesis involves the formation of an aza-butadienylium intermediate, formed due to alkenylation of the nitrile using a vinyliodonium salt and are catalyzed by CuBr. The major advantage of this synthesis is its high flexibility in the substitution pattern and can be extended to the use of alkenes instead of alkynes, as they are expensive and relatively scarce (Scheme 59) [61].



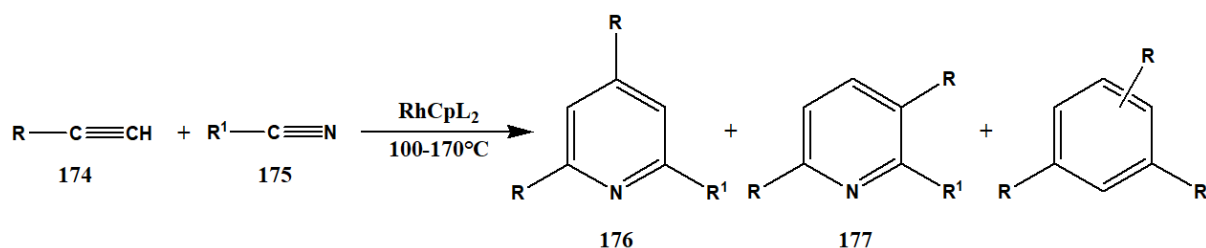
Scheme 59

Contd.

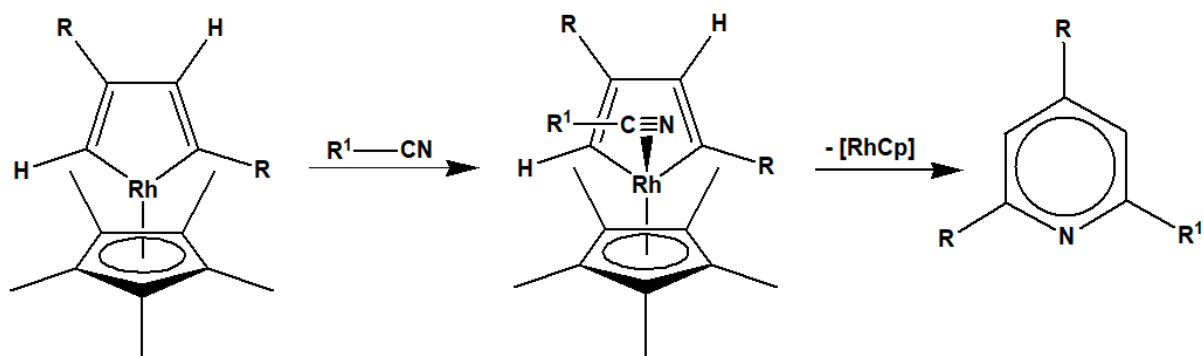


### Possible Reaction Pathway for Scheme 59

Cioni et al. devised a rhodium-catalyzed synthesis of pyridine derivatives **176** & **177** by cocyclization of alkynes **174** and nitriles **175** at temperatures between 110 to 170°C. Complexes of the general formula [RhCpL<sub>2</sub>] are administered, as they are excellent long-lived catalyst precursors. The catalytic activity of the precursor depends on the nature of both the ligands viz. Cp and L. Experimental findings suggested that the activity is highest when Cp = C<sub>5</sub>H<sub>5</sub> and L = C<sub>2</sub>H<sub>4</sub> and it remains unaffected due to the presence of different functional groups in the substrates. The simultaneous formation of benzene derivatives can be lowered by increasing the nitrile-to-alkyne ration to more than 5. Additional findings implies that the cocyclization of terminal alkynes and nitriles results in a mixture of 2,4,6- and 2,3,6-trisubstituted pyridinic isomers (Scheme 60) [62].

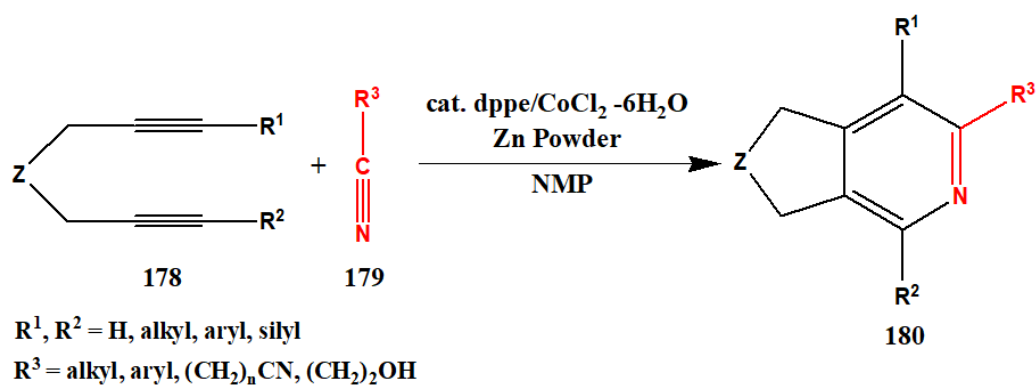


Scheme 60



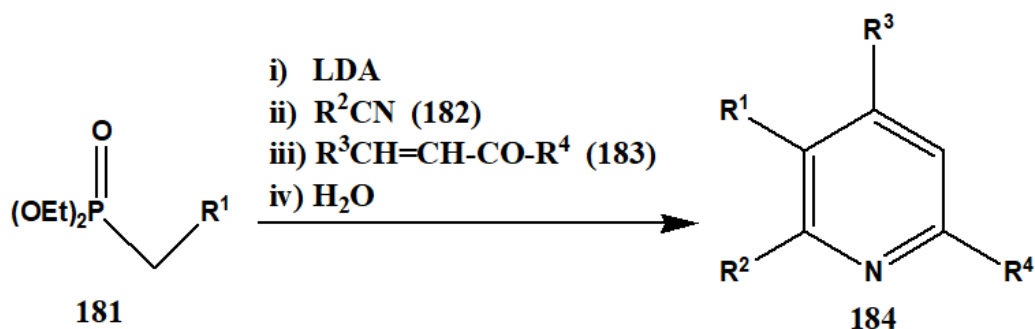
Possible Reaction Pathway for Scheme 60

Kase et al. reported a highly practical on-demand synthetic method for the catalytic generation of polysubstituted pyridines **180** with high regioselectivity and functional group compatibility, obtained from a range of  $\alpha,\omega$ -diynes **178** and unactivated nitriles **179**. The synthesis is catalyzed by 5 mol% of  $dppe/CoCl_2 \cdot 6H_2O$  in the presence of Zn dust (10 mol%) and is carried at a temperature range of rt to  $50^\circ C$ . The active catalyst is generated in situ and this alleviates the difficulty associated with the preparation and isolation of the catalyst and also reduces waste generation (Scheme 61) [63].

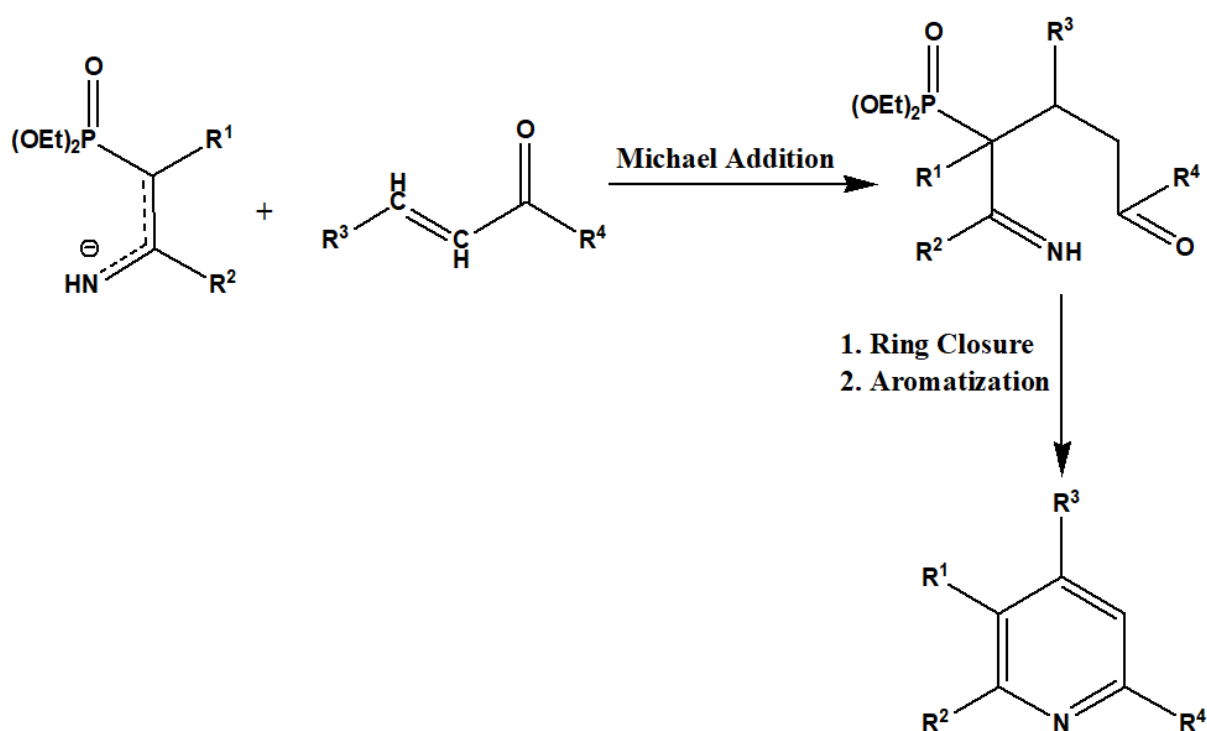


Scheme 61

Palacios et al. developed a highly efficient yet simple one-pot reaction for the synthesis of polysubstituted pyridines **184**. The synthesis proceeds from the readily available phosphonates **181**, which are straight way metalated by using lithium diisopropylamide (LDA) in THF followed by the subsequent addition of nitriles **182** and unsaturated ketones **183**. The synthesis also requires an additional aqueous work-up for generation of the final product. The synthesis is highly regioselective and is carried out under mild reaction conditions (Scheme 62) [64].



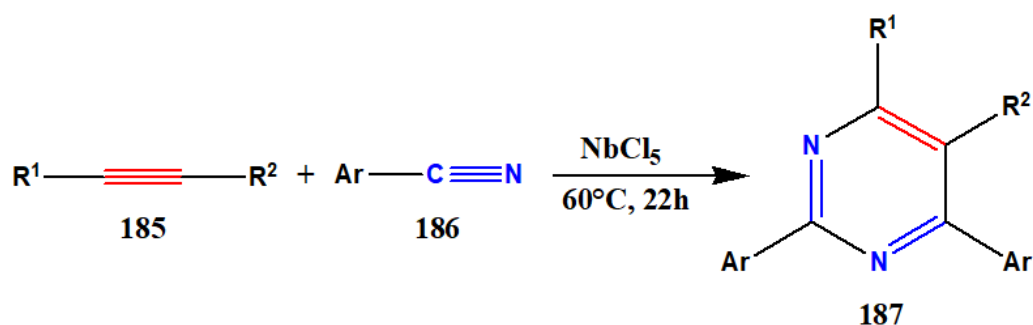
Scheme 62



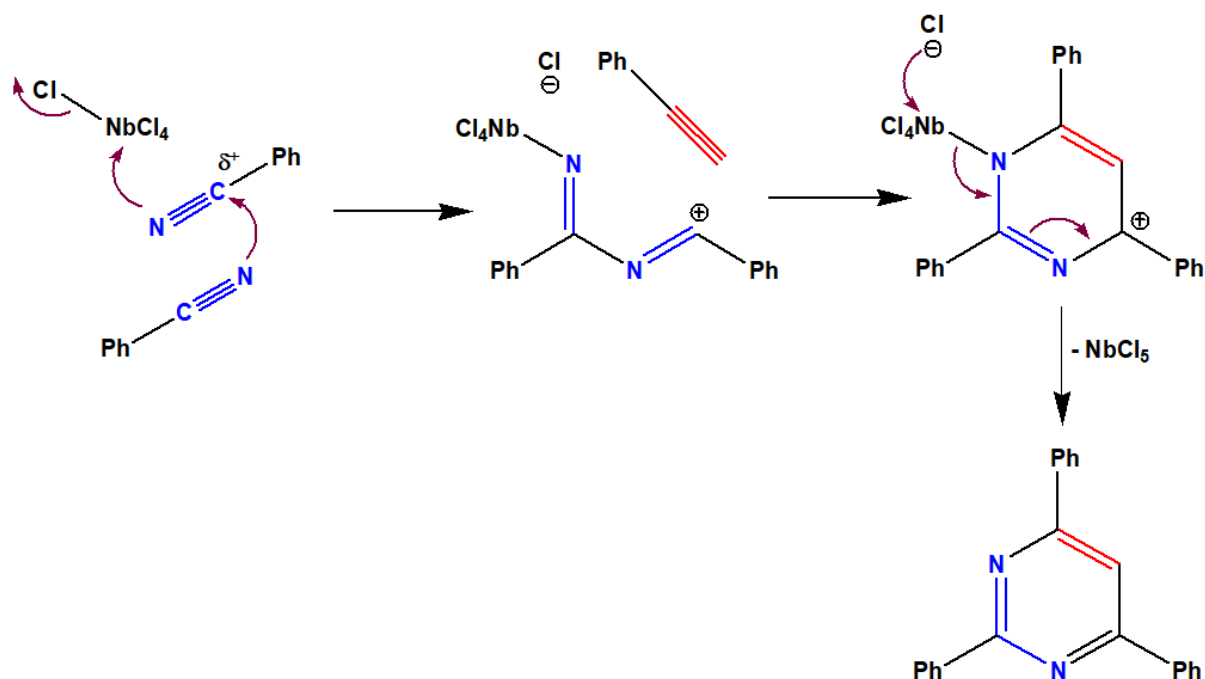
Possible Reaction Pathway for Scheme 62

### 5.3 Pyrimidine and its derivatives

Sato et al. reported an intermolecular cycloaddition based synthetic pathway for the generation of substituted pyrimidines **187** in high yields using alkynes (both terminal and internal alkynes) **185** and aryl nitriles **186** with the complex  $\text{NbCl}_5$  (a strong Lewis Acid) as the catalyst. It is a practical and highly efficient synthetic pathway that exhibits excellent chemo- and regioselectivity and is one of the first examples of the use of transition metals to catalyse cycloaddition reactions (Scheme 63) [65].

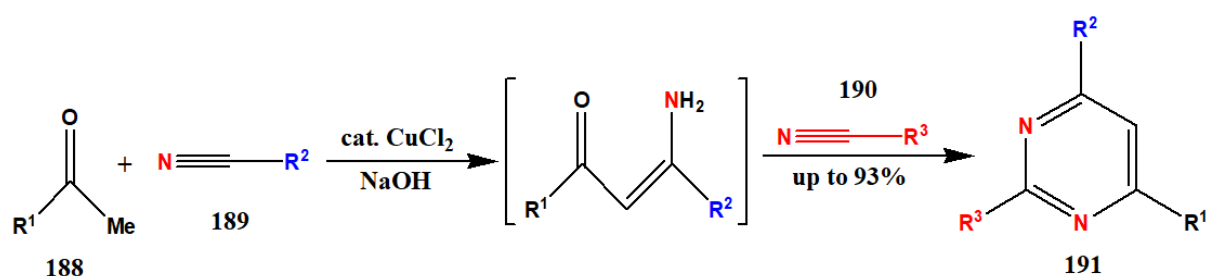


Scheme 63



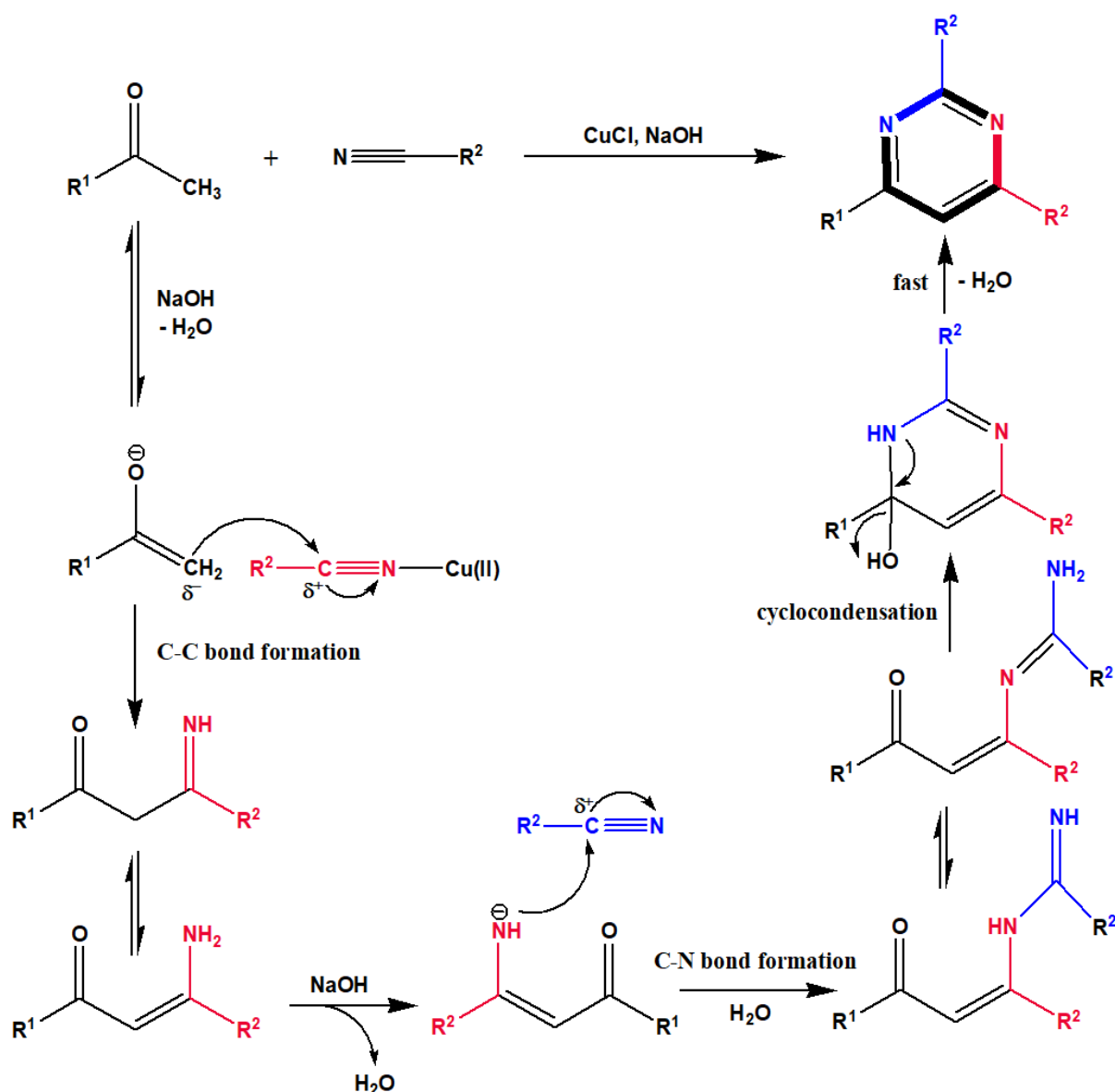
Possible Reaction Pathway for Scheme 63

Su et al. developed a facile and general copper catalyzed reaction for the generation of diversely functionalized pyrimidines **191** via the cyclization of ketones **188** and nitriles **189** & **190**. It is novel and economical synthetic pathway that is carried out under basic conditions. the reaction proceeds with the use of nitriles as electrophiles and the consecutive formation of a C–C and two C–N bonds, there exhibiting excellent substrate scope and tolerance to a range of functionalities and is thus used extensively in chemical research and industry (Scheme 64) [66].



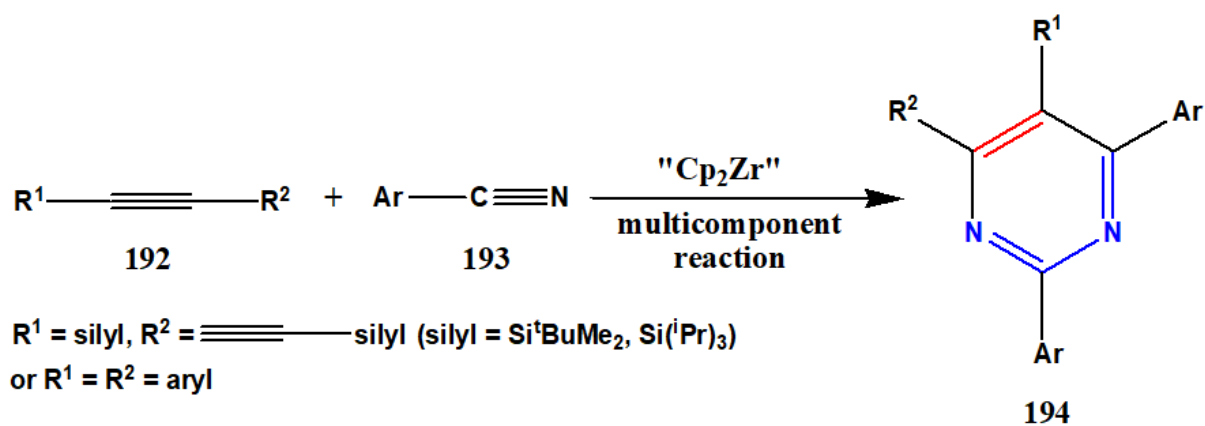
**Scheme 64**

**Contd.**

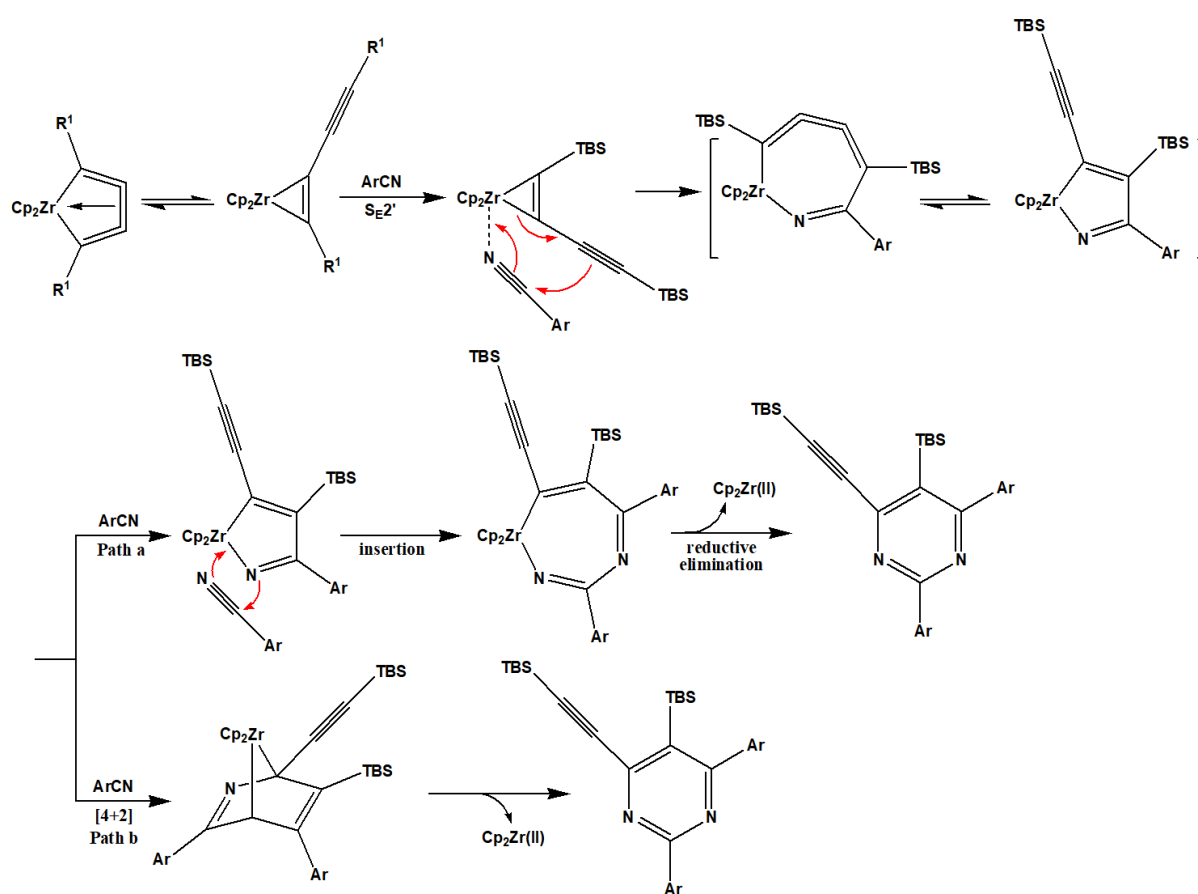


#### Possible Reaction Pathway for Scheme 64

You et al. reported a one-pot synthesis for the regioselective generation of polysubstituted pyrimidines **194** using a zirconium-mediated multicomponent reaction between silylbutadienes **192** and two molecules of aryl nitriles **193**. A similar kind of reaction occurs on using zirconocene monoyne instead of zirconocene butadiyne. The use of aliphatic nitriles is avoided as it results in the formation of enynyl ketones on hydrolysis. Clarification of the proposed reaction mechanism and its application are in constant progress (Scheme 65) [67].



Scheme 65

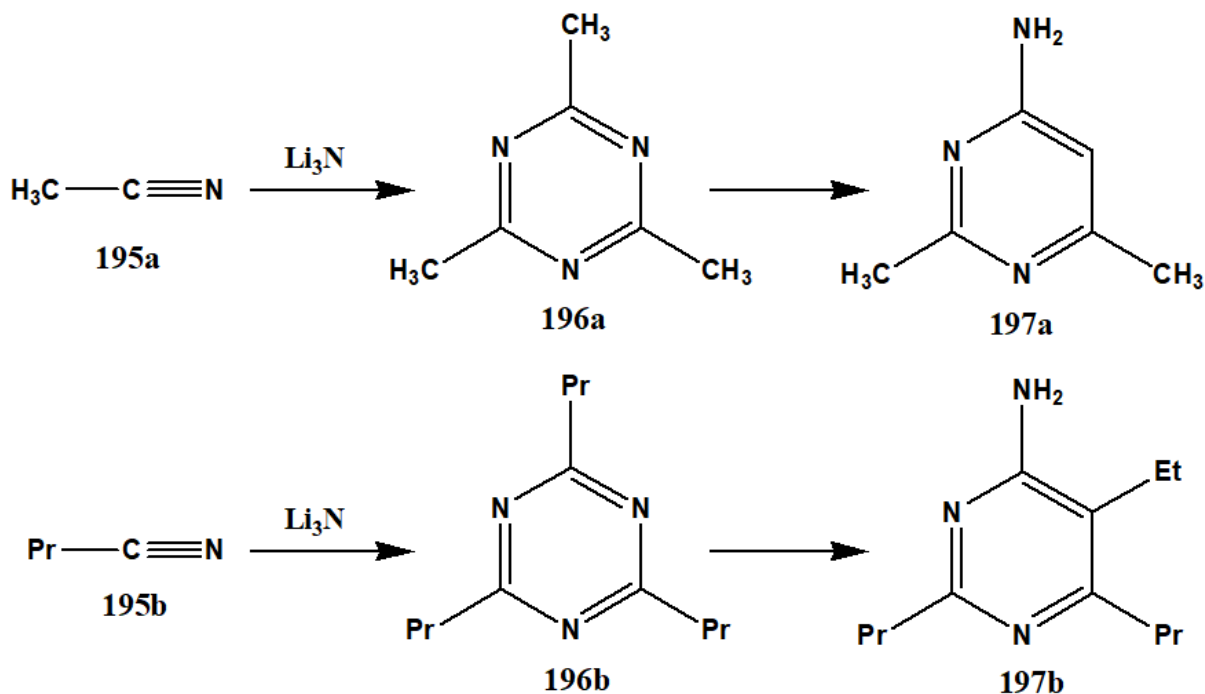


Possible Reaction Pathway for Scheme 65

Zhaoxiang et al. reported the unexpected yet highly efficient synthesis of substituted pyrimidines **197** via the formation of s-triazines **196** using cyclotrimerization of nitriles **195** in the presence of  $\text{Li}_3\text{N}$  as the catalyst. It is simple, solvent-free, one-pot synthesis which is easy to scale up and does not require the use of extremely high reaction pressure. Additionally,

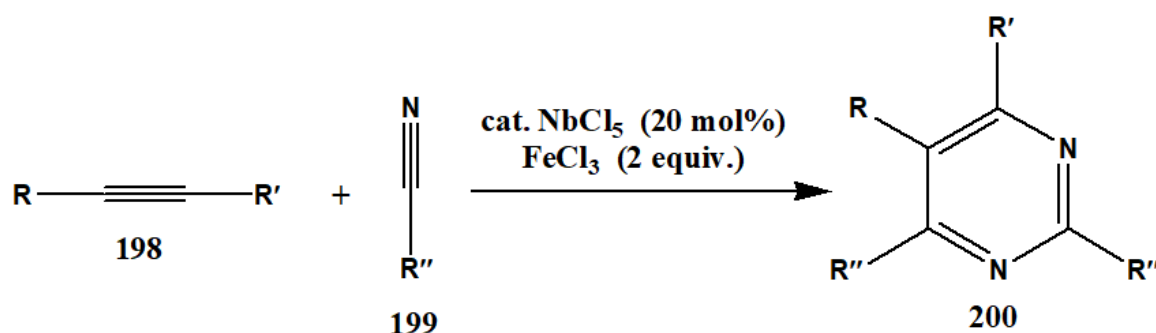


it also eliminates the use of large amounts of co-catalyst such as amine, alcohols and acids. This reaction contributes immensely to the present works of finding new functional molecules having triazine or pyrimidine unit (Scheme 66) [68].

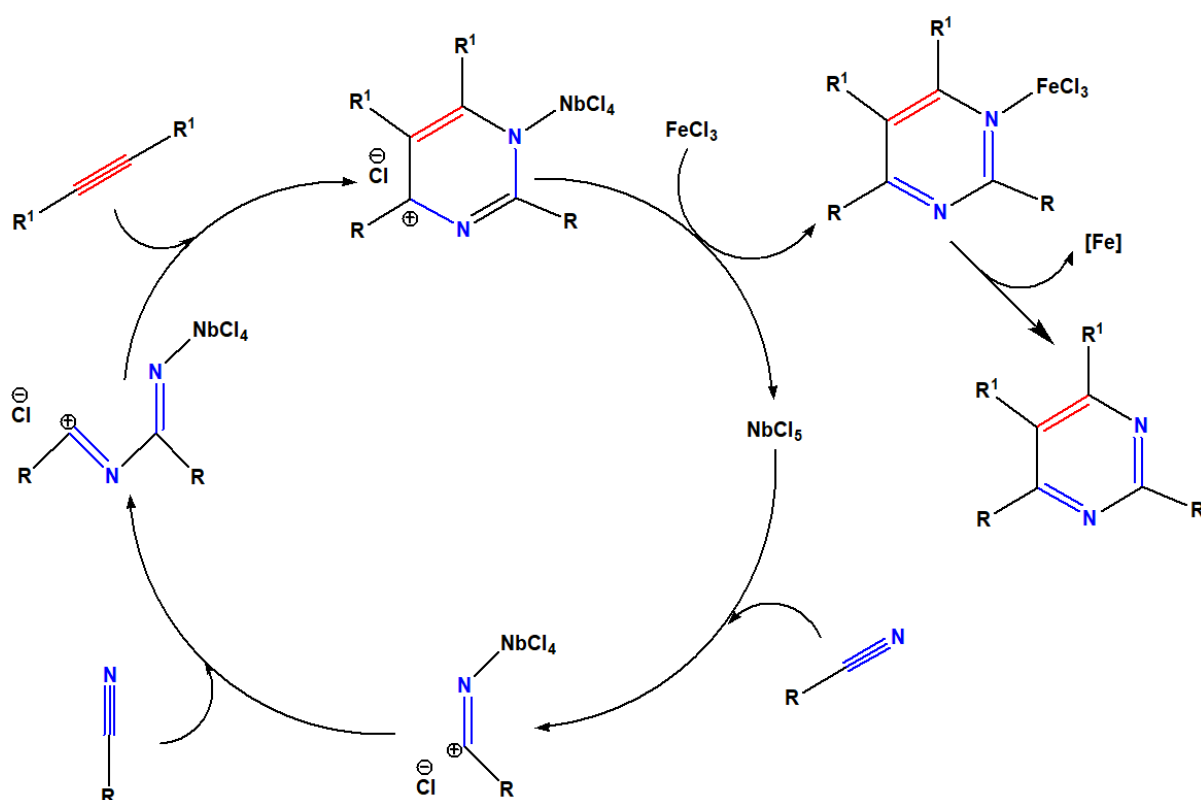


Scheme 66

Fuji and Obora reported the [2+2+2] cycloaddition-based synthesis of alkyl- and arylpyrimidines **200** using alkynes **198** and nitrile **199**. The reaction was catalyzed by  $\text{NbCl}_5$  assisted with  $\text{FeCl}_3$ . The strategy behind using the two Lewis acids individually, was to complete the synthesis using only a catalytic amount of  $\text{NbCl}_5$ . The role of both of the used Lewis acids was determined by FT-IR spectroscopy. It suggested that,  $\text{NbCl}_5$  was involved in the activation of nitriles, whereas  $\text{FeCl}_3$  exhibited the stronger Lewis acidity towards the product pyrimidines thereby regenerating free  $\text{NbCl}_5$  for repeating the catalytic cycle (Scheme 67) [69].



Scheme 67

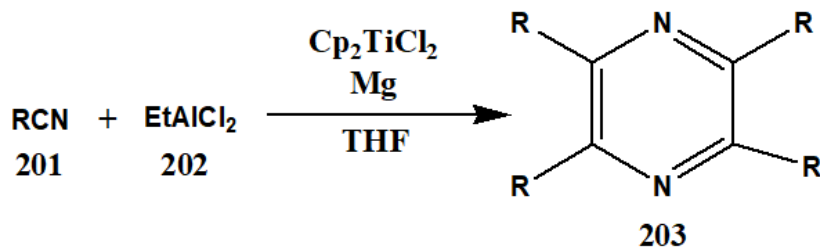


Possible Reaction Pathway for Scheme 67

## 5.4 Pyrazine and its derivatives

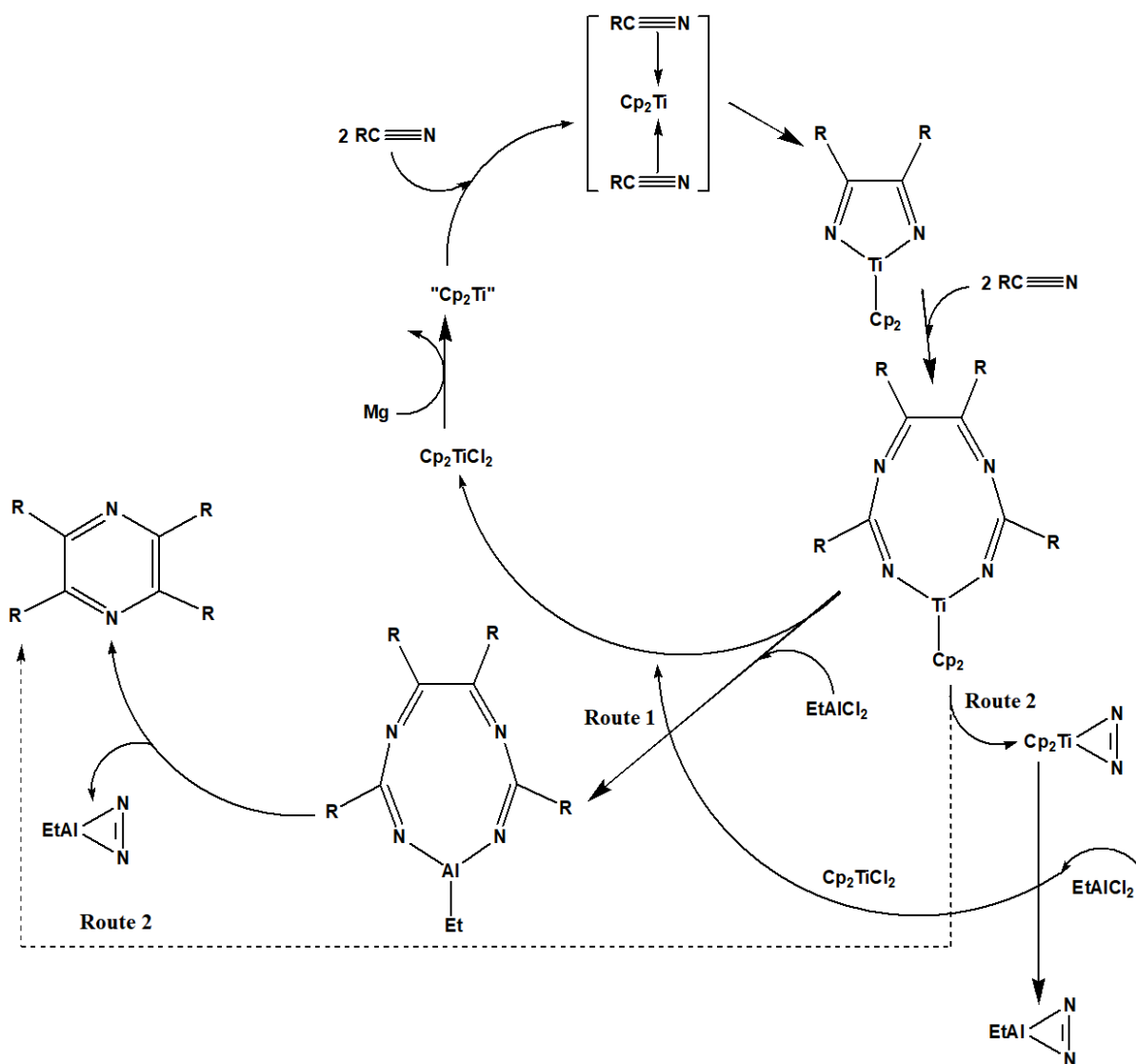
Khafizova et al. reported a titanium-catalyzed one-pot synthetic pathway for the generation of tetrasubstituted pyrazines **203** using nitriles **201** and  $\text{EtAlCl}_2$  **202**. The reaction proceeds with a short reaction time (8h) in the presence of metallic Mg and  $\text{Cp}_2\text{TiCl}_2$  catalyst to generate the final product with excellent yields of about 60 to 90%. Moreover, the synthetic work-up is very

simple and uses a relatively inexpensive catalyst and exhibits appreciable diversity. Mechanistic studies suggested that the substituted pyrazines are formed via the initial formation of tetraazatitanacyclononatetraene intermediate (Scheme 68) [70].



R = Ph (90%); 2-MePh (84%); 3-MePh (88%); 4-MePh (90%); 4-PriPh (70%);  
3,5-Me<sub>2</sub>Ph (65%); 4-MeOPh (82%); BnPh (77%); 4-MeBn (76%)

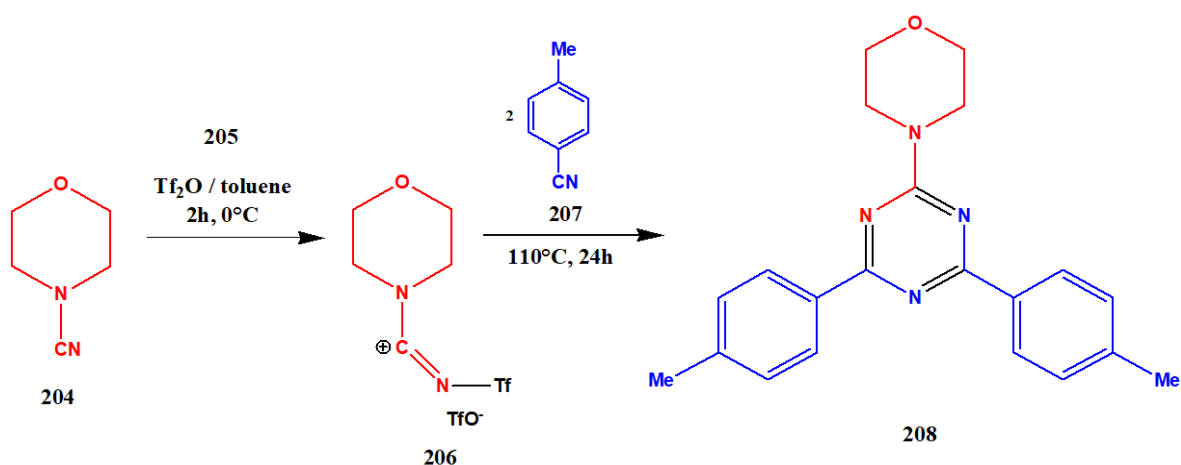
Scheme 68



Possible Reaction Pathway for Scheme 68

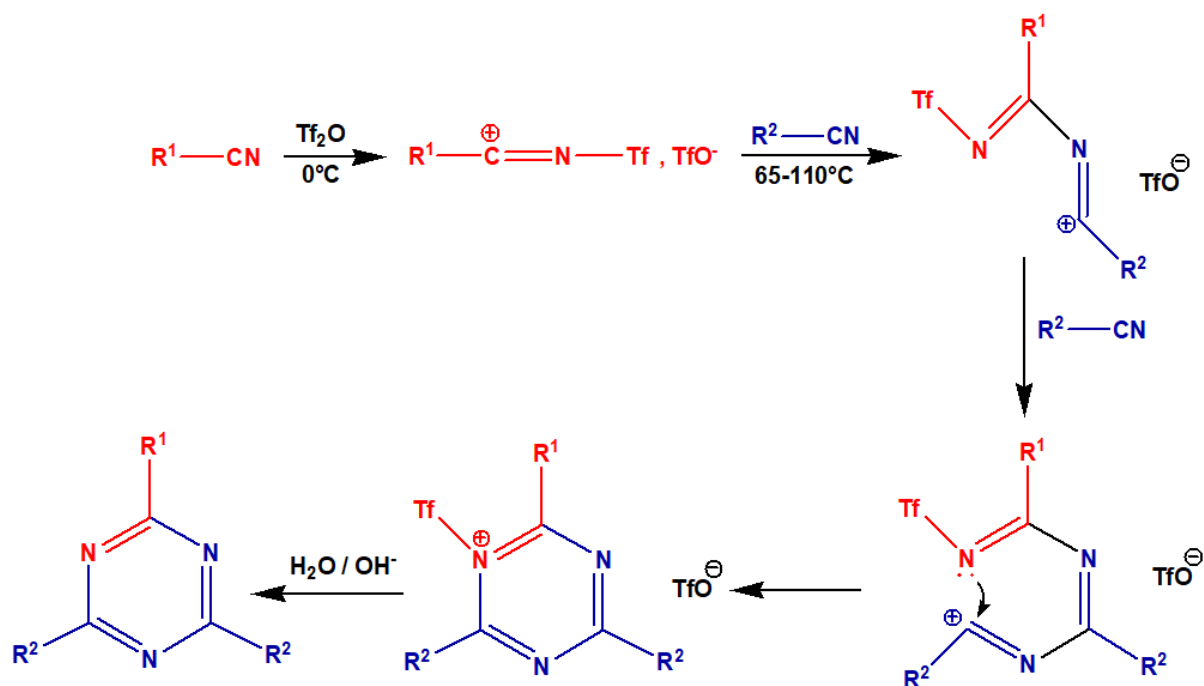
## 5.5 Triazine and its derivatives

Herrera et al. devised a one-pot synthesis involving the cyclotrimerization of nitriles to generate 1,3,5-Triazine in moderate to good yields. This method is also used to produce 1,3,5-triazine with various substituents. It involves the low temperature reaction between the equimolar amounts of a nitrile **204** and triflic anhydride or triflic acid **205** to generate the nitrilium salt intermediate **206** which then further reacts at a higher temperature with two equivalents of another nitrile **207** to yield the 2,4-disubstituted-6-substituted 1,3,5-triazines **208**. The reaction mechanism depends on the relative stability of the intermediate formed via a reversible pathway (Scheme 69) [71].



Scheme 69

Contd.

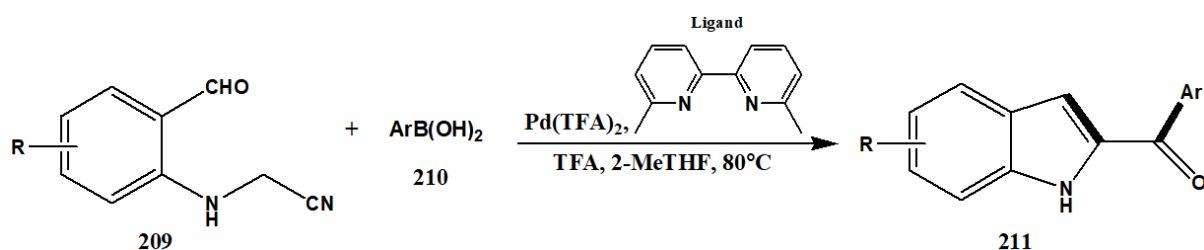


Possible Reaction Pathway for Scheme 69

## 6. Synthesis of fused heterocyclic compounds

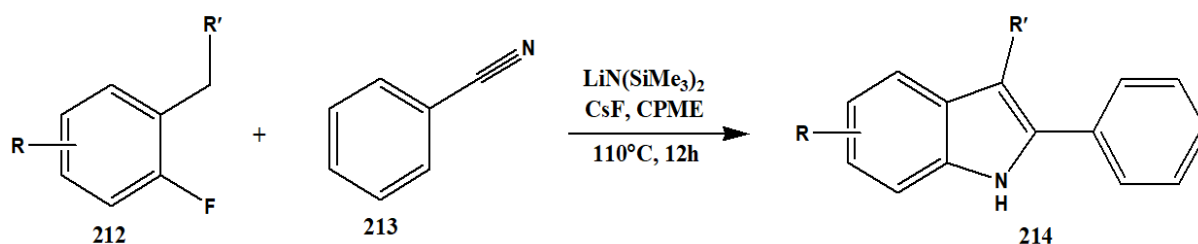
### 6.1 Indole and its derivatives

Gong et al. reported the first example of a palladium-catalyzed tandem addition / cyclization reaction to generate 2-aryl indoles **211** using 2-(2-acylphenoxy)acetonitriles **209** and arylboronic acid **210**. The synthesis exhibits excellent chemoselectivity and high compatibility with a variety of functional groups. Mechanistic studies suggested that the synthesis initially includes a nucleophilic addition to produce 2-(2-acylphenoxy)-1-phenylethan-1-one and is then followed by an intramolecular cyclization to yield the desired product (Scheme 70) [72].

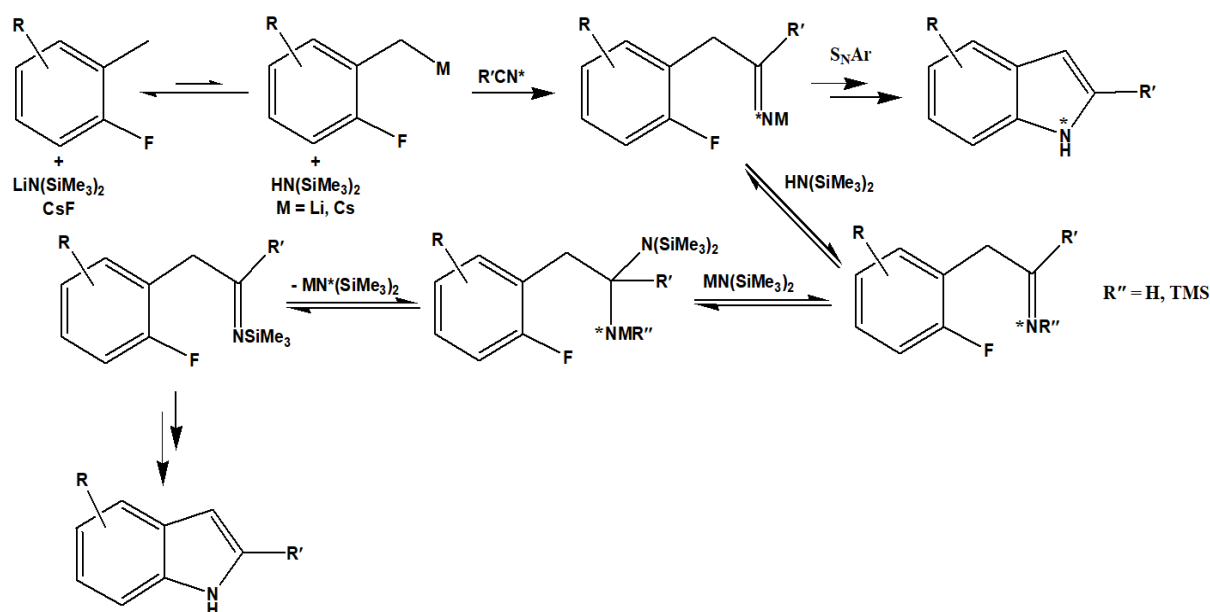


Scheme 70

Mao et al. reported the synthesis of indoles via a transition-metal-free pathway. The synthesis proceeds by the simple combination of readily available substrates viz. 2-fluorotoluenes **212**, nitriles **213**, LiN(SiMe<sub>3</sub>)<sub>2</sub> and CsF thereby producing a wide variety of indoles **214** with good yield ranging from 48-92%. Moreover, it enables us to introduce various substituents at different positions on the indole structure. It is a brief synthesis that avoids the requirement of low temperatures that are not easily accessible (Scheme 71) [73].

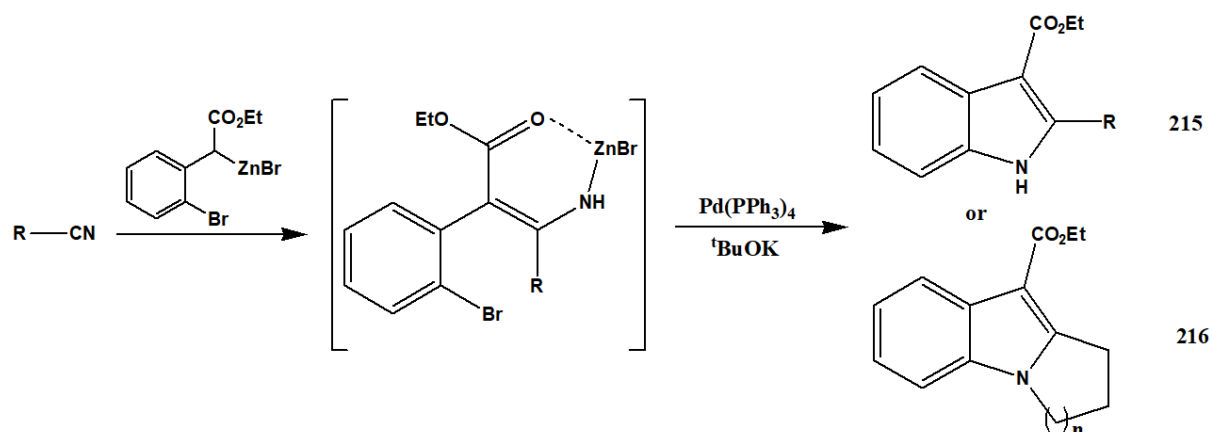


Scheme 71

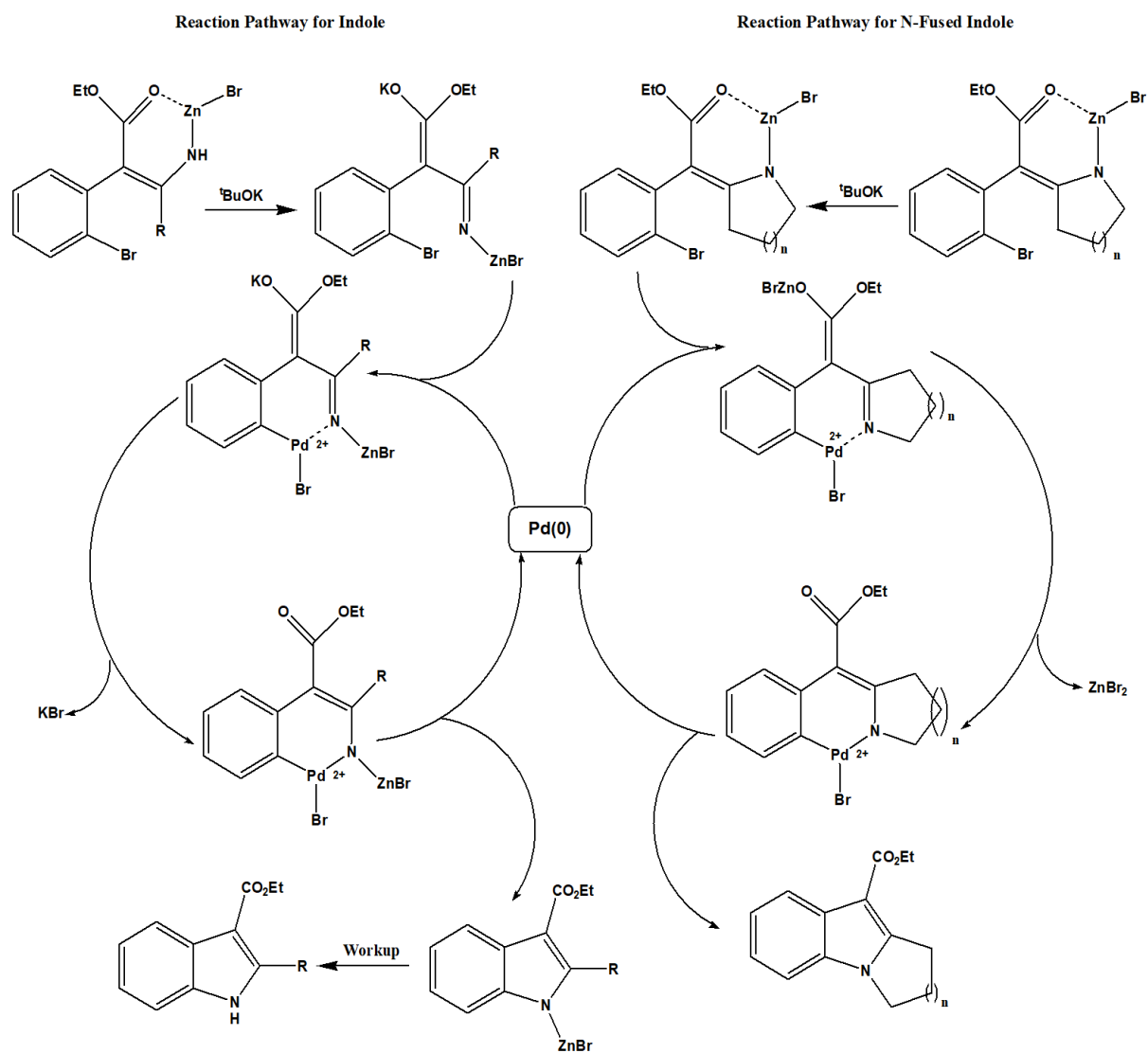


Possible Reaction Pathway for Scheme 71

Kim and Lee reported the synthesis of indole **215** and N-fused indole **216** derivatives via a one-pot process that involves the intramolecular N-alkylative or N-arylate trapping of the Blaise reaction intermediate using palladium as the catalyst. The synthesis uses readily available nitriles along with the Reformatsky reagents to carry the process of trapping the intermediate. This synthesis provides a platform for further studies regarding the applications of the Blaise reaction intermediate (Scheme 72) [74].



Scheme 72

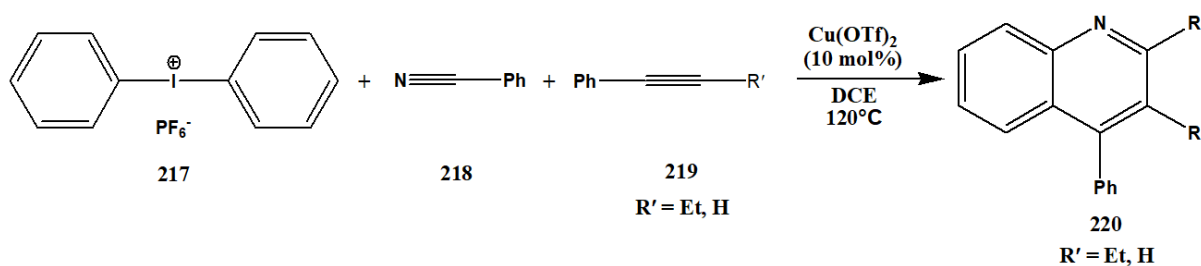


Possible Reaction Pathway for Scheme 72



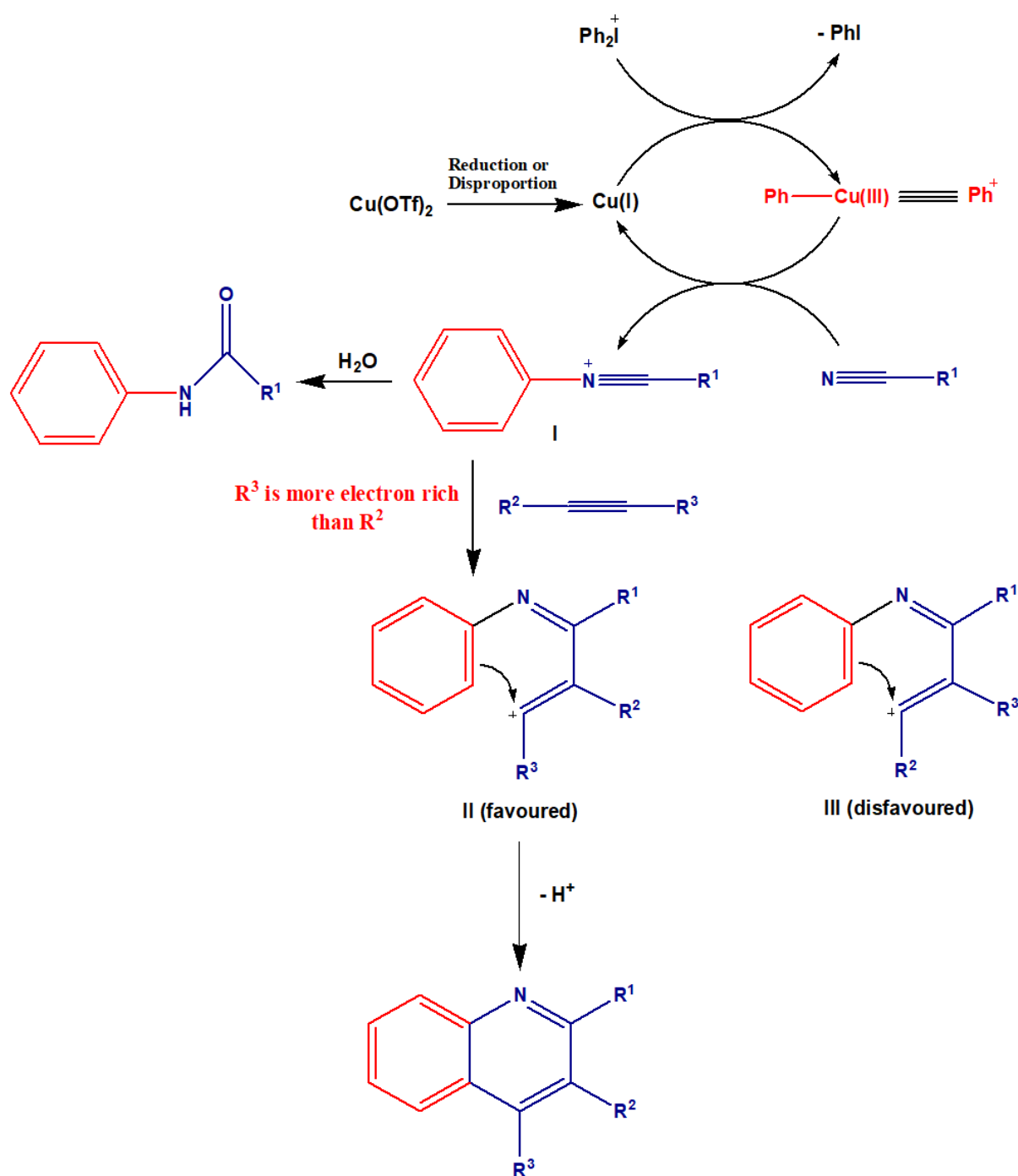
## 6.2 Quinoline and its derivatives

Wang et al. reported a regioselective synthetic pathway to generate polysubstituted quinolines **220** using a three-component annulation reaction involving diaryliodoniums **217**, nitriles **218** and alkynes **219** and is catalyzed by copper(II). The reaction proceeds with a [2+2+2] cyclization using  $\text{Cu}(\text{OTf})_2$  as the catalyst and the aryl group in diaryliodoniums acts as a  $\text{C}_2$  building block. This protocol exhibits an appreciable departure from that of the other ones that involves condensation chemistry (Scheme 73) [75].



Scheme 73

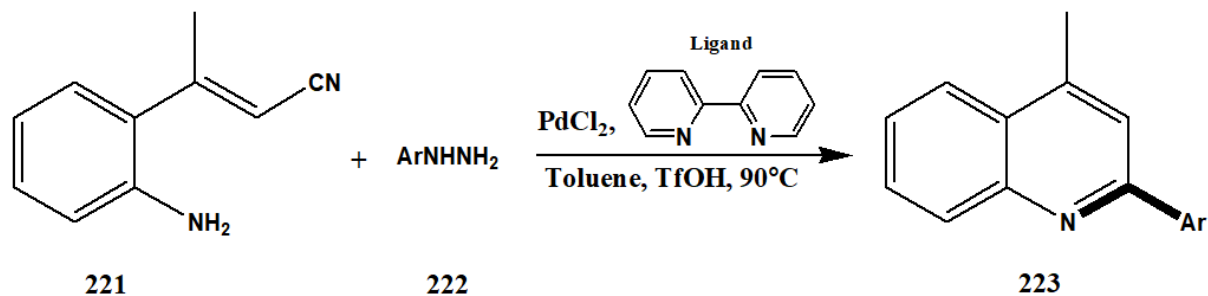
Contd.



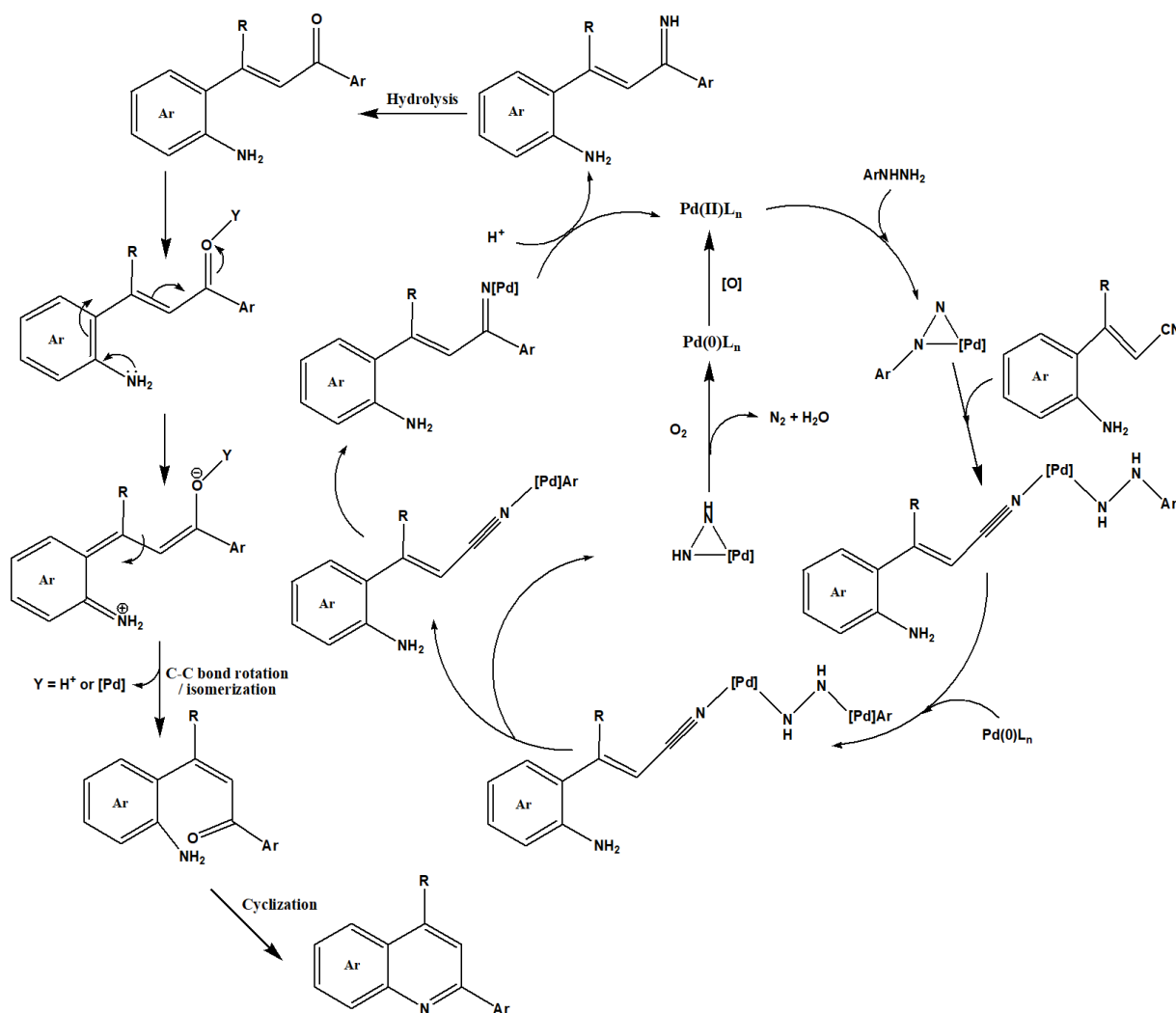
### Possible reaction Pathway for Scheme 73

Xie et al. reported the first case of denitrogenative cascade reaction using O-aminocinnamionitriles **221** and arylhydrazines **222** using palladium catalyst to produce quinolines **223**. The synthesis exhibits high efficiency and generates products with good yields.

Mechanistic studies have inferred that the synthesis involves a denitrogenative addition reaction with subsequent intramolecular cyclization (Scheme 74) [76].

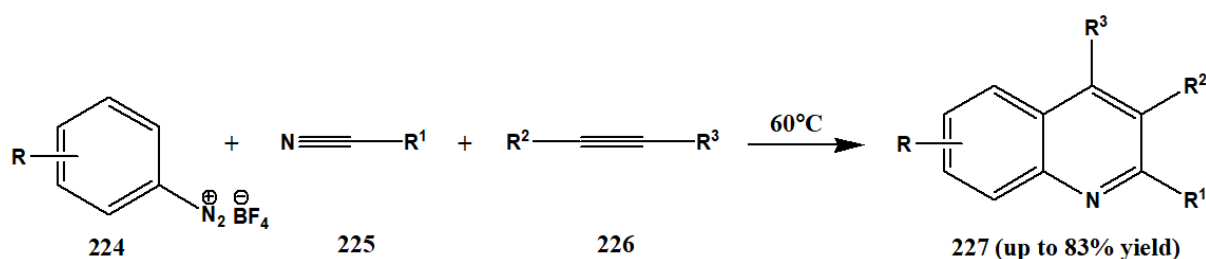


**Scheme 74**



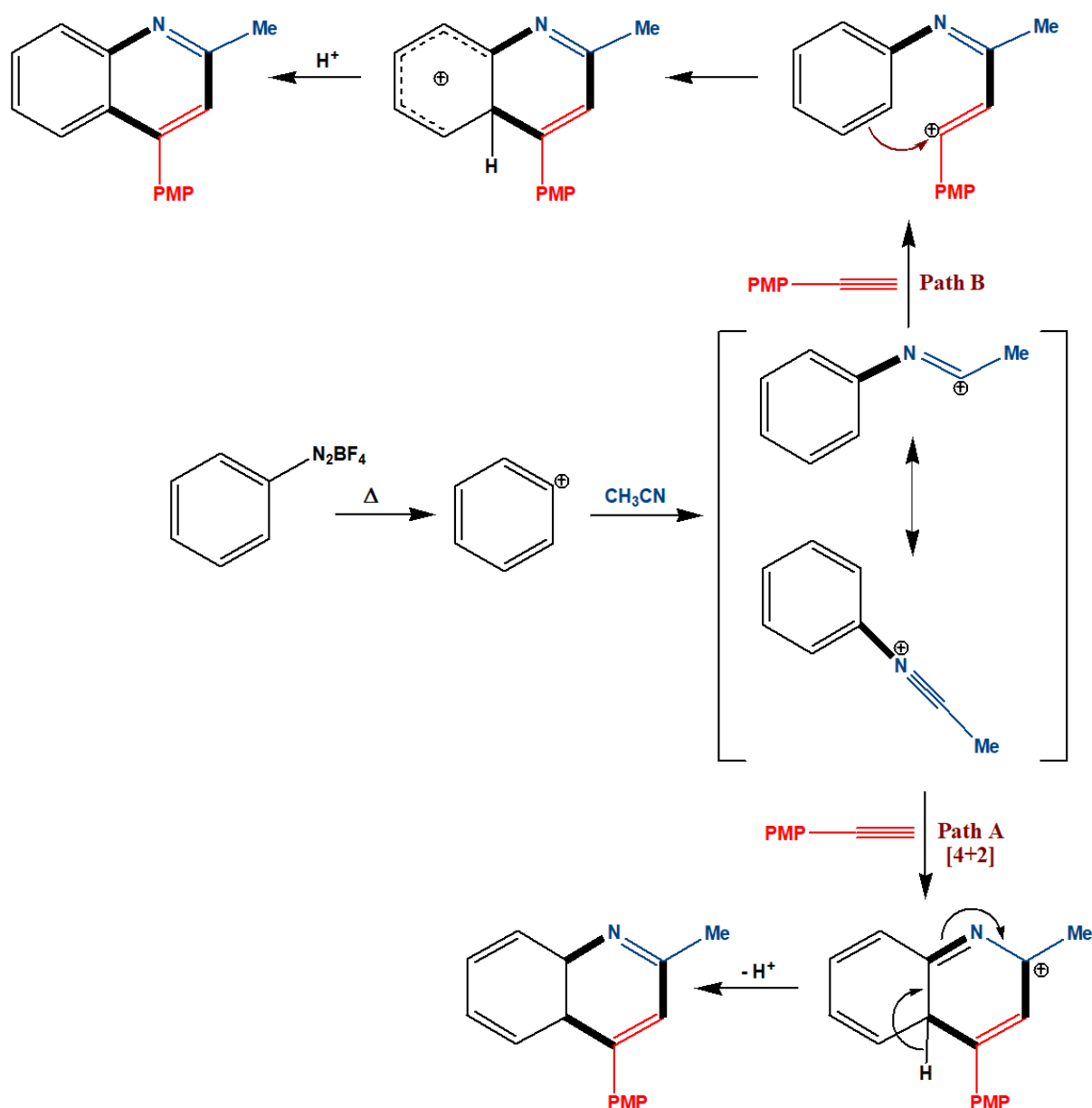
**Possible Reaction Pathway for Scheme 74**

Wang et al. reported an efficient and rapid three-component cascade synthetic pathway to generate polysubstituted quinolines **227**. It involves the cascade annulation of the aryl diazonium salts **224**, nitriles **225** and alkyne **226** without the aid of any catalyst or additive to generate the product quinolines with high yields up to 83%. Moreover, it demands a very short reaction time (1h) at a temperature of about 60°C. It is highly economic and being environmentally benign it has high future developmental potential for both industrial and chemical faction (Scheme 75) [77].



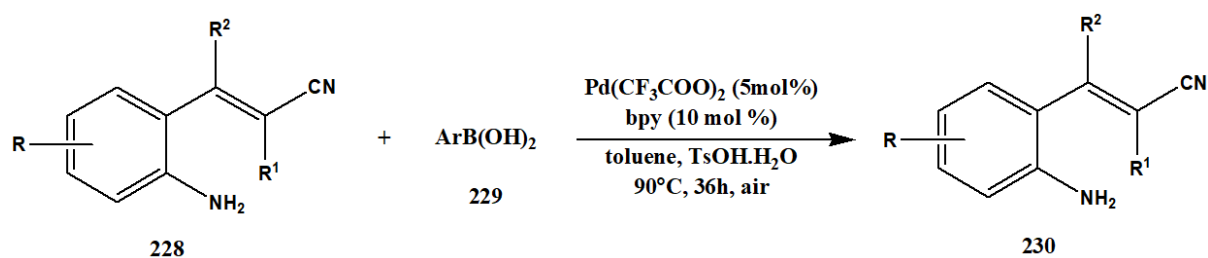
Scheme 75

Contd.

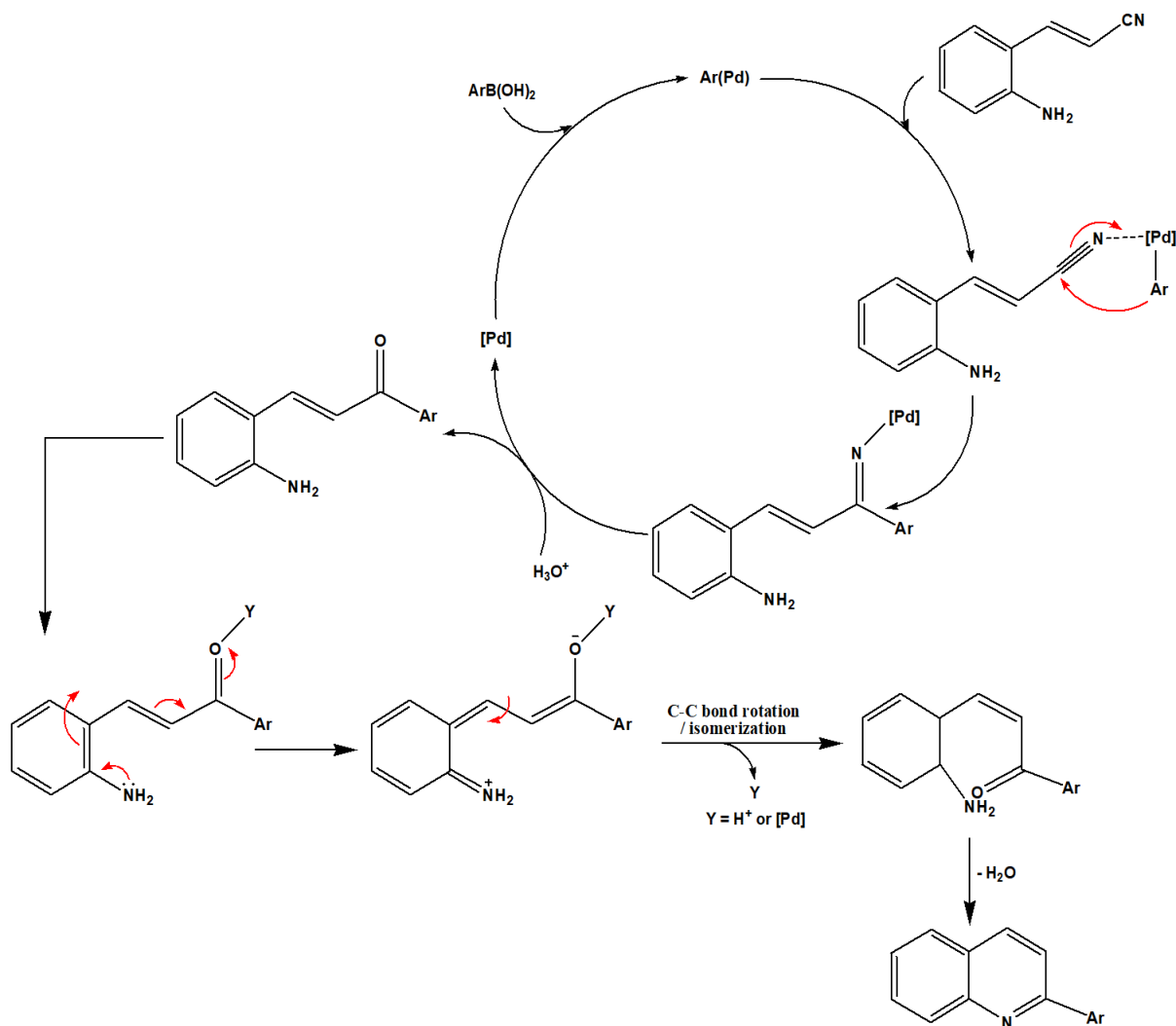


### Possible Reaction Pathway for Scheme 75

Xu et al. reported a novel tandem reaction using 2-aminostyryl nitriles **228** and arylboronic acids **229** and palladium as the catalyst to generate 2-arylquinolines **230** with excellent yield and high tolerance for a variety of functional groups. The synthesis provides an advantage of easy upscaling to gram quantities and offers a new pathway in comparison to the existing condensation reactions. Mechanistic studies suggested that the synthesis involves the nucleophilic addition of the aryl palladium species to the corresponding nitrile to yield the aryl ketone intermediate which subsequently undergoes intramolecular cyclization and dehydration to generate the quinoline ring (Scheme 76) [78].



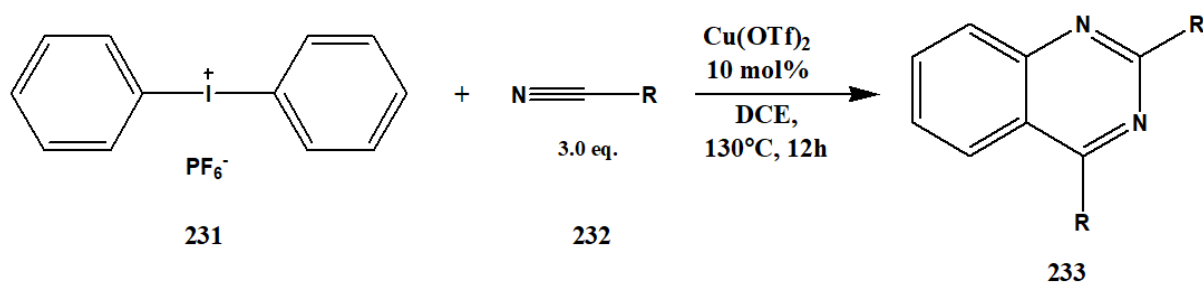
Scheme 76



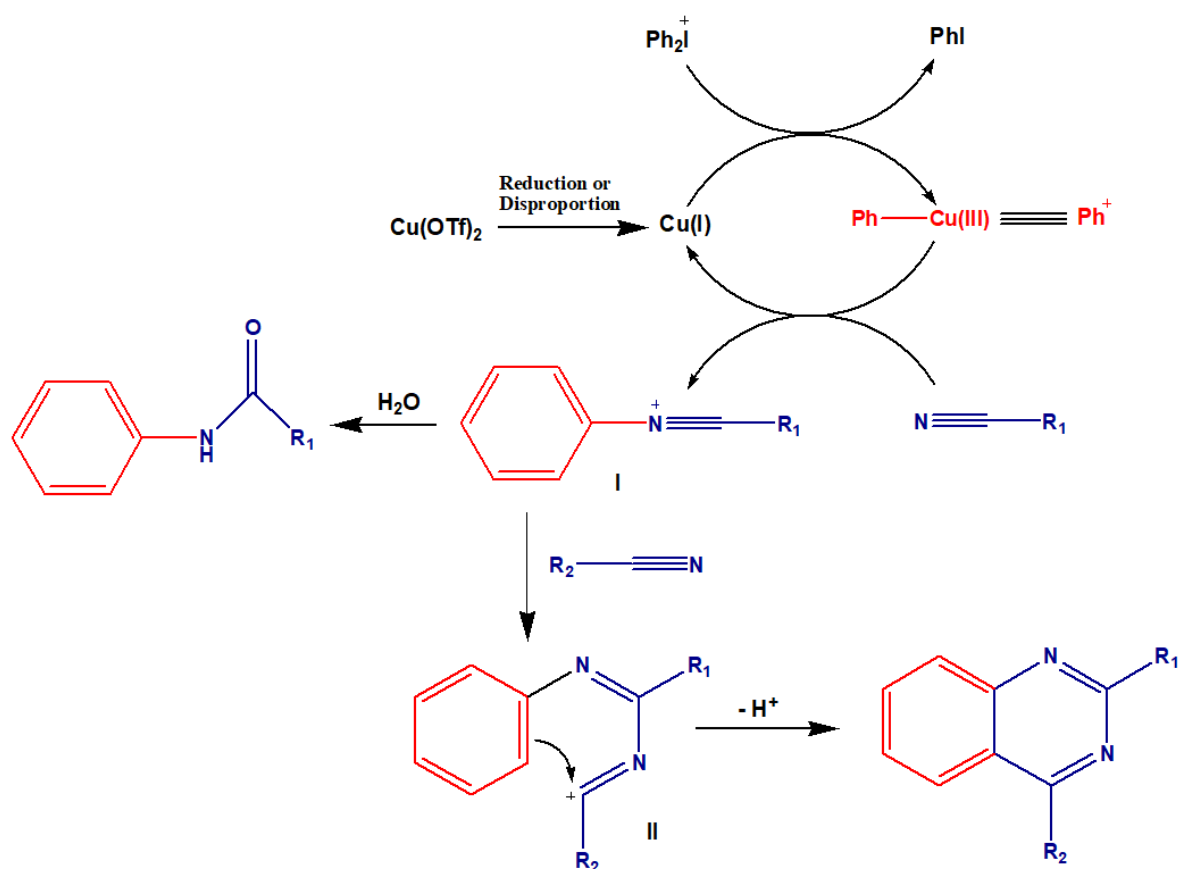
Possible Reaction Pathway for Scheme 76

### 6.3 Quinazoline and its derivatives

Su et al. devised an efficient one-pot synthesis of polysubstituted quinazolines **233** using diaryliodonium salts **231** and two nitriles **232**. The synthesis proceeds via a [2+2+2] cascade annulation reaction and offers high flexibility in substitution. Moreover, one can use two different nitriles to yield a regioselective product. This facile synthetic pathway lays the foundation to the generation of a quinazolines' library (Scheme 77) [79].

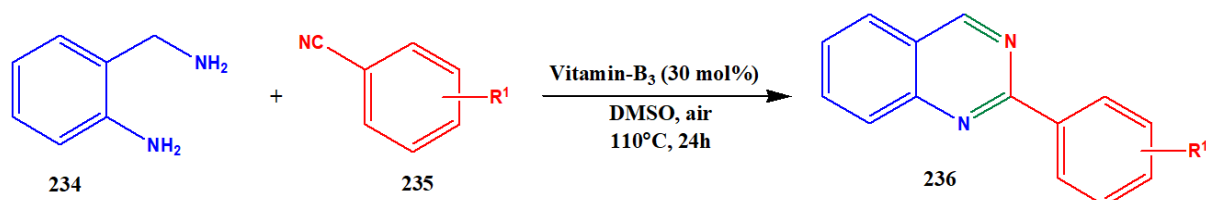


Scheme 77

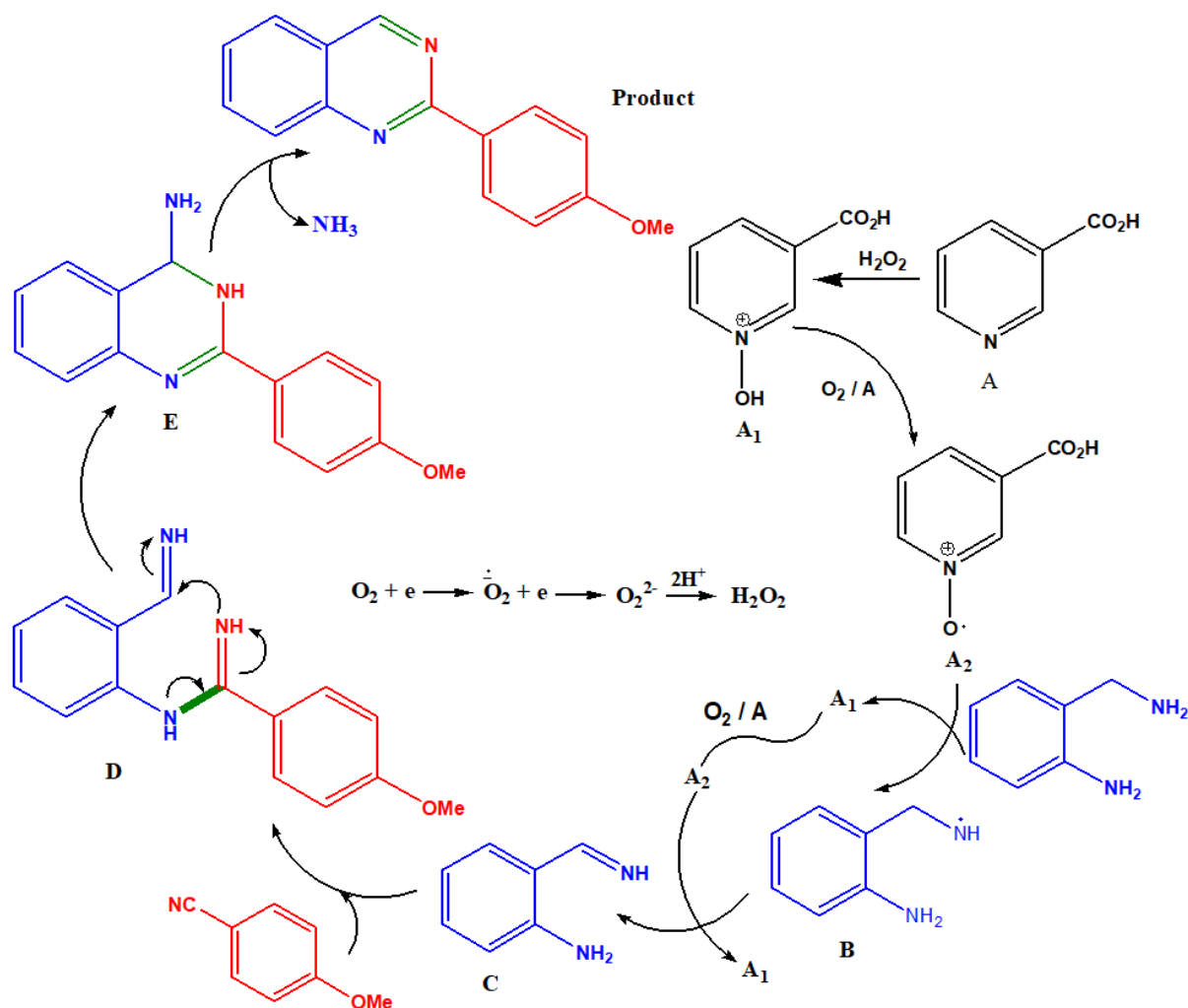


Possible Reaction Pathway for Scheme 77

Gujjarappa et al. reported an efficient and cost-efficient synthesis of substituted quinazolines **236** in high yields from 2-aminobenzylamines **234** and nitriles **235** that uses niacin (vitamin-B<sub>3</sub>) as a potent organocatalyst and nitriles as the source of the C–N bond. This methodology is pertinent to a wide variety of nitriles and 2-aminobenzylamines and also offers high tolerance to a range of functionalities (Scheme 78) [80].



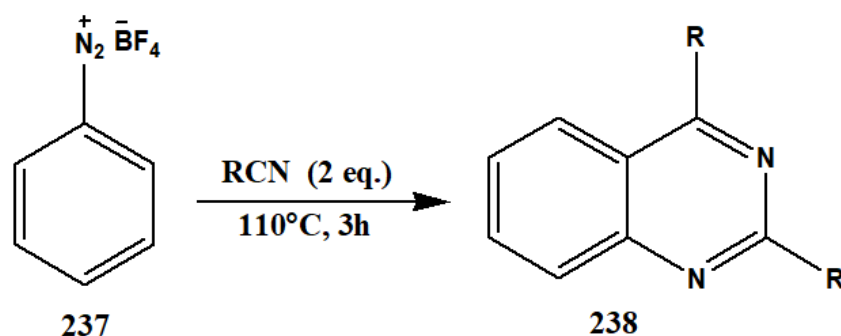
Scheme 78



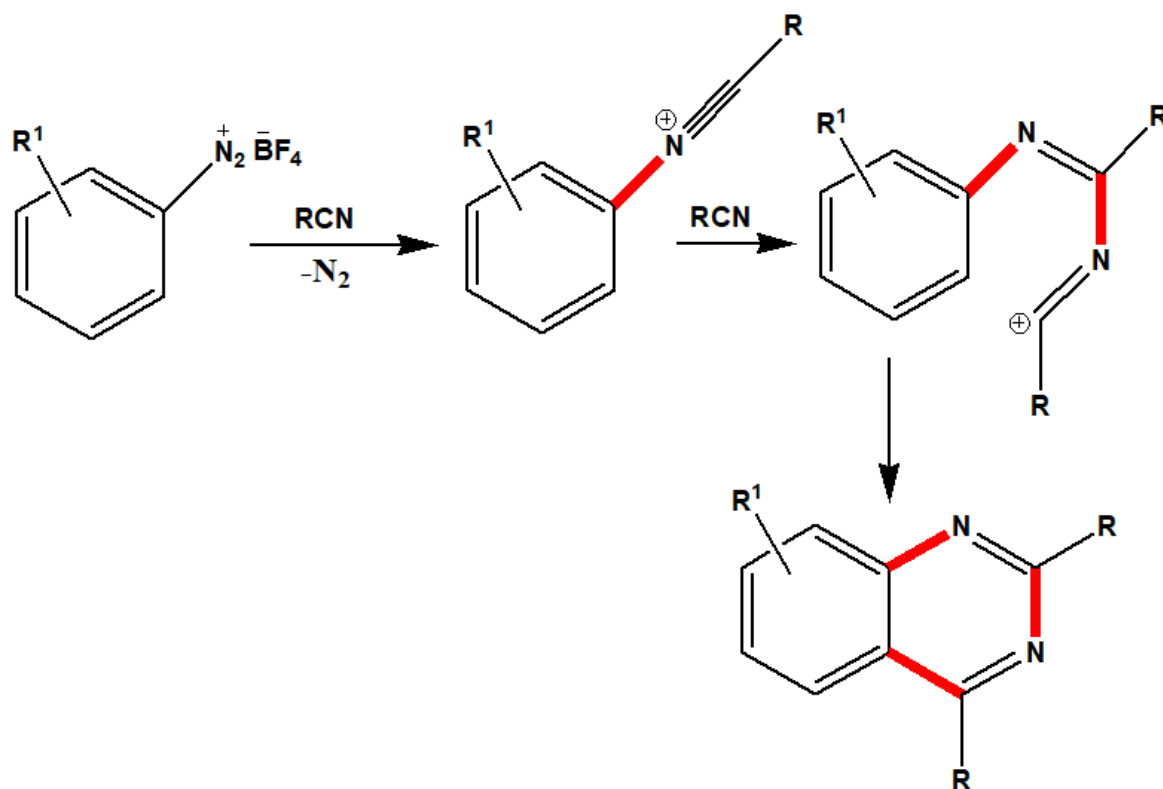
Possible Reaction Pathway for Scheme 78



Ramanathan and Liu developed a preparative scheme to produce polysubstituted quinazolines **238** using aryldiazonium salts **237** and two equivalent of nitriles. It involves a [2+2+2] annulation reaction that proceeds with the initial formation of the reactive nitrilium ion which is then attacked by the second nitrile molecule. The resulting species then undergoes electrophilic cyclization to yield the product. The synthesis uses readily available substrates and requires a short reaction duration and can be used in gram-scale synthesis. Additionally, it exhibits significant flexibility in substitution and proceeds via a transition metal-free pathway (Scheme 79) [81].



Scheme 79



Possible Reaction Pathway for Scheme 79

## 7. Conclusion

Nitriles have exhibited their supreme importance in the synthesis of heterocyclic compounds having varying heteroatoms and ring sizes. Many of these heterocycles hold important positions in the discovery of biologically active compounds and also have numerous applications in many different fields. This review mainly focusses on summarizing the available synthetic pathways involving nitriles for the generation of numerous heterocyclic compounds with great efficiency, high yields, innovative reaction pathways etc.

This field of study is highly extensive and demands even higher attention and exploration. Most of the synthetic pathways mentioned in this review is accompanied by a plausible reaction pathway, however, some others remain undescribed and are under further studies. The greatest advantage of the present study is that it paves a way for a relatively cost-effective way of heterocycle synthesis as nitriles are analogously easily synthesized. However, care must be taken while handling nitriles during synthesis as exposure to them may cause several hepatic issues which includes bile duct hyperplasia, megalocytosis and fibrosis etc.

## 8. Reference

1. Elgazwy, A.S.S.H. and Refaee, M.R.M. The chemistry of alkenyl nitriles and its utility in heterocyclic synthesis. *Org. Chem. Curr. Res.* **2013**, 2: 117.
2. Mowry, D.T. The preparation of nitriles. *Chem.Rev.* **1948**, 42(2): 189-283.
3. Friedman, L. and Shechter, H. Preparation of nitriles from halides and sodium cyanide. An advantageous nucleophilic displacement in dimethyl sulfoxide. *J. Org. Chem.* **1960**, 25(6): 877-879.
4. Martin, A. and Kalevaru, V.N. Heterogeneously catalyzed ammoxidation: A valuable tool for one-step synthesis of nitriles. *Chem. Cat. Chem.* **2010**, 2: 504-1522.
5. Narsaiah, A.V. and Nagaiah, K. An efficient and improved method for the preparation of nitriles from primary amides and aldoximes. *Adv. Synth. Catal.* **2004**, 346: 1271-1274.
6. Wang, E.C., Huang, K.S., Chen, H.M., Wu, C.C. and Lin, G.J. An efficient method for the preparation of nitriles via the dehydration of aldoximes with phthalic anhydride. *J. Chin. Chem. Soc.* **2004**, 51: 619-627.
7. Alcaraz, G., Wecker, U., baceiredo, A., Dahan, F. and Betrand, G. Synthesis of a 2H-Azirine by [1+2] cycloaddition of a phosphinocarbene with a nitrile and its ring-expansion to a 1,2λ<sup>5</sup>-Azaphosphete. *Angew. Chem. Int. Ed. Engl.* **1995**, 34(11): 1246-1248.
8. König, H., Metzger, H. and Seelert, K. Reactions of dimethyl-oxo-sulfonium methylide with azomethines, azines, hydrazones and nitriles. *Chem. Ber.* **1965**, 98(11): 3724-3732.
9. Bunescu, A., Wang, Q. and Zhu, J. Synthesis of functionalized epoxides by copper-catalyzed alkylative epoxidation of allylic alcohols with alkyl nitriles. *Org. Lett.* **2015**, 17: 1890-1893.

10. Mahmoud, M.R., Madkour, H.M.F., El-Bordany, E.A. and Soliman, E.A. Activated nitriles with ammonium benzyldithiocarbamate, synthesis of thietane derivatives. *Phosphorus Sulfur Silicon Relat. Elem.*, **2009**, 184: 156-163.
11. Senter, T.J., O'Reilly, M.C., Chong, K.M., Sulikowski, G.A. and Lindsley, C.W. A general, enantioselective synthesis of N-alkyl terminal aziridines and C2-functionalized azetidines via organocatalysis. *Tetrahedron Lett.* **2015**, 56: 1276-1279.
12. Guchhait, S.K., Sisodiya, S., Saini, M., Shah, Y.V., Kumar, G., Daniel, D.P., Hura, N. and Chaudhary, V. Synthesis of polyfunctionalized pyrroles via a tandem reaction of Michael addition and intramolecular cyanide-mediated nitrile-to-nitrile condensation. *J.Org. Chem.* **2018**, 83: 5807-5815.
13. Moss, T.A. and Nowak, T. Synthesis of 2,3-dicarbonylated pyrroles and furans via the three-component Hantzsch reaction. *Tetrahedron Lett.*, **2012**, 53: 3056-3060.
14. Wang, K. and Dömling, A. Design of a versatile multicomponent reaction leading to 2-amino-5-ketoaryl pyrroles. *Chem. Biol. Drug Des.* **2010**, 75: 277-283.
15. Das, P., Ray, S. and Mukhopadhyay, C. Exploitation of dual character of CN moiety in the synthesis of uniquely decorated 3H-pyrroles: A rare observation. *Org. Lett.* **2013**, 15(22): 5622-5623.
16. Zhao, M.N., Liang, H., Ren, Z.H. and Guan, Z.H. Iron-catalyzed tandem one-pot addition and cyclization of the Blaise reaction intermediate and nitroolefins: Synthesis of substituted NH-pyrroles from nitriles. *Adv. Synth. Catal.* **2013**, 355: 221-226.
17. Feng, X., Wang, Q., Lin, W., Dou, G.L., Huang, Z.B. and Shi, D.Q. Highly efficient synthesis of polysubstituted pyrroles via four-component domino reaction. *Org. Lett.* **2013**, 15(10): 2542-2545.
18. Rao, H.S.P. and Desai, A. Zinc and trimethylsilyl chloride mediated synthesis of 2,3,5-trisubstituted pyrrole diesters from nitriles and ethyl bromoacetate. *Synlett.* **2014**, 26: A-D.

19. Chen, J., Li, C., Zhou, Y., Sun, C. and Sun, T. An efficient, scalable and eco-friendly synthesis of 4,5-substituted pyrrole-3-carbonitriles by intramolecular annulation on Pd/C and HZSM-5. *Chem.Cat.Chem.* **2019**, 11(7): 1943-1948.
20. Zhou, Y., Zhou, L., Jesikiewicz, L.T., Liu, P. and Buchwald, S.L. Synthesis of pyrroles through the CuH-catalyzed coupling of enynes and nitriles. *J. Am. Chem. Soc.* **2020**, 142(22): 9908-9914.
21. Pagadala, R. and Anugu, S. Synthesis of polyfunctionalized pyrroles via green chemical methods. *J. Heterocycl. Chem.* **2017**, 55(1): 181-186.
22. Sabnis, R.W., Rangnekar, D.W. and Sonawane, N.D. 2-Aminothiophenes by the Gewald reaction. *J. Heterocyclic Chem.* **1999**, 36: 333-345.
23. Elgazwy, A.S.S.H. and Refaee, M.R.M. The chemistry of alkenyl nitriles and its utility in heterocyclic synthesis. *Organic Chem. Curr. Res.* **2013**, 2(2): 117.
24. Middleton, W.J., Engelhardt, V.A. and Fisher, B.S. Cyanocarbon chemistry VIII. Heterocyclic compounds from tetracyanoethylene. *J. Amer. Chem. Soc.* **1957**, 80: 2822-2829.
25. Kandeel, Z.E.S. Nitriles in heterocyclic synthesis: A novel synthesis of some thieno[2,3-d]pyrimidine and thieno[2,3-b]pyridine derivatives. *Heteroat. Chem.* **1996**, 7(1): 29-33.
26. Abdelrazek, F.M. and Ead, H. Heterocyclic synthesis with nitriles: A new approach to thiophene and thieno-[2,3-d]-pyrimidine derivatives. *J. Prakt. Chem.* **1988**, 330(4): 585-589.
27. Volovenko, Y.M. and Volovenko, T.A. New method of synthesis of 2-Amino-4(5H)-Oxothiophenes. *Chem. Heterocycl. Compd.* **2005**, 41(2): 173-176.
28. Elgazwy, A.S.S.H. and Refaee, M.R.M. The chemistry of alkenyl nitriles and its utility in heterocyclic synthesis. *Organic Chem. Curr. Res.* **2013**, 2(2): 117.

29. Lambu, M.R. and Judeh, Z.M.A. Efficient, one-step, cascade synthesis of densely functionalized furan from unprotected carbohydrates in basic aqueous media. *Green Chem.* **2019**, 21: 821-829.
30. Wang, X., Liu, M., Xu, L., Wang, Q., Chen, J., Ding, J. and Wu, H. Palladium-catalyzed addition of potassium aryltrifluoroborates to aliphatic nitriles: Synthesis of alkyl aryl ketones, diketone compounds, and 2-arylbenzo[b]furans. *J. Org. Chem.* **2013**, 78(11): 5273-5281.
31. Komogortsev, A.N., Melekhina, V.G., Lichitsky, B.V. and Minyaev, M.E. Novel one-pot approach to 2-aminofuran derivatives via multicomponent reaction of 3-hydroxy-4H-pyran-4-ones,  $\alpha$ -ketoaldehydes and methylene active nitriles. *Tetrahedron Lett.* **2020**, 61: 152384.
32. Shoji, T., Nagai, D., Tanaka, M., Araki, T., Ohta, A., Sekiguchi, R., Ito, S., Mori, S. and Okujima T. Synthesis of 2-aminofurans by sequential [2+2] cycloaddition-nucleophilic addition of 2-propyn-1-ols with tetracyanoethylene and amine-induced transformation to 6-aminopentafulvenes. *Chem. Eur. J.* **2017**, 10.1002.
33. Das, U.K., Shimon, L.J.W. and Milstein, D. Imidazole synthesis by transition metal free, base-mediated deaminative coupling of benzylamines and nitriles. *Chem. Commun.* **2017**, 53: 13133-13136.
34. Yang, D., Shan, L., Xu, Z.F. and Li, C.Y. Metal-free synthesis of imidazole by  $\text{BF}_3 \cdot \text{Et}_2\text{O}$  promoted denitrogenative transannulation of N-sulfonyl-1,2,3-triazole. *Org. Biomol. Chem.* **2018**, 16: 1461-1464.
35. Garcia, J.J., Silva, P.Z., Rios, G.R., Crestani, M.G., Arévalo, A. and Francisco, R.B. One-pot synthesis of imidazoles from aromatic nitriles with nickel catalyst. *Chem. Commun.* **2011**, 47: 10121-10123.
36. Wang, Q., Chen, X., Wang, X.G., Liu, H.C. and Liang, Y.M. Base-promoted nitrile-alkyne domino-type cyclization: A general method to trisubstituted imidazoles. *Org. Lett.* **2019**, 21(24): 9874-9877.

37. Horneff, T., Chuprakov, S., Chernyak, N., Gevorgyan, V. and fokin, V.V. Rhodium-catalyzed transannulation of 1,2,3-triazoles with nitriles. *J. Am. Chem. Soc.* **2008**, 130: 14972-14974.
38. Harisha, M.B., Dhanalakshmi, P., Suresh, R., Kumar, R.R., Muthusubramanian, S. and Bhuvanesh, N. TMSOTf-catalyzed synthesis of 2,4,5-trisubstituted imidazoles from vinyl azides and nitriles. *Chemistry Select.* **2019**, 4: 2954-2958.
39. Pearce, A.J., Harkins, R.P., Reiner, B.R., Wotal, A.C., Dundcomb, R.J. and Tonks, I.A. Multicomponent pyrazole synthesis from alkynes, nitriles, and titanium imido complexes via oxidatively induced N–N bond coupling. *J. Am. Chem. Soc.* **2020**, 142: 4390-4399.
40. Chen, B., Zhu, C., Tang, Y. and Ma, S. Copper-mediated pyrazole synthesis from 2,3-allenoates or 2-alkynoates, amines and nitriles. *Chem. Commun.* **2014**, 50: 7677-7679.
41. Jang, S.S., Chang, J.Y., Kang, G.Y. and Youn, S.W. Oxidant-controlled divergent syntheses of pyrazoles and pyrroles by copper(I)-catalyzed oxidative coupling of  $\beta$ -enamino esters. *Asian J. Org. Chem.* **2019**, 8: 1-7.
42. Suri, M., Jousseume, T., Neumann, J.J. and Glorius, F. An efficient copper-catalyzed formation of highly substituted pyrazoles using molecular oxygen as the oxidant. *Green Chem.* **2012**, 14: 2193-2196.
43. Hori, M., Nogi, K., Nagaki, A. and Yorimitsu, H. Annulative synthesis of thiazoles and oxazoles from alkenyl sulfoxides and nitriles via additive Pummerer reaction. *Asian J. Org. Chem.* **2019**, 8(7): 1084-1087.
44. Johnson, F. and Nasutavicus, W.A. Polyfunctional Aliphatic Compounds. IV. The cyclization of nitriles by halogen acids: A new synthesis of thiazoles. *J. Org. Chem.* **1963**, 28(7): 1877-1883.
45. Doyle, K.J. and Moody, C.J. Diazo-sulfones and nitriles in oxazole synthesis; three step preparation of a bis-oxazole. *Tetrahedron Lett.* **1992**, 33(50): 7769-7770.

46. Li, X., Huang, L., Chen, H., Wu, Q., Huang, H. and Jiang, H. Copper-catalyzed oxidative [2+2+1] cycloaddition: regioselective synthesis of 1,3-oxazoles from internal alkynes and nitriles. *Chem. Sci.* **2012**, 3: 3463-3467.
47. Zhang, D., Song, H., Cheng, N. and Liao, W.W. Synthesis of 2,4,5-trisubstituted oxazoles via Pd-catalyzed C–H addition to nitriles/cyclization sequences. *Org. Lett.* **2019**, 21(8): 2745-2749.
48. Saito, A., Hyodo, N. and Hanzawa, Y. Synthesis of highly substituted oxazoles through Iodine(III)-mediated reactions of ketones with nitriles. *Molecules* **2012**, 17: 11046-11055.
49. Hori, M., Nogi, K., Nagaki, A. and Yorimitsu, H. Annulative synthesis of thiazoles and oxazoles from alkenyl sulfoxides and nitriles via additive Pummerer reaction. *Asian J. Org. Chem.* **2019**, 8(7): 1084-1087.
50. Wang, L.Y., Tsai, H.J., Lin, H.V., Kaneko, K., Cheng, F.Y., Shih, H.S., Wong, F.F. and Huang, J.J. One-flask synthesis of 1,3,5-trisubstituted 1,2,4-triazoles from nitriles and hydrazonoyl chlorides via 1,3-dipolar cycloaddition. *RSC Adv.* **2014**, 4: 14215-14220.
51. Xu, H., Ma, S., Xu, Y., Bian, L., Ding, T., Fang, X., Zhang, W. and Ren, Y. Copper-catalyzed one-pot synthesis of 1,2,4-triazoles from nitriles and hydroxylamine. *J. Org. chem.* **2015**, 80(3): 1789-1794.
52. Demko, Z.P. and Sharpless, K. B. Preparation of 5-substituted 1H-tetrazoles from nitriles in water. *J. Org. Chem.* **2001**, 66: 7945-7950.
53. Koguro, K., Oga, T., Mitsui, S. and Orita, R. Novel synthesis of 5-substituted tetrazoles from nitriles. *Synthesis.* **1998**, 6: 910-914.
54. Chai, L., Xu, Y., Ding, T., Fang, X., Zhang, W., Wang, Y., Lu, M., Xu, H. and Yang, X. *Org. Biomol. Chem.* **2017**, 15: 8410-8417.
55. Noei, J. and Khosropour, A.R. A novel process for the synthesis of 3,5-diaryl-1,2,4-thiadiazoles from aryl nitriles. *Tetrahedron Lett.* **2013**, 54: 9-11.



56. Elagamey, A.G.A., Sawllim, S.Z., El-Taweel, F.M.A. and Elnagdi, M.H. Nitriles in heterocyclic synthesis: Novel syntheses of benzo[b]pyrans, naphtho[1,2-b]pyrans, naphtho[2,1-b]-pyrans, pyrano[3,2-h]quinolines and pyrano[3,2-c]quinolines. *Collect. Czech. Chem. Commun.* **1988**, 53: 1534-1538.
57. Shaabani, A., Samadi, S. and Rahmati, A. One-pot, three-component condensation reaction in water: An efficient and improved procedure for the synthesis of pyran annulated heterocyclic systems. *Synth. Commun.* **2007**, 37: 491-499.
58. Devi, I. and Bhuyan, P.J. Sodium bromide catalysed one-pot synthesis of tetrahydrobenzo[b]pyrans via a three-component cyclocondensation under microwave irradiation and solvent free conditions. *Tetrahedron Lett.* **2004**, 45: 8625-8627.
59. Honarmand, M., Tzani, A. and Detsi, A. Synthesis of novel multi-OH functionalized ionic liquid and its application as dual catalyst-solvent for the one-pot synthesis 4H-pyrans. *J. Mol. Liq.* **2019**, 290: 111358.
60. Varela, J.A., Castedo, L. and Saá, C. Scope of Ru(II)-catalyzed synthesis of pyridines from alkynes and nitriles. *J. Org. Chem.* **2003**, 68: 8595-8598.
61. Sheng, J., Wang, Y., Su, X., He, R. Chen, C. Copper-catalyzed [2+2+2] modular synthesis of multisubstituted pyridines: Alkenylation of nitriles with vinylidonium salts. *Angew. Chem. Int. Ed.* **2017**, 56: 1-6.
62. Cioni, P., Diversi, P., Ingrosso, G., Lucherini, A. and Ronce, P. Rhodium-catalyzed synthesis of pyridines from alkynes and nitriles. *J. Mol. Catal.* **1987**, 40: 337-357.
63. Kase, K., Goswami, A., Ohtaki, K., Tanabe, E., Saino, N. and Okamoto, S. On-demand generation of an efficient catalyst for pyridine formation from unactivated nitriles and  $\alpha,\omega$ -diynes using  $\text{CoCl}_2 \cdot 6\text{H}_2\text{O}$ , dppe, and Zn. *Org. Lett.* **2007**, 9(5): 931-934.
64. Palacios, F., Retana, A.M.O.D. and Oyarzabal, J. A “one-pot” synthesis of polysubstituted pyridines from metalated alkylphosphonates, nitriles and  $\alpha,\beta$ -unsaturated ketones. *Tetrahedron Lett.* **1996**, 37(26): 4577-4580.

65. Satoh, Y., Yasuda, K. and Obora, Y. Strategy for the synthesis of pyrimidine derivative: NbCl<sub>5</sub>-mediated cycloaddition of alkynes and nitriles. *Organometallics*. **2012**, 31(15): 5235-5238.
66. Su, L., Sun, K., Pan, N., Liu, L., Sun, M., Dong, J., Zhou, Y. and Yin, S.F. Cyclization of ketones with nitriles under base: A general and economical synthesis of pyrimidines. *Org. Lett.* **2018**, 20: 39099-3402.
67. You, X., Yu, S. and Liu, Y. Reactions of zirconocene butadiyne or monoyne complexes with nitriles: Straightforward synthesis of functionalized pyrimidines. *Organometallics*. **2013**, 32(19): 5273-5276.
68. Zhaoxiang, D., Wenfeng, Q., Weijia, L. and Yadong, L. Cyclotrimerization of nitriles catalyzed by Li<sub>3</sub>N. *Chin. Sci. Bull.* **2004**, 49(2): 127-130.
69. Fuji, M. and Obora, Y. FeCl<sub>3</sub>-assisted niobium-catalyzed cycloaddition of nitriles and alkynes: Synthesis of alkyl- and arylpyrimidines base on independent functions of NbCl<sub>5</sub> and FeCl<sub>3</sub> Lewis acid. *Org. Lett.* **2017**, 19: 5569-5572.
70. Khafizova, L.O., Shaibakova, M.G. and Dzhemilev, U.M. A new one-pot synthesis of tetrasubstituted pyrazines by the Ti-catalyzed reaction of aromatic and benzyl-substituted nitriles with EtAlCl<sub>2</sub>. *ChemistrySelect*. **2018**, 3: 11451-11453.
71. Herrera, A., Riano, A., Moreno, R., Caso, B., Pardo, Z.D., Fernández, I., Sáez, E., Molero, D., Vazquez, A.S. and Alvarez, R.M. One-pot synthesis of 1,3,5-triazine derivatives via controlled cross-cyclotrimerization of nitriles. A mechanism approach. *J.Org. Chem.* **2014**, 79(15): 7012-7024.
72. Gong, J., Hu, K., Shao, Y., Li, R., Zhang, Y., Hu, M. and Chen, J. Tandem addition/cyclization for synthesis of 2-aryl benzofurans and 2-aryl indoles by carbopalladation of nitriles. *Org. Biomol. Chem.* **2020**, 18: 488-494.
73. Mao, J., Wang, Z., Xu, X., Liu, G., Jiang, R., Guan, H., Zheng, Z. and Walsh, P.J. Synthesis of indoles through domino reactions of 2-fluorotoluenes and nitriles. *Angew. Chem. Int. Ed.* **2019**, 58(32): 11033-11038.

74. Kim, J.H. and Lee, S.G. Palladium-catalyzed intramolecular trapping of the Blaise reaction intermediate for Tandem one-pot synthesis of indole derivatives. *Org. Lett.* **2011**, 13(6): 1350-1353.
75. Wang, Y., Chen, C., Peng, J. and Li, M. Copper(II)-catalyzed three-component cascade annulation of diaryliodoniums, nitriles, and alkynes: A regioselective synthesis of multiply substituted quinolines. *Angew. Chem. Int. Ed.* **2013**, 52: 1-6.
76. Xie, J., Huang, H., Xu, T., Li, R., Chen, J. and Ye, X. The synthesis of quinolines via denitrogenative palladium-catalyzed cascade reaction of o-aminocinnamitriles with arylhydrazines. *RSC Adv.* **2020**, 10: 8586-8593.
77. Wang, H., Xu, Q., Shen, S. Yu, S. Synthesis of quinolines through three-component cascade annulation of aryl diazonium salts, nitriles, and alkynes. *J. Org. Chem.* **2017**, 82(1): 770-775.
78. Xu, T., Shao, Y., Dai, L., Yo, S., Cheng, T. and Chen, J. Pd-catalyzed tandem reaction of 2-aminostyryl nitriles with arylboronic acids: synthesis of 2-arylquinolines. *J. Org. Chem.* **2019**, 84(21): 13604-13614.
79. Su, X., Chen, C., Wang, Y., Chen, J., Lou, Z. and Li, M. One-pot synthesis of quinazoline derivatives via [2+2+2] cascade annulation of diaryliodonium salts and two nitriles. *Chem. Commun.* **2013**, 49(60): 6752-6754.
80. Gujjarappa, T., Vodnala, N., Reddy, V.G. and Malakar, C.C. Niacin as a potent organocatalyst towards the synthesis of quinazolines using nitriles as C–N source. *Eur. J. Org. Chem.* **2020**, 2020(7): 803-814.
81. Ramanathan, M. and Liu, S.T. Preparation of quinazolines via a 2+2+2 annulation from aryldiazonium salts and nitriles. *J. Org. Chem.* **2017**, 82(15): 8290-8295.

# A LITERATURE REPORT ON “MECHANO-RESPONSIVE METAL COMPLEXES”



Submitted by

Pirbika Engtipi

Roll No. PS-191-808-0078

Registration No. 240354

M.Sc 4th Semester

Department of Chemistry

Gauhati University

Supervised by

Dr. Rupam Jyoti Sarma

Associate Professor

Department Of Chemistry

Gauhati University

# • CONTENTS:

## PAGE NO.

1. Abstract	( 3-4)
2. INTRODUCTION	( 5-6)
3. DIFFERENT TYPES OF MECHANO –RESPONSIVE SYSTEM	
(a). Chemical and Mechano Responsive Metal –Organic Gels Of Bis (benzimidazole) -Based Ligands With Cd(II) and Cu(II) Halide Salts.	( 6-13)
(b). Supercooled liquid beta –diketones with mechano responsive emission	(14- 20)
(c). Mechanoresponsive material of AIE-Active dihydropyrrolo[3,2-b] pyrrole luminophores	(20-26)
(d). Mechanoresponsive materials for drug delivery	(26-27)
4. Conclusion	(28-29)
5. Acknowledgement	30
6. References	( 31-33)

**ABSTRACT:** The pyridine-3,5-bis(benzimidazole-2-yl) ligand (L) with metal salts (Cu(II) or Cd(II)) has been found to gelate several aliphatic alcohols to generate multi functional metal–organic gels(MOGs). The anions of the metal salt were found to play an important role in the gelation property; halides (chlorides or bromides) and sulphates were found to be more effective than other univalent ions such as nitrate, acetate, perchlorate, and tetra fluoro borate. The microscopic investigation with FESEM, TEM, POM, and AFM confirmed the formation of inter winding 3D gel fibrous networks, which have immobilized the large volume of solvent. The coordination of the metal to the ligand L was found to play a vital role in the construction of gel fibers. Rheology studies on the MOGs revealed that these MOGs have significantly high mechanical strengths and therefore exhibit self sustainability. The porous nature of the MOGs has been explored by gas sorption studies; xerogels show the type-III N<sub>2</sub>-sorption isotherm. The MOGs have also shown a tendency as potent dye removal agents. These gels also exhibited thermo irreversibility but mechano reversibility. The sol–gel transformations were observed through applying external chemical stimuli, that is, by adding metal capturing agents.

Shear-induced crystallization of dyes in the amorphous state is an effective strategy for generating higher energy emission after mechanical perturbation—a rare phenomenon in mechanoresponsive materials. Recently, we reported that a  $\beta$ -diketone with a 3,4,5-trimethoxy substituted phenyl ring formed a stable supercooled liquid (SCL) phase after melting and cooling in air. To tune the lifetime of  $\beta$ -diketones in the SCL phase, a series of dyes with 3,4,5-trimethoxysubstituted phenyl rings were synthesized. Derivatives with naphthyl and phenyl rings were prepared in order to modulate crystallization through arene interactions. Additionally, dyes were substituted with alkoxy chains of varying length to promote crystallization through increased van der Waals interactions. Video screening in conjunction with differential scanning calorimetry and X-ray diffraction studies indicated that naphthyl-substituted derivatives exhibited increased melted state life times and that increasing the alkoxy chain length can induce crystallization. Analysis of molecular packing of single crystals of PH, PC1, PC3, and PC5 revealed that the central para-substituted methoxy group of the trimethoxy-substituted ring was forced out of the increasing the alkoxy chain length can induce crystallization. Analysis of molecular packing of single crystals of PH,

PC1, PC3, and PC5 revealed that the central para-substituted methoxy group of the trimethoxy-substituted ring was forced out of the molecular plane because of steric interactions with neighboring methoxy groups.

A new tetraphenylethylene (TPE) functionalized 1,4-dihydropyrrolo[3,2-b]pyrrole derivative (APPTPECN) was synthesized with obvious aggregation-induced emission (AIE) active by simple synthetic method. APPTPECN exhibited reversible mechanofluorochromic (MFC) behavior. The powder X-ray diffraction (PXRD) and scanning electron microscopy (SEM) investigations exhibited that the MFC nature is originated through a conversion from the microcrystalline to amorphous phase under the stimulus of external force. The results obtained would be of major help in understanding the MFC mechanism and designing new MFC materials. Compound APPTPECN has the potential possibility to employ in rewritable data storage and is of assistance in the rational design of smart luminescent materials.

Mechanically –activated delivery systems harness existing physiological and / or externally applied forces to provide spatiotemporal control over the release of active agents .Current strategies to deliver therapeutic proteins and drugs use three types of mechanical stimuli: compression, tension and shear. Shear –activated systems are based on nano assemblies or micro aggregates that respond to and withstand cyclic compressive loading wherease, tension–responsive system use composite to compartmentalize payloads

## Introduction:

Supramolecular self assembly of small molecules has been established as an active area of research and in the past few years by using the phenomena, many successful synthesis of new materials with a very wide range of functional properties have been reported. In particular, an exponential growth has been observed in the synthesis of materials, which can capture various solvents by gelation due to the inherent self-assembling nature of low molecular weight organic gelator (LMOGs) molecules. The supramolecular gels have a wide range of diverse applications such as foods, drug delivery, optical devices, cosmetics, tissue engineering, cleaning agent, and wastewater treatment. The non covalent forces such as electrostatic, van der Waals, hydrophobic, hydrogen bonding, and  $\pi$ - $\pi$  stacking interactions play a major role in assembling LMOGs to form three-dimensional (3D) gel networks. The supramolecular gels were found to be very responsive for a wide range of external stimuli such as pH, addition of salts, sonication, shearing and irradiation by light.

Fluorescent mechanofluorochromic (MFC) is a phenomenon where solid and liquid crystalline materials change their photoluminescence properties upon applying mechanical stimulation, such as grinding, ball-milling, and crushing. Fluorescence emission and color change could often recover by another stimulation or more, such as heating, organic solvent vapor, and light. Mechanofluorochromic materials as a kind of “smart material” have its potential applications in mechanosensors, fluorescence switches, and data storage soon. Recently, rationally controlling the design of molecular mechanofluorochromic behavior is still a huge challenging, two main problems restrict the development of this kind of materials: the lack of deep understanding for the structure-property relationship of such materials and the fluorescent quenching effect in the solid state. It is exciting that a major breakthrough came from an unusual aggregation-induced emission (AIE) phenomenon in the study of 1-methyl-1,2,3,4,5-pentaphenylsilole. Since then, AIE concept has been extensively used to design efficient solid-state fluorescent materials and MFC materials because of highly twisted backbone structures bearing rotatable units. Also, the twisted molecular conformations which not only enable them to emit strong fluorescence in the aggregated state by weakening intermolecular close stacking and intense  $\pi$ - $\pi$  interactions, but also easily lead to the formation of MFC properties by changing the molecular packing modes upon pressure. In order to obtain excellent MFC materials with strong fluorescence emission in the solid state and aggregated state, an artful design of the molecule was important for tuning molecular MFC properties. Typically, 1,4-dihydropyrrolo[3,2-b]pyrroles (PPs), a class of 10  $\pi$ -electron aromatic dihydro heteropentalenes, were discovered by Hemetsberger and Knittel in 1972. Importantly, Gryko and co-workers developed a one-step synthetic method to acquire tetraaryl-pyrrolo[3,2-b]pyrroles in 2013. Moreover, these compounds have received increasing attention because PPs have a lot of advantages including high thermal, photostability, good absorptivity, bright fluorescence and high quantum yields. Meanwhile, molecules and the modifications of TPE have been proved an efficient



way to construct new aggregation-induced emission (AIE) luminogens with high solid-state efficiency.

Luminescent materials that exhibit color changes in response to mechanical stimuli are desirable for a variety of applications including security inks, force sensors, and optical storage devices. Most of these mechanochromic luminescent (ML) materials exhibit shifts toward lower energy wavelengths after mechanical perturbation because of crystalline-to-amorphous phase transitions. In other cases, color changes are produced by mechanically generated transitions between different crystalline polymorphs.<sup>8,9</sup> For example, Ito et al. have shown that arene-substituted gold complexes can undergo crystal-to-crystal transitions with tunable emission through donor and acceptor substitution.<sup>10</sup> Systems such as these benefit from the fact that single crystal analysis can be used to probe both initial and post smearing states.

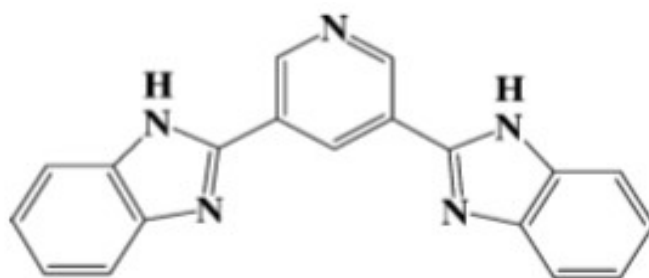
The delivery of therapeutic agents to a specific location with optimal dose and duration remains a significant clinical challenge. This multifaceted problem is being investigated using a myriad of drug delivery strategies because of systemic drug administration although widely used in clinic typically requires multiple doses to treat diseased tissue. However, this leads to significant and widespread off target side effects due to exposure of healthy tissue. Stimuli responsive materials are well suited for application in drug delivery, actively releasing their drug payloads in response to either physiological or externally applied triggers. There are relatively few reports of mechanoresponsive drug delivery systems; they cover the breadth of mechanical forces: compression, tension and shear.

## 2. DIFFERENT TYPES OF MECHANO-RESPONSIVE KNOWN:

(a). Chemical and mechano responsive metal-organic gels of Bis (benzimidazole)-based ligands with Cd(II) and Cu(II) Halide salts:

The molecules containing pyridyl bis (urea), terpyridyl, or bis (benzimidazole) moieties have been explored for their gelation properties with metal salts. For example, the pyridyl bis(urea)-based ligand has been shown to form a shear induced metal-organic gel with Cu(II) bromide salt. The terpyridyl-based ligands have been effectively shown to form gels with platinum salts, and their photo physical properties were investigated. Further, electronic absorption and luminescent properties of gels of alkyl platinum(II) complexes of tridentate bis (N-alkylbenzimidazole-2'-yl) pyridine have also been well demonstrated. The catalytic activity of imidazole-based gels has also been explored recently. In very few cases, gas adsorption and dye adsorption phenomena have also been studied with gel materials. In all these MOGs, the N-containing unit of gelator molecule plays a crucial role in the formation of gel. Although the research in the field of gels is growing enormously, the rational design of gelator molecules is still elusive.

In the laboratory, it has designed and synthesized the pyridine-3,5-bis(benzimidazole-2-yl) molecule (L) to explore its potential to form MOFs with various metal salts. However, it is surprise, to found that this molecule has an excellent capability to form gels with various metal halide salts in alcohols. The molecule L was chosen due to the following reasons that promote the self assembly process : (1) it is coplanar with V shape geometry and contains only aromatic moieties; (2) multiple the self assembly process : (1) it is coplanar with V shape geometry and contains only aromatic moieties; (2) multiple coordination sites with possibility of 6 symmetry ;(3) in addition to three N-atoms for coordination ,it also contain two imine – NH groups for aggregation of molecules through hydrogen bonding interactions ; (4) and lastly, the extended n backbone of ligand L might be of great use in the supra molecular of self–aggregation process.



Scheme1.Molecular Structure of Pyridine-3,5 bis(benzimidazole-2-yl) (L)

Here, in this article, we would like to present the gelation properties of L with copper(II) and cadmium(II) halide salts in alcohols and their characterizations by various microscopic and spectroscopic techniques. The gelation was observed even in the presence of low concentration of the metal salt with respect to the ligand that is at a 0.1:1.0 ratio of metal salt and L. The gelation capacity was found to increase with the increase of metal concentration that is up to a 1:2 ratio of metal to ligand and remains constant for a further increase in metal salt.

The halide ions as counterions were chosen for this study due to their ability to form metal clusters via halide bridges.<sup>9</sup> Indeed, our results suggest that the halide ions have higher propensity to form gels with L in MeOH compared to the other anions such as  $\text{NO}_3^-$ ,  $\text{I}^-$ ,  $\text{OAc}^-$ ,  $\text{ClO}_4^-$ , and  $\text{BF}_4^-$ . The  $\text{SO}_4^{2-}$  salts of Cu(II) have also been explored in the gel formation with L and found that they form gels but that the formation ability differs from those of halides salts. In this article, the role of anions informing the MOGs, effect of various external chemical stimuli on MOGs, mechanical strength of these gels, dye and gas sorptionability, and self-sustainability of MOGs will be addressed in detail. The ligand L was synthesized by a condensation reaction of o-phenylene diamine and pyridine-3,5-dicarboxylic acid in the presence of polyphosphoric acid. The divalent transition metals such as Cu(II) and Cd(II) halide salts have been chosen for the gelation studies. For a typical gel formation reaction ,a certain amount of the ligand L was dissolved in a specific amount of MeOH in several vials .To these vials ,methanol solutions of metal (II) salt with varied concentrations from 0.1 to 1.0

equiv with respect to the ligand have been added such that the total volume is 2 mL in each vials. The vials were closed with a screw cap and left at room temperature. The gelation was found to occur in most of the cases instantly or in less than two minutes (except for  $\text{CuCl}_2$  gel, which takes  $\sim 2\text{h}$ ).

In the case of  $\text{CuBr}_2$  gel (MOG-1), 1mL MeOH solutions containing 10mg (0.03 mmol) of ligand L have been prepared in ten different glass vials. To this solution, 1mL methanol solutions of  $\text{CuBr}_2$  containing different concentrations, 0.1 to 1.0 equiv with respect to L, have been added and mixed thoroughly. Almost instantly, a yellow colored thick gel was formed from the vials that contain 0.2 to 1.0 equiv of metal salt. The formation of gel was confirmed by the inverted vial method (Figure1). The vial containing 0.1 equiv of  $\text{CuBr}_2$  has the same appearance but is not strong enough to hold in the inverted vial.

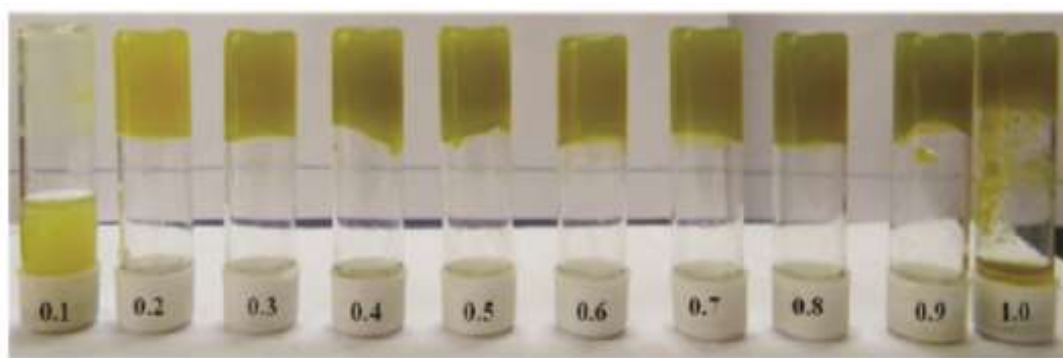


Figure1. Snapshots of inverted vials of  $\text{CuBr}_2$  gel (MOG-1). Numbers on the cap indicates the equivalents of metal salt with respect to L present in the respective vial

However, green and white colored metallo gels have been produced when the above reactions were carried out with  $\text{CuCl}_2$  (MOG-2, Figure S1, Supporting Information) and  $\text{CdBr}_2$  (MOG-3, Figure S2, Supporting Information) or  $\text{CdCl}_2$  (MOG-4, Figure S3, Supporting Information), respectively.

. For MOG-2, the gelation occurs from 0.3 equiv onward, whereas, the vials containing 0.1 and 0.2 equiv of metal salts produced weak gel-like materials. Similar to MOG-1, MOG-3 also forms good gels in the vials containing 0.2 equiv or more. In the case of MOG-4, interestingly, the gelation occurred with as low as 0.1 equiv of metal salt itself. This clearly indicates the high gelation tendency of  $\text{CdCl}_2$  with the ligand L even at very low concentration. Further, the increase in the equivalents of metal (0.1 to 0.5 equiv) with respect to ligand (1 equiv) was found to increase the gelation capacity rapidly from 2 to 6 mL. For example, in the case of MOG-1, the vial that has only 0.2 equiv of metal salt can hold a maximum of 2mL of MeOH, whereas the vial that has 0.5 equiv metal salt can hold a maximum of 6 mL of MeOH. No significant increase in gelation capacity was observed by further increasing the metal equivalents. In the case of MOG-1 and MOG-3, 0.1 equiv of metal salt with respect to L seems to be insufficient to form a stable gel as we observed that

even the use of a less amount methanol (total 1 mL) could not yield the stable gel. All the MOGs were found to be stable for several months at room temperature. These MOGs can be synthesized in bulk scale in similar manner. The gels found to be thermo irreversible as it was evidenced by the fact that the heating of the gels up to 90–95 °C neither changed its appearance nor leaked any solvent. Notably, the reversibility of the gelation process was found to occur through mechanical stimuli as the gels exhibit thixotropic behavior. For example, shaking of the vial containing gel for 2 min turns the gels into free-flowing liquids, which take 15–20 h to reform the gel depending on the nature of the materials (Figure 2). Generally, the gel reformation time was found to depend on the amount of metal salt along with the gelator molecule present in the system. For instance, in the case of MOG-1, the reformation time was 15 h when the vial contains 0.3 equiv metal, but it was 6 h when the vial contains 1 equiv of metal salt.

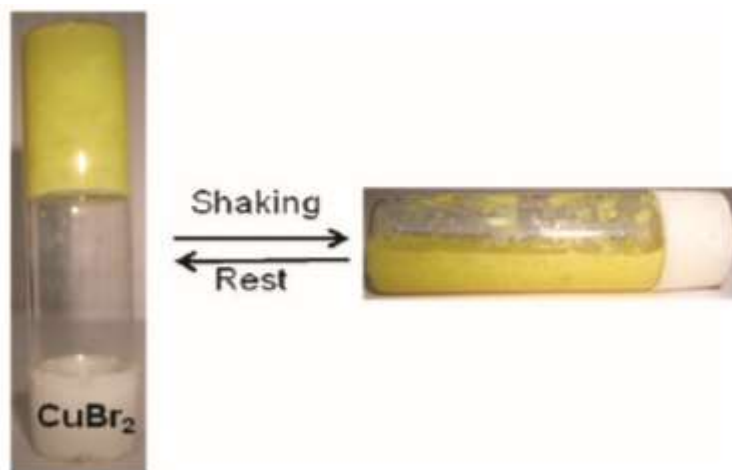


Figure 2. Illustration for mechano responsive nature of MOG-1.

**Gelation of Solvents Other than MeOH.** The gelation of solvents such as ethanol, n-butanol, n-hexanol, n-heptanol, isopropanol, and t-butanol has been also explored to understand the solvent effect. The commonality of these solvents is to have –OH groups that can hydrogen bond with the L, but contains different sizes and shapes of alkyl groups. It was found that the ligand L in combination with Cu(II) or Cd(II) halides can easily gelate any of the above solvents. Interestingly, the gelation times found to increase as the aliphatic portion of the alcohol increases. Moreover, these components failed to gelate the nonalcoholic solvent such as THF, probably due to the lower tendency to form hydrogen bonds. The efforts to gelate MeNH<sub>2</sub> failed understandably due to its strong coordination ability to Cu(II) or Cd(II), which inhibits formation of the metal–L complex.

**Gelation with Counterions Other than Halides.** In order to explore the counterion effect on the gelation process, several other metal salts of Cd(II) and Cu(II) with monovalent anions such as NO<sub>3</sub><sup>–</sup>, OAc<sup>–</sup>, ClO<sub>4</sub><sup>–</sup>, and BF<sub>4</sub><sup>–</sup> were used to try to gelate with L in MeOH under similar conditions mentioned above. However, it was found that none of these reactions resulted in the gel

formation, but resulted in the formation of precipitates. Interestingly, the use of a divalent counterion such as  $\text{SO}_4^{2-}$  in the form of  $\text{CuSO}_4$  resulted in the gel (MOG-5) formation similar to the halide salts. However, some important differences were observed in the formation and stability of the MOG-5 when compared with those of MOGs 1–4. In the case of MOGs 1–4, it was stated above that the gradual increase of metal concentration increases the capacity of gelation. In contrast, reverse tendency was observed in the case of MOG-5, that is the vials containing metal to ligand ratios of 0.1:1, 0.2:1, and 0.3:1 form gels, whereas the vials containing the metal equiv above 0.3 with respect to the ligand do not form gels but form precipitates (Figure S5, Supporting Information). Another, noteworthy difference is the stability of the gels, the MOGs 1–4 are stable for longer periods (months), whereas on standing for less than a month, MOG-5 yields a fine crystalline material, which is not suitable for single crystal X-ray studies. These observations indicate that the counterions play a crucial role in the formation of the MOGs 1–5. The halide ions and  $\text{SO}_4^{2-}$  ions have a greater tendency to bridge metal atoms to form metal clusters than the other counterions  $\text{NO}_3^-$ ,  $\text{OAc}^-$ ,  $\text{ClO}_4^-$ , and  $\text{BF}_4^-$ . This fact explains why the other counterions failed to form MOGs.

**Infrared Spectroscopy.** To gain some insight into the coordination of imine N-atoms and the involvement of N–H groups in hydrogen bonding, the IR spectra of the dried gels of MOGs have been analyzed. The FTIR spectra of L and all MOGs contain a broad area near 3049 to 3188  $\text{cm}^{-1}$ , indicating the participation of NH in hydrogen bonding. Another broad area was observed near 3400  $\text{cm}^{-1}$ , which could be assigned to the hydrogen bonding of a –OH group of solvent. The C=N stretch of pyridyl and imidazole moieties are observed at 1593  $\text{cm}^{-1}$  in the case of the L, which has been blue-shifted by 11–13  $\text{cm}^{-1}$  in the xerogels of MOGs. Similar blue shifts for C=N frequencies, due to coordination of the metal to the N-atom, have been previously observed in the coordination complexes of pyridine or imidazole containing ligands.

**Sol–Gel Transformations of MOG by Chemical Stimuli.** The transformation of gel material to liquid form and back again to gel form has been observed by the addition of appropriate chemicals. For example, the addition of a few drops of  $\text{NH}_4\text{OH}$  to MOGs resulted in the clear blue and colorless solutions in the cases of MOG-1/2/5 (Figure 4) and MOG-3/4, respectively. This transformation could be the result of the formation of the metal ammonia complex breaking the metal–ligand (L) coordination, which resulted in the clear solutions. The above result suggested that we study the effect of the metal trapping reagent to trap the metal atom single matrixes.

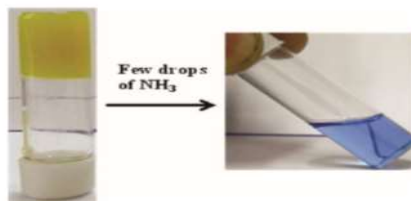


Figure 3. Illustration for gel-sol transformation of MOG-1 by the addition of external chemical stimuli (ammonia)

For that purpose, a well-known chelating agent ethylene di amine tetra acetic acid (EDTA) was chosen. The crystalline EDTA was added on the surface of the gels; the vials were sealed and left at room temperature. The same number of equiv of EDTA was added to the gel as the equivalents of the metal salt in the gel. In the case of MOG-1, MOG2, and MOG-5, which contain Cu (II) metal, the solid EDTA found to penetrate slowly into the gel materials and thereby gradually transferring the gel into a clear liquid state from top to bottom. In one week time, the whole gel turns into a clear transparent liquid containing a blue colored precipitate at the bottom of the vial. Our investigations reveal that the blue color precipitate is a EDTA and L complex of Cu (II), while the clear solution is the MeOH solution of the remaining ligand. It was found that the clear solution can be turned into a yellow color thick gel, similar to the beginning, by adding  $\text{CuBr}_2$ , which confirms that the colorless solution is nothing but the solution of the L (Figure 3 for MOG-1; see Supporting Information Figure S16 and S17 for MOG-2 and MOG-5, respectively). We note here that the gel-sol-gel transformations, by subsequent additions of EDTA and  $\text{CuBr}_2$ , can be repeated in the same vial until the ligand is exhausted.

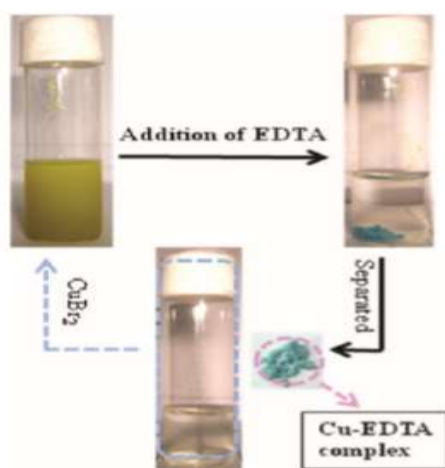


Figure 4. Illustration for reversible gel-sol transformation of MOG-1 by the addition of EDTA and  $\text{CuBr}_2$

However, similar additions of EDTA to MOG-3 and MOG-4 have shown no influence on the gel. Even after standing for one month, the solid crystalline EDTA remains unchanged at the top of the gel. Therefore, Cd (II) containing gels exhibited stability even in the presence of EDTA. The failure of EDTA to extract Cd(II) from the gel could be due to the apparent differences in the nature of Cd(II) and Cu(II). The crystal field effects for Cu(II) may be driving Cu(II) (d9-system) in MOG1/2/5 to form a stable complex with EDTA, whereas in the cases of MOG-3 and 4, the Cd(II)L complex was not disturbed by EDTA as there are no crystal field effects in the case of Cd(II) (d10-system). In general, it can also be noted that the formation constant of the cadmium-EDTA complex ( $2.9 \times 10^{16}$ ) is less



than the copper–EDTA complex ( $6.3 \times 10^{18}$ ). These studies first show that MOG-1/2/5 are responsive to metal trapping agents but not MOG-3/4. Second, it is evident that the metal coordination with ligand (L) resulted in the formation of gel materials.

**Dye Adsorption by MOGs.** The removal of toxic dye substances from wastewater has been a major concern. In the literature, several types of smart materials such as dendritic polymers, clays, and supramolecular gels were shown to act as efficient dye adsorbing agents.<sup>13</sup> Generally, the dye absorbing agents should contain two domains: hydrophilic domain to interact with water and hydrophobic domain to absorb the dye. The ligand L possesses both features, and therefore, the MOGs of L may have a potential to act as a dye adsorbing agents. With this intention, xerogels of all the MOGs (MOGs 1–5) were tested for methyl orange dye adsorption. Stock solution of the dye was prepared by dissolving 6 mg of methyl orange dye in 200 mL of distilled water. In a typical reaction, 8 mg of xerogel was immersed in 3 mL of the dye stock solution in a vial and left undisturbed for 24 h. After 24 h, it was observed that almost the entire dye was transferred from aqueous solution to xerogel, resulting in an almost clear water solution in the glass vial (Figure 5). At various time intervals during 24 h, the adsorption of dye from aqueous solution by xerogel was monitored by UV-visible spectroscopy. The MOG-1/2 and MOG-3/4 exhibits the dye absorption of 10.7mg/g and 9.56mg/g, respectively. However, MOG-5 exhibited lower dye absorption capability of 7.30mg/g

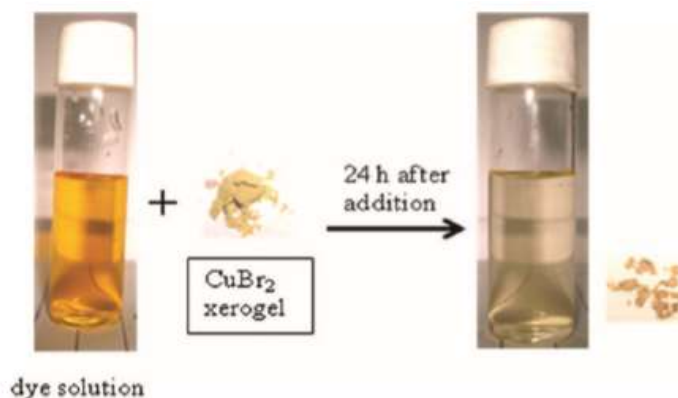
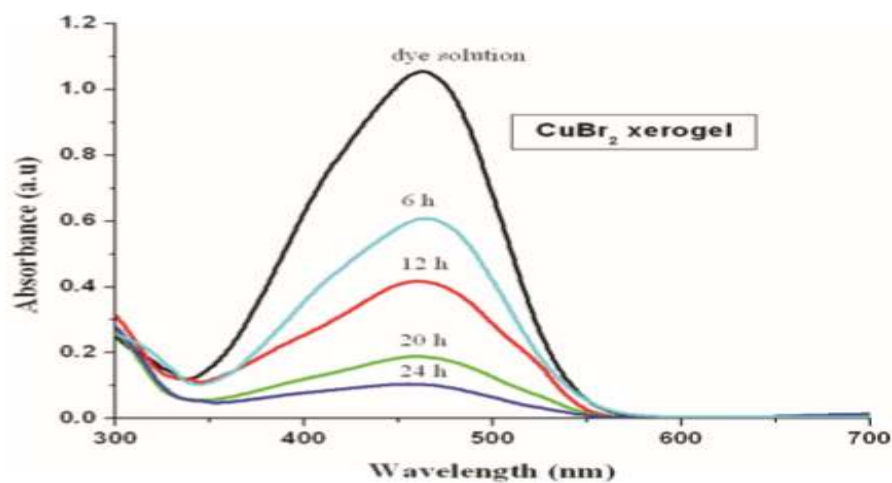
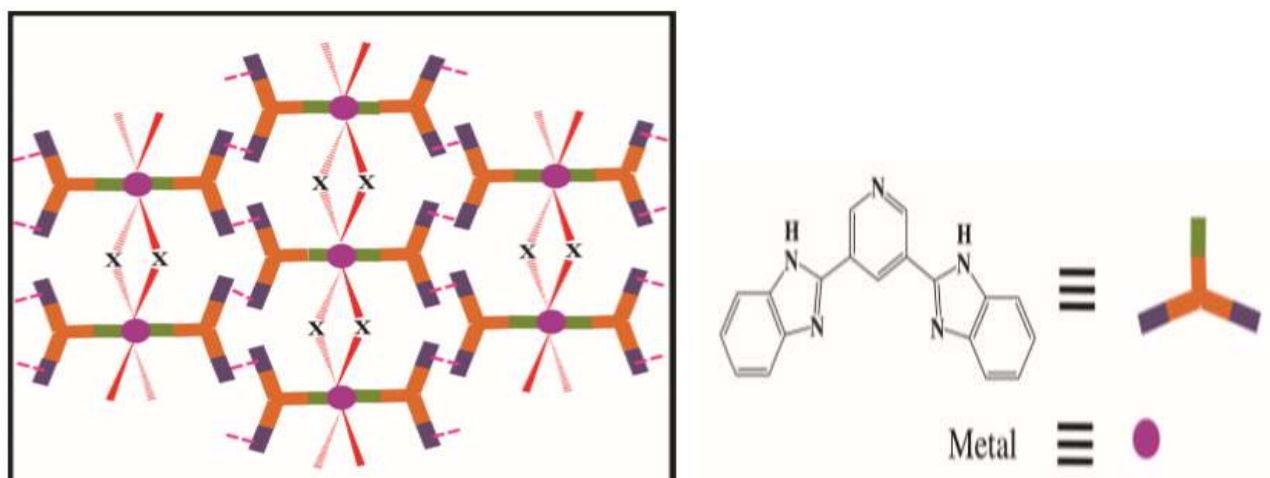


Figure5. Illustration for dye adsorption by the xerogel of MOG-1;



Fig; UV-vis spectra of dye solution (black in line) after the addition of MOG at various time intervals

**Model for Self-Aggregation.** Existing literature on the coordination complexes of L with  $\text{Cd}(\text{NO}_3)_2$ ,  $\text{Zn}(\text{NO}_3)_2$ , and  $\text{Zn}(\text{CH}_3\text{COO})_2$  has shown that L is capable of forming discrete metal complexes.<sup>10</sup> In all the three complexes, only the pyridine N atom of the ligand L is coordinated to the metal, while the imidazole N-atoms participate in hydrogen bonding. Recently, we have reported that the related bis (benzimidazole)-based ligand forms coordination polymers with metal halides in which halide bridging of metal centers play a significant role in the propagation of polymeric networks.<sup>9e</sup> Further, the optimum gelation of MeOH was found at the M–L ratio of 1:2, that is, the gelation of amount of MeOH gradually increased as the M–L ratio changes from 1:10 to 1:2. However, no significant increase in the amount of gelation of MeOH was found from the M–L ratio of 1:2 to 1:1. On the basis of these inputs, the probable model of self-aggregation in forming gel fibers and gel fibril networks could be proposed as shown in Scheme 2.



Scheme 2. Proposed Model of the Self-Aggregation of L and Metal Halides (X)

The shape of the 1D coordination networks is such that the self assembling of these nets through weak interactions creates a plethora of voids and channels for holding the solvent molecules.



(b). Supercooled Liquid  $\beta$ -Diketones with Mechanoresponsive Emission:  $\beta$ -diketones (bdk) are a particularly promising class of stimuli responsive materials because of their facile synthesis from commercially available starting materials and tunable optical properties. Their emission properties are tunable via boron coordination, alkyl chain length, substituent ring size, heavy atom, and donor and acceptor substitution,, as well as heteroatom and steric effects. However, the mechano responsive emission of these materials is due to crystalline-to-amorphous phase transitions. Amorphous-to crystalline transitions have yet to be broadly established. Recently, we reported the mechanochromic luminescence properties of gbmOMe, a  $\beta$ -diketone with a 3,4,5-trimethoxysubstituted phenyl ring. In addition to rapidly recovering blue to-green mechanochromic luminescence, we discovered that gbmOMe also forms a green-emissive Supercooled liquid (SCL) phase after melting which is stable for up to 24 h. According to the crystal structure of gbmOMe, the methoxy group in the 4-position of the tri methoxy-substituted ring extends out of the plane of the molecule which may provide the steric bulk needed for the formation of the SCL state. Hence, synthesizing other molecules with this motif may be an effective strategy to form SCL phases.

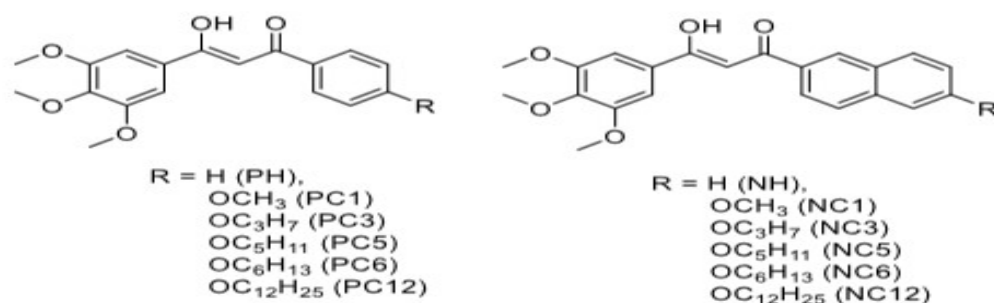


Figure 1. Chemical structures of di ketones. Dyes are named for the arene ring (P = phenyl and N = naphthyl) and the length of the alkyl chain (e.g., C1=methyl and C3=propyl). For example, PC1 is a phenyl dye with a methoxy substituent.

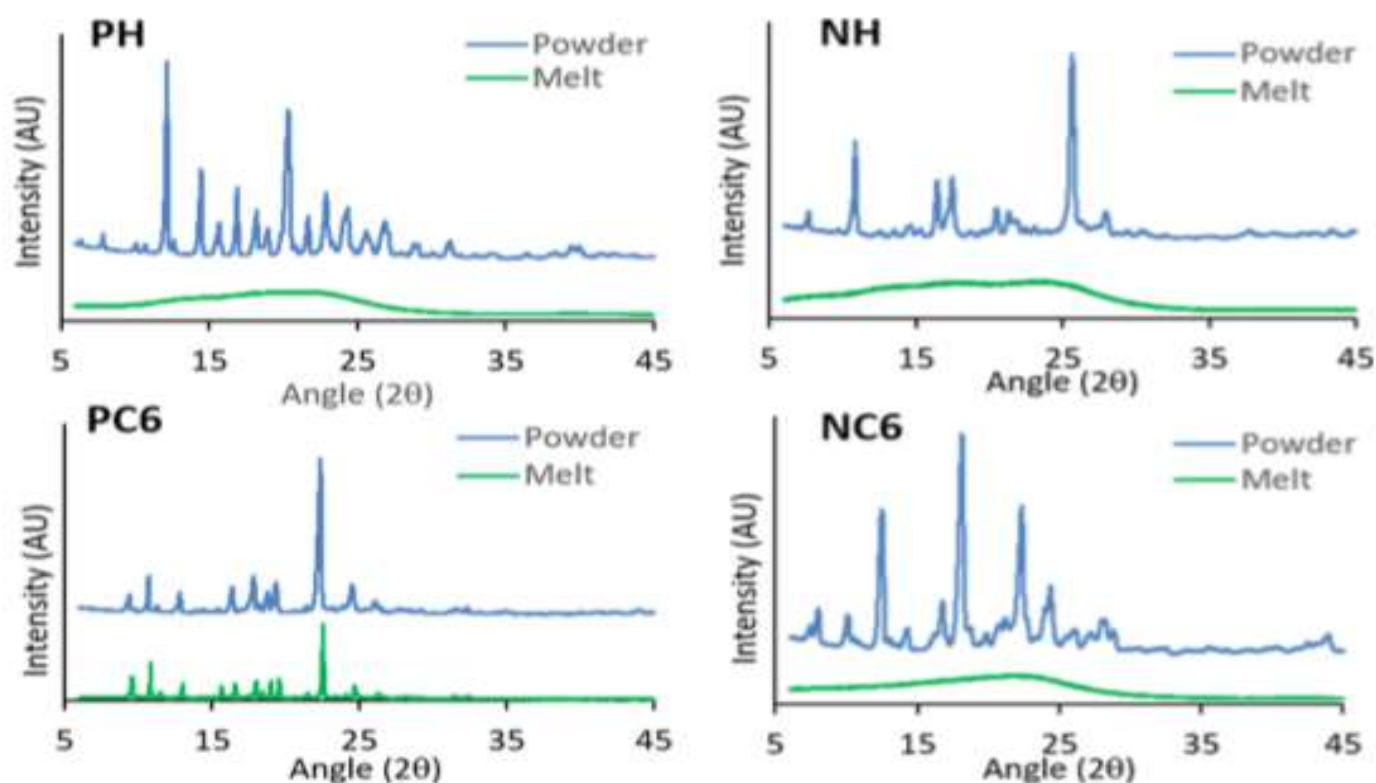
Inspired by the design strategy of Kimetal, a series of trimethoxyphenyl bdk were synthesized, incorporating phenyl and naphthyl rings, to probe arene effects on the lifetime of SCL phases (Figure 1). Additionally, both sets of dyes (phenyl and naphthyl) were substituted with alkoxy groups of varying alkyl length ( $n = 0, 1, 3, 5, 6$ , and  $12$ ) in order to induce van der Waals interactions and drive crystallization. Previous reports of alkyl chain lengths and arene size effects on the mechanochromic luminescence of BF2bdk materials indicate that the stimuli-responsive optical properties of spin-cast films (e.g., thermal, ML) may be affected in addition to the stability of SCLs. Thermal and structural characterization of these dyes was performed using differential scanning calorimetry (DSC) and X-ray diffraction (XRD), respectively. When possible, single crystals were grown and assessed by XRD to provide insight into the intermolecular and packing interactions that

influence the lifetime of the melted phase. Solid state optical properties, including shear-induced crystallization, were investigated for bulk powders and melted films. Additionally, thin films were fabricated in order to investigate the mechanochromic luminescence response of each dye.

**Synthesis.** In order to investigate the stability of SCL states and mechanochromic luminescence properties of  $\beta$ -diketone dyes, a series of phenyl (Scheme S1) and naphthyl (Scheme S2) derivatives were synthesized via Claisen condensation with the appropriate ketone /ester pair. The ketone starting materials for both phenyl and naphthyl derivatives were synthesized via Williamson ether synthesis using a previously described method.<sup>34</sup> Diketones were soluble in common organic solvents (e.g.,  $\text{CH}_2\text{Cl}_2$ , THF, and  $\text{CHCl}_3$ ); however, solubility in hexanes varied depending on the length of the alkoxy chain, that is, longer chains corresponded to greater hexane solubility. Peaks near 17.0 ppm were observed in the NMR spectra for all dyes, which indicate the enol form is present in solution. Given the possibility of three tautomers (i.e., diketo and two different enols, given dye asymmetry) and different rotamers (i.e., rotation about the naphthyl-keto bond), 45 NMR spectra can be complex.

**Optical Properties in Solution.** The optical properties of the dyes were measured in dilute (10–5 M) dichloromethane solutions (Figures S11, S12, and Table S1). As a result of increased conjugation, red-shifted absorption and emission were observed for naphthyl derivatives versus phenyl dyes. With the exception of the hydrogen-substituted derivatives that were slightly blue-shifted compared to other dyes, little deviation in peak absorbance ( $\lambda_{\text{abs}}$ ) was detected within each set of dyes (i.e., phenyl and naphthyl). As expected and previously observed, alkoxy substitution results in red-shifted emission because of increased electron donation versus H; however, the alkyl chain length has little effect on absorption. All dyes exhibited similar molar absorptivities ranging from 55000 for NC3 to 81000 for NC5 regardless of phenyl or naphthyl substitution. Typically, increasing conjugation results in larger absorbing cross-sections and increased molar absorptivity; however, no such trend was observed for these trimethoxy dyes. One potential explanation could be that twisting of arene rings in the ground state limits the absorbing cross-section of both sets of dyes. Visual inspection of UV excited samples indicated that dyes are essentially non emissive in solution, further evidenced by low quantum yields ( $\phi < 3\%$ ) irrespective of increased conjugation or alkoxy substitution. Similar to their absorption in solution, the emission of naphthyl dyes was red-shifted compared to phenyl substituents via fluorescence spectroscopy. Phenyl derivatives PH and PC12 show red-shifted emission compared to other derivatives of this kind. Similarly, no trends in emission with the alkyl chain length could be established for naphthyl dyes. Relatively, short life times ( $<0.5$  ns) were observed for both sets of dyes, which is consistent with other bdk derivatives (e.g., bromo and methoxy dinaphthoylethane dyes;  $<0.23$  ns;<sup>22</sup> and 3,4,5-trimethoxy derivatives with fluoro, iodo, and cyano substituents:  $<0.23$  ns).

**Powder XRD Characterization of Melted Thin Films;** Analysis of powder patterns for phenyl dyes indicated that derivatives with shorter alkyl chains (<C6) were crystalline as bulk powders, but mostly amorphous as thin films that were melted and then cooled to room temperature. With the exception of PC3, no diffraction peaks were observed in the powder patterns of the melted films for these dyes, which indicates that they are amorphous. For PC3, small peaks were observed in the melted phase which may be because of the formation of small crystalline regions during the course of the measurement. The XRD patterns for bulk powders and melted films of phenyl dyes with longer alkoxy chains, PC6 and PC12, indicated that both states were populated with crystalline species. Therefore, melted PC6 and PC12 films rapidly converted to a crystalline blue-emissive phase which is consistent with video characterization. Comparison of the bulk powder and melted patterns of PC6 shows that the same crystalline phase is present in both states, whereas the XRD data for PC12 show several peaks in the bulk powder pattern that are absent when melted, and crystallization occurs afterward. This suggests that multiple crystalline phases are present in the bulk powder of PC12, some of which were not formed when PC12 was melt-quenched. The XRD patterns of bulk powders and melted films of naphthyl compounds showed similar behavior to their phenyl counterparts. With the exception of NC12, all dyes exhibited crystalline powder phases, and no peaks were observed after melt quenching, thereby demonstrating that the melted phases formed by naphthyl dyes are amorphous. Similar to PC 12 melted NC12 films form crystalline phase after cooling; however, it is composed of the same crystalline species as the corresponding bulk powder.



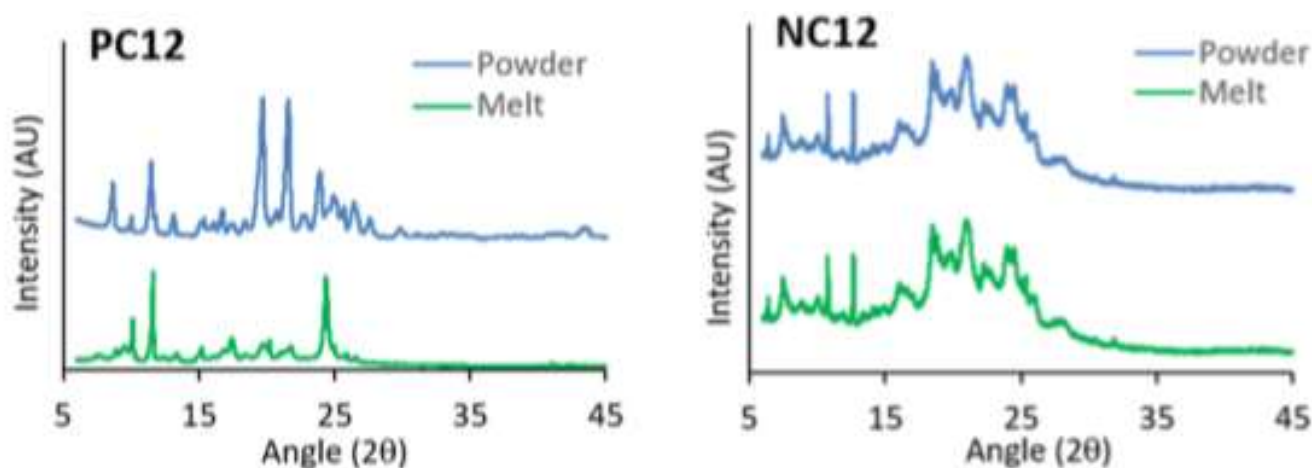


Figure 2. Powder XRD patterns of selected phenyl and naphthyl dyes as powders and melted films.

**Mechanochromic Luminescence.** The mechanochromic luminescence properties of bdk and BF2bdk dyes typically involve a red shift in emission that is the result of a crystalline-to-amorphous phase transition. PC1 showed blue-to-green mechanochromic luminescence with rapid self-erasing ( $\sim 30$  s to 5 min, depending on the sample). To test the mechanochromic luminescence properties of phenyl and naphthyl derivatives, spin-cast films were prepared with dilute (0.18 M) dye solutions in dichloromethane. The emission of each film was measured in as spun (AS), thermally annealed (TA), and SM states (Table 3). In general, phenyl dyes were annealed at 75 °C for 10 min to produce films in the TA state. With the exception of PH and PC1, this was sufficient to produce a crystalline phase with maximally blue shifted emission. To anneal PH and PC1, films were smeared with a Kimwipe by applying gentle pressure to the sample and rubbing in a single direction before subsequent heating at 75 °C for another 10 min.

	cycle 1 <sup>a</sup>		cycle 2 <sup>b</sup>	
	$T_m^c$	$T_c^d$	$T_m^c$	$T_c^d$
PH	101.5			
PC1	112.4		116.5	
PC3	123.6		121.5	54.1, 90.8, (84.2)
PC5	105.4	(62.3)	104.3	(69.6)
PC6	98.5	(41.6)	97.4	(65.5)
PC12	95.2	(63.0)	94.7	(78.1)
NH	89.5			
NC1	134.1		133.3	102.5, (107.5)
NC3	116.3		114.4	87.5
NC5	102.0		101.6	78.9
NC6	120.1		119.2	67.0, (94.3)
NC12	77.0	(42.9)	79.6	43.4, (44.6)

Table 1. Optical Properties of SCLs on Glass

For all naphthyl dyes but NC12, films were heated at 85°C for 10min, followed by gentle smearing with a Kimwipe and additional heating at 85 °C for another 10 min to make TA films. The smearing and reheating step was omitted for NC12 as blue-shifted emission was observed after heating at 85°C for only 10min. With the exception of PH and PC1, films glowed blue in the AS state (Figures 3 and S19). Green emission was observed for PH ( $\lambda_{em}$  = 471 nm) and PC1 ( $\lambda_{em}$  = 471 nm). The differences observed in PH and PC1 are in accordance with XRD and DSC studies and indicate that dyes substituted with longer alkoxy chains have a greater propensity to crystallize. No trend in the emission wavelength with the alkoxy chain length was observed for AS films of blue-emissive dyes as PC3 ( $\lambda_{em}$  = 441 nm) exhibited the maximally blue-shifted emission, and the lowest energy emission was observed for PC6 ( $\lambda_{em}$  = 451 nm). Thermal annealing of phenyl dye films resulted in a large blue shift for PC1; however, little change in emission was observed for all other phenyl dyes, which indicates that they are likely crystalline in the AS phase. The emission of PH bulk powder suggest that higher energy emission should be achievable ; however annealing and gently smearing was insufficient to produce blue emission. For all phenyl dyes but PC6, peak emission of annealed film is similar to the emission of the monomer in dichloro methane, which suggest that dye-dye interactions that modulate emission are very weak or absent for annealed films. The peak emission of PC6 is red-shifted relative to emission in dichloromethane; therefore, interactions between PC6 molecules are likely present in these films. Smearing resulted in red-shifted emission for all dyes; however, the extent of the mechanochromic luminescence shift was highly dependent on the alkoxy chain length. The mechanochromic luminescence shifts ( $\Delta\lambda_{ML}$ ) varied depending on the alkoxy chain length; however, no clear trend could be established. The smallest mechanochromic luminescence shifts were observed for PH and PC6 ( $\Delta\lambda_{ML}$  < 26 nm), and the largest

mechanochromic luminescence shifts for phenyl dyes were observed in PC1 and PC5 ( $\Delta\lambda_{ML} > 43$  nm). With the exception of PC1, no evidence of self-erasing was observed for phenyl dyes 24 h after smearing, which indicates that room temperature recovery is hindered in derivatives with longer alkoxy chains. The same trend was observed in BF2bdk dyes with differing alkoxy chains.

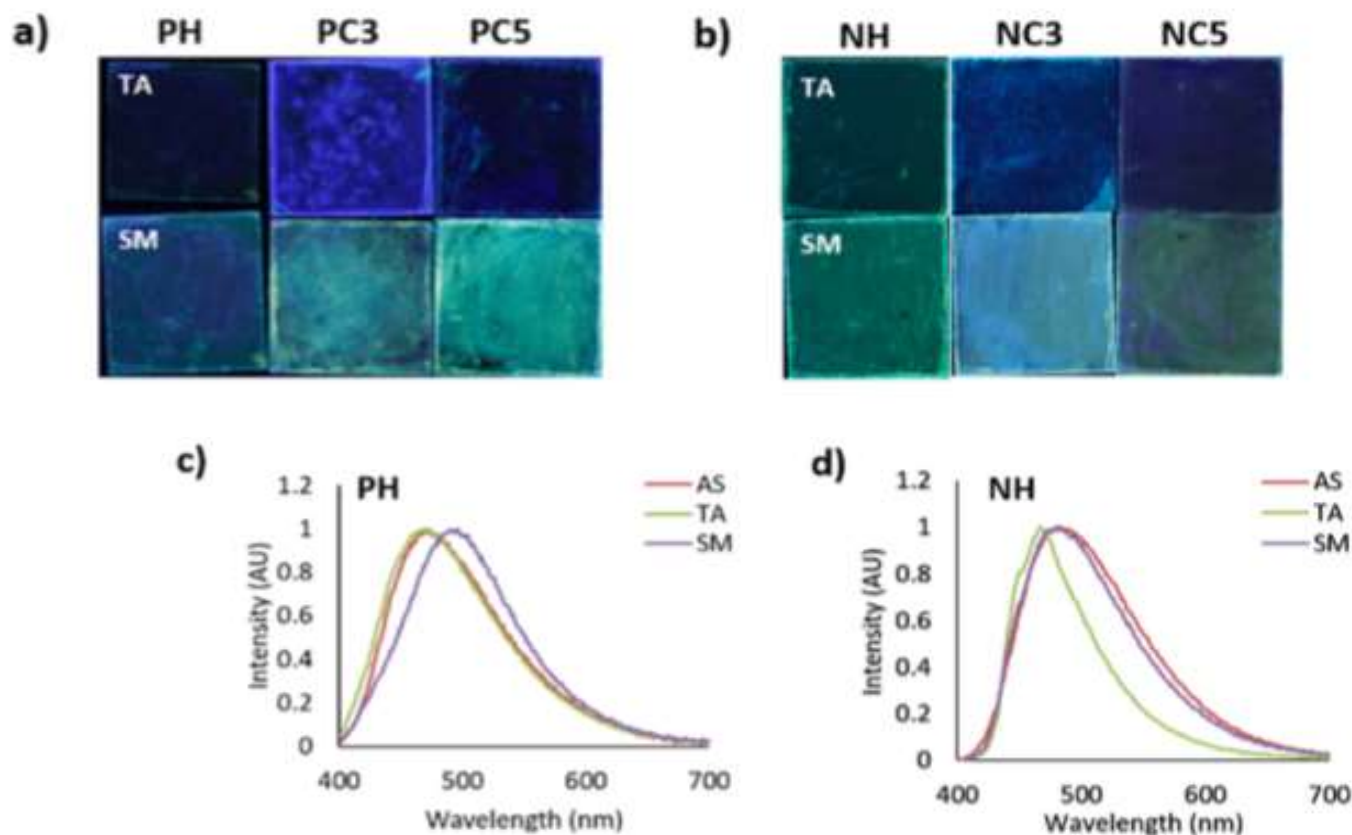
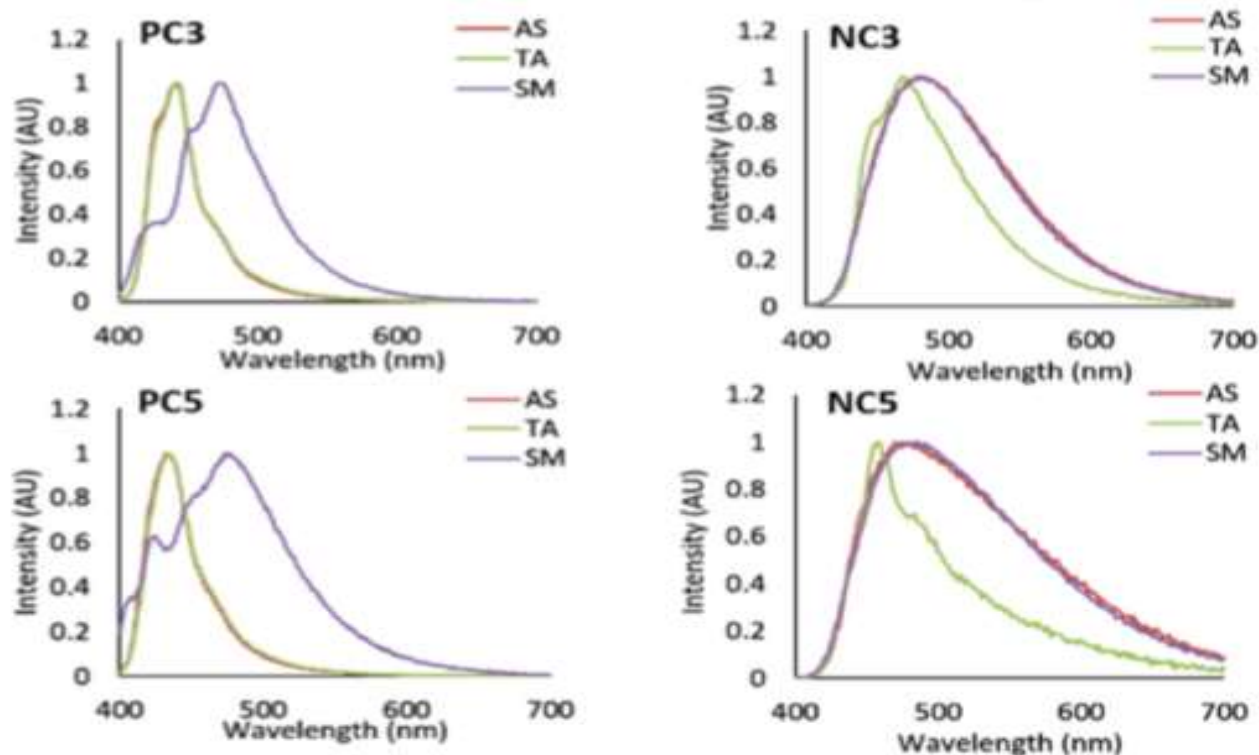


Figure 3. Images under UV irradiation of TA and SM thin films of phenyl (a) and naphthyl dyes. Normalized emission spectra of selected phenyl (c) and naphthyl (d) dye films in AS,TA, and SM

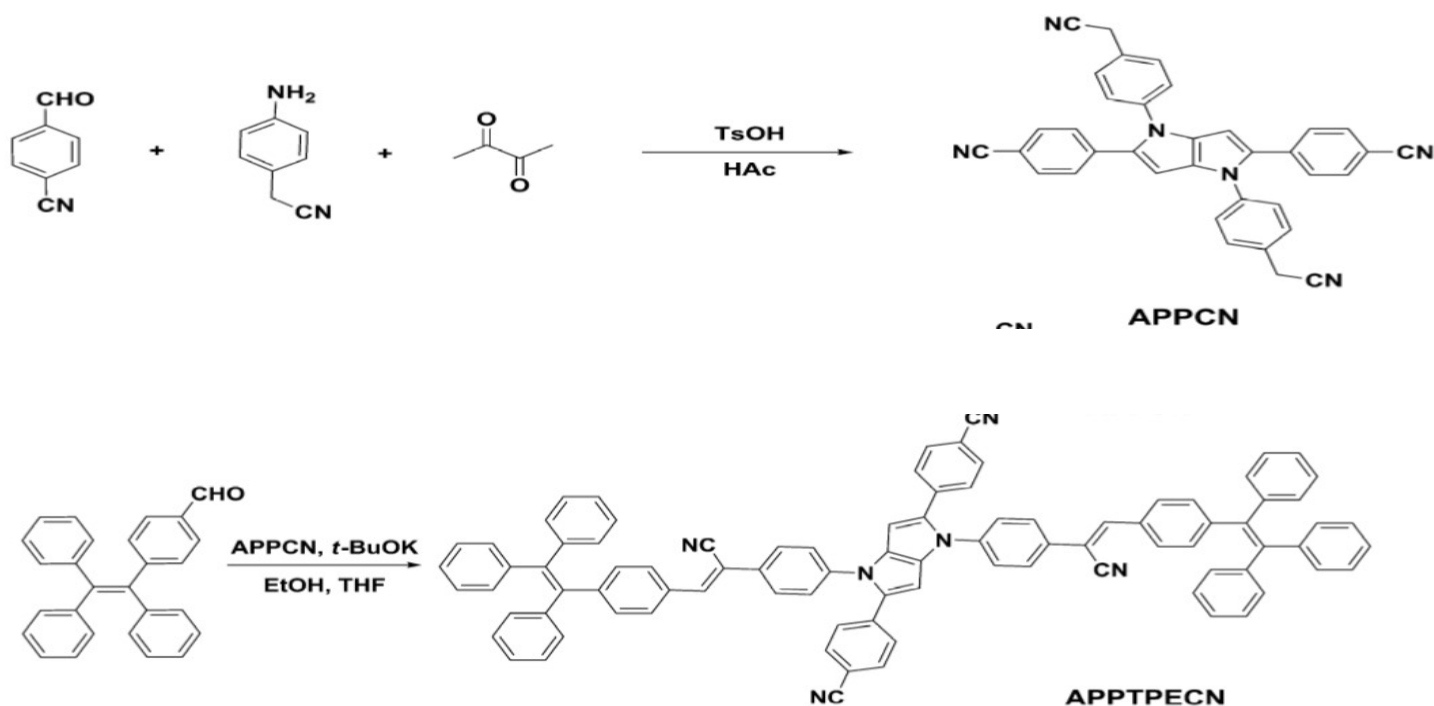




For films of naphthyl dyes, the AS state glowed green under UV irradiation. Compared to phenyl dyes, broader emissions profiles were observed regardless of the alkoxy chain length. Thermal annealing of naphthyl films resulted in very little change in peak emission for NC1 and NC6. Relatively small changes in the peak wavelength were observed compared to phenyl dyes; however, there were substantial reductions in full width at half-maxima especially for NH, NC3, NC5, and NC12. With the exception of NH, which showed similar peak emission with respect to dichloromethane solutions, large deviations in peak emission between solution and solid-state spectra were observed for naphthyl dyes. This is indicative of more significant intermolecular interactions between dyes for all alkoxy-substituted naphthyl dyes. With the exception of NC5, changes in peak emission and spectral broadening were observed for naphthyl dyes indicating mechanochromic luminescence activity. No evidence of room temperature self recovery was observed for naphthyl dyes. Much smaller mechanochromic luminescence shifts and lower contrast emission changes were detected in comparison to phenyl derivatives.

(C) MECHANO-RESPONSIVE MATERIAL OF AIE-ACTIVE 1,4-Dihydropyrrolo[3,2-b]pyrrole Luminophores: A simple method to discover MFC compound of novel 1,4-dihydropyrrolo[3,2-b]pyrroles derivative containing TPE unit, We have been trying our best knowledge to grow crystal to explain the phenomenon why the material fluorescence enhanced after grinding, unfortunately, we still unable to successfully cultivate crystal. APPTPECN showed strong AIE property. Also, the obtained APPTPECN exhibited reversible MFC behaviors. It was shown that interconversion between the microcrystalline and amorphous phase, and the MFC mechanism was proved by PXRD

and SEM. MFC materials with strong fluorescence emission in the solid state and aggregated state, an artful design of the molecule was important for tuning molecular MFC properties. Typically, 1,4-dihydropyrrolo[3,2-b]pyrroles (PPs), a class of 10  $\pi$ -electron aromatic dihydroheteropentalenes, were discovered by Hemetsberger and Knittel in 1972 . Importantly, Gryko and co-workers developed a one-step synthetic method to acquire tetraaryl-pyrrolo[3,2-b]pyrroles in 2013 . Moreover, these compounds have received increasing attention because PPs have a lot of advantages including high thermal , photostability , good absorptivity , bright fluorescence and high quantum yields .Meanwhile , molecules and modifications of TPE have been proved an efficient way to construct new aggregation-induced emission (AIE) luminogens with high solid-state efficiency. Synthesis of the APPCN and APPTPECN: The synthesis of APPCN was carried out using one –step method and compound APPTPECN was synthesized using a classical Knoevenagel condensation reaction .The chemical structure and synthetic route of the compounds are shown in scheme1. The detailed procedure is listed as follows.



Scheme1. Synthetic route of APPCN and APPTPECN

Considering the miscibility of DMF and H<sub>2</sub>O, for the purpose of checking whether APPTPECN is AIE active , we used a standard approach to investigate UV–Vis absorption and FL spectra. Concentration of APPTPECN were kept at  $1.0 \times 10^{-5}$  mol/L in DMF and water mixture solution .For UV-vis spectra , obviously , with the increasing water fraction, the solubility of the compound gradually decreased and the molecules gradually shifted from the free state to the aggregation state, forming



the molecular aggregated particles. Meanwhile the level –off tail suggested that the aggregates have been formed in mixture. DLS experiment showed the formation of aggregates with average hydrodynamic diameter of 265 nm (polydispersity index = 0.342). For FL spectra, APPTPECN showed very weak visible light excited by 365 nm UV light in pure DMF because of the intramolecular rotation of tetraphenylene core. FL intensity remarkably increases from 30% to 99% water fraction and reaches its peak at 90% (fig 1b-d). Also, there is a significant red-shift of APPTPECN fluorescence wavelength. The bright yellow-green light emitting of APPTPECN (located at 532 nm) was observed for the aggregates, which was about 30 times higher than that in pure DMF, likely due to the intramolecular rotation restriction of tetraphenylethene unit. These results indicated a typical AIE activity that the non-radiative processes were restrained because the restriction of intramolecular rotation and intramolecular interaction. FL spectra were utilized to investigate the MFC behavior of APPTPECN in the solid state. As shown in Figure 2a, The pristine solid APPTPECN emitted green fluorescence in 512 nm ( $\Phi F = 14\%$ ,  $\tau < 0.1$  ns, Figure S5). Interestingly, APPTPECN exhibited an obvious red-shift upon grinding (34 nm) yellow emission ( $\lambda_{em} = 546$  nm,  $\Phi F = 22\%$ ) with a long life time ( $\tau = 1.15$  ns, Figure S7). Higher  $\Phi F$  values indicated a higher average excited state life time compared to the pristine sample.

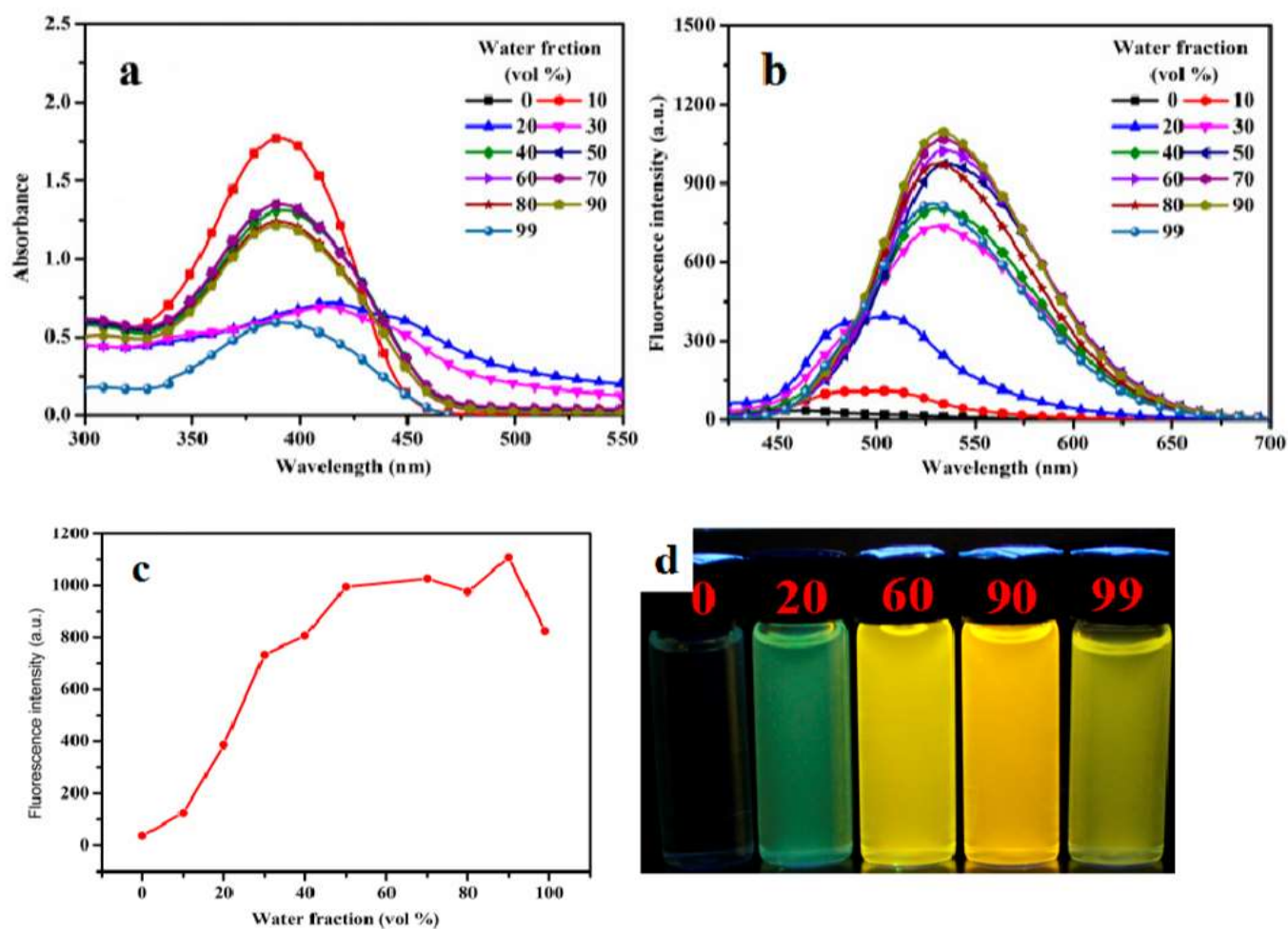
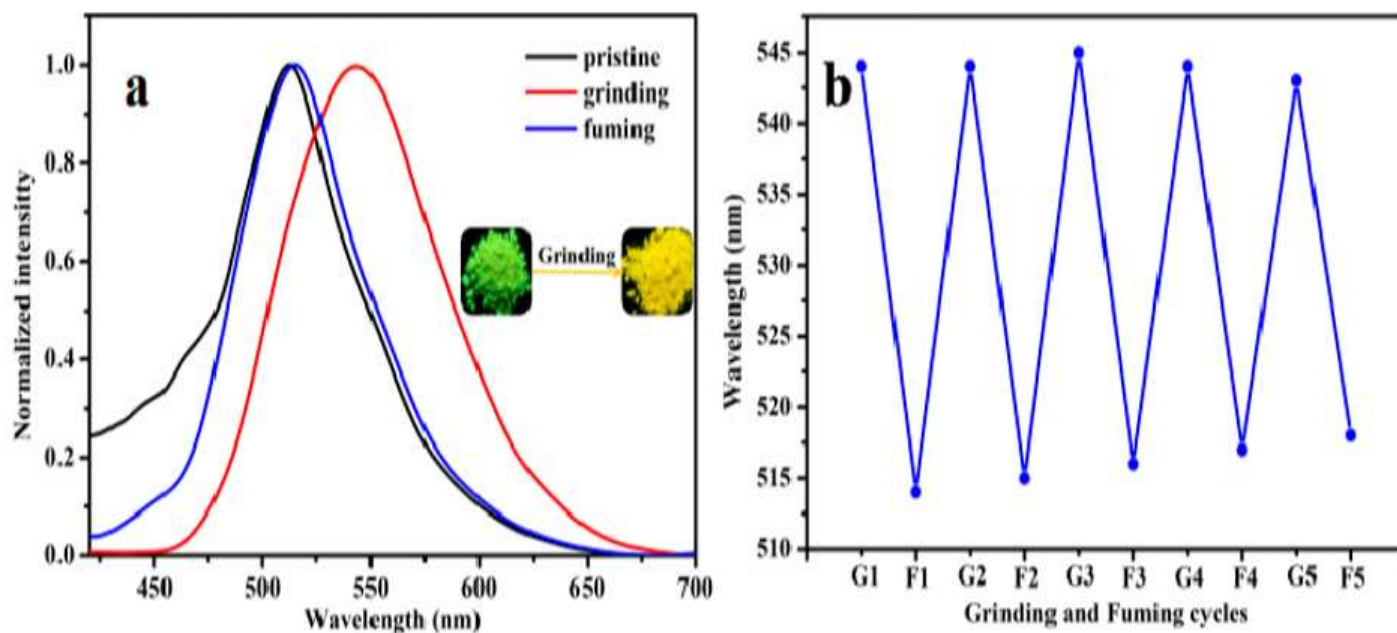


Figure 1. The UV-vis absorption (a) and FL spectra (b) of APPTPECN in DMF/water mixtures with different water volume fractions; the effect of the water volume fraction on the maximum emission intensity (c); optical photographs recorded fractions; the effect of the water volume fraction on the maximum emission intensity (c); optical photographs recorded under 365 nm UV irradiation with various fractions of water (d).

This result is worth noting that only a few materials have been reported to display higher fluorescence quantum yield for the pristine sample than that for the grinding sample in the field of smart materials. Additionally, we take insight to determine the self-reversible mechanofluorochromic fluorescence conversion by alternating grinding and EtOH fuming, the fluorescence emission and colour of grinding powder could be nearly converted numerous times between the green and yellow emissions. It was possible that an external mechanical force resulted in a change in the molecular morphology, indicative an outstanding reversibility of the MFC process. Owing to the excellent mechanofluorochromic properties of the smart fluorescent materials. We further explore the practical application, a simple and portable ink-free rewritable paper were conducted on Figure 2c, the pristine sample was dissolved in  $\text{CH}_2\text{Cl}_2$  (DCM), then a Whatman filter paper was immersed into the solvent for approximately 30 min. Afterwards, Whatman filter paper was taken out and dried at room temperature. Intriguingly, they were very clear and discernible under 365 nm irradiation and filter paper emitted green emission. When the APPTPECN-loaded paper was crushed, the fluorescence emission significantly red-shift. The letter “light” can be erased after the “paper” was exposed to DCM vapor. Further more, a Chinese letter “light” was easily written in the Whatman filter paper again. As a result, the material has great potential for application in ink-free rewritable paper.



c



Figure 2. FL spectra of APPTPECN as pristine, grinding and fuming samples (a); Repeated switching of the solid-state fluorescence of APPTPECN (b) by repeated grinding and fuming cycles; (c) Photos of the luminescence writing/erasing process on the APPTPECN-loaded paper under a 365nm UV lamp.

The excellent rewritable paper further promotes us explore the application of rewritable storage ,as shown in figure 3,compared to green background , the preparation of Whatman filter paper was crushed and appear yellow 'H' and 'Y' letter. Then the background is easily also converted into a yellow background with crushing .Next , 'H' and 'Y' letters were written using a specially made 'pen' with DCM vapour as 'ink' which exhibiting green fluorescence emission due to the grinding sample back to the original state after DCM treatment Last , exposure of the Whatman filter paper to DCM vapor can readiy erase the fluorescent letters and return to original green fluorescence background Herein, compound APPTPECN is employed in rewritable data storage and is of assistance in the rational design of smart luminescent materials . To, further understand and evaluate the origin and MFC properties in the powder state, PXRD was investigated forthe sample before and after grinding . As shown in figure 4, the diffraction curves of the pristine sample revealed many sharp and intense reflections , indicative of the well ordered crystalline structures . In contrast , after grinding , the diffraction peaks nearly disappeared and only some diffuse, broad and weak band were observed, exhibiting disordered molecular packing or amorphous states.

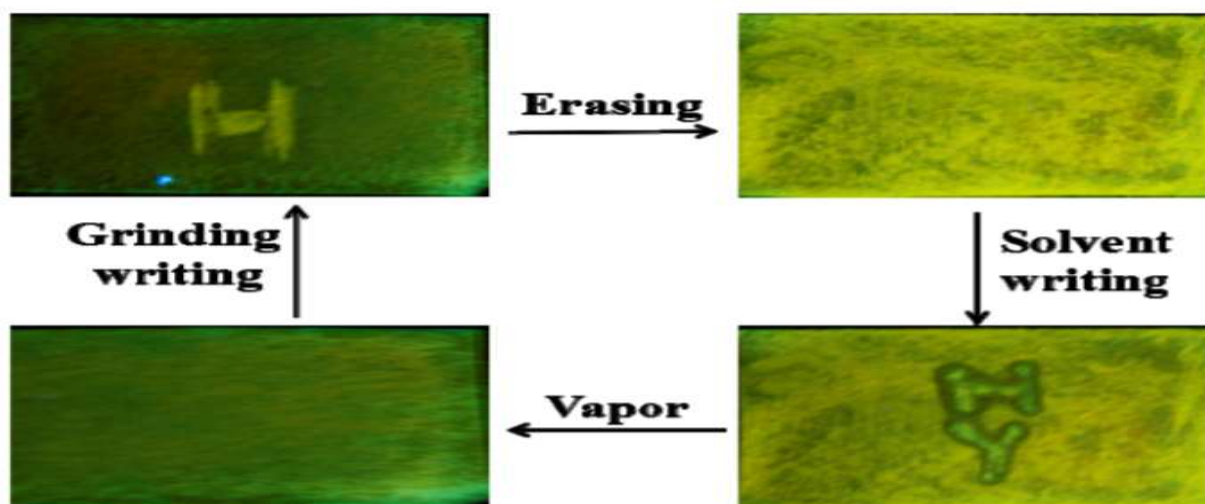


Fig3: photographs of the writing or erasing cycle under UV light

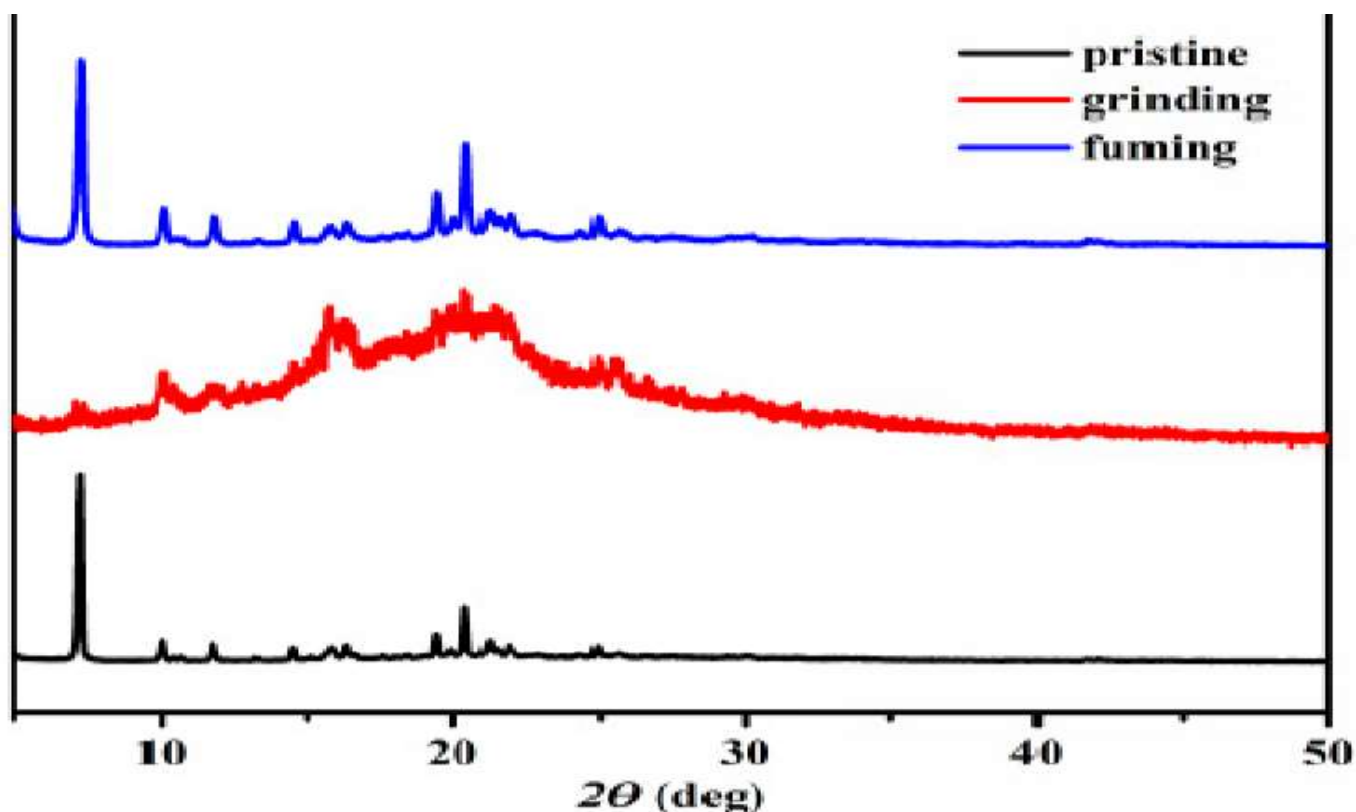


Figure 4. PXRD patterns of pristine, grinding and fuming samples of APPTPECN.

The aggregation morphology of APPTPECN before and after grinding were investigated by scanning electron microscopy (SEM) investigations. As performed in Figure 4, the APPTPECN exhibits an analogue “magnesium” structure (figure 5a), whereas the irregular and rough aggregates were observed for the grinding APPTPECN (figure 5b). When the grinding sample was fumed by EtOH, it essentially reverted to its original microcrystalline state (figure 5c). It is further proved that a microcrystalline to amorphous phase conversion of solid after grinding.

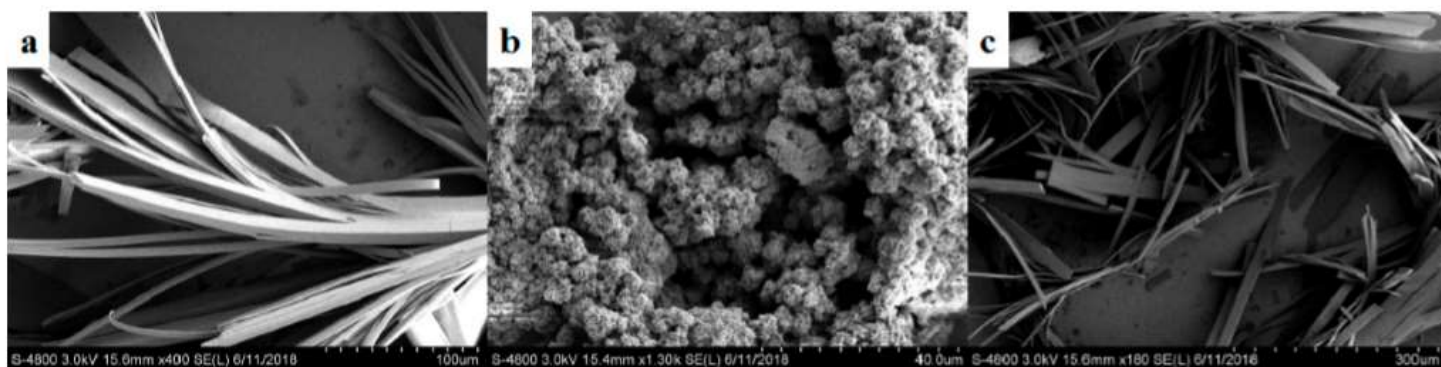


Figure 5: SEM image of pristine sample (a); grinding sample (b) and fuming sample (c).



TG analysis curves revealed that the degradation temperature ( $T_d$ ) of 5% weight loss of APPTPECN before and after grinding are 438 °C, 440 °C, respectively (Figure 6a). This result revealed that APPTPECN has an excellent thermal stability. In addition, DSC thermograms demonstrated that a new exothermic peak at 159 °C was observed for grinding sample. This exothermic peak could be attributed to the cold crystallization transition of the amorphous APPTPECN caused by mechanical grinding (Figure 6b). Hence, PXRD, SEM and DSC experiments verified that phase transformation between the microcrystalline and amorphous states should be responsible for MFC behavior.

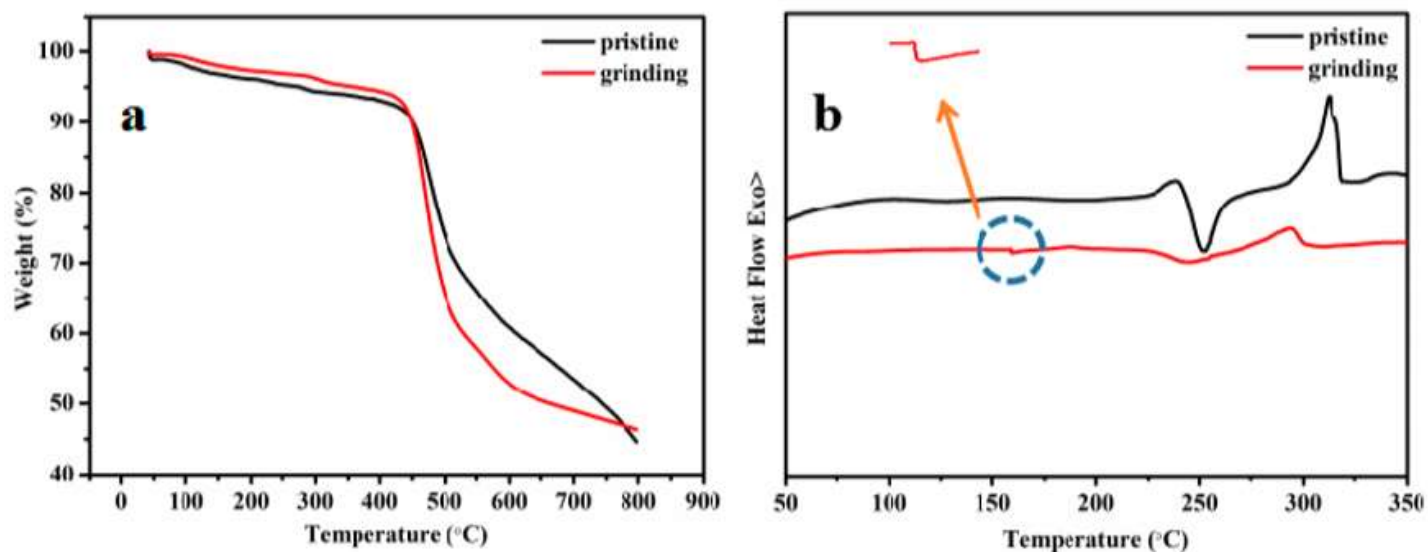


Figure6: TGA curves (a) and DSC curves of APPTPECN in different states (b)

(d). Mechano responsive materials for drug delivery: Stimuli- responsive materials are well suited for applications in drug delivery, actively releasing their drug payloads in response to either physiological or externally applied triggers. This spatiotemporal control over drug release is widely demonstrated for stimuli such as Ph, temperature ,light, ionic strength ,electrical potential and applied magnetic fields .While some of these systems ultimately undergo a mechanical change such as deformation, swelling or change in modulus.

Mechanically –activated systems are triggered by mechanical forces in the body that either occur physiologically or are exerted on the body by external devices , both over a wide magnitude .Generally an unopposed force exerted an object accelerates its motion. The distribution of the force on the object is described as the mechanical stress, which can result in deformation. Microscopic cellular forces are present and coordinate into macroscopic forces for processes such as wound repair and

inflammation. Further coordination results in the exertion of even greater forces by various system such as the musculoskeletal ,cardiovascular and respiratory systems. Alternatively ,external triggers are applied by medical devices such as stents and catheters that mechanically open blocked or narrowed structures ,or are applied by another user or self – exerted to control administration. Therefore, drug and protein delivery system that respond to mechanical forces serve as innovative solutions to control on demand release within a physiological environment . Designing such mechanoresponsive systems that account for the dynamic nature of the human body will bring about novel solutions to clinical challenges. systems that account for the dynamic nature of the human body will bring about novel solutions to clinical challenges. Mechanically stimuli are quantified by force and displacement . In compression a force is applied resulting in an equal but opposing force along the same axis , generally reducing the object’s length along that direction.Similarly , an object under tension is pulled or stretched, lengthening the object along the axis. This force , and resulting deformation, can be converted into stress and strain. For engineering stress ( $\sigma$ ), the force is normalized by the cross-sectional area while engineering strain calculates the relative change in displacement – the difference in length divided by thr original length. Instead , of applying forces normal to the cross section , shear forces areapplied parallel to the objects cross section. Shear strain is the strain in parellel direction. The overall , elastic material property is expressed by Young’s modulus ;  $E = \text{STRESS} / \text{STRAIN}$  .The shear modulus is defined as  $G = E / (2(1 + \nu))$ , where  $\nu$  is Poisson’s ratio, which describes the expansion of the material along the axis compared to compression perpendicular to the axis. Mechanoresponsive drug delivery is attractive due to the ease of applying compressive, tensile, and shear stimuli, and to the ubiiquity of these forces in the human body . While ultrasound is also considered a mechanical stimulus , several recent reviews have been published on ultrasound – triggered drug delivery and thus will not be discussed here. The scope of the current review focuses on drug delivery systems that utilize compression ,tension, and shear and are categorized according to the respective forces used for the respective forces used for mechanical stimulation of drug release.

**Conclusion :** The gelling properties of pyridine containing the bis(benzimidazole) ligand in the presence of transition metal(II) salts have been thoroughly investigated. It was demonstrated that the coordination of metal to ligand play a very important role in the formation of metal–organic gels. The anions were found to influence profoundly the gelation properties as well as the property of the gels. Our studies indicate that the chloride and bromide anions promoted the gel formation better than other univalent ions such as nitrate, perchlorate, acetate, and tetra fluoro borate. The gels were characterized using various microscopic and spectroscopic techniques. FESEM images of the gel samples confirmed the formation of 3D entangled gel networks. Rheological experiments on MOGs reveal significantly high mechanical strength of these soft materials. The MOG-1, 2, and 5 were found to be responsive with external chemical stimuli such as the addition of EDTA and NH<sub>3</sub> solutions. These experiments proved the importance of the coordination bond in the gelation process. These components have shown the versatility in gelating several alcohols other than MeOH. Further, the gels reported here have exhibited gas sorption, dye absorption, and significant self-sustainability properties.

Based on video characterization and DSC and powder XRD results, all dyes formed SCL phases when melted and cooled in air. The lifetime of trimethoxy-substituted diketone SCL phases could be tuned using a combination of alkoxy chain length and arene effects. In general, naphthyl SCLs exhibited longer lifetimes than their phenyl counterparts. Additionally, dyes substituted with longer alkoxy chains exhibited faster crystallization compared to unsubstituted derivatives or dyes with shorter chains. For certain derivatives, mechanically induced crystallization was observed at room temperature (PH, PC1, PC3, and NC6). Single crystal analysis of selected phenyl derivatives indicated that the para-substituted methoxy groups of the trimethoxy rings were out of the molecular plane. Mechanochromic luminescence was also observed for most derivatives. While dyes exhibited blue to out of the molecular plane. Mechanochromic luminescence was also observed for most derivatives. While dyes exhibited blue to green emission changes upon mechanical perturbation, the degree of the wavelength shift was dependent on the alkoxy chain length.

In this work, a novel molecular design of 1,4-dihydropyrrolo[3,2-b]pyrrole derivative (APPTPECN) containing TPE was synthesized, The incorporation of TPE unit in the backbone endows the APPTPECN an obvious aggregation-induced emission (AIE) behaviour. Effective MFC behavior with the red-shifts of 34 nm in FL spectra upon grinding is observed and indicative of reversible performance. Moreover, compound APPTPECN has the potential possibility to employ rewritable data storage and is of assistance in the rational design of smart luminescent materials. The present study provides valuable information for designing new AIEMFC materials with desired properties.

The field of mechanically stimulated delivery is rapidly expanding with a number of reports demonstrating the promise of releasing pharmaceutical or active agents in a controlled manner.

These mechanoresponsive systems are designed to be clinically relevant through physiological force triggers or externally applied clinically devices. The dynamic nature of the human body is constantly subjected to forces; therefore determining triggers distinguishable from the mechanical forces routinely present in daily activities are key to targeting and maximizing release.



# ACKNOWLEDGEMENT

I would like to express my special thanks of gratitude to Dr. Citrani Medhi (HOD) for giving me the golden opportunity to this wonderful project at home.

Secondly, I would like to thank to my esteemed guide, Dr. Rupam Jyoti Sarma, Associate Professor for his inspiring and guidance on carrying out my literature review. I acknowledge the kind support, time spent, effort and guidance on him and I take the opportunity to extend my heartfelt gratitude for his valuable time and support.

My heartfelt thanks goes to Anima Deori and Abhisek Saikia for their constant help and encouragement in this literature review.

Date: 09/09/2021

Pirbika Engtipi

Place: Department of Chemistry

M.Sc 4th Semester

Gauhati University

**REFERENCES:** 1.(a) Terech, P.; Weiss, R. G. *Chem. Rev.* 1997, 97, 3133–3160. (b) Sangeetha, N. M.; Maitra, U. *Chem. Soc. Rev.* 2005, 34, 821–836. (c) Abdallah, D. J.; Weiss, R. G. *Adv. Mater.* 2000, 12, 1237–1247. (d) Dastidar, P. *Chem. Soc. Rev.* 2008, 37, 2699–2715. (e) Estroff, L. A.; Hamilton, A. D. *Chem. Rev.* 2004, 104, 1201–1217. (f) Hirst, A. R.; Smith, D. K. *Langmuir* 2004, 20, 10851–10857. (g) Steed, J. W. *Chem. Commun.* 2011, 47, 1379–1383.

2. (a) George, M.; Weiss, R. G. *Acc. Chem. Res.* 2006, 39, 489–496. (b) Ajayaghosh, A.; Praveen, V. K. *Acc. Chem. Res.* 2007, 40, 644–656. (c) van Esch, J.; Feringa, B. L. *Angew. Chem., Int. Ed.* 2000, 39, 2263–2266. (d) Steed, J. W. *Chem. Soc. Rev.* 2010, 39, 3686–3699. (e) Smith, D. K. *Adv. Mater.* 2006, 18, 2773–2778. (f) Hirst, A. R.; Smith, D. K. *Chem. Eur. J.* 2005, 11, 5496–5508. (g) Heeres, A.; van der Pol, C.; Stuart, M.; Friggeri, A.; Feringa, B. L.; van Esch, J. J. *Am. Chem. Soc.* 2003, 125, 14252–14253. (h) Smulders, M. M. J.; Schenning, A. P. H. J.; Meijer, E. W. *J. Am. Chem. Soc.* 2008, 130, 606–611.

3. (a) Maitra, U.; Mukhopadhyay, S.; Sarkar, A.; Rao, P.; Indi, S. S. *Angew. Chem., Int. Ed.* 2001, 40, 2281–2283. (b) Lin, Y.; Kachar, B.; Weiss, R. G. *J. Am. Chem. Soc.* 1989, 111, 5542–5551. (c) Grownwald, O.; Shinkai, S. *Chem. Eur. J.* 2001, 7, 4328–4334. (d) Tiller, J. C. *Angew. Chem., Int. Ed.* 2003, 42, 3072–3075. (e) Samai, S.; Dey, J.; Biradha, K. *Soft Matter* 2011, 7, 2121–2126. (f) Bag, B. G.; Dinda, S. K.; Dey, P. P.; Mallia, V. A.; Weiss, R. G. *Langmuir* 2009, 25, 8663–8671. (g) Braga, D.; d’Agostino, S.; D’Amen, E.; Grepioni, F. *Chem. Commun.* 2011, 47, 5154–5156. (h) Byrne, P.; Lloyd, G. O.; Applegarth, L.; Anderson, K. M.; Clarke, N.; Steed, J. W. *New J. Chem.* 2010, 34, 2261–2274.

4. Hu, C.; Englert, U. *Angew. Chem., Int. Ed.* 2005, 44, 2281–2283.

5. (a) Denoyel, R.; Rey, E. S. *Langmuir* 1998, 14, 7321–7323. (b) Bekiari, V.; Lianos, P. *Chem. Mater.* 2006, 18, 4142–4146. (c) Inomaru, K.; Kiyoto, J.; Yamanaka, S. *Chem. Commun.* 2000, 903–904. (d) Sayari, A.; Hamoudi, S.; Yang, Y. *Chem. Mater.* 2005, 17, 212–216. (e) Arkas, M.; Tsiourvas, D.; Paleos, C. M. *Chem. Mater.* 2005, 17, 3439–3444. (f) Tu, T.; Bao, X.; Assenmacher, W.; Peterlik, H.; Daniels, J.; Dötz, K. H. *Chem.–Eur. J.* 2009, 15, 1853–1861. (g) Piepenbrock, M.-O. M.; Lloyd, G. O.; Clarke, N.; Steed, J. W. *Chem. Rev.* 2010, 110, 1960–2004.

6. (a) Zhang, S.; Yang, S.; Lan, J.; Yang, S.; You, J. *Chem. Commun.* 2008, 6170–6172. (b) Sambri, L.; Cucinotta, F.; Paoli, G. D.; Stagni, S.; Cola, L. D. *New J. Chem.* 2010, 34, 2093–2096. (c) Piepenbrock, M.-O. M.; Clarke, N.; Steed, J. W. *Soft Matter* 2011, 7, 2412–2418.

7. (a) Pal, A.; Shrivastava, S.; Dey, J. *Chem. Commun.* 2009, 6997–6999. (b) Lloyd, G. O.; Steed, J. W. *Nat. Chem.* 2009, 1, 437–442. (c) Piepenbrock, M.-O. M.; Clarke, N.; Steed, J. W. *Soft Matter* 2010, 6, 3541–3547.

8. Teng, M.J.; Jia, X.R.; Yang, S.; Chen, X.F.; Wei, Y. Reversible tuning luminescent color and emission intensity: A dipeptide-based light-emitting materials. *Adv. Mater.* 2012, 24, 1255–1261. [CrossRef] [PubMed]

9. Chi, G.; Zhang, X.Q.; Xu, B.J.; Zhou, X.; Ma, C.P.; Zhang, Y.; Liu, S.W.; Xu, J.R. Recent advances in organic mechanofluorochromic materials. *Chem. Soc. Rev.* 2012, 41, 3878–3896. [CrossRef] 9

10. Zhang, X.Q.; Chi, Z.G.; Zhang, Y.; Liu, S.W.; Xu, J.R. Recent advances in mechanochromic luminescent metal complexes. *J. Mater. Chem. C* 2013, 1, 3376–3390. [CrossRef]

11. Sagara, Y.; Yamane, S.; Mitani, M.; Weder, C.; Kato, T. Mechanoresponsive luminescent molecular assemblies: An emerging class of materials. *Adv. Mater.* 2016, 28, 1073–1095. [CrossRef] [PubMed]

12. Reus, C.; Baumgartner, T. Stimuli-responsive chromism in organo phosphorus chemistry. *Dalton Trans.* 2016, 45, 1850–1855. [CrossRef] [PubMed]

13. Wiggins, K.M.; Brantleya, J.N.; Bie-lawski, C.W. Methods for activating and characterizing mechanically responsive polymers. *Chem. Soc. Rev.* 2013, 42, 7130–7147. [CrossRef] [PubMed]
14. Zhao, J.; Chi, Z.H.; Zhang, Y.; Mao, Z.; Yang, Z.Y.; Ubba, E.; Chi, Z.G. Recent progress in the mechanofluoro chromism of cyano ethylene derivatives with aggregation-induced emission. *J. Mater. Chem. C* 2018, 6, 6327–6353. [CrossRef]
15. Teng, M.J.; Jia, X.R.; Yang, S.; Chen, X.F.; Wei, Y. Reversible tuning luminescent color and emission intensity: A dipeptide-based light-emitting materials. *Adv. Mater.* 2012, 24, 1255–1261. [CrossRef] [PubMed] 2. Chi, G.; Zhang, X.Q.; Xu, B.J.; Zhou, X.; Ma, C.P.; Zhang, Y.; Liu, S.W.; Xu, J.R. Recent advances in organic mechanofluorochromic materials. *Chem. Soc. Rev.* 2012, 41, 3878–3896. [CrossRef] 3. Zhang, X.Q.; Chi, Z.G.; Zhang, Y.; Liu, S.W.; Xu, J.R. Recent advances in mechanochromic luminescent metal complexes. *J. Mater. Chem. C* 2013, 1, 3376–3390. [CrossRef] 4. Sagara, Y.; Yamane, S.; Mitani, M.; Weder, C.; Kato, T. Mechanoresponsive luminescent molecular assemblies: An emerging class of materials. *Adv. Mater.* 2016, 28, 1073–1095. [CrossRef] [PubMed]
16. Reus, C.; Baumgartner, T. Stimuli-responsive chromism in organophosphorus chemistry. *Dalton Trans.* 2016, 45, 1850–1855. [CrossRef] [PubMed] 6. Wiggins, K.M.; Brantleya, J.N.; Bie-lawski, C.W. Methods for activating and characterizing mechanically responsive polymers. *Chem. Soc. Rev.* 2013, 42, 7130–7147. [CrossRef] [PubMed]
17. Luo, J.D.; Xie, Z.L.; Lam, J.W.Y.; Cheng, L.; Chen, H.Y.; Qiu, C.F.; Kwok, H.; Zhan, X.W.; Liu, Y.Q.; Tang, B.Z. Aggregation-induced emission of 1-methyl-1,2,3,4,5-pentaphenylsilole. *Chem. Commun.* 2001, 21, 1740–1741. [CrossRef]
18. Jadhav, T.; Dhokale, B.; Mobin, S.M.; Misra, R. Mechanochromism and aggregation induced emission in benzothiazole substituted tetraphenylethylenes: A structure function correlation. *RSC Adv.* 2015, 5, 29878–29884. [CrossRef]
19. Tang, C.; Feng, H.; Huang, Y.Y.; Qian, Z.S. Reversible luminescent nano switches based on aggregation-induced emission enhancement of silver nanoclusters for luminescence turn-on assay of inorganic pyro phosphatase activity. *Anal. Chem.* 2017, 89, 4994–5002. [CrossRef] [PubMed]
20. Liu, L.Y.; Wen, T.; Fu, W.Q.; Liu, M.; Chen, S.M.; Zhang, J. Structure-dependent mechanochromism of two Ag (I) imidazolate chains. *CrystEngComm* 2016, 18, 218–221. [CrossRef] 58. Sudhakar, P.; Neenar, K.K.; Thilagar, P. H-Bond assisted mechanoluminescence of borylated aryl amines: Tunable emission and polymorphism. *J. Mater. Chem. C* 2017, 5, 6537–6546. [CrossRef]
21. Jiang, Y. An Outlook Review: Mechanochromic Materials and Their Potential for Biological and Healthcare Applications. *Mater. Sci. Eng. C* 2014, 45, 682–689.
22. Zhang, X.; Chi, Z.; Zhang, Y.; Liu, S.; Xu, J. Recent Advances in Mechanochromic Luminescent Metal Complexes. *J. Mater. Chem. C* 2013, 1, 3376–3390.
23. Sagara, Y.; Yamane, S.; Mitani, M.; Weder, C.; Kato, T. Mechanoresponsive Luminescent Molecular Assemblies: An Emerging Class of Materials. *Adv. Mater.* 2016, 28, 1073–1095.
24. Sagara, Y.; Kato, T. Mechanically Induced Luminescence Changes in Molecular Assemblies. *Nat. Chem.* 2009, 1, 605–610.
25. Chung, K.; Kwon, M. S.; Leung, B. M.; Wong-Foy, A. G.; Kim, M. S.; Kim, J.; Takayama, S.; Gierschner, J.; Matzger, A. J.; Kim, J. Shear-Triggered Crystallization and Light Emission of a Thermally Stable Organic Supercooled Liquid. *ACS Cent. Sci.* 2015, 1, 94–102

26. Nguyen, N. D.; Zhang, G.; Lu, J.; Sherman, A. E.; Fraser, C. L. Alkyl Chain Length Effects on Solid-State Difluoroboron  $\beta$ -Diketonate Mechanochromic Luminescence. *J. Mater. Chem.* 2011, 21, 8409–8415.
27. Morris, W. A.; Sabat, M.; Butler, T.; Derosa, C. A.; Fraser, C. L. Modulating Mechanochromic Luminescence Quenching of Alkylated Iodo Difluoroboron Dibenzoylmethane Materials. *J. Phys. Chem. C* 2016, 120, 14289–14300
28. Butler, T.; Wang, F.; Sabat, M.; Fraser, C. L. Controlling SolidState Optical Properties of Stimuli Responsive Dimethyl amino Substituted Dibenzoylmethane Materials. *Mater. Chem. Front.* 2017, 1, 1804–1817.
29. Morris, W. A.; Butler, T.; Kolpaczynska, M.; Fraser, C. L. Stimuli Responsive Furan and Thiophene Substituted Difluoroboron  $\beta$ -Diketonate Materials. *Mater. Chem. Front.* 2017, 1, 158–166.
30. (a) Pal, A.; Shrivastava, S.; Dey, J. *Chem. Commun.* 2009, 6997– 6999. (b) Lloyd, G. O.; Steed, J. W. *Nat. Chem.* 2009, 1, 437–442. (c) Piepenbrock, M.-O. M.; Clarke, N.; Steed, J. W. *Soft Matter* 2010, 6, 3541–3547.
31. (a) Zhang, S.; Yang, S.; Lan, J.; Yang, S.; You, J. *Chem. Commun.* 2008, 6170–6172. (b) Sambri, L.; Cucinotta, F.; Paoli, G. D.; Stagni, S.; Cola, L. D. *New J. Chem.* 2010, 34, 2093–2096. (c) Piepenbrock, M.-O. M.; Clarke, N.; Steed, J. W. *Soft Matter* 2011, 7, 2412–2418.
32. (a) Denoyel, R.; Rey, E. S. *Langmuir* 1998, 14, 7321–7323. (b) Bekiari, V.; Lianos, P. *Chem. Mater.* 2006, 18, 4142–4146. (c) Inomaru, K.; Kiyoto, J.; Yamanaka, S. *Chem. Commun.* 2000, 903– 904. (d) Sayari, A.; Hamoudi, S.; Yang, Y. *Chem. Mater.* 2005, 17, 212–216. (e) Arkas, M.; Tsiourvas, D.; Paleos, C. M. *Chem. Mater.* 2005, 17, 3439–3444. (f) Tu, T.; Bao, X.; Assenmacher, W.; Peterlik, H.; Daniels, J.; Dötz, K. H. *Chem.–Eur. J.* 2009, 15, 1853–1861. (g) Piepenbrock, M.-O. M.; Lloyd, G. O.; Clarke, N.; Steed, J. W. *Chem. Rev.* 2010, 110, 1960–2004
- 33 Hu, C.; Englert, U. *Angew. Chem., Int. Ed.* 2005, 44, 2281–2283.
34. Jadhav,T.;Choi,J.M.; Shinde,J.;Lee,J.Y.;Misra,R.Mechanochromismandelectroluminescenceinpositional isomers of tetraphenylethylene substituted phenanthroimidazoles. *J. Mater. Chem. C* 2017, 5, 6014–6020. [CrossRef49. Jadhav,T.;Choi,J.M.; Shinde,J.;Lee,J.Y.;Misra,R.Mechanochromismandelectroluminescenceinpositional isomers of tetraphenylethylene substituted phenanthroimidazoles. *J. Mater. Chem. C* 2017, 5, 6014–6020. [CrossRef]
- 35 . Jadhav,T.;Choi,J.M.; Shinde,J.;Lee,J.Y.;Misra,R.Mechanochromismandelectroluminescenceinpositional isomers of tetraphenylethylene substituted phenanthroimidazoles. *J. Mater. Chem. C* 2017, 5, 6014–6020. [CrossRef(1)30. Liu, T.; Chien, A. D.; Lu, J.; Zhang, G.; Fraser, C. L. Arene Effects on Difluoroboron  $\beta$ -Diketonate
36. Jadhav,T.;Choi,J.M.; Shinde,J.;Lee,J.Y.;Misra,R.Mechanochromismandelectroluminescenceinpositional isomers of tetraphenylethylene substituted phenanthroimidazoles. *J. Mater. Chem. C* 2017, 5, 6014–6020. [CrossRef

# SYNTHESIS AND APPLICATION OF GUANIDINES



## A LITERATURE REVIEW REPORT

SUBMITTED TO THE DEPARTMENT OF CHEMISTRY, GAUHATI UNIVERSITY  
AS A PART OF PARTIAL FULLFILMENT OF THE REQUIREMENTS FOR THE  
DEGREE OF MASTERS OF SCIENCE IN CHEMISTRY

Submitted By,

**PRIYANKU PROTEEM BORAH**

ROLL NO: PS-191-808-0079

REGISTRATION NO : 18096048 (2018-2019)

MSC 4<sup>TH</sup> SEMESTER

DEPARTMENT OF CHEMISTRY,  
GAUHATI UNIVERSITY

*Under the supervision of*

---

**Prof. Prodeep Phukan, Ph.D,**  
**Department Of Chemistry,**  
**Gauhati Univerity**

## **DECLARATION**

I hereby declare that the matter embodied in this literature review entitled, ***“Synthesis and Application of Guanidines”*** is the result of survey of scientific literature carried out by me at the Department of Chemistry, Gauhati University, Guwahati, Assam under the supervision of Prof. Prodeep Phukan, and that it has not been submitted elsewhere for the award of any degree or diploma.

As a general practice of writing scientific reports, due acknowledgement has been made to all the authors whose works have been discussed in this survey and unintentional omission, if any, is highly regretted.

Date: 06/09/2021

Place: Department Of Chemistry,  
Gauhati University.



**(Priyanku Proteem Borah)**

M.Sc. 4<sup>th</sup> Semester

**Prodeep Phukan, PhD**

**Professor, Department Of Chemistry,  
Gauhati University, Guwahati-781014, Assam, India  
Ref \_\_\_\_\_**

**Email:pphukan@gauhati.ac.in  
Tel +91-361-2570535(O)**

**Date:**

**To whom it may concern**



This is to certify that **Priyanku Proteem Borah**, a student of the Department Of Chemistry, Gauhati University, Assam has completed this literature review for the partial fulfillment of the requirements for the award of the degree of Masters of Science in Chemistry, 2021 under my guidance on the topic entitled, “ **Synthesis and Application of Guanidines**”.

.....

**Prodeep Phukan**

## **ACKNOWLEDGEMENT**

First and foremost, I would like to thank **Dr.Citrani Medhi**, professor and HOD, to provide us with the opportunity to conduct this literature review in home .

I feel immensely privileged in expressing deep sense of gratitude to my esteemed guide, **Prodeep Phukan**, for his inspiring and invaluable guidance rendered in carrying out my literature review. He has been a constant source of inspiration and invaluable guidance and supervision without which my tasks of performing the literature review wouldn't have been possible. I wish to express my deep sense of gratitude and heartfelt thanks to him.

My heartfelt thanks goes to **Krishnamoni Deka** for his constant help and encouragement in this literature review.

Date: 06/09/2021

Place: Department Of Chemistry

Gauhati University



**(Priyanku Proteem Borah)**

M.Sc. 4<sup>th</sup> semester



## CONTENT

<b>1. INTRODUCTION</b>	<b>6-7</b>
1.1. Chemical Structure	
<b>2. SYNTHESIS OF GUANIDINES</b>	<b>8-13</b>
2.1. Various Synthetic Routes	
2.2. General Procedure For The Guanylation	
2.3. Importance Of Guanidines	
<b>3. APPLICATIONS OF GUANIDINES</b>	<b>14-36</b>
3.1. Industry	
3.2. Biochemistry	
3.3. Medicinal And Drugs Developement	
3.3.1. Muscle Weakness And Tiredness	
3.3.2. Drugs For Central Nervous System	
3.3.3. $\beta$ Secretase Inhibitors	
3.3.4. Other CNS Agents	
3.3.5. Cardiovascular Drugs & Antihypertensive Drugs	
3.3.6. Antihistamine Drugs & Histamine Receptors	
3.3.7. Antidiabetic Drugs	
3.3.8. Antibiotic Drugs	
3.3.9. Anti-inflammatory Drugs	
3.3.10. Antithrombotic Drugs	
3.3.11. Anticancer Guanidines	
3.3.12. Antiviral Guanidines	
3.3.13. Antibacterial Drugs	
3.3.14. Antiprotozoal Drugs	
3.3.15. Treatment Of Pain: Analgesic Agents	
3.3.16. Influenza Inhibitors	
3.3.17. Anti Obesity Drugs	
3.3.18. Anticoagulant	
3.3.19. Fungicidal Guanidines	
3.3.20. Inhibitors of $\text{Na}^+/\text{H}^+$ Exchanger	
3.3.21. Inhibitors of NO Synthase	
3.3.22. Guanidinium Based Transporters & Vectors	
3.4. Guanidinium Derivative As Catalysts	
3.5. Guanidinium Sweeteners	
3.6. Polymers & Dendrimers Bearing Guanidine Moieties	
3.7. Metal Complexes & Organoelement Derivatives Of Guanidine	
<b>4. CONCLUSIONS</b>	<b>37</b>
<b>5. REFERENCES</b>	<b>38-42</b>

## 1.INTRODUCTION

Guanidine, also known as Carbamide is a nitrogenous organic base with the formula  $\text{HNC}(\text{NH}_2)_2$ . By property, it is a colourless solid that dissolves in polar solvents. It is found in urine as a normal product of protein metabolism. A guanidine moiety sometimes appears in large organic molecules such as on the side chains of Arginine and it plays an important role in the interaction with enzymes as well as receptors through hydrogen bonding (H-Bonding) and/or electrostatic interaction [1].

The Guanidine functionality is a privileged structure in many natural products, biochemical processes and pharmaceuticals, playing key roles in various biological functions. It has been widely used in the synthesis of heterocyclic compounds incorporating at least two nitrogen atoms, and in the production of plastics and explosives.

Guanidines are found ubiquitously in nature [2-4] where they involve as mediators of specific non-covalent binding in ground state recognition events. They also take part in binding in various catalytic processes. [5]

### 1.1.Chemical Structure:

Guanidine can be thought of as a nitrogenous analogue of carbonic acid by replacing the carbonyl group ( $\text{C}=\text{O}$ ) by a  $\text{C}=\text{NH}$  group and each hydroxyl ( $\text{OH}$ ) is replaced by a  $\text{NH}_2$  group [6]. A detailed crystallographic analysis of guanidine was carried out 148 years after its first synthesis, despite its simplicity [7]. In 2013, the positions of the hydrogen atoms along with their displacement parameters were determined accurately with the use of single crystal neutron diffraction. [8]

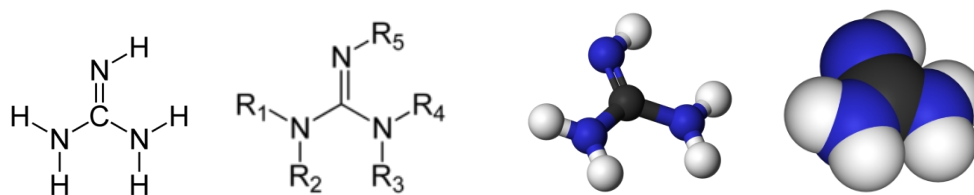


**Figure 1 :** Various 2D and 3D structures of Guanidine and substituted Guanidine

Considering the viewpoint of structural chemistry, Guanidines and its derivatives can be represented as the molecules consisting simultaneously of two functionalities- amination and imine as shown as the following figures

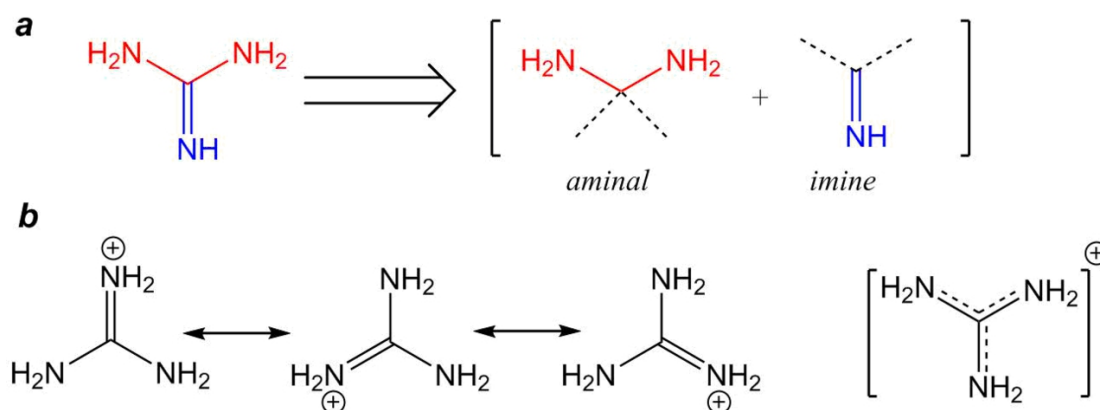


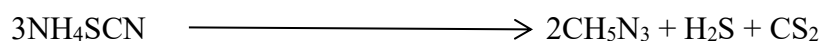
**Figure 2.** Formal presentation of the guanidine structure (**a**) and the resonance structures of its protonated form (**b**).

The kind of presentation cited above gives an insight into the chemical properties of guanidine as well as its derivatives, featuring both its nucleophilic and electrophilic properties[9].

## 2. SYNTHESIS OF GUANIDINES

Guanidine can be obtained from natural sources, being first isolated via the degradation of guanine by Adolph Strecker[10]. In 1861, it was first synthesised by oxidative degradation of an aromatic natural product, the guanine which was isolated from Peruvian guano (accumulated excrement of seabirds and bats, as a manure, guano is highly effective fertilizer due to its exceptionally high content of nitrogen, phosphate and potassium).[11]

A gentle preparation method of guanidine is the thermal decomposition of dry ammonium thiocyanate in anhydrous condition:



The commercial route involves a two step process which starts with the reaction of dicyandiamine with ammonium salts. Via the intermediacy of biguanidine, this ammonolysis step affords salts of the guanidinium cation. Second step involves the treatment of salt with base such as sodium methoxide.[10]

The nitrates, hydrochloride, carbonates and sulfates are the most popular guanidine salts which are very much stable crystalline solids. They are produced industrially either by the chemical method (melting of ammonium salt with urea) or from the urea production wastes. One of the guanidinium salt viz. guanidinium isocyanate was tested against COVID-19 as a lysis buffer[12].

## 2.1. Various Synthetic Routes

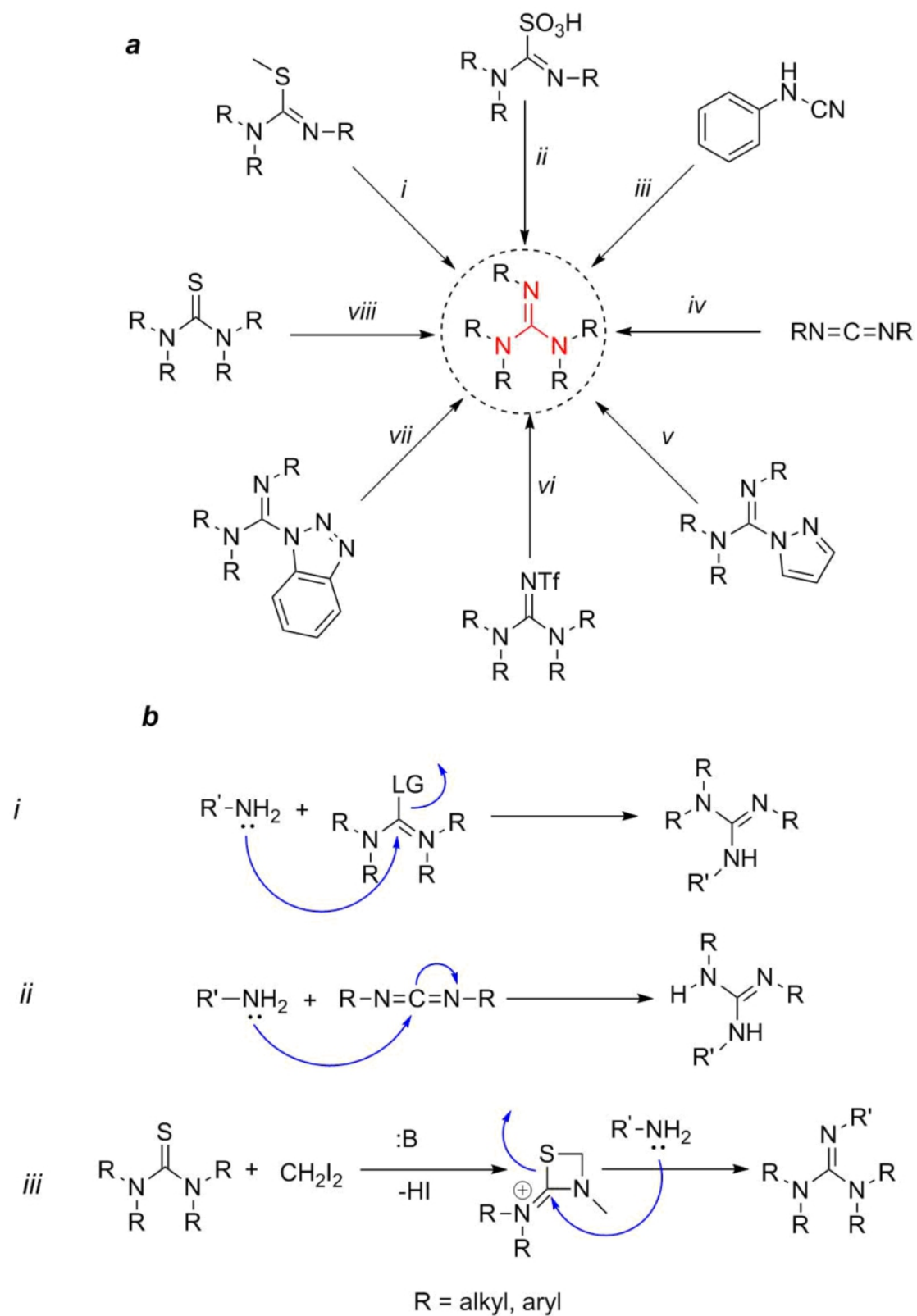
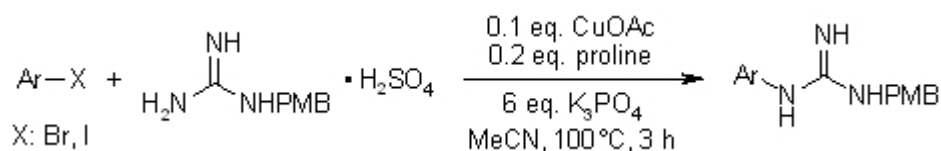


**Figure 3.** Main methods for the synthesis of guanidine derivatives (**a**) and mechanisms of the presented reactions (**b**).

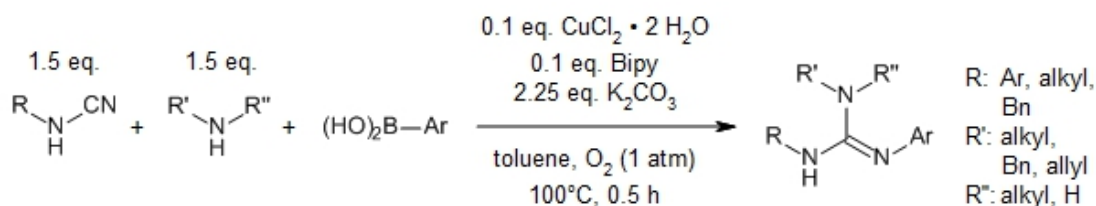
All the reactions cited above, in general, can be classified into two types viz. Nucleophilic substitution and nucleophilic addition (Figure 3b).

- I. Hence, method (i) is the classical method of substitution of thiourea ylides with amine [13] or an analogous process with thiourea and Mukaiyama's reagent [14].
- II. Method (ii) consists of substitution of thiourea trioxide with amines [15,16].
- III. Method (v) is the substitution of a pyrazole derivative with amine [17].
- IV. Methods (vi) [18] and (vii) [19] are the nucleophilic substitution of a leaving group of guanilating reagent with an amino group.
- V. Method (iii) is the addition of amines to cyanamides [20].
- VI. Method (iv) is attributed to the addition to carbodiimides [21].
- VII. Method (viii) consists of addition of diiodomethane to a thiourea derivative in the presence of a base followed by the opening of the four membered ring 1,3-thiazetidine ring with an amine [22].

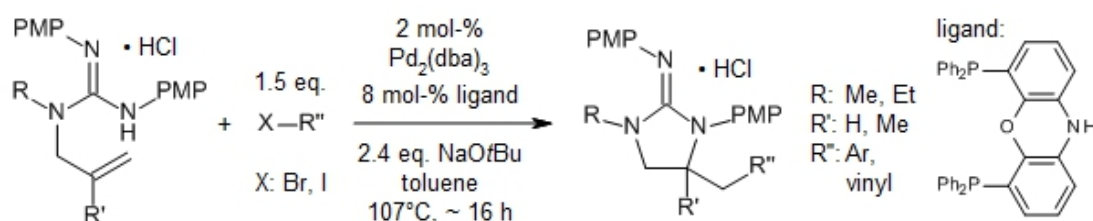
P-methoxybenzyl (PMB) guanidines are used as guanidinylation agents to give prominent yields of various aryl and heteroaryl guanidines (modified Ullmann reaction) [23].



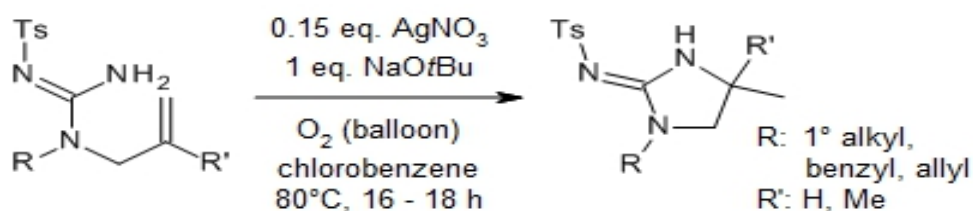
A simple and rapid three component copper catalysed synthesis of trisubstituted N-aryl guanidines involving cyanamides, arylboronic acids and amines is carried out in the presence of  $\text{K}_2\text{CO}_3$ , a catalytic amount of  $\text{CuCl}_2 \cdot 2\text{H}_2\text{O}$ , bipyridine and oxygen (1 atm) [24].



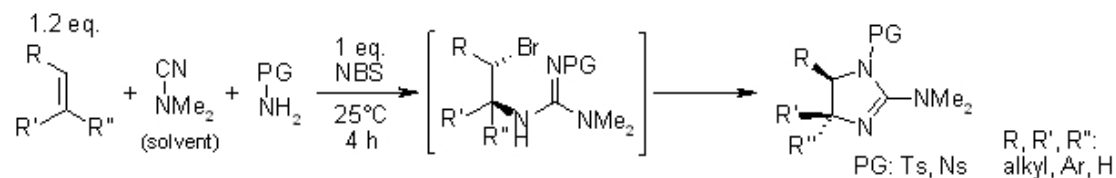
Alkene carboamination reactions catalysed by Palladium between acyclic N-allyl guanidines and aryl or alkenyl halides gives substituted 5-membered cyclic guanidines in good yield.[25]



A hydroamination of tosyl protected N-allylguanidines catalysed by Silver provides substituted cyclic guanidines in good yield.[26].

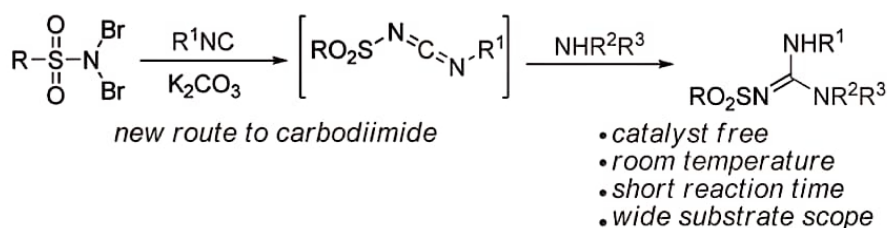


A novel electrophilic one pot reaction of an olefin, a cyanamide, an amine, and N-bromosuccinimide enables the synthesis of a large number of guanidine derivatives in very prominent yield.[27]

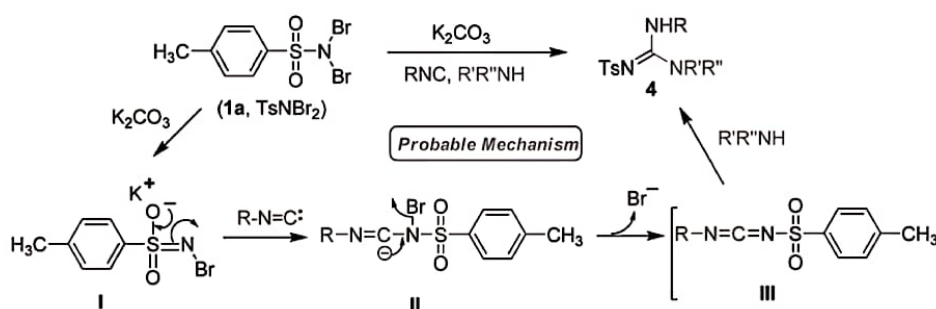


According to Phukan *et al.* N,N',N''-trisubstituted acyclic guanidines can be synthesised by utilizing N,N-dibromoarylsulfonamides without the use of any catalyst. This reaction proceeds through the generation of carbodiimide intermediate

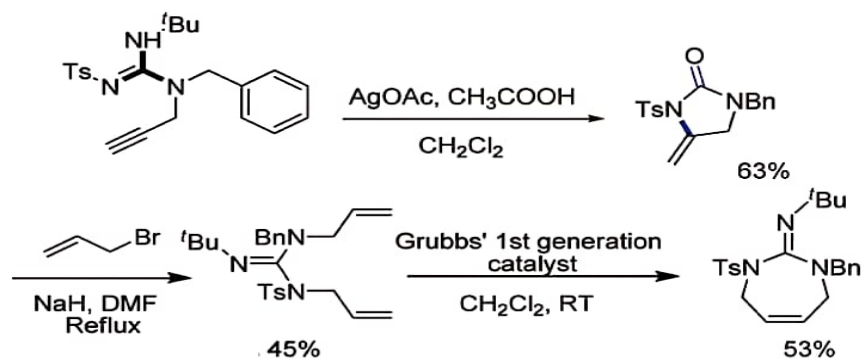
in-situ at room temperature.(Cascade synthesis of N,N',N''-trisubstituted acyclic guanidines.[28]



Another probable route for the synthesis of guanidine is through the generation of a carbodiimide intermediate(III) as shown in the following schematic reaction,[28]



Another method includes synthesis of seven membered cyclic guanidines via a diallylation along with ring metathesis to generate 1,3-diazapine derivative.[28]





## **2.2.General Procedure For The Guanylation**

The starting thiourea, the amine (1,1 equiv) and triethylamine (2.2 equiv) is to be dissolved in dimethyl formamide (5 mL / mmol substrate) and the mixture is to be cooled down in an ice bath. Mercury (II) chloride (1.1 equiv) is to be added and the mixture is to be stirred for 20 Min. On completion of the reaction, (judged by TLC) the reaction mixture is to be diluted with ethyl acetate and filtered through celite, washing the celite cake with additional ethyl acetate. The filtrate is to be washed with water, then with brine and then the organic phase drying with  $\text{MgSO}_4$ . [29,30]

## **2.3.Importance Of Guanidine Group**

The Guanidine moiety is found in arginine amino acids which is found in a number of enzyme active sites and cell recognition motifs. Horseradish peroxidase, fumarate reductase and creatine kinase [31] are some examples of enzymes that contain arginine containing active sites. The tripeptide sequence Arg-Gly-Asp (RGD) is a common cell recognition motif which is responsible for the binding of the integrin receptors. This sequence has been used as a lead structure for the development of different integrin antagonists, while carboxylic guanidino analogs are used as influenza neuroaminidase inhibitors. Guanidinium based molecules are also extensively used as cardiovascular drugs, antihistamines, anti-inflammatory agents, antidiabetic, antibacterial, antifungal, antiprotozoal and other antiparasitic drugs and antiviral drugs.

### 3. APPLICATIONS OF GUANIDINES

Over the past couple of decades, the interest of guanidinium group in industrial, biological, pharmaceutical and supramolecular applications has been ignited. They are valuable precursors of numerous medically important molecules and are assets in biological research. A large number of natural and synthetic guanidine compounds are being used as therapeutic compounds having broad spectrum of medical activity. The biguanidine group also appears in a number of important therapeutic agents [32]. A general explanation of the usefulness of guanidines and its derivatives are discussed as below:

#### 3.1. Industry

The main salt of commercial interest is the nitrate  $[C(NH_2)_3]NO_3$ . It is used as a propellant for example in the airbags.

#### 3.2. Biochemistry

Guanidine exists protonated, as guanidinium in solution at physiological pH. Guanidinium Chloride has chaotropic properties and is used to denature proteins. Guanidinium Chloride is known to denature proteins with a linear relationship between concentration and free energy of unfolding. In aqueous solutions containing 6M Guanidinium Chloride, almost all proteins lose entirely their secondary structure and become randomly coiled peptide chains. Guanidinium thiocyanate is also used on various biological samples due to its denaturing effect. Guanidinium chloride [33] is used as an adjuvant in the treatment of botulism, introduced in 1968 [34].

### **3.3. Medicinal and Drugs Development**

#### **3.3.1. Muscle Weakness And Tiredness**

Guanidine is used to treat muscle weakness and tiredness that is caused by the Eaton Lambert syndrome. The Eaton-Lambert syndrome is an autoimmune disorder which affects directly the nervous system. Guanidine works on the nervous system to restore the muscle strength.

#### **3.3.2. Drugs For Central Nervous System**

Neuropeptide Y (NPY) plays a significant role as a neurotransmitter in the central as well as peripheral nervous system. In human, four receptor subtypes referred as NPY-Y1, Y2, Y4 and Y5 receptors, mediate the biological effects of NPY. NG-Acyl argininamides are NPY Y1 receptors (Y1R) antagonist. In Central Nervous System activation of Y1R produces the sedative effects and it is involved in the stimulation of food intake.

#### **3.3.3. $\beta$ -secretase Inhibitors:**

Alzheimer's disease (AD) is the most common form of Dementia that affects more than 20M people worldwide.  $\beta$ -secretase (BACE-1, Beta Amyloid Cleaving Enzyme-1) is a member of the pepsin like membrane-anchored aspartic protease which generates the N-terminus of amyloid  $\beta_{42}$ .

BACE-1 is considered to be the molecular target for the therapeutic intervention in AD and both of its active as well as inhibitor-bound forms have been elucidated by X-ray crystallography[35]. Recently low molecular weight, non-peptide non substrate related thiazol-2-yl-guanidine which contains compounds (formula 1, figure 4) and their pharmaceutically acceptable salt has been

patented for the prevention of A $\beta$ -related pathologies, such as AD, Down's syndrome pre-senile and senile dementia,  $\beta$ -amyloid angiopathy, cerebral amyloid angiopathy, mild cognitive impairment (MCI), memory loss, neurodegradation, dementia of mixed vascular and degenerative origin, hereditary cerebral hemorrhage, progressive supranuclear palsy or cortical basal degradation.[36]

Along with these, a series of substituted acylguanidine derivatives (formula 1 and 2, figure 4) are found to be the effective inhibitors for the production of the  $\beta$ -amyloid peptide from the  $\beta$ -amyloid precursor protein ( $\beta$ -APP)[37-41]. These compounds are useful for the treatment of conditions responsive to inhibition of  $\beta$ -AP in patients suffering AD and Down's syndrome.

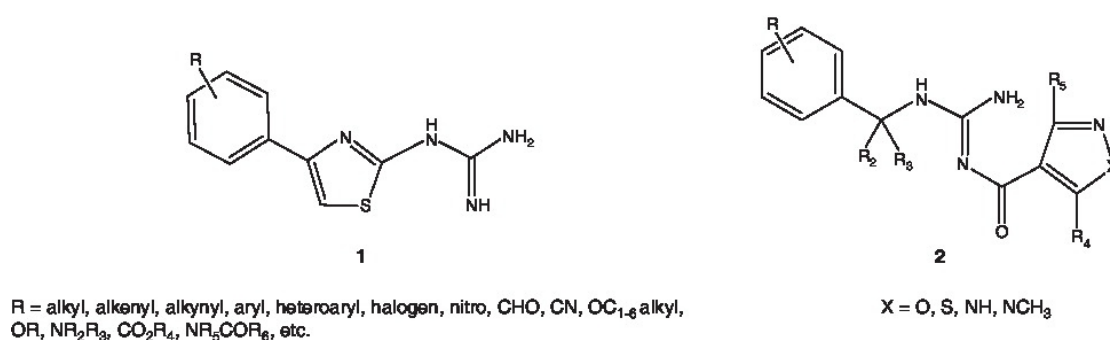


**Figure 4 : Some substituted guanidines acting as CNS agents**

### 3.3.4. Other CNS Agents

N,N' disubstituted guanidine derivatives eg. N-(adamantan-1-yl)-N'-(p-iodophenyl) guanidine is found to show high binding affinity to the sigma-receptor of isolated mammalian brain membrane and were claimed to be effective for the treating human beings who have been suffering from psychiatric mental illness.[42]

### **3.3.5.Cardiovascular Drugs & Antihypertensive Drugs**

Some of the widely used and well known examples of guanidine based cardiovascular and antihypertensive drugs include- Triamterene (potassium sparing diuretic that promotes the loss of sodium and water from the body without depleting potassium), Guanfacine(lower the blood pressure by activating alpha receptors in the central nervous system which opens then peripheral arteries), Doxazosin mesylate, Amiloride, Prazosin, Clonidine, Guanabenz, Guanethidine, Terazosin(alpha blockers that lowers the blood pressure by relaxing blood vessels), Moxonidine, Aproclonidine, Guanaxone, Guanazodine, Trimazosin, Guanadrel and Guanochlor.[43]

### **3.3.6.Antihistamine Drugs And Histamine Receptors**

Cimetadine,Famotidine and Dispacamide are well known medicines used for the treatment of ulcer.

Histamine H<sub>1</sub>,H<sub>2</sub>,H<sub>3</sub> and H<sub>4</sub> receptors which belong to one family of rhodopsin like class A GPCRs and those strongly differ in various fields such as ligand binding , signaling pathways as well as their functions. Ligands of H<sub>1</sub> and H<sub>2</sub> receptors have been utilised in medical practices for treating allergic diseases and gastric ulcer respectively, whilst H<sub>3</sub> receptor agonists have been in the clinical phase with probable indications for treating numerous diseases such as cognitive impairment,schizophrenia,narcolepsy, attention deficit hyperactivity disorder(ADHD),seizure and obesity[44].

Recently,N<sup>G</sup>-acetylated imidazolylpropylguanidine (AIPGs) 14 (figure 5) has been synthesized as a new form of H<sub>2</sub> receptor agonists which is analogous to a prototypic arpromidine(ARP), and it was utilised for probing ligand - specific histamine H<sub>1</sub> and H<sub>2</sub> receptor conformations[45]. In addition, Change in the quality

of the effect have been observed and the newly designed compounds have been proved to be the potent H<sub>2</sub>R agonists and partial hH<sub>4</sub>R agonists.[46,47]

Histamine H<sub>4</sub> receptors are important for the human immune system and H<sub>4</sub> agonists are potential drugs for treating inflammatory diseases for example asthma and allergy. Guanidine compounds that act as human  $\beta$ -tryptase inhibitors i.e. inhibitors of a structurally unique serine protease with trypsin like activity that is released from mast cell secretory granules, may find medical and pharmaceutical applications as anti-inflammatory drugs or anti-allergic drugs. Recently, a new tryptase inhibitor has designed which is based on a library of 2,5-diketopiperazine group by the Spanish researchers[48].

### **3.3.7.Antidiabetic Drugs**

Some of the effective guanidine based drugs against diabetes are : Phenformin, 3-guanidinopropionic acid and Metformin. It is reported that, hetero-aryl guanidine derivatives also found to exhibit the antidiabetic activity. Several substituted guanidines including N-(2-methyl,5-Chloro-1H-indol-3-yl)-guanidine are founds as effective anti-diabetic compound via several studies.[49]

B-Carbolide derived guanidine alkaloid viz. tiruchenduramine along with its derivatives extracted from Indian ascidian *Synocium macroglossum* have been proved to be effective as  $\alpha$ -glucosidase inhibitors(it retards the use of dietary carbohydrates for suppressing the postprandial hyperglycemia,PPHG) and are claimed to be effective in the management of diabetic disorders in human[50].Cyclic guanidines having 2-iminobenzimidazole structure have also been designed and claimed as effective agents for the treatment, prevention and delaying the onset of type2 diabetes mellitus [51].Novel trisubstituted guanidine, urea or thiourea derivatives have also been claimed to be useful in treating muscular edema related to diabetic retinopathy[52].

### 3.3.8. Antibiotic Drug

Some of the antibiotic drugs are: Streptomycin, Chlorhexidine and Trimethoprim which are mainly used for the urinary tract infection. These are the guanidine derivatives.

Another derivative Polyhexamethylene biguanidine is utilised as a disinfectant for swimming pools, wound care and fabric conditioning. Pyrrolidine bis-cyclic guanidines have been reported to be active against Gram positive methicillin-resistant pathogens viz. *Staphylococcus aureus* (MRSA) [53]. C. Kratzer *et al.* reported a novel polymeric guanidine Akacid plus which exhibits prominent in vitro antimicrobial activity against various strains of bacteria and fungi [54]. Another copolymer of guanidine hydrochloride and hexamethylene diamine along with crosslinking of epichlorohydrin have reported by L. Qian *et al.* That have antimicrobial activity. The presence of four membered ring having the quaternary ammonium group was found to enhance the antimicrobial activity.

### 3.3.9. Anti-inflammatory Drugs

Leucettamine that is extracted from a type of sponge and then synthesised has been shown to possess a significant role as a mediator of inflammation [55]. H. MavarManga *et al.* extracted N1,N2-diisopentylguanidine and N1,N2,N3-triisopropylguanidine from an African plant *Alchornea cordifolia* that exhibited significant anti-inflammatory activity. 3,4-dimethoxyphenethyl-B-guanidine extracted from another plant *10 Aplidium orthium* (New Zealand) is being reported as potential anti-inflammatory compound. [56]

A series of quinoline and quinazoline containing guanidines is described as p56 tyrosine kinase inhibitors, inhibitors of T-cell activation and proliferation and inhibitors of cytokin production. These compounds find its medical uses for the

treatment of autoimmune conditions eg. T-cell mediated inflammatory diseases such as transplant rejection or rheumatoid arthritis, glomerulonephritis and lung sclerosis, psoriasis, inflammatory bowel disease, hypersensitivity reactions of the skin, insulin independent diabetes, atherosclerosis, allergic asthma and the acute rejection of transplant organs.[57].

### **3.3.10. Antithrombotic Agents**

Excessive blood clotting (thrombosis) is a significant factor in cardiovascular diseases eg. acute myocardial infarction, ischemic stroke, disseminated intramuscular coagulation, unstable angina etc. A central role in the thrombosis and homeostasis is being played by thrombin (THR), which is a multifunctional serine protease with the trypsin like specificity along with procoagulant congeners: factor Xa and prothrombinase (pTase).[58]

### **3.3.11. Anticancer Guanidines**

Recent advances in the understanding of physiological and pathological processes that involve cell adhesion molecules (CAMs) including integrins, cadherins, selectins and immunoglobulins that have led to the development of the novel biotherapeutics[59,60]. Therapeutic applications of soluble RGD which contains RGD mimetic compounds include tumor growth, cancer metastasis, osteoporosis and rheumatoid arthritis, thrombosis, occlusive cardiovascular disease, diabetic retinopathy, renal failure, macular degeneration, inflammation and wound healing[58]. Recently a stable RGD peptidomimetic 2-amino-6-[(2-amino-5-guanidino-pentanoyl)amino]hexanoic acid (AAGPAHA) which has been described in patent literatures as a coating of biomaterials and implants with prominent medicinal use as the treatment of cancer[61].



Guanidine containing compounds have also been claimed to inhibit the binding of lymphocyte function associated antigen-1 (LFA-1) to ICAM(cellular adhesion molecules ) and hence could be therapeutically effective for the treatment of diseases or conditions that are mediated by LFA-activity .[62]

1-isoquinolinyguanidine derivative 1 (figure 5) is found to be a suitable candidate for the preclinical evaluation fo treating chronic dermal ulcers[63]. Small nonpeptide diaryl phosphonate 2 (figure5) are significant in antimetastatic therapy[64]. Guanidine Derivative 3 (Figure5) is found to possess a broad spectrum antitumorial activity towards the six cancer cell lines in human- SKBR3 (breast cancer), BT 474 and T47D( breast carcinoma),PC-3 and Ln CAP(prostate carcinoma) along with HT-29(colon Carcinoma).

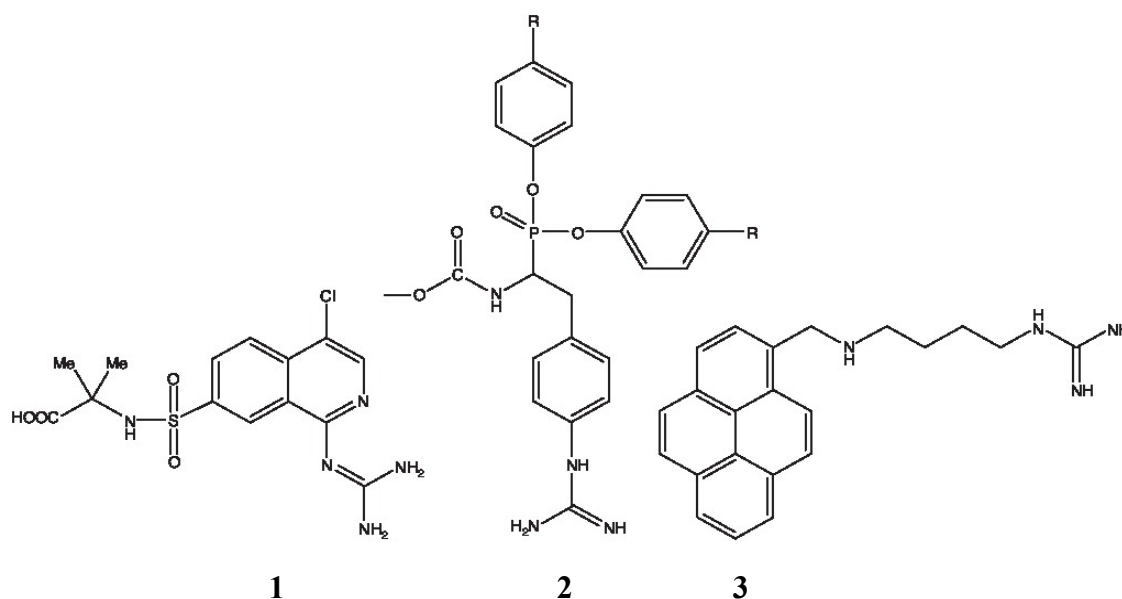


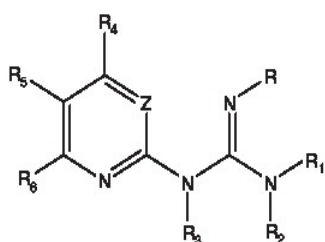
**Figure 5:** Some anticancer guanidine moiety

### 3.3.12. Antiviral Guanidines

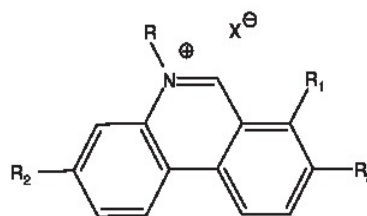
Fomivirsen is being used to treat cytomegalovirus CMV, retinitis and AIDS. 4-carbamoyl-5-(4,6-diamino-2,5-dihydro-1,3,5-triazin-2-yl)imidazole-1- $\beta$ -D-ribofuranoside is also reported to exhibit activity against various viral strands.

A series of pyrimidine-2-yl-guanidines (Figure 6a) has been described in patent literature as the prominent and selective inhibitors of HCV (hepatitis c) replication [65,66]. Chemical modification of ethidium, the well known laboratory strain for double stranded DNA and RNA which shows antiviral and anticancer activity has led to the discovery of new guanidine containing compounds (figure 6b) which binds to DNA less effectively and is therefore less toxic and/or mutagenic but it maintains a high level of antiviral activity. [67]

Since the 1960s, it has been known that guanidine hydrochloride effectively inhibits the replication of many animal and plant viruses. However, zanamivir-the first antiviral drug having guanidine moiety resulting from the structural based drug design discovered by van Itzstein and received FDA approval in 1999 [68]. Guanidinoglycosides, 2deoxystreptamine, paronomycin, neomycin and glucosamine act as potential anti-HIV agents [69]



R = H, C<sub>1</sub>-C<sub>6</sub> alkyl, CN, SO<sub>3</sub>H, SO<sub>2</sub>(C<sub>1</sub>-C<sub>6</sub> alkyl)  
R<sub>1</sub> = Ph, naphthyl, indanyl, 9H-fluorenyl, aryloxy, aryloamino, etc.  
R<sub>2</sub>, R<sub>3</sub>, R<sub>4</sub>, R<sub>5</sub>, R<sub>6</sub> are independently H, halogen, OH, CN, amino, acetyl, alkyl, etc.  
Z = CH, N



R, R<sub>1</sub> = functionalized or unfunctionalized alkyl, alkenyl, alkynyl, aryl, arylalkyl, alkylheteroaryl  
R<sub>2</sub>, R<sub>3</sub> = guanidine, diBoc-guanidine

**Figure 6a and 6b** Antiviral Guanidines

### 3.3.13. Antibacterial Drug

Recently, in view of the rising incidence of a lot of infections caused by antibiotic-resistance bacteria, the discovery and development of novel classes of antibacterial agents is being critically important[70]. Guanidine containing agent with significant activity against MRSA cephalosporin is an example of antibacterial drug bearing 4-[3-(aminoalkyl)-ureido]-1-pyridinium moiety at c-3' carbon atom. The replacement of guanidine with another polar functionality eg. hydroxyl or amino group have led to reduction of antimicrobial activity[71].

Numerous modified guanidine polymers having antimicrobial activity are obtained by the two step synthesis using hexamethylene diamine, guanidine hydrochloride and epichlorohydrin[72]. AKACID Plus is a novel member of cationic family of polymeric antibacterials which is consist of a 3:1 mixture of poly-[2-(2-ethoxy)-ethoxymethyl]-guanidinium chloride. It shows low acute toxicity, antiproliferative effects and broad antimicrobial spectrum against various bacteria, yeasts and filamentous fungi.[73]

### 3.3.14. Antiprotozoal Drug

Guanidine based drugs are also used against the disease that are produced by protozoa or other lower animals. Paludrine and Chlorguanidine are the example antimalarial drugs. Melarsoprol is effectively used for the last stage treatment of human african trypanosomiasis(HAT) or the 'sleeping sickness' that is caused by the protozoan parasites *Trypanosoma brucei*[74]. Woster and coworkers have reported some alkylpolyaminobiguanidines as prominent antiparasomal compounds H Berber et al. synthesised 5-benzyl-6-trifluoromethyl-2,4-diaminopyrimidines and 6-aryl-5-trifluoroethyl -2,4-diaminopyrimidines and these are tested for their in vitro anti-toxoplasmosis activity ( disease produced by protozoa *Toxoplasma gondii*)

Purine derivative of guanidine moiety has been described in patent literature as an agent that is suitable for the treatment and/or prevention of various parasitic infections or infestation in mammalian subjects.[75]

Ptilocaulin derivatives are known as tricyclic guanidine alkaloids extracted from the sponge *Monachora unguifera* has been known to show inhibitory activity against the malaria parasite *Plasmodium falciparum* as well as antiprotozoal activity against *Leishmania donovani* [76].

Novel dicationic diphenyl compounds eg. bisguanidine and bis(2-aminoimidazoline) DNA minor grooves binders is known to show in vitro activity against *Trypanosoma brucei* rhodesiense and *P.falciparum* at the nanomolar concentration range.[77]

High prophylactic antimalarial activity has been described for two novel guanidinoimidazoline-dione derivatives, which can be regarded as cyclic dicarboxamides of chlorproguanil.[78,79]

### **3.3.15.Treatment Of Pain: Analgesic Agents**

Guanidine compounds of general formula 1[80] and 2 (figure 7) have been claimed to act as blockers of neuropeptide FF1 receptor and hence increase the effect of the administered opioids and prevent the development of tolerance to these analgesic drugs.[81,82]

Other cyclic guanidine compounds such as 2-imino-1,2-dihydrobenzimidazole derivatives are potent sodium channel blockers in neuronal mammalian cells and show anesthetic and analgesic activity in the rat. They also block spinal, epidural and/or somatic or autonomic nerve conduction that renders them promising agents for

the treatment and prophylaxis of convulsions, brain or spinal cord trauma or ischemia, neuropathic pain, epilepsy and stroke[83]

Recently, researchers of Roche Palo Alto have developed analgesic and anti-inflammatory agents with guanidine moiety that is incorporated into 2-iminoimidazoline ring system.[84]

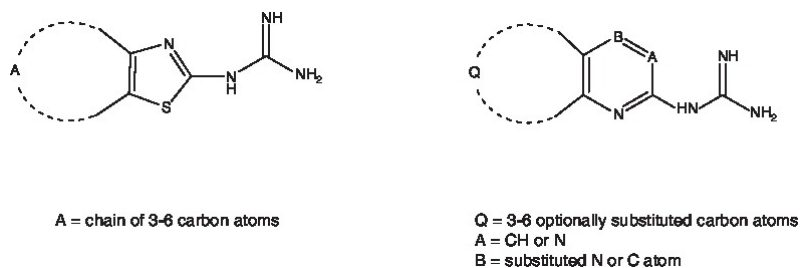


**Figure 7: Analgesics**

### 3.3.16 influenza Inhibitor

Zanamivir-the guanidine containing drug is found to be effective against all types of flu. P.Chand et al. synthesised guanidine derivatives of pyridine and reported as influenza inhibitors.[85]

### 3.3.17 Anti Obesity Drug

Metformin and 3-guanidinopropionic acid are used to control obesity. Aminoguanidines and diaminoguanidines analogues of 3-guanidinopropionic acid are also synthesized and found to be effective as anti-obesity drug[86]. Biguanidines and NG-Acyl argininamides are also reported to regulate the food intake and obesity control.

### 3.3.18. Anticoagulant

Substituted guanidines especially acylguanidines have been reported as thrombin inhibitor (Factor Xa inhibitor) for treating uncontrolled blood coagulation.[87]

### 3.3.19. Fungicidal Guanidines

During the past few decades, because of the increase in HIV infections, organ transplantation, extensive use of broad spectrum antibiotics, hemodialysis and glucocorticosteroids or chemotherapy induced neutropenia along with fungal infections have become potential medical threat[88].

Perhaps one of the most interesting discovery in recent years lies in the area of fungicidal drugs have dealt with novel fungicidal lipopeptide-1[89]. Chitinase is a major structural component of fungi and insects. Mammalian chitinase is implicated in triggering asthma. Chitinase inhibitors have attracted attention as prominent insecticides, fungicides and anti asthmatic drug[90]. A series of simple 4-substituted phenylguanidium derivatives also possess antifungal activity although much lesser than that of dodine(1-dodecylguanidinium acetate) and ketoconazole used as reference compound[91].

### 3.3.20. Inhibitors Of $\text{Na}^+/\text{H}^+$ Exchanger

$\text{Na}^+/\text{H}^+$  exchanger(NHE) system is a mechanism which is utilised in maintaining the intracellular physiological pH. During injuries the accumulation of intracellular protons lead to the activation of  $\text{Na}^+/\text{H}^+$  exchanger, that acts by exchanging intracellular  $\text{Na}^+$  to regulate intracellular pH. Although it is an essential mechanism but the excessive stimulation of NHE enhances  $\text{Na}^+$  concentration. Most of the NHE-1 inhibitors contains acylguanidines structure with quite diverse aryl ring templates having benzene, quinoline, pyrazole and indole etc.[92]

The  $\text{Na}^+/\text{H}^+$  exchanger (NHE) is expressed in different mammalian cell types and is also responsible for intracellular pH and volume regulation. The  $\text{Na}^+/\text{H}^+$  exchanger is activated at the post-ischemic reperfusion and lead to causes  $\text{Ca}^{2+}$  overload that in turn, known to be associated with cellular dysfunction, damage and eniporide necrosis. Inhibitors of  $\text{Na}^+/\text{H}^+$  exchanger eg. Acylguanidines (amiloride, capiporide, sabiporide and azaniporide) act as cardioprotective agents. Along with these inhibitors of NHE1, NHE4 and NHE5 has been known to show cardioprotective activity and NHE3 inhibitors and have been investigated in ischemia induced acute renal failure[93-95]

Guanidines with a condensed tricyclic ring can also be used as effective drug for the treatment of organ disorders which are associated with ischemia and reperfusion, cell proliferative disorders, cardiac hypertrophy and hypertension and diabetes.[96]

Another group of  $\text{Na}^+/\text{H}^+$  exchange inhibitors have been designed and synthesised include N-(3-oxo-3,4-dihydro-2H-benzol[1,4]oxazine-6-carbonyl)guanidines[97], substituted benzoylguanidines[98] and (benzimidazole-2-yl) or (benzimidazol-2-ylthiomethyl)benzoylguanidines[99], which inhibit NHE1-mediated platelet swelling in a concentration dependent manner.

### **3.3.21. Inhibitors Of NO Synthase**

Although NO is an important regulator of various physiological processes such as neurotransmission, smooth muscle contractility, platelet reactivity along with cytotoxic activity of immune cells, but NO over production is responsible for a lot of disease states.

The best known inhibitors of NOS are the non amino acid based compounds eg. guanidine and aminoguanidines derivatives.

Recently, N<sup>G</sup>-aminoguanidine containing amino acid moiety in the side chain have been proved to be a potent NOS inhibitor[100]. Other NOS inhibitor are 2-amino-guanidino-purine[101] , [3-(1H-imidazol-4-yl)propyl]guanidines[102] and *trans*-3,4-cyclopropyl-L-arginine analogues.[103]

### 3.3.22.Guanidinium Based Transporters And Vectors

Guanidinium containing cationic lipids include bis-guanidinium cholesterol derivative eg. BGSC(bis-guanidinium n=spermidine-cholesterol) as well as BGTC(bis-guanidinium-tren-cholesterol) both of them are proved to be highly effective for the gene transformation *in vitro* into a variety of mammalian cell lines when in form cationic liposomers with colipid DOPE(dioleoyl phosphatidylethanolamine)[104]. Lipoplex which is composed of BGDA {pentacosanoic acid (2-[bis-(2-guanidinoethyl)amino]ethylamide)}, DOPE and DNA also demonstrated a high level of transfection *in vitro* as well as resistance to serum.

### 3.4.Guanidinium Derivative As Catalysts

The strong basic properties are the distinctive features of guanidine and its alkyl and cycloalkyl derivatives. These guanidine derivatives are organic bases and are often referred to as the superbases or proton sponges due to its high Bronsted basicity[105,106].

Substituted or sterically hindered guanidine derivatives are potentially used in the fields which require the application of strong nucleophilic bases featuring high solubility in organic solvents , high efficiency, low toxicity and recyclability[107].

The Examples of these bases (compounds 1-14) are presented in the following figure(8) in which guanidine bases 1-8 are widely used in organic synthesis and compounds 9-14 have been obtained recently but hold great promise.



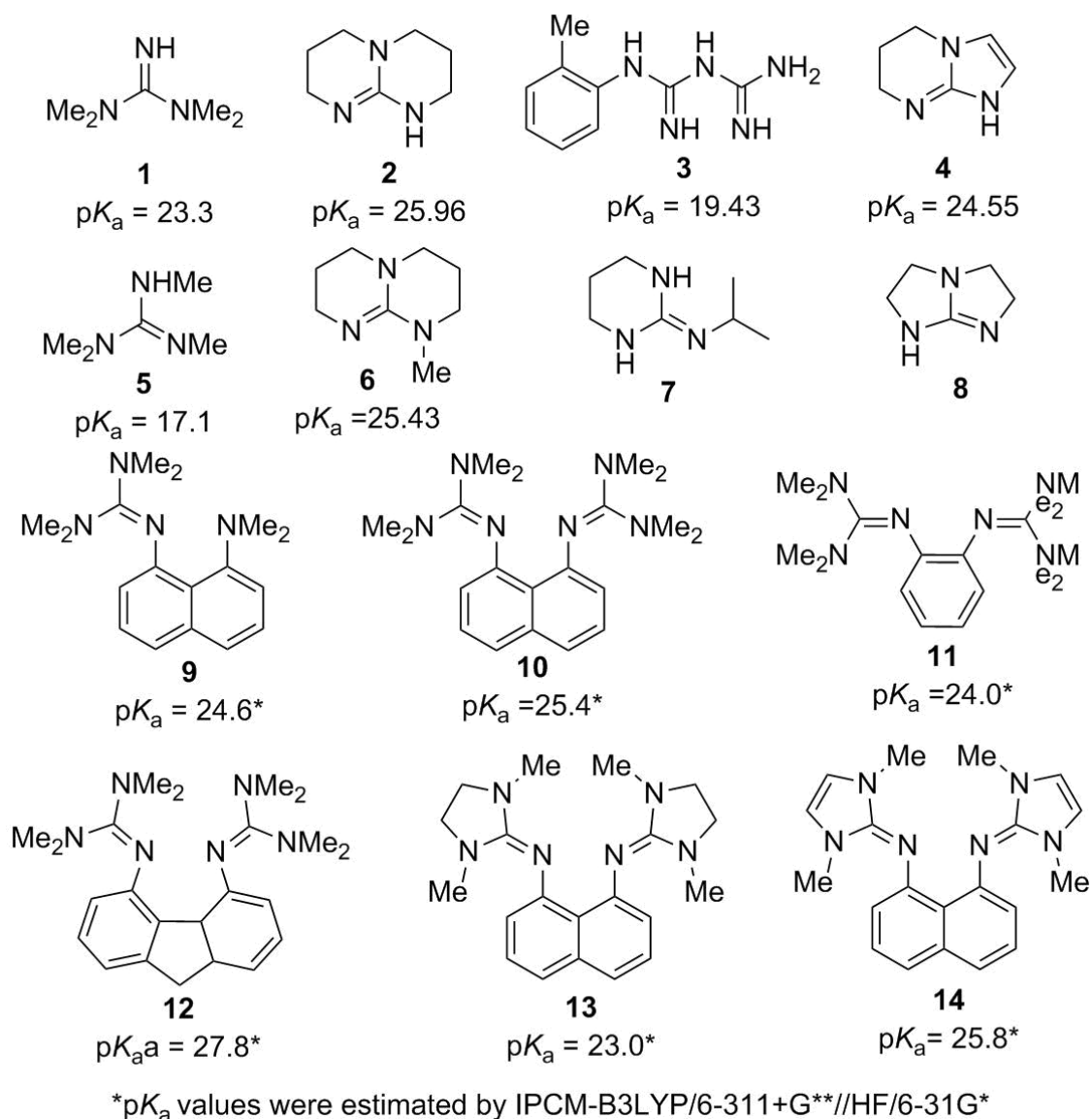


**Figure 8:** Superbases based on guanidine and the values of  $pK_a$  of the conjugated acids.

Bases and superbases derived from guanidine have been found wide application in organic synthesis[108-110] eg. the michael addition of organophosphorous compound[111] , aza-Henry[112], Baylis-Hillman[113] and numerous other classical; reactions including Aldol condensation, Mannich reaction, Claisen rearrangement, Strecker reaction, azidation, silylation of alcohols[114,115].

Most prominent reactions are enantioselective additions of C-,O-,N-,S-, and P-nucleophiles to olefins, $\alpha$ - $\beta$ -unsaturated carbonyl compounds as well as aliphatic esters,lactones,amides and nitro compounds.[116]

In Polymer chemistry these catalysts are extensively used for the controlled living ring opening polymerization of cyclotrisiloxanes[117], ring opening polymerization of caprolactone[118], ring opening polymerization of lactide[119] and living radical polymerization[120].

Guanidine exhibits moderate electrophilic properties .Due to the presence of lone pair at the Nitrogen atom the guanidine units can readily form hydrogen bonding with different substrates including organic and bearing polar electron withdrawing groups.This property of guanidine and its derivatives is actively used in asymmetric catalysis harnessing chiral guanidinium salts.

Several reviews provide detailed consideration of these and other guanidine containing catalyst[121,122].

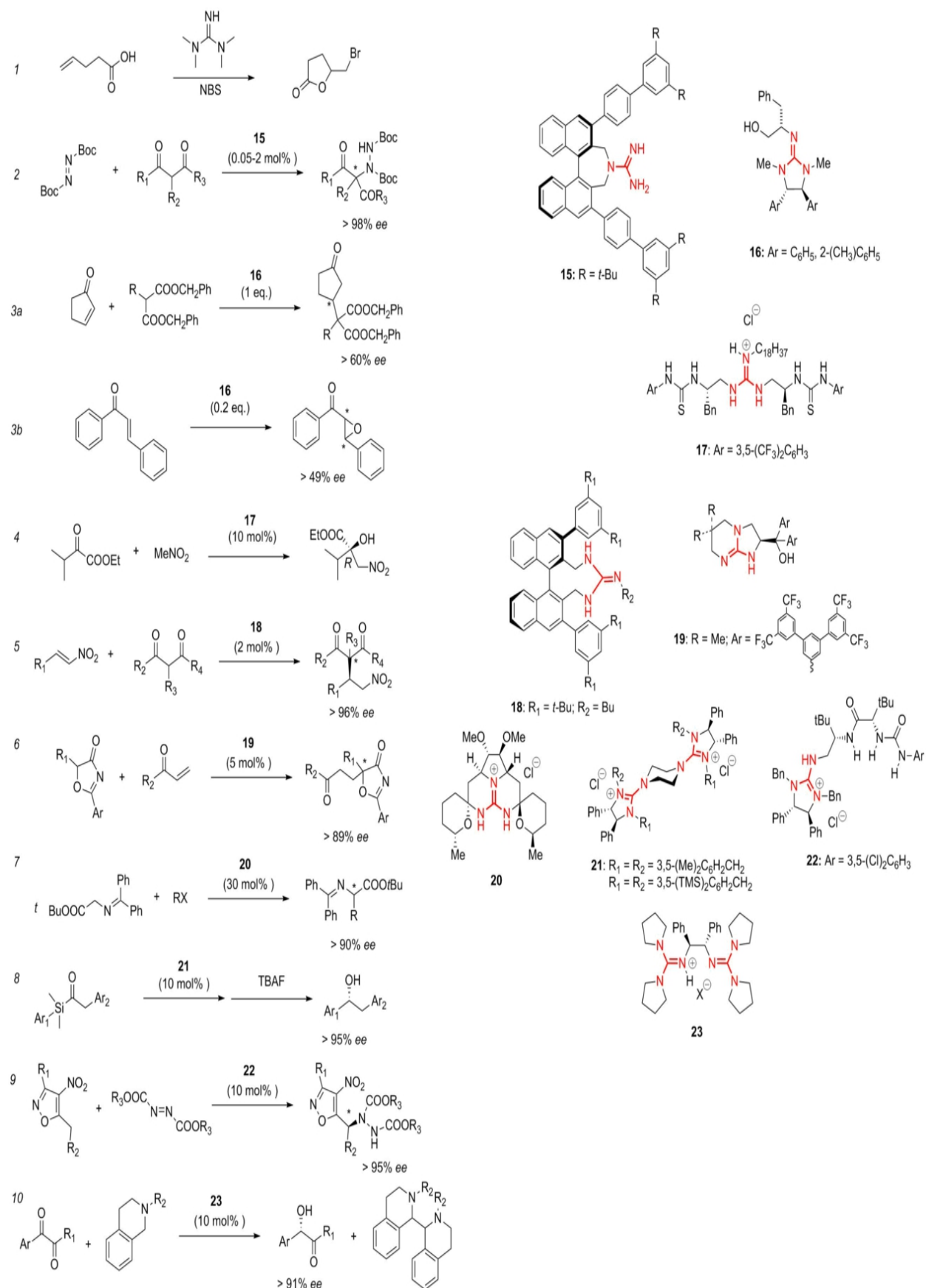


**Figure 9:** Schemes of the reaction catalysed by different guanidine derivatives and the structures of these derivatives.

A recent trend is the functionalisation of the surface of magnetite or ferrite nanoparticles with guanidine moieties. An advantage of these catalytic systems is the simplicity of the production, easy handling and separation by magnetic removal, high catalytic activity, high yields and the possibility of recycling and using green solvents. These heterophase catalysts are effectively used for example for the oxidation of sulfides to sulfoxides[123].

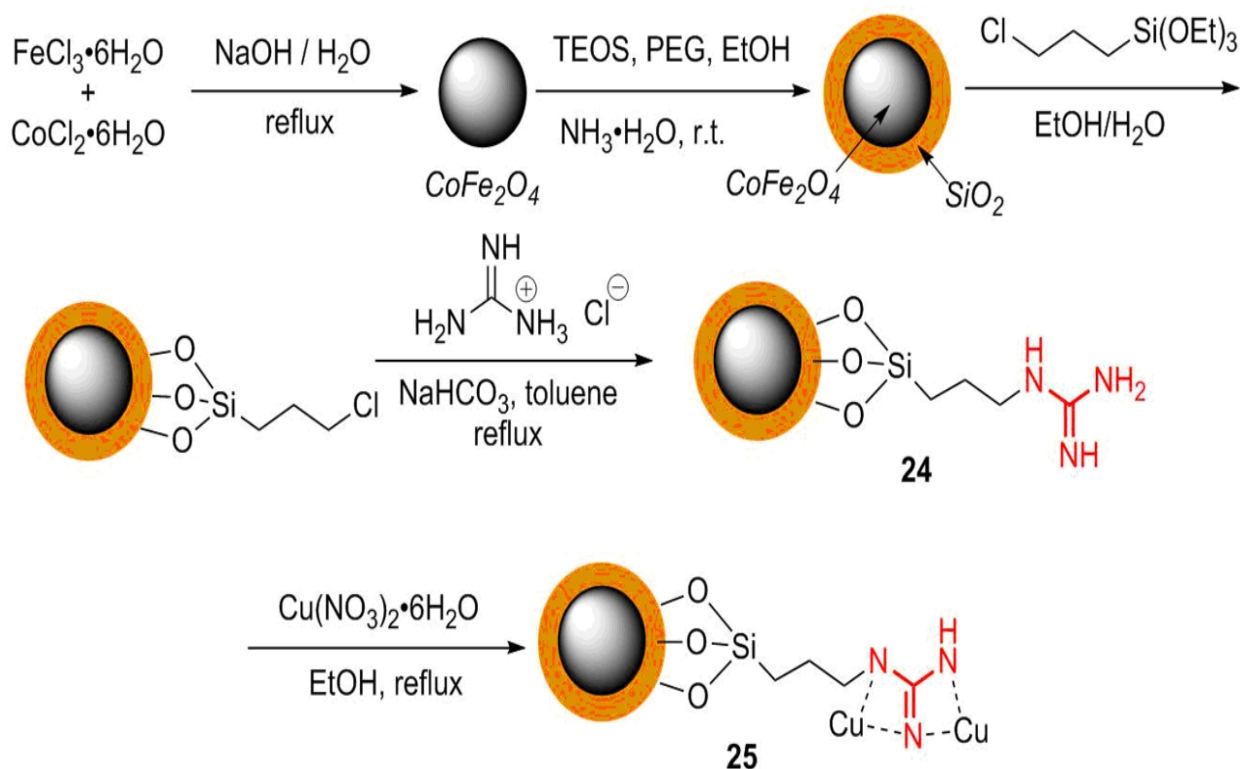


**Figure 10 :** Scheme for the synthesis of  $\text{CoFe}_2\text{O}_4 @ \text{SiO}_2$ -CPTES-guanidine-Cu(II) catalyst nanoparticles

### 3.5. Guanidine Sweeteners

In 1986, Nofre, Tinti and colleagues reported a new series of highly efficient sweeteners viz N-(Carboxymethyl)guanidines. A library of promising and efficient sweeteners were produced [124,125].

To gain further insight into the structure-activity relations of guanidine acting as sweeteners, a series of N-(aryl/alkyl)-N-carboxymethyl-1) substituted guanidines were prepared.

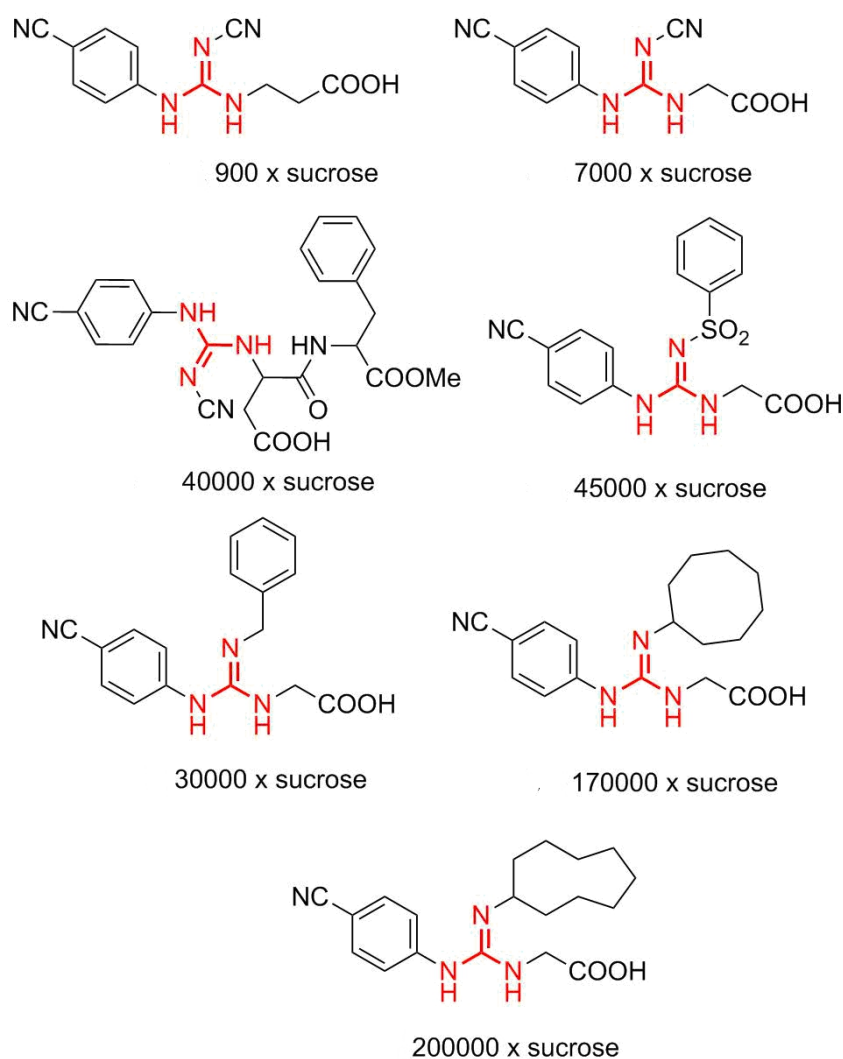


**Figure 11 :** Structures of the sweeteners based on N-(carboxymethyl)guanidines.

### 3.6. Polymers And Dendrimers Bearing Guanidine Moieties

Polyhexamethylene guanidine hydrochloride (PHMG) was one of the first and simplest copolymer which was synthesised in 1954[126] .PHMG is extensively used in various commercial fields such as cosmetics, contact lens solutions, hand cleaners, disinfectants for medical and dental utensils and trays, personal hygiene products, fabric softeners, agricultural equipment, potable water for animals along with surfaces in medical organisations and hospitals. Another uses PHMG is to disinfect beer glasses, in the food processing, to disinfect water in pools as a chlorine free polymer disinfectant, and equipment at brewing plants[127].PHMG exhibits high biological activity against most of the pathogenic microorganisms viz. bacteria,viruses and fungi[128].

During covid-19 pandemic(SARSCoV-19),it was found that PHMG exhibits antiviral activity against coronavirus. Therefore , use of solutions of PHMG with a concentration of 0.2% and above is recommended by the Russian Federal Service for Surveillance on Consumer Rights Protection and Human Wellbeing.

The simplest Guanidine macromolecular systems that can be used as molecular glues are represented in the following figure as polymer brushes and dendrons.

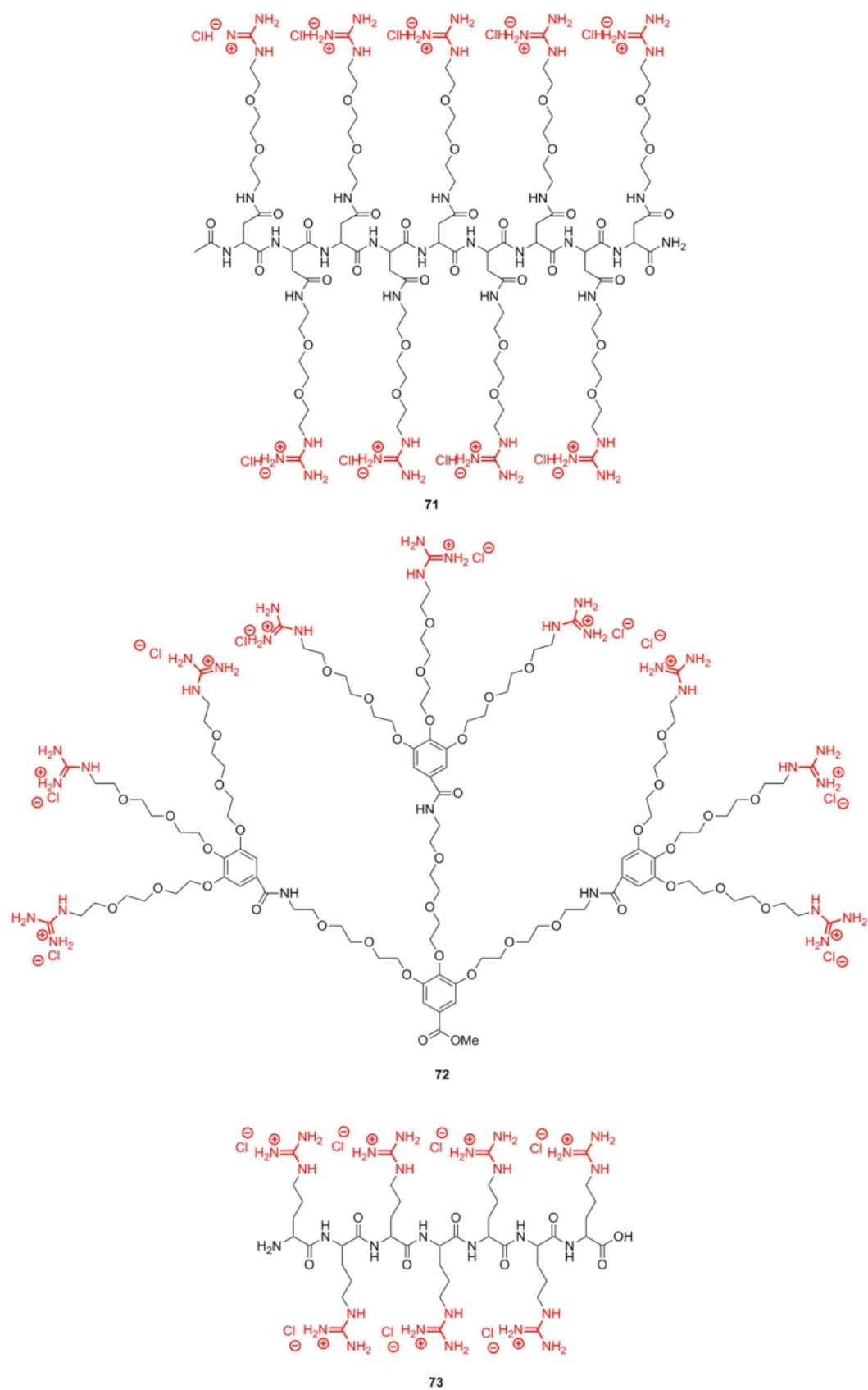


**Figure 11:** Simple macromolecular guanidine system acting as molecular glues

### **3.7. Metal Complexes And Organoelement Derivatives Of Guanidine**

Murillo[129] reported the synthesis of molybdenum and tungsten complexes based on bicyclic guanidine ligands which serve as the strong reducing agent. Based on the bicyclic guanidine ligands, the complexes of tin and mercury[130] and bridges complexes of manganese and nickel are also known[131].



#### 4. CONCLUSION

Despite the fact that this review provides only a quick and limited information regarding the synthesis, importance, properties, chemical nature and various applications, the performed analysis allowed us to follow the main directions of investigations in the rapidly developing field and outline most promising areas of further development. In this review report, guanidine and its various substituted derivatives, their structures, chemistry, and practical importance as well as their widespread applications in various fields starting from daily life to medicinal and drug development and to polymer and metal complex design are highlighted. In a general statement, it may be concluded that Guanidine with its unique and promising properties can be act as the versatile chemical in various field of chemistry satisfying the needs and the further research and development will be a blessing for the entire humankind.

## References

1. Assunção L, Marinho E, Proença F, Arkivoc 2010; 2010: 82-91
2. Berlinck RGS, Burtoloso ACB, Kossuga MH. Nat Prod Rep 2008;25:919-54
3. Mori A, Cohen BD, Lowenthal. Plenum, New York, 1985
4. Greenhill JV, Lue L. In: Prog Med Chem 1993;30:203
5. Ishikawa T. Superbases for organic synthesis: guanidines, amidines, phosphazenes and related organocatalysts. J Wiley & Sons, 2009
6. Goebel M, Klapoetke M, Chem. Commun 2007; 43: 3180-2. Goebel M, Klapoetke M, Chem. Commun 2007; 43: 3180-2.
7. Yamada T, Liu X, Englert U, Yamane H, Dronskowski R, Chem. Eur. J 2009; 15: 5651-5.
8. Sawinski K, Meven M, Englert U, Dronskowski R, Cryst. Growth Des 2013; 13: 1730-5.
9. B. Cho, M. W. Wong, *Molecules*, **2015**, 20, 15108–15121. DOI: [10.3390/molecules200815108](https://doi.org/10.3390/molecules200815108)
10. Güthner, Thomas; Mertschenk, Bernd; Schulz, Bernd. "Guanidine and Derivatives". Ullmann's Encyclopedia of Industrial Chemistry. Weinheim: Wiley-VCH. doi:10.1002/14356007.a12\_545.pub2
11. Strecker, A. (1861). Liebigs Ann. Chem. 118 (2): 151–177. doi:10.1002/jlac.18611180203
12. E. Z. Ong, Y. F. Z. Chan, W. Y. Leong, N. M.Y. Lee, S. Kalimuddin, S. M. H. Mohideen, K. S. Chan, A. T. Tan, A. Bertolotti, E. E. Ooi, J. G. H. Low, *Cell Host Microbe*, **2020**, 27, 879–882. DOI: [10.1016/j.chom.2020.03.021](https://doi.org/10.1016/j.chom.2020.03.021)
13. N. Aoyagi, Y. Furusho, T. Endo, *Synlett*, **2014**, 25, 983–986. DOI: [10.1055/s-0033-1340904](https://doi.org/10.1055/s-0033-1340904)
14. J. Zhang, Y. Shi, P. Stein, K. Atwal, C. Li, *Tetrahedron Lett.*, **2002**, 43, 57–59. DOI: [10.1016/S0040-4039\(01\)02071-8](https://doi.org/10.1016/S0040-4039(01)02071-8)
15. C. A. Maryanoff, R. C. Stanzione, J. N. Plampin, J. E. Mills, *J. Org. Chem.*, **1986**, 51, 1882–1884. DOI: [10.1021/jo00360a040](https://doi.org/10.1021/jo00360a040)
16. A. E. Miller, J. J. Bischoff, *Synthesis*, **1986**, 9, 777–779. DOI: [10.1055/s-1986-31777](https://doi.org/10.1055/s-1986-31777)
17. M. S. Bernatowicz, Y. Wu, G. R. Matsueda, *J. Org. Chem.*, **1992**, 57, 2497–2502. DOI: [10.1021/jo00034a059](https://doi.org/10.1021/jo00034a059)
18. K. Feichtinger, H. L. Singh, T. J. Bakery, K. Matthews, M. Goodman, *J. Org. Chem.*, **1998**, 63, 8432–8439. DOI: [10.1021/jo9814344](https://doi.org/10.1021/jo9814344)
19. A. R. Katrizky, B. V. Rogovoy, C. Chassaing, V. Vvedensky, *J. Org. Chem.*, **2000**, 65, 8080–8082. DOI: [10.1021/jo0006526](https://doi.org/10.1021/jo0006526)
20. N. L. Reddy, W. Fan, S. S. Magar, M. E. Perlman, E. Yost, L. Zhang, D. Berlove, J. B. Fischer, K. Burke-Howie, T. Wolcott, G. J. Durant, *J. Med. Chem.*, **1998**, 41, 3298–3302. DOI: [10.1021/jm980134b](https://doi.org/10.1021/jm980134b)
21. G. Panda, N. V. Rao, *Synlett*, **2004**, 4, 714–716. DOI: [10.1055/s-2004-817770](https://doi.org/10.1055/s-2004-817770)
22. N. Okajima, Y. Okada, *J. Heterocycl. Chem.*, **1991**, 28, 177–185. DOI: [10.1002/jhet.5570280131](https://doi.org/10.1002/jhet.5570280131)

23. H. Hammoud, M. Schmitt, F. Bihel, C. Antheaume, J.-J. Bourguignon, *J. Org. Chem.*, **2012**, *77*, 417-423.
24. J. Li, L. Neuville, *Org. Lett.*, **2013**, *15*, 6124-6127.
25. B. P. Zavesky, N. R. Babij, J. A. Fritz, J. P. Wolfe, *Org. Lett.*, **2013**, *15*, 5420-5423.
26. Z. J. Garlets, M. Silvi, J. P. Wolfe, *Org. Lett.*, **2016**, *18*, 2331-2334.
27. L. Zhou, J. Chen, J. Zhou, Y.-Y. Yeung, *Org. Lett.*, **2011**, *13*, 5804-580
28. P. Phukan, D. Hazarika, A. J. Borah, Chemcomm, Royal Society Of Chemistry, New York, 2019, DOI:10.1039/c8cc08564a
29. Kumar S, kumar D, Renu R. A Fast Route for the Synthesis of Cyclic Guanidine Derivatives. *Orient J Chem* 2011;27(1).
30. R.E. Dickerson, *J. Mol. Biol.*, **57**, 1 (1971).
31. Wang P, McLeish J, Kneen M, Lee G, Kenyon L, *Biochemistry* 2001; **40**: 11698 - 11705
32. J Greenhill; P Lue, G.P. Eillis, D.K. Luscombe, Elsevier Science, New York, 1993,
33. Kaplan, J. E.; Davis, L. E.; Narayan, V.; Koster, J.; Katzenstein, D. (1979) **6** (1): 69–71. doi:10.1002/ana.410060117. PMID 389150. S2CID 42901888."
34. Puggiari, Marcello; Cherington, Michael (1978). *J. Am. Med. Assoc.* **240** (21): 2276–7. doi:10.1001/jama.1978.03290210058027. PMID 702753.
35. Shimizu H, Tosaki A, Kaneko K, et al. *Mol Cell Biol* 2008;28:3663-71
36. AstraZeneca AB. WO-120096; 2007
37. Gerritz S, Shi S, Zhu S, et al. US-0287287; 2006
38. Bristol-Myers Squibb Company. WO-002220; 2007
39. Bristol-Myers Squibb Company. WO-002214; 2007
40. Gerritz S, Good AC, Thompson III LA, et al. US-0015754; 2007
41. Yong-Jin WU, Gerritz S, Shi S, et al. US-0232581; 2007
42. Keana JFW, Weber E. US-5574070
43. A Katritzky; N Khashab; S Bobrov. *Helv Chim Acta*, 2005, 1664-1675.
44. Stark H. Histamine receptors: review No1. *Biotrend Rev* 2007;1-9
45. Sheng-Xue xie, Ghorai P, Qi-Zhuang YE, et al. *J Pharmacol Exp Ther* 2006;317:139-46
46. Ghorai P, Kraus A, Keller M, et al. *J Med Chem* 2008;51:7193-204
47. Igel P, Schneider E, Schnell D, et al. *J Med Chem* 2009 :Article ASAP
48. Fresno MD, Fernandez-Fornier D, Miralpeix M, et al. *Bioorg Med Chem Lett* 2005;15:1659-64
49. R Bahekar; M Jain; A Goel; D Patel; V Prajapati; A Gupta; P Jadav; P Patel. *Bioorgan Med Chem*, 2007, **15**, 3248.
50. Venkateswarlu Y. US-0222168; 2005
51. Parmee ER. US-0105930; 2007
52. Karageozian VH. US-0105950; 2007
53. M Sibrian-Vazquez; I Nesterova; T Jensen; M Vicente. *Bioconjugate Chem*, 2008, **19**, 705.
54. V Gade; P Nilkanth; G Mhaske; R Manjul; V Shinde; S Kushare; S Shelke, *Int J Innov Res Sci Eng Technol*, 2014, **3**, 7.

55. G Bentabed-Ababsa; M Rahmouni; F Mongin; A Derdour; J Hamelin; J Bazureau. *Behav Sci Public Health*, 2007, 37, 2935
56. J Stanek; T R€osener; A Metz; J Mannsperger; A Hoffmann; S Herres-Pawlis, *Top Heterocycl Chem*, 2015, 173
57. AstraZeneca AB. US-7001904; 2006
58. Vlasuk GP In: Sasahara AA, Loscalzo J, editors, Marcel Dekker; Chapter 15. New York, 1997
59. Mousa SA, Cheresch DA 1997;2:187-99
60. Wiesner S, Legate KR, Fässler R. Review. Integrin-acting interactions. *Cell Mol Life Sci* 2005;62:1081-99
61. Massia SP, Ehteshami G. US-0246104; 2006
62. Burdick DJ, Stanley MS, Oare D, et al. US-6667318; 2003
63. Fish PV, Barber CG, Brown DG, et al. *J Med Chem* 2007;50:2341-51
64. Joossens J, Ali OM, El-Sayed I, et al. *J Med Chem* 2007;50:6638-46
65. Chen XI, Liu C, Thurkauf A, Louise-May S. US-0100225; 2006
66. Achillion Pharmaceuticals, Inc. WO-095345; 2005
67. The Regents of the University of California. WO-016343; 2005
68. Itzstein MV, Wen-Yang WU, KOK GB, et al. *Nature* 1993;363:418-23
69. Goodman M, Tar Y, Baker T, et al. US-6525182; 2003
70. Hensler ME, Bernstein G, Nizet V, Nefzi A. *Bioorg Med Chem Lett* 2006;16:5073-9
71. Yoshizawa H, Kubota T, Itani H, et al. *Bioorg Med Chem* 2004;12:4221-31
72. Qian L, Guan Y, Xiao H, et al. *Polymer* 2008;49:2471-5
73. Kratzer C, Tobudic S, MacFelda K, et al. *Antimicrob Agents Chemother* 2007;51:3437-9
74. L de Assunção; E Marinho; F Proença. *Turk J Chem*, 2014, 38, 345.
75. David L. WO-135380; 2007
76. Hui-Hang Hua, Peng J, Fronczek MTFR, et al. *Bioorg Med Chem* 2004;12:6461-4
77. Rodríguez F, Rozas I, Kaiser M, et al. *J Med Chem* 2008;51:909-23
78. Guan J, Zhang Q, Montip G, et al. *Bioorg Med Chem* 2005;13:699-704
79. Jian Guan, Xihong Wang, Smith K, et al. *J Med Chem* 2007;50:6226-31
80. Caroff E, Steger M, Valdenaire O, et al. US-0194788; 2006
81. Actelion Pharmaceuticals Ltd. WO-023781; 2005
82. Actelion Pharmaceuticals Ltd. US-0123510; 2007
83. Taktix Corporation. WO-105779; 2003
84. Clark RD, Jahangir A, Severance D, et al. *Bioorg Med Chem Lett* 2004;14:1053-6
85. M Coles; M Khalaf; P Hitchcock. *Inorganica Chimica Acta*, 2014, 422, 228.
86. S Larsen; M Connell; M Cudahy; B Evans; P May; M Meglasson; T O'Sullivan; H Schostarez; J Sih; F Stevens; S Tanis; C Tegley; J Tucker; V Vaillancourt T; Vidmar W Watt; J Yu. *J Med. Chem*, 2001, 44, 1217.
87. M. Khalaf. *Iraqi Nat J Chem*, 2014, 55, 328 -339
88. Bossche HV. Echinocandins – an update. *Exp Opin Ther Patents* 2002;12:151-67

89. Weibo Wang, Qun Li, Hasvold L, et al. *Bioorg Med Chem Lett* 2003;13:489-93
90. Sakuda S, Isogaim A, Suzuki A, Yamada Y. 1993;7:50-7
91. Braunerová G, Buchta V, Palát K Jr, et al. *Il Farmaco* 2004;59:443-50
92. S Lee; K Yi; S Youn; B Lee; S Yoo. *Bioorg. Med. Chem. Lett.*, 2009, 19, 1329.
93. Masereel B, Pochet L, Laeckmann D. An overview of inhibitors of Na<sup>+</sup>/H<sup>+</sup> exchanger. *Eur J Med Chem* 2003;38:547-54
94. Rui Zhang, Lei L, Yun-Gen Xu, et al. *Bioorg Med Chem Lett* 2007;17:2430-3
95. Juno Kim, Yi-Sook Jung, Vonsun Han, et al. *Eur J Pharmacol* 2007;567:131-8
96. Nicholas Piramal India Limited. WO-051476; 2006
97. Bao Xin-Hua, Lu Wen-Cong, Liu Liang, Chen Nian-Yi. *Acta Pharmacol Sin* 2003;24:472-6
98. Wen-Ting Xu, Ning Jin, Jing Xu, et al. *Bioorg Med Chem Lett* 2009;19:3283-7
99. Rui Zhang, Lin Lei, Yun-Gen XU, et al. *Bioorg Med Chem Lett* 2007;17:2430-3
100. Martin NI, Beeson WT, Woodward JJ, Marletta MA. *J Med Chem* 2008;51:924-31
101. Cesnek M, Holý A, Masojídková M, Zidek Z. *Bioorg Med Chem* 2005;13:2917-26
102. Bertinaria M, Stilo AD, Tosco P, et al. *Bioorg Med Chem* 2003;11:1197-205
103. Fishlock D, Perdicakis B, Montgomery HJ, et al. *Bioorg Med Chem* 2003;11:869-73
104. Martin B, Sainlos M, Aissaoui A, et al. *Curr Pharm Des* 2005;11:375-94
105. *Superbases for Organic Synthesis*, T. Ishikawa (Ed.), Wiley, Chippenhams, **2009**. DOI: [10.1002/9780470740859](https://doi.org/10.1002/9780470740859)
106. D. Barić, I. Dragičević, B. Kovačević. *J. Org. Chem.*, **2013**, 78, 4075–4082. DOI: [10.1021/jo400396d](https://doi.org/10.1021/jo400396d)
107. I. P. Selig (Ed.), *Top. Heterocycl. Chem.*, Springer, Cham, **2017**, vol. 50. DOI: [10.1007/978-3-319-52725-3](https://doi.org/10.1007/978-3-319-52725-3)
108. D. Leow, C.-H. Tan, *Chem. Asian J.*, **2009**, 4, 488–507. DOI: [10.1002/asia.200800361](https://doi.org/10.1002/asia.200800361)
109. D. Leow, C.-H. Tan, *Synlett*, **2010**, 11, 1589–1605. DOI: [10.1055/s-0029-1219937](https://doi.org/10.1055/s-0029-1219937)
110. T. Ishikawa, T. Isobe, *Chem. Eur. J.*, **2002**, 8, 552–557. DOI: [10.1002/1522-3765\(20020201\)8:3<552::AID-CHEM552>3.0.CO;2-T](https://doi.org/10.1002/1522-3765(20020201)8:3<552::AID-CHEM552>3.0.CO;2-T)
111. D. Simoni, F. P. Invidiata, M. Manferdini, I. Lampronti, R. Rondanin, M. Roberti, G. P. Pollini, *Tetrahedron Lett.*, **1998**, 39, 7615–7618. DOI: [10.1016/S0040-4039\(98\)01656-6](https://doi.org/10.1016/S0040-4039(98)01656-6)
112. L. Bernardi, B. F. Bonini, E. Capitò, G. Dessole, M. Comes-Franchini, M. Fochi, A. Ricci, *J. Org. Chem.*, **2004**, 69, 8168–8171. DOI: [10.1021/jo0488762](https://doi.org/10.1021/jo0488762)
113. R. S. Graunger, N. E. Leadbeater, M. A. Pamies, *Catal. Commun.*, **2002**, 3, 449–452. DOI: [10.1016/S1566-7367\(02\)00178-4](https://doi.org/10.1016/S1566-7367(02)00178-4)
114. T. Ishikawa, T. Kumamoto, *Synthesis*, **2006**, 5, 737–752. DOI: [10.1055/s-2006-926325](https://doi.org/10.1055/s-2006-926325)
115. J. E. Taylor, S. D. Bull, J. M. J. Williams, *Chem. Soc. Rev.*, **2012**, 41, 2109–2121. DOI: [10.1039/C2CS15288F](https://doi.org/10.1039/C2CS15288F)

- 116.J. L. Vicario, D. Badia, L. Carrillo, E. Reyes, *RSC, Cambridge*, **2010**. DOI: [10.1039/9781849732185](https://doi.org/10.1039/9781849732185)
- 117.K. Fuchise, M. Igarashi, K. Sato, S. Shimada, *Chem. Sci.*, **2018**, 9, 2879–2891. DOI: [10.1039/c7sc04234e](https://doi.org/10.1039/c7sc04234e)
- 118.R. Yuan, Q. Shou, Q. Mahmood, G. Xu, X. Sun, J. Wan, Q. Wang, *Synlett*, **2019**, 30, 928–931. DOI: [10.1055/s-0037-1611766](https://doi.org/10.1055/s-0037-1611766)
- 119.M. K. Kiesewetter, M. D. Scholten, N. Kirn, R. L. Weber, J. L. Hedrick, R. M. Waymouth, *J. Org. Chem.*, **2009**, 74, 9490–9496. DOI: [10.1021/jo902369g](https://doi.org/10.1021/jo902369g)
- 120.L. Lei, M. Tanishima, A. Goto, H. Kaji, *Polymers*, **2014**, 6, 860–872. DOI: [10.3390/polym6030860](https://doi.org/10.3390/polym6030860)
- 121.I. P. Selig (Ed.), *Top. Heterocycl. Chem.*, Springer, Cham, **2017**, vol. 50. DOI: [10.1007/978-3-319-52725-3](https://doi.org/10.1007/978-3-319-52725-3)
- 122.S. Dong, X. Feng, X. Liu, *Chem. Soc. Rev.*, **2018**, 47, 8525–8540. DOI: [10.1039/c7cs00792b](https://doi.org/10.1039/c7cs00792b)
- 123.L. Heidari, L. Shiri, *Appl. Organomet. Chem.*, **2019**, 33, e4636. DOI: [10.1002/aoc.4636](https://doi.org/10.1002/aoc.4636)
- 124.D. Glaser, *Pure Appl. Chem.*, **2002**, 74, 1153–1158. DOI: [10.1351/pac200274071153](https://doi.org/10.1351/pac200274071153)
- 125.A. R. Katritzky, R. Petrukhin, S. Perumal, M. Karelson, I. Prakash, N. Desai, *Croat. Chem. Acta*, **2002**, 75, 475–502.
- 126.G. E. Davies, J. Francis, A. R. Martin, F. L. Rose, G. Swain, *Br. J. Pharmacol. Chemother.*, **1954**, 9, 192–196. DOI: [10.1111/j.1476-5381.1954.tb00840.x](https://doi.org/10.1111/j.1476-5381.1954.tb00840.x)
- 127.K. Schedler, O. Assadian, U. Brautferger, G. Müller, T. Koburger, S. Classen, A. Kramer, *BMC Infect. Dis.*, **2017**, 17, 143. DOI: [10.1186/s12879-017-2220-4](https://doi.org/10.1186/s12879-017-2220-4)
- 128.Z. Zhou, A. Zheng, J. Zhong, *Acta Biochim. Biophys. Sin.*, **2011**, 43, 729–737. DOI: [10.1093/abbs/gmr067](https://doi.org/10.1093/abbs/gmr067)
- 129.C. A. Murillo, *Aust. J. Chem.*, **2014**, 67, 972–979. DOI: [10.1071/CH13694](https://doi.org/10.1071/CH13694)
- 130.S. M. El-Hamruni, S. E. Sözerli, J. D. Smith, M. P. Coles, P. B. Hitchcock, *Aust. J. Chem.*, **2014**, 67, 1071–1080. DOI: [10.1071/CH14255](https://doi.org/10.1071/CH14255)
- 131.F. A. Stokes, L. Kloo, P. J. Harford, A. J. Peel, R. J. Less, A. E. H. Wheatley, D. S. Wright, *Aust. J. Chem.*, **2014**, 67, 1081–1087. DOI: [10.1071/CH14271](https://doi.org/10.1071/CH14271)



**SYNTHESIS, PROPERTIES AND APPLICATIONS OF TETRAZOLES****A LITERATURE REVIEW REPORT**

SUBMITTED TO THE DEPARTMENT OF CHEMISTRY, GAUHATI UNIVERSITY AS A  
PART OF PARTIAL FULLFILMENT OF THE REQUIREMENTS FOR THE DEGREE OF  
MASTERS OF SCIENCE IN CHEMISTRY 2021

Submitted By:

**RITWIK KASHYAP**

ROLL NO: PS-191-808-0086

REGISTRATION NO: 19000066 (2019-2020)

MSC 4TH SEMESTER

DEPARTMENT OF CHEMISTRY, GAUHATI UNIVERSITY

*Under the supervision of,*

-----

Prof. Prodeep Phukan,  
Department Of Chemistry,  
Gauhati University



**DECLARATION**

I hereby declare that the matter embodied in this literature review entitled, **“Synthesis, Properties and Applications of Tetrazoles”** is the result of survey of scientific literature carried out by me at the Department of Chemistry, Gauhati University, Guwahati, Assam under the supervision of Prof. Prodeep Phukan, and that it has not been submitted elsewhere for the award of any degree or diploma.

As a general practice of writing scientific reports, due acknowledgement has been made to all the authors whose works have been discussed in this survey and unintentional omission, if any, is highly regretted.

Date: 06/09/2021

Place:

(Ritwik Kashyap)  
MSc 4<sup>TH</sup> Semester  
Department Of Chemistry,  
Gauhati University.

In my capacity as supervisor of the candidate's work, I certify that the above are true to the best of my knowledge

Date.....

Prof. Prodeep Phukan, PhD  
Department Of Chemistry,  
Email: pphukan@gauhati.ac.in  
Gauhati University, Guwahati  
781014, Assam, India  
Tel +91-361-2570535(O)

**DEPARTMENT OF CHEMISTRY**  
**GAUHATI UNIVERSITY,**  
**GUWAHATI: 781014, ASSAM INDIA**

**CERTIFICATE**

This is to certify that **Ritwik Kashyap**, a student of the Department Of Chemistry, Gauhati University, Assam has completed this literature review for the partial fulfillment of the requirements for the award of the degree of Masters of Science in Chemistry, 2021 under my guidance on the topic entitled, “**Synthesis, Properties and Applications of Tetrazoles**”.

**Prof. Prodeep Phukan**  
**Dept. of Chemistry.**  
**Gauhati University.**

### **ACKNOWLEDGEMENT**

I consider it my privilege to express my gratitude to all those individuals and my institution without whose support, encouragement and cooperation, this review work would not have been possible.

First of all, I would like to extend my heartfelt gratitude to Prof. Prodeep Phukan Department of Chemistry, Guwahati University, my advisor, for his valuable guidance, assistance and encouragement which helped complete my review work. I would like to thank him for his time, advice, constant support and encouragement throughout my work.

Next, the Department of Chemistry, Gauhati University, the institution which provided me a platform for the completion of my post-graduation. I would also like to thank the Department for proving us students this opportunity to do a Review Project during our M.Sc. course, thereby exposing us to the colossal amount of work which are being processed everyday both in the academic research and on the industrial fabrication. This opportunity has indeed been very beneficial for us students as this has allowed us to connect our theoretical knowledge of our course to the practical applications in the laboratories.

I also convey my gratitude, to all the staff members of Department of Chemistry for their help and support.. Last but not the least I would like to express my thankfulness from the bottom of my heart to all my classmates, my parents and the almighty for their support and blessings.

Date: 06/09/2021

Place:

(Ritwik Kashyap)  
MSc 4<sup>TH</sup> Semester  
Department Of Chemistry,  
Gauhati University

## **CONTENTS**

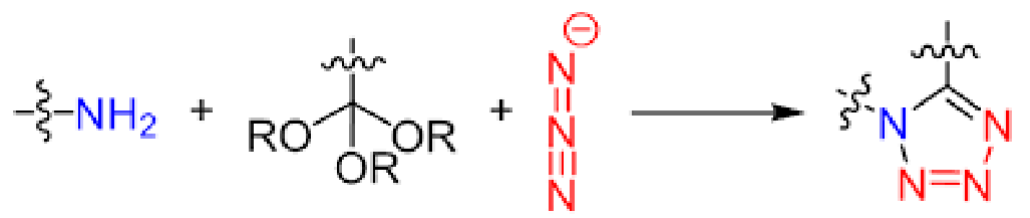
<b><u>Serial no.</u></b>	<b><u>Title</u></b>	<b><u>Page no.</u></b>
1.	Brief introduction of Tetrazoles and its Derivative Compounds -----	7
2.	Extraction of Tetrazoles from nature And Synthetic process of -----  Tetrazole compounds	8
3.	Chemical Properties of Tetrazoles. -----	14.
4.	Tetrazole coordination complexes. -----	22
5.	Use of Tetrazole and its derivatives in pharmaceutical uses. -----	30.

### **Abstract**

In this literature survey report we see about the process of synthesizing Tetrazole and its derivative compounds. Then we see about various chemical properties of Tetrazoles specially we saw about the Thermal decomposition of tetrazole and its derivative compounds. After that we have seen the detail study of Tetrazole coordination complexes along with the application of Tetrazole coordination complexes in organic synthesis. Finally we prepare a report on various applications of tetrazole and its derivative compounds in pharmaceutical uses.

## 1. Introduction

The current development in the designing of new energetic materials is largely associated with synthesizing of tetrazoles and its derivatives. Tetrazoles possess a unique combination of properties – significant thermal stability along with high positive values of the enthalpy of formation and the highest nitrogen content among organic compounds (80% for tetrazole itself). Due to these properties, tetrazoles are considered as components of highly effective propellants, explosives, pyrotechnics, as well as gas generating compositions. The main product of their thermal decomposition is nitrogen, and this fact motivates the interest toward tetrazoles as "green" energetic materials.



Tetrazole is a five membered ring (four nitrogen atoms with one carbon atom) in same structure, the compound is found in standard conditions as a soluble solid in water and ethanol; but it is difficult to dissolve in ether. Tetrazole exhibits weak acidic properties in solutions [31-40], and has a (pKa)- value of dissociation of acid (4.89) close to acetic acid. Tetrazole is a heterocyclic organic compound having the chemical formula (CH<sub>2</sub>N<sub>4</sub>), in white solid form. Structurally, the compound is composed of an unsaturated five-membered ring containing four nitrogen atoms

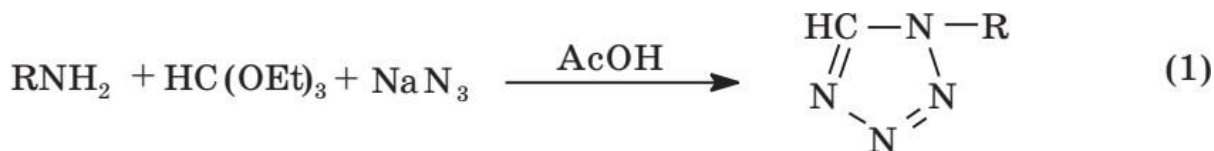
This review provides comprehensive analysis of literature data on the heterocyclization reaction of primary amines, orthoesters, and azides, which can be used for the preparation of tetrazole, its 1-mono- and 1.5-disubstituted derivatives.

## 2. SYNTHESIS OF TETRAZOLES

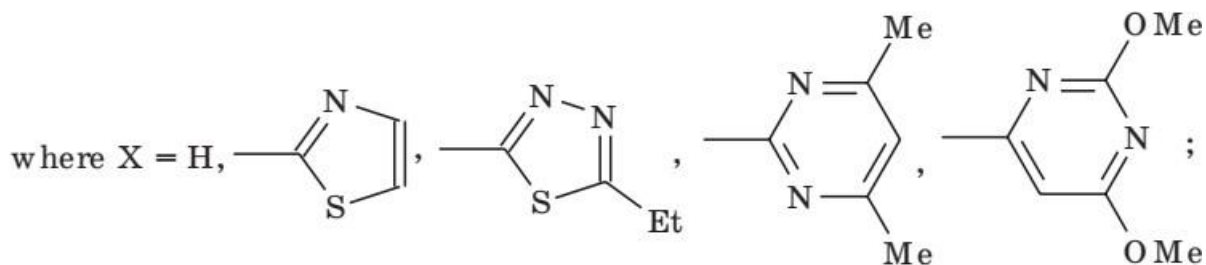
The development of novel procedures for the synthesis of tetrazoles as well as for the improvement of known methods of their preparation have been carried out in our laboratory mainly within the framework of two following approaches: the heterocyclization of readily available nitrogen-containing substrates and the functionalization of heterocycles and substituents of the simplest tetrazoles.

### Synthesis of 1-mono- and 1, 5-disubstituted tetrazoles based On reactions of heterocyclization

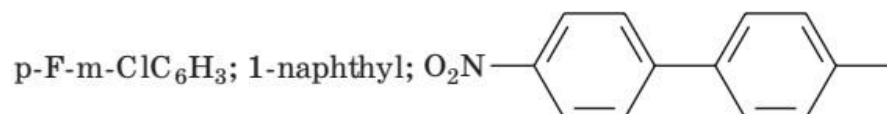
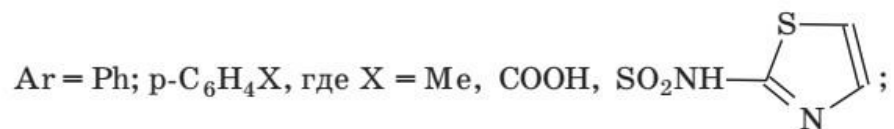
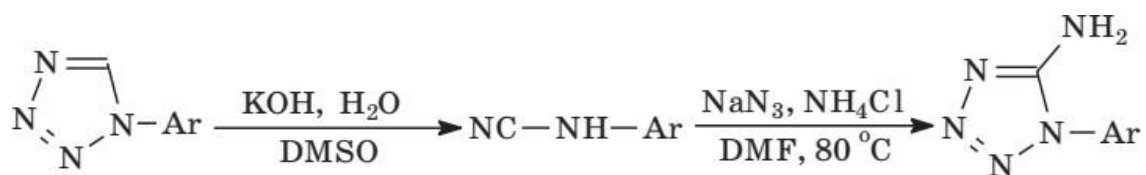
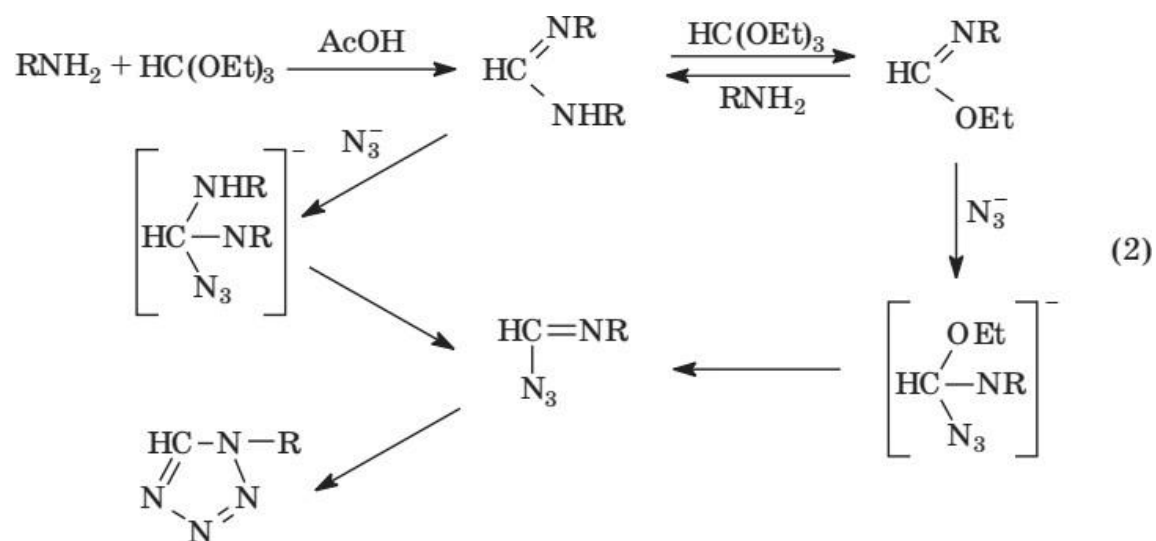
The interaction of a wide variety of primary amines of different natures with ethylorthoformate and sodium azide resulting in formation of 1-monosubstituted tetrazoles has been studied



R = Me; Et; Bu; t-Bu; Allyl;  $\text{CH}_2\text{CF}_3$ ;  $(\text{CH}_2)_2\text{X}$ , where  $\tilde{\text{O}}$  = Ph, OH, COOH,  $\text{NMe}_2$ ,  $\text{N}_3$ ;  $\text{CH}_2\text{COOH}$ ;  $\text{C}(\text{CH}_2\text{Cl})_3$ ;  $\text{CH}(\text{COOH})\text{CH}_2\text{Ph}$ ; cyclo-Pr; cyclo- $\text{C}_6\text{H}_{11}$ ;  $\text{CH}_2\text{Ph}$ ; Ph;p- $\text{XC}_6\text{H}_4$ , where  $\tilde{\text{O}}$  = Me, MeO, MeCO, p- $\text{NO}_2\text{C}_6\text{H}_4$ , Cl, Br, OH, COOH,  $\text{NO}_2$ ; m- $\text{XC}_6\text{H}_4$ , where  $\tilde{\text{O}}$  = MeO, MeCO,  $\text{CH}=\text{CH}(\text{COOH})$ , Cl, Br, OH,  $\text{NO}_2$ ; o- $\text{XC}_6\text{H}_4$ , where  $\tilde{\text{O}}$  = OH, COOH,  $\text{NO}_2$ ; 2-OH-5- $\text{NO}_2\text{C}_6\text{H}_3$ ; 2-OH-4- $\text{NO}_2\text{C}_6\text{H}_3$ ; 2-Me-4- $\text{JC}_6\text{H}_3$ ; 3-Cl-4- $\text{FC}_6\text{H}_3$ ; 2,4,6- $\text{Me}_3\text{C}_6\text{H}_2$ ; 2-OH-3,5- $(\text{NO}_2)_2\text{C}_6\text{H}_2$ ; p- $\text{C}_6\text{H}_4\text{SO}_2\text{NHX}$ ,



naphthyl;  $\text{NH}_2$  (from  $\text{Ph}-\text{CH}=\text{N}-\text{NH}_2$ ); 2-thiazolyl; 1-adamantyl (Ad); AdCHMe

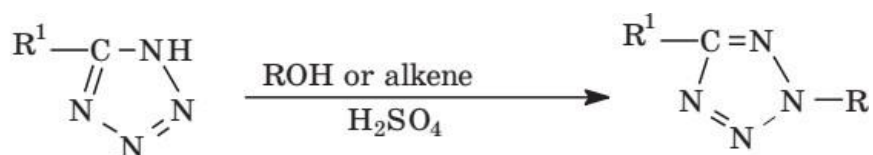
**Mechanism:**



### Alkylation of tetrazoles

#### 2-Mono- and 2,5-disubstituted tetrazoles starting with N-unsubstituted tetrazoles and alcohols (olefines) in acidic media

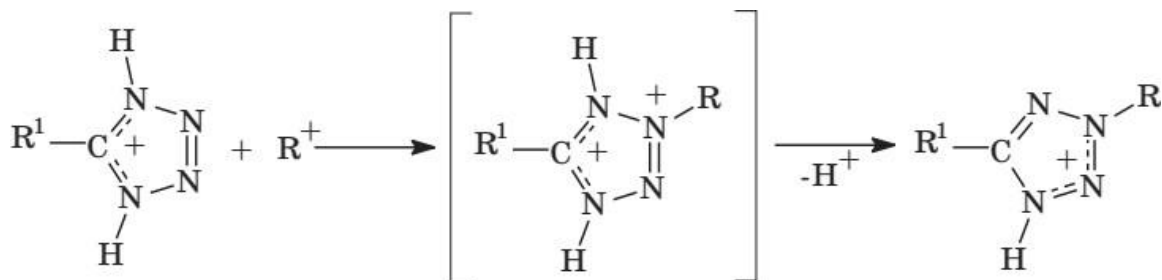
The reactions of tetrazoles alkylation in strong acidic media have been studied for the first time. It has been shown that the interaction of tetrazoles with alcohols and olefines having the structures which are favourable for the stabilization of the formed carbocations including tert-butyl-, isopropyl- and cyclohexyl alcohols, propylene, iso-butylene and cyclohexene proceeds readily without heating in sulphuric acid media. In all cases, independently on the nature and the size of the substituents at position «5» of the tetrazole cycle, the formation of solely 2-substituted tetrazoles with high yields (up to 100%) is observed.



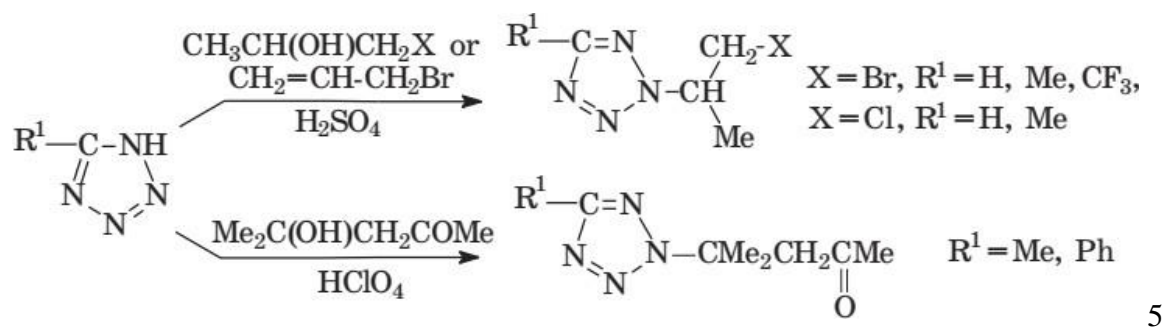
$\text{R} = i\text{-Pr}$ ,  $\text{R}^1 = \text{H}$ ,  $(\text{CH}_2)_2\text{NMe}_2$ , Ph, p-MeC<sub>6</sub>H<sub>4</sub>, p-ClC<sub>6</sub>H<sub>4</sub>, m-BrC<sub>6</sub>H<sub>4</sub>, p-NO<sub>2</sub>C<sub>6</sub>H<sub>4</sub>;  $\text{R} = t\text{-Bu}$ ,  $\text{R}^1 = \text{H}$ , Me,  $t\text{-Bu}$ ,  $(\text{CH}_2)_2\text{NMe}_2$ , CF<sub>3</sub>, Ph, NH<sub>2</sub>;  $\text{R} = \text{R}^1 = \text{H}$ , Ph

4

The study of kinetics and mechanism of the alkylation process by the example of isopropyl alcohol and substituted 5-phenyltetrazoles with invoking of quantum-chemical calculations has demonstrated that the fully protonated symmetrical 1-H,4-H,5-R1-tetrazolium cation act as a substrate of protonation, only one of the two equal atoms at the positions «2» and «3» of the ring characterized by the negative p-charges being accessible for the attack of electrophile.



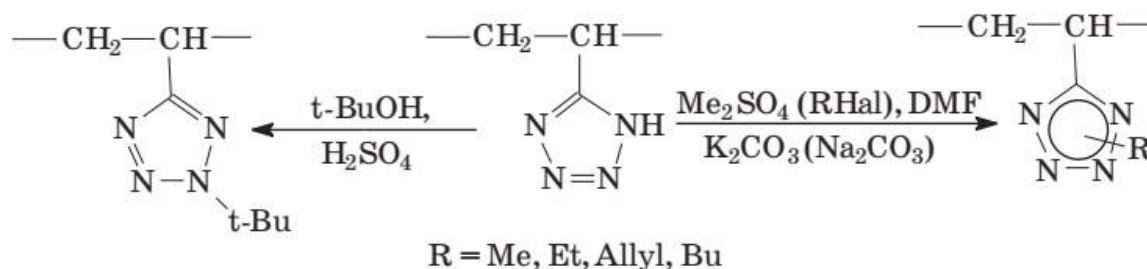
The main factor determining the possibility of reaction proceeding and its rate is the valid concentration of the carbocation, which depends on its stability, all other factors being equal. Therefore, the alkylation of tetrazoles with tert-butyl alcohol proceeds with higher rate than with isopropyl and cyclohexyl alcohols in media of the same acidity. When using alcohols which are unexplored in the considered reaction, it is necessary to take into account the conditions of generation of the corresponding carbocations. For example, in the case of halogen-containing alcohols, high yields of resulting products were obtained only under their long-term interaction with tetrazoles (scheme 5). Diacetone alcohol which form easily the corresponding carbocation, reacts with tetrazoles as rapidly as tert-butyl alcohol.



5

### Synthesis of polyvinyl- and vinyltetrazoles by alkylation reactions

Polymers based on vinyltetrazoles characterized by unique combination of physico-chemical and operating properties are considered as prospective materials for many purposes. However, until recently, the initial monomers for synthesis of polyvinyltetrazoles have not been easily accessible. Taking this into account, we have studied in detail some polymeranalogous transformations leading to formation of polyvinyltetrazoles, namely, polyacrylonitrile (PAN) tetrazolation and alkylation of the formed poly-5-vinyltetrazole (PVT)



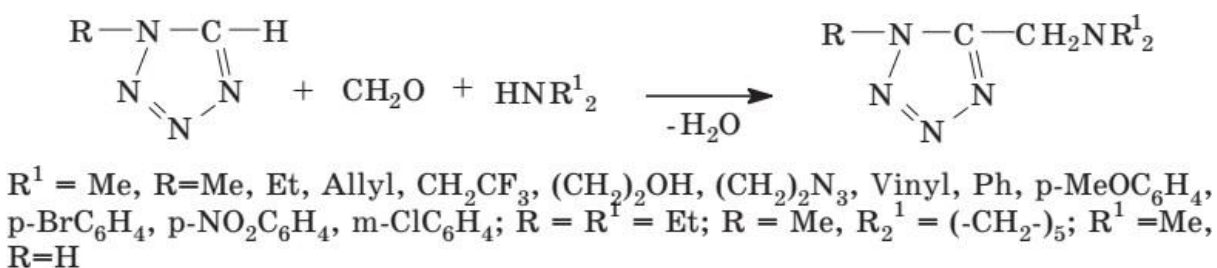
6

A simple and convenient method of PVT synthesis using inexpensive and available PAN was developed. The method allows to obtain polymeric products with a wide range of PVT fragments content including PVT with structure and properties which are practically identical to that of 5-vinyltetrazole homopolymer. The use of the method permits to obtain PVT with a required molecular weight distribution by means of selection of the initial PAN with appropriate molecular weight characteristics.

### Synthesis of 1,5-disubstituted tetrazoles by substitution at the cycle carbon atom

Because of the ease of synthesis of 1R-tetrazoles, they attract an attention as initial substances for the synthesis of different functionally substituted tetrazoles by reactions at the carbon atom of the tetrazole cycle. Earlier, such reactions have been poorly known because the electrophilic substitution of hydrogen atom at the carbon atom was considered to be hinder as a consequence of deactivation of this position by annular nitrogen atoms. At the same time, the data on rates of H/D exchange as well as evaluation of C-H-acidity using spectroscopic and quantum-chemical methods gave grounds to expect that such reactions are practicable for 1-substituted tetrazoles.

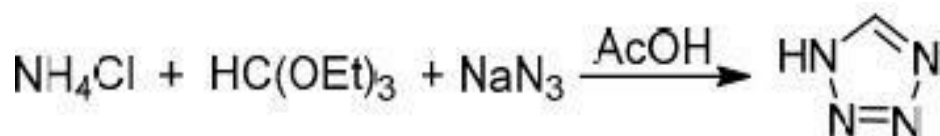
1-R-tetrazoles are found to enter readily into aminomethylation reaction as C-H-acidic component.





### **SYNTHESIZING OF SIMPLEST 1H-TETRAZOLE**

- The synthesizing of simplest 1H tetrazole is done by heating ammonium chloride, sodium azide and triethyl orthoformate (TEOF), in glacial acetic acid medium. The optimal reaction condition include maintaining for 2-3 h at a temp above 70°C. The chemical reaction for the synthesis is-



In this process approximately 90% yields of 1 H tetrazole were reported for crude product that had not been purified by very stallization. The synthesise of 1H-tetrazole by researchers is very much beneficial, since it is valuable precursor for the synthesis of various derivatives, including energetic tetrazoles.

### **3. CHEMICAL PROPERTIES OF TETRAZOLES**

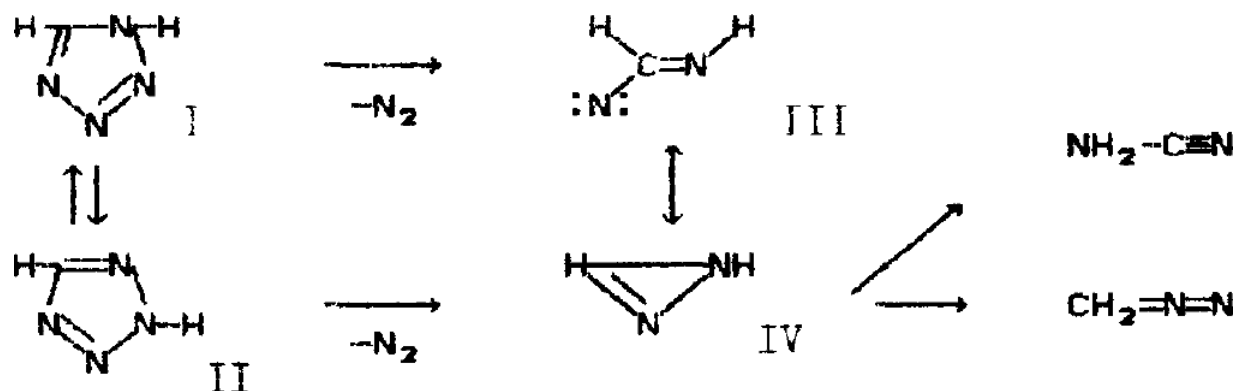
#### **Thermal decomposition of Tetrazole:**

Tetrazole and its derivatives were first obtained more than a century ago when the study of the thermal decomposition of tetrazoles began, owing to the surprisingly high thermostability of these compounds that have four nitrogen atoms in the heterocycle. Further systematic studies of tetrazole thermolysis, which began in the 1950s, included both purely scientific and applied problems.

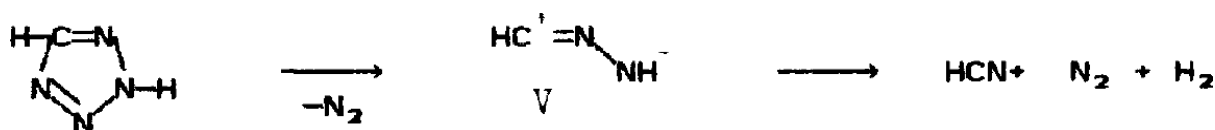
#### **THERMAL DECOMPOSITION OF TETRAZOLE AND ITS 5SUBSTITUTED DERIVATIVES**

The thermal decomposition of tetrazole has been studied in the gas phase and in a melt. With slow heating the tetrazole vapour slowly decomposes from  $T = 225^\circ\text{C}$  into hydrogen azide and hydrogen

cyanide. At a higher temperature,  $T = 280^\circ\text{C}$ , an alternative thermolysis pathway takes place, with elimination of the nitrogen molecule from the tetrazole cycle. Under flash-thermolysis conditions ( $500^\circ\text{C}$ ), elimination of nitrogen molecules predominates. Because tetrazole mainly exists in the 2-H form (II) in vapours, then, as the quantum-mechanical calculation has shown, the decomposition can involve a metastable intermediate of isodiaziridine (IV). With decomposition of the 1-H form, formation of nitrene (III) precedes that of isodiaziridine (IV)

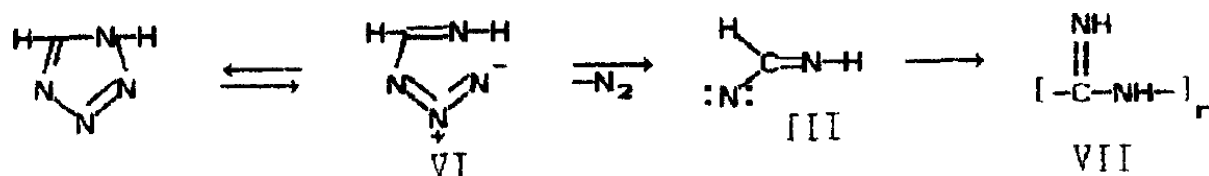


It is assumed that the intermediate product decomposition is nitrilimine (V)



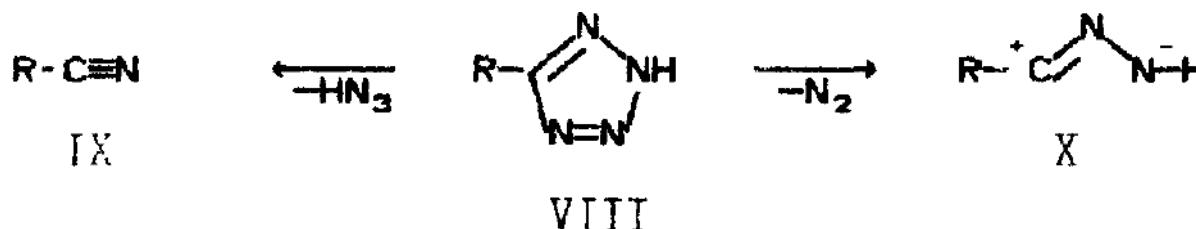
In a melt, tetrazole is less thermally stable than in a vapour and begins to decompose at  $170^\circ\text{C}$  [El.

It is assumed that the 1-H form of tetrazole is in equilibrium with its azide form (VI) from which a nitrogen molecule splits off



In this case, in a condensed phase, the polycyanamide (VII) formed as the result of nitrene implantation in the C-H bond of tetrazole [15] is accumulated.

5 substituted tetrazole derivatives (VIII) decompose by two alternative mechanisms with formation of nitrogen or hydrogen azide



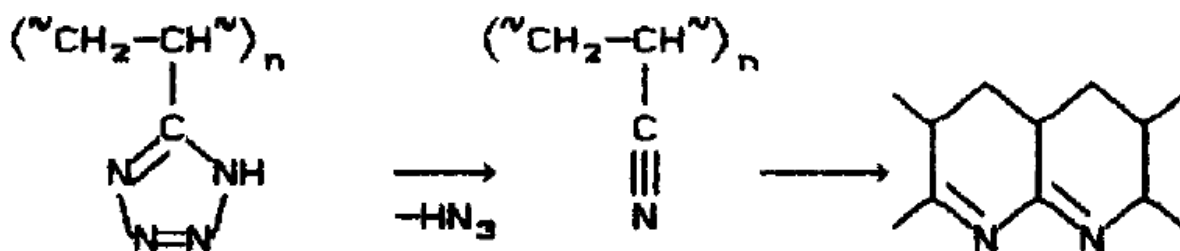
Depending on the character of the substituent R and the conditions of thermolysis, either one or both of the above-mentioned pathways are followed. The variety of products accumulated in the residue (Scheme 1) is determined by nitrile (IX) cyclotrimerization or by nitrilimine (X) stabilization. If thermolysis of VIII is carried out in a melt, then the nitrile formed as a result of  $\text{HN}_3$  loss is capable of cyclotrimerization. In the mesitylene solution ( $164^\circ\text{C}$ ), the benzonitrile formed by the decomposition of 5-phenyltetrazole trimerizes. The decomposition of 5-mercaptotetrazoles in a melt is accompanied exclusively by the formation of  $\text{HN}_3$ ; in this case, thiocyanates and a slightly soluble tar residue, perhaps the product of polymerization of the latter, are formed.

If a nitrogen atom is eliminated from the heterocycle of 5-substituted tetrazoles, the nitrilimine (X) is observed independently of whether the thermolysis proceeds in the gas phase or in solution. However, their further transformation depends on the experimental conditions. During the pyrolysis of 5-substituted tetrazoles in the gas phase, the nitrilimine decomposes, as a rule, with the formation of very active particles, in particular carbenes, whose stabilization leads to many reaction products. In a solution, the nitrilimine is stabilized by cycloaddition due to interaction of two molecules, or it reacts with nitriles with formation of 1,2,4-triazoles.

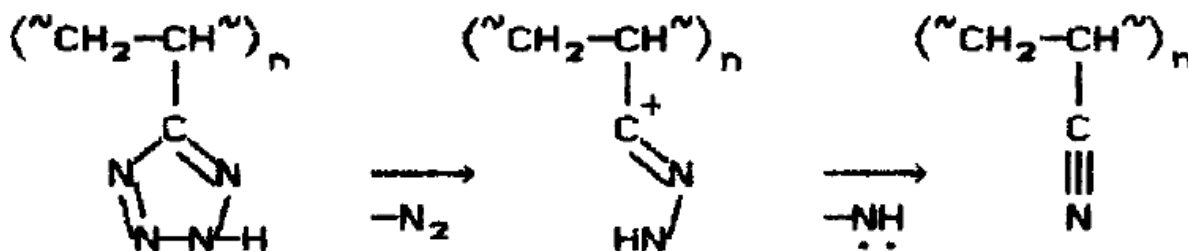
### **THERMAL DECOMPOSITION OF POLYVINYLTETRAZOLES**

In the literature, there is no information on the thermal decomposition of poly-1-vinyltetrazoles. The thermolyses of 1- or 2-alkylsubstituted poly-5-vinyltetrazoles have mainly been studied. The mechanism of thermal splitting of the tetrazole cycle fixed on a carbon-chain matrix is similar, to

a great extent, to the thermolysis of low molecular weight compounds, but there are also differences. The thermolysis of the investigated polyvinyl tetrazoles occur in the solid phase without polymer melting. By analogy with 5-substituted tetrazoles, poly-5-vinyltetrazole can decompose in two alternative pathways with elimination of HN, or N<sub>2</sub>, depending on the temperature. The nitrile groups formed following loss of HN, interact to yield polycyclic structures.



It is assumed that the nitrile groups may also arise by the elimination of nitrene from intermediate nitrilimine

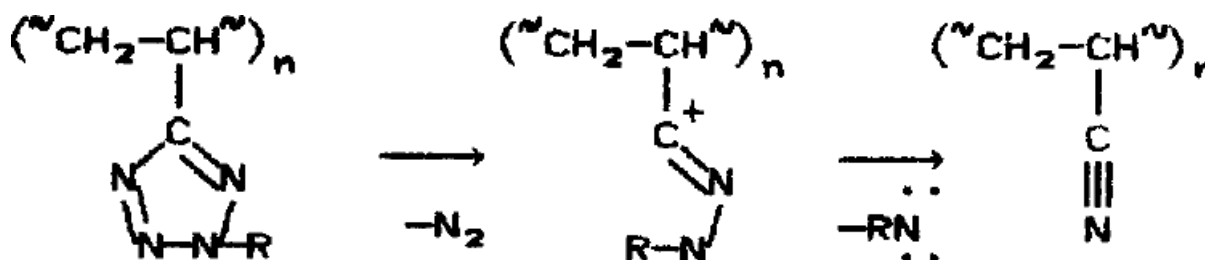


The crosslinking of the polymer chains observed 'during the thermolysis of poly-5-vinyltetrazole is attributed to either the joining of active nitrene to the neighbouring polymer chain or the



interaction of nitriles with intermediate nitrilimines by the mechanism of 1,3-dipolar addition. Poly-1-methyl-5-vinyltetrazole decomposes by analogy with 1,5-disubstituted tetrazoles, but the nitrene formed is stabilized owing to the interaction with the neighbouring carbon chains, which leads to their crosslinking.

Poly-2-alkyl-5-vinyltetrazoles are less thermostable than poly-1-alkyl-5-vinyltetrazoles. At an initial stage of their decomposition, N<sub>2</sub> splits off and nitrilimine is formed. Further stabilization of nitrilimine by the mechanism of cycle-addition is impeded by the low elasticity of the polymer chains in the solid state; therefore, part of the nitrilimine eliminates from nitrene and passes into nitrile



If a tert-butyl group is the alkyl substituent, then simultaneously with nitrogen elimination, detachment of the substituent from a part of the tetrazole cycle occurs, after which the polymer with non-substituted heterocycles undergoes thermolysis.

### Spectroscopic study of tetrazoles

The obtained data on the electron density distribution in the ring of 1- (1,5)- and 2- (2,5)-substituted tetrazoles suggest a sufficient difference in some spectral parameters of the mentioned tetrazole derivatives. This can be used for both the evaluation of their reactivity and identification. Therefore, it seemed expedient to carry out a systematical study of vibrational and NMR spectra of a wide range of tetrazoles.

For the correct assignment of the absorption bands of the ring in IR spectra of tetrazole derivatives, we carried out a comparative study of the theoretical and the experimental spectra of tetrazole and

deuteriotetrazole, tetrazolate-anion (the experimental spectra of tetrazolates of ammonium, alkali and earth-alkalimetals have been analyzed), as well as of a series of N-substituted and 5-substituted tetrazoles. The theoretical study included calculations of distribution of potential energy of vibrations which is necessary for the quantitative evaluation of the contribution of one or another type of vibrations into the spectroscopic pattern. Besides, a systematical analyses of the experimental IR spectra of 1- and 2-alkyltetrazoles with  $R=CH_3 \div n-C_8H_{17}$  and their complexes with some Cu(II) salts, vinyltetrazoles and some other tetrazole derivatives have been studied.

The obtained data allowed us to reveal several features, peculiar to the IR spectra of tetrazoles. Firstly, a mixing of different types of vibrations is observed for all the absorption bands attributed to the tetrazole cycle. Only in specific cases, one can identify the frequencies characterized by the predomination of contribution of definite type of vibrations into the distribution of their potential energy. Within the tetrazole-N-substituted tetrazoles series, among them are the stretching vibrations of C-H bonds which appear at  $3100-3145\text{ cm}^{-1}$  and  $1225-1289\text{ cm}^{-1}$ , respectively. Within tetrazole-5substituted tetrazoles series, deformation vibrations  $\rho_{N-H}$  are the most characteristic by the frequency. Secondly, in spite of sufficient differences in the force field of molecules of 1- (1,5)- and 2- (2,5)- substituted tetrazoles determined by features of electron density distribution in the cycle, the IR spectra of both 1- and 2-substituted tetrazoles contain, as a rule, a closely related set of absorption bands attributed to the tetrazole cycle which differ mainly by the intensity distribution. Nevertheless, the detailed analysis of IR spectra of individual and coordinated N-monosubstituted tetrazoles allow us to establish that absorption bands at  $1204-1309\text{ cm}^{-1}$  and  $1273-1289\text{ cm}^{-1}$  in spectra of 1- and 2-monosubstituted tetrazoles, respectively, determined mainly by the stretching vibrations of the cycle N-N bonds. In spectra of individual 1-monosubstituted tetrazoles,  $\nu_{N-N}$  appear as a set ( $2 \div 4$ ) of bands of low intensity, whereas in spectra of individual and coordinated 2-isomers,  $\nu_{N-N}$  is recorded as a singlet. These features permit one to identify the position of the substituent in the tetrazole cycle of isomers. The IR spectra of 1-methyl-5-vinyltetrazole (1-MVT) and 2-methyl-5-vinyltetrazole (2-MVT) were found to contain absorption bands at  $1098\text{ cm}^{-1}$  and  $735\text{ cm}^{-1}$ , correspondingly, which are characteristic of only each isomer. This allowed us to elaborate the method for the determination of the content

of 1-MVT and 2-MVT chains in their copolymers which are of great practical importance, because the commonly used elemental analysis is unsuitable in this case .

The performed analysis allowed to refine and to identify a number of absorption bands in the IR spectra of tetrazole and some its derivatives. In particular, it has been shown that the band at 1570  $\text{cm}^{-1}$  in the IR spectra of tetrazole is caused solely by the  $\text{C}=\text{N}$  and  $\text{N}=\text{N}$  vibrations rather than by  $\text{N}-\text{H}$  ones as expected previously. The assignment has been carried out also for absorption bands at 1688–1690  $\text{cm}^{-1}$  and 1792–1794  $\text{cm}^{-1}$  in IR spectra of tetrazolates of ammonium and alkali metals, which are considered earlier for sodium tetrazolate as combined bands. A special experiments on the temperature dependence of the maxima and the shape of absorption bands in IR spectra of ammonium tetrazolate in the crystal state and in the melt when using different samples (pellets with KBr, emulsions with Vaseline oil) allow one to conclude that the considered bands are determined by the influence of salts crystal lattice . The data of  $^1\text{H}$  and  $^{13}\text{C}$  NMR spectra allow one to clearly recognize the isomeric N monosubstituted tetrazoles. The chemical shifts (CSs) of the cycle carbon atoms in the  $^{13}\text{C}$  NMR spectra were found to be acutely sensitive to the isomer type. The CSs of 2-monosubstituted tetrazoles are displaced to a weak field by 10,4±1,8 ppm comparative to those of the corresponding 1-isomers, the nature of the N-substituent being exert insignificant influence on CS values. For a rich series of 1-monosubstituted tetrazoles, CS values of the cycle carbon atom appear within 140–145 ppm, whereas in the case of 2-monosubstituted tetrazoles these values amount to 152–154 ppm. In the case of 1,5- and 2,5-substituted tetrazoles, CS of the cycle carbon atom depends substantially on the nature of the substituent at the C(5) atom . The CSs of hydrogen atom at the carbon atom of the tetrazole cycle in  $^1\text{H}$  NMR spectra are displaced to a weak field comparative to those of the corresponding 2-isomers. However, CSs of these atoms in the case of 1-isomers, in contrary to 2-isomers, depend significantly on the nature of solvent and, in some cases, on the solution concentration. This is conditioned by the ability of molecules of 1-substituted tetrazoles to association and specific solvation . The obtained data on  $^{13}\text{C}$  NMR spectra of tetrazolium salts show the significant difference between CSs of the cycle carbon atom of 1,4- (1,4,5)- and 1,3- (1,3,5)-substituted tetrazolium salts identical to that for N-substituted tetrazoles.

An analysis of  $^1\text{H}$  and  $^{13}\text{C}$  NMR spectra of a wide series of p- and m-substituted 1-phenyltetrazoles and the establishment of linear correlations ( $r=0,992$ ) between the CSs of C(5)-H proton and CSs of protons of phenyl groups allowed us to evaluate precisely the Hammett constants  $\sigma_m=0,53\pm0,04$ ;  $\sigma_p=0,50\pm0,04$ ;  $\sigma_I=0,56\pm0,03$  and the Taft constants  $\sigma_R=-0,04\pm0,04$ ;  $\sigma_R^0=-0,04\pm0,01$  of 1-tetrazolyl group [119]. The data of  $^{13}\text{C}$  NMR spectra of a series of 1- and 2-alkyl(allyl)-tetrazoles and the comparison of CSs of carbon atoms of alkyl substituents with CSs of the corresponding atoms of unsubstituted alkanes allowed one to estimate the values of increments of N-tetrazolyl groups which amount to  $\alpha=+36,3\pm2,0$ ;  $\beta=+9,1\pm1,5$ ;  $\gamma=-3,3\pm1,1$  for the 1-tetrazolyl group and  $\alpha=+40,8\pm1,3$ ;  $\beta=+8,1\pm1,2$ ;  $\gamma=-3,4\pm1,1$  for the 2-tetrazolyl group. The obtained values are close to those of NHR and NR<sub>2</sub> groups, respectively.

#### **4. Tetrazole coordination complexes (TCC)**

According to the mechanism proposed by Sharpless and co-workers, the intermediates in the [2+3] cycloaddition of an azide anion to a nitrile group should involve a 1-metal-coordination compound. However the reaction mechanism seems much more complicated based on subsequent works by us and others. Most of the coordination compounds, which were synthesized by the in situ hydrothermal method, were found not only to possess the 1-coordination mode but also several other modes. Thus, before we describe the structures of these coordination compounds, we will first discuss their coordination modes

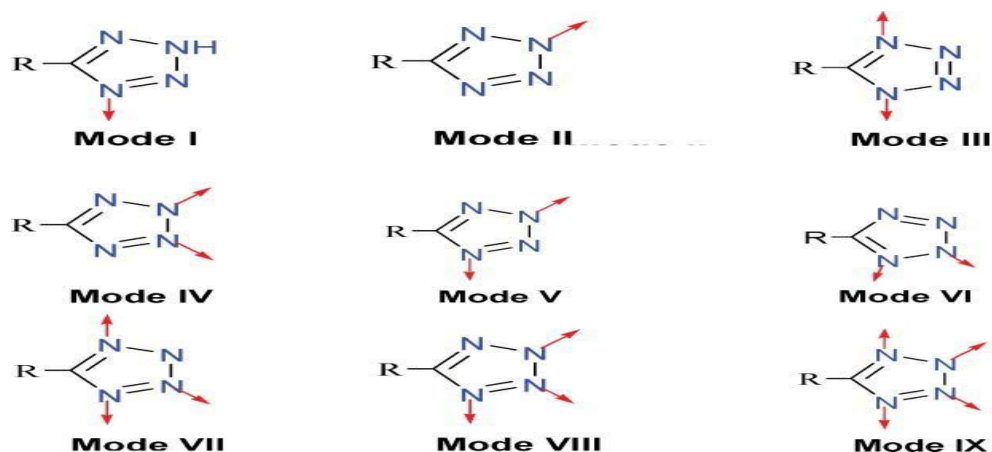
##### **Coordination modes**

Putting aside the mechanism of the [2+3] cycloaddition and in situ hydrothermal method, the tetrazole ligand has been shown to be able to participate in at least nine distinct types of coordination modes with metal ions in the construction of metal–organic frameworks . Tetrazoles have attracted increasing attention in recent years in coordination chemistry due to the excellent coordination ability of the four nitrogen atoms of the functional group to act as either a multidentate or a bridging building block in supramolecular assemblies. Thus, it is not difficult to find numerous examples in the literature of tetrazole coordination compounds with these nine coordination modes.

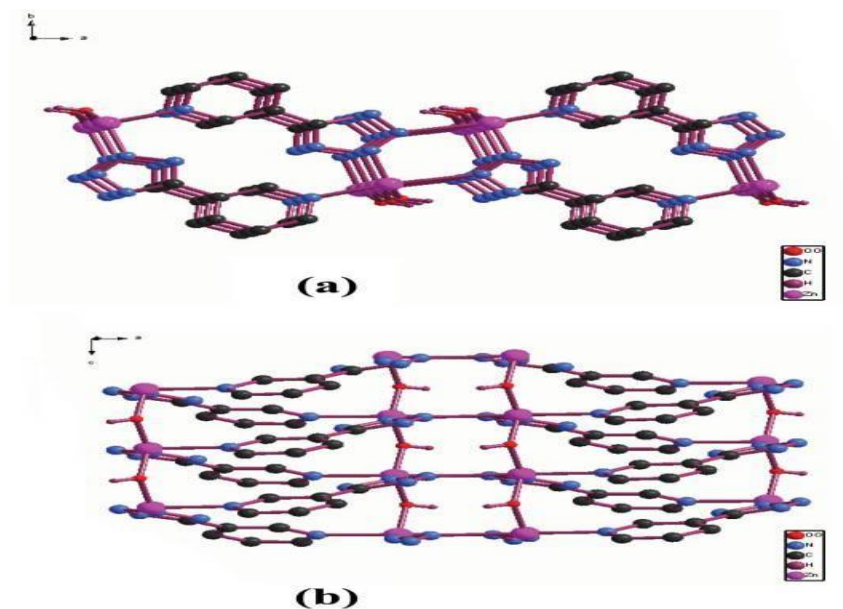
##### **Pyridyl-tetrazole (PTZ) coordination compounds**

There are a myriad study in the literature of tetrazole coordination compounds containing the pyridyl functionality. They can be prepared from the corresponding cyanopyridine,  $\text{NaN}_3$ , and  $\text{MX}_2$ . Due to the donor–acceptor system between the pyridine and cyano groups, the azide anion can easily attack the N atom of the cyano group. This reactivity means that the reaction can be carried out at room temperature.<sup>11</sup> In this review, we will mainly focus on complexes synthesized

under hydrothermal conditions.  $[\text{Zn}(\text{OH})(3\text{-PTZ})]$  (1) (3-PTZ 5 5-(3-pyridyl)tetrazolate) was prepared by reaction of 3-cyanopyridine with  $\text{NaN}_3$  and  $\text{ZnCl}_2$  under hydrothermal condition at 160 uC.<sup>12</sup> This complex is a two-dimensional (2D) polymer (Fig. 1). It should be



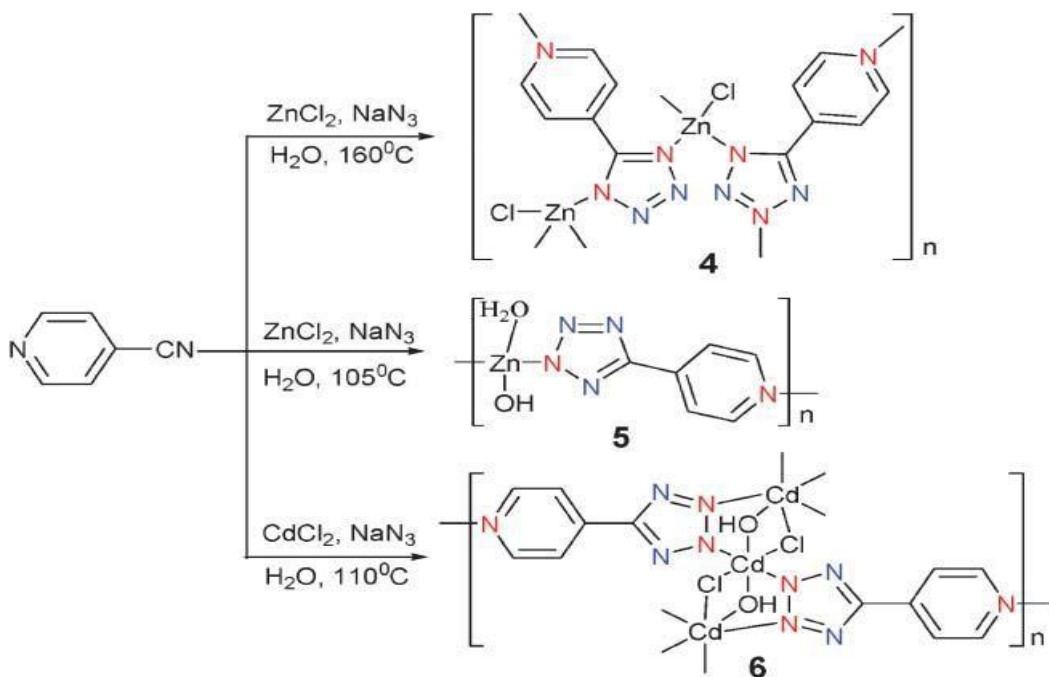
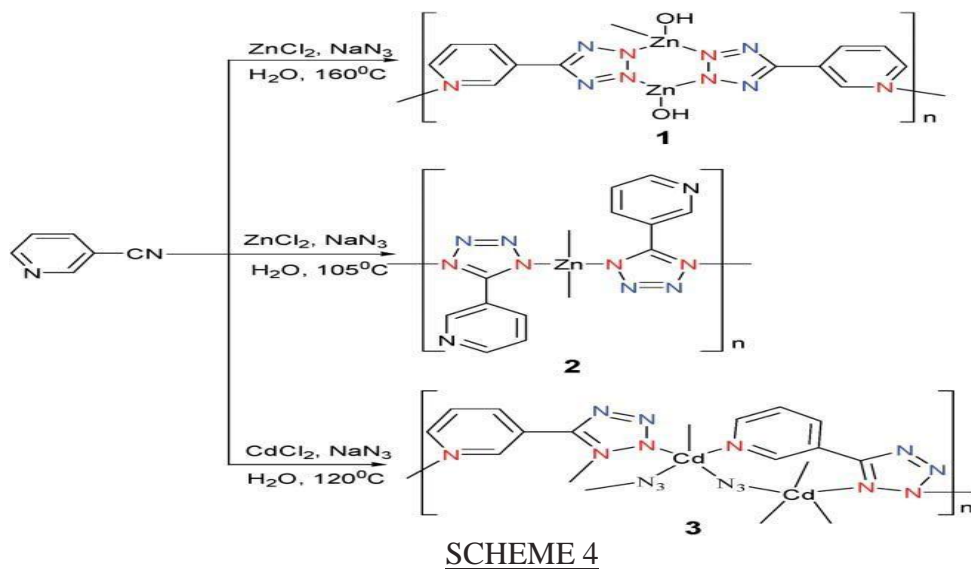
**SCHEME 3**



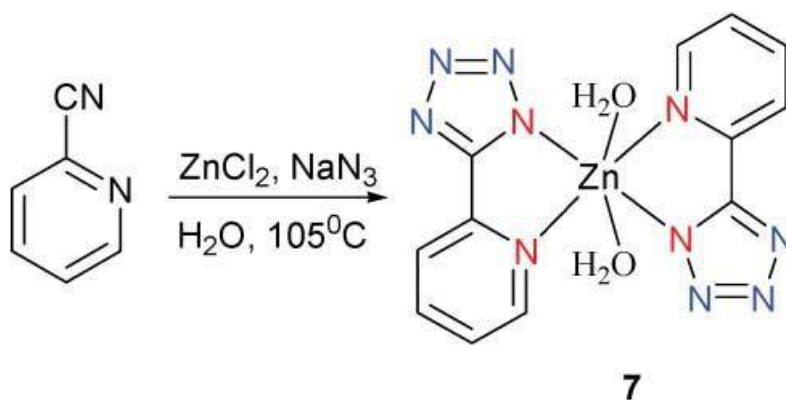
**Fig. 1** 2D structure of (a) A view almost normal to the axis of the two fold helices that extend In the C direction. (b) A perspective view of the sheet structure from a direction parallel to the C axis.

It should be emphasized that the 3-PTZ ligand acts as a bidentate bridge through the 2,3 N atoms of the tetrazole (Mode IV). Its coordination mode does not agree with the mechanism proposed by Sharpless and co-workers. Using the same reactants as for 1 but at a lower temperature (105 °C) afforded [(3-PTZ)<sub>2</sub>Zn]. The solid structure of complex 2 revealed the Zn atom to coordinate only to four of the N atoms from the tetrazoles of the 3-PTZ ligands (Mode III). This results in the formation of a 3D diamondoid framework. Similarly, [CdN<sub>3</sub>(3-PTZ)] was prepared in the same manner as that for 1 but with CdCl<sub>2</sub> to replace ZnCl<sub>2</sub>. However, 3 was shown to contain azide ligands and a 3D polymer structure in which these ligands adopted two distinct bridging modes based on X-ray analysis. The complex structure is perhaps best understood by considering zig-zagging chains of cadmium atoms extending in the c direction (Fig. 2). The two unique types of azide ions alternate as bridging ligands along the chain. The complex also contains one tetrazole–metal coordination in Mode VI [ZnCl(4-PTZ)] was prepared in the same manner as that for 1 at 160 °C but with 4-cyanopyridine to replace 3-cyanopyridine.<sup>12</sup> Interestingly, with this small change, a different coordination environment was obtained. Compound 4 has a 3D network structure (Fig. 3a). This complex coordination polymer is perhaps best understood in terms of [ZnCl(4-PTZ)] strips that extend in the c direction, that possess two distinct kinds of tetrazole coordination modes (Modes III & V). Inspection of Fig. 3b reveals large channels with an approximate hexagonal cross section. These intraframework voids are occupied by a second identical network. The two networks are represented in Fig. 3c. Simply changing the reaction temperature from 160 to 105 °C was found to give [(4-PTZ)Zn(OH)(H<sub>2</sub>O)]. The solid state structure of compound 5 showed that the Zn atom not only coordinates to two atoms from the pyridyl ring and tetrazole of the 4-PTZ ligand (Mode II), but also binds to two hydroxy groups that are presumably formed in situ from water. Thus, compound 5 shows a two-dimensional layered structure with an intercalated water molecule through hydrogen bonding between the two layers. This result is unexpected, probably suggesting that water is also a reactant. [Cd<sub>3</sub>(OH)<sub>2</sub>Cl<sub>2</sub>(4-PTZ)<sub>2</sub>] was obtained by the treatment of CdCl<sub>2</sub> with 4-cyanopyridine in the presence of NaN<sub>3</sub> and water under hydrothermal conditions at 110

<sup>0</sup>C. The structure incorporates not only the anticipated PTZ ligand which acts as a tridentate bridging ligand but also hydroxide and chloride ions.







SCHEME 6

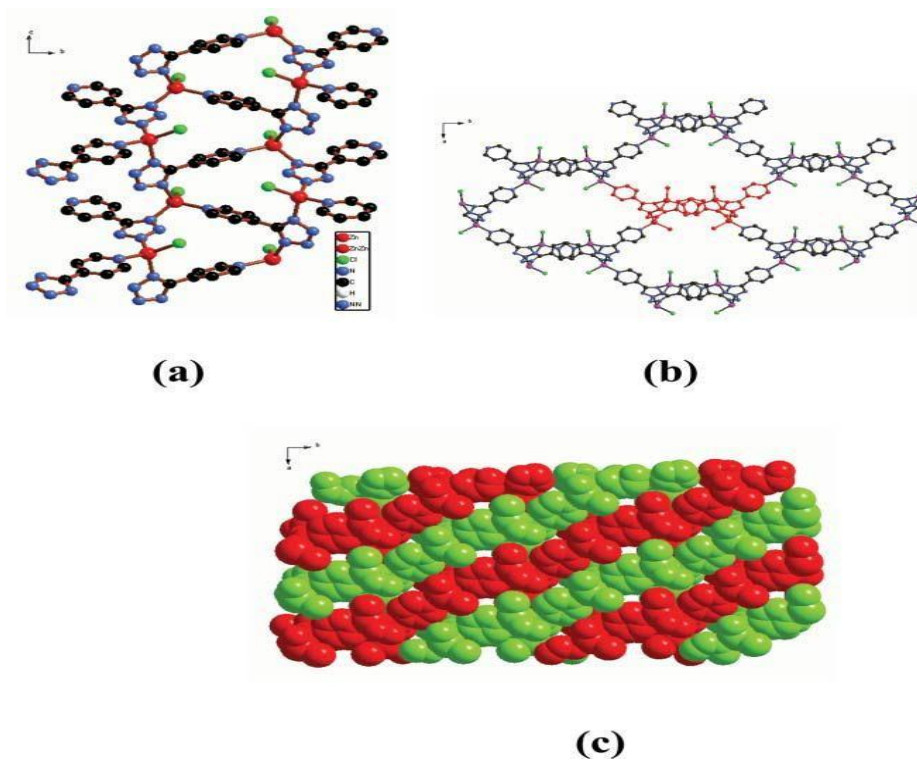
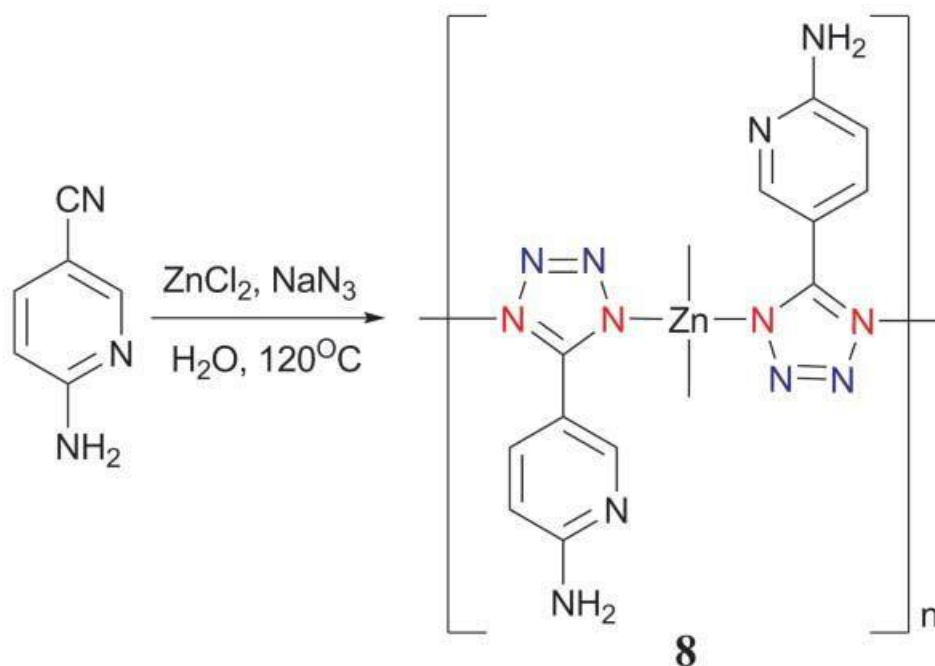


**Fig. 3.** 3D interpenetrating structure of 4. (a)  $[\text{ZnCl}(4\text{-PTZ})]$  strips extending in the  $c$  direction. (b) A view down the  $c$  axis of 4 showing the connections between strips. The central strip is highlighted with red spheres. (c) A space-filling model showing the interpenetration of the independent networks within the crystal

For each Cd, the trans chloride and trans hydroxide ions form an approximate square planar arrangement while the remaining trans positions are occupied by N atoms from the two 4-PTZ ligands (Mode IV) (Scheme 5).

$[(2\text{-PTZ})_2\text{Zn}(\text{H}_2\text{O})_2]$  was prepared by hydrothermal reaction of 2-cyanopyridine,  $\text{NaN}_3$ , and  $\text{ZnCl}_2$  at  $105^\circ\text{C}$  (Scheme 6). The local coordination geometry around the Zn center can be best described as a slightly distorted octahedron with four equatorial nitrogen atoms from two 2-PTZ ligands (Mode I) and two apical water molecules, resulting in the formation of a monomeric Zn complex.  $[(2\text{-NH}_2\text{-5-PTZ})_2\text{Zn}]$  was prepared under hydrothermal conditions by reacting 2-amino-5-cyanopyridine with  $\text{ZnCl}_2$  in the presence of  $\text{NaN}_3$  (Scheme 7). The three-dimensional diamondoid polymeric structure of **8** was determined by X-ray crystallography (Fig. 4). The Zn(II) center is bonded to the four N atoms of the four 2-NH<sub>2</sub>-5-PTZ ligands (Mode III). It is worth noting that the amino and pyridyl groups present in **8** are uncoordinated to the Zn atom.



SCHEME 7

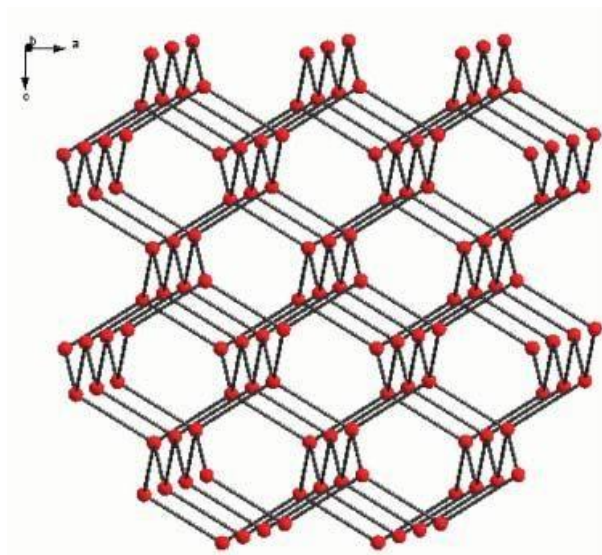
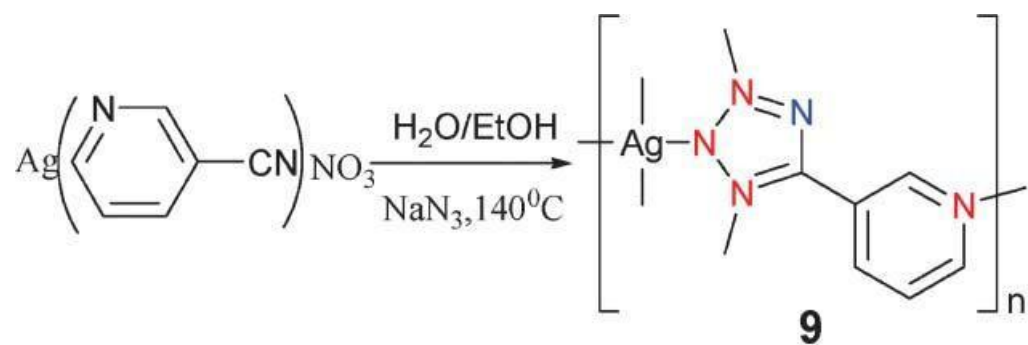


**Fig. 4.** 3D diamondoid-like network (the ligands between Zn atom are simplified as bonds).



SCHEME 8

[(3-PTZ)Ag] was prepared under very different conditions. In view of the fact that Ag(I) can be easily reduced in the in situ [2+3] tetrazole reaction system, the expected product cannot be obtained by directly reacting the silver salt with other reactants. A solution to this synthetic problem is the use of a Ag<sup>+</sup> coordination polymer with cyanopyridine to replace AgNO<sub>3</sub> as the Lewis acid for the in situ [2+3] cycloaddition reaction of the cyano and azide groups in the presence of water (Scheme 8). This gave the anticipated Ag tetrazole coordination polymer. The local coordination geometry around each Ag center is a slightly distorted tetrahedron defined by four N atoms from three different tetrazole (Mode VIII) and one pyridyl groups. Thus, each 3-pyridyltetrazole acts as a tetradentate ligand coordination to four different silver centers leading to the formation of the 2D layered network.

#### **Application of Tetrazole coordination complexes in organic synthesis**

A key application of TCC is in organic synthesis, where they are used as the starting and intermediate compounds for the preparation of valuable and practical substances. The synthesis of N-substituted tetrazoles N-alkyl-, N-aryl- and N-heteroaryl tetrazoles from various metal tetrazolates, and as a method for introducing tetrazolyl groups into complex biologically active compounds, are prominent examples of can be accomplished with this synthetic strategy.

## 5. Uses of Tetrazole and its derivative compounds in pharmaceuticals

### uses

Tetrazoles and triazoles are used for their hotheaded or combustive belongings, for instance tetrazole itself with 5-aminotetrazole, which are sometimes used as a component of gas generators in automobile airbags. Its derivatives represent a connecting ring and a raw material for many interactions of synthetic chemistry, chemistry of coordination complexes and reagents, because of the hybrid atoms they contain within their composition, which gave them extremely important being that they contain atoms characterized by biological and pharmacological activities and the basic nucleus of many life compounds, vitamins and medicines. Tetrazole created energetic materials yield high-temperature and non-toxic reaction products for instance water besides to nitrogen gas and have a high burn rate and relative stability to all of which are desirable properties.

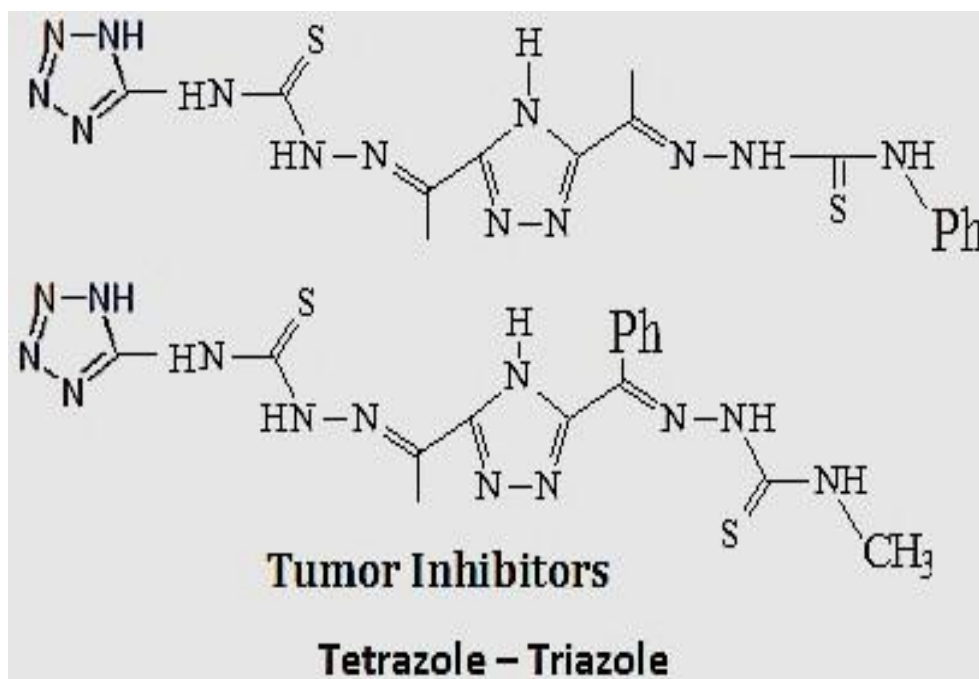


**Fig.** Tetrazole and Triazole compound as tumor inhibitors

## **Tetrazole compounds as anticancer drugs**

Different tetrazole derivatives containing isoxazole has been synthesized. 5-phenyl tetrazoles was cyclized using sodium azide and ammonium chloride and benzonitrile. The 5-phenyl tetrazoles on treatment with acetic anhydride forms 5-phenyl 1-acetyl Tetrazole which on reaction with different aromatic aldehydes forms chalcones. The chalcones further undergo cyclisation with hydroxylamine hydrochloride in presence of KOH to form 5-phenyl-1-(5-substituted phenyl isoxazol-3-yl)-1*H*-tetrazole. The chemical structures were confirmed by means of FT-IR, <sup>1</sup>H-NMR and elemental analysis. Among the synthesized tetrazole derivatives, eight compounds have been selected and evaluated for their anticancer activity at the National Cancer Institute for testing against a panel of approximately 60 different human tumor cell lines derived from nine neoplastic cancer types.

## **Tetrazole derivatives having various pharmaceutical properties.**

Tetrazole derivatives possess very interesting pharmacological and biological properties and are reported to exhibit variety of biological activities like antibacterial antifungal and anticonvulsant, analgesic, anti-inflammatory, antitubercular activity and anticancer activity . Similarly, 1, 5 disubstituted tetrazoles have long been known for their pharmaceutical activity as stimulants or depressants on the central nervous system and are reported to show oral antidiabetic and antithrombotic and antimicrobial properties. Isoxazoles may show interesting medicinal or crop protection properties or have some other industrial utility. Various pharmacologically important isoxazoles with antimicrobial . anti-inflammatory, analgesic , antitubercular activity , antitumoral and antimycobacterial activity .have already been reported. Isoxazoles are unique in their chemical behavior, not only among heterocyclic compounds in general, but also among related azoles.

**REFERENCES:-**

1. (a) He, P.; Zhang, J.-G.; Yin, X.; Wu, J.-T.; Wu, L.; Zhou, Z.-N.; Zhang, T.-L. *Chem.–Eur. J.* 2016, 22, 7670. (b) Klapötke, T. M. *Chemistry of High-Energy Materials*; Walter de Gruyter: Berlin, 2012, 2nd ed., p. 273. (c) Gao, H.; Shreeve, J. M. *Chem. Rev.* 2011, 111, 7377. (d) Singh, R. P.; Verma, R. D.; Meshri, D. T.; Shreeve, J. M. *Angew. Chem., Int. Ed.* 2006, 45, 3584. (e) Gao, H.; Shreeve, J. M. *Chem. Rev.* 2011, 111, 7377.
2. (a) Ostrovskii, V. A.; Koldobskii, G. I.; Trifonov, R. E. In *Comprehensive Heterocyclic Chemistry III*; Katritzky, A. R.; Ramsden, C. A.; Scriven, E. F. V.; Taylor, R. J. K., Eds.; Elsevier: Oxford, 2008, Vol. 6, p. 257. (b) Ostrovskii, V. A.; Pevzner, M. S.; Kofman, T. P.; Shcherbinin, M. B.; Tselinskii, I. V. *Targets Heterocycl. Syst.* 1999, 3, 467.
3. Trifonov, R. E.; Ostrovskii, V. A. *Russ. J. Org. Chem.* 2006, 42, 1599. [*Zh. Org. Khim.* 2006, 42, 1585.]
4. Gaponik, P. N.; Voitekhovich, S. V.; Ivashkevich, O. A. *Russ. Chem. Rev.* 2006, 75, 507. [*Usp. Khim.* 2006, 75, 569.]
5. Voitekhovich, S. V.; Gaponik, P. N.; Ivashkevich, O. A. *Russ. Chem. Rev.* 2002, 71, 721. [*Usp. Khim.* 2002, 71, 818.]
6. Zhang, Q.; Shreeve, J. M. *Chem. Rev.* 2014, 114, 10527.
7. Kamiya, T.; Saito, Y. JP Patent 7247031; *Chem. Abstr.* 1973, 78, 111331.
8. (a) Kamiya, T.; Saito, Y. US Patent 3767667; *Chem. Abstr.* 1974, 80, 27262a. (b) Kamiya, T.; Saito, Y. DE Patent 2147023; *Chem. Abstr.* 1973, 79, 5346. (c) Kamiya, T.; Saito, Y. FR Patent 2153772; *Chem. Abstr.* 1973, 79, 78807u.
9. (a) Bison, G.; Heinzelmann, W.; Linkat, N. DE Patent 2348802; *Chem. Abstr.* 1975, 83, 58836. (b) Bison, G.; Linkat, N.; Wolfes, W. DE Patent 2854015; *Chem. Abstr.* 1981, 94, 15739n. (c) Janda, L.; Martvon, A. CZ Patent 259379; *Chem. Abstr.* 1989, 111, 134166.

10. (a) Gaponik, P. N. Dissert. of Doctor of Chemical Sciences; Minsk, 2000. (b) Grigor'ev, Yu. V. Dissert. of Candidate of Chemical Sciences; St.Petersburg, 1998. (c) Voitekhovich, S. V.; Ivashkevich, O. A.; Gaponik, P. N. Russ. J. Org. Chem. 2013, 49, 635. [Zh. Org. Khim. 2013, 49, 655.].
11. *Gaponik P. N., Karavai V. P.* USSR Patent 915423 (1981).
12. *Gaponik P. N., Karavai V. P.* Khimiya Geterotsiklicheskikh Soedinenii, 1983, <sup>1</sup> 6, pp. 841–842. (in Russ.) // Chemistry of Heterocyclic Compounds (Engl. Transl.), 1983, Vol. 19, No. 6, P. 681–682.
13. *Gaponik. P. N., Karavai V. P., Chernavina N. I.* Vestnik Belorusskogo Universiteta. Seriya 2, 1983, <sup>1</sup> 2, P. 23–25.
14. *Gaponik P. N., Karavai V. P.* Khimiya Geterotsiklicheskikh Soedinenii, 1985, <sup>1</sup>10, P. 1422–1424. (in Russ.) // Chemistry of Heterocyclic Compounds (Engl. Transl.), 1985, Vol. 21, <sup>1</sup> 10, P. 1172–1174.
15. *Gaponik P. N., Karavai V. P., Grigoriev Y. V.* Khimiya Geterotsiklicheskikh Soedinenii, 1985, <sup>1</sup>11, P. 1521–1524. (in Russ.) // Chemistry of Heterocyclic Compounds (Engl. Transl.), 1985, Vol. 21, <sup>1</sup> 11, P. 1255–1258.
16. *Grigoriev Y. V., Maruda I. I., Gaponik P. N.* Vestsi NAN Belarusi. Seriya Khimichnikh Navuk, 1997, <sup>1</sup> 4, P. 86–90.
17. *Gaponik P. N.* Doctoral Thesis in Chemical Sciences, Research Institute for Physical Chemical Problems of Belorussian State University, Minsk, 2000.
18. *Voitekhovich S. V., Gaponik P. N., Lyakhov A. S., Ivashkevich O. A.* Polish Journal of Chemistry, 2001, Vol. 75, <sup>1</sup> 2. P. 253–264.
19. *Voitekhovich S. V., Vorobiev A. N., Gaponik P. N., Ivashkevich O. A.* Khimiya Geterotsiklicheskikh Soedinenii, 2003, in press, (in Russ.) // Chemistry of Heterocyclic Compounds (Engl. Transl.), 2003, in press.
20. Gibbs J. B., Science ,287, 1969,(2000).
21. Unger C., Drug Future,22, 1337,(1997).
22. Heffeter P., Jakupec M. A., W. Orner, S. Wild, N. G. Keyserlingk, L. Elbling, H. Zorbas, A. Korynevskaya, S. Knasmüller, H. Sutterluty, M. Micksche, B. K. Keppler, W. Berger, Biochem. Pharmacol. 71, 426(2006) .
23. Menta E., Palumbo M., Exp. Opin. Ther. Patents ,7, 1401,(1997) .



24. Boyd M.R., Paull K. D., Drug Dev. Res. 34, 91 (1995).
25. Shwartsmann G., Winograd B.,Pinedo H.H.' ,12, 301,(1988).
26. Kemajl, K., Idriz V., Arben ,H., Sevdije,G., Muharrem I. and Sefkija M.,The FASEB Journal. 21:790-795,(2007).
27. Mulwad, V. V. ;Pawar, Rupesh ,B. ; Chaskar, Atul ,C. J. Korean Chem.Soc. 52,3, 249-256,(2008).
28. Upadhayaya, R. S.; Jain, S.; Sinha, N.; Kishore, N.; Chandra, R.; and Arora, S. K.; Eur. J. Med. Chem. 39, 579-592, (2004).
29. Rajasekaran, A. ;Sankar,N.; Murugesh, A.; Kalasalingam, Rajagopal A.; Archives of Pharmacal Research. 29,7,535-540(2006).
30. Mohite, P., B., Pandhare, R. B., Khanage, S.G., Bhaskar V.H., Journal of Pharmacy Research. 3,(1),43-46,(2010).
31. Adamec ,J.;Waisser K.; Kunes J.; Kaustova, J.; ArchPharm.2005;338: 385- 389.
32. De, Souza, AO., Pedrosa, MT., Alderete, JB., Cruz AF., Prado MA., Alves, RB., Silva CL.; Pharmazie.60,(5),396-397,(2005).
33. Dabholkar V.V.,and Faisal ,Y. A. . J. Serb. Chem. Soc. ,74 (11) 1219–1228,(2009).
34. Karbasanagouda T.,A.,Vasudeva A.,Girisha M, Indian .J.Chem.,48B:430-437, (2009).
35. Tangallapally R.J.,, Dianqing Sun, R., Nageshwar B., Robin E.B. Lee, Anne J.M. Lenaerts, Bernd M. and Richard E. Lee. Bioorg Med Chem Lett. 17:(23):6638, (2007).
36. Ray, S.M. ;Lahiri, S.C.; J. Ind. Chem. Soc., 67, 324-326(1990).
37. National Cancer Institute, <http://dtp.nci.nih.gov>.
38. Furniss, B.S.; Hennafor, A, J; Smith, P.W.G.; Tatchell, A.R. In: Vogel Text Book of Practical organic chemistry, 5th edn, Addison-Wesley, England, pp. 692: 1261-1262, (1998).
39. Mann, F.G. and Saunder, B.C. Practical Organic Chemistry, 4th edn, Orient Longman Private Limited, New Delhi-110002. pp 118-119, (2003).
40. Popat ,K.H .,Nirmavat, K.S., Kachhadia ,V.V., Joshi H.S. J Indian Chem Soc.,80,707-778, (2003)..
41. Sherif ,A.F., Rostom, Hayam M.A., Ashour, Heba A., Abd El, Razik, Abd El Fattah H. Abd El Fattah and Nagwa N. El-Din; Bioorg Med Chem . 17:6: 2410-2422, (2004).
42. Rajasekaran A. ,Sankaranarayanan ,M., Kalasalingam A. R., Archives of Pharmacal

Research.29:7:535-540(2006).

43. Mohite ,P. B., Pandhare, R. B., Khanage, S. G. , Bhaskar, V. H. Digest Journal Of Nanomaterials And Biostructures , 4: 4:803 -807(2009).

44. J. A. Bladin, Ber. Dtsch. Chem. Ges., 1885, 18, 1544.

45. (a) F. R. Benson, Chem. Rev., 1947, 41, 1; (b) F. R. Benson, Heterocycl. Compd., 1967, 8, 1; (c) R. N. Butler, Adv. Heterocycl. Chem., 1977, 21, 323; (d) R. N. Butler, in Comprehensive Heterocyclic Chemistry, ed. A. R. Katritzky, Elsevier, Amsterdam, 1984, vol. 5, p. 791; (e) S. J. Wittenberger, Org. Prep. Proced. Int., 1994, 26, 499; (f) R. N. Butler, in Comprehensive Heterocyclic Chemistry II, ed. A. R. Katritzky, C. W. Rees and E. F. V. Scriven, Pergamon Press, Oxford, 1996, vol. 4, p. 621.

46. P. N. Gaponik, S. V. Voitekhovich and O. A. Ivashkevich, Russ. Chem. Rev., 2006, 75, 507.

47. H. Singh, A. S. Chawla, V. K. Kapoor, D. Paul and R. K. Malhotra, Prog. Med. Chem., 1980, 17, 151.

48. (a) V. A. Ostrovskii, M. S. Pevzner, T. P. Kofmna, M. B. Shcherbinin and I. V. Tselinskii, Targets Heterocycl. Syst., 1999, 3, 467; (b) M. Hiskey, D. E. Chavez, D. L. Naud, S. F. Son, H. L. Berghout and C. A. Bome, Proc. Int. Pyrotech. Semin, 2000, 27, 3.

49. A. Hantzsch and A. Vagt, Justus Liebigs Ann. Chem., 1901, 314, 339.

50. Z. P. Demko and K. B. Sharpless, J. Org. Chem., 2001, 66, 7945.

51. (a) F. Himo, Z. P. Demko, L. Noodleman and K. B. Sharpless, J. Am. Chem. Soc., 2002, 124, 12210; (b) F. Himo, Z. P. Demko, L. Noodleman and K. B. Sharpless, J. Am. Chem. Soc., 2003, 125, 9983.

52. J. Blake, N. R. Champness, S. S. M. Chung, W.-S. Li and M. Schroder, Chem. Commun., 1997, 1675.

53. X.-M. Zhang, Coord. Chem. Rev., 2005, 249, 1201.

- 54.(a) P. Lin, W. Clegg, R. W. Harrington and R. A. Henderson, Dalton Trans., 2005, 2388; (b) Z.-X. Yu, X.-P. Wang, Y.-Y. Feng and X.-H. Zhong, Inorg. Chem. Commun., 2004, 7, 492; (c) X.-J. Mo, E.-Q. Gao, Z. He, W.-J. Li and C.-H. Yan, Inorg. Chem. Commun., 2004, 7, 353; (d) F. A. Mautner, C. Gspan, K. Gatterer, M. A. S. Goher, M. A. M. Abu-Youssef, E. Bucher and W. Sitte, Polyhedron, 2004, 23, 1217.
55. R.-G. Xiong, X. Xue, H. Zhao, X.-Z. You, B. F. Abrahams and Z.-L. Xue, Angew. Chem., Int. Ed., 2002, 41, 3800.
56. L.-Z. Wang, Z.-R. Qu, H. Zhao, X.-S. Wang, R.-G. Xiong and Z.-L. Xue, Inorg. Chem., 2003, 42, 3969.
57. X. Xue, X.-S. Wang, L.-Z. Wang, R.-G. Xiong, B. F. Abrahams, X.-Z. You, Z.-L. Xue and C.-M. Che, Inorg. Chem., 2002, 41, 6544.
58. Q. Ye, Y.-H. Li, Y.-M. Song, X.-F. Huang, R.-G. Xiong and Z.-L. Xue, Inorg. Chem., 2005, 44, 3619.
- 16 X.-S. Wang, Y.-Z. Tang and R.-G. Xiong, Chin. J. Inorg. Chem., 2005, 21, 1025.
59. X.-S. Wang, Y.-Z. Tang, X.-F. Huang, Z.-R. Qu, C.-M. Che, P. W. H. Chan and R.-G. Xiong, Inorg. Chem., 2005, 44, 5278.
60. T. Wu, B.-H. Yi and D. Li, Inorg. Chem., 2005, 44, 4130.
61. L.-Z. Wang, X.-S. Wang, Y.-H. Li, Z.-P. Bai, R.-G. Xiong, M. Xiong and G.-W. Li, Chin. J. Inorg. Chem., 2002, 18, 1191.
- Scheme 27
62. (a) H. Zhao, Q. Ye, Q. Wu, Y.-M. Song, Y.-J. Liu and R.-G. Xiong, Z. Anorg. Allg. Chem., 2004, 630, 1367; (b) Y.-C. Wang, H. Zhao, Y.-M. Song, X.-S. Wang and R.-G. Xiong, Appl. Organomet. Chem., 2004, 18, 494.
63. X.-F. Huang, Y.-M. Song, Q. Wu, Q. Ye, X.-B. Chen, R.-G. Xiong and X.-Z. You, Inorg. Chem. Commun., 2005, 8, 58.
64. X.-S. Wang, X.-F. Huang and R.-G. Xiong, Chin. J. Inorg. Chem., 2005, 21, 1020.

65. X.-H. Huang, T.-L. Sheng, S.-C. Xiang, R.-B. Fu, S.-M. Hu, Y.-M. Li and X.-T. Wu, *Inorg. Chem. Commun.*, 2006, 9, 1304.
66. (a) T. J. Marks and M. A. Ratner, *Angew. Chem., Int. Ed. Engl.*, 1995, 34, 155; (b) C. Janiak, *Dalton Trans.*, 2003, 2781; (c) S. L. James, *Chem. Soc. Rev.*, 2003, 32, 276; (d) B. Kesanli and W. Lin, *Coord. Chem. Rev.*, 2003, 246, 305; (e) Q. Ye, X.-S. Wang, H. Zhao and R.-G. Xiong, *Chem. Soc. Rev.*, 2005, 34, 208.
67. Z.-R. Qu, H. Zhao, X.-S. Wang, Y.-H. Li, Y.-M. Song, Y.-J. Liu, Q. Ye, R.-G. Xiong, B. F. Abrahams, Z.-L. Xue and X.-Z. You, *Inorg. Chem.*, 2003, 42, 7710.
68. Q. Ye, Y.-Z. Tang, X.-S. Wang and R.-G. Xiong, *Dalton Trans.*, 2005, 1570.
69. Q. Ye, Y.-M. Song, G.-X. Wang, K. Chen, D.-W. Fu, P. W. H. Chan, J.-S. Zhu, S.-P. D. Huang and R.-G. Xiong, *J. Am. Chem. Soc.*, 2006, 128, 6554.
70. T. Wu, R. Zhou and D. Li, *Inorg. Chem. Commun.*, 2006, 9, 341.
71. X.-S. Wang, Y.-M. Song and R.-G. Xiong, *Chin. J. Inorg. Chem.*, 2005, 21, 1030.
72. (a) L. Pu, *Chem. Rev.*, 2004, 104, 1687; (b) P. C. Ford, E. Cariati and J. Bourassa, *Chem. Rev.*, 1999, 99, 3625.
73. (a) *Nonlinear Optical properties of Organic Molecules and Crystals*, vol. 1, ed. J. Zyss and D. S. Chemla, Academic Press, New York, 1989, p. 23; (b) N. J. Long, *Angew. Chem., Int. Ed. Engl.*, 1995, 34, 21; (c) J. Zyss and J. F. Nicoud, *Curr. Opin. Solid State Mater. Sci.*, 1996, 1, 533; (d) M. C. Etter and K. S. Huang, *Chem. Mater.*, 1992, 4, 824; (e) D. Y. Curtin and C. Paul, *Chem. Rev.*, 1981, 81, 525; (f) *Nonlinear Optical Effects and Materials*, Springer Series in Optical Sciences, ed. P. Gunter, vol. 72, Berlin, Germany, 2000.
74. K. M. Ok, E. O. Chi and P. S. Halasyamani, *Chem. Soc. Rev.*, 2006, 35, 710.
75. P. A. Franken, A. E. Hill, C. W. Peters and G. Wienrich, *Phys.*

Rev. Lett., 1961, 7, 118.

76. S. Endo, T. Chino, S. Tsuboi and K. Koto, *Nature*, 1989, 340, 452.

77. R. P. Lemieux, *Acc. Chem. Res.*, 2001, 34, 845.

78. K. E. Maly, M. D. Wand and R. P. Lemieux, *J. Am. Chem. Soc.*, 2002, 124, 7898.

79. T. Lee and I. A. Aksay, *Cryst. Growth Des.*, 2001, 1, 409.

80. (a) Z.-R. Qu, H. Zhao, Y.-P. Wang, X.-S. Wang, Q. Ye, Y.-H. Li, R.-G. Xiong, B. F. Abrahams, Z.-G. Liu, Z.-L. Xue and X.-Z. You, *Chem.-Eur. J.*, 2004, 10, 54; (b) Y.-R. Xie, H. Zhao, X.-S. Wang, Z.-R. Qu, R.-G. Xiong, X. Xue, Z.-L. Xue and X.-Z. You, *Eur. J. Inorg. Chem.*, 2003, 20, 3712; (c) H. Zhao, Z.-R. Qu, Q. Ye, B. F. Abrahams, Y.-P. Wang, Z.-G. Liu, Z.-L. Xue, R.-G. Xiong and X.-Z. You, *Chem. Mater.*, 2003, 15, 4166; (d) Y.-H. Li, Z.-R. Qu, H. Zhao, Q. Ye, L.-X. Xin, X.-S. Wang, R.-G. Xiong and X.-Z. You, *Inorg. Chem.*, 2004, 43, 3768.

81. (a) H. Zhao, Y.-H. Li, X.-S. Wang, Z.-R. Qu, L.-Z. Wang, R.-G. Xiong, B. F. Abrahams and Z.-L. Xue, *Chem.-Eur. J.*, 2004, 10, 2386–2390; (b) Q. Ye, Y.-H. Li, Q. Wu, Y.-M. Song, J.-X. Wang, H. Zhao, R.-G. Xiong and Z. Xue, *Chem.-Eur. J.*, 2005, 11, 988.

82. T. A. Vanderah, *Science*, 2002, 298, 1182.

83. C. C. Homes, T. Vogt, S. M. Shapiro, S. Wakimoto and A. P. Ramirez, *Science*, 2001, 293, 673.

84. (a) A. Palazzi, S. Stagni, S. Selva and M. Monari, *J. Organomet. Chem.*, 2003, 135, 669; (b) A. Hammerl, G. Holl, T. M. Klapotke, P. Mayer, H. Noth, H. Piotrowski and M. Warchhold, *Eur. J. Inorg. Chem.*, 2002, 834; (c) I. P. Beletskaya, D. V. Davydov and M. S. Gorovov, *Tetrahedron Lett.*, 2002, 43, 6221; (d) A. Palazzi, S. Stangi, S. Bordoni, M. Monari and S. Selva, *Organometallics*, 2002, 21, 3774; (e) K.-H. Chang, Y.-C. Lin, Y.-H. Lui and Y. Wang, *J. Chem. Soc., Dalton Trans.*, 2001, 3154.

85. (a) D. V. Davydov, I. P. Beletskaya, B. B. Semenov and Y. I. Smushkevich, *Tetrahedron Lett.*, 2002, 43, 6217; (b) D. E. Chavez and M. A. Hickey, *J. Heterocycl. Chem.*, 1998, 35, 1329.
86. L. J. GooBen, G.-J. Deng and L. M. Levy, *Science*, 2006, 313, 662.
87. (a) D. W. Fu and H. Zhao, *Chin. J. Inorg. Chem.*, 2007, 23, 122; (b) D. W. Fu and H. Zhao, *Chin. J. Inorg. Chem.*, 2007, 23, 281; (c) Z.-R. Qu, *Chin. J. Inorg. Chem.*, 2007, 23, 1117.
88. M. Dinca, A. Dailly, Y. Liu, C. M. Brown, D. A. Neumann and J. R. Long, *J. Am. Chem. Soc.*, 2006, 128, 16876.
89. Nagham Mahmood Aljamali, Nemah Sahib Mohammed Husien, Fatimah A. Wannas, Radhiyah Abdul Baqi Aldujaili, Nemah S M . Review on preparation & applications of thiadiazole derivatives., *International Journal of Chemical Synthesis and Chemical Reactions*, 2020, 6, 1.

**THANK YOU**

A literature survey  
on

# **MEDICINAL MECHANOCHEMISTRY AND SUSTAINABLE DEVELOPMENT**



**Submitted By**

**GARIMA SAIKIA**

**Roll number: PS-191-808-0089**

**Registration number: 283813 of 2016-17**

**M.Sc. 4<sup>th</sup> semester**

**Gauhati University**

**Under the supervision of**

**Dr. RANJIT THAKURIA**

**Assistant professor**

**Department of chemistry, Gauhati University**



## **Certificate**

This is to certify that the literature survey report, entitled “**Medicinal Mechanochemistry and Sustainable Development**” is submitted by **GARIMA SAIKIA**, M. Sc 4<sup>th</sup> semester, Gauhati University in partial fulfillment of the requirement for the degree of Master in Science in Chemistry. The literature survey is a bonafide work carried out by her under my supervision and guidance.

I wish her success in life

**Dr. Ranjit Thakuria**  
**Assistant Professor**  
**Department of Chemistry**  
**Gauhati University**

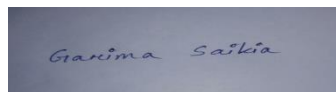
## **DECLARATION**

I, Garima Saikia student of M.Sc. 4<sup>th</sup> semester, studying at Gauhati University, Guwahati, hereby declared that the M.Sc. project report on “Medicinal Mechanochemistry and Sustainable Development” submitted to Gauhati University is the work conducted by me.

This report is not being submitted to any other University for award of any other Degree, Diploma and Fellowship.

Date: 07/09/2021

Place: Guwahati

A rectangular box containing a handwritten signature in blue ink that reads "Garima Saikia".

(Garima Saikia)

## **ACKNOWLEDGEMENT**

I would like to express my special appreciation to my project supervisor **Dr. Ranjit Thakuria**, Assistant Professor, Department of chemistry, Gauhati University, for his constant guidance, congenial help and unfailing support throughout my literature survey work.

I would like to take the opportunity to thank **Dr. Chitrani Medhi**, Head of the Department, Chemistry, for giving me the opportunity to do the literature survey work and providing timely support.

I am pleased to convey my hearty thanks to research scholar Poonam Deka and my friend Krishnamoni Deka for their help and encouragements during various stages of completion of the literature survey.

Date: 7-09-2021

Garima Saikia

Roll no: PS-191-808-0089

M. Sc. 4th Semester

Department of Chemistry

Gauhati University

# ***CONTENTS***

page no.

1. Introduction	1
2. Mechanochemical techniques	
2.1 Neat grinding and Liquid-assisted grinding (LAG)	4
2.2 Ion- and liquid-assisted grinding (ILAG)	5
2.3 Polymer-assisted grinding (POLAG)	6
2.4 Polymer-assisted grinding (POLAG)	6
3. Mechanistic studies	7
4. Sustainability	9
5. Enabling technologies to eco-friendly access to medicinal Mechanochemistry	11
6. Mechanochemical synthesis of pharmacologically active compounds	15
7. Mechanoenzymatics, a greener strategy in medicinal mechanochemistry	21
8. Medicinal mechanochemistry in the battlefield	25
9. Conclusion	26
10. References	28

## 1. Introduction

The mechanochemical reactions are defined as chemical transformations induced by the direct absorption of mechanical energy<sup>1</sup> via compression, shear, or friction in which the energy input to laboratory-scale reactions is performed by grinding, using a mortar and pestle, or by energy shocks in planetary ball milling, vibrational ball milling, and extrusion<sup>2</sup>. The application of mechanical force to influence chemical reactions has been called by various names<sup>3</sup> such as mechanochemistry, tribochemistry, mechanical alloying, the continued development of which promises to revolutionize the chemical industry, providing synthetic routes devoid of environmentally harmful solvents. Mechanochemistry offers a possibility to remove the need for the use of bulk solvent and thus reduce the generation of waste and also opens the door to a different reaction environment previously not accessible in solution, can be achieved.<sup>4</sup>

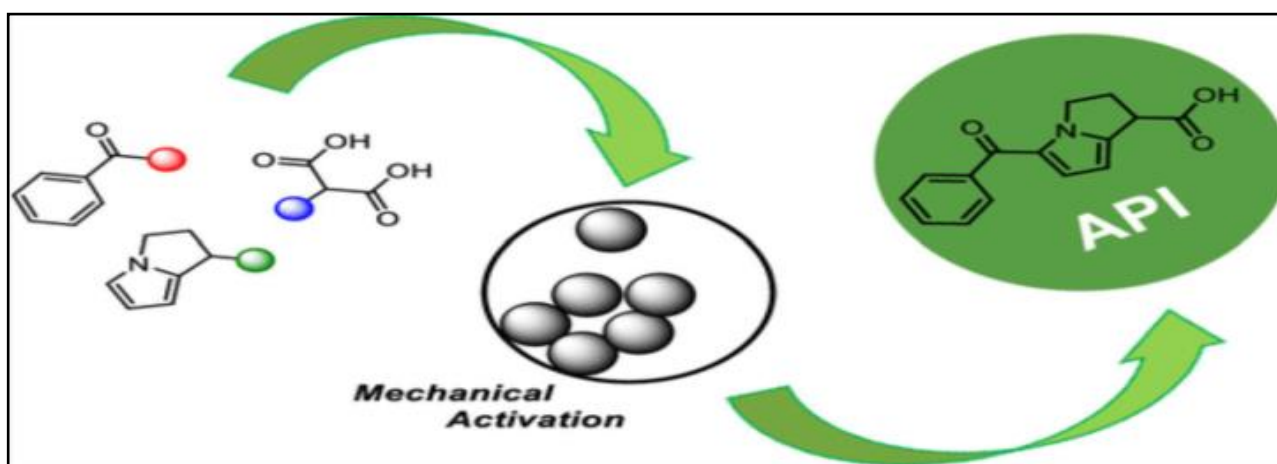


**Figure1.** Mechanical activation of active pharmaceutical ingredient<sup>1</sup>

The reproducibility of mechanochemical transformations using ball milling instrument (high-speed ball milling or high-speed vibration milling) and mixer mills systems requires the optimization of multiple factors, namely, milling frequency, material and size of the milling balls and jars, and also the number of balls.<sup>5</sup> Mechanical treatment of a single powder particle will still involve geometric distortion of its molecular substituents and there remains the potential for molecular or atomic electronic excitation or emission processes to occur. This kind of behavior is clear in high pressure experiments of molecular solids where mechanical action of the bulk lattice yields the geometric and electronic distortions or excitations at the molecular or at atomic level. The dynamical stressing of solids like compression or shearing can also cause chemical species within the solid state to approach each other at high velocities similar to molecular collisions in fluids.<sup>3</sup>

Recent awareness of the highly polluting and unsustainable ways in which many industrial processes are carried out has led to the establishment of more strict but necessary policies that regulate industrial activities in several chemical areas including fine chemistry and pharmaceutical enterprises. Thus, rather than discouraging or obstructing research and development in such industries the new regulations have motivated innovations in the pursuit of more sustainable chemistry by paying increased attention to the development of cleaner and more efficient synthetic pathways according to the “12 principles of green chemistry” (Figure 5).<sup>1</sup> Recently, mechanochemistry has been acknowledged by the International Union of Pure and Applied Chemistry (IUPAC) as one of the “top ten emerging technologies in chemistry” answering to the increasing demand for clean processes and ecoconscious reaction conditions.<sup>6</sup> Now a days, mechanochemistry is seen as an excellent method of green chemistry that offers way to greatly reduce or even completely avoid solvent use. However, the absence of bulk solvent also creates new synthetic opportunities: improved or new selectivity, fast reactions and quantitative yields – augmented by absence of extensive workup, and access to tantalizing molecules, materials and reactions.<sup>4</sup> The extraordinary advantages of protocols that avoid the use of bulk solvent or that can be carried out under solvent-free conditions,<sup>7</sup> as well as the development of elegant organometallic reactions via a recyclable source of metal catalysts and the real-time analysis of mechanochemical processes have converted mechanochemistry into one of the most attractive methodologies for sustainable synthetic chemistry. EcoScale<sup>8</sup> and E-factor<sup>9</sup> values for them also support the excellent sustainability of these mechanochemical synthetic processes.

There is a strong link exists between solid-state chemistry and the pharmaceutical sciences. For organic molecules a number of solid-state properties such as solubility, dissolution rate, tabletability, thermal and moisture stability etc. are critically depends on their structure at molecular (e.g. crystal structure) and macroscopic (e.g. particle size and morphology) levels. Therefore, significant effort in solid-state pharmaceutical materials science has been dedicated to developing strategies to impact solid-state properties of active pharmaceutical ingredients (APIs) by modifying their molecular arrangement in solids, e.g. by amorphisation, formation of polymorphs, solvates, salts and, more recently, of pharmaceutical cocrystals.<sup>10</sup> The recent development of new mechanochemical approaches based on twin-screw extrusion (TSE),<sup>6</sup> a technique already employed in the formulation of pharmaceutical products and also in food manufacture. It has also been employed successfully for the synthesis of organic compounds, MOFs<sup>2</sup> and peptides<sup>11</sup> upto kg hr<sup>-1</sup> scales under solvent-free or minimal-solvent conditions. A successful synthesis of nitrofurantoin is resulted in by using TSE, with very high conversions and stereoselectivities. The work indicates the

potential of TSE for the efficient production of APIs, with some additional advantages compared to solution-based procedures (Figure 2).<sup>6</sup>

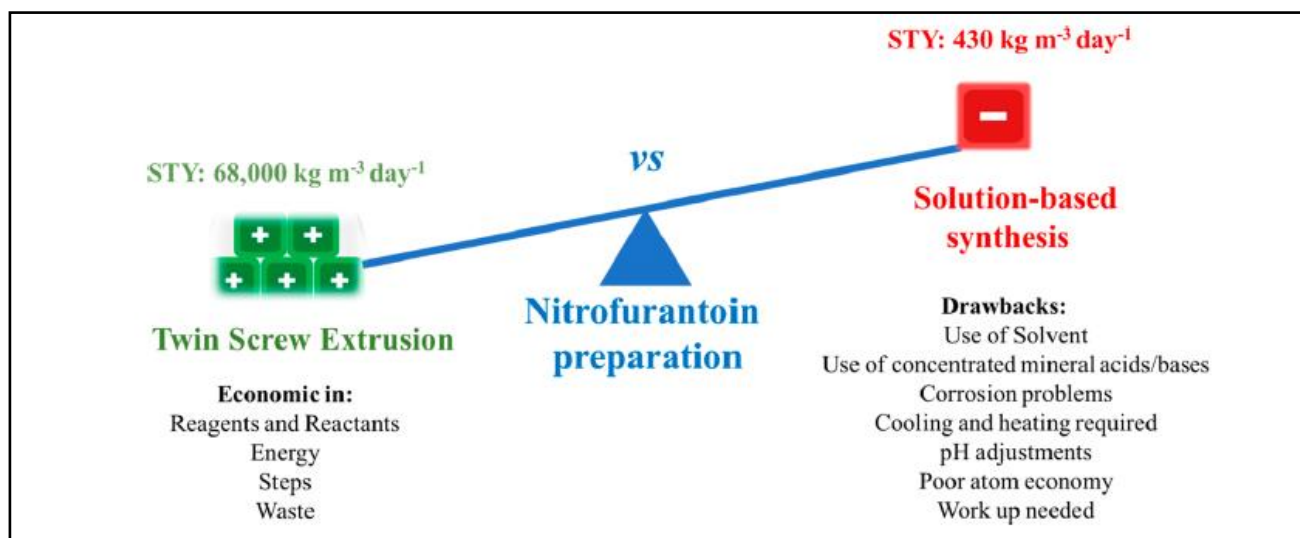


**Figure2.** Advantages of TSE vs solution-based procedures for the preparation of nitrofurantoin<sup>6</sup>

Through medicinal mechanochemistry, medicinal synthetic processes have taken the advantage not only of being efficient, clean and solvent-free nature of mechanochemical synthesis, but also of its emerging benefits, as well as previously unknown reactions and excellent selectivity. Such a development is in line with the very vocal demands of modern pharmaceutical industry for the development of cleaner and more efficient synthetic approaches. In this overview, the continuing development of mechanochemistry is highlighted from a screening technique in pharmaceutical materials science to approach a clean and versatile methodology in medicinal synthesis. In particular, medicinal mechanochemistry utilises mechanochemistry<sup>10</sup> for: (i) controlling, manipulating and manufacturing of solid forms of APIs, (ii) the synthesis of APIs themselves and their large-scale manufacture, and (iii) the systematic screening of molecular recognition properties of active pharmaceutical ingredients and the biomolecules. The applications of mechanochemistry in organic synthesis recently have drawn the attention of both the academic and the industrial chemical communities. The processes performed by mechanical activation has high efficiency and the low environmental impact which placed mechanical methods among salient green techniques since it allows the accomplishment of most sustainable chemistry principles. Mechanochemistry has been used as a tool for synthesizing APIs via chemical synthesis or by using enzymes through biocatalytic protocols with outstanding results, while at the same time increasing the efficiency and sustainability of the process.

## 2. Mechanochemical techniques:

A symbol for mechanochemistry in chemical equations was proposed by the Hanusa group (Figure 3a).<sup>3</sup> The mechanochemical reactions can be performed using a range of equipment in batch (shaker, planetary, attritor mills) or by using continuous mode (twin screw extrusion, TSE). The currently most popular devices used in mechanochemistry are shaker and planetary mills, with rising interest in TSE. These types of instruments are commercially available and their characteristics, advantages and limitations have been addressed in various reviews and research papers.

### 2.1. Neat grinding and Liquid-assisted grinding (LAG)

One of these technique is liquid-assisted grinding (LAG),<sup>4,7</sup> which is now established as a powerful screening and synthesis technique. The scope of mechanochemistry in the development of solid form of API has been strongly expanded by LAG. LAG transformations are conducted by automated ball milling, wherein a small amount of a liquid, is introduced into a milling jar along with reactants and milling media (balls), while the technique analogous to it which is based on an open mortar-and-pestle setup is known as kneading. This provides an enclosed environment in which the additive and milling conditions are controllable and can include milling frequency, time, light, temperature, and gas. As the liquid can accelerate or enable reactions that do not proceed by neat milling, LAG can offer a powerful method to optimize solid-state reactions. The LAG technique was introduced initially as solvent-drop grinding (SDG), and is sometimes also referred to as solvent-assisted grinding.<sup>10</sup> Liquid-assisted grinding offers an energy- efficient and elegant solution to optimizing and controlling mechanochemistry. In 2002, Shan *et al.* reported that the rate of grinding cocrystallization is increased by addition of a few drops of a liquid, facilitating the synthesis of cocrystals difficult to access by neat grinding.<sup>7</sup>

The parameter,  $\eta$  gives the ratio of liquid additive to the weight of solid reactants and it is typically expressed in mL mg<sup>-1</sup>, that was introduced to quantitatively describe the LAG reaction conditions and it enables a direct quantitative comparison of neat grinding with LAG, slurry and solution cocrystallisation (Fig. 3b) <sup>4</sup>. The LAG reaction conditions can be defined as those reactions that corresponding to the  $\eta$  value at which reactivity does not depend of reactant solubility. An empirical definition of LAG is leaded by a systematic study of cocrystallization by milling as the  $\eta$  range of ca. 0-2  $\mu$ L/mg, in which the reactant solubility does not affect reaction outcome. At higher  $\eta$  (in slurry or solution), cocrystallization becomes hindered or prevented by incongruent solubility of reactants. LAG can also be used to direct polymorphism of the product while it is being synthesized,



as shown for the active pharmaceutical ingredient (API) Tolbutamide. The polymorphism of the product can be manipulated by seeding-assisted grinding (SEAG).<sup>4</sup> Products that arising from neat grinding are more commonly contain an amorphous phase, whereas LAG products are often found to be highly crystalline. One negative outcome for using LAG is the (unintentional) formation of crystal solvates, which is observed frequently, for example, in a recent study five different cocrystal solvates of caffeine and anthranilic acid were formed by LAG during a screening study for different (nonsolvated) polymorphic forms.<sup>12</sup>

LAG was empirically associated with  $\eta$  values between 0 and 1 mL mg<sup>-1</sup> and within this range, higher  $\eta$  values led to faster cocrystal formation kinetics. By definition, neat grinding experiments correspond to  $\eta = 0$  mL mg<sup>-1</sup>.<sup>10</sup>

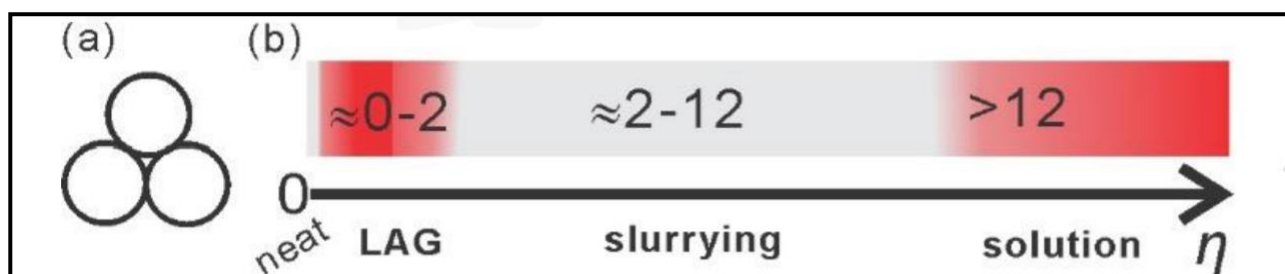


**Figure3.** a) Symbol proposed for mechanochemical activation by Hanusa b) the  $\eta$ -scale

## 2.2. Ion- and liquid-assisted grinding (ILAG)

The ILAG methodology<sup>4,10</sup> is a technique which utilises catalytic amounts of a simple salt additive, in addition to a liquid, which was developed from LAG, with the aim to enable the direct conversion of mineral-like feedstocks to metal-organic materials. In ILAG, small amounts of a salt (5 mol% or less) and a liquid are used to activate systems that react only partially or not at all by LAG, quantitatively yielding pillared MOFs,<sup>13</sup> zeolitic imidazolate frameworks (ZIFs), or API bismuth subsalicylate directly from a metal oxide.<sup>14</sup> Ionic liquids have also been used in organic mechanosynthesis, *e.g.* in a Knoevenageldomino reaction of isatin, malononitrile and 1,3-diketone.<sup>4</sup> Although ILAG is used more in the clean synthesis of microporous metal– organic frameworks, it also found use in the development of a simple and clean procedure for the synthesis of bismuth salicylates, including the active ingredient of Pepto-Bismols.<sup>10</sup>

## 2.3. Polymer-assisted grinding (POLAG)

To avoid formation of solvate in LAG cocrystallization, Hasa *et al.* used liquid or solid polymers, *e.g.* polyethylene glycols (PEGs) as additives<sup>4</sup> to accelerate cocrystallization and direct

formation of polymorphs. Hasa and co-workers demonstrated that a small amount (1–2.5% by weight) of poly(ethyleneglycol) (PEG) polymer can exert a strong effect on the course of mechanochemical cocrystallisation. Such polymer-assisted grinding (POLAG) allows for the formation of cocrystals in systems that aren't reactive upon neat milling (e.g. caffeine and citric acid), and it permits the control over the polymorphic composition of the cocrystal product.

POLAG enables efficient screening and control over cocrystal formation and polymorphism without the risk of undesired solvate formation which is an important advantage of it. Polymer additives also have been used in organic mechanosynthesis, *e.g.* Lamaty group using PEG additives in mechanosyntheses of variety of hydantoins, including the API ethotoin.<sup>15</sup>

#### **2.4. Accelerated and re-activated aging (RAging)**

The aim of accelerated aging is to simplify reaction design and scale-up, while minimizing energy and solvent use, by conducting reactions in static mixtures. Such diffusion-controlled reactivity is promoted by moisture or organic vapor, as shown by the reaction of 1,1'-bis(4-pyridyl)ferrocene and pimelic acid, driven towards a cocrystal or a salt upon exposure to vapors of solvents of different polarity, while aldimine condensation is, counterintuitively, promoted by moisture. Aging reactions can be facilitated by gas phase additives, *e.g.* by the utilization of triethylamine as a basic gas-phase catalyst in Schiff base synthesis. Aging also can be mechanically activated by brief milling: Qi *et al.* used five minutes of ball milling to significantly reduce the time required to convert metal oxides to oxalates, in some cases 16-fold. This was exploited by Hammerer *et al.* who achieved efficient, fast solvent free enzyme catalysis by introducing RAging, a methodology based on repeating cycles of brief milling activation and aging.<sup>16</sup>

Aging reactions are often directed by templating, as was shown by Kaabel *et al.* who combined milling and aging with chloride or perchlorate ions to form 6- or 8-membered hemicucurbituril macrocycles, respectively.<sup>17</sup> Accelerated aging is also a simple, low-energy way to form MOFs from metal oxides. Such syntheses also are readily templated and catalyzed, as shown by Qi *et al.* who templated oxalate MOFs by alkylammonium salts or Mottillo *et al.* who used caffeineium salts to regulate ZIF synthesis. In that context, the Yuan group has shown that aging also enables the conversion of trivalent metal oxides into MOFs.

### 3. Mechanistic studies

Mechanochemical conversions of organic molecules can be conveniently described via the three-stage model put forward by Kaupp involving the activation of solid reactants, their reaction and crystallisation of the product. In such a three step process, mass transfer that occurs during a mechanochemical reaction can proceed through a gas, a liquid, a solid phase, or any combination of those (Fig. 4). It has been proposed that mechanochemical processes moves forward through participation of hot spots which are short-lived and highly localized areas of high temperature. The mechanochemical reactivity can be explained by using magma-plasma or hot-spot models explains in terms of frictionally induced, short-lived (ca. 10 ns) microscopic areas of high temperature (>1000 °C).<sup>18</sup> The appearance of hot spots has been directly observed by the Suslick and Dlott groups in crystals of sucrose and molecular explosives exposed to mechanical stress employing a high-frequency (20 kHz) ultrasonic hammer. However, it is, becoming more and more clear that mechanochemical processes are highly complex and sometimes can't be described using one kind of mechanism only. Mechanochemical milling reactions are normally carried out in closed and rapidly moving reaction vessels, preventing a direct insight into the reaction course and, for many years, limited reaction monitoring to enable stepwise *ex situ* analysis. These limitations can be avoided by *in situ* techniques which are introduced recently that enable reaction monitoring in real time.<sup>[19,20]</sup> The first two *in situ* monitoring techniques probing the chemical composition of the reaction mixture, which are based on powder X-ray diffraction (PXRD) and Raman spectroscopy as well as their use in tandem. *In situ* monitoring allows for investigating the fundamental aspects of reactivity that are well understood in solution, but have remained largely unexplored in mechanochemistry, e.g., reaction kinetics or the temperature effect on reactivity. The mechanochemical preparation of two marketed APIs, silver sulfadiazine and dantrolene, was investigated using *in situ* Raman spectroscopy.<sup>19</sup> For the first time, the mechanochemical transformations involving highly fluorescent compounds might be studied *in situ* with a high-resolution Raman system combined with a suitable unique Raman probe.

A recent report by the Stolle group showed the high temperature dependence for the reaction rate of a mechanochemical Knoevenagel condensation. Temperature dependence suggests that hot spots do not play a major role in determining reactivity.<sup>10</sup> Indeed, observed thermal sensitivity suggests that such high-energy environments may not be critical for mechanochemical reactions, a minimum of not of organic and metal–organic solids. A variable temperature *in situ* diffraction study showed that mechanochemical mechanisms can be readily changed with a modest temperature change and that reaction rates can be strongly temperature-dependent. This is in accordance with *ex*

*situ* studies of Knoevenagel condensation by milling challenging the view that mechanochemical reactions need localized “hot spots” with temperatures exceeding 1000 °C.<sup>20</sup> A hot spot mechanism is more relevant for grinding hard and abrasive inorganic materials compared to mechanically agitated transformations of soft molecular substances.

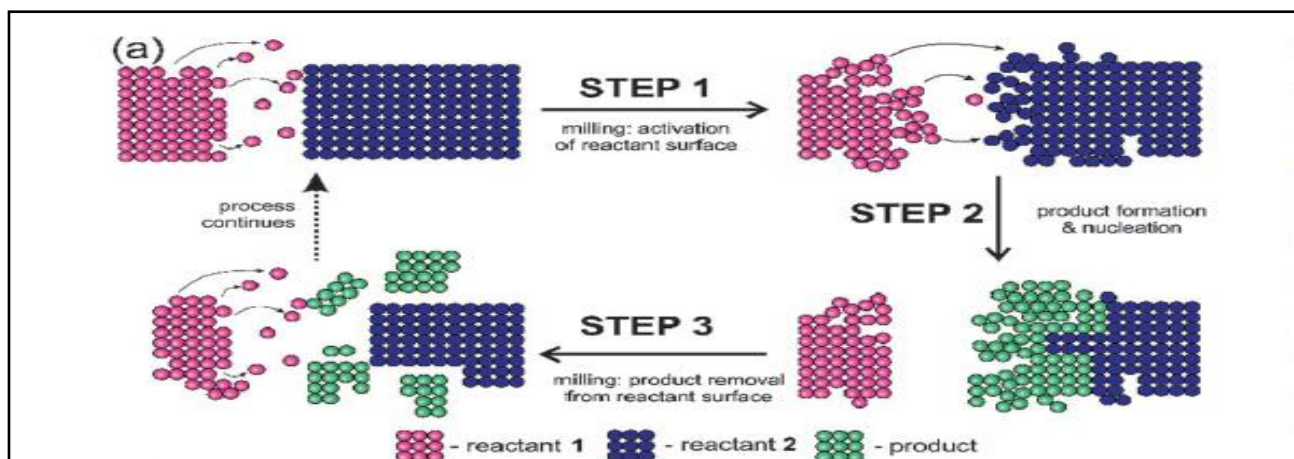


**Figure 4.** Schematic representation of the three-step mechanism for mechanochemical reactions by milling or grinding.<sup>10</sup>

## 4. Sustainability

Sustainable development was basically defined by the Agenda 21: “Sustainable development is development that meets the needs of the present without compromising the ability of future generations to meet their own needs.”<sup>21</sup> One of the contributions of chemistry to meet the challenge of more sustainability in the development of our society is the promotion of a sustainable chemistry, in the fields of research and industrial production. Under the name of green chemistry (or in Europe also sustainable chemistry) a lot of effort has been undertaken to make future chemistry less poisonous and fewer hazardous. The aim of green chemistry is to make chemistry more energy efficient, at reducing waste disposal, and/or producing innovative products with less consumption of natural resources. Designing of alternative processes and reaction pathways and development of new materials and products are contributing to satisfy our needs today, but with taking more care of the interests of future generations.

The E-factor is a metric of how environmentally or harmful a chemical process is and is defined as the ratio of the mass of waste generated per kilogram of product synthesized i.e.  $E\text{-factor} = (\text{total mass of waste} / \text{mass of the product})$ .<sup>5</sup> A higher E-factor is related to more waste and consequently, greater negative impact on the environment. The E-factor is zero for ideal processes whereas lower E-factors correspond to reduced manufacturing costs of APIs which is a reflection of

lower process materials input and output, reduced costs of hazardous and toxic waste disposal thus improved capacity utilisation and reduced energy demand.<sup>8</sup> The EcoScale is a postsynthetic tool that evaluates other aspects of the synthetic process such as the toxic effects of the reactants, energy input (time and temperature of the reaction), and procedure safety. The transparency and user-friendliness are the basic requirements for designing EcoScale and an ideal reaction has the EcoScale value of 100.<sup>22</sup> All of the procedures to be analyzed start with 100 points, and the points are subtracted as each of the evaluated parameters deviates from the ideal of sustainability. Therefore, higher the EcoScale value, more the sustainability of the process will be.<sup>5</sup> The primary substantial green efficiency goal for any manufacturing process to a given drug is represented by the Green Aspiration Level (GAL) which has the marked advantage over other conventional waste metrics that quantifies environmental impact for producing any pharmaceutical agent by considering the complexity of its ideality for producing the target molecule. An integral part of green chemistry implementation and communication strategy is the Green Scorecard that holds the potential to cascade broad adoption of the GAL all over the pharmaceutical industry and its supply chain into process chemists and engineers daily routine, since it forcefully yet fairly communicates the objective value added of green process chemistry via quantitative and goal-driven data, unlike the other green chemistry metric so far.<sup>23</sup> The utilization of a solvent either in the multicomponent acid-catalyzed reaction or a two-step methodology using a base as a catalyst leads to a deviation from the ideal values of sustainability. The values calculated for both E-factor and EcoScale, regarding the synthesis of chalcones, show that the use of the SSD device and solvent-free conditions increases the sustainability of the process.<sup>5</sup>

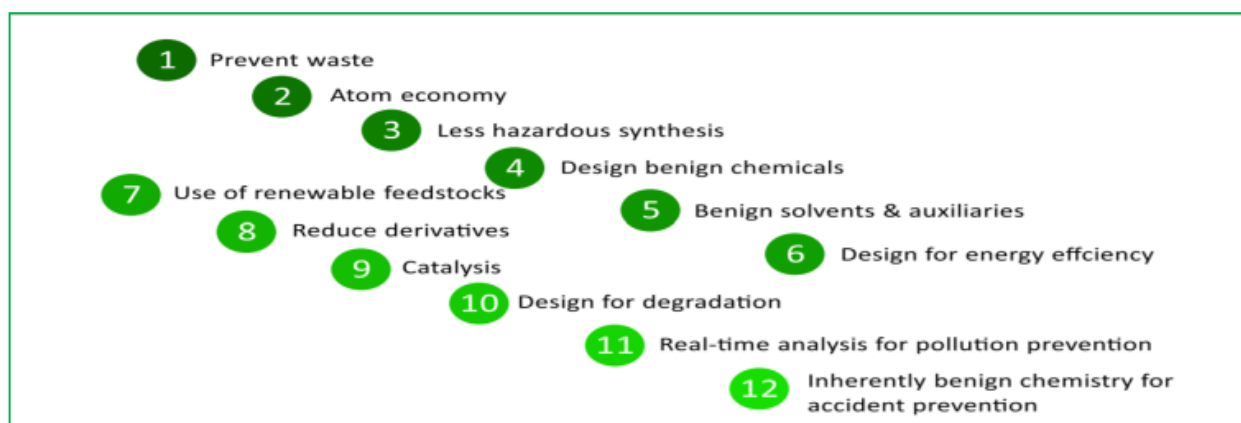


**Figure5.** 12 principles of green chemistry.<sup>1</sup>

Finally, the sustainability scores for porphyrins synthesis, in the two-step methodology under mechanical activation were calculated and compared it with those previously described for methodologies employing a ball milling device, showing the improvement achieved by drilling. These values are found below the Efactor and EcoScale values previously obtained by utilizing the water-microwave methodology. In summary, these metric calculations intensify the effective improvement in the reaction sustainability under mechanical activation, using the SSD device, by drilling at room temperature, in solvent-free conditions. Green chemistry aims at making chemistry more energy efficient, at reducing waste disposal and producing innovative products with less consumption of natural resources by using 12 principles of it (figure 5).<sup>1</sup>

## 5. Enabling technologies to eco-friendly access to medicinal mechanochemistry

The growing interest in designing processes with minimum environmental impact and high sustainability has recently encouraged the search for innovative technologies capable to transfer energy to reacting molecules in the most effective and efficient ways possible. In addition, the ecological footprint of a process can be improved more by developing, implementing and enacting sustainable technologies, aimed to minimize scientific and technical difficulties and complementing the REACH (Registration, Evaluation, Authorization and Restriction of Chemicals) legislation. Industrial and academic researchers have become aware of the importance to design environmentally benign chemical process accordingly adopting a radically different approach to the organic synthesis. One of the challenges faced by the scientific community is to “*think chemistry differently*” translating green synthetic methodologies to the field of drug discovery, to arrange in a sustainable way drug candidates, active pharmaceutical ingredients (APIs) and in general, commodity chemicals for the industry.

The hydantoin scaffolds preparation utilizing modern nonconventional activation methods, for the preparation of hydantoin-based Active Pharmaceutical Ingredients (APIs) by mechanochemistry, highlighting its advantages compared to classical solution procedures, giving new perspectives for the sustainable preparation of useful scaffolds for the pharmaceutical industry.

Many hydantoin-containing structures exhibit remarkable biological properties with relatively low toxicity and side effects (Figure 6).<sup>24</sup> Hydantoin derivatives are also found in toothpaste, cosmetics and oral hygiene products and perform important activities as herbicides and fungicides.

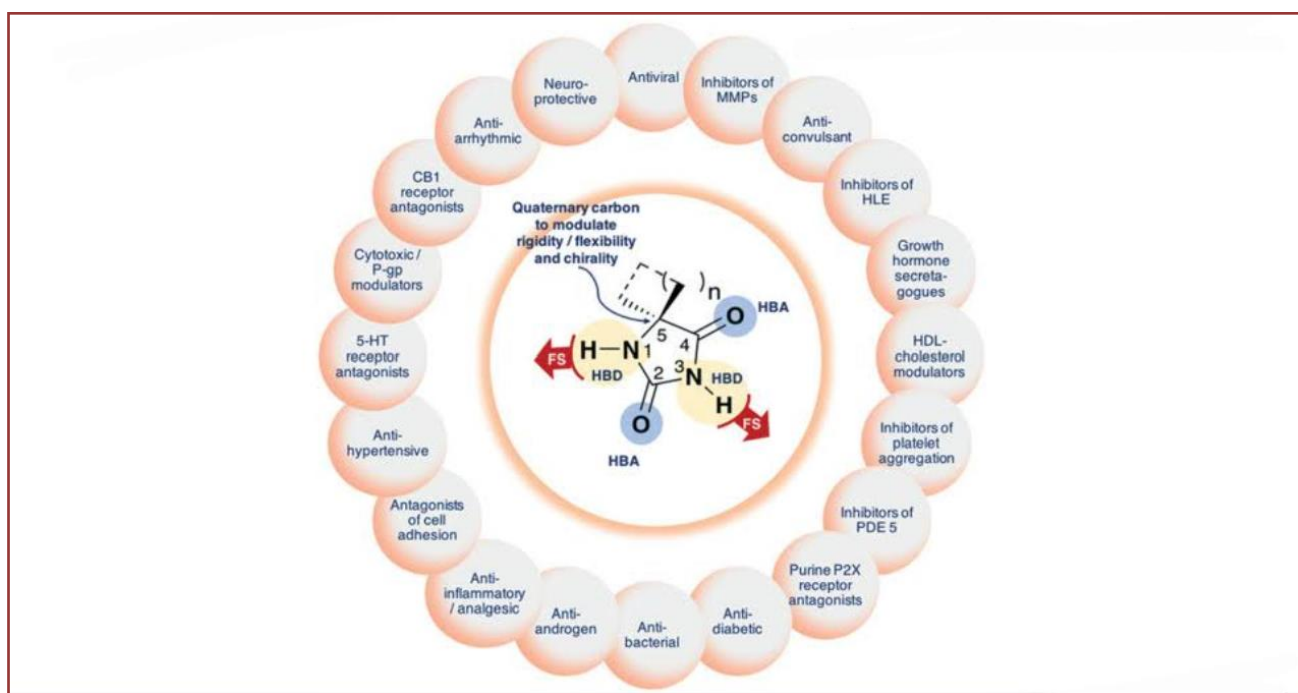
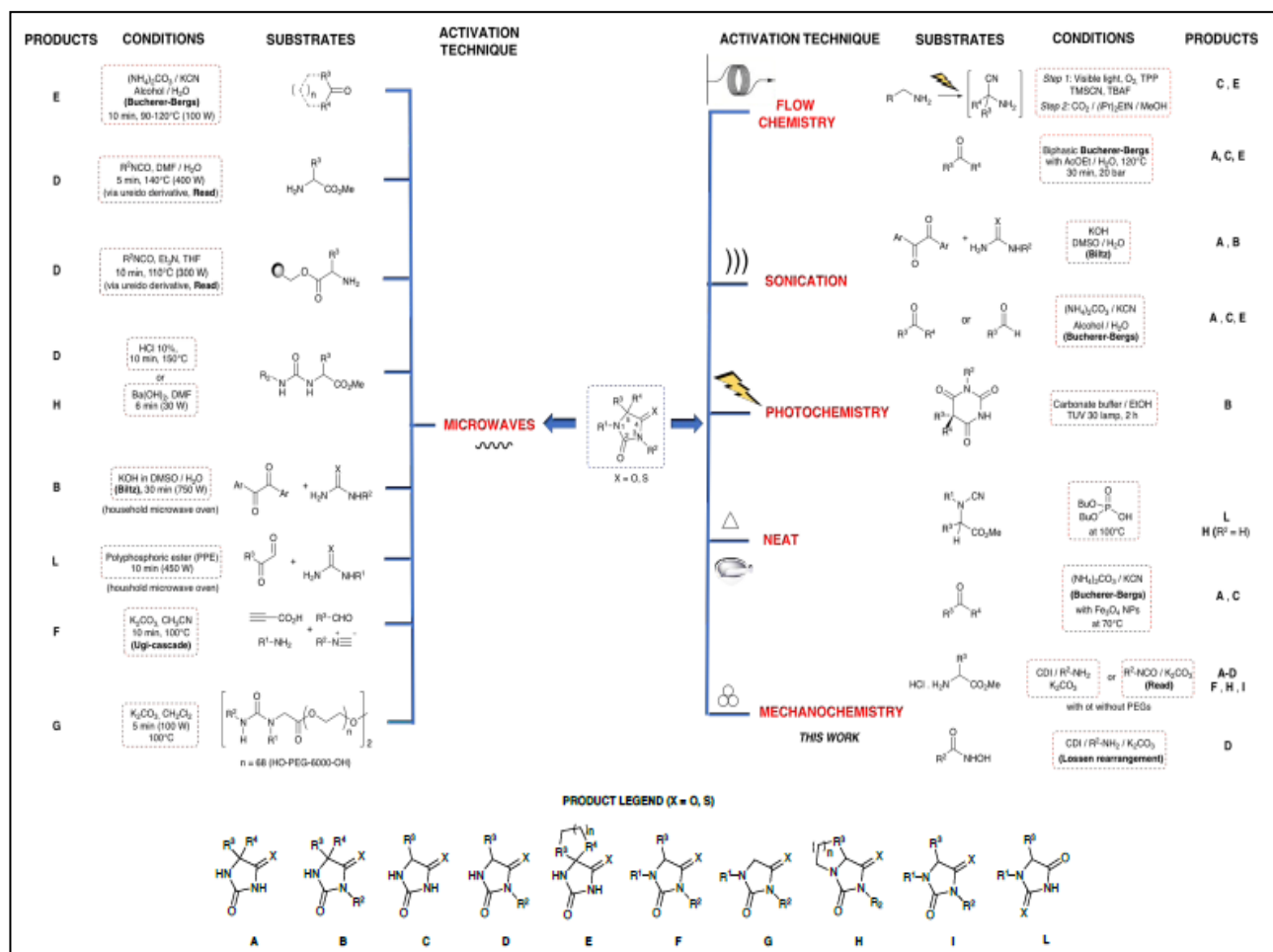


**Figure 6.** Chemical structural properties of hydantoin scaffold and their biological and pharmacological effects.<sup>24</sup>

The synthetic and pharmaceutical interest for imidazolidine-2,4-diones, or hydantoins, has not faded over the past decade, and has given rise to over 3000 publications and patents in methodological and medicinal chemistry. Several reviews have concentrated on the synthesis of those five-membered heterocycles referencing their preparation methods from the main, historical ones like the Read, Bucherer–Bergs or Biltz syntheses to more modern ones, like multicomponent reactions (MCRs), which enabled libraries of hydantoinic compounds to be obtained through simple routes.<sup>25</sup>

The Biltz reaction is a straightforward procedure for the preparation of 5,5-disubstituted (thio)hydantoins **A** and **B**, while Bucherer–Bergs and Read syntheses are used commonly to access C-5-substituted hydantoins **C** and **D**. The difficult reaction conditions, long reaction times, solubility problems, unsustainable substrates, poor yields, along with environmental concerns limited the potential of these methodologies. More recently, some of these drawbacks have partially been solved by the use of non-conventional activation techniques (*e.g.* microwaves, photochemistry, continuous flow such as TSE and tribochemical processes like ultrasounds or solvent-free related procedures like grinding and mechanochemistry), under the framework of ‘Green Chemistry’.

The microwave-activated reactions generally allowed for a cleaner reaction conditions, led to rapid reaction rates and better yields, thereby overcoming a number of the disadvantages of the Bucherer-Bergs reaction conditions, like longer reaction time, requirement of high temperature to attain acceptable yields, together with a large excess of cyanide.



**Scheme1.** Preparation of C- and/or N-substituted hydantoins **A-L** using various non-conventional activation methods.<sup>24</sup>

Among the environmentally friendly synthetic tools to prepare valuable complex organic molecules, photochemistry has also earned an important place as it is attractive for its operational simplicity and the mild reaction conditions and also not requiring any activation except the absorption of a photon.

The only example reported designated the formation of 3,5,5- trisubstituted hydantoins **B** by photolytic ring contraction of barbituric acid derivatives (Scheme 1). Solvent-free procedures have also been reported to access hydantoin scaffolds **H** and **L** from methyl N-cyano-Nalkyl/



arylaminoacetate derivatives upon heating (at 100°C) in the presence of dibutyl phosphate. The reaction goes through the formation of mono-substituted urea which is further cyclized in acidic medium to hydantoins (Scheme 1). However, even if ‘*solvent economy*’ is attained for this step, this approach is not effortless, because the *N*-cyano-*N*-alkyl/ aryl aminoacetate derivatives are not commercially available, their preparation is far from being sustainable and therefore the whole procedure suffers from poor atom economy and waste generation (tetrabutyl pyrophosphate).

Alternative energy sources based on sonochemical procedures were also investigated as promising heating technique for accessing hydantoins **A-C** and **E** (Scheme 1).

Among the various energy input processes, mechanochemistry offers unique opportunities for the development of more sustainable synthetic processes, to access hydantoin-based Active Pharmaceutical Ingredients (APIs),<sup>15</sup> enzymes inhibitors and advanced silicon based nanomaterials for potential biomedical applications. “*Benign by design*” mechanochemistry is a valid alternative to several solution-based procedures, avoiding the utilization of solvents and the high temperatures (sometimes responsible for API degradation), providing reagent and waste economy, a sustainable, operationally simple and a low-energy chemical processing, also at a manufacturing scale through twin screw extrusion processes.<sup>6</sup>

In this context, the successful symbiosis of mechanochemistry and APIs has driven the development of an innovative, green and active area of investigations referred to as “*medicinal mechanochemistry*”<sup>10</sup> to access organic molecules and Active Pharmaceutical Ingredients (API) in the absence of solvent, with cleaner reaction profiles and simplified work-up procedures, highly reducing the environmental impact for the production of biomolecules as a valid and reliable alternative to chemistry in solution for the preparation of marketed drugs or prepare hybrid nanoparticles *via* a mechanochemical process, without using harmful reaction conditions, reagents or solvents, even in the work-up.

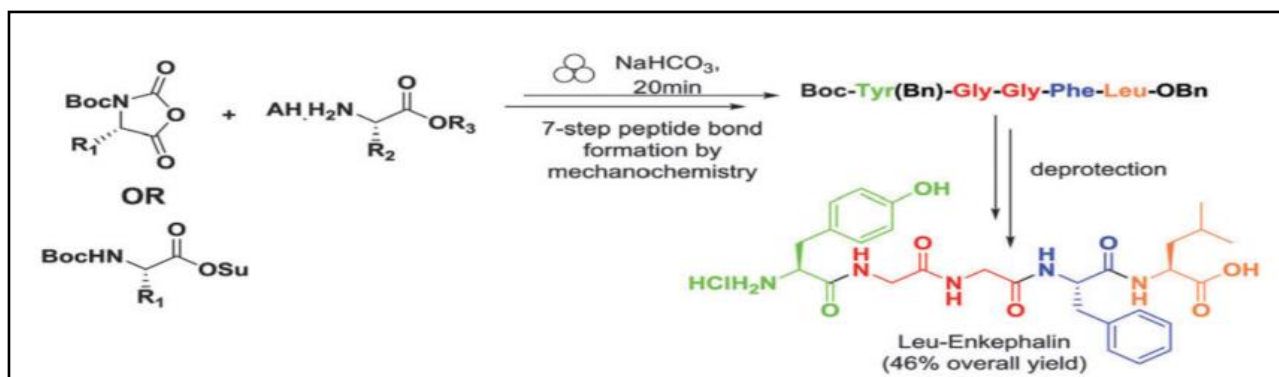
Medicinal mechanochemistry endeavours offering new perspectives for a sustainable thinking of drug development and drug discovery, stimulating the interests not only of the scientists and engineers of the future, but also politics, economists, business leaders and stakeholders and opening new frontiers for safe and eco-friendly synthesis of pharmaceutically interesting drugs on large scale, inspiring sustainable and cost-effective drug manufacturing by mechanochemistry.

## 6. Mechanochemical synthesis of pharmacologically active compounds

Organic synthesis of pharmacologically active or fine chemical compounds is frequently coupled with complex chemical transformations that require mild, specific, and highly controlled reaction conditions. Nevertheless, the optimal procedures for the synthesis of relevant bioactive molecules can often be achieved through diverse nonconventional methods.<sup>26</sup> The mechanical force can be produced by not automatic or automatic manual grinding, or through an automatized milling equipment with vibrational or planetary configuration, or via reactive extrusion that is used for promoting the continuous production of valuable products and to carry out a wide range of organic chemical transformations with remarkable results.<sup>1</sup> Whereas the literature addressing the mechanosynthesis of pharmaceutically-relevant molecular fragments is relatively rich, reflecting the high level of interest in and development of mechanochemical organic synthesis, the mechanosynthesis of a small number of real APIs was only recently demonstrated. An early report of a mechanochemically synthesised API was a metal–organic compound, the metallodrug bismuth subsalicylate, active ingredient of Pepto-Bismols.<sup>14</sup> Friščić and his coworkers pointed out the advantages of the use ion- and liquid- assisted grinding (ILAG) as adjuvants in a mechanochemical reaction. To obtain the active bismuth subsalicylate complex, commercially available as Pepto-Bismol, the authors used a mixture of water and nitrite salts as ILAG in the reaction of bismuth oxide and salicylic acid and have completed it in a short reaction time (60 min) and with a better yield<sup>14</sup> providing a clean route to the API, without resorting to the formerly ubiquitous toxic soluble bismuth (III) nitrate or chloride salts. This protocol introduced the use of mechanical force as an efficient strategy for synthesizing pharmaceutically active compounds and actually established a new field, the so-called “medicinal mechanochemistry” field<sup>1,10</sup> in mechanochemistry.

Mechanochemical synthetic procedures act as a bridge between the application of mechanical force to carry out a particular chemical transformation and the synthesis of valuable biologically active compounds or relevant pharma intermediates. The pioneering work of Lamaty and co-workers had demonstrated the successful use of mechanochemical solvent-free strategies in peptide synthesis using activated urethanes.<sup>27</sup> This work set the basis for the development of a remarkable mechanochemical pathway for the synthesis of Leu-enkephalin<sup>28</sup> an endogenous opioid produced in vertebrates, had previously been synthesized using enzymatic and chemical routes. By contrast, Lamaty and co-workers developed a mechanochemical procedure for conducting peptide coupling with benzyl-protected amino acids in the presence of NaHCO<sub>3</sub> applying the model reaction described in Scheme 2. The power of this procedure was illustrated by a seven-step, solvent-free procedure for making the covalent backbone of Leu-enkephalin.<sup>18</sup> In the new application, ethyl

acetate was used for liquid-assisted grinding and subsequent deprotection steps completed the peptide synthesis.<sup>1</sup>

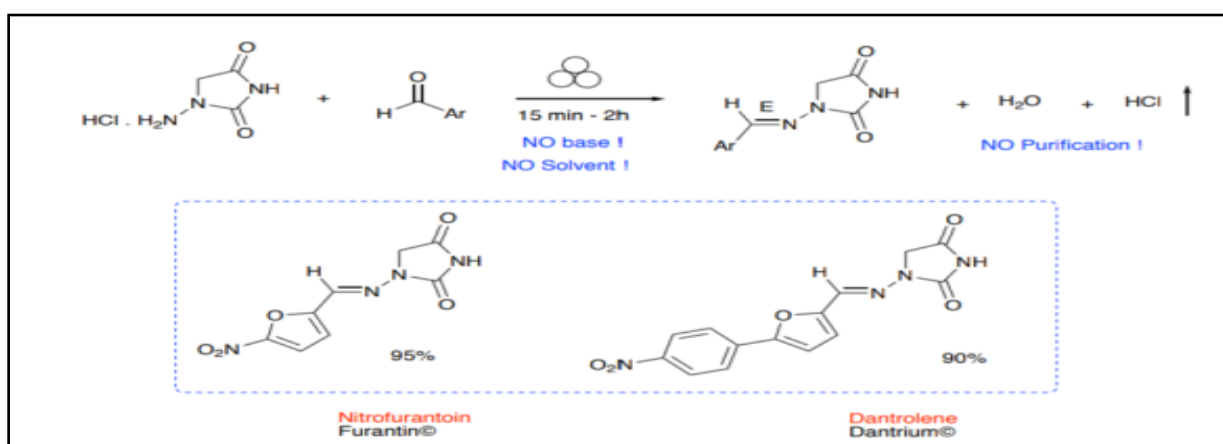


**Scheme2.** Mechanochemical synthesis of Leu-Enkephalin.

Mechanochemistry proved to be particularly satisfactory for the preparation of APIs such as the antibacterial agent Nitrofurantoin (Furantin) and Dantrolene (Dantrium). Dantrolene is a prescribed muscle relaxant that is used to treat malignant hyperthermia,<sup>29</sup> while nitrofurantoin is a prescribed antibiotic used particularly for the treatment of urinary tract infections.<sup>30</sup> Conventional routes for the synthesis of both compounds involve the use of toxic solvents such as DMF, a solvent class 2 (according to the Q3C Guidance of FDA), that should be limited in pharmaceutical products because of its inherent toxicity; moreover, the industrial synthesis of these compounds involves the use of strong acids and bases (H<sub>2</sub>SO<sub>4</sub>, HNO<sub>3</sub>, NaOH), several pH adjustments, and needed thermal heating and cooling cycles. The mechanochemical approach carried out by Colacino keep away those drawbacks.<sup>1</sup> By synthesizing nitrofurantoin and dantrolene, Colacino and collaborators expanded the application of mechanical force in the preparation of relevant hydantoin.<sup>31</sup> Stoichiometric milling of 1-amino hydantoin hydrochloride and the suitable aldehyde reacted quantitatively and exclusively to give the corresponding *E*-stereoisomers without any post-synthetic work-up procedures, thus allowing an easy recovery of the final APIs by just scratching them out from the jar even on gram scale, thus supporting *waste economy* (Scheme 3).<sup>24</sup> In this case, the nucleophilic free amine was generated *in situ* without any additional base or reagent (*reagent economy*) probably by a proton exchange between the reactants, possibly achieved by the strong activation provided during the mechanochemical activation. Compared to solution-based procedures the mechanochemical preparation of nitrofurantoin and dantrolene<sup>31</sup> presents several other advantages:<sup>24</sup> i) it reduces number of synthetic steps and excess of reactants (*reagent economy*) thus reducing overall footprint of the process ii) increases throughput/hour due to its shorter reaction times and absence of work-up

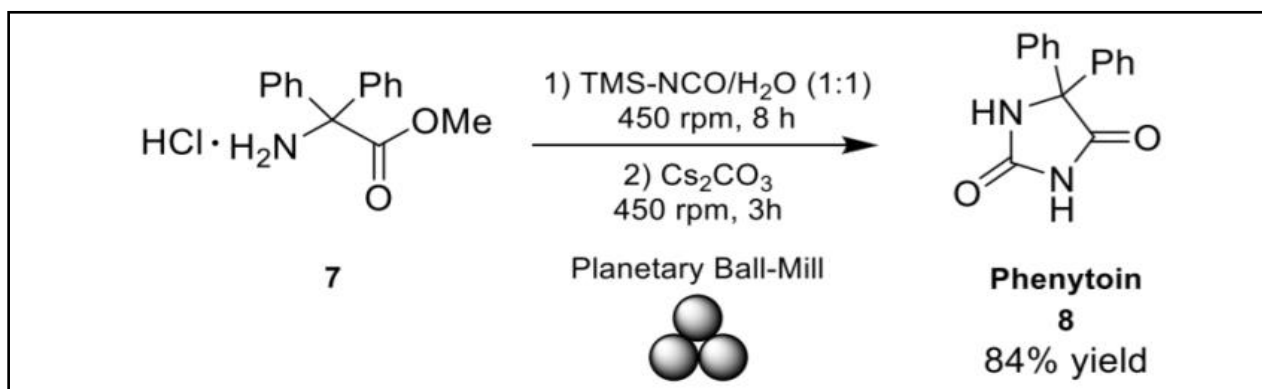
(*time and waste economy*) iii) improves green chemistry metrics by eliminating the utilization of solvents (*e.g.* DMF, CH<sub>3</sub>CN and EtOH, *solvent economy*) iv) safer reaction conditions eliminating the use of highly concentrated acidic or basic solutions (*e.g.* NaOH, HCl 30%, HNO<sub>3</sub>-H<sub>2</sub>SO<sub>4</sub>), at the same time preventing the corrosion problems usually encountered and v) reduces costs of chemical and in terms of energy by avoiding heating (up to 90°C) or controlled cooling (between -2 and -4°C) of the mixture.

Twin-screw extrusion (TSE) can also be used for the synthesis of hydantoin-based APIs like nitrofurantoin and dantrolene, employing minimal or no solvent.<sup>6</sup>



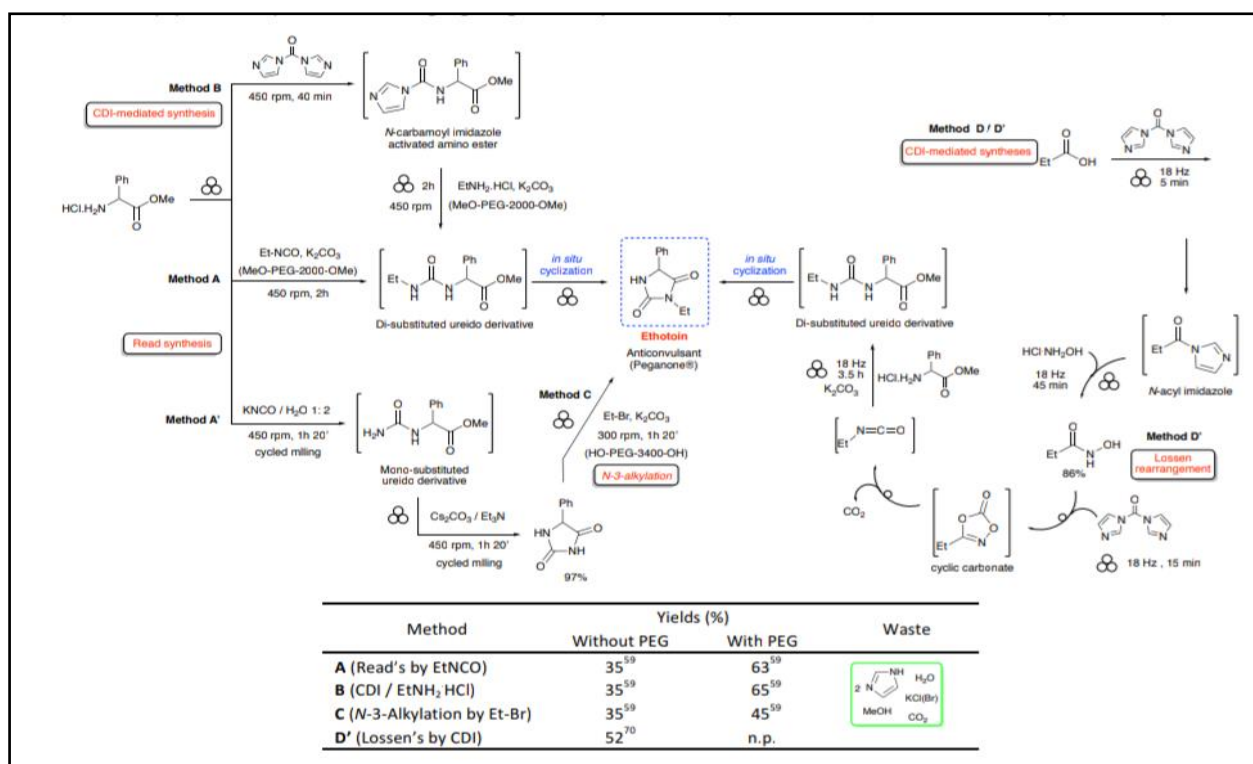
**Scheme3.** Preparation of *N*-acylhydrazone APIs by mechanochemistry.<sup>24</sup>

A mechanochemical procedure for the preparation of relevant hydantoin-based APIs such as phenytoin<sup>32</sup> and ethotoin<sup>15</sup> was recently described by Colacino and co-workers. Konnert *et al.* synthesise antiepileptic drug Phenytoin (Phenytek) by utilizing a biphenyl-based amino acid in a one-pot two-step mechanosynthesis process. The use of a significantly less toxic trimethylsilylisocyanate in place of KOCN, in the presence of water, enabled the activation of the methyl-protected biphenyl amino acid salt to form the *N*-urea moiety. Subsequent cyclisation was attained by grinding with Cs<sub>2</sub>CO<sub>3</sub> thus giving the required API with a far better yield.<sup>10</sup> (Scheme 4)<sup>1</sup>



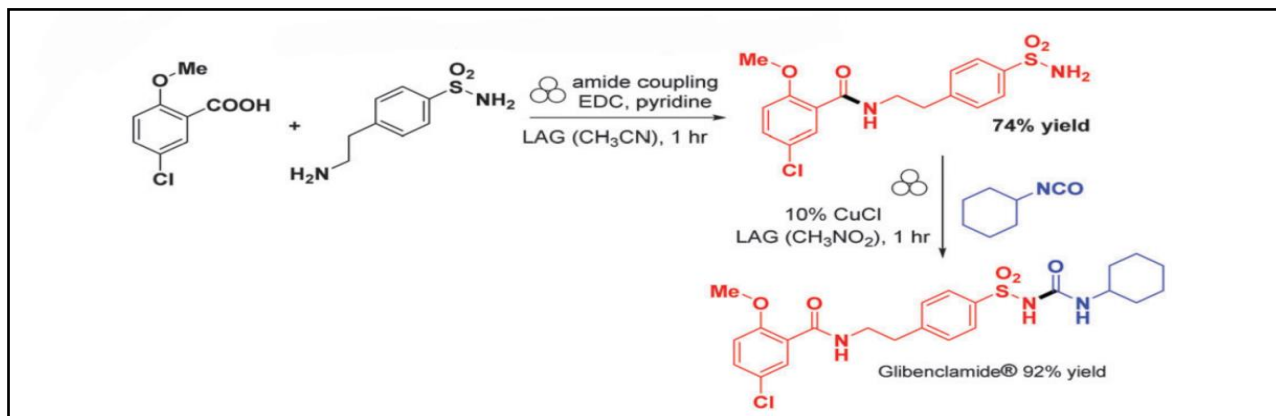
**Scheme 4.** Mechanochemical Procedure for the Synthesis of Active Pharmacologically Active Phenytoin.<sup>1</sup>

Furthermore, the synthesis of ethotoin,<sup>1</sup> an anticonvulsant drug, was possible by following a similar mechanochemical procedure, utilizing isocyanates. The preparation of ethotoin, an anticonvulsant drug, by utilization of other nonconventional methods for activation was never reported so far with the only exception of ball-milling procedures. For the preparation of ethotoin according to straightforward and safer procedures, mechanochemistry was the unprecedented tool used to move a step forward displaying a lower environmental impact. Four alternate methods **A-D** were reported by mechanochemistry from commercially available substrates (Scheme 5).<sup>24</sup>



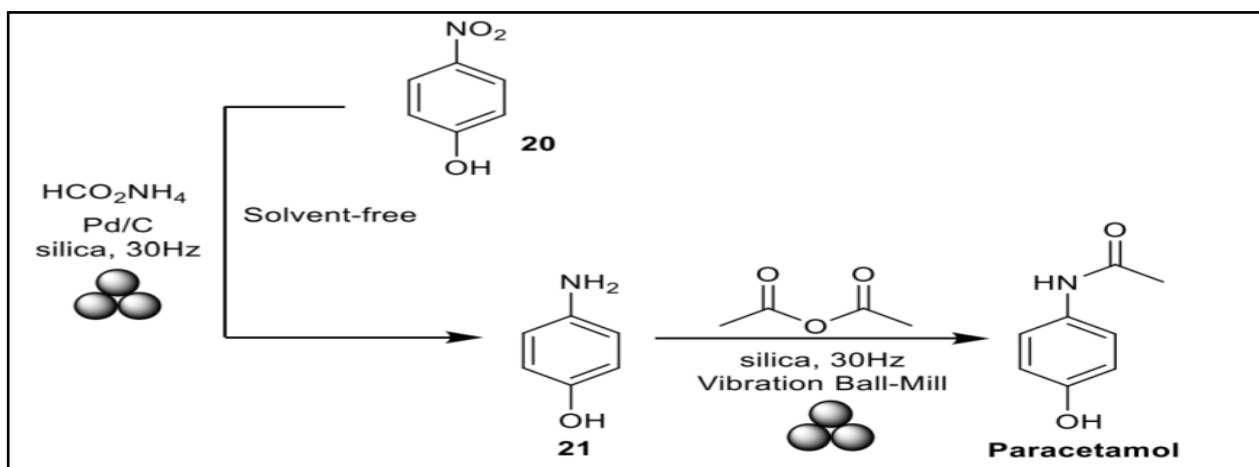
**Scheme 5.** Different mechanochemical methods for the preparation of the anticonvulsant drug Ethotoin.

The copper-catalysed procedure are often combined with mechanochemical approaches for carbodiimide mediated amide synthesis to get the more complex 2<sup>nd</sup> generation drug molecule, Glibenclamide<sup>10</sup> the synthesis of which required of two mechanochemical steps, the first one involving a condensation reaction affording precursor and the second one, the mechanochemical copper-catalyzed coupling reaction to give the product (Scheme 6).



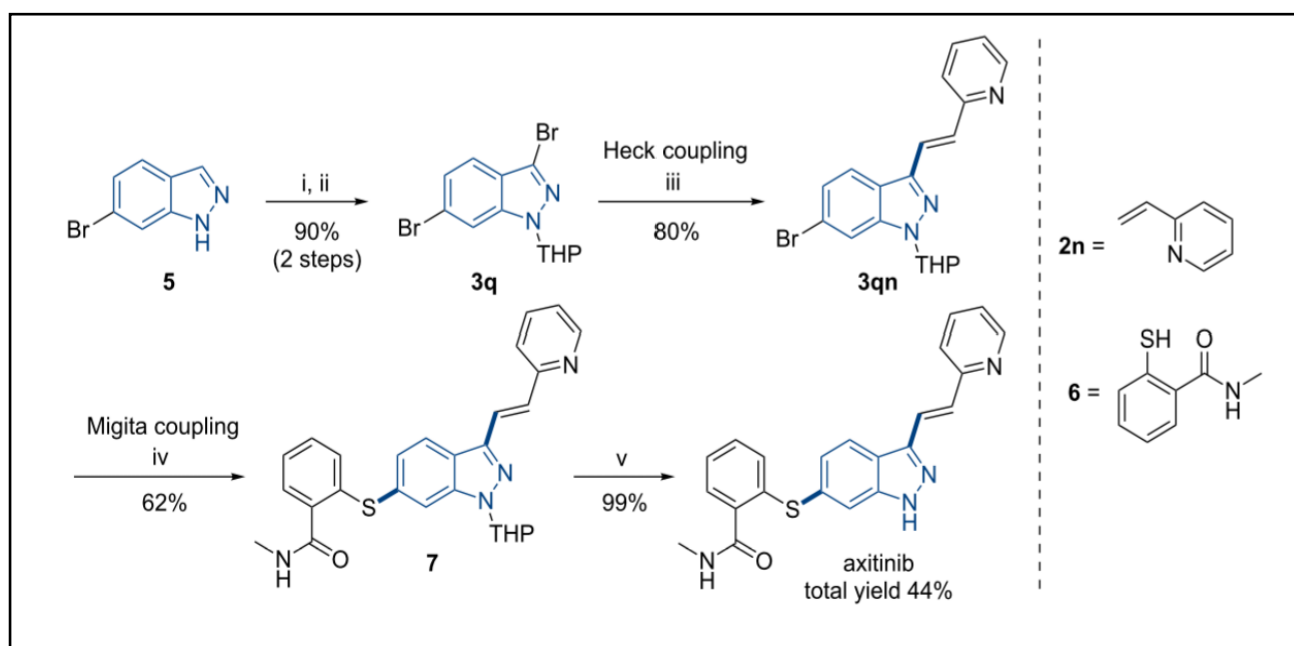
**Scheme6.** Glibenclamide syntheses reported by Tan *et al.*<sup>10</sup>

On the other hand, paracetamol was synthesized following the hydrogenation strategy utilizing 4-nitrophenol (20), ammonium formate, palladium, and using silica as a grinding auxiliary. The amine product 21 was then acylated under mechanical conditions to gain paracetamol in quantitative yield (Scheme 7).<sup>1</sup>



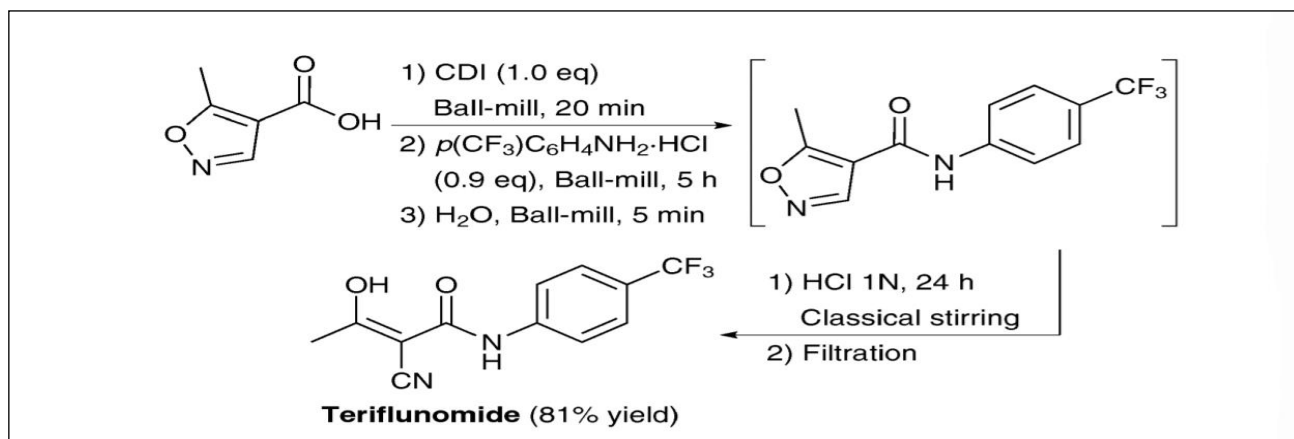
**Scheme7.** Synthesis of and Paracetamol by Catalytic Transfer Hydrogenation Mediated by Mechanical Force.<sup>1</sup>

Su and co-workers<sup>33</sup> used mechanochemical metal catalysis processes in the synthesis of axitinib, a potent drug used for treatment of renal cell carcinoma. The synthetic strategy started with mechanochemical bromination of 6-bromo-1H-indazole, using NBS, and subsequent protection of the amine group, followed by a Heck-Migita coupling reaction to obtain, after deprotection, Axitinib in 44% overall yield. This five-step solvent-free mechanochemical pathway made use of silica gel as a grinding auxiliary<sup>1</sup> (Scheme 8).<sup>33</sup>



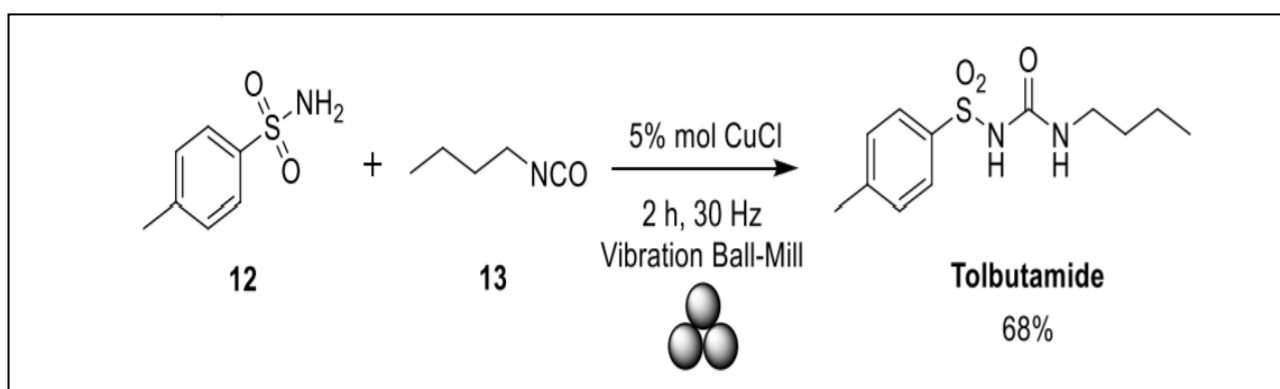
**Scheme 8.** Mechanochemical synthesis of axitinib by Heck-Migita coupling. Reagents and conditions: (i) NBS, NaOH, silica gel (ii)  $\text{CH}_3\text{SO}_3\text{H}$ , dihydropyran, silica gel (iii) compound **2n**,  $\text{Pd}(\text{OAc})_2$ ,  $\text{PPh}_3$ , TBAB, TEA, NaBr (iv) compound **6**,  $\text{Pd}_2(\text{dba})_3$ , Xantphos,  $\text{Cs}_2\text{CO}_3$ , silica gel (v)  $p$ -TsOH, silica gel a gel.<sup>33</sup>

Amide bond formation via mechanical activation was also applied in the synthesis of teriflunomide,<sup>34</sup> an active pharmaceutical ingredient used for multiple sclerosis therapy. The synthesis of teriflunomide was achieved by a two-step mechanochemical coupling reaction using 5-methyl-4-isoxazolecarboxylic acid, CDI, and 4-(trifluoromethyl)aniline hydrochloride. The reaction's intermediate was hydrolyzed with aqueous HCl, and the product was filtered to obtain the pharmaceutical ingredient in 81% of yield (Scheme 9).<sup>34</sup>



**Scheme 9.** Synthesis of teriflunomide via three mechanochemical steps.<sup>34</sup>

In 2014, Tan and co-workers presented two mechanochemical synthetic routes for making anti-diabetic sulfonylurea APIs.<sup>10</sup> The elegant mechanochemical protocols for the synthesis of antidiabetic sulfonylurea tolbutamide have been reported by Frišić and collaborators. In this study, copper catalysis was used to carry out the coupling reaction between arylsulfonamides and isocyanates (Scheme 10). Tolbutamide was synthesized with a better yield by the use of 5% mol of CuCl and acetonitrile (LAG), reaching a 90% yield of the desired product (Scheme 10).<sup>1</sup>



**Scheme 10.** Mechanochemical synthesis of Tolbutamide under solvent-free conditions.<sup>1</sup>

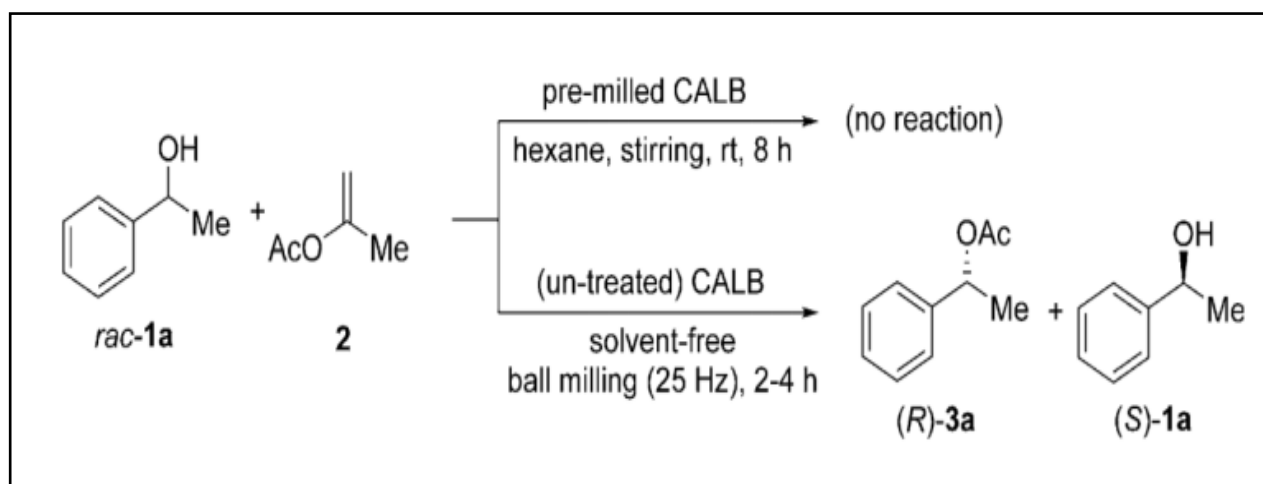
## 7. Mechanoenzymatics, a greener strategy in medicinal mechanochemistry

The amide and peptide bond formation by mechanochemical methods is a highly relevant topic in mechanochemistry, particularly in the medicinal mechanochemistry field. This field has attracted the attention of the scientific community for two reasons: (1) the fact that the energy produced by mechanical grinding is high enough to activate the coupling reaction between two amino acids but sufficiently mild to prevent denaturation of the synthesized peptides, even when



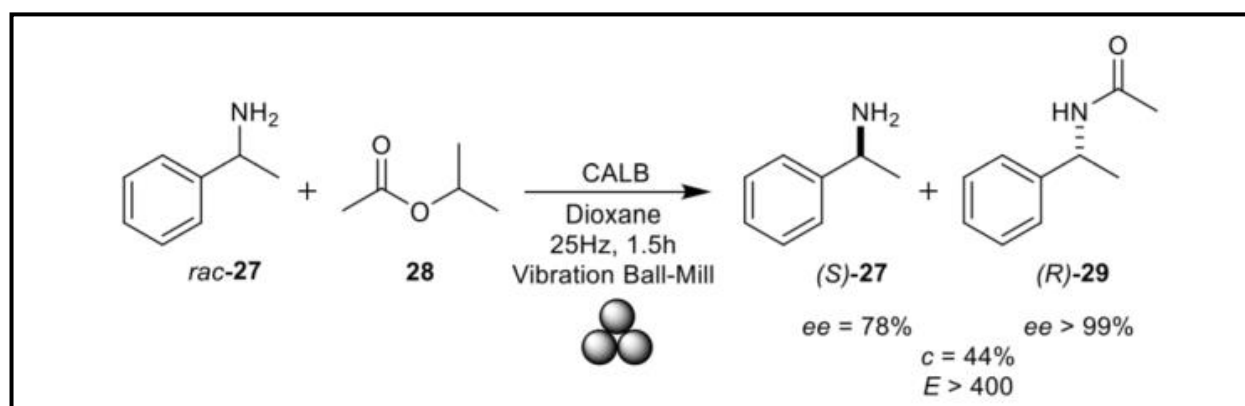
susceptible polypeptide structures are prepared and (2) the excellent results achieved when peptides are used as organocatalysts in enantioselective mechanochemical reactions, including their easy recovery from the reaction medium.

The first example of a mechanoenzymatic reaction to obtain pharmaceutical derivatives was published very recently <sup>35</sup> using immobilized *Candida antarctica* lipase B (CALB) as a biocatalyst. Indeed one of the most widely used lipases in both academia and industry is immobilized CALB (commercially available as Novozym 435). The higher efficiency of CALB to carry out regio-, chemo-, and enantioselective transformations, as well as relevant enzymatic properties like resilience to harsh conditions, and the observed high recyclability when the enzyme is immobilized has converted CALB into a highly useful biocatalyst.<sup>1</sup>



**Scheme 11.** Top: Enzymatic kinetic resolution of *rac*-1a in hexane using premilled CALB; bottom: mechanochemical resolution of *rac*-1a catalyzed by CALB in the ball mill.<sup>35</sup>

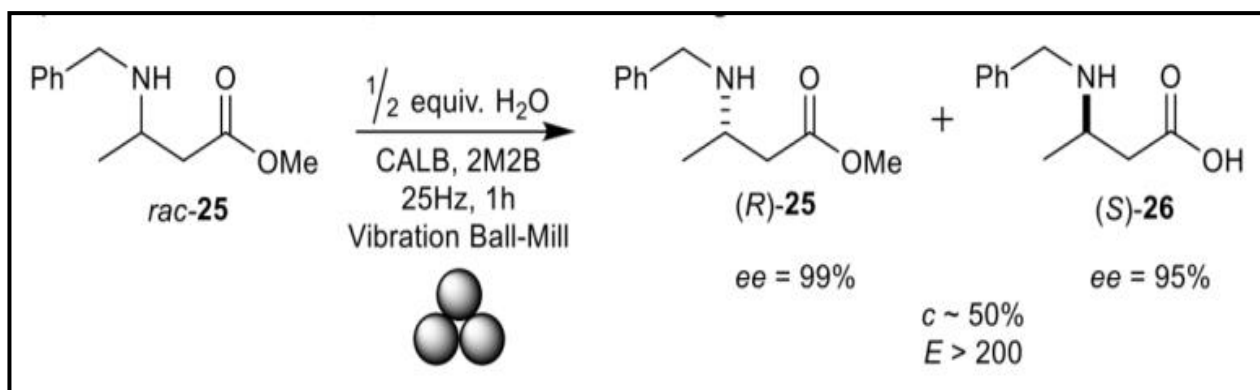
In the past few years, deracemization protocols that utilise immobilized CALB have been applied for the synthesis of commercially available pharmacologically active compounds. Pérez-Venegas and Juaristi developed a mechanoenzymatic strategy in this regard for the deracemization of primary amines directly bonded to a stereogenic carbon (Scheme 12).<sup>1</sup>



**Scheme 12.** Deracemization of Chiral Amines via Mechanoenzymatic Kinetic Resolution.<sup>1</sup>

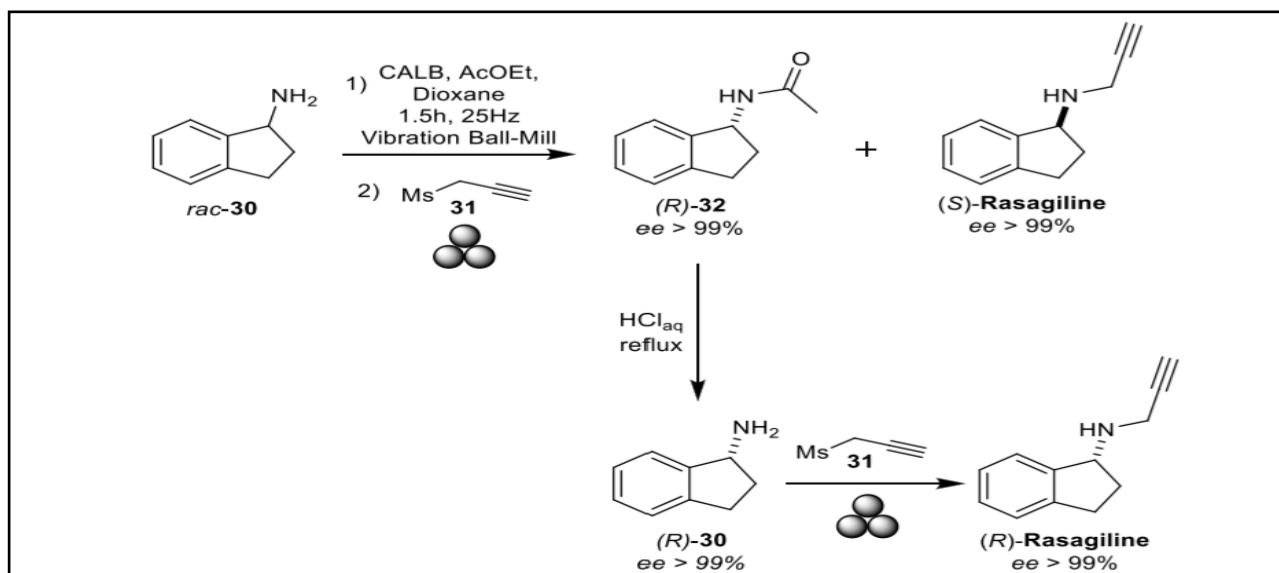
The decay in catalytic activity of the CALB upon recycling could either stem from partial denaturation of the biocatalyst upon milling, or be due to leaching of the lipase from the solid support. This phenomenon is very usual when working with physically adsorbed biocatalysts like CALB. Besides, lipase B from *Candida antarctica*, Amano lipase PS-IM from *Burkholderia cepacia* immobilized on diatomaceous earth catalyzed the mechanochemical kinetic resolution, indicating the general compatibility between lipases and ball milling techniques.<sup>36</sup>

Chiral alcohols are present in a wide number of pharmacologically active compounds such as nifenalol, salbutamol, isoproterenol, ezetimibe, among others, which promotes the interest in the development of sustainable protocols for the preparation of enantiopure alcohols. Similarly, the enantioselective synthesis of  $\beta$ -amino acid is currently a research field of significant interest in medicinal chemistry. In this regard, Pérez-Venegas *et al.* reported a mechanoenzymatic strategy for the enantioselective synthesis of  $\beta^3$ -amino acids<sup>37</sup> very recently, using kinetic resolution mediated by N435 and LAG (Scheme 13).



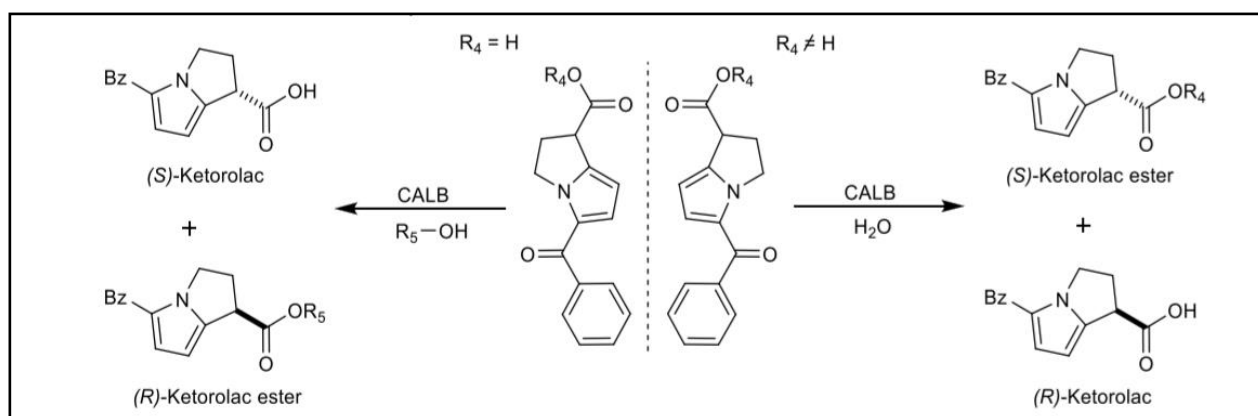
**Scheme 13.** Mechanoenzymatic Resolution of  $\beta^3$ -Amino Esters Using Immobilized CALB and Mechanical Activation (2M2B = 2-methyl-2-butanol).<sup>1</sup>

The new and highly effective mechanoenzymatic deracemization process of chiral amines was applied also in the synthesis of the enantioselective active (R) enantiomer of rasagiline, a monoamine oxidase inhibitor used in the treatment of the Parkinson's disease. The synthesis of (R)-rasagiline (Scheme 14) started with the mechanoenzymatic (CALB) deracemization of 1-aminoindan (*rac*-30) utilizing ethyl acetate as the acylating agent. Once the kinetic resolution was completed, propargyl mesylate(31) was added to the milling jar and the reaction was milled for 15 min to obtain the acylated product (R)-32 and the (S)-enantiomer of rasagiline. The acylated product was deprotected under acidic conditions, and the resulting amine was milled with propargyl mesylate to obtain the active (R)-rasagiline in enantiopure form (*ee* > 99%).



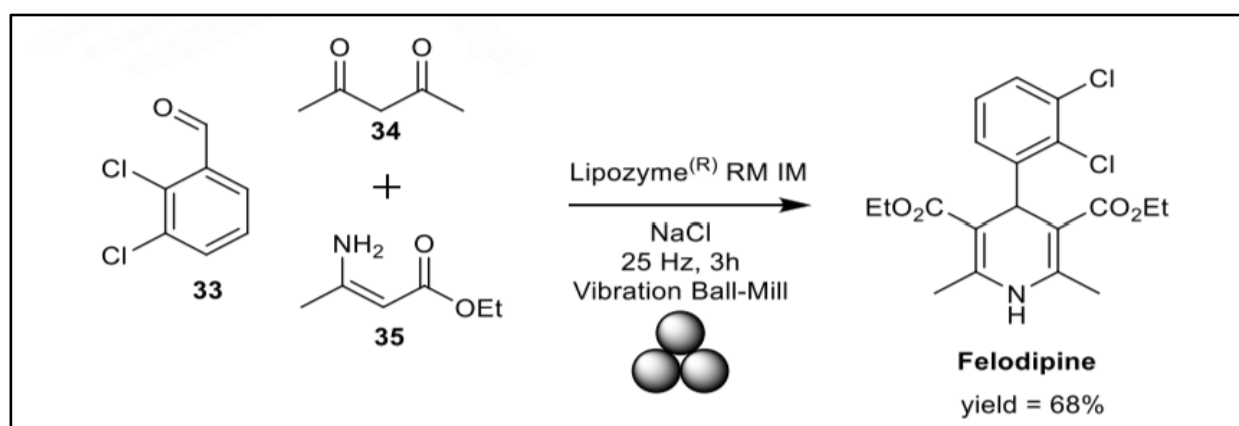
**Scheme 14.** Synthesis of (R)-Rasagiline via Mechanoenzymatic Kinetic Resolution.<sup>1</sup>

An analogous mechanoenzymatic kinetic resolution procedure utilizing N435 was employed in the synthesis of both enantiomers of ketorolac using two alternative approaches (Scheme 14).<sup>1</sup> The first strategy (left side in Scheme 14) that involves the CALB mediated enantioselective esterification of the carboxylic function in racemic ketorolac. The alternative strategy (right side in Scheme 15) unlike to the former consisted of the enantioselective hydrolysis of racemic ketorolac alkyl esters using water as LAG. Both strategies were carried out with good enantioselectivity (*ee* > 83%) for the anti-inflammatory (S)-enantiomer and simultaneously producing the enantiopure form (*ee* > 99%) of the less active (R)-isomer which is being used as a potential drug in the management of ovarian cancer.



**Scheme 15.** Dual Mechanochemical Enzymatic Resolution of rac-Ketorolac.<sup>1</sup>

Very recently Jiang *et al.* developed a mechanoenzymatic method, along similar lines, for the synthesis of 1,4-DHP calcium antagonists felodipine,<sup>38</sup> using an immobilized lipase from *Rhizomucor miehei* commercially available as lipozyme RM IM (Scheme 16).



**Scheme 16.** Mechanoenzymatic Synthesis of Felodipine.<sup>1</sup>

In addition to the substantial advantages offers by mechanoenzymatic protocols for synthesizing of pharmacologically active compounds, that include a significant reduction in reaction time and amount of solvent used, the application of a nonconventional and more efficient energy sources like mechanical force and the use of a biocatalyst that can be accessed through renewable sources lead to the fulfillment of the majority of the 12 green chemistry principles thus affording a truly sustainable process.

## 8. Medicinal mechanochemistry in the battlefield

The field of medicinal mechanochemistry has expanded during the past few years, from the development of novel crystalline structures to the development of innovative protocols for the synthesis of pharmacologically active compounds using biocatalysts.<sup>37</sup> Nevertheless, grinding and milling techniques have existed during most of pharmacy's history. Furthermore, dry and wet milling, mixing, granulation, and tableting are some of the most commonly used techniques in the pharmaceutical field involving the use of mechanical force that can produce useful modifications in the components of a substrate.

Relevant studies of how mechanical force produced during the tableting process can modify the crystallinity or even change the crystalline form of a pharmaceutical active ingredient have been reported with notable results.<sup>39</sup> In the same context, when pharmaceutically relevant enzymes were tableted, a reduction in the residual activity of the protein was observed, suggesting an inactivation mechanism owing to the mechanical force applied during tableting.<sup>40</sup> Moreover, mechanical force has been used as a strategy to inactivate aged pharmaceuticals; in a particular report,<sup>41</sup> ibuprofen was used as a model drug.

Finally, the medicinal mechanochemistry field can help understand and correct when necessary the fluctuations that happen throughout the production process of an active pharmaceutical ingredient. Clearly, this potential leads to an increase in the interest of the study of mechanical force as an inducer of physical and chemical transformations and to a greater interconnection of the medicinal mechanochemistry field with the pharmaceutical enterprise.

## 9. Conclusion

Several research groups in various countries have adopted mechanochemistry, including medicinal mechanochemistry, as one of their principal research fields that are leading to the establishment of mechanochemistry as an important tool for synthetic applications in fine chemistry and green chemistry. When comparing with classical thermal methods in solution, the preparation by mechanochemistry is particularly advantageous: yields are improved, the reaction conditions and therefore the work-up procedures are simplified, reduce the reaction times and the formation of by-products usually encountered in solution is avoided. These advantages perfectly match the design of a benign chemistry to achieve 'economy', not only of solvents but also in terms of time, reagents and waste, avoiding harmful reaction conditions and complex experimental settings and provides a cheap and sustainable alternative to prepare APIs at a reduced cost and with low environmental impact. The future of pharmaceutical and medicinal chemistry will extremely dependent on the

development of medicinal mechanochemistry field. It doesn't only provide access to reactivity or materials that are difficult or even impossible to achieve in solution, but provides a general answer to the demands of pharmaceutical industry for greener and more effective approaches of chemical synthesis and materials processing. The further development of the field, in particular towards: 1) creating standard protocols for solvent-free research and chemical engineers interested in this area and 2) educating and encouraging chemists and chemical engineers interested in this area and 3) designing further mechanistic studies whose results can be deployed to build a systematic understanding of mechanochemical reactions which are the three steps that are necessary to achieve what we perceive as the ultimate goal of mechanochemistry: creating a foundation for a cleaner, safer, solvent-free approach to chemistry in the laboratory and in the industry.

## References

1. Pérez-Venegas, M.; Juaristi, E. Mechanochemical and Mechanoenzymatic Synthesis of Pharmacologically Active Compounds: A Green Perspective. *ACS Sustainable Chem. Eng.* **2020**, *8*, 8881-8893.
2. Crawford, D.; Casaban, J.; Haydon, R.; Giri, N.; McNally, T.; James, S. L. Synthesis by extrusion: Continuous, large-scale preparation Of MOFs using little or no solvent. *Chem. Sci.* **2015**, *6*, 1645-1649.
3. Michalchuk, A. A. L.; Boldyreva, E. V.; Belenguer, A. N.; Emmerling F.; Boldyrev, V.V. Tribochemistry, Mechanical Alloying, Mechanochemistry: What is in a Name? *Front. Chem.* **2021**. doi: 10.3389/fchem.2021.685789.
4. Friščić, T.; Mottillo, C.; Titi, H. M. Mechanochemistry for Synthesis. *Angew. Chem. Int. Ed.* **2019**, *59*, 1018-1029.
5. Gomes, C.; Vinagreiro, C. S.; Damas, L.; Aquino, G.; Quaresma, J.; Chaves, C.; Pimenta, J.; Campos, J.; Pereira, M.; Pineiro, M. Advanced Mechanochemistry Device for Sustainable Synthetic Processes. *ACS Omega.* **2020**, *5*, 10868-10877.
6. Crawford, D. E.; Porcheddu, A.; McCalmont, A. S.; Delogu, F.; James, S. L.; Colacino, E. Solvent-Free, Continuous Synthesis of Hydrazone-Based Active Pharmaceutical Ingredients by Twin-Screw Extrusion. *ACS Sustainable Chem. Eng.* **2020**, *8*, 12230-12238.
7. Do, J.-L.; Friščić, T. Chemistry 2.0: Developing a New, Solvent-Free System of Chemical Synthesis Based on Mechanochemistry. *Synlett.* **2017**, *28*, 2066–2092.
8. Sheldon, R. A. The *E* factor 25 years on: the rise of green chemistry and sustainability. *Green Chem.* **2017**, *19*, 18–43.
9. Aken, K. V.; Strekowski, L.; Patiny, L. EcoScale, a semi-quantitative tool to select an organic preparation based on economical and ecological parameters. *Beilstein J. Org. Chem.* **2006**, *2*, 1–7.

10. Tan, D.; Loots, L.; Friščić, T. Towards medicinal mechanochemistry: evolution of milling from pharmaceutical solid form screening to the synthesis of active pharmaceutical ingredients (APIs). *Chem. Commun.***2016**, 52, 7760–7781.
11. Yebooue, Y.; Gallard, B.; Moigne, N. L.; Jean, M.; Lamaty, F.; Martinez, J.; Métro, T.-X. CMR-free and solid-tolerant peptide couplings by reactive extrusion. *ACS Sustainable Chem. Eng.***2018**, 6, 12, 16001-16004.
12. Hasa, D.; Rauber, G. S.; Voinovich, D.; Jones, W. Cocrystal Formation through Mechanochemistry: from Neat and Liquid-Assisted Grinding to Polymer-Assisted Grinding. *Angew. Chem. Int. Ed.***2015**, 54, 7371-7375.
13. Friščić, T.; Reid, D. G.; Halasz, I.; Stein, R. S.; Dinnebier, R. E.; Duer, M. J. Ion- and Liquid-Assisted Grinding: Improved Mechanochemical Synthesis of Metal–Organic Frameworks Reveals Salt Inclusion and Anion Templating. *Angew. Chem. Int. Ed.***2010**, 49, 712 –715.
14. André, V.; Hardeman, A.; Halasz, I.; Stein, R. S.; Jackson, G. J.; Reid, D. G.; Duer, M. J.; Curfs, C.; Duarte, M. T.; Friščić, T. Mechanosynthesis of the Metallodrug Bismuth Subsalcylate from Bi<sub>2</sub>O<sub>3</sub> and Structure of Bismuth Salicylate without Auxiliary Organic Ligands. *Angew. Chem. Int. Ed.***2011**, 50, 7858–7861.
15. Konnert, L.; Dimassi, M.; Gonnet, L.; Lamaty, F.; Martinez, J.; Colacino, E. Poly(ethylene) glycols and mechanochemistry for the preparation of bioactive 3,5-disubstituted hydantoins. *RSC Adv.***2016**, 6, 36978–36986.
16. Hammerer, F.; Loots, L.; Do, J.-L.; Therien, J. P. D.; Nickels, C. W.; Friščić, T.; Auclair, K. Solvent-free enzyme activity: quick, high-yielding mechanoenzymatic hydrolysis of cellulose into glucose. *Angew. Chem.***2018**, 57, 2621-2624.
17. Kaabel, S.; Stein, R. S.; Fomitšenko, M.; Järving, I.; Friscic, T.; Aav, R. Size-control by anion templating in mechanochemical synthesis of hemicucurbiturils in the solid state. *Angew. Chem.***2019**, 58, 6230-6234.
18. Tan, D.; Friščić, T. Mechanochemistry for Organic Chemists: An Update. *Eur. J. Org. Chem.***2017**, 18-33.
19. Sović, I.; Lukin, S.; Meštrović, E.; Halasz, I.; Porcheddu, A.; Delogu, F.; Ricci, P. C.; Caron, F.; Perilli, T.; Dogan, A.; Colacino, E. Mechanochemical Preparation of Active Pharmaceutical Ingredients Monitored by In Situ Raman Spectroscopy. *ACS Omega.***2020**, 5, 28663-28672.
20. Do, J.-L.; Friščić, T. Mechanochemistry: A Force of Synthesis. *ACS Cent. Sci.***2017**, 3, 13–19.
21. Eilks, I.; Rauch, F. Sustainable development and green chemistry in chemistry education. *Chem. Educ. Res. Pract.***2012**, 13, 57–58.
22. Konnert, L.; Lamaty, F.; Martinez, J.; Colacino, E. Recent Advances in the Synthesis of Hydantoins: The State of the Art of a Valuable Scaffold. *Chem. Rev.***2017**, 117, 13757–13809.

23. Roschangar, F.; Colberg, J.; Dunn, P. J.; Gallou, F.; Hayler, J. D.; Koenig, S. G.; Kopach, M. E.; Leahy, D. K.; Mergelsberg, I.; Tucker, J. L.; Sheldon, R. A.; Senanayake, C. H. A deeper shade of green: inspiring sustainable drug manufacturing. *Green Chem.***2016**, *19*, 281-285.
24. Colacino, E.; Porcheddu, A.; Charnay, A. C.; Delogu, F. From enabling technologies to medicinal mechanochemistry: an eco-friendly access to hydantoin-based Active Pharmaceutical Ingredients. *React. Chem. Eng.***2019**, *4*, 1179-1188.
25. Konnert, L.; Lamaty, F.; Martinez, J.; Colacino, E. Recent Advances in the Synthesis of Hydantoins: The State of the Art of a Valuable Scaffold. *Chem. Rev.***2017**, *117*, 13757-13809.
26. Kappe, C. O.; Dallinger, D. The impact of microwave synthesis on drug discovery. *Nat. Rev. Drug Discovery.***2006**, *5*, 51-63.
27. Declerck, V.; Nun, P.; Martinez, J.; Lamaty, F. Solvent-Free Synthesis of Peptides. *Angew. Chem. Int. Ed.***2009**, *48*, 9318-9321.
28. Bonnamour, J.; Métro, T.-X.; Martinez, J.; Lamaty, F. Environmentally benign peptide synthesis using liquid-assisted ball-milling: application to the synthesis of Leu-enkephalin. *Green Chem.* **2013**, *15*, 1116-1120.
29. Krause, T.; Gerbershagen, M. U.; Fiege, M.; Weißhorn, R.; Wappler, F. Dantrolene – A review of its pharmacology, therapeutic use and new developments. *Anaesthesia.***2004**, *59*, 364-373.
30. Guay, D. R. An Update on the Role of Nitrofurans in the Management of Urinary Tract Infections. *Drugs.***2001**, *61*, 353-364.
31. Colacino, E.; Porcheddu, A.; Halasz, I.; Charnay, C.; Delogu, F.; Guerra, R.; Fullenwarth, J. Mechanochemistry for “no solvent, no base” preparation of Hydantoin-based Active Pharmaceutical Ingredients: Nitrofurantoin and Dantrolene. *Green Chem.***2018**, *20*, 2973-2977.
32. Konnert, L.; Reneaud, B.; Figueiredo, R. M.; Campagne, J.-M.; Lamaty, F.; Martinez, J.; Colacino, E. Mechanochemical Preparation of Hydantoins from Amino Esters: Application to the Synthesis of the Antiepileptic Drug Phenytoin. *J. Org. Chem.***2014**, *79*, 10132-10142.
33. Yu, J.; Hong, Z.; Yang, X.; Jiang, Y.; Jiang, Z.; Su, W. Bromide-assisted chemoselective Heck reaction of 3-bromoindazoles under high-speed ball-milling conditions: synthesis of axitinib. *Beilstein J. Org. Chem.***2018**, *14*, 786-795.
34. Métro, T.-X.; Bonnamour, J.; Reidon, T.; Sarpoulet, J.; Martinez, J.; Lamaty, F. Mechanochemical synthesis of amides in the total absence of organic solvent from reaction to product recovery. *Chem. Commun.***2012**, *48*, 11781-11783.
35. Hernández, J. G.; Frings, M.; Bolm, C. Mechanochemical Enzymatic Kinetic Resolution of Secondary Alcohols under Ball-Milling Conditions. *ChemCatChem.***2016**, *8*, 1769-1772.
36. Bolm, C.; Hernández, J. G. From Synthesis of Amino Acids and Peptides to Enzymatic Catalysis: A Bottom-Up Approach in Mechanochemistry. *ChemSusChem.***2018**, *11*, 1410-1420.
37. Pérez-Venegas, M.; Reyes-Rangel, G.; Neri, A.; Escalante, J.; Juaristi, E. Mechanochemical enzymatic resolution of *N*-benzylated-β3-amino esters. *Beilstein J. Org. Chem.***2017**, *13*, 1728-1734.



38. Jiang, L.; Ye, L.-d.; Gu, J.-l.; Su, W.-k.; Ye, W.-t. Mechanochemical enzymatic synthesis of 1,4-dihydropyridine calcium antagonists and derivatives. *J. Chem. Technol. Biotechnol.***2019**, *94*, 2555–2560.
39. Otsuka, M.; Matsuda, Y. Effects of Environmental Temperature and Compression Energy on Polymorphic Transformation during Tableting. *Drug Dev. Ind. Pharm.***1993**, *19*, 2241–2269.
40. Picker, K. M. Influence of tableting on the enzymatic activity of different  $\alpha$ -amylases using various excipients. *Eur. J. Pharm. Biopharm.***2002**, *53*, 181–185.
41. Andini, S.; Bolognese, A.; Formisano, D.; Manfra, M.; Montagnaro, F.; Santoro, L. Mechanochemistry of ibuprofen pharmaceutical. *Chemosphere***2012**, *88*, 548–553.